From: [redacted]
To: ManstonAirport@pins.gsi.gov.uk
Subject: Fwd: Manston PINS interested party : 20012763
Date: 14 February 2019 16:21:35
Attachments: Modeling Aircraft NoiseInduced Sleep Disturbance.pdf

---

“I oppose this DCO as it is not in the national interest and is flawed”

In the interest of brevity I will only write about a few facets of the arguments put forward by RSP.

“Night flights will be kept to a minimum” they say. This is a meaningless and casuist statement at best. The customers will dictate when they buy flight time. The industry that produces perishable food stuffs and cut flowers uses the day time hours to harvest their produce. The night time is ‘dead’ time to them, so best used for transporting the goods. This aspect needs thorough investigation by the inspectorate to identify exactly what RSPs plans are for night flights.

The promise of jobs holds no real details of job roles and where the will actually be, locally at Manston or are they including jobs at other sites and undefined jobs in related industries. How many will be full time and above the living wage? Please investigate this for full details from RSP.

I have lived on and off in Ramsgate since 1963 and if any real jobs were created at Manston airport in the past they were in the dozens, and were generally low grade, zero hours and on call 24/7”.

I have lived under the flight path, when Manston was an airport, at various distances from the runway. The pollution of chemical pollution was evident by the residue of aircraft fuel floating on pond surfaces. We could smell it on the washing that was hung outside to dry. Then there was the noise pollution. You could not continue a conversation either with another person or on the telephone. It was a nightmare being woken suddenly at night when there were breaches of the previous no night flight restrictions. The aircraft were very old, noisy types that were not maintained to the point where they even appeared very dirty and unkempt. Humanitarian and emergency night flight are never an issue. However, night flights would cause sleep disturbance, which would affect our quality of life negatively. This is well researched. See attached.

Project paper attached: Modelling Aircraft Noise- Induced Sleep Disturbance 2013 concludes on page 294, paragraph 1:

9. SUMMARY, OUTCOMES AND RECOMMENDATIONS FOR FUTURE

WORK

‘Night time aircraft noise can disturb sleep in communities, causing a decrease in rapid

eye movement and slow wave sleep and an increase in the number of awakenings and

time spent awake. These changes in sleep may lead to both next day and long term

health effects’.

The Nethercourt estate and many surrounding properties are made up of many bungalows, housing a high proportion of elderly residents. To be faced with the prospect that we may face our last years under the blight of a 24-hour freight airport that is not even required and of national need, will be a devastating blow for myself and thousands of others.

Please ensure RSP stick to their consultation mantra that night flights are not needed. I request that the night flights are therefore removed from their documentation. Their consultation document indicates a 24hr freight services including freight vehicle movements 24hrs a day.

This email has been scanned by the Symantec Email Security.cloud service.
For more information please visit http://www.symanteccloud.com

PARTNER

Partnership for AiR Transportation
Noise and Emissions Reduction
An FAA/NASA/Transport Canada-
sponsored Center of Excellence

Modeling Aircraft Noise-Induced Sleep Disturbance

A PARTNER Project 24 and 25A Report

prepared by
Sarah McGuire, Patricia Davies

December 2013

REPORT NO. PARTNER-COE-2013-004

Modeling Aircraft Noise-Induced Sleep Disturbance

A PARTNER Project 24 Report

Sarah McGuire, Patricia Davies

PARTNER-COE-2013-004

December 2013

This work was funded by the US Federal Aviation Administration Office of Environment and Energy under FAA Award No. 07-C-NE-PU, Amendment Nos. 013 and 028, and Award No. 09-C-NE-PU, Amendment Nos. 001, 008, 009, 014, and 019. This project was managed by Mehmet Marsan of the FAA.

Opinions, findings, and conclusions or recommendations expressed in this material are those of the authors and do not necessarily reflect the views of the FAA, NASA, Transport Canada, the U.S. Department of Defense, or the U.S. Environmental Protection Agency

The Partnership for AiR Transportation Noise and Emissions Reduction — PARTNER — is a cooperative aviation research organization, and an FAA/NASA/Transport Canada-sponsored Center of Excellence. PARTNER fosters breakthrough technological, operational, policy, and workforce advances for the betterment of mobility, economy, national security, and the environment. The organization's operational headquarters is at the Massachusetts Institute of Technology.

The Partnership for AiR Transportation Noise and Emissions Reduction
Massachusetts Institute of Technology, 77 Massachusetts Avenue, 33-240
Cambridge, MA 02139 USA
http://partner.mit.edu

TABLE OF CONTENTS

Page

LIST OF TABLES vii

LIST OF FIGURES xii

GLOSSARY xxvii

ABSTRACT xxxi

1. INTRODUCTION 1
   1.1 Motivation 2
   1.2 Objective 4
   1.3 Research Approach 6
   1.4 Thesis Outline 7

2. NOISE INDUCED SLEEP DISTURBANCE AND THE POTENTIAL HEALTH EFFECTS 10
   2.1 Normal Sleep 10
   2.2 Sleep Stage Classification 11
   2.3 Auditory Processing During Sleep 22
      2.3.1 Auditory Awakening Thresholds 22
      2.3.2 Auditory Processing During Rapid Eye Movement Sleep . . 24
   2.4 Measurement Methods 26
   2.5 Noise Induced Sleep Disturbance 30
   2.6 Mediating Factors 36
      2.6.1 Laboratory vs Field 36
      2.6.2 Habituation 38
      2.6.3 Noise Sensitivity 40
      2.6.4 Inter-Individual Variability 41
   2.7 Short Term Effects of Sleep Disturbance 42
      2.7.1 Sleepiness and Tiredness 42
      2.7.2 Performance 45
      2.7.3 Annoyance 47
      2.7.4 Coping Strategies 47
   2.8 Long-Term Health Effects and Potential Pathways 48
      2.8.1 Sympathetic Tone 48
      2.8.2 Cardiac Arousals 49
      2.8.3 Stress Hormones 50
      2.8.4 Appetite Regulation Hormones Leptin and Ghrelin 51

Page
2.8.5 Increased Blood Pressure . . . 52
2.8.6 Glucose Tolerance and Diabetes . . . 53
2.8.7 Myocardial Infarction and Stroke . . . 54
2.8.8 Mental Health . . . 55
2.9 Effects of Noise on Children . . . 56
2.10 Conclusions . . . 58

3. NOISE INDUCED SLEEP DISTURBANCE MODELS . . . 59
3.1 Obtained Survey Data . . . 59
3.1.1 US Sleep Disturbance Survey Data . . . 59
3.1.2 1999 UK Sleep Study Data . . . 62
3.1.3 1999 UK Sleep Study Data Used for Analysis . . . 64
3.2 Sleep Disturbance Models . . . 65
3.2.1 Single Event Awakening Models . . . 65
3.2.2 Models Based on Reported Sleep Disturbance . . . 69
3.2.3 Multiple Events Awakening Model . . . 70
3.2.4 Spontaneous vs Noise-Induced Awakenings . . . 72
3.2.5 Noise Protective Measures . . . 73
3.3 Model Comparisons . . . 74
3.3.1 Awakening Model Comparison . . . 74
3.3.2 Multiple Events Model Evaluation . . . 75
3.4 Conclusions . . . 81

4. MARKOV MODELS AND AIRCRAFT NOISE INDUCED SLEEP DISTURBANCE . . . 82
4.1 Description of Markov Model . . . 82
4.2 Modification of Sleep Structure Model . . . 85
4.3 Comparison of Markov Model Predictions to Behavioral Awakening US Survey Data . . . 93
4.4 Comparison of Markov Model Predictions to Data from UK Study . . . 95
4.5 Conclusions . . . 99

5. NON-NOISE DISTURBED SLEEP MODELS . . . 101
5.1 Markov Models . . . 101
5.2 Simple Dynamic Models . . . 106
5.2.1 Sleep Patterning Model . . . 106
5.2.2 Sleep Package Model . . . 106
5.2.3 Random Walk Sleep Model . . . 108
5.3 Flip-Flop Sleep-Wake Nonlinear Dynamic Models . . . 111
5.3.1 Phillips and Robinson's Sleep-Wake Model . . . 112
5.3.2 Rempe, Best, and Terman's Sleep Model . . . 115
5.4 Reciprocal Interaction REM Models . . . 116
5.4.1 McCarley and Hobson Lotka-Volterra REM Sleep Model . . . 118
5.4.2 REM Limit Cycle Reciprocal Interaction Model (LCRIM) . . . 128

Page
5.5 Two Process Model of Slow Wave Activity . . . 132
5.6 Combined Two Process SWA and Reciprocal Interaction REM Models 142
5.6.1 REM and Slow Wave Activity LCRIM-Based Integrated Sleep Control Model . . . 142
5.6.2 Acherman and Borbély's Combined REM and Slow Wave Activity Model . . . 149
5.6.3 Additional Combined REM and Slow Wave Activity Models 150
5.7 Use of Nonlinear Dynamic Models to Predict Noise-Induced Sleep Disturbance . . . 154
5.8 Conclusions . . . 158

6. ARTIFACT REMOVAL AND SLEEP STAGE CLASSIFICATION . . . 159
6.1 Overview of EEG Artifacts . . . 159
6.2 Description of Artifact Removal Methods . . . 162
6.3 Review of Existing Sleep Stage Classification Methods . . . 170
6.3.1 Slow Wave Sleep Detection . . . 170
6.3.2 Rapid Eye Movement Detection . . . 170
6.3.3 Sleep Spindle Detection . . . 174
6.3.4 Additional Features . . . 179
6.4 Sleep Stage Classification Algorithm . . . 180
6.5 Conclusions . . . 190

7. NONLINEAR SLEEP MODEL DEVELOPMENT AND PARAMETER ESTIMATION . . . 191
7.1 Limitations of Massaquoi and McCarley Model . . . 191
7.2 Altering Ultradian Oscillator-Slow REM Model . . . 208
7.3 Fast REM Model . . . 211
7.3.1 REM Density Calculation . . . 211
7.3.2 Form of Fast REM Model . . . 214
7.4 Model Parameter Estimation . . . 229
7.4.1 The Homeostatic Process S Model . . . 229
7.4.2 Slow Wave Activity . . . 233
7.4.3 The Wake Term . . . 240
7.4.4 Slow REM Sleep . . . 243
7.5 Overview of The Model So Far . . . 253
7.6 Thresholds for Scoring Sleep Stages . . . 254
7.7 Adding Noise Dependence to Model . . . 258
7.8 Combined Model . . . 260
7.9 Conclusions . . . 265

8. NOISE MODEL COMPARISONS FOR AIRPORT OPERATIONS . . . 270
8.1 Airport Noise Modeling . . . 270
8.2 Awakening Model Comparisons . . . 272
8.3 Sleep Disturbance Comparisons for Different Time Scenarios . . . 277

Page

8.3.1 Addition of Quadratic Dependence on Noise Level to Markov Model . . . 277
8.3.2 Time-Dependent Model Comparisons . . . 280
8.4 Conclusions . . . 290

9. SUMMARY, OUTCOMES AND RECOMMENDATIONS FOR FUTURE WORK . . . 294
9.1 Outcomes of This Research . . . 295
9.2 Recommendations for Future Work . . . 297

LIST OF REFERENCES . . . 299

APPENDICES
Appendix A. Noise Metrics . . . 314
Appendix B. Laboratory and Field Studies . . . 316
Appendix C. Coefficients for Basner's Markov Model . . . 322
Appendix D. Model Parameters Estimated for Each Subject . . . 323
Appendix E. Range for Nonlinear Model Parameters Estimated for Each Subject . . . 342
Appendix F. Equations and Coefficients of Nonlinear Dynamic Models . . . 344
F.1 Massaquoi and McCarley Model . . . 344
F.2 The Nonlinear Model Developed as Part of This Research. . . . 345
Appendix G. Code for Nonlinear Dynamic Model . . . 351
Appendix H. Code for Feature Extraction and Sleep Stage Scoring . . . 373

VITA . . . 393

LIST OF TABLES

Table		Page
2.1	EEG frequency bands.	13
2.2	Characteristics of sleep stages.	21
2.3	The number of studies that used the listed measurement techniques and measured the listed variables.	27
3.1	Number of locations and subjects that took part in the 3 US sleep studies.	61
3.2	Number of events and awakenings for each noise level for the 3 US field studies.	62
3.3	UK Data used in analysis. (Dark gray indicates that data was used in all analysis, light gray indicates data was not used in noise analysis. Y-data available, N-data not available).	66
3.4	Average number of awakenings per person. Highlighted in dark gray are situations where on average approximately 0.5 awakenings occur, light gray highlights where on average approximately one awakening occurs. Events were all indoor $SELA$=57 dB(A).	78
4.1	Coefficients of Basner's Markov models that were not estimated well due to a low probability of the transition occurring and thus a lack of observations on which to make a good estimate of the probability.	87
4.2	Mean time spent in each sleep stage for baseline no noise nights. The standard deviation of the data is in parenthesis.	99
5.1	Average (entire night) transition rates from Stage s_i to Stage s_j for Kemp and Kamphuisen's model (1986): (dark gray) highest transition rate, (light gray) second highest transition rate.	104
5.2	Average (entire night) transition rates from Stage s_i to Stage s_j for Basner's baseline model (2006): (dark gray) highest transition rate, (light gray) second highest transition rate.	104
5.3	The transition probabilities for the Semi-Markov model developed by Yang and Hursch (1973).	105
5.4	Values of the model parameters for the Fulcher, Phillips and Robinson sleep model (2008).	115

Table Page

5.5 Coefficients of the REM Reciprocal Interaction model (McCarley and Hobson, 1975). 123

5.6 Duration of REM sleep and period of X in minutes for different coefficient values. (See Table 5.5 for original values of a, b, c, and d). 127

5.7 Coefficients of the Two Process Model (Achermann and Borbély, 1990). 135

5.8 Effect of an increase in coefficient value on the solution of the Two Process Model. 140

5.9 Coefficients of Massaquoi and McCarley's LCRIM/I Model (1992). . . . 147

5.10 Coefficients of Achermann and Borbély's Combined REM and Slow Wave Activity model (1992). 151

5.11 Comte et al.'s model cofficients (2006). 153

5.12 Summary of nonlinear dynamic sleep model structures. 157

6.1 Artifacts in EEG signals. PCA-Principal Components Analysis, ICA-Independent Components Analysis, Regression-Linear regression using other recorded signals such as ECG and EOG. 160

6.2 Key features of sleep stages and characteristics of polysomnography data that were extracted. 181

6.3 Sensitivity and Specificity for identifying sleep stages. 189

7.1 Coefficients of Massaquoi and McCarley's LCRIM/I Model (1992). . . . 192

7.2 Positions of the equilibrium points for the baseline fast REM sleep model. 218

7.3 Coefficients of the SWA model estimated from data taken from 76 subject nights of the 1999 UK study. Mean and standard deviation of these estimates, based on the data, and original values from Achermann, Dijk, Brunner, and Borbély (1993). 240

7.4 Estimated values for the statistics of the impulsive excitation ($N(t)$) that leads to the spontaneous wake model based on the UK dataset and original values from Massaquoi and McCarley (1992). 243

7.5 Statistics of slow wave activity during different sleep stages for 76 subject nights in the 1999 UK dataset. 255

7.6 Overall statistics of the fraction of times there was agreement in sleep stage classification between scoring of the original data and automated scoring of simulated data for each of 76 subject nights. 255

Table Page

7.7 Statistics of the fraction of times that there was agreement in sleep stage classification between scoring of the original data and automated scoring of simulated data for each of the 76 subject nights, for each sleep stage. 258

7.8 Parameters of the nonlinear model. *Parameters varied according to a Gaussian distribution, + parameters varied according to a uniform distribution, and x parameter varied according to an exponential distribution. 264

8.1 Aircraft at Airport A. 271

8.2 Aircraft at Airport B. 272

8.3 Number of people within awakening contours for Airport A, with 150 events during the night. 282

Appendix Table

B.1 Laboratory studies-sleep measurements. 316

B.2 Laboratory studies-additional measurements. 317

B.3 Field studies-sleep measurements. 318

B.4 Field studies-additional sleep measurements. 319

B.5 Field studies-noise measurements. 320

B.6 Field studies-additional noise measurements. 321

C.1 Coefficients for Basner's Four Markov Models (2006). 322

D.1 Estimated parameters for Process S and SWA models for field subjects 1 through 12 in the 1999 UK study. 324

D.2 Estimated parameters for Process S and SWA Models for field subjects 13 through 18 in the 1999 UK study. 325

D.3 Estimated parameters to define the random noise term $n(t)$ for field subjects 1 through 12 in the 1999 UK study. 326

D.4 Estimated parameters to define the random noise term $n(t)$ for field subjects 13 through 18 in the 1999 UK study. 327

D.5 Estimated Slow REM parameters for the 1st REM period for field subjects 1 through 12 in the 1999 UK study. 328

D.6 Estimated Slow REM parameters for the 1st REM period for field subjects 13 through 18 in the 1999 UK study. 329

D.7 Estimated Slow REM parameters for the 2nd REM period for field subjects 1 through 12 in the 1999 UK study. 330

Appendix Table Page

D.8 Estimated Slow REM parameters for the 2nd REM period for field subjects 13 through 18 in the 1999 UK study. 331

D.9 Estimated Slow REM parameters for the 3rd REM period for field subjects 1 through 12 in the 1999 UK study. 332

D.10 Estimated Slow REM parameters for the 3rd REM period for field subjects 13 through 18 in the 1999 UK study. 333

D.11 Estimated Slow REM parameters for the 4th REM period for field subjects 1 through 12 in the 1999 UK study. 334

D.12 Estimated Slow REM parameters for the 4th REM period for field subjects 13 through 18 in the 1999 UK study. 335

D.13 Estimated parameters for Process S and SWA Models for laboratory subjects in the 1999 UK study. 336

D.14 Estimated parameters to define the random noise term $n(t)$ for laboratory subjects in the 1999 UK study. 337

D.15 Estimated Slow REM parameters for the 1st REM period for laboratory subjects in the 1999 UK study. 338

D.16 Estimated Slow REM parameters for the 2nd REM period for laboratory subjects in the 1999 UK study. 339

D.17 Estimated Slow REM parameters for the 3rd REM period for laboratory subjects in the 1999 UK study. 340

D.18 Estimated Slow REM parameters for the 4th REM period for laboratory subjects in the 1999 UK study. 341

E.1 Range of estimated parameter values for Process S and SWA Models for all field subject nights in the 1999 UK study. 342

E.2 Range of estimated parameter values for $n(t)$ for all field subject nights in the 1999 UK study. 342

E.3 Range of estimated parameter values for the Slow REM model for all field subject nights in the 1999 UK study. 342

E.4 Range of estimated parameter values for Process S and SWA Models for all laboratory subject nights in the 1999 UK study. 343

E.5 Range of estimated parameter values for $n(t)$ for all laboratory subject nights in the 1999 UK study. 343

E.6 Range of estimated parameter values for the Slow REM model for all laboratory subject nights in the 1999 UK study. 343

Appendix Table		Page
F.1	Coefficients of Massaquoi and McCarley's LCRIM/I Model (1992). . . .	347
F.2	Parameters of the nonlinear model. *Parameters varied according to a Gaussian distribution and + parameters varied according to a uniform distribution, x parameter varied with an exponential distribution. . . .	350
G.1	Subroutines of the nonlinear dynamic model.	351
H.1	Subroutines of the feature extraction code and sleep stage scoring algorithm.	373

LIST OF FIGURES

Figure		Page
1.1	Diagram of the steps involved in assessing the effect of nighttime aircraft noise on communities.	5
1.2	Diagram of the steps involved in developing a nonlinear dynamic sleep model and comparing its performance in predicting community sleep disturbance with that of other models.	8
2.1	An example of a normal sleep pattern.	12
2.2	The percent of time spent in each of the 6 sleep stages for different age groups. Each bar represents a different age group. The age groups are 3-5 yrs, 6-9 yrs, 10-12 yrs, 13-15 yrs, 16-19 yrs, 20-29 yrs, 30-39 yrs, 40-49 yrs, 50-59 yrs, 60-69 yrs, and 70-79 yrs. The bars are shown in order of increasing age; 3-5 yrs (black) to 70-79 yrs (light gray) (Williams, Karacan, and Hursch, 1974).	12
2.3	The standard placement of EEG electrodes, based on a diagram in Spriggs (2008).	14
2.4	An example of the EEG and EOG signals for Stage Wake. (a) C3-A2 EEG channel, (b) Right EOG channel, and (c) Left EOG channel.	16
2.5	An example of the EEG and EOG signals for Stage 1. (a) C3-A2 EEG channel, (b) Right EOG channel, and (c) Left EOG channel.	17
2.6	An example of vertex waves, a characteristic feature of Stage 1 sleep.	17
2.7	An example of sleep spindles, a characteristic feature of Stage 2 sleep.	18
2.8	An example of a K-complex with sleep spindles, a characteristic feature of Stage 2 sleep.	18
2.9	Examples of the EEG signals for (a) Stage 3 and (b) Stage 4 sleep.	19
2.10	An example of EEG, EMG, and EOG signals during REM sleep. (a) C3-A2 EEG channel, (b) EMG, (c) Right EOG channel, and (d) Left EOG channel.	20

Figure Page

3.1 Output of various awakening models for each 5 dB grouping of *SELA* values. From left to right; 1) Anderson and Miller (2005), 2) ANSI dose response curve (2008), 3) Finegold and Elias (2002), 4) Passchier-Vermeer et al. (2002), 5) Ollerhead et al. (1992), 6) FICAN (1997), and 7) Basner et al. (2006) model predictions. 69

3.2 Example of the ANSI standard method of calculating percent awakened at least once for a full night of aircraft events. 71

3.3 The percent awakened in Fidell et al.'s surveys (red-circles) and model predictions (blue-x). (a) Anderson and Miller (2005), (b) Finegold and Elias (2002), (c) FICAN (1997), (d) Basner et al. (2006), (e) Passchier-Vermeer et al. (2002), and (f) Ollerhead et al. (1992) model predictions. 76

3.4 The effect of increasing the number of nighttime noise events on DNL and percent awakened at least once. (a) Increase in DNL and (b) increase in percent awakened at least once predicted using different awakening models. Indoor *SELA*=57 dB(A). 77

3.5 The percent awakened at least once for different numbers of events from 1 (thin line) to 200 (thick line). Each line represents 1, 2, 5, 10, 20, 50, 100, 150, or 200 nighttime events. (a) ANSI standard Model (2008), (b) Finegold and Elias (2002), (c) FICAN (1997), (d) Basner et al. (2006), (e) Passchier-Vermeer et al. (2002), and (f) Ollerhead et al. (1992) model predictions. 79

3.6 The average number of awakenings for different numbers of events from 1 (thin line) to 200 (thick line). Each line represents 1, 2, 5, 10, 20, 50, 100, 150, or 200 nighttime events. (a) ANSI standard Model (2008), (b) Finegold and Elias (2002), (c) FICAN (1997), (d) Basner et al. (2006), (e) Passchier-Vermeer et al. (2002), and (f) Ollerhead et al. (1992) model predictions. 80

4.1 Method for determining what sleep stage an individual is in using Basner's Markov model. 84

4.2 Sleep hypnogram, the output of the sleep structure model using the no noise model for one person. 85

4.3 (a) Probability of being in a particular sleep stage throughout the night predicted using Basner's baseline model. Stage 5 is REM, Stages 3 and 4 are slow wave sleep, Stage 0 is awake. (b) A close up of the plots for Stage 0, 1, 3, and 4. 86

Figure Page

4.4 Change in coefficients $c(s_i,s_1)$ (i=0, 1, 3, 4, 5) with noise level for transitions from Stage 1 to each sleep stage. Noise 1-First noise model, Noise 2-Second noise model, and Noise 3-Third noise model. 89

4.5 Change in the transition probabilities of the first noise model with noise level: (a) to (f) transitions to s_o thru s_5 for each stage. Bars further to the right are results for higher noise levels. The bar all the way to the left is for the baseline model. Levels are $SELA$ = 53, 63, 73, 83, 93, and 103 dB(A). * denotes unlikely scenario. 90

4.6 Change in the transition probabilities of the second noise model with noise level: (a) to (f) transitions to s_o thru s_5 for each stage. Bars further to the right are results for higher noise levels. The bar all the way to the left is for the baseline model. Levels are $SELA$ = 53, 63, 73, 83, 93, and 103 dB(A). 91

4.7 Change in the transition probabilities of the third noise model with noise level: (a) to (f) transitions to s_o thru s_5 for each stage. Bars further to the right are results for higher noise levels. The bar all the way to the left is for the baseline model. Levels are $SELA$ = 53, 63, 73, 83, 93, and 103 dB(A). 92

4.8 Coefficients of the first noise model. Basner's Original model coefficients (black triangles) and the estimated coefficients from the simulated noise-level dependent model (gray squares). Bars show the 5th and 95th percentile of estimates. 94

4.9 The percent awakened in the three US studies (light gray x) of Fidell et. al (1995, 2000) and that predicted by a modified version of Basner's model (dark gray circles) with 95% confidence intervals, the percent awakened predicted by Passchier-Vermeer et al.'s model (2002) is shown by the black dashed line. (a,b) A conscious awakening was defined as lasting at least 2 and half minutes. (c,d) A conscious awakening was defined as lasting at least 3 minutes. 96

4.10 Baseline Markov model predictions of the probability of being in Wake, REM, and NREM (red line). The estimated probability of being in these sleep stages calculated using the 1999 UK sleep data (blue circles). . . 97

4.11 Comparison of Markov model predictions for the probability of being in REM (red line), and the probability of being in the same sleep stages calculated using the (a) 1999 UK sleep data (blue circles) and (b) extracted from Basner (2006) (blue circles). 98

Figure Page

5.1 (a) Probability of being in a particular sleep stage throughout the night, from Zung et al.'s model: (light gray) model for 20-29 yr olds, (dark gray) model for 30-39 yr olds, and (black) model for 20-39 yr olds. (b) Probability of being in a particular sleep stage throughout the night predicted using Basner's baseline model. 103

5.2 Example of the results obtained from one simulation with Lawder's Model (1984). (a) The ramp (red-dotted line) and triangular waveform (blue-solid line) and (b) estimated sleep stages. 107

5.3 Example of the results obtained from one simulation with Lo et al.'s model. (a) Output of model and (b) classification of sleep stages. 110

5.4 (a) Predicted probability of awakening using Lo et al.'s model for (black) original values of Δ and (gray) decreased values of Δ. (b) Predicted probability of awakening using Basner's Baseline Markov model. 111

5.5 An example of an output of Phillips and Robinson's model (2007). (a) V_v the cell potential for VLPO neurons, (b) V_m, the cell potential for MA neurons, (c) the Homeostatic Process and (d) the Circadian Process. . 114

5.6 An example of the output of Rempe, Best, and Terman's model (2010). (a) Firing rate of aminergic wake promoting x_A (black) and VLPO sleep promoting x_V neurons (red dashed line), (b) firing rate of wake promoting x_A (black), NREM sleep promoting x_N (red dashed line) and REM sleep promoting x_R neuron activity (light gray),(c) firing rate of wake promoting x_A (black), NREM sleep promoting x_N (red dashed line) and REM sleep promoting x_R neuron activity (light gray) between 15 and 28 hours, and (d) scored sleep stages between 15 and 28 hours. 117

5.7 Solutions in the phase plane for different initial values of REM-ON (X) and REM-OFF (Y) activity. 121

5.8 REM-ON (X) (green/light gray) and REM-OFF (Y) (blue/black) activity for different initial conditions, (a) 0.5 times the original initial conditions, (b) the original initial conditions, and (c) 1.5 times the original initial conditions. 122

5.9 Results for different values of a, (a) $a = 0.75$ times the original coefficient, (b) $a =$ the original coefficient value, and (c) $a = 1.25$ times the original coefficient. REM-ON (X) (green) and REM-OFF (Y) (blue). See Table 5.5 for original values. Note the decrease in the X-Y period with increased a. 124

5.10 Example of how the threshold for REM sleep is determined. REM-ON (X) (green) and REM-OFF (Y) (blue). 125

Figure Page

5.11 Results for different values of b, (a) $b = 0.75$ times the original coefficient, REM duration = 4.5 minutes and REM period = 38.3 minutes, (b) $b =$ the original coefficient value, REM duration = 5.1 minutes and REM period = 45.0 minutes and (c) $b = 1.25$ times the original coefficient, REM duration = 5.5 minutes and REM period = 52.2 minutes. REM-ON (X) (green) and REM-OFF (Y) (blue). See Table 5.5 for original values. Note the increase of the X-Y period with increased b. 128

5.12 Results for different values of c, (a) $c = 0.75$ times the original coefficient, (b) $c =$ the original coefficient value, and (c) $c = 1.25$ times the original coefficient. REM-ON (X) (green) and REM-OFF (Y) (blue). See Table 5.5 for original values. Note the decrease in the X-Y period with increased c. 129

5.13 Results for different values of d, (a) $d = 0.75$ times the original coefficient, (b) $d =$ the original coefficient value, and (c) $d = 1.25$ times the original coefficient. REM-ON (X) (green) and REM-OFF (Y) (blue). See Table 5.5 for original values. Note the small change in the X-Y period with increased d. 130

5.14 Coefficient and saturation functions for the REM Limit Cycle Reciprocal Interaction model; (a) $a(X)$, (b) $b(X)$, (c) $S_1(X)$, and (d) $S_2(X)$. . . . 132

5.15 Solutions for a different phase of d_{circ}; (a) 0.5 times the original phase, (b) original phase = 2.3, and (c) 1.5 times the original phase. REM-ON (X) (green/light gray) and REM-OFF (Y) (blue/black). 133

5.16 Example of results from Achermann and Borbéy's Two Process Model (1990). Process S (Green), slow wave activity (SWA) (Blue), and scaled $REMT$ (Red). (a) Example 1 and (b) Example 2. 135

5.17 Slow wave activity for different values of rc. (a) Slow wave activity for the entire night and (b) slow wave activity between 50 and 150 minutes. . . 136

5.18 Slow wave activity for different values of fc. (a) Slow wave activity for the entire night and (b) slow wave activity between 40 and 150 minutes. 137

5.19 Results for different values of gc. (a) Slow wave activity, (b) slow wave activity from 50 and 150 minutes, and (c) Process S. 138

5.20 (a) Slow wave activity and (b) Process S for different initial values of Process S (S_o). (c) A close-up of slow wave activity between 0 and 50 minutes for different initial values of SWA (SWA_o). 139

Figure Page

5.21 Illustration of the effect of the extra S term on the outcome of slow wave activity, without the extra term (blue/black) and with the extra term (green/light gray). (a) SWA and (b) level of Process S for the entire night. 141

5.22 An example of the terms for excitation, N and E, ($k = 10$). 144

5.23 An example of using Massaquoi and McCarley's LCRIM/I model (1992) to classify sleep stages, (a) REM-ON (X) (green) and REM-OFF (Y) (blue) activity, (b) Process S and SWA, (c) Excitatory Activity (E), and (d) sleep stages. Thresholds used for scoring sleep stages (red-dashed lines). 146

5.24 The effect of changing the amplitude of N on the level of X (REM-ON) (green), Y (REM-OFF) (blue), and slow wave activity (SWA). (a,c,e,g) variation of amplitudes was based on the original model parameters, (b,d,f,h) amplitudes of N used to obtain E was increased by 50%, (Thresholds used for scoring sleep stages, red-dashed lines). 148

5.25 An example of the outcome of the combined Limit-Cycle Reciprocal Interaction Model and the Two Process Model by Achermann and Borbély (1992). (a) REM-ON (green) and REM-OFF Activity (blue), (b) Process S (green) and SWA (blue), (c) the circadian oscillator, and (d) scored sleep stages. 152

5.26 An example of the output of Comte et al.'s model (2006). (a) Wake neuron activity (w), (b) REM neuron activity (p), (c) SWS neuron activity (sw), and (d) sleep stages. 155

5.27 An example of the output of Diniz Behn and Booth's model (2010). (a) Firing rate of different neuron populations. Wake promoting neurons locus coeruleus and dorsal raphe (green), sleep promoting neurons VLPO (red), and REM promoting neurons (blue). (b) Homeostatic sleep drive (h) and (c) sleep stages. 156

6.1 (a) The ECG signal and (b) the EEG signal where the heart beats are being picked up in addition to the EEG information. 161

6.2 An example of an EOG artifact in an EEG signal, (a) EOG and (b) corresponding EEG signal with artifact. 162

6.3 An example of a movement artifact in the (a) EEG, (b) EMG, (c) Right EOG, and (d) Left EOG signal. 163

6.4 A diagram of the process used to remove ECG artifacts from the EEG signal. 164

Figure Page

6.5 An example of an outcome obtained using an RLS adaptive filter to remove ECG artifacts. The (a) ECG, (b) EEG with artifact, and (C) EEG after minimizing artifact signals. 166

6.6 An example of the use of Brunner et al.'s (1996) method to remove muscle and movement artifacts. (a) Power between 26.0 and 32.0 Hz of an EEG signal with artifacts present and (b) power after removing epochs which exceeded the threshold. 169

6.7 An example of slow wave sleep detection. (a) An EEG signal filtered between 0.5 and 2.0 Hz (blue) and zero crossings (red x) and (b) detected slow wave sleep. 171

6.8 The percent of each epoch containing slow wave sleep (SWS). 171

6.9 Cumulative power of 1,166 samples of rapid eye movement (black-dash line is at 0.5 Hz). 174

6.10 Correlation between right and left EOG Channels for one subject night in 1999 UK study. 175

6.11 (a) Scored sleep stages for one subject night from the 1999 UK Dataset and (b) the frequency with lowest decay rate calculated using an AR(4) model. 178

6.12 (a) EEG Segment and (b) the frequency with lowest decay rate for each 1 second segment determined from an adaptive AR(4) model. 179

6.13 Percentage of the total power in an EEG signal in the (a) Delta_1 band, (b) Theta band, (c) Alpha band, (d) Sigma band, and (e) Gamma frequency bands. 183

6.14 Average percentage of power for 76 subject nights in each of the frequency bands for sleep stages Wake (0), NREM Stages 1 through 4, and REM sleep (5). 184

6.15 The average (a) ratio of power in the alpha frequency band to the power in the theta frequency band, (b) percentile of the EMG and (c) percent of an epoch occupied by slow wave sleep (SWS) for 76 subject nights for sleep stages Wake (0), NREM Stages 1 through 4 and REM sleep (5). . 185

6.16 Steps used in developing sleep stage classification algorithm. 185

6.17 Rules used in scoring sleep stages. 186

6.18 Probability of being in (a) Stage Wake/S1, (b) Stage 2, (c) Stage 3/4 and (d) REM calculated using the developed algorithm. 187

Figure Page

6.19 (a) Original Sleep Stages from the UK dataset and (b) sleep stages scored using the developed algorithm. 188

7.1 Probability of being in Wake, REM, and NREM sleep predicted using the original parameters of the Massaquoi and McCarley model (blue), with the parameter c increased by 40% (green) and with Basner's Markov model (red). 193

7.2 Probability of being in Wake (light gray), REM (dark gray), and NREM sleep (black) predicted using, (a) and (b) the Massaquoi and McCarley model and (c) and (d) Basner's Markov model. (a) and (c) All individuals retired at 11:00 pm and (b) and (d) Gaussian variation in sleep onset was assumed. Results based on 100 simulations. 195

7.3 Example of a REM sleep period and the change in sleep stages within that period. 196

7.4 The time varying frequencies of the Massaquoi and McCarley model. (a) X model and (b) Y model. 198

7.5 Massaquoi and McCarley model predictions for 16 events of 1 minute duration occurring during the night. (a) Low amplitude (E_{max}=2.4, N_{max}=4) and (b) high amplitude (E_{max}=6.0, N_{max}=10) impulses. 200

7.6 The duration of REM, NREM and Wake stages predicted using the Massaquoi and McCarley model for nights with 16 events of different amplitudes of $N(t)$. The duration of the impulses in $N(t)$ was 1 minute and spacing between impulses was 30 minutes. 201

7.7 Massaquoi and McCarley model predictions for 64 events of 1 minute duration occurring during the night. (a) Low amplitude (E_{max}=1.8, N_{max}=3) and (b) high amplitude (E_{max}=3.6, N_{max}=7) impulses. 202

7.8 The duration of REM, NREM and Wake stages predicted using the Massaquoi and McCarley model for nights with 64 events of different amplitudes of $N(t)$. The duration of the impulses in $N(t)$ was 1 minute and spacing between impulses was 7.5 minutes. 203

7.9 Prediction of the Massaquoi and McCarley model when an excitation term (EX) was introduced in the REM-ON (X) equation. 204

7.10 Saturation function $f(X)$ used in Equation (7.7) to turn on E effects only when $X > 1.3$. 205

Figure Page

7.11 Prediction of the Massaquoi and McCarley model when an excitation term with a saturation function was added to the REM-ON (X) equation. A and B mark times when there are awakenings during the REM sleep period. (a) X (green) and Y (blue); (b) Process S (green) and SWA (blue); (c) excitatory term (E) (filtered rectangular pulses with uniformly distributed amplitudes and durations and exponentially distributed arrival times); and (d) sleep stage classification. 206

7.12 Prediction of the Massaquoi and McCarley model when an excitation term with a saturation function was added to the REM-ON (X) equation. Less desirable changes in sleep were obtained. (a) X (green) and Y (blue); (b) Process S (green) and SWA (blue); (c) excitatory term (E) (filtered rectangular pulses with uniformly distributed amplitudes and durations and exponentially distributed arrival times); and (d) sleep stage classification. 207

7.13 REM-ON activity (X) with (a) added sinusoidal noise with frequency of 4 oscillations per minute and amplitude of 40. (b) Added uniformly distributed (between -50 and 50) band-passed noise between frequencies of 1 and 4 oscillations per minute. 209

7.14 An example of rapid eye movement activity. (a) 30 second correlation between right and left EOG signals and the -0.2 threshold used (red dashed line), (b) REM density measurement-proportion of the 30 second epoch occupied by rapid eye movement activity, and (c) an indicator of Phasic and Tonic REM sleep. 213

7.15 A Duffing oscillator with two stable points at 0.5 and -0.5 and one unstable point at 0, $\delta = 0.06$ and $\omega = 2\pi(0.1)$. (a) Beam analogy, (b) potential function, (c) oscillations about one stable equilibrium (A=0.01), (d) chaotic jumps between equilibrium (A=0.4), and (e) periodic oscillations about both stable equilibria (A=0.6). 216

7.16 (a) REM period model beam analogy. A Duffing oscillator with 3 stable and 2 unstable equilibrium positions, ($\delta = 0.06$, $\omega = 2\pi(0.3)$, A=0.5) (b) $w(t)$=0, (c) 8 evenly spaced events of 1 minute, $-2 + \gamma w(t)$=-0.6 when events were occurring. 217

7.17 Phase plane for Duffing equation. Unstable equilibrium points (red/light gray), stable equilibrium points (black) ($\delta = 0.06$, $\omega = 2\pi(0.3)$, A=0.5), $y = \dot{x}$. 219

Figure Page

7.18 The potential function for the 5th order stiffness Duffing equation for different positions of the unstable equilibrium point between Wake and Tonic REM sleep, (a) -2.0, (b) -1.5, and (c) -1.0. m1, m2, m3 represent the magnet locations in the beam system analogy corresponding to "Phasic REM","Tonic REM" and "Wake" respectively. 221

7.19 (a) Solution of the Duffing equation, oscillations are about 3 stable equilibria, (red-dashed line) thresholds used to assign sleep stages. (b) Unstable equilibrium position $(-2+\gamma N)$ and (c) classified sleep stages. The driving frequency $\omega = 2\pi(0.3)$, $\delta = 0.06$ and the amplitude (A) was 0.5. 222

7.20 Statistics of Tonic and Phasic REM sleep for simulations (red) and survey data (blue). (a) Inter-arrival time of Phasic activity, (b) proportion of REM period (without awakenings) occupied by Tonic REM sleep and (c) proportion of REM period (without awakenings) occupied by Phasic REM sleep. 224

7.21 Proportion of the REM period defined as awake for (a) 2, (c) 4, and (e) 8 events as a function of level. Probability of awakening to, (b) 2, (d) 4, and (f) 8 noise events as a function of level. 225

7.22 Proportion of the REM period defined as Phasic REM sleep for (a) 2, (c) 4, and (e) 8 events as a function of level. Proportion of the REM period defined as Tonic REM sleep for (b) 2, (d) 4, and (f) 8 events as a function of level. 226

7.23 An example of Sleep Stages (blue) and identified REM periods (red dashed line). 231

7.24 (a) Sleep Stages. The start of each REM period is indicated by a red dot and the end of each REM period is marked by a black dot. (b) Estimated SWA (blue), 95th percentile of SWA for each NREM period (red dot) and the estimated Homeostatic Process S (black-dashed line). 232

7.25 SWA activity (blue), REM periods (black) and (a) portion of segment used to calculate rc (red) and (b) portion of segment used to calculate fc (red). 234

7.26 (a) Estimated noise term $n\tilde{(}t)$, (b) the original SWA (blue), and smoothed SWA (red). 237

7.27 Probability density function of $n(t)$ (black) and Gaussian distribution resulting from a fit to the data (red). 237

7.28 Statistics of $n(t)$ with tails of the distribution removed. Gray to black results from eliminating 1% to 5% of the tails of the distribution of $n(t)$ before calculating the statistics for each 30 minute segment. 238

Figure Page

7.29 Range of values for the (a) mean, (b) standard deviation, (c) skewness, and (d) kurtosis for all subjects based on statistics calculated from each moving 30 minute segment of the estimated random noise term $n(t)$. The results are shown as a boxplot: red line median, edge of each box is the lower and upper quartile, the red plus signs are outliers. 239

7.30 An example of gamma activity, arrows indicate inter-arrival time, duration and amplitude of the excitations. 241

7.31 (a) Distribution of inter-arrival times between estimated $N(t)$, (b) distribution of the duration of $N(t)$, and (c) distribution of the amplitude of $N(t)$ in the UK dataset. 242

7.32 (a) REM sleep duration and (b) NREM sleep duration. Mean values and $\pm$ one standard deviation of the estimated mean, estimated from the 1999 UK study. 244

7.33 An example of creating REM-ON (X) and REM-OFF (Y) signals based on the timing of REM sleep periods in the 1999 UK study data and Equations (7.33) and (7.34). 246

7.34 An example of the fitting of REM sleep model parameters of (a) the REM-ON model and (b) the REM-OFF model. Blue line is based on created signals and the red line is the linear model using the estimated parameters. 248

7.35 (a) Error between the estimated start time of each REM sleep period and the value derived from the UK dataset. (b) Error between the estimated duration of the REM sleep period and the value derived from the UK study data. The NREM duration is for the NREM period just before the REM period. 249

7.36 The created REM signal based on data and a simplified REM model (Equations 7.31 and 7.32) (blue/dark gray) and the simulated REM signal (green/light gray) using model parameters obtained from a linear fit to the study data. 250

7.37 Estimated parameters of slow REM model versus the duration of REM sleep. 251

7.38 Estimated parameters of the slow REM model versus the duration of the NREM sleep period prior to the REM period. 252

7.39 Mean and standard deviation of the estimated REM model parameters for each REM period. 253

Figure Page

7.40 Best agreement between simulated and actual slow wave activity for one subject night of the 1999 UK dataset, thresholds used for scoring sleep stages (red-dashed lines). 256

7.41 Worst agreement between simulated and actual slow wave activity for one subject night of the 1999 UK dataset, thresholds used for scoring sleep stages (red-dashed lines). 257

7.42 Diagram of impulsive noise as used in nonlinear dynamic model. 259

7.43 Example of the parameters for the developed nonlinear sleep model, which include slow wave activity (SWA), REM which is the X or REM-ON activity, REM sleep period indicator, Fast REM model and the spontaneous and noise induced excitation terms. 262

7.44 Sleep stages calculated using the developed nonlinear model. (a) No aircraft events, and (b) 32 events of an L_{Amax} of 60 dB(A). 263

7.45 Probability of being in each sleep stage predicted for a baseline no noise night using the developed nonlinear model (blue) and Basner's Markov model (red): (a) Wake/S1, (b) REM, (c) S2, (d) S3/S4 Stages. 266

7.46 Percent awakened predicted with the nonlinear dynamic model developed in this research (blue/dark gray) and the modified version of Basner's Markov model (red/light gray). 267

7.47 Change in duration of Wake/S1, SWS, and REM sleep for (a,c,e) 16 evenly spaced events and (b,d,f) 32 evenly spaced events. The nonlinear dynamic model predictions are shown in blue/dark gray and the predictions from the modified version of Basner's Markov model are shown in red/light gray. 268

8.1 Gray-scale shading indicates percent awakened at least once. Black to dark gray 75%, dark gray to light gray 50%, and light gray to white 25%. (a,b,c) Scenario 1 and (d,e,f) Scenario 2 for Airport A. (a,d) ANSI, (b,e) FICAN and (c,f) Basner et al. model. Red contours are the 40 and 55 dB(A) $L_{night,outside}$ contours. 274

8.2 Population distribution living around the Airports. (a) Airport A and (b) Airport B. Red contours are the 40 to 55 dB(A) $L_{night,outside}$ contours. . 275

8.3 Number of people awakened at least once around the Airports, predicted using Basner et al.'s awakening model. (a) Airport A and (b) Airport B. Red contours are the 40 to 55 dB(A) $L_{night,outside}$ contours. 276

Figure Page

8.4 (a) Percent awakened predicted when using Basner's Markov model for different values of the multiplier. (b) The relationship between L_{Amax} and the multiplier, based on Basner's field dose-response relationship. . . . 278

8.5 The obtained relationship between L_{Amax} and the percent awakened using the modified version of Basner's Markov model. Basner et al.'s (2004) dose-response curve is shown in blue,the mean of the simulated results in (green/light gray), and the results of 100 simulations in black. 279

8.6 The occurrence of events for six nighttime scenarios that were examined. Each bar represents the number of events during an hour of the night. There are eight bars per scenario representing each hour from 11 pm to 7 am. (a) Peak in operations in two hours in the middle of the night, (b) an even distribution, (c) most events in the middle of the night, (d) a U-shaped distribution, (e) most events at the beginning of the night, and (f) most events occurring at the end of the night. 280

8.7 Average number of awakenings for the 6 time scenarios predicted using the ANSI standard model with time dependence. Black to dark gray 1.5, dark gray to light gray 1.0 and light gray to white 0.5 awakenings. (a) Peak in operations in two hours in the middle of the night, (b) an even distribution, (c) most events in the middle of the night, (d) a U-shaped distribution, (e) most events at the beginning of the night, and (f) most events occurring at the end of the night. 281

8.8 Average number of awakenings for the 6 time scenarios predicted using Basner's Markov model with added quadratic dependence on noise level. Black to dark gray 1.5, dark gray to light gray 1.0, and light gray to white 0.5 awakenings. (a) Peak in operations in two hours in the middle of the night, (b) an even distribution, (c) most events in the middle of the night, (d) a U-shaped distribution, (e) most events at the beginning of the night, and (f) most events occurring at the end of the night. 283

8.9 Average number of awakenings for the beginning of the night (black to dark gray 1.5, dark gray to light gray 1.0 and light gray to white 0.5 awakenings) and end of the night (blue contours) for (a) the ANSI standard model with time dependence and (b) Basner's Markov model with added quadratic dependence on noise level. 284

8.10 Predictions of the average number of awakenings using Basner's Markov model with added quadratic dependence on noise level for the scenario in which most events are at the beginning of the night (black to dark gray 1.5, dark gray to light gray 1.0 and light gray to white 0.5 awakenings) and the $L_{night,outside}$ contours (red). 285

Figure Page

8.11 SQI predictions for the 6 nighttime flight operation scenarios. (a) Peak in operations in two hours in the middle of the night, (b) an even distribution, (c) most events in the middle of the night, (d) a U-shaped distribution, (e) most events at the beginning of the night, and (f) most events occurring at the end of the night. Red contours are the 40 to 55 dB(A) $L_{night,outside}$ contours. 287

8.12 Reduction in time spent (minutes) in slow wave sleep for the 6 nighttime flight operation scenarios. (a) Peak in operations in two hours in the middle of the night, (b) an even distribution, (c) most events in the middle of the night, (d) a U-shaped distribution, (e) most events at the beginning of the night, and (f) most events occurring at the end of the night. . . 288

8.13 Increase in time spent (minutes) in Wake for the 6 nighttime flight operation scenarios. (a) Peak in operations in two hours in the middle of the night, (b) an even distribution, (c) most events in the middle of the night, (d) a U-shaped distribution, (e) most events at the beginning of the night, and (f) most events occurring at the end of the night. 289

8.14 Average number of awakenings for 6 flight operation scenarios predicted using the nonlinear dynamic model for (a) grid point at (-1 nmi, 5 nmi) and (b) grid point at (1 nmi, -4 nmi). The scenarios are: (1) Peak in operations in two hours in the middle of the night, (2) an even distribution, (3) most events in the middle of the night, (4) a U-shaped distribution, (5) most events at the beginning of the night, and (6) most events occurring at the end of the night. 291

8.15 Change in sleep stage durations for the 6 flight operation scenarios predicted using the nonlinear dynamic model for (a) grid point at (-1 nmi, 5 nmi) and (b) grid point at (1 nmi, -4 nmi). The scenarios are: (1) Peak in operations in two hours in the middle of the night, (2) an even distribution, (3) most events in the middle of the night, (4) a U-shaped distribution, (5) most events at the beginning of the night, and (6) most events occurring at the end of the night. 292

Appendix Figure

A.1 A-weighted noise level (dB(A)) of aircraft noise event. The maximum noise level (L_{Amax}) and the portion of the sound used to calculate the Sound Exposure Level ($SELA$) (red arrow) are indicated. 315

Appendix Figure Page

F.1 An example of using Massaquoi and McCarley's LCRIM/I model to classify sleep stages, (a) REM-ON (X) (green) and REM-OFF(X) (blue) activity, (b) Process S (green) and SWA (blue), (c) Excitatory activity E, and (d) sleep stages. Thresholds used for scoring sleep stages (red-dashed lines). 346

F.2 An example of the parameters for the developed nonlinear sleep model, which include slow wave activity (SWA), REM, REM sleep period indicator, fast REM model and the spontaneous and noise induced excitation terms. 349

H.1 An example of some of the characteristics that are extracted including; (a) the percent of an epoch occupied by movement artifacts, (b) the percent of an epoch occupied by Slow Wave Sleep (SWS), (c) the frequency that has the lowest decay rate identified using an AR(4) model, (d) correlation between the right and left EOG channels, and (e) the root-mean-square (RMS) of the EMG activity for each epoch. 374

H.2 Probability of being in Stage Wake/S1, Stage 2, Stage 3/4, and REM sleep calculated using the developed sleep stage scoring algorithm. 375

GLOSSARY

Actigraph	A device worn on the wrist. It contains an accelerometer and is used for measuring motility during the night.
Adaptation	Decrease in response, occurs at the level of the sensory organ.
Alpha Activity	Activity in the EEG signal between 8-12 Hz.
Arousal	Consists of EEG activity in the 8 to 12 Hz range. There will also be an increase in muscle activity. They last for at least 3 seconds but not more than 15 seconds.
A-weighting	Frequency weighting. It was derived from the 40-phon equal loudness curve. It's use was meant for sounds of low levels.
Autonomic Arousal	Elevation in the sympathetic tone. May occur with or without a cortical arousal. It is associated with elevations in blood pressure and heart rate.
Behavioral Awakening	An individual must perform a task when awakened such as pressing a button.
Beta Activity	Activity in the EEG signal between 15-25 Hz.
Blood Pressure Dipping	The nighttime blood pressure level decreases below 10% of its average daytime level.
Circadian Rhythm	24 hour variation in biological rhythms such as body temperature.
Day Night Average Sound Level (DNL)	An average A-weighted sound pressure level which has a 10 dB penalty for noise events occurring between the hours of 10:00 pm and 7:00 am. (See Appendix A)
ECG Artifact	Artifact in the EEG signal, heart activity is picked up due to the electrode being positioned close to a vein or artery.
Electrocardiogram (ECG)	Measurement of electrical activity of the heart.
Electroencephalogram (EEG)	Measurement of electrical activity in the brain.
Electromyogram (EMG)	Measurement of muscle activity.

Electrooculogram (EOG)	Measurement of eye movement.
EOG Artifact	Artifact in the EEG signal caused by eye movements.
Gamma 1 Activity	Activity in the EEG signal between 25-35 Hz.
Gamma 2 Activity	Activity in the EEG signal between 35-45 Hz.
Ghrelin	A hormone for regulating appetite. An increased level leads to an increase in appetite.
Glucose Tolerance	Rate of decline of glucose levels in the body. Those with impaired glucose tolerance would have a slower rate of decline.
Habituation	Decrease in response, happens at the central nervous system.
Homeostatic Sleep Process	Indicator of an individual's need for sleep. Increases when an individual is awake, decreases while asleep.
Hypertension	High blood pressure.
K-complex	A characteristic feature of Stage 2 sleep. They last for at least half a second and consist of a sharp decrease in EEG activity followed by a longer increase in level. Usually a sleep spindle will occur before, after, or during a K-complex.
L_{Aeq}	Average A-weighted sound pressure level of a sound.
L_{Amax}	Maximum A-weighted sound pressure level of a sound.
Leptin	A hormone for regulating appetite. An increased level leads to a decrease in appetite.
L_{night}	Average A-weighted sound pressure level between 11:00 pm and 7:00 am.
Motility	A measurement of body movement.
Multiple Sleep Latency Test	An objective measure of sleepiness. The time it takes for an individual to fall asleep is measured 4 to 5 times throughout the day.
Noise Sensitivity	How bothered someone is by noise in general, not just aircraft noise. It is typically measured using a multi-item questionnaire.
Obstructive Sleep Apnea	A sleep disorder in which the airflow and respiratory effort either completely stops for a few seconds or is reduced.
Odds Ratio	Ratio of an exposed population having a certain condition to a non-exposed population having a certain condition.

Phasic Rapid Eye Movement Sleep	Rapid eye movement sleep in which there is irregular occurrence of events such as rapid eye movement.
Polysomnography	The simultaneous measurement of the electroencephalogram (EEG), electromyogram (EMG), and electrooculogram (EOG).
Pupillographic Sleepiness Test (PST)	A measurement of the oscillation in pupil size. A change less then 0.3 mm indicates a subject is alert.
Rapid Eye Movement Sleep (REM)	A sleep stage which is characterized by theta activity in the EEG signal, and the lowest amount of muscle activity during the night. Also there will be rapid oscillations in the EOG signal.
Sawtooth Waves	Sawtooth shaped waves that occur in the EEG signals during Stage REM. The fundamental frequency is between 2 to 6 Hz.
Sigma Activity	Activity in the EEG signal between 12-15 Hz.
Sleep Efficiency	Total sleep time divided by the total time in bed.
Sleepiness	Indicated by difficulty remaining awake and falling asleep.
Sleep Latency	Time from lights out to the first occurrence of Stage 2.
Sleep Spindles	Fast oscillations, between 12 to 14 Hz, in the EEG signal. They are a characteristic feature of Stage 2 sleep.
Slow Wave Activity	Power in the spectrum of the electroencephalogram (EEG) signal in the frequency range of 0.5-4.5 Hz.
Sound Exposure Level ($SELA$)	A measure derived from the A-weighted sound level time history of a noise event. $SELA$ is determined by considering only the portion of the noise event 10 dB down from the maximum A-weighted sound pressure level. (See Appendix A)
Spontaneous Awakening	An awakening that is not associated with a noise (or other external stimulus) event.
Stage Wake	In this stage the activity in the EEG signal will be primarily between 8 and 12 Hz (alpha activity). The level of EMG activity will be high and if the individual is relaxed, there will be slow eye rolling.
Stage 1	This stage is primarily a transition stage. Most of the EEG activity is between 4 to 8 Hz. The muscle tone decreases from Stage Wake.
Stage 2	The background activity in Stage 2 is theta activity, however there are two characteristic features sleep spindles and K-complexes.

Stage 3	This stage is considered deep sleep. Twenty to 50% of the epoch contains slow waves of less than 2 Hz with a peak to peak amplitude greater then 75 microvolts.
Stage 4	This is the deepest stage of sleep. At least 50% of the epoch contains slow waves of less than 2 Hz with a peak to peak amplitude greater than 75 microvolts.
Stage REM	This stage consists of theta activity in the EEG signal. The muscle activity reaches a minimum in this stage and there are rapid eye movements. Also sawtooth waves may occur.
Theta Activity	Activity in the EEG signal between 4-8 Hz.
Tiredness	Lack of energy, fatigue.
Tonic Rapid Eye Movement Sleep	Rapid eye movement sleep in which there are no rapid eye movements however, the low mixed frequency EEG activity and the low EMG activity means the sleep stage is still classified as Stage REM.
Ultradian Cycle	Cyclic variations in sleep between NREM and REM sleep.
Vertex Wave	Sharp transient increase in EEG activity during sleep Stage 1.
Vigilance Task	A task that involves sustained attention. An individual has to detect stimuli that occur at random intervals. The reaction time is measured.

ABSTRACT

McGuire, Sarah M. Ph.D., Purdue University, August 2012. Modeling Aircraft Noise Induced Sleep Disturbance. Major Professor: Patricia Davies, School of Mechanical Engineering.

One of the primary impacts of aircraft noise on a community is its disruption of sleep. Aircraft noise increases the time to fall asleep, the number of awakenings, and decreases the amount of rapid eye movement and slow wave sleep. Understanding these changes in sleep may be important as they could increase the risk for developing next-day effects such as sleepiness and reduced performance and long-term health effects such as cardiovascular disease. There are models that have been developed to predict the effect of aircraft noise on sleep. However, most of these models only predict the percentage of the population that is awakened. Markov and nonlinear dynamic models have been developed to predict an individual's sleep structure during the night. However, both of these models have limitations. The Markov model only accounts for whether an aircraft event occurred not the noise level or other sound characteristics of the event that may affect the degree of disturbance. The nonlinear dynamic models were developed to describe normal sleep regulation and do not have a noise effects component. In addition, the nonlinear dynamic models have slow dynamics which make it difficult to predict short duration awakenings which occur both spontaneously and as a result of nighttime noise exposure. The purpose of this research was to examine these sleep structure models to determine how they could be altered to predict the effect of aircraft noise on sleep. Different approaches for adding a noise level dependence to the Markov Model was explored and the modified model was validated by comparing predictions to behavioral awakening data. In order to

determine how to add faster dynamics to the nonlinear dynamic sleep models it was necessary to have a more detailed sleep stage classification than was available from visual scoring of sleep data. An automatic sleep stage classification algorithm was developed which extracts different features of polysomnography data including the occurrence of rapid eye movements, sleep spindles, and slow wave sleep. Using these features an approach for classifying sleep stages every one second during the night was developed. From observation of the results of the sleep stage classification, it was determined how to add faster dynamics to the nonlinear dynamic model. Slow and fast REM activity are modeled separately and the activity in the gamma frequency band of the EEG signal is used to model both spontaneous and noise-induced awakenings. The nonlinear model predicts changes in sleep structure similar to those found by other researchers and reported in the sleep literature and similar to those found in obtained survey data. To compare sleep disturbance model predictions, flight operations data from US airports were obtained and sleep disturbance in communities was predicted for different operations scenarios using the modified Markov model, the nonlinear dynamic model, and other aircraft noise awakening models. Similarities and differences in model predictions were evaluated in order to determine if the use of the developed sleep structure model leads to improved predictions of the impact of nighttime noise on communities.

1. INTRODUCTION

Currently in the United States the Day Night Average Sound Level (DNL) is used to quantify aircraft noise around an airport. This metric is based on the average A-weighted sound pressure level of the aircraft noise events for an entire day and has a 10 dB penalty which is applied to nighttime events occurring between 10:00 pm and 7:00 am. This 10 dB penalty is applied to account for the adverse affects of nighttime noise. The Federal Aviation Administration's (FAA) noise policy is based on DNL. The FAA considers communities within the 65 dB(A) DNL contour to be adversely affected by aircraft noise and eligible for noise insulation. They adopted the use of DNL because they felt it provided a reliable relationship between noise exposure and the reactions of people to noise (FICON, 1992).

Research on the use of DNL as a metric for predicting community impact has primarily focused on examining its relationship to annoyance. Many dose-response models, which relate the percent highly annoyed to DNL, have been developed using social survey data. One of the most widely used models was developed by Schultz (1978) who combined responses to road, rail, and aircraft noise to generate the model. According to the model a DNL level of 65 dB(A) corresponds to about 15% of the population being highly annoyed. A more recent model, in which response to aircraft noise was modeled seperately, has been developed by Miedema and Oudshoorn (2001). This model is used in the European Union. However, there have been arguments made against the use of DNL to predict impacts other than annoyance. The results of studies on sleep disturbance support the hypothesis that DNL is not a good predictor of noise induced awakenings, and that awakenings are better estimated when using

the level of each individual noise event (Fidell, Pearsons, Tabachnick, Howe, Silvati, and Barber, 1995). It also should be noted that awakenings are just one of many possible characteristics of sleep disturbance.

1.1 Motivation

The results of numerous field and laboratory studies have provided evidence that aircraft noise causes an increase in the number of awakenings and a reduction in the amount of rapid eye movement and slow wave sleep (Griefahn, Robens, Bröde, and Basner, 2008b). Noise-induced sleep disturbance may lead to next day effects including an increase in annoyance (Quehl and Basner, 2006) and sleepiness (Basner, 2008), and a decrease in performance (Elmenhorst and Basner, 2008). Also there is evidence presented in the sleep literature that fragmented sleep may lead to long term health effects by causing an increase in blood pressure (Haralabidis, Dimakopoulou, Vigna-Taglianti, Giampaolo, Borgini, Dudley, Pershagen, Bluhm, Houthuijs, Babisch, Velonakis, Katsouyanni, and Jarup, 2008), impairing glucose tolerance (Tasali, Leproult, Ehrmann, and Van Cauter, 2008), and affecting appetite (Spiegel, Tasali, Penev, and Van Cauter, 2004) and stress hormone levels (Ekstedt, Åkerstedt, and Söderström, 2004).

Several models have been developed in order to predict the impact of noise on sleep. Most of the models are simplistic dose-response relationships relating the indoor noise level of a single event to the percent awakened (e.g. FICAN (1997); Finegold and Elias (2002)). The majority of these models are based on behavioral awakening data, where an individual is instructed to press a button when they are awakened by noise. Behavioral awakenings are not a sensitive measure of sleep as it requires that an individual regain full consciousness. Behavioral awakenings are also a subjective measure of sleep because individuals can decide whether or not to press the button.

Therefore, models based on behavioral awakening data may under-predict the amount of sleep disturbance in communities. Only one dose-response relationship has been developed based on awakenings measured using electroencephalography (EEG) in the field. EEG is a more sensitive measure by which to determine sleep state (Basner, Samel, and Isermann, 2006) because it measures brain wave activity. EEG measured awakenings are as brief as 15 seconds in duration. Models based on awakenings measured with EEG do predict a higher degree of disturbance than those based on behavioral awakenings. To predict the percent awakened at least once for an entire night of aircraft events, an ANSI standard (2008) has also been developed. However, a limitation of this standard is that it is based on the behavioral awakenings dose-response models.

One limitation of all of these models is that they only predict awakenings, but aircraft noise also changes the structure of sleep. A Markov model has been developed which can be used to predict the effect of noise on sleep structure (Basner, 2006) however, it is not without limitations. The model only accounts for whether an aircraft event occurs, not the noise level. This model also has many parameters making it difficult to fully validate because a large amount of data is needed to produce low variance estimates of the parameters. Also it is not intuitive in terms of how to change the model coefficients in order to predict sleep disturbance for different age groups, or other sub-populations of interest. Another limitation of Markov models is that they do not provide information on the physical processes behind sleep.

There are nonlinear dynamic sleep models which are based on a more physical understanding of the sleep process (Achermann and Borbély, 1990; Massaquoi and McCarley, 1992). The nonlinear dynamic models predict the interactions that have been found between rapid eye movement (REM) sleep promoting neurons and REM sleep inhibiting neurons which cause the ultradian oscillation between non-REM (NREM)

and REM sleep during the night. Also the change in slow wave activity (power in the EEG signal between 0.5 and 4.5 Hz) during the night can be predicted with these models. The amount of slow wave activity is related to the depth of sleep. One limitation of the nonlinear dynamic models, in their current form, are that they only predict normal non-noise disturbed sleep.

1.2 Objective

As noted above, there is evidence from studies that aircraft noise affects sleep and that these changes in sleep may lead to health effects. Because the current community impact metric DNL is not a measure of sleep disturbance even with the 10 dB night penalty, and existing awakening and sleep structure models all have limitations, there is a need to develop a new sleep model that could be used to create sleep and health effect contours, which are maps indicating noise impact in communities. The process involved in developing these contour maps involves several steps as outlined in Figure 1.1. Sound propagation and transmission modeling is needed so that indoor noise levels can be predicted. Different characteristics of the sound in addition to maximum level such as the rise time and spectral balance may also affect the degree of sleep disturbance and therefore should be predicted (Marks, Griefahn, and Basner, 2008). Also there needs to be an improved understanding of what changes in sleep best relate to potential health effects. Developing useful sleep contours is a complex problem involving research in many different areas. It would not be feasible to address all of these issues within this research. This research has been focused on one step involved in predicting the impact of nighttime noise on communities: developing a more comprehensive aircraft noise induced sleep disturbance model which predicts not only the increase in number of awakenings due to noise but also the change in sleep structure.

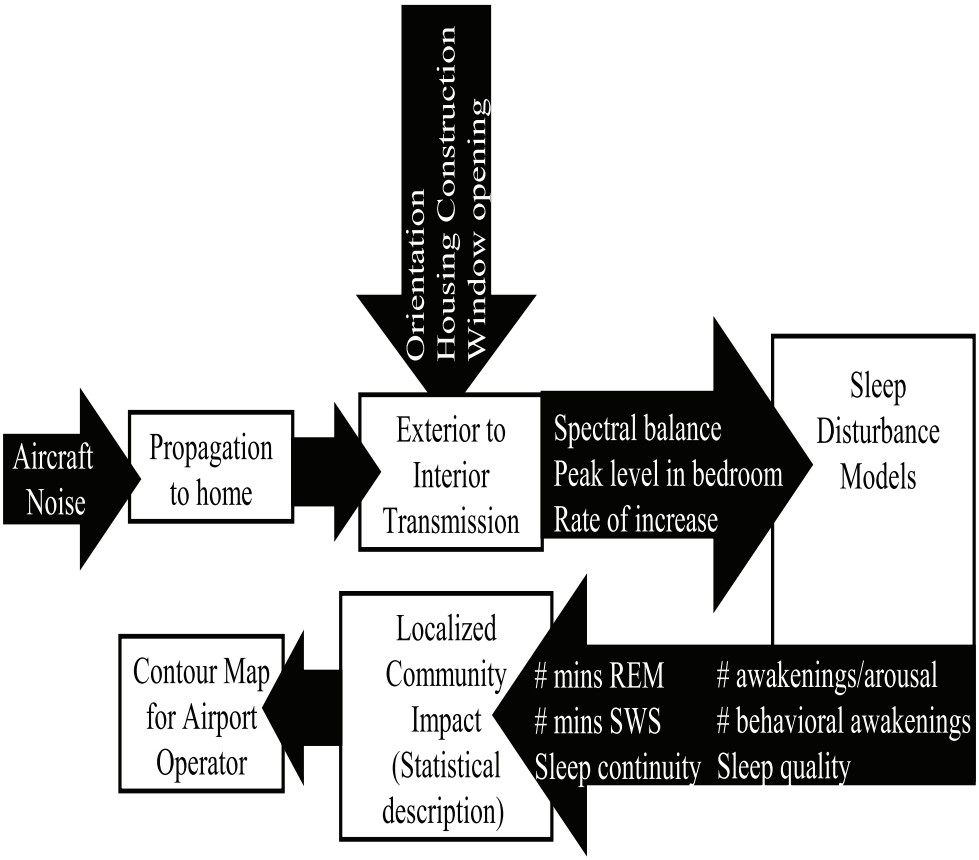

Figure 1.1. Diagram of the steps involved in assessing the effect of nighttime aircraft noise on communities.

1.3 Research Approach

The approach of this research was to modify the nonlinear dynamic sleep models in order to predict noise induced sleep disturbance, specifically the model developed by Massaquoi and McCarley (1992). This model is based on physiological sleep processes and requires less parameters than Markov models. Although, the dynamics of the Massaquoi and McCarley (1992) model accurately describes the slow 90 minute ultradian cycling between NREM and REM sleep the model does not allow awakenings during all stages of sleep to be predicted, yet from observing physiological data it is known that this is possible. Basner (2006) found that the probability of transitioning from REM to Wake when a noise event occurred was 0.14. In addition the model only predicts normal sleep patterns, therefore a way of introducing the effects of being exposed to different noise levels needs to be incorporated into the model so that the observed increase in sleep disturbance with noise level can be predicted.

In order to develop and validate nonlinear sleep models, data from existing studies in which sleep was measured using polysomnography have been obtained from other researchers. A sleep stage classification algorithm was developed to define sleep stages on a more refined scale in order to identify brief awakenings. The current standard is to score sleep stages according to 30 second segments of sleep. The algorithm developed defines a sleep stage for each 1 second of sleep. Different features of the polysomnography data are extracted including rapid eye movements and slow wave activity. The occurrence of these features were used to determine how to introduce faster dynamics and a noise dependence into the nonlinear models, and the extracted data was also used to estimate the parameters in the model.

By using various elements shown in Figure 1.1, and the developed sleep disturbance model, a prediction of sleep changes in a population around an airport can be made. To do this, data from two US airports was obtained. Noise metrics were pre-

dicted for single aircraft noise events. Different nighttime operation scenarios were generated and sleep disturbance was predicted using the nonlinear models. Sleep disturbance was also predicted using existing noise induced awakening models and Markov models. These models were examined, and limitations of the models were addressed such as adding a noise dependence to the Markov model, so that a fair comparison of model predictions could be made. The different model predictions were examined to determine whether the nonlinear dynamic models may lead to improved predictions of sleep disturbance. The steps involved in this research are shown in Figure 1.2

1.4 Thesis Outline

The outline of this thesis is as follows: In Chapter 2 a literature review of the basics of sleep and how it is measured is provided. Also auditory processing during sleep, changes in sleep that occur due to noise exposure, and possible next day and longer term health effects caused by sleep disturbance are described. The information in Chapter 2 provides a rationale for why a model that predicts awakenings and the effect of noise on an individuals sleep structure may be useful. A description of the survey data that was obtained and used throughout the analysis is described in Chapter 3. Chapter 3 also contains a review and evaluation of existing awakening models by comparing predictions from those models to obtained survey data. In Chapter 4 Basner's Markov model (2006) is described. An approach to adding a noise level dependence to the Markov model was examined and predictions using the modified model are compared to survey data. Chapter 5 consists of a review on nonlinear dynamic sleep models. The results of a parameter variation study performed on the Massaquoi and McCarley (1992) model, that is used as the basis of the model developed in this research, is described. In Chapter 6 an analysis of the obtained sleep

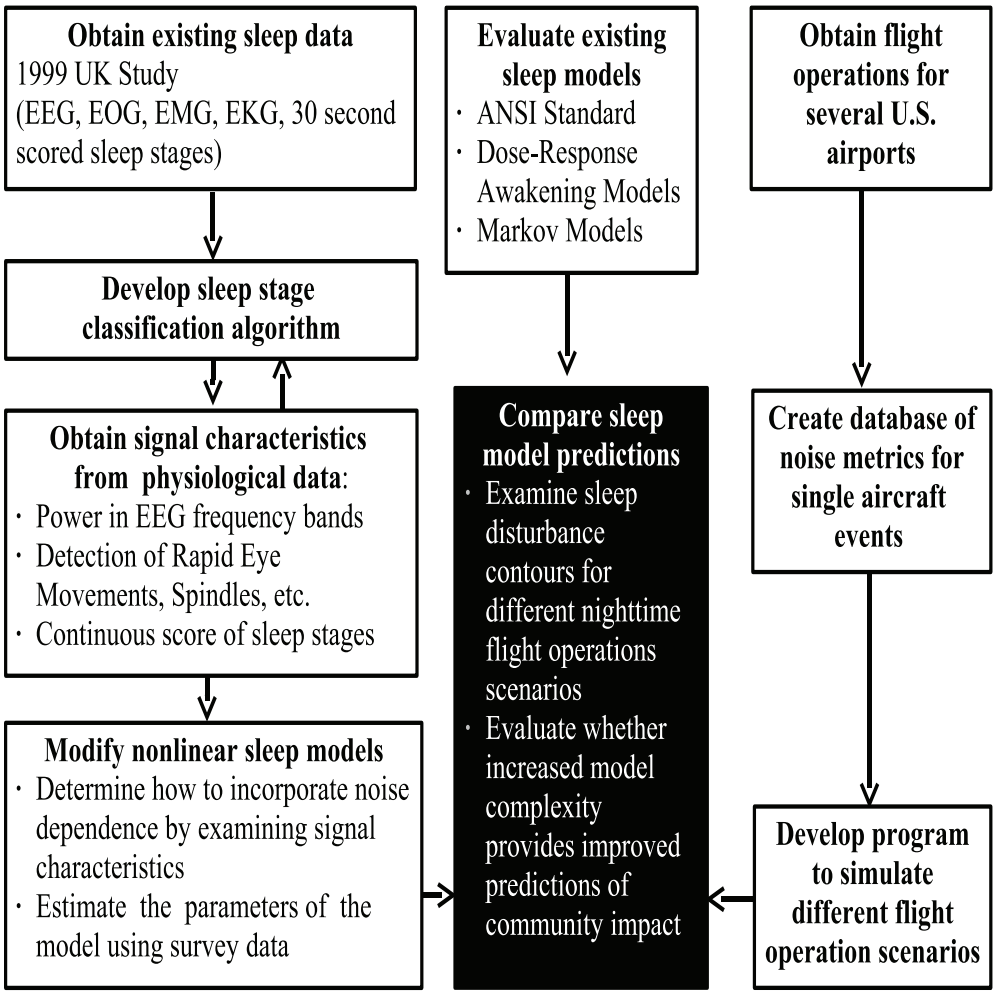

Figure 1.2. Diagram of the steps involved in developing a nonlinear dynamic sleep model and comparing its performance in predicting community sleep disturbance with that of other models.

physiological data is provided including an examination of artifact removal methods and the development of a sleep stage classification algorithm. In Chapter 7 the steps taken to develop the nonlinear dynamic sleep model is provided. Methods for overcoming the limitations of the model and for estimating model parameters are described. In Chapter 8 a comparison of sleep disturbance model predictions using the awakening models, Markov models and the developed nonlinear dynamic model are described for different airport noise scenarios. Chapter 9 consists of a review of the research findings and a proposal for future work that should be done in the area of noise-induced sleep disturbance modeling.

2. NOISE INDUCED SLEEP DISTURBANCE AND THE POTENTIAL HEALTH EFFECTS

This chapter consists of a literature review on noise induced sleep disturbance. A description of normal sleep and how it is measured is provided. A review of studies on how noise is processed during sleep, how it affects sleep structure, and the implications of these disturbances on both short term and long term health will also be discussed.

2.1 Normal Sleep

For a normal healthy individual it will take between 10 to 20 minutes to fall asleep. If an individual is tired this sleep onset latency will become shorter. A latency of less than 5 minutes is considered to be pathologic sleepiness (Spriggs, 2008). A sleep onset latency greater than 20 minutes indicates difficulty initiating sleep. Sleep is a time varying process and periodic in nature. Periods of rapid eye movement (REM) and non rapid eye movement (NREM or non-REM) sleep alternate throughout the night in about 90 minute cycles, with the first REM period occurring about 80 minutes after an individual retires to bed. The duration of the first REM sleep period is typically between 5-10 minutes in duration. The duration of REM sleep periods increases throughout the night (Carskadon and Dement, 2005), with the largest increase in duration occurring between the first and second REM periods (McCarley and Massaquoi, 1986). NREM sleep consists of 4 different stages numbered 1 through 4. Sleep is considered to be deeper, more restorative, as the NREM sleep stage number increases. In the beginning of the night, slow wave sleep (SWS), Stages 3 and 4, is more prevalent.

An average young adult in their twenties, will spend less than 5% of the night awake, 5% will be spent in Stage 1, 50-55% will be spent in Stage 2, 10% will be spent in Stage 3, 10% in Stage 4, and 20 to 25% will be spent in REM sleep (Kales and Kales, 1970). An example of a typical sleep pattern is shown in Figure 2.1. During the night a young adult will spontaneously awaken about 20 times and will have approximately 80 arousals as measured with EEG (electroencephalogram – measurement of electrical activity in the brain) (Bonnet and Arand, 2007). Arousals and awakenings are characterized by higher frequencies of brain wave activity (alpha activity 8-12 Hz) and there is often an increase in the muscle tone seen in the electromyogram (EMG – measurement of activation signals in muscles). The difference between arousals and awakenings is primarily based on their duration: arousals last at least 3 seconds but no more than 15 seconds, while awakenings are greater than 15 seconds in duration (Bonnet et al., 1992). Another type of arousal are autonomic arousals; which are elevations in the sympathetic tone, which is the normal activity level of the sympathetic nervous system. An autonomic arousal can occur with or without an EEG arousal and includes a change in heart rate and an increase in blood pressure (Griefahn, Bröde, Marks, and Basner, 2008a).

As individuals age, sleep lightens and there is a decrease in the amount of Stage 3 and 4 sleep and an increase in the number of awakenings and arousals. In Figure 2.2 the percent of time spent in each of the 6 different stages of sleep for different age groups is shown (Williams, Karacan, and Hursch, 1974).

2.2 Sleep Stage Classification

Sleep stage classification rules were developed by Rechtschaffen and Kales (1968) and became the standard for scoring sleep physiological data. Sleep stages are determined by examining the signals of the EEG, EMG, and electroocculogram (EOG– measure-

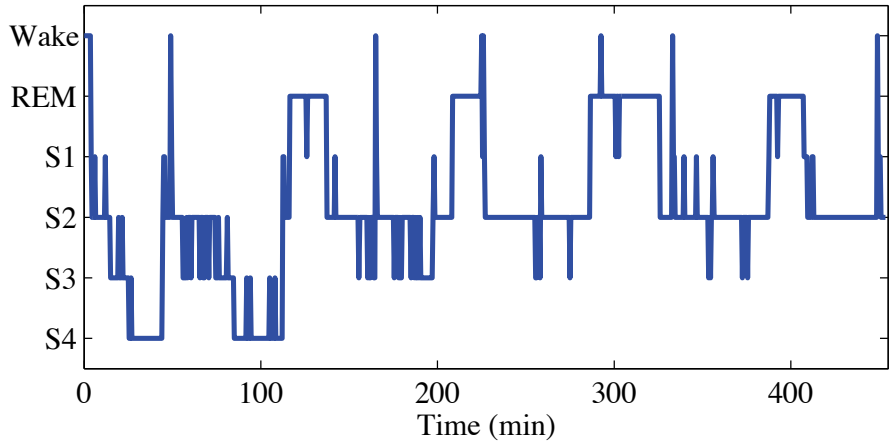

Figure 2.1. An example of a normal sleep pattern.

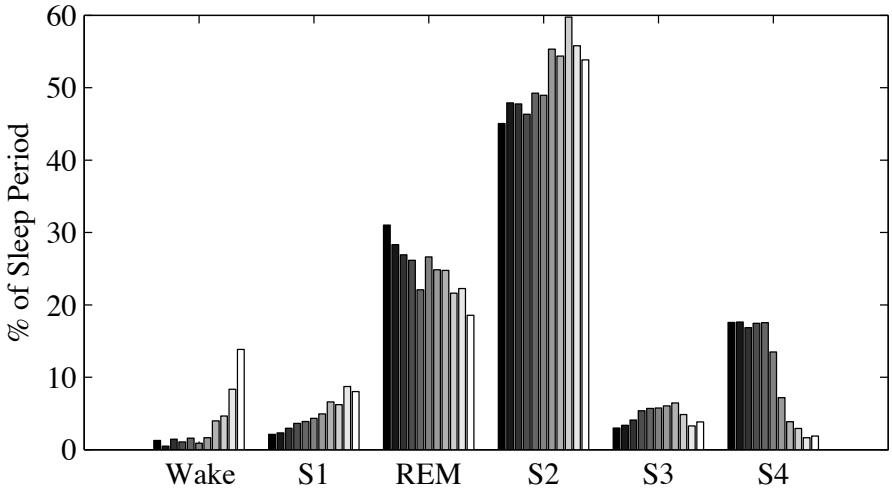

Figure 2.2. The percent of time spent in each of the 6 sleep stages for different age groups. Each bar represents a different age group. The age groups are 3-5 yrs, 6-9 yrs, 10-12 yrs, 13-15 yrs, 16-19 yrs, 20-29 yrs, 30-39 yrs, 40-49 yrs, 50-59 yrs, 60-69 yrs, and 70-79 yrs. The bars are shown in order of increasing age; 3-5 yrs (black) to 70-79 yrs (light gray) (Williams, Karacan, and Hursch, 1974).

ment of eye movements). EEG is measured by attaching electrodes to the scalp. A diagram of the positions for placing electrodes is shown in Figure 2.3. There are several different regions of measurement; Frontal (F), Central (C), Parietal (P), Occiptal (O), and Temporal (T). Most of the aircraft noise studies have measured EEG at the central locations, C3 and C4. These locations are referenced to A2 and A1, respectively. EMG is usually measured with 3 electrodes. One electrode is placed in the middle of the chin, and the other two are placed underneath the chin, approximately 2 cm from the top of the chin and 2 cm from the center line, one on the left of the center line and one on the right (Spriggs, 2008). EOG is measured by having one electrode placed about 1 cm out and 1 cm up from the corner of the right eye. The electrode for the left eye is placed 1 cm out and 1 cm down from the corner of the eye. Looking away from an electrode will result in a negative signal, while looking toward the electrode will result in a positive signal (Spriggs, 2008). By having one electrode above the eye and one electrode below the eye, the occurrence of eye movements can be distinguished as the two channels of EOG will be negatively correlated.

Table 2.1. EEG frequency bands.

Frequency Bands	Range
Delta	0-4 Hz
Theta	4-8 Hz
Alpha	8-12 Hz
Sigma	12-16 Hz
Beta	16-25 Hz
Gamma 1	25-35 Hz
Gamma 2	35-45 Hz

It is standard practice to assign a sleep stage to each 30 second segment of sleep. Most sleep stages are related to EEG activity in a specific frequency band. The frequency bands are listed in Table 2.1. For Stage Wake, when an individual is

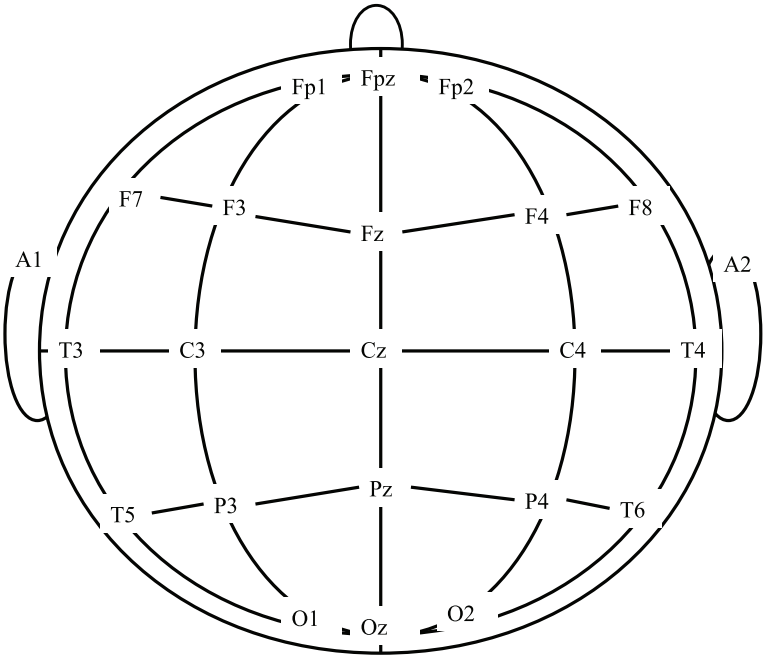

Figure 2.3. The standard placement of EEG electrodes, based on a diagram in Spriggs (2008).

relaxed there is often alpha activity in the EEG signal which is activity in the 8 to 12 Hz range (alpha activity). There is also high EMG activity and slow eye rolling. An example of the EEG and EOG signals for Stage Wake are shown in Figure 2.4. If an individual is moving when awake, high amplitude artifacts will appear in most of the other physiological measurements.

Stage 1 appears in the EEG as a low voltage mixed frequency signal. Most of the activity is in the 4 to 8 Hz range (theta activity). An example of the EEG and EOG signals for Stage 1 is shown in Figure 2.5. Also sharp vertex waves can occur which are sharp transient waves in the EEG signal which last less than 0.5 seconds and are of a high amplitude typically greater than 100 μV, an example is shown in Figure 2.6. The amount of muscle activity will also decrease compared to Stage Wake.

Stage 2 also consists of theta activity but has two characteristic features, sleep spindles and K-complexes. Sleep spindles last for one half second or more but not longer than approximately two seconds and are bursts of activity between 12 to 14 Hz in the EEG signal, an example is shown in Figure 2.7. K-complexes are waves which have a sharp negative followed by a slower positive component. K-complexes also last for at least one half second and have sleep spindles occurring either before, after, or during it (Fisher and Cordova, 2006). An example of a K-complex with a sleep spindle is shown in Figure 2.8.

Stage 3 is classified by the amount of low frequency activity; at least 20% but not more than 50% of the epoch consists of oscillations of 2 Hz or a lower frequency and has a peak to peak voltage of 75 μV or more. Stage 4 is classified in a similar manner as Stage 3, but the slow wave behavior must occur for more than 50% of the epoch. Examples of EEG signals during Stage 3 and 4 is shown in Figure 2.9.

Rapid eye movement (REM) sleep has a similar EEG pattern as Stage 1 in that it is a low voltage, mixed frequency signal. Therefore to catergorize an epoch as

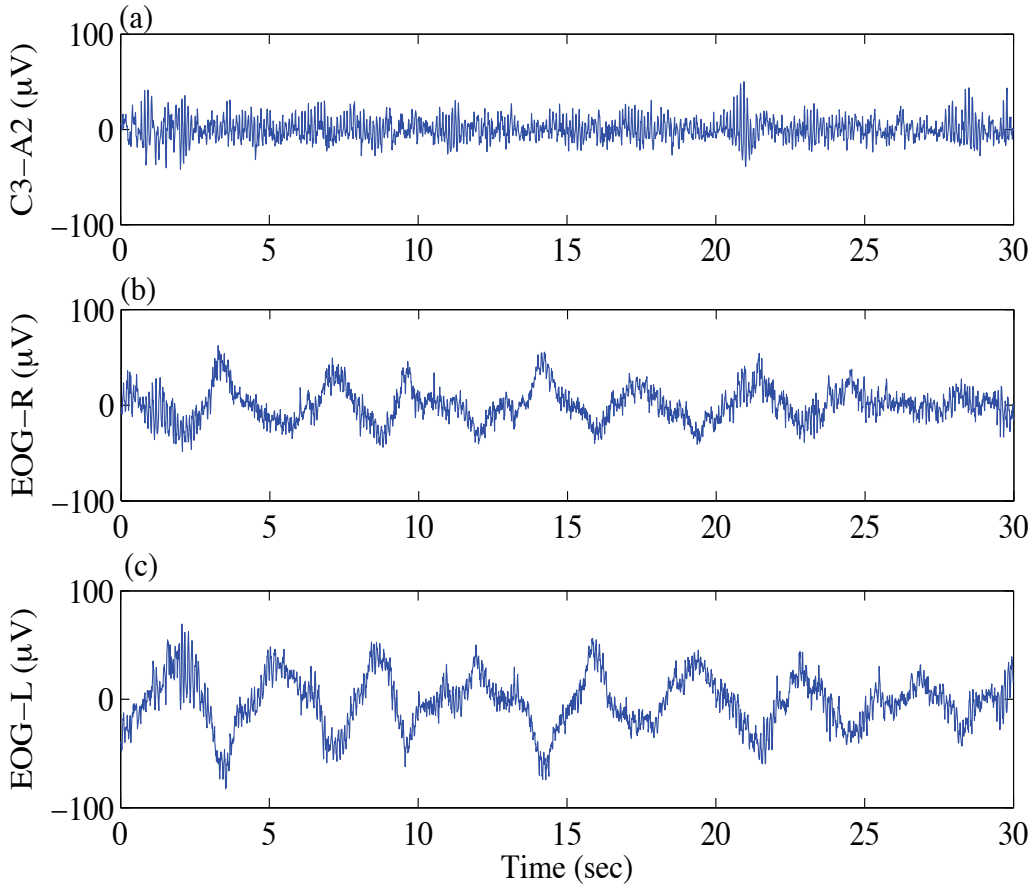

Figure 2.4. An example of the EEG and EOG signals for Stage Wake. (a) C3-A2 EEG channel, (b) Right EOG channel, and (c) Left EOG channel.

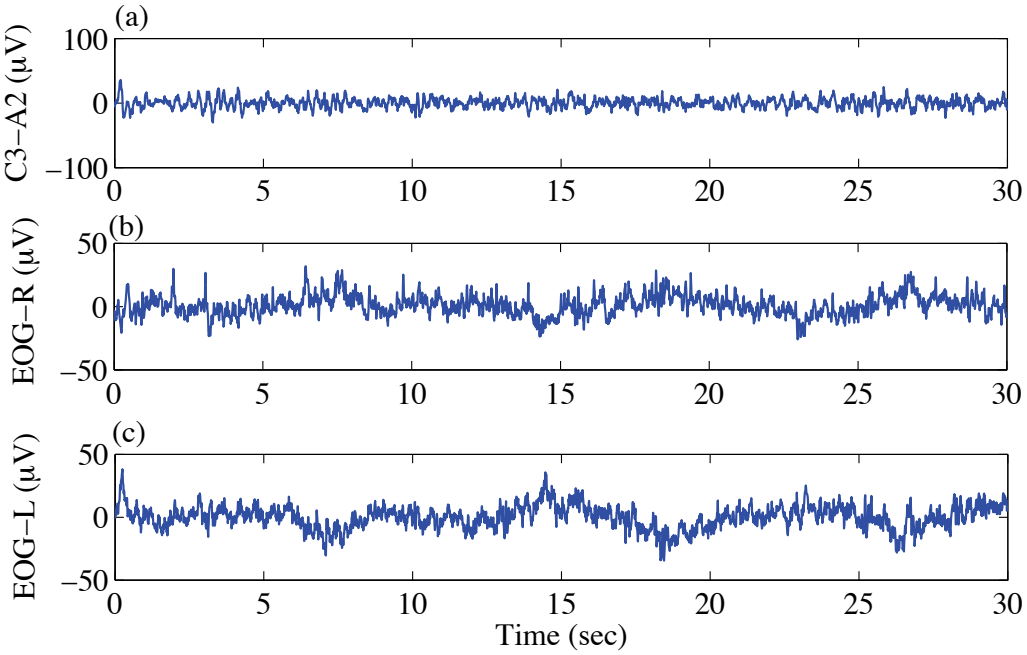

Figure 2.5. An example of the EEG and EOG signals for Stage 1. (a) C3-A2 EEG channel, (b) Right EOG channel, and (c) Left EOG channel.

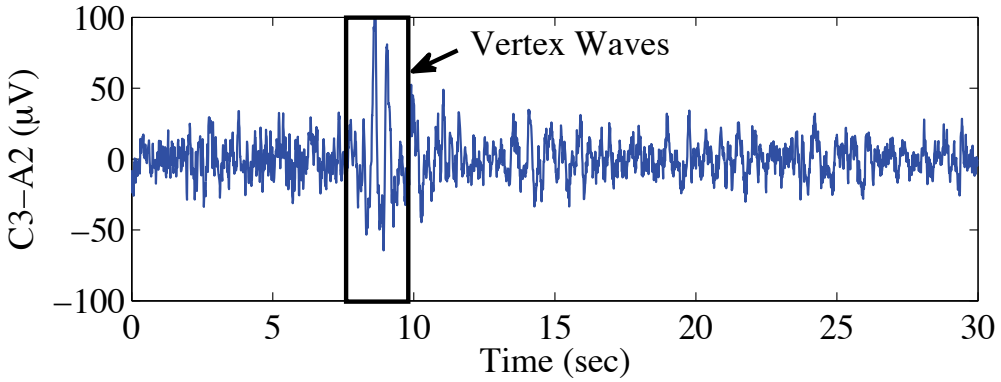

Figure 2.6. An example of vertex waves, a characteristic feature of Stage 1 sleep.

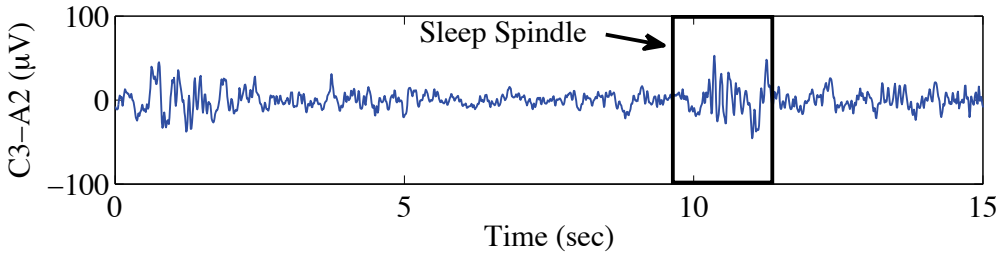

Figure 2.7. An example of sleep spindles, a characteristic feature of Stage 2 sleep.

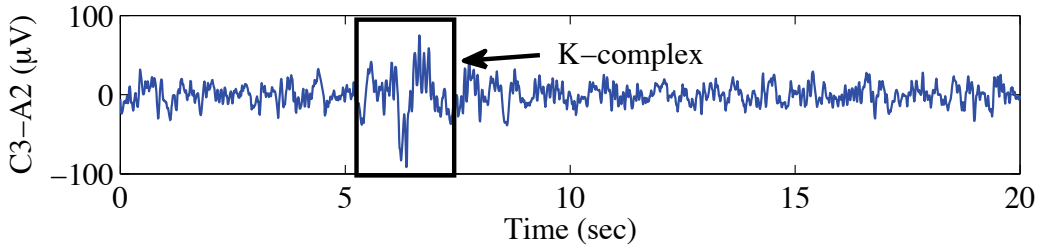

Figure 2.8. An example of a K-complex with sleep spindles, a characteristic feature of Stage 2 sleep.

consisting of REM sleep, an examination of the EOG and the EMG signals is needed. EMG, which is a measure of muscle activity, will be at its lowest level during REM sleep. Also sawtooth waves may occur in the EEG signal which are sharp, triangular waves between 2 and 6 Hz (Silber et al., 2007). An example of Stage REM is shown in Figure 2.10. REM sleep in which there is low EMG activity and low mixed frequency EEG activity, but no transient activity like sawtooth waves and rapid eye movements are called Tonic REM sleep. REM sleep with rapid eye movements or other transient activity is referred to as Phasic REM sleep. There is no standard method to classify

Tonic and Phasic REM sleep. The characteristics for each of the 6 sleep stages are summarized in Table 2.2.

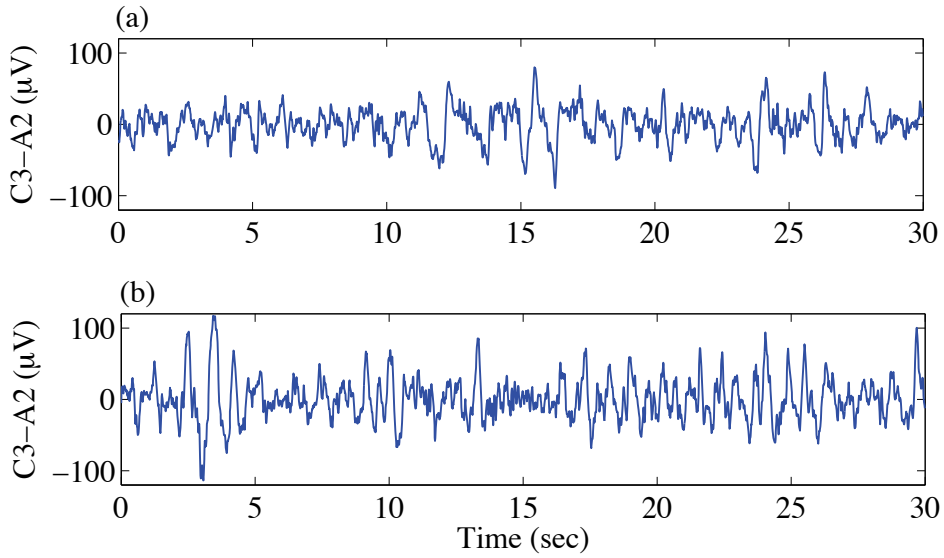

Figure 2.9. Examples of the EEG signals for (a) Stage 3 and (b) Stage 4 sleep.

A review of the sleep stage scoring rules developed by Rechtshaffen and Kales began in 2004 and in 2007 a new manual for visual sleep scoring was published by the American Academy of Sleep Medicine (Silber et al., 2007). The characteristics of the sleep stages largely remain the same. One of the changes made is that Stage 3 and Stage 4 were combined. Also the rules for scoring the beginning and end of Stage 2 and REM sleep were clarified. For example there used to be a 3-minute rule; 3 minutes of sleep between sleep spindles and K-complexes could be scored as Stage 2 as long as there were no movements, arousals, or transitions to other sleep stages. After 3 minutes the stages were classified as Stage 1. This rule was changed and now once Stage 2 begins, epochs can continue to be scored as Stage 2 as long as there is not an apparent transition to another sleep stage. Also, in order to not confuse sleep

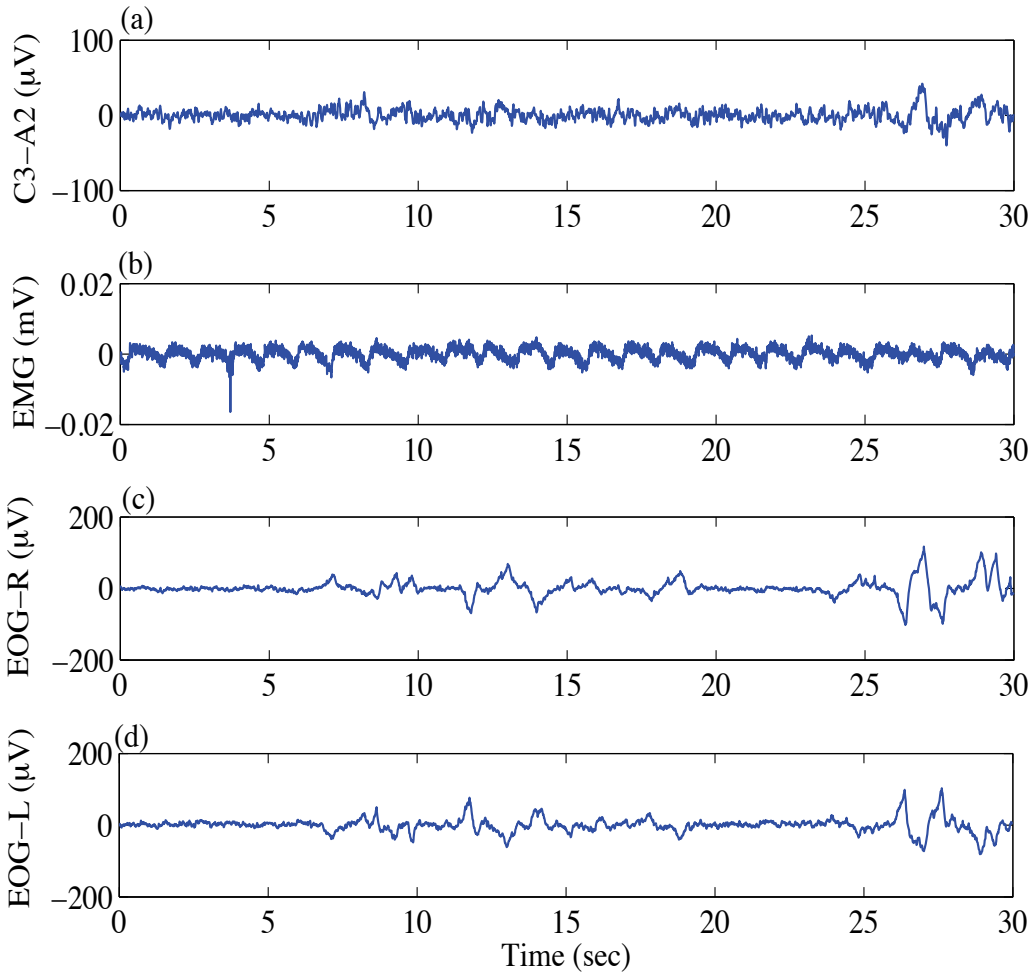

Figure 2.10. An example of EEG, EMG, and EOG signals during REM sleep. (a) C3-A2 EEG channel, (b) EMG, (c) Right EOG channel, and (d) Left EOG channel.

Table 2.2. Characteristics of sleep stages.

Sleep Stage	EEG	EMG	EOG
Stage Wake	Alpha activity	Increase in activity	Slow eye rolling
Stage 1	Theta activity Vertex waves	Decrease in level compared to Stage Wake	Slow eye rolling
Stage 2	Theta activity Sleep Spindles K-complexes	Level varies	Varies
Stage 3	20-50% oscillations below 2 Hz peak to peak voltage $\geq$ 75 micro-volts	Level varies	Small movement
Stage 4	>50% oscillations below 2 Hz peak to peak voltage $\geq$ 75 micro-volts	Level varies	Small movement
REM	Theta activity Sawtooth waves	Lowest level	Rapid oscillations

stage scoring using the old and new system, each stage has a new name. Stage 1 is referred to as N1, Stage 2 is N2, and Stage 3 and 4 are now referred to as N3. Since the results and models discussed use the former labeling of stages the new labeling will not be used throughout this report.

2.3 Auditory Processing During Sleep

Auditory processing continues during sleep, however not at the same level as during awake states. In the brain almost all sensory information passes through the thalamus on its way to the cortex. During sleep, the transmission of information to the cortex is reduced compared to the amount of information that reaches the thalamus. This phenomenon has often been called "thalamic or sensory gating"(Coenen, 2010).

2.3.1 Auditory Awakening Thresholds

Several studies have evaluated the level of a sound needed to awaken an individual during the night. The sleep stage that an individual is in affects whether they will be awakened. Zeplin, McDonald, and Zammit (1984) determined the auditory awakening thresholds of subjects of different ages. The three age groups that were studied was 18 to 25, 40 to 48, and 52 to 71 years. They played an 800 Hz tone of 5 seconds duration during the night, the intensity of the tone was increased until an individual awakened. The subjects had to press a buzzer to signal they were awakened. Auditory awakening thresholds for Stage 2, 4, and REM sleep were measured. They found that auditory awakening thresholds decreased with age. Also the sleep stage with the highest threshold was Stage 4, which is considered the deepest stage of sleep. In men, they found that the auditory awakening threshold for Stage REM was similar to the threshold for Stage 2 sleep. However, in women, while similar results as men

were found for the 18 to 25 age group, for the 40 to 48 and 52 to 71 age group, the auditory awakening threshold for REM sleep was closer to the threshold for Stage 4. They stated this difference in response to sounds during REM sleep may be due to the incorporation of the auditory stimuli in dreams or that the tones were played during Phasic REM sleep when auditory awakening thresholds may be higher.

Rechtschaffen, Hauri, and Zeitlin (1966) also measured auditory awakening thresholds. Seven subjects took part in the study and they were between 20 to 30 years in age. The sound stimulus that was used was a 2000 Hz tone of 5 seconds duration. After each sound stimuli was played a series of short repetitions of the tone were played. The subjects had to verbally respond how many repetitions of the tone were played. If their answer was correct they were considered to have awakened. Rechtschaffen, Hauri, and Zeitlin (1966) used the method of constant stimuli; they calculated the percent of trials that resulted in an awakening for different sleep stages. They found that more awakenings occurred in REM and Stage 2 sleep than Stage 3 and 4 sleep during the first three hours of the night. A similar number of awakenings occurred in Stage 2 and REM sleep.

Through the night, the depth of sleep lightens, which means that the auditory thresholds may decrease through the night. Basner (2010) reviewed the research of Ernst Otto Heinrich Kohlschütter who over 150 years ago investigated the sound intensity required to wake 6 students throughout the night. The sound was generated by having a pendulum hammer strike a slate slab. The intensity of the sound was varied by increasing the elevation of the hammer. The subjects gave some sort of signal to indicate that they were awakened. The stimulus intensity needed to awaken subjects increased for the first 90 minutes of sleep and then decreased throughout the remaining part of the night. This follows trends that would be expected due to the variation in sleep depth during the night.

Brain activity response to noise, not just behaviorally indicated awakenings has also been evaluated. Czisch, Wetter, Kaufmann, Pollmächer, Holsboer, and Auer (2002) evaluated responses to noise during sleep using EEG and fMRI. The stimuli used was an excerpt from a novel. They found using fMRI that a reduction in activity in the primary and auditory cortices during NREM sleep occurred. Issa and Wang (2011) collected neuron activity data from the auditory cortex in marmosets monkeys. They also measured EEG activity in order to determine which sleep state the marmosets were in. During the night tones and narrow-band noise of different levels were played. The levels used were not high enough to cause an awakening. They found that during slow wave sleep when quiet sounds below 40 dB were played neuron firing rates were less than when subjects were awake. However, for louder sounds, greater than 40 dB, neuron firing for the SWS and Wake states was similar.

2.3.2 Auditory Processing During Rapid Eye Movement Sleep

Awakening thresholds found in previous studies are not consistent; it is unclear from these studies whether the auditory awakening threshold for REM sleep is more similar to the awakening thresholds of Stage 2 or Stage 4. The contradictory findings may be due to the fact that awakenings during the two different substates of REM sleep, Phasic and Tonic, were not distinguished. During Tonic REM sleep muscle tone is low and EEG amplitude is low and consists of mixed frequency activity primarily in the theta band similar to Stage 1 sleep. During Phasic REM sleep there are spikes in neuron activity which can be observed in the occipital cortex and are called ponto-geniculo-occipital spikes, there is also rapid eye movement, contractions of the muscles of the middle ear similar to the contractions that occur to protect against loud noise, other muscle twitches and irregularity in respiration and heart rate (Seigl,

2005). Also dreams may be more intense and emotional during Phasic REM sleep (Sallinen, Kaartinen, and Lyytine, 1996).

Ermis, Krakow, and Voss (2010) examined whether the different auditory awakening thresholds found in previous studies was due to the non differentiation between the two types of REM sleep. They classified a state as being Tonic REM sleep if rapid eye movements were absent for at least 15 seconds prior to a 30 second epoch. The acoustic stimulus used was a 1000 Hz tone that began at 35 dB and the level was increased until the subject pressed a switch taped to their palm to indicate that they were awake. They measured behavioral awakening thresholds during Stage 2, 3, 4, and Phasic and Tonic REM sleep. During Phasic REM the sound stimuli began being played when rapid eye movement activity was occurring. Ten subjects completed the study. They found that the awakening threshold or level of sound needed to awaken a subject increased with NREM stages. The auditory awakening threshold was lowest for Stage 2 sleep and highest for Stage 4 sleep. They also found that the awakening threshold during Phasic REM sleep was similar to that for Stage 4 and the awakening threshold during Tonic REM was similar to that for Stage 2. These differences cannot be explained by the frequency spectrum of the EEG signal, as the EEG activity level during both Tonic and Phasic REM sleep is similar to the EEG activity levels during light NREM sleep.

Wehrle, Kaufmann, Wetter, Holsboer, Auer, Pollmächer, and Czisch (2007) used functional magnetic resonance imaging (fMRI) and polysomnography to evaluate the differences in processing of auditory stimuli during REM sleep. Data from 7 subjects was used in the analysis. They used different stimuli including narrative text, a beep, and piano music during the test. The purpose of this test was not to determine the awakening threshold but to evaluate differences in auditory processing, so stimuli were played at a non-arousing threshold. REM density was calculated by determining the

presence of rapid eye movements in 3 second epochs. The regions of the brain that were the focus of the imaging were the thalamus and the auditory cortex. They found that activation of the auditory cortex was reduced in Tonic REM sleep compared to that during wakefulness and at its lowest level in Phasic REM sleep. They also found that auditory stimuli that began in Phasic REM sleep sometimes led to Tonic REM sleep. They stated that their work supports that of Llinas and Pare (1991) who argued that the thalamus is as excited by external stimuli during REM sleep as during awake states but the information is ignored and not passed to the cortex during Phasic REM sleep. They stated that the thalmacortical network must act as a closed loop during Phasic REM sleep.

2.4 Measurement Methods

There is substantial evidence that sounds are processed during sleep and that they can cause awakenings during the night. Therefore, there has been concern over whether aircraft noise at night will lead to significant amounts of sleep disturbance in communities surrounding airports. In Appendix B are detailed lists of laboratory and field studies that have been conducted to understand the effect of aircraft noise on sleep. Twelve laboratory and 12 field studies have been identified. The reports for each study were examined to determine what methods were used to measure awakenings and what additional measurements were made; the results are summarized in Table 2.3. It can be seen that a wide range of methods have been used to measure awakenings. Sleep has been measured by using polysomnography in few field studies, which is considered the most sensitive measure of sleep. In addition, in most field studies heart rate, blood pressure, or hormone levels have not been measured. Data collected from these type of measurements could aid in understanding the relationship between sleep and health.

Table 2.3. The number of studies that used the listed measurement techniques and measured the listed variables.

	Laboratory	Field
>than 20 subjects	3	11
Social Survey	0	5
am/pm Questionnaires	7	7
Behavioral Awakenings	3	4
Actimetry	3	6
Motility-Other	1	1
Polysomnography	12	3
ECG	7	2
Blood Pressure	1	1
Hormone Levels	3	1
Objective Sleepiness	2	0
Subjective Sleepiness	6	8
Performance	5	3

One method that has been used to quantify sleep disturbance is to use social surveys or next day questionnaires. These surveys have included questions on the number of awakenings, difficulty falling asleep, annoyance caused by nighttime noise, window closing habits, etc. A correlation between objective measures of sleep and subjective evaluations has been found. Ollerhead et al. (1992), for example, found a strong inverse relationship between arousal rate (measured with actimetry) and subjects' evaluations of sleep quality, indicating that subjects with a higher number of arousals did report poorer sleep. A problem with the use of social surveys or questionnaires to evaluate sleep is that subjects will only remember awakenings in which they regained full consciousness, which means the awakening lasted at least two and a half minutes (Ollerhead et al., 1992). Shorter arousals will not be remembered in the morning, but they may be an important factor in long or short term health effects.

One method used, particularly in US field studies on aircraft noise and sleep disturbance, is the measurement of signaled awakenings, also often referred to as behavioral awakenings. In US studies subjects pressed a button when they were awakened. This method is less intrusive than other measurements of sleep such as polysomnography which involves many electrodes, and it can easily be implemented in the field. However, it is an insensitive measure of disturbance compared to measurements made with EEG. A person has to be consciously awake to press the button. Also it is a subjective measure as subjects can decide whether or not to press the button. The result is a measurement of far fewer awakenings then might actually occur during the night.

In a study by Fidell, Pearsons, Tabachnick, Howe, Silvati, and Barber (1995) it was found, when measuring behavioral awakenings of subjects living around airports, that on average two spontaneous awakenings and less than one noise induced awakening occurred during the night. This is much less then the approximately 20 EEG measured spontaneous awakenings that occur. In addition, behavioral awakenings may underestimate sleep disturbance due to habituation. There is evidence that the number of behavioral or signaled awakenings decreases over subsequent study nights while other physiological measurements such as cardiac arousals do not (Griefahn, Bröde, Marks, and Basner, 2008a). Thiessen (1978) conducted a laboratory study in which subjects were exposed to noise from road vehicles. Seven truck passbys were played during the first six hours of sleep. Ten subjects slept 24 consecutive nights in the laboratory. There was clear habituation in signaled awakening responses, i.e., fewer occurred as the length of time in the study increased, however there was never full habituation.

The measurement of motility has been used in several studies to evaluate sleep disturbance. Movement is often measured using actimeters, which are devices worn on

the wrist and contain an accelerometer. Different algorithms are used to determine when awakenings occur making it difficult to compare results across studies (Luz, Nykaza, Stewart, and Pater, 2008). As part of a study conducted by Ollerhead et al. (1992), comparisons were made between arousals, determined by using actimeters and EEG measured awakenings. It was found that 88% of all EEG awakenings coincided with actimetric arousals. Another less intrusive method for evaluating movement has been developed by Brink, Müller, and Schierz (2006). In this technique, called seismosomnography, force sensors are placed underneath bed posts. Heart rate, respiration, and body movement can be estimated from these measurements. However, this method has not been used often, and still needs further validation.

In order to evaluate the effect of noise on sleep stages and to determine the number of smaller arousals polysomnography is used. This method involves the simultaneous measurement of EEG, EOG, and EMG. Additional measurements such as electrocardiogram (ECG – measurement of electrical activity of the heart) and respiration measurements are also often made. For polysomnography, the ECG usually involves only two electrodes. The two electrodes can either be placed directly below the collarbone on both the left and right side, or one electrode is placed under the right collarbone and the other electrode is placed on the left side of the ribcage. Respiration measurements are made with a strap around the lower abdomen (Spriggs, 2008).

While polysomnography provides detailed information about an individual's sleep, it is costly to perform. A trained individual is needed to apply the electrodes. Also the standard practice is to visually score sleep stages, which is time consuming and expensive. In addition, the number of electrodes that are used may affect the quality of sleep, causing an individual's sleep to be lighter and therefore more likely to be awakened by noise.

Less intrusive methods have been used to obtain information on changes in sleep state. LeVere, Bartus, and Hart (1972) only used one EEG electrode (plus reference) for their study. This meant that they could not distinguish sleep stages since EOG and EMG are needed to define REM sleep; however they did perform a spectral analysis of the EEG signal to quantify the effect of noise on sleep. The frequency bands they analyzed were; Delta, Theta, Alpha and Beta. LeVere et al. (1972) defined 5 levels of activation. Level 0 was the highest level of activation and, although not stated in the paper, one would assume this corresponds to the waking state. Levels 1 and 2 were associated with 30% of the epoch containing theta and alpha activity and could be thought of as light sleep such as Stage 1 and 2, Level 3 occured when the epoch contained 20-50% delta activity which is Stage 3 sleep, and Level 4 was associated with 50% delta activity which corresponds to Stage 4 sleep. The results of their study were that the level of activation did increase when an aircraft sound occurred.

Another less invasive method for measuring sleep has been developed by Basner, Müller, Elmenhorst, Kluge, and Griefahn (2008c). They have evaluated cardiac activations, measured with an electrocardiogram. It involves fewer electrodes and participants in a study can be trained to apply their own electrodes. They found that very similar dose-response relationships for EEG awakenings and ECG (cardiac) arousals can be obtained. This method is less expensive to implement than polysomnography and is a more sensitive measure of awakenings than other low cost options such as actimetry or button pressing.

2.5 Noise Induced Sleep Disturbance

Regardless of the method used to evaluate sleep, overall an increase in sleep disturbance with noise level has been found in most studies designed to examine the effect of aircraft noise on sleep. The differences in the results between studies is primarily

the number of awakenings measured, which is important when trying to understand potential health effects. For example, Ollerhead et al. (1992) found that 4.2% of events caused an EEG awakening, while only 0.9% of events caused an actimetric arousal.

Noise not only increases the number of awakenings but also the duration of the awakening. Basner, Samel, and Isermann (2006) found that compared to spontaneous awakenings, the duration of a noise induced awakening increases for sounds that have a maximum noise level above 70 dB(A) (L_{Amax}). Researchers who have used polysomnography, have also evaluated the effect of noise on the amount of time spent in specific sleep stages. Griefahn, Marks, and Robens (2006) found a significant decrease in the amount of REM sleep and SWS for nights with noise compared to nights without noise. The reduction in total minutes of REM sleep was found to be 6.4 minutes and 5.3 minutes for SWS. For an average young adult about 96 minutes is spent in both Slow Wave and REM sleep (Kales and Kales, 1970). The result of Griefahn et al. (2006) would suggest a 5-7% decrease in duration of these sleep stages occured due to noise. Basner and Samel (2005) also found that noise exposure resulted in a significant reduction in average time spent in SWS, although not for REM sleep.

The overall effect of noise on awakenings and sleep structure was summarized by Griefahn, Robens, Bröde, and Basner (2008b). Noise has been found to cause:

1. an increase in time to fall asleep
2. an increase in time until Stage 4 is reached
3. an increase in time spent awake
4. an increase in the number of awakenings which last longer than three minutes (these would constitute conscious awakenings)

5. an increase in time spent in Stage 1 sleep

6. a decrease in time spent in slow wave sleep (SWS, Stages 3 and 4)

7. a decrease in time spent in rapid eye movement sleep (REM).

Basner, Glatz, Griefahn, Penzel, and Samel (2008b) indicate it may be useful not only to examine awakenings but also to examine the effect of noise on arousals. They evaluated 3 nights of data from 10 subjects, two of the nights were noise exposure nights. For one noise exposure night, 64 aircraft events were played with a maximum noise level of (L_{Amax}) 65 dB(A). For the second noise exposure night, 64 aircraft events were played with a maximum noise level of (L_{Amax}) 45 dB(A). One finding of the study was that for louder sounds of 65 dB(A), awakenings were the best indicator of the changes in sleep due to noise, while for quieter sounds of 45 dB(A) arousals were the best indicator of the impact of noise on sleep.

The usefulness of measuring arousals is supported by the findings of Saremi, Grenéche, Bonnefond, Rohmer, Eschenlauer, and Tassi (2008). In their test, there were two experimental nights in which subjects were exposed to train noise. On one night train noise with a $L_{Aeq,8hr}$ (8-hour A-weighted equivalent noise level) of 40 dB(A) was presented and the other night train noise with a $L_{Aeq,8hr}$ of 50 dB(A) was presented. The only significant effects of noise on sleep that were found were an increase in latency to SWS (the time from sleep onset until Stage 3 or Stage 4 occurs) and an increase in the number of arousals. The increase in both latency and number of arousals was found to increase with noise level.

There is still not a clear understanding of how different characteristics of noise affect whether an individual will be disturbed. Currently models are based on the assumption that single event indoor metrics L_{Amax} or A-weighted Sound Exposure Level ($SELA$) are the best predictors of the disturbance. There is, however evidence

that sound characteristics in addition to the noise level affect whether an individual awakens. Bruck, Ball, Thomas, and Rouillard (2009) examined awakening thresholds for different types of signals including; square waves of different fundamental frequencies, a sound consisting of three pure tones, white noise, and sounds that had a higher noise level in a given frequency band. All sounds were presented 4 times during the night when the participant was in Stage 4 sleep. To indicate an awakening, subjects had to press a button three times. A 20 dB difference in mean awakening thresholds was found across the different signals.

A study on low frequency noise and cortisol levels was conducted by Ising and Ising (2002). In this study the levels of cortisol in children ages 7 to 13 years old who were exposed to road noise were measured. Cortisol levels were determined from urine samples, one sample was obtained 1 hour after falling asleep and another was obtained after awakening at the end of the night. The maximum noise levels were measured using both A-weighting and C-weighting (L_{Amax}, L_{Cmax}). Fifty-six children took part in the study. There was some correlation between the secretion of cortisol in the first half of the night and the C-weighted noise levels.

In addition to low frequency content, the rise time of the noise affects the degree of arousal. Levere, Davis, Mills, Berger, and Reiter (1976) investigated the effect of rise time on arousal. The stimuli used were band-passed random noise, one-third octave band centered at 125 Hz. The stimuli had a duration of 15 seconds and 80 dB peak intensity. For one sound the rise time was "instantaneous" and was approximately 3.24 ms. The second stimuli had a linear rise time and approached the maximum noise level after 7.5 seconds. The response to events of different rise times was not found to be consistent throughout all stages of sleep. When the EEG was occupied by fast wave activity, which would coincide with light sleep, both fast and slow-rise time events produced similar levels of activation. During slow wave sleep the

sounds with the faster rise time produced the greatest response. Marks, Griefahn, and Basner (2008) found that for aircraft and railway noise, people were more likely to be awakened by sounds with faster rise times. This finding is also supported by the work of Brink, Lercher, Eisenmann, and Schierz (2008). The subjects in their experiment were exposed to aircraft sounds reproduced by a loudspeaker. The aircraft events occurred during a period of 90 minutes, either at the beginning or end of the night. They found that the faster the rise time the greater the motility.

Related to noise metrics, two studies have been conducted in order to evaluate the difference in sleep disturbance caused by aircraft, road, and rail noise. Basner, Elmenhorst, Maass, Müller, Quehl, and Vejvoda (2008a) found that aircraft noise caused fewer awakenings and changes to Stage 1 than the other types of transportation noise. Marks, Griefahn, and Basner (2008) also found that sleep disturbance was dependent on the noise source. They found that train noise caused the most awakenings, followed by aircraft, and then road noise. They stated that a possible reason for these results is a difference in sound characteristics such as duration, rise time and spectral balance. These characteristics should be considered along with the maximum level as candidate terms in a more comprehensive sleep disturbance model.

LeVere, Bartus, Morlock, and Hart (1973) examined whether equal loudness or equal sound pressure level dictated whether an individual would awaken to noise. Acoustical stimuli used were three one-third octave band noise centered on the frequencies of 125 Hz, 250 Hz, and 1000 Hz. The sounds were equated for equal loudness of 80 dB measured with A-weighting. The actual sound pressure of the sounds was 93 dB for 125 Hz, 87 dB for the 250 Hz sound, and 80 dB for the 1000 Hz sound. During high cortical activity response to all three stimulus was the same however, during slow wave sleep the sound with the highest sound pressure and lowest frequency (125 Hz) caused the greatest degree of arousal. They suggest that certain neural centers

which normally are involved in auditory processing are perhaps inhibited during sleep resulting in a difference in processing during deep sleep.

LeVere, Morlock, Thomas, and Hart (1974) conducted a second study to further examine processing of sounds of equal loudness during sleep. The sounds used were band-passed random noise for one-third octave bands centered at 50, 250, and 1000 Hz. Subjects during the day used the method of adjustment to match the loudness of the 50 and 250 Hz sound to the level of the 1000 Hz sound. The average SPL of the 50 Hz sound was approximately 100 dB, the average SPL of the 250 Hz sound judged to be equally loud as the 1000 Hz sound was 90 dB, and the reference 1000 Hz tone was played at 80 dB. Similar results to the 1973 study were found in that the three stimuli produced almost equal amounts of arousal during fast activity while the amount of response varied according to sound pressure level in slow wave sleep.

It has been shown that the meaning of sounds also affects whether an individual will be awakened. Oswald, Taylor, and Treisman (1960) played a recording of 56 different names. This list included the names of the subjects involved in the study. The subjects were told to awaken when they heard their name or a control name and to clench their fist upon awakening. Oswald et al. (1960) found that subjects moved their hand more when their name was presented, and they also had more K-complexes than when other names were played. Portas, Karakow, Allen, Josephs, Armony, and Frith (2000) used fMRI and EEG to examine sensory processing during NREM sleep. The stimuli used were a pure tone beep and the subject's name. More awakenings occurred when the subject's name was presented than when the tone was presented. They stated that the pattern of activation of brain activity in both sleep and waking was similar. However, there was reduced activity in different regions of the brain including the left parietal, bilaterally in the prefrontal cortex, thalamus, and part of the limbic system compared to the activity present in the awake state.

During sleep when the subjects name was presented certain areas of the brain were more responsive than when the tone was played.

2.6 Mediating Factors

There are several factors that may affect the level of sleep disturbance in addition to the sound characteristics. Of particular interest in noise studies, is whether the testing environment affects the level of disturbance. A person sleeping in a laboratory may be more likely to be awakened because of an unfamiliar sleeping environment. Therefore, results from a laboratory study may not be directly applicable to communities around airports. There has also been interest in habituation and whether those living in communities will become less likely to awaken over time. This could also be another reason why results in the laboratory and in the field studies are different.

2.6.1 Laboratory vs Field

There have been several field and laboratory studies conducted to evaluate the effect of noise on sleep. However, whether the results from the two environments can be directly compared has been a subject of debate, particularly because the methods used in the two studies are often different. Pearsons, Barber, Tabachnick, and Fidell (1995) combined data from several existing studies and examined the difference in dose-response relationships between the noise level and percent awakened in the laboratory tests and in the field tests. It was found that for the same noise level, the percent awakened was higher in the laboratory. For example, an A-weighted Sound Exposure Level ($SELA$) of 80 dB(A) would cause 33% of people in a laboratory study to be awakened while only 4% awakened in the field. However, one of the main problems with their analysis is that they combined data from studies that used different noise

sources including aircraft, railway, white noise, pure tones, and sonic booms. It has been found in several studies that noise induced sleep disturbance is dependent on the sound source. Therefore, if the sound sources used in the laboratory studies and in the field studies are not the same, attributing differences in sleep disturbance to the study environment alone is highly questionable. However, higher responses to noise in the laboratory than in the field were also found by Basner et al. (2004). They even found a higher degree of disturbance in the laboratory for the group of 20 people who participated in both the laboratory and the field studies.

Iber et al. (2004) investigated the difference in sleep parameters for subjects undergoing unsupervised recording in the home and supervised recording in the laboratory. In both circumstances the application of the sensors was performed by a trained individual. Also, the same individuals were tested in both environments. The responses in the home environment were compared to those in the laboratory and it was found that in the laboratory test, sleep duration decreased by 38 minutes, sleep efficiency (total sleep time divided by the total time in bed) decreased by 7.8%, the percent time spent in REM sleep decreased by 2.6% and the amount of Stage 1 sleep increased by 1.2%, however,they did not find a significant difference in the arousal index (the number of arousals per hour of sleep) in the two environments. In other studies, such as those by Flindell et al. (2000) and Skånberg and Öhrström (2006), large differences in sleep disturbance between the two testing environments (laboratory and field) were not found. Skånberg and Öhrström (2006) used actimeters to evaluate sleep and found that in the laboratory there was an increase in sleep onset latency of 3.3 min and a slight decrease in time awake of 1 minute. They also found a slight decrease in sleep quality and increase in tiredness when subjects slept in the laboratory.

2.6.2 Habituation

It has often been argued that the differences in results in the two testing environments is due to habituation, i.e., that individuals living near airports have become accustomed to the noise and therefore, are less likely to be awakened. Habituation within a single night and over the course of many nights has been examined by researchers. Brink, Lercher, Eisenmann, and Schierz (2008) found that motility in response to a noise event decreased with the number of events. They found a decrease of approximately 20% between the motility for the first event and the motility for the sixteenth event during a single night.

Basner and Samel (2004) also found a decrease in the probability of awakening as the number of events increased in a laboratory study. This decrease began with 8 events and there seemed to be a threshold reached in which the probability of awakening remained constant after 32 events. Öhrström (1995) measured movement of subjects, with an accelerometer attached to the bed, when they were exposed to noise from a passing truck. Different numbers of truck operations from 16 to 128 were played. It was found that movements induced by noise decreased when subjects were exposed to 64 and 128 noise events compared to when subjects were exposed to 16 and 32 events. Griefahn and Muzet (1978) in a review paper stated that for up to 35 stimuli a night the probability of awakening seems to increase with the number of events, however after that the percent awakened either no longer increased or began to decrease. Griefahn (1977) stated that a decrease in response with number of events is not due to habituation, but is caused by adaptation. Adaptation can occur if stimuli occur too close together as neurons may be in a refractory period, which means that they are unable to respond to the next stimuli. In adaptation the neurons at the level of the sensory organ cannot respond. However, for habituation the individual can

fully sense it, the lack of response happens at the level of the central nervous system (Domjan, Grau, and Krause, 2010).

Habituation over the course of several nights has also been examined. Kuroiwa, Xin, Suzuki, Saszawa, and Kawada (2002) had 9 subjects undergo 17 nights of sleep measurements. For 10 nights, subjects were exposed to road traffic noise. They used polysomnography to evaluate sleep disturbance. They also had subjects complete a questionnaire in which they rated sleepiness, sleep maintenance, worry, integrated sleep feeling, and sleep initiation. Over the ten days it was found that polysomnographic sleep parameters did not change, however, there was some evidence of habituation in the subjective sleep parameters. Thiessen (1978) also conducted tests to evaluate habituation to noise from trucks. Sleep disturbance was evaluated using both EEG and behavioral awakenings. In one test, 5 subjects slept for 12 nights in the laboratory while in another test 10 subjects were tested for 24 nights. It was found that behavioral awakenings did decrease over the number of nights. This decrease though, could be due to a lack of motivation to press the button.

Vallet, Gagneux, Blanchet, Favre, and Labiale (1983) conducted a study with subjects who had lived in the same house for at least four years. Sleep was evaluated in the home of the subjects. They slept in their normal nighttime arrangement for part of the study and they also moved their bed to a room on the quieter side of the house for several nights. The subjects' sleep did improve in the quieter setting, less time was spent awake, and the amount of REM sleep and subjective sleep quality increased. This provides evidence that even after living near a noise source for several years sleep is still disturbed by noise. Therefore, while there is evidence from awakenings and subjective evaluations of sleep that subjects do habituate to some degree, no full habituation occurs. By reducing noise, an individual's sleep can be improved. Also it is important to note that lesser degrees of arousal have shown no

habituation. Griefahn, Bröde, Marks, and Basner (2008a) found that the number of cardiac arousals caused by noise both within a night and across nights did not decrease with increased exposure.

2.6.3 Noise Sensitivity

Noise sensitivity has been found to explain part of the variation in annoyance due to noise, and so the relationship between noise sensitivity and sleep has also been investigated. Marks and Griefahn (2007) assessed noise sensitivity by using the Noise Sensitivity Questionnaire (NoiSeQ) which is a list of 35 questions, seven questions in each of 5 different categories related to work, sleep, communication, leisure, and habituation. The scores for each question are averaged and the results can range from 0 to 3. The noise sensitivity for subjects in their study ranged from 0.37 to 1.77. They found that noise sensitivity did not seem to relate to any physiological measures but was related to subjective assessment of sleep. Specifically, it was related to reported difficulty falling asleep, calmness, restoration, estimated body movements and sleep quality.

Öhrström and Björkman (1988) evaluated responses to noise using an accelerometer attached under the bed and also measured heart rate using ECG. For the test they had 12 very noise-sensitive subjects and 12 non noise-sensitive subjects. This was determined by using a sensitivity scale from 0 to 100. During the night subjects were exposed to road noise. The difference in heart rate and body movements between sensitive and non-sensitive subjects was small. However, there was a difference in self-reported sleep. Noise sensitive subjects reported a longer sleep onset latency and a higher number of awakenings. Based on the results of these two studies it seems that noise sensitivity affects subjective measures of disturbance but not physiological measures.

Dang-Vu, McKinney, Buxton, Solet, and Ellenbogen (2010) found that there is possibly a biological marker that indicates whether a person will be more likely to awaken to noise during the night than another person. They found that individuals with a high number of sleep spindles were less likely to awaken due to noise (which consisted of commonly heard sounds of road and air traffic, telephone ringing, and hospital based sounds), than individuals who had less sleep spindles during the night. The number of sleep spindles a person had during the night seemed to be a stable characteristic over three nights of testing.

2.6.4 Inter-Individual Variability

When evaluating sleep disturbance it is important to keep in mind the large inter-individual differences that occur. While the average change in the duration of sleep stages or number of awakenings when exposed to noise may be small, there is often a large spread in the data, with some individuals being affected significantly more than others. Therefore, in order to understand how noise affects both short-term and long term health, it may be useful to examine the data on an individual basis rather than on a population average basis. This was advocated by Vallet, Gagneux, Blanchet, Favre, and Labiale (1983). They evaluated the effect of road traffic noise on the sleep of each person. They stated that "averaging the results gives only a mediocre indication of these differences and it is more fruitful to follow the procedure of examining the classification of pattern responses to noise (Vallet, Gagneux, Blanchet, Favre, and Labiale, 1983)." When they state "classification of pattern response", the authors are referring to evaluating the change in sleep stage duration, sleep onset latency, and number of awakenings for each subject.

It is also important to keep in mind that the subjects taking part in noise studies are almost always in good health. They are not a representative population of those

living in communities around airports. Therefore the amount of disturbance due to noise could vary even more then what is observed in sleep studies on the effects of aircraft noise. For example, subjects with high anxiety have poorer sleep. Fuller, Waters, Binks, and Anderson (1997) found that subjects with high anxiety have a longer sleep latency, decreased slow wave sleep, a greater amount of Stage 1 sleep, lower REM density, and were more prone to arousal especially in the first half of the night. Also health and weight problems could lead to increased disturbance. Dixon, Schachter, and O'Brien (2005) conducted a sleep study in which the subjects underwent laparoscopic gastric band surgery. Sleep was evaluated using polysomnography both before surgery and on average about 17 months after surgery. It was found that weight loss led to a lower Apnea-Hypopnea index and an increase in slow wave sleep and REM sleep. In addition, it should be noted that 50 to 70 million people have sleep problems (National Institute of Health, 2003). It is unknown how noise interacts or compounds preexisting sleep issues.

2.7 Short Term Effects of Sleep Disturbance

Sleep disturbance during the night can lead to several next day effects. It can increase an individual's sleepiness. Also, it may lead to decrements in performance and increased annoyance to aircraft noise. A description of these next day effects follows.

2.7.1 Sleepiness and Tiredness

The effect of aircraft noise on sleepiness has been evaluated objectively as well as subjectively. Basner (2008) used the Pupillographic Sleepiness Test (PST). Data was collected for 24 out of the 128 subjects from the DLR laboratory sleep study. PST involves measuring the oscillations in pupil size. The change in size will be

below 0.3 mm for alert subjects, while for sleepy subjects the change could be several millimeters. Basner (2008) calculated the pupillary unrest index (PUI), which is a measure of the oscillation in pupil size per unit of time. They found that the natural log of PUI did increase with levels of noise events and also with the number of events that people were exposed to over the preceding night. The results were compared to PUI values for people with obstructive sleep apnea (OSA). It was found that the levels of sleepiness caused by aircraft noise never reached the levels found for those with OSA.

Another test used to evaluate sleepiness is the Multiple Sleep Latency Test (MSLT). This test involves evaluating how long it takes for an individual to fall sleep. Each test period is 20 minutes long, 4 to 5 sessions are completed throughout the day, with approximately 2 hours between tests. For a normal subject it takes between 10 to 20 minutes to fall asleep. The less time it takes to fall asleep, the higher an individual's sleepiness. MSLT tests were performed as part of the laboratory study conducted by Flindell et al. (2000). They did not find any statistically significant difference between the data from subjects following a control night and following a noise exposure night.

In many studies sleepiness is evaluated subjectively. There are three scales that are often used in sleep research, although they are not typically implemented in studies by researchers investigating effects of aircraft noise on sleep. These scales include the Epworth Sleepiness Scale (ESS) (Johns, 1991), Karolinska Sleepiness Scale (KSS) (Åkerstedt and Gillberg, 1990), and the Stanford Sleepiness Scale (SSS) (Flindell et al., 2000).

The Epworth Sleepiness Scale (ESS) is derived from answers to questions on how likely subjects are to fall asleep while in different situations which include: 1) reading, 2) watching TV, 3) sitting in a public place, 4) as a passenger in a car, 5) lying down to rest in the afternoon, 6) sitting and talking to someone, 7) sitting after a lunch, and 8)

in a car while stopped. Each scale is rated from 0 to 3, and the results for each question are added together to obtain an overall score. A test in which the use of the ESS was examined was conducted by Johns (1991). The subjects for this test included a control group as well as those with sleep disorders including snoring, obstructive sleep apnea, narcolepsy, idiopathic hypersomnia, and periodic limb movement disorder. Several patients not only filled out the ESS but also underwent Multiple Sleep Latency Tests. It was found that there was a correlation between MSLT and ESS scores.

The Karolinska Sleepiness Scale (KSS) is a 9 point scale, which has verbal labels for every odd scale number. The verbal labels are: 1) extremely alert, 3) alert 5) neither alert nor sleepy 7) sleepy but no difficulty remaining awake and 9) extremely sleepy-fighting sleep (Åkerstedt and Gillberg, 1990). The Stanford Sleepiness Scale (SSS) has 7 detailed descriptions of the degree of sleepiness. For example, a rating of 1 is associated with "feeling active, vital, alert, or wide awake" while a rating of 7 is associated with "No longer fighting sleep, sleep onset soon, having dream like thoughts." This scale was used in the aircraft noise study conducted by Flindell et al. (2000). However, they found no effect of aircraft noise on sleepiness as evaluated by using the SSS. Passchier-Vermeer, Vos, Steenbekkers, van der Ploeg, and Froothuis-Oudshoorn (2002) had subjects evaluate sleepiness with a 9 point scale. They found that nighttime noise was related to sleepiness ratings but only when the rating was completed first thing in the morning.

Tiredness has been examined in other studies. In a social survey conducted around Heathrow and Gatwick Airports, a large variation in reports of tiredness was found. Tiredness was evaluated by using a five point scale marked from "very refreshed" to "very tired" (DORA, 1980). The reported tiredness was compared to the average A-weighted night-time noise levels between 10:00 pm and 7:00 am and no relationship was found below 65 dB(A), however above 65 dB(A) there was an increase in reported

tiredness with noise level. Fidell et al. (1995) used a 5 point scale to evaluate tiredness (1 "not at all tired", 5 "extremely tired"). They found that tiredness was positively correlated with the number of behavioral awakenings.

2.7.2 Performance

Sleep disturbance might also decrease next day performance. Wilkinson and Campbell (1984) evaluated performance after sleep disturbance caused by traffic noise. Performance was evaluated both before and after double glazed windows were installed. They used several different performance tests including a reaction time test, short term memory tests, and vigilance tests. After installing double glazed windows they found that reaction time improved. They showed that this decrease in reaction time also coincided with an increase in Stage 4 sleep and an improvement in the subjects' evaluations of sleep. However, the relationship between these three variables was not statistically significant. The association between SWS and performance has also been shown by Marks and Griefahn (2005) after nights where subjects were exposed to rail traffic noise.

Elmenhorst and Basner (2008) have found small but statistically significant differences in performance after noise exposure. A decrease in performance with L_{Aeq} levels was found. An increase in reaction time of 0.13 ms/dB was found in the laboratory studies and a 0.3 ms/dB increase in reaction time in the field studies. Flindell et al. (2000) also evaluated next day performance. They used several tests that were completed every two hours during the day. The tests included a sustained attention task, a digit memory recall task, and a choice reaction task. They found that performance did not decrease with increased noise exposure. In the field study, performance improved for all three tasks over the course of three days (following nights of noise exposure). However, it was noted by the authors that few of the field subjects completed

all of the required training and therefore the results could represent a learning effect. In their laboratory tests, for most performance tests and testing times, a statistically significant effect of noise on performance could not be found. Schapkin, Falkenstein, Marks, and Griefahn (2006) also found no statistically significant results that would indicate that noise affects next day performance. It was mentioned that this could have been due to the tasks being too easy, which was indicated by the low false alarm rates. These results are also further supported by Passchier-Vermeer et al. (2002) who used a reaction time task to evaluate performance and found that neither the reaction time nor mistakes made during the test were affected by sleep disturbance caused by nighttime aircraft noise.

As a result of the negative findings found in many studies, there is the question of what type and what amount of sleep disturbance would lead to next day performance decrements? Guilleminault, Abad, Philip, and Stoohs (2006) conducted a study in which a 1000 Hz tone was used to excite cardiac arousals but not EEG arousals during one night. For a second night they excited EEG arousals. For both nights, once an arousal was obtained, at least 1 minute of sleep had to occur before another tone was played. The following morning, after each experimental night, subjects completed a psychomotor vigilance task. They found that an increase in reaction time only occurred for the test condition in which EEG arousals were evoked.

Decrements in performance are found after nights in which sleep time is greatly reduced. However, even in studies in which subjects are completely deprived of sleep, there are large variations in performance and not all tests indicate a decrease in performance. Frey, Badia, and Wright Jr. (2004) evaluated the performance of subjects after two nights of sleep deprivation. The subjects completed 22 different performance tests that included psychomotor vigilance tasks and reaction time tasks. The tasks were completed every three hours during the sleep deprivation period. Performance

compared to that on baseline nights was worse for 17 out of the 22 tasks. Performance for individual subjects was highly task dependent. The subject that performed the worst on one test did not consistently perform the worst on all tests. There was also a large variability in response between subjects. Thus, when evaluating next day performance, it is important to use multiple tests as well as evaluate the change in performance on an individual basis.

2.7.3 Annoyance

Sleep disturbance can also lead to increased annoyance. Using laboratory and field data, Quehl and Basner (2006) examined annoyance due to nighttime noise. Annoyance was evaluated each morning using the standardized 5 point annoyance scale (1 "Not at all Annoyed" to 5 "Extremely Annoyed") (Fields et al., 2001). They found that annoyance in the laboratory was greater than in the field. They also found that it was important to include the number and level of events when assessing annoyance. Basner, Elmenhorst, Maass, Müller, Quehl, and Vejvoda (2008a) also evaluated annoyance due to sleep disturbance caused by aircraft, road, and train noise. They found that aircraft noise caused the greatest amount of annoyance but it caused the least number of transitions to Wake or Stage 1 sleep.

2.7.4 Coping Strategies

Coping strategies such as taking sleeping pills and closing windows to reduce the noise are both used in the short term to improve sleep for a particular night, and in the long term when their use becomes a continuous habit for an individual. Griefahn, Schuemer-Kohrs, Schuemer, Moehler, and Mehnert (2000) found that the probability that an individual slept with the windows closed increased with outdoor noise level.

They also found that those exposed to road noise were less likely to sleep with windows closed compared to those exposed to train noise of the same outdoor noise level. Passchier-Vermeer et al. (2002) found that an increase in age as well as noise level contributed to an increase in the percentage of people taking sleeping pills.

2.8 Long-Term Health Effects and Potential Pathways

In addition to next day effects, noise induced sleep disturbance may lead to long-term health effects. One of the largest studies examining the health effects caused by aircraft and road traffic noise is the Hypertension and Exposure to Noise near Airports study (HYENA) (Jarup et al., 2008). This study was conducted in order to evaluate the risk of developing hypertension due to aircraft and road traffic noise exposure. The study was conducted in communities surrounding six airports: London Heathrow, Berlin Tegel, Amsterdam Schiphol, Stockholm Arlanda, Milan Malpensa and Athens Elpheterios Venizelos Airports. Researchers compared both $L_{Aeq,16hr}$ and L_{night} measures of aircraft noise with the odds ratio for hypertension and found that only the relationship with L_{night} was statistically significant. Therefore, it seems that nighttime noise and sleep disturbance may be an important pathway through which noise may affect an individual's health.

2.8.1 Sympathetic Tone

In response to a stressor, an increase in activity in the sympathetic nervous system occurs. This includes an increase in heart rate and blood pressure among other effects. Elevations in activity of the parasympathetic nervous system cause the opposite reactions. There have been a few studies conducted in which the effect of noise on these levels has been investigated. Graham, Janssen, Vos, and Miedema (2009) conducted

a study to investigate the effect that train and road noise have on sympathetic and parasympathetic tone. They found no relationship between traffic noise and cardiac sympathetic tone but they did find a relationship with cardiac parasympathetic tone; there seemed to be a reduced level but only for the second half of the night.

Carter, Henderson, Lal, Hart, Booth, and Hunyor (2002) conducted a laboratory study in which the subjects were 9 nurses who were night-shift workers. The effect of noise on heart rate, blood pressure, and sympathetic tone was evaluated. They played military aircraft, trucks, tones, and civilian aircraft sounds to the subjects during an 80 minute period at the beginning of night. They found that military aircraft and pure tones increased systolic and diastolic blood pressure. To evaluate the effect of noise on sympathetic tone they performed a frequency analysis of the heart rate and blood pressure measures. They found that there was an increase in sympathetic tone for military aircraft when assessing the data on blood pressure, but did not find an increase when analyzing the heart rate data.

2.8.2 Cardiac Arousals

In addition to EEG arousals, the effect of noise on autonomic arousals has been investigated. One of the main indicators of an autonomic arousal is a change in heart rate. Griefahn, Bröde, Marks, and Basner (2008a) examined cardiac arousals caused by road, rail, and aircraft noise. Cardiac arousals both with and without an awakening were assessed. With an awakening the changes in heart rate were monophasic (an increase from baseline to a maximum followed by a decrease to baseline). The maximum heart rate was greatest when awakening from SWS and lowest when awakening from REM sleep. For autonomic arousals not associated with an awakening, the behavior was biphasic with an increase in heart rate followed by a deceleration and then a gradual increase back to baseline. The sleep stage the person was in affected the

extent of the arousal; this time it was greatest during REM sleep and lowest during SWS. A greater heart rate elevation was found when an awakening occurred.

Di Nisi, Muzet, Ehrhart, and Libert (1990) also found that noise affects heart rate. They conducted a laboratory test in which subjects were exposed to five different sounds: a jet, truck, motorcycle, train, and a telephone. They conducted two tests, one in which subjects were exposed during the day and another study where subjects were exposed at night. For the daytime experiment, each of the signals were presented six times. They measured ECG, finger-pulse, respiratory movements, and body movements. For the nighttime tests they used all of the sounds except the telephone ringing and they reduced the average noise levels of the sounds by 15 dB(A). Eight sounds per hour were played, the inter-arrival time of the stimuli was random. In addition to the measurements made during the day, they also used polysomnography to evaluate sleep. They found that the heart rate response at night was much greater than that during the day, which was especially significant because the sounds during the night were 15 dB(A) quieter than the sounds heard during the day.

2.8.3 Stress Hormones

The effect of sleep disruption on stress hormones has been investigated in several studies. Understanding the effect of noise on cortisol levels, for example, is important as an elevated level could affect glucose functions, increase protein and bone degeneration, and could affect blood pressure raising hormones (Spreng, 2004). In a normal night cortisol levels will decrease during the first half of the night and will increase in the second half of the night, reaching a peak shortly after awakening. Elevated levels are due to a stress response (Born and Fehm, 2000). Spiegel, Leproult, and Van Cauter (1999) found, after restricting sleep to 4 hours, that morning cortisol levels obtained from saliva samples were elevated. In addition to sleep length, there

is also evidence that the number of arousals during the night may be related to an increase in cortisol levels. Ekstedt, Åkerstedt, and Söderström (2004) separated their data into two groups, results for those that experienced more than 9 arousals per hour and those that experienced less than 9 per hour. For subjects with a higher frequency of arousal a statistically significant increase in heart rate, blood pressure, and cortisol level was found.

Carter, Hunyor, Crawford, Kelly, and Smith (1994) evaluated the sleep of 9 subjects who had a history of cardiac arrhythmia. The subjects spent four nights in the laboratory, two of which included exposure to noise. For one night road traffic noise was presented, while for the other night aircraft noise was played. They measured levels of noradrenaline, adrenaline, and dopamine at the end of the night and found that all levels were in the normal range and were unaffected by noise. MaaB and Basner (2006) found similar results to Carter et al. (1994). For both the laboratory and field studies they assessed the levels of stress hormones cortisol, adrenaline, noradrenaline, and the electrolytes potassium, calcium, sodium, and magnesium. They found that aircraft noise exposure did not have a large affect on any of these levels.

2.8.4 Appetite Regulation Hormones Leptin and Ghrelin

Fragmented sleep may also have an affect on appetite. Spiegel, Tasali, Penev, and Van Cauter (2004) evaluated the level of leptin and ghrelin after sleep restriction. Elevated levels of ghrelin are related to increased appetite while increased levels of leptin are associated with a decrease in appetite. Spiegel et al. (2004) had 6 subjects spend 10 hours in bed, while 6 subjects had their sleep restricted to 4 hours in bed. The following morning blood samples were obtained. They also had subjects evaluate their hunger and appetite using a questionnaire. Spiegel et al. found that after the 4 hour sleep condition there was an increase in appetite especially for sweet or salty

foods. Also, they found that leptin levels were 18% lower and ghrelin levels were 28% higher compared to the results for subjects who spent 10 hours in bed. The results found by Spiegel et al. are supported by results from a much larger study conducted by Taheri, Lin, Austin, Young, and Mignot (2004). This study was part of the Wisconsin Sleep Cohort Study. They found that ghrelin and leptin levels are related to sleep duration. They also found an increase in Body Mass Index (BMI) for reduced sleep duration, although BMI also increased for sleep durations greater than 8 hours and therefore there seems to be a U-shaped relationship between BMI and sleep duration.

2.8.5 Increased Blood Pressure

Haralabidis et al. (2008), as part of the HYENA Study, examined nighttime blood pressure. Subjects around four airports were investigated: Athens, Malpensa, Arlanda and Heathrow Airport. Blood pressure and heart rate were measured every 15 minutes during the night. They found that there was a 0.6 mmHg increase in systolic and diastolic blood pressure for a 5 dB increase in noise level as measured using the $L_{Aeq,15min}$ which is the average A-weighted level during a 15 minute time period. Also, they found that the mean increase in blood pressure when an aircraft noise event occurred was 6.2 mmHg for systolic blood pressure and 7.4 mmHg for diastolic blood pressure. In addition, they found that heart rate increased by 5.4 beats per minute.

This increase in blood pressure is troubling as during normal sleep the blood pressure level should become lower. A person is classified as a "dipper" if blood pressure during the night drops by more than 10%, compared to its daytime level. The "non-dipping" of blood pressure may increase the risk for developing cardiovascular and renal disease (Pickering and Kario, 2001). Loredo, Nelesen, Ancoli-Israel, and Dimsdale (2004) determined that dipping was associated with a greater amount of

slow wave sleep (SWS). In another study conducted by Loredo, Ancoli-Israel, and Dimsdale (2001), the blood pressure of subjects with sleep apnea was measured during the night. Their results indicate that time in SWS and the number of arousals may be related to the variance seen in the diastolic blood pressure.

Guilleminault and Stoohs (1995) evaluated the blood pressure and heart rate for both control subjects as well as those with sleep apnea when aroused by auditory stimuli. The auditory stimuli caused an increase in blood pressure of approximately 20%. Their results also indicated that the greatest change in blood pressure occurred when aroused from SWS.

2.8.6 Glucose Tolerance and Diabetes

Disturbed sleep may also increase the risk for developing type 2 diabetes. Spiegel, Tasali, Penev, and Van Cauter (2004) had subjects sleep 4 hours for 6 nights and 12 hours for 7 nights. They found that glucose effectiveness was 30% lower when subjects were sleep deprived. They also found that there was a decrease in insulin response. They stated that the cause of the decrease in insulin response could be due to an elevation in sympathetic and a decrease in parasympathetic activity during the sleep deprivation nights, which might affect pancreatic function.

Tasali, Leproult, Ehrmann, and Van Cauter (2008) found similar results in a more recent study. They suppressed SWS in subjects for three nights using acoustic stimuli of different frequencies and intensities. They did not want to cause awakenings but just a sleep stage change so that total sleep time and amount of REM sleep would remain the same while the amount of Stage 2 sleep would increase. They assessed glucose tolerance after the three nights. It was found that glucose tolerance was decreased by 23% and insulin sensitivity was decreased by 25%. Glucose tolerance is a measure of the decrease in glucose levels, it is measured in terms of the percent

decrease per minute. They also performed spectral analysis of ECG recordings and evaluated the amount of high and low frequencies, which is a measure of sympathetic activity. They found that sympathetic activity had increased.

The study by Tasali et al. (2008) was conducted in a laboratory, with an unnatural suppression of slow wave sleep. However, similar findings have been found in large epidemiological studies. Gottlieb, Punjabi, Bewman, Resnick, Redline, Baldwin, and Nieto (2005) used data from two cohort studies, which were a part of the Sleep Heart Health Study, to evaluate glucose tolerance. A significant odds ratio for impaired glucose tolerance and the development of diabetes was found for those sleeping less than 6 hours or greater than 9 hours.

2.8.7 Myocardial Infarction and Stroke

One of the overall longterm effects of noise on health is that it may lead to cardiovascular disease and Myocardial Infarction. A possible pathway which has been discussed is the repeated elevation in the sympathetic nervous system which may cause elevated heart rate and blood pressure.

Huss, Spoerri, Egger, and Röösli (2010) conducted a study to examine whether aircraft noise and air pollution due to flight operations caused an increase in risk of death from myocardial infarction in Switzerland. They used data from the Swiss National Cohort which contains national census data and national mortality data. They found that increased aircraft noise was associated with a higher risk of dying from myocardial infarction and that the risk increased with the duration that an individual had lived in the area. They found no relationship with increased risk and air pollution which was a measure of particulate matter.

Sørensen, Hvidberg, Andersen, Nordsborg, Lillelund, Jakobsen, Tjønneland, Overvad, and Raaschou-Nielsen (2011) examined the risk of stroke and exposure to trans-

portation noise. The data used was from a diet, cancer and health study that was conducted between 1993 to 1997. Subjects were between 50 and 64 years in age and lived in the Copenhagen or Aarhus area. A questionnaire was completed as well as subject's height, weight, and blood pressure were measured. Sørensen et al. (2011) were able to link the data from the cohort study to the Danish National Hospital Registry and were able to identify those individuals who were in the hospital and who had suffered a stroke. The road noise levels L_{Aeq} for the day, evening, night and L_{den} were predicted. They also predicted train and aircraft noise, and air pollution. They found that a 10 dB increase in road traffic noise was associated with a 14% increased risk of stroke. The increased risk was greater for older subjects. These results are applicable for L_{den} (which is average A-weighted sound pressure level with different weightings for noise during the day, evening, and night) levels greater than 60 dB(A). Air pollution and train and aircraft noise exposure did not result in an increased risk of stroke.

2.8.8 Mental Health

Stansfeld and Matheson (2003) stated that aircraft noise causes annoyance and that annoyance may lead to long term mental health issues. Several early studies were conducted to investigate the effect of aircraft noise on admissions to mental hospitals. Meecham and Smith (1977) examined the mental hospital admissions in a census tract near Los Angeles International airport and a control census tract further away. The two areas had similar socioeconomic conditions. They found a 29% increase in admissions in the area closer to the airport. However the total number of admissions in both areas was low.

More recently, the pathway from annoyance to mental health has been examined using survey questionnaires. Schrenkenberg, Meis, Kahl, Peschel, and Eikmann

(2010) examined the self reported quality of life of those living around Frankfurt airport. They found no relationship between ratings of mental health and noise level. However, there was a relationship between ratings of aircraft annoyance and mental health as well as between noise sensitivity and mental health.

Noise may also effect the mental health of children. Stansfeld, Clark, Cameron, Alfred, Head, Haines, van Kamp, van Kempen, and Lopez-Barrio (2009) examined the effect of noise on children's health and cognition as part of the RANCH study. They used a questionnaire, The Strengths and Difficulties Questionnaire, to evaluate mental health. The questionnaire had four scales relating to emotional symptoms, conduct problems, hyperactivity, and peer relations problems. They found no relationship between the overall score of mental health and noise. However, they did find that aircraft noise was associated with a higher rating of hyperactivity. Contradictory evidence though was found for road noise where a lower amount of conduct disorders was associated with higher noise levels. While there are no conclusive findings from this study, the authors did state that due to the transitory nature of aircraft noise it would be expected that it would have a stronger affect on attention than road traffic noise.

2.9 Effects of Noise on Children

For most of the studies mentioned the subjects have been adults. However, as found in the RANCH study, noise also effects children. Öhrström, Hadzibajramovic, Holmes, and Svensson (2006) conducted a study to examine the effect of road traffic noise on sleep in adults and children. They conducted a main study involving a questionnaire as well as a more detailed study in which subjects filled out sleep logs and wore actimeters for 4 days. They found that children had better sleep quality and less awakenings then adults when analyzing the subjective responses. However, they found

that children had worse sleep as determined by actimeter data. They stated that children may naturally have higher motility which could have caused the difference between the objective and subjective measurements of sleep. For children whose sleep was disturbed by noise, a large percentage indicated a problem with daytime sleepiness. Lukas (1972) conducted a study in order to evaluate sleep disturbance caused by sonic booms and jet aircraft noise. Subjects indicated awakenings by using a switch. Their sleep was also evaluated using polysomnography. It was found that the age of the subjects greatly affected the degree of disturbance. Children in the study were found to be relatively insensitive to the noise. A survey conducted around Heathrow and Gatwick airport (DORA, 1980) contained questions in which parents were asked to state whether aircraft noise disturbed the sleep of their children. It was found that children seemed to be far less disturbed by noise at night, it was reported that 89% of children were not awakened by the noise. From the results of these three studies it was concluded that children are less likely to be awakened by noise then adults.

However, just because children are less likely to be awakened, it does not mean that noise does not cause negative effects. Ising and Ising (2002) conducted a study with children between the ages of 7 to 10 years. The children were exposed to heavy truck noise approximately every 2 minutes during the night. The effect of noise on sleep was evaluated by measuring cortisol levels. Two urine samples were collected from each subject. One sample was taken in the morning, while the other was obtained during the night. They found that noise seemed to cause an increase in cortisol levels in the first half of the night. They also found that memory and concentration problems were higher in the quarter of the group with the highest cortisol level. This study provides some evidence that noise at night is affecting children despite the low number of awakenings found in other studies. Also Sadeh, Gruber, and Raviv (2002)

conducted a study involving children in second, fourth, and sixth grades. The children were classified as either good or bad sleepers; a bad sleeper was defined as someone that had at least three awakenings lasting more than 5 minutes and at least 10% of the night was spent awake. They found significant differences in the performance of children on tests as well as significant differences in behavior. Therefore, there is still a need for studies in the future to further examine the effect of noise on children's sleep and next day performance.

2.10 Conclusions

Aircraft noise can cause an increase in awakenings and a decrease in slow wave and REM sleep. These changes in sleep could lead to short term effects such as an increase in sleepiness and a decrease in performance. Fragmented sleep due to noise could also lead to long term effects such as hypertension, diabetes, and a change in appetite which could contribute to obesity. However, there have been no studies that have investigated directly the long term effects of noise-induced sleep disturbance. It still needs to be determined whether the disturbance that occurs due to nighttime noise is significant enough to lead to these adverse health effects.

3. NOISE INDUCED SLEEP DISTURBANCE MODELS

Several models have been developed which predict noise induced sleep disturbance. Most only predict the percent awakened to a single noise event. However, an ANSI standard has been developed to predict the percent of the population that is awakened at least once due to multiple events. A description of these models will be provided. In order to evaluate these sleep models data was obtained from four sleep disturbance surveys. A description of the data that was obtained and comparisons between model predictions and behavioral awakening survey data is described.

3.1 Obtained Survey Data

As discussed in Chapter 2, there have been several studies conducted which have provided information on the relationship between noise and sleep disturbance. It was desired to obtain several of these datasets in order to develop new sleep disturbance models because conducting a new sleep study would be expensive and require a significant amount of time, and it is not guaranteed whether any new information would be gained. Data from four sleep studies were obtained. A description of the obtained data is provided and limitations of the datasets are discussed.

3.1.1 US Sleep Disturbance Survey Data

Data from the three most recent sleep studies conducted in the US were obtained. The studies were conducted around Los-Angeles International Airport and Castle Air-Force Base (Fidell, Pearsons, Tabachnick, Howe, Silvati, and Barber, 1995), DeKalb-

Peachtree Airport, and Stapleton International and Denver International Airport (Fidell, Pearsons, Tabachnick, and Howe, 2000). For the study conducted around Los-Angeles International Airport and Castle-Air-Force Base, 1887 nights of data were collected. Sleep was assessed by having subjects use push buttons; subjects pressed a button when they were awakened. To quantify the noise, they measured one half second L_{Aeq} levels (A-weighted equivalent noise level, the average noise level for the defined time period). The recording of events was triggered based on a threshold. To account for variation in the level of background noise from site to site, this threshold was set specific to each site. However, to be classified as a noise event the threshold only had to be exceeded for 2 seconds so other loud sounds may also have been classified as aircraft noise events. The main result of this study was that the A-weighted Sound Exposure Level ($SELA$) correlated best to the number of awakenings, although the relationship was weak. They also found that the probability of awakening increased with the time since retiring.

The purpose of the other two US studies, conducted by Fidell et al. (2000), was to evaluate sleep disturbance when a change in airport operations occurred. One study was conducted around Stapleton International Airport before and after it closed, and around Denver International Airport before and after it opened. Fidell et al. (2000) also completed a study around DeKalb-Peachtree airport before, during, and after the 1996 Atlanta Olympics. The primary method used for evaluating sleep disturbance was again the use of push buttons, although actimeters were also used. Both indoor and outdoor L_{Aeq} levels were obtained. The result for all testing sites was that there was a very low probability of awakening due to an aircraft event. For the DeKalb-Peachtree study they also found no change in the number of awakenings for the three different testing periods. However, behavioral awakenings are extremely insensitive

measures of sleep disturbance and therefore the method used to measure awakenings may be the reason for the negative findings.

The data that was obtained for these 3 studies include information on the gender and age of the subjects. In terms of sleep data, the number of spontaneous awakenings and button presses which corresponded to noise events are included in the dataset. The timing of the noise-induced awakenings are indicated but not the timing of spontaneous awakenings. Data for subjective evaluations of sleep was also obtained including evaluations of tiredness, recalled sleep latency, and recalled time awake.

The information on noise events in the dataset include indoor noise levels, *SELA* and L_{Amax}, for each aircraft event. The timing of the events is also known. A difficulty with the dataset is that very few of the subjects experienced the same noise scenario, as well as subjects were not all tested for the same number of nights. A summary of the number of locations and subjects for each of the three studies is listed in Table 3.1. The maximum number of noise events at a location is also listed.

Table 3.1. Number of locations and subjects that took part in the 3 US sleep studies.

Survey	Number of Locations	Number of People	Maximum Number of Noise Events
(1995) LAX and Castle Air Force Base	43	72	435
(1994/1995) DEN and DIA airport	65	113	153
(1996) PDK airport	12	22	136

The number of events and awakenings for each indoor $SELA$ level for the three studies conducted by Fidell et al. (1995, 2000) are summarized in Table 3.2.

Table 3.2. Number of events and awakenings for each noise level for the 3 US field studies.

$SELA$	Number of Events	Number of Awakenings
52	2222	20
55	4399	36
58	3378	28
61	2716	48
64	4374	67
67	3703	71
70	4302	83
73	4984	109
76	4354	85
79	4274	95
82	4299	81
85	3096	76
88	1809	44
91	1230	34
94	680	35
97	396	15
100	166	3
103	40	1

3.1.2 1999 UK Sleep Study Data

Data from a study in which sleep was measured using polysomnography was also obtained. This study was conducted in the UK in 1999 and involved both a laboratory study conducted in Farnborough and a field study conducted around Manchester airport (Flindell, Bullmore, Robertson, Wright, Turner, Birch, Jiggins, Berry, Davison, and Dix, 2000). It was funded by the UK Department for Transport and the data is owned by the Civil Aviation Authority. Both laboratory and field were considered trial studies. The three main objectives were to examine noise during the shoulder hours to see if they led to premature awakenings or delayed sleep onset, to compare sleep patterns of individuals living in high and low noise exposed areas, and to study sleep disturbance in a group of people that considered themselves sensitive to noise.

The field test was conducted around Manchester airport. Eighteen participants took part in the study, 9 were from a low noise area and 9 were from a high noise area. Only data from 12 subjects was suitable though to use for analysis. All subjects were in the age range of 30-40 years. Also, all subjects were considered to have high noise sensitivity as evaluated by the Weinstein scale. The high noise area was located 500 to 2500 meters from the airport, while the low noise area was located 4000 to 7000 meters from the airport. One problem with the study was that while the high and low areas had different outdoor noise levels, there was little variation in the indoor noise levels.

For the field study subjects participated for 5 consecutive nights. Sleep was recorded using polysomnography. Recordings of 4 channels of EEG, 2 channels of EOG, ECG, EMG and respiratory measurements were obtained. Sleep stages for each subject were scored. The noise levels that were collected were A-weighted sound pressure level noise time histories, measured both indoors and outdoors and a voltage signal that was synchronized with the physiological measurements. The voltage signal was not a sound recording, it only had a 10 Hz sampling rate. Information from the airport on the timing of arrivals and departures and type of aircraft were obtained. Also, for four sites, 10 second recordings (stored in .wav files) of the events and one third octave band data through time were also collected.

Nine people living near Farnborough took part in the laboratory test. The subjects were tested one night per week over a period of five weeks. In addition to an adaptation night, one night was a baseline night and consisted of no noise. There was three noise exposure nights; one noise condition was supposed to be representative of a night around Manchester airport, for one night the noise exposure was similar to that at Manchester airport but with more noise events added during the beginning of the night, and for one night the noise exposure was like that at Manchester airport

but with more events at the end of the night. Five aircraft recordings were used in the study. As in the field study, sleep was recorded using polysomnography and a voltage measurement of the noise was also recorded.

For both laboratory and field studies, tests to evaluate sleepiness and performance decrements were also performed; no significant differences in results between nights of noise exposure and baseline nights were found. In general, there was not a large difference between results in the laboratory study and those in the field study. A similar number of awakenings, sleep stage changes, and slow wave sleep was found for the Manchester typical noise night in the laboratory and in the field study. Those who participated in the laboratory study, though, did have less REM and more stage 2 sleep during the noise exposure nights.

3.1.3 1999 UK Sleep Study Data Used for Analysis

For several of the subject nights data was either missing or a recording was not acceptable for use because an electrode most likely became loose during the night. Only subject nights which had a C4-A1 and C3-A2 EEG recording, EOG left and right recordings, EMG recording and scored sleep stages were used for analysis. A list of subjects, and the subject nights used in the analysis throughout this report are listed in Table 3.3. Subjects 1 through 18 were in the field study and Subjects 19 through 27 were in the laboratory study. A total of 76 subject nights were used for the sleep stage classification algorithm development and for estimating the parameters of the nonlinear dynamic models. However, when evaluating the changes in sleep due to noise events data from subjects 1 through 7 were not used. The reason for this elimination is that for these subjects a voltage recording of the noise event that is time locked with the polysomnography data was not made. The timing of the noise events were only obtained from the separate sound level meter measurements. However,

from reviewing the data there seems to be a drift in time that occurred over the 5 days of testing in the sound level meter data. Therefore to insure that the time of events coincides with the activity in the physiological data these subjects was not used in the noise analysis. Also the data for subjects 26 and 27 for night 2 were not used in the noise analysis as the timing of noise events did not match the noise scenario that was supposed to be played that evening.

3.2 Sleep Disturbance Models

Several models have been developed to predict the effect of aircraft noise on sleep. Many of these models predict the percent awakened due to a single noise event. A standard has also been developed which predicts the effect of an entire nighttime scenario of events on a population. Models have also been developed based on responses to social survey questionnaires. A review of these existing models is provided.

3.2.1 Single Event Awakening Models

Most of the models that have been developed are simple dose response relationships between the indoor noise level of an event and the percent awakened. In these models it is assumed that the response to each event during the night is independent of its previous responses. The noise level is measured by using either L_{Amax} or *SELA*. L_{Amax} is the maximum A-weighted noise level of the event, *SELA* takes into account the energy of the event within 10 dB of the peak of the noise event. Both metrics are highly correlated to one another.

Finegold, Harris, and von Gierke (1994) analyzed data from several studies in order to create an awakening model. They grouped the number of awakenings by counting the number in each 5 dB interval. For their regression, each noise interval

Table 3.3. UK Data used in analysis. (Dark gray indicates that data was used in all analysis, light gray indicates data was not used in noise analysis. Y-data available, N-data not available).

	Subject	Adaptation Night	Night 1	Night 2	Night 3	Night 4
Field	1	N	N	Y	N	Y
	2	N	Y	N	Y	Y
	3	N	N	N	Y	Y
	4	N	N	N	N	N
	5	N	N	N	N	N
	6	N	Y	Y	Y	N
	7	N	N	N	N	N
	8	N	N	N	N	Y
	9	N	Y	N	Y	Y
	10	Y	Y	N	Y	N
	11	N	N	N	N	N
	12	Y	Y	Y	Y	Y
	13	N	Y	Y	Y	Y
	14	Y	Y	N	Y	Y
	15	Y	Y	Y	Y	Y
	16	N	N	Y	Y	Y
	17	N	N	Y	N	Y
	18	Y	Y	N	Y	N
Laboratory	19	Y	Y	Y	N	N
	20	N	Y	Y	Y	N
	21	N	N	N	N	N
	22	Y	Y	Y	Y	Y
	23	Y	Y	Y	Y	Y
	24	N	Y	Y	Y	Y
	25	Y	Y	N	Y	Y
	26	Y	Y	Y	Y	Y
	27	Y	Y	Y	Y	N

had equal weight even though there was a different number of data points in each interval. Another weakness in this model is that the data sets were from studies that used different noise sources and were conducted in different testing environments, both laboratory and field. Two further analyses were done to create an updated dose response relationship. Finegold and Elias (2002) used data from more recent surveys, however, as in the development of the previous model, data from different noise sources were combined. The equation for the model developed by Finegold et al. (1994) is,

$$\%Awake = (7.1e^{-6})SELA^{3.5}, \tag{3.1}$$

and the model by Finegold and Elias (2002) is,

$$\%Awake = 0.58 + (4.3e^{-8})SELA^{4.11}. \tag{3.2}$$

FICAN (1997), the Federal Inter-Agency Committee on Aircraft Noise, developed a curve based on 6 datasets examined by Pearsons et al. (1995) as well as the data from the Ollerhead et al. (1992) study and from the Denver and Los Angeles sleep studies by Fidell et al. (1995, 2000). In contrast to Finegold et al.'s models, the dose response relationship that was developed predicts the *upper limit* of the percent awakened found in the data. The equation for the FICAN model is,

$$\%Awake = 0.0087(SELA - 30)^{1.79}. \tag{3.3}$$

Several other models that predict the probability of awakening because of a noise event have been developed including: Anderson and Miller's (2005) model

$$z = -10.7383 + 0.0874SELA; \quad \%Awake = \frac{100}{1 + e^{-z}}, \tag{3.4}$$

the dose response relationship used in the ANSI (2008) Standard,

$$z = -6.8884 + 0.04444SELA; \quad \%Awake = \frac{100}{1 + e^{-z}}, \tag{3.5}$$

Basner et al.'s model (2006),

$$\%Awake = (1.894e^{-3})L_{Amax}^2 + (4.008e^{-2})L_{Amax} - 3.3243, \tag{3.6}$$

Passchier-Vermeer et al.'s model (2002),

$$\%Awake = 0.51 + 0.000353SELA^2, \tag{3.7}$$

and Ollerhead et al.'s model (1992),

$$\%Awake = 0.4(-2.96 + 0.162SELA). \tag{3.8}$$

The predictions of the different awakening models are shown in Figure 3.1. The FICAN and Basner et al. models predict the highest percent awakened. The FICAN model was meant to be an upper bound of the survey data from which it was derived. The model developed by Basner et al. is based on awakenings from a study conducted around Cologne-Bonn airport where they measured awakenings by using polysomnography which is a more sensitive measure of awakenings. Most of the other models were developed based on behavioral awakenings data which are a less sensitive measure of sleep and occur less often during the night.

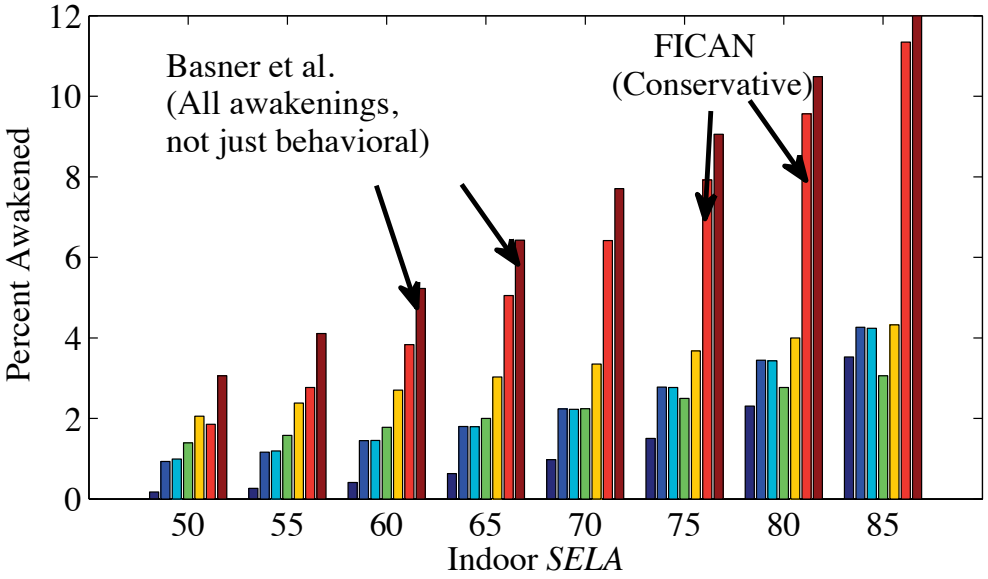

Figure 3.1. Output of various awakening models for each 5 dB grouping of *SELA* values. From left to right; 1) Anderson and Miller (2005), 2) ANSI dose response curve (2008), 3) Finegold and Elias (2002), 4) Passchier-Vermeer et al. (2002), 5) Ollerhead et al. (1992), 6) FICAN (1997), and 7) Basner et al. (2006) model predictions.

3.2.2 Models Based on Reported Sleep Disturbance

The models that were described were based on measures of awakenings from polysomnography, button pressing to measure behavioral awakenings, or from actigraphy measurements. However, dose response models have also been developed based on subjective reports of sleep disturbance. In addition to the sleep studies that have been conducted, many large social surveys on the effects of aircraft noise on communities have been conducted. General questions on sleep disturbance that are often asked include whether an individual's sleep was disturbed and how often, or whether they were annoyed because their sleep was disturbed. Miedema, Passchier-Vermeer, and Vos (2002) developed dose-response curves based on data from these social surveys. The models relate L_{night} to the percent of the population that are a little sleep dis-

turbed (LSD), sleep disturbed (SD), or highly sleep disturbed (HSD). They developed curves for aircraft, road, and train noise. For aircraft noise, the models are based on seven different community surveys. The three equations are:

$$\%HSD = 18.147 - 0.956L_{night} + 0.01482L^2_{night}, \tag{3.9}$$

$$\%SD = 13.714 - 0.807L_{night} + 0.01555L^2_{night}, \tag{3.10}$$

$$\%LSD = 4.465 - 0.411L_{night} + 0.01395L^2_{night}. \tag{3.11}$$

One of the problems with these dose-response models are that they are based on responses to different types of questions. For example, for most of the aircraft noise studies, the questions on sleep were related to how annoyed an individual was if they were awakened by aircraft noise. However, they combined data on annoyance caused by sleep disturbance with data from another study in which the question was how often an individual was awakened by noise. These questions are asking two different things and thus it is questionable whether the responses can be combined. Also, annoyance should not be considered synonymous with sleep disturbance. Therefore, these dose-response relationships do not predict the percent of the population that is sleep disturbed but rather they are an indication of how sleep disturbance may relate to annoyance.

3.2.3 Multiple Events Awakening Model

In 2008, an ANSI (American National Standards Institute) standard for predicting the probability of awakening at least once due to multiple events was published. The use of this standard has been recommended by FICAN. It is based on behavioral

awakening data. In the model, the probability of awakening due to a single event is dependent on the noise level, as measured by indoor *SELA*. There is also a model which accounts for the time the noise event occurred. The equation for the time dependent model is:

$$z = -7.594 + 0.04444SELA + 0.00336T_{retire}; \quad \%Awake = \frac{100}{1 + e^{-z}}, \tag{3.12}$$

where T_{retire} is the time (in minutes) an event occurred relative to the time an individual went to bed. The process for calculating the probability of awakening at least once for an entire night using the ANSI model is shown in Figure 3.2. It is determined by multiplying the probabilities of not awakening to each individual event,

$$\%Not\ Awake = (1 - P1)(1 - P2)... \tag{3.13}$$

and subtracting this result from 1,

$$\%Awakened\ at\ Least\ Once = 1 - (1 - P1)(1 - P2)... \tag{3.14}$$

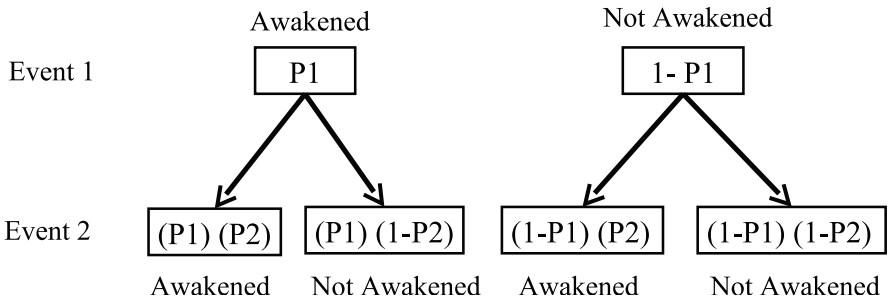

Figure 3.2. Example of the ANSI standard method of calculating percent awakened at least once for a full night of aircraft events.

The ANSI standard is based on the work of Anderson and Miller (2007). One component of their model that was not included in the standard is the sensitivity to awakening. Anderson and Miller evaluated the data from Fidell et al.'s surveys (1995, 2000) and found a large inter-individual difference in the number of noise induced awakenings. They modeled this variation as a Gaussian distribution and added a coefficient to their model to account for this.

3.2.4 Spontaneous vs Noise-Induced Awakenings

When comparing model predictions to survey data one of the challenges is defining what an awakening is. To determine how many noise-induced awakenings occur, a time window about each noise event has to be defined. Within the time window, sleep disturbance is attributed to the noise. The length of the time window varies depending on the study and the technique used to evaluate sleep. For example, Basner et al. (2004) defined a noise-induced awakening when it occurred within 90 seconds of a noise event in the field study and within 60 seconds in the laboratory study. Ollerhead et al. (1992) defined a time window as beginning 16 seconds before the start of a noise event and having a width of 64 seconds. Fidell et al. (1995), who used behavioral (signaled) awakenings, found the strongest relationship between noise and awakenings when using a time window of 5 minutes.

Also, there is a challenge in separating noise-induced awakenings from spontaneous awakenings, which are awakenings that occur naturally during a non-noise disturbed night. Brink and Basner (2009) have discussed two ways to define the probability of awakening to just the noise events. The first is what they call $P_{\text{additional}}$ which is equal to the probability of awakening due to noise events minus the probability of a spontaneous awakening occurring. However, they recognize that a noise awakening and a spontaneous awakening may not be mutually exclusive. A person may be in the

process of awakening spontaneously and then an aircraft event occurs and they are awakened by the noise. Therefore, they also defined P_{induced}, which is the probability of awakening due to a noise event which is not confounded with the probability that a spontaneous awakening was jointly occurring. The practice that is most commonly used is to calculate $P_{\text{additional}}$.

3.2.5 Noise Protective Measures

Different noise metrics have also been proposed for predicting and preventing sleep disturbance in communities. In the US only DNL is used for predicting noise impact. However, in Europe, the noise metric, L_{night} is used in order to protect communities from adverse effects of nighttime noise. L_{night} is the average nighttime noise level for 11:00 pm to 7:00 am. It is stated in the World Health Organization's Night Noise Guidelines for Europe (2009) that noise leads to additional awakenings and movements above an $L_{night,outside}$ of 30 dB. For an $L_{night,outside}$ between 40 to 55 dB most of the population will be affected by the noise and for an $L_{night,outside}$ above 55 dB adverse health effects may occur. WHO has issued a recommendation that outside noise levels be below 40 dB at night to prevent adverse health effects. However, as such a limit would be difficult to obtain a target goal of 55 dB has been proposed.

A protection criteria based on the number of awakenings has been developed by Basner, Samel, and Isermann (2006). They defined three goals to achieve by creating this criteria: 1) Limit effects to less (on average) than 1 additional noise induced awakening, 2) Prevent awakenings that will be remembered the next day, 3) Prevent increases in latency of falling asleep again during the night. To obtain these goals they defined a contour which is based on a region in which 1 or more additional awakenings occur and 1 or more events have a L_{Amax} greater than or equal to 80 dB(A). The dose-response curve developed by Basner, Samel, and Isermann (2006)

was used to create these contours. This method was implemented around Leipzig-Halle airport. Another protection criteria, the Frankfurt Night Index (FNI), is also based on the dose-response relationship developed by Basner et al. (2006). An area that needs to be protected is defined as one in which 0.5 or more additional noise induced awakenings occur on average (Schreckenberg, Thomann, and Basner, 2009).

3.3 Model Comparisons

To evaluate how well awakening models predict the percent awakened found in survey data comparisons were made between the US behavioral awakening survey data and six dose-response awakening models. The performance of the ANSI standard method was also examined. Comparisons were made between the ANSI model and *DNL* for different numbers of nighttime aircraft noise events.

3.3.1 Awakening Model Comparison

To examine how well the dose-response models predict the percent awakened in survey data, comparisons were made with the results from Fidell et al.'s surveys. As part of this analysis a Monte Carlo simulation was performed in order to determine whether enough data was collected in these surveys to validate the awakening models. For each $SELA$, a vector of uniformly distributed random numbers in the range from 0 to 1 was created. The length of the vector was equal to the number of events that were experienced in the survey data for that particular $SELA$ level. Then using one of the awakening models, the number of values in the vector below the specific probability of awakening was calculated. This value is equal to the number of people awake. The percent awakened was then calculated and this procedure was repeated 10,000 times in order to evaluate the variation in predictions for different sampling. The results

of the simulation were then compared to the actual percent awakened in the survey data. The comparisons are shown in Figure 3.3. The error bars for the simulations indicate that 95% of all outcomes of the Monte Carlo simulation were within that range, while for the survey data the error bars are the 95% confidence intervals. From the results of performing this analysis, shown in Figure 3.3, it is evident that there was not a lot of data collected in the survey at the higher noise levels. Lack of data at high noise levels was the reason why, for this analysis, the data from all three of the studies conducted by Fidell et al. were combined. Also, the predictions of the Passchier-Vermeer et al. model most closely matched the awakenings in the survey data. Although most of the models predicted the percent awakened at low noise levels reasonably well.

3.3.2 Multiple Events Model Evaluation

The process described in the ANSI standard was used to compare the change in awakenings and the corresponding change in *DNL* when the number of nighttime events are increased. For simplicity it was assumed that 1 aircraft event occurred every 2 minutes during the day and that initially there were no nighttime events. The number of daytime operations was 450 which is similar to the number of operations at a medium sized airport such as Indianapolis International Airport. It was assumed all the aircraft events were of the same noise level for simplicity. The noise level of the events was an indoor *SELA* level of 57 dB(A). This level results in an initial *DNL* of 60 dB(A) for this number of events. Nighttime events were then added. The new *DNL* level and the percent awakened at least once, using the method of the ANSI standard and the different awakening models (without time dependence), was calculated for each additional nighttime event. The results of this simulation are shown in Figure 3.4. When 110 nighttime events were added the *DNL* level

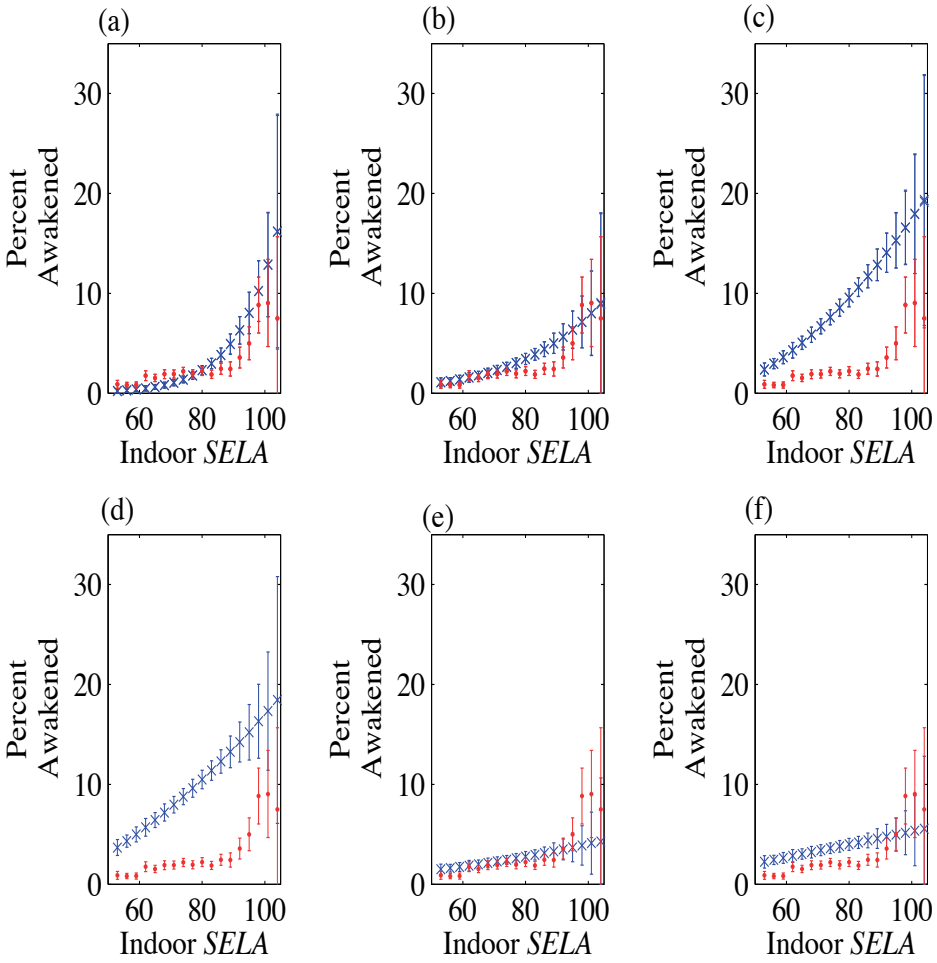

Figure 3.3. The percent awakened in Fidell et al.'s surveys (red-circles) and model predictions (blue-x). (a) Anderson and Miller (2005), (b) Finegold and Elias (2002), (c) FICAN (1997), (d) Basner et al. (2006), (e) Passchier-Vermeer et al. (2002), and (f) Ollerhead et al. (1992) model predictions.

increased by about 5 dB while the percent awakened at least once varied from 30% to approximately 98% depending on the awakening model that is used. The average number of awakenings per individual as predicted by the different awakening models are in Table 3.4. The awakening model by Basner et al. (2006) predicts on average two noise-induced awakenings per person when there are 50 nighttime events.

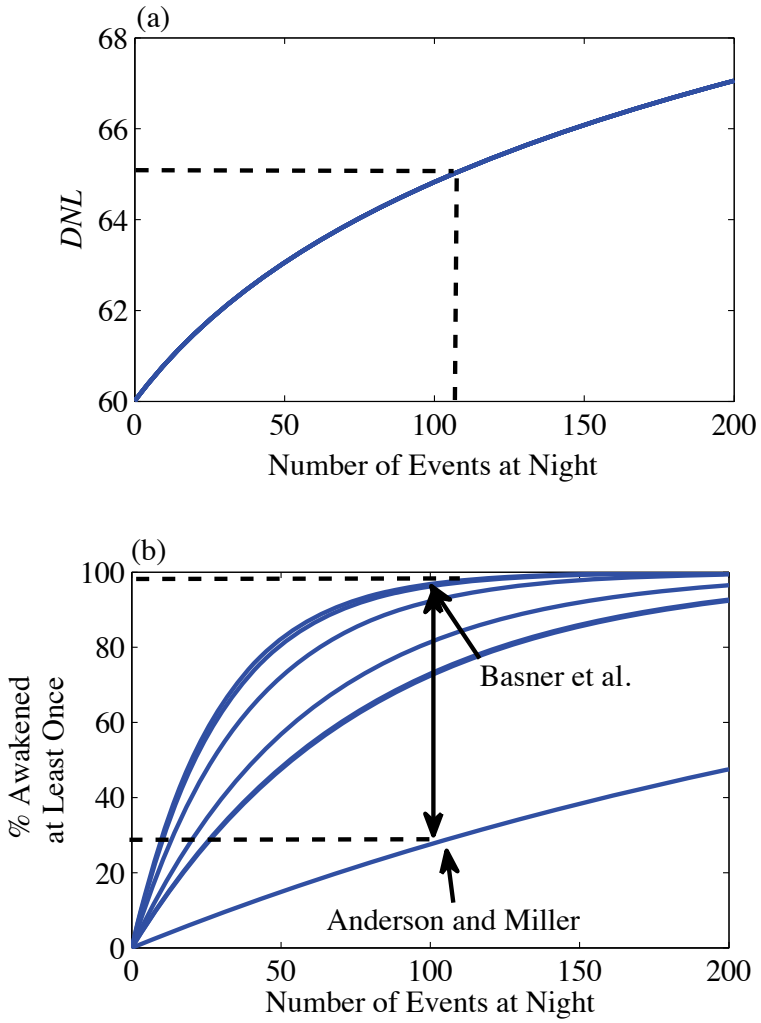

Figure 3.4. The effect of increasing the number of nighttime noise events on DNL and percent awakened at least once. (a) Increase in DNL and (b) increase in percent awakened at least once predicted using different awakening models. Indoor $SELA$=57 dB(A).

Table 3.4. Average number of awakenings per person. Highlighted in dark gray are situations where on average approximately 0.5 awakenings occur, light gray highlights where on average approximately one awakening occurs. Events were all indoor *SELA*=57 dB(A).

Awakening Models/Number of Events	10	20	30	40	50
Anderson and Miller (2005)	0.03	0.06	0.10	0.13	0.16
ANSI Standard (2008)	0.12	0.26	0.38	0.50	0.65
Finegold and Elias (2002)	0.13	0.25	0.39	0.53	0.65
Passcher-Vermeer et al. (2002)	0.17	0.33	0.51	0.66	0.83
Ollerhead et al. (1992)	0.25	0.49	0.74	1.01	1.25
FICAN (1997)	0.32	0.64	0.95	1.27	1.60
Basner et al. (2006)	0.45	0.89	1.38	1.82	2.26

The results of this analysis demonstrate that a model other then DNL is needed to predict the impact of noise on sleep. However, the method described in the ANSI standard is not without limitations. Several airports have a large number of freight aircraft operations at night and can have well over a hundred flights. Data that was obtained for two US airports, for example, showed that there were 150 and 280 nighttime flights at these airports. In order to assess the predicted percent awakened at least once for different noise levels and numbers of nighttime flights, the ANSI method with the different dose-response relationships were used. The results are shown in Figure 3.5. When there are greater than 100 nighttime events, the models all predict that the entire population (100%) will be awakened at least once and that there is no longer any noise level dependence. However, when the average number of awakenings is predicted, there still is a noise level dependence. The results for the average number of awakenings is shown in Figure 3.6.

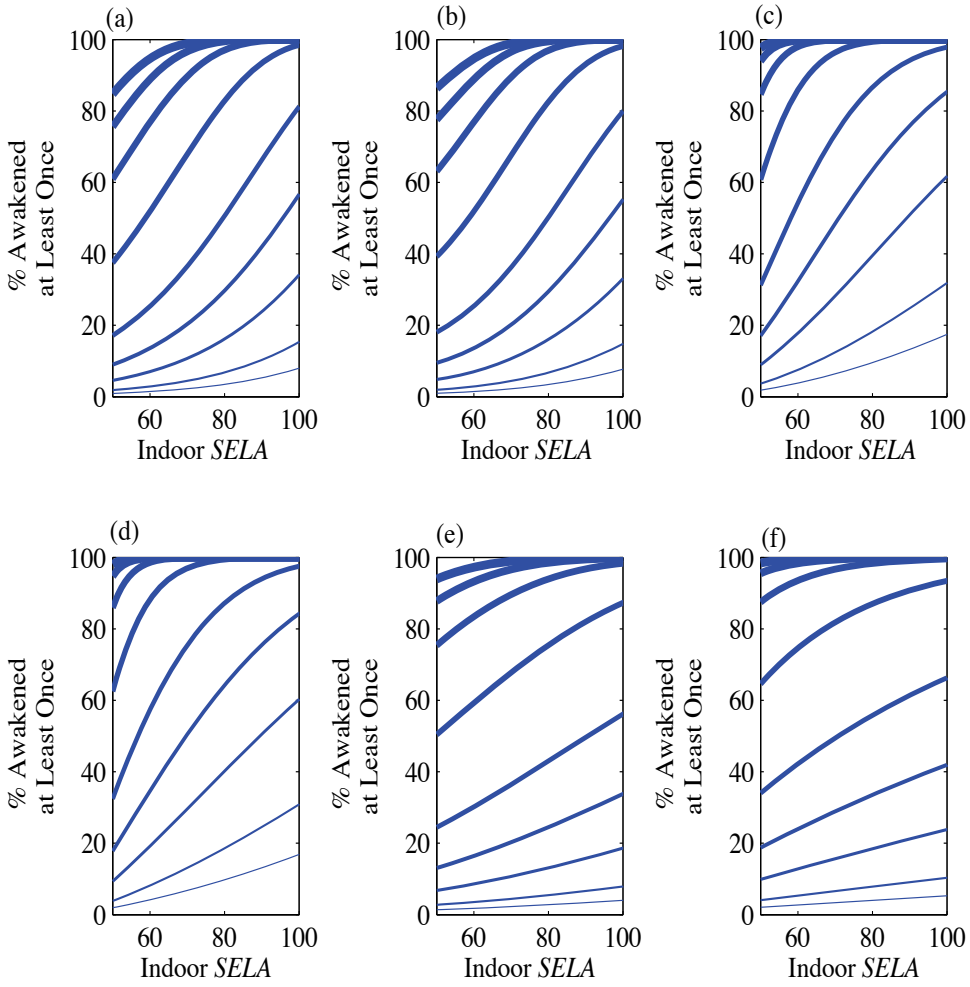

Figure 3.5. The percent awakened at least once for different numbers of events from 1 (thin line) to 200 (thick line). Each line represents 1, 2, 5, 10, 20, 50, 100, 150, or 200 nighttime events. (a) ANSI standard Model (2008), (b) Finegold and Elias (2002), (c) FICAN (1997), (d) Basner et al. (2006), (e) Passchier-Vermeer et al. (2002), and (f) Ollerhead et al. (1992) model predictions.

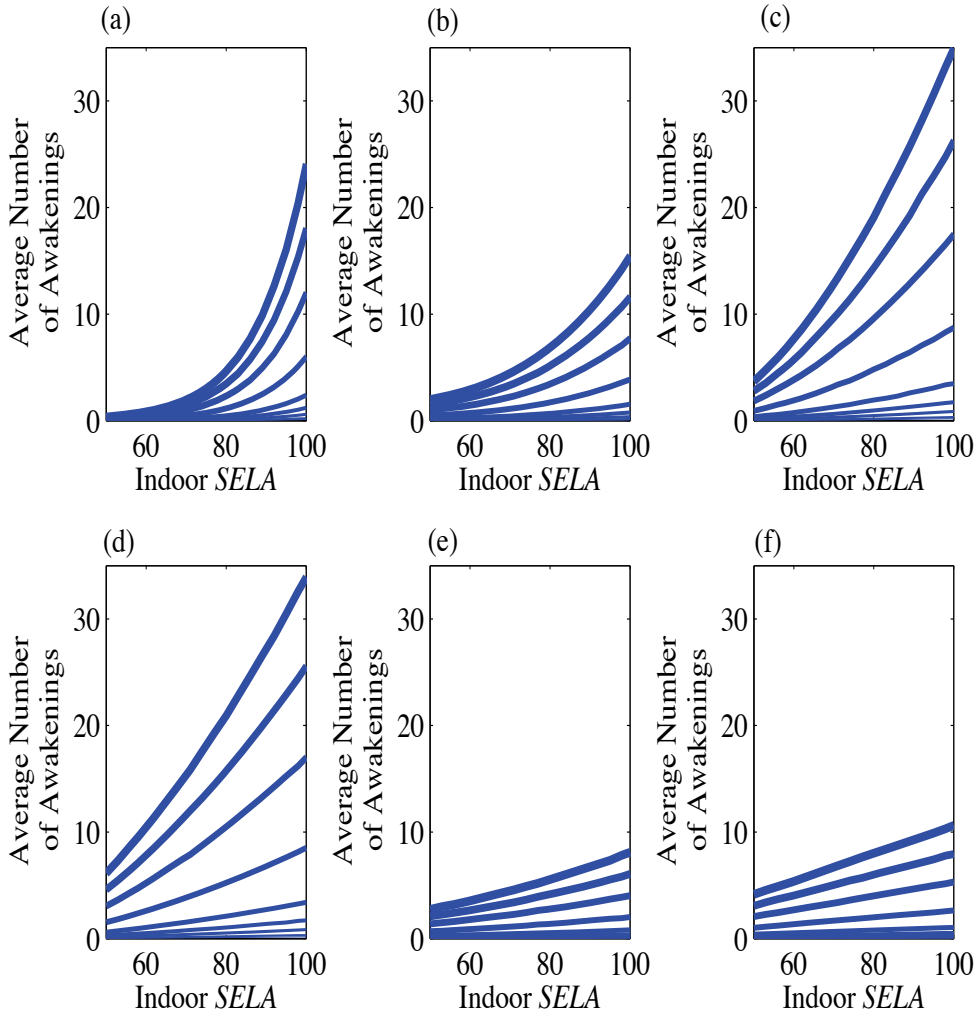

Figure 3.6. The average number of awakenings for different numbers of events from 1 (thin line) to 200 (thick line). Each line represents 1, 2, 5, 10, 20, 50, 100, 150, or 200 nighttime events. (a) ANSI standard Model (2008), (b) Finegold and Elias (2002), (c) FICAN (1997), (d) Basner et al. (2006), (e) Passchier-Vermeer et al. (2002), and (f) Ollerhead et al. (1992) model predictions.

3.4 Conclusions

Several models have been developed in order to predict the percent of the population that is awakened from nighttime aircraft events. While these models are a better predictor of nighttime disturbance than using DNL, they are not without limitations. There are significant differences in the predictions of various models even when removing the FICAN and Basner et al. models. Also only the Passchier-Vermeer et al. model predicted the behavioral awakenings in the Fidell et al. studies to any degree of accuracy for noise event levels above an *SELA* indoor of 80 dB(A). Also the ANSI standard was found to no longer predict differences in sleep disturbance for different aircraft operations when the number of events was greater than 100. This is because of the use of the percent awakened at least once. The use of the average number of awakenings per person per night may be more useful especially for busier airports.

4. MARKOV MODELS AND AIRCRAFT NOISE INDUCED SLEEP DISTURBANCE

Aircraft noise not only causes an increase in awakenings, but also decreases the amount of time spent in rapid eye movement (REM) and slow wave sleep (SWS) (Griefahn, Robens, Bröde, and Basner, 2008b). These changes in sleep may be important to predict around airports, as they may lead to next day or long term health effects. A more sophisticated model of sleep disturbance has been developed by Basner (2006) which would allow these changes in sleep structure to be predicted, however this model does not have a dependence on noise level. A review of this model and how a noise level dependence was introduced into the model is described. Comparisons made between model predictions and survey data are also discussed.

4.1 Description of Markov Model

Basner's (2006) Markov model is based on the data from a laboratory experiment that was conducted at the German Aerospace Center between 1999 and 2003. 128 subjects took part in the study. Sixteen were in the control group (no noise) and 112 were in the experimental group. Each subject slept in the laboratory for 13 consecutive nights. The first night was an adaptation night, subjects became acquainted with sleeping in the laboratory setting, the second night was a no noise night which was used to establish a baseline measurement of normal non-noise disturbed sleep. Nights 3 to 11 were noise experimental nights and nights 12 and 13 were no noise recovery nights. For the experimental nights, the number of aircraft sound events varied from 4 per night to 128. For a given night, the events were evenly spaced in time and all

events were of the same noise level. Playback of the events began after 11:00 pm, the exact starting time though varied depending on the number of nighttime events. The maximum noise levels used in the study ranged from a maximum noise level (L_{Amax} indoor) of 45 dB(A) to 80 dB(A). Polysomnography was used to measure sleep.

By using the data from the baseline and noise-exposure nights, the coefficients for four Markov models were estimated. These sleep disturbance models predict the probability of transitioning from sleep stage s_j to stage s_i given the time of night (t is measured in the number of 30 second epochs since the first occurrence of Stage 2, and ranges from 1 to 820). The models are of the form:

$$p_k(s_i|s_j) = \frac{e^{a_k(s_i)+b_k(s_i)t+c_k(s_i,s_j)}}{\sum_{i=0}^{5} e^{a_k(s_i)+b_k(s_i)t+c_k(s_i,s_j)}} \tag{4.1}$$

where the subscripts i=0, 1, 3,...5, and j=1, 2, ...5. In the notation s_o refers to wake, s_1 to s_4 refers to Stage 1 though Stage 4, and s_5 refers to REM. The subscript k=1, 2, 3, 4 and refers to one of the four noise models. The inclusion of four noise models came from an examination of the data and refer to: 1-no noise, 2-noise event just begun, 3-flyover in progress, and 4-flyover just completed. Stage 2 is the reference stage and so

$$a_k(s_2) = b_k(s_2) = c_k(s_2, s_j) = 0. \tag{4.2}$$

The data from the experiments were used to estimate the 4 x (5+5+25)= 140 coefficients by using a multinomial logistic regression model estimation process. Basner used the $CATMOD$ program in SAS to complete this estimation. For reference in Appendix C a list of the estimated coefficients values for all four models are provided.

Using the Markov models and given the stage (s_j) that a person is in, the time of night, and what noise situation is occurring, the probabilities of moving to each of the six stages can be computed, P0, P1,...P5, where the sum of the probabilities

is equal to 1. A sample (X) from a random process uniformly distributed from 0 to 1 is generated and the sleep stage is determined as depicted in Figure 4.1. By repeating this process for each 30 second interval during the night a hypnogram can be generated, an example is shown in Figure 4.2. The sleep stage an individual is in for each 30 second segment of sleep is indicated by the hypnogram. The probability of being in each of the six sleep stages during the night, as predicted by the baseline, no noise model, is shown in Figure 4.3.

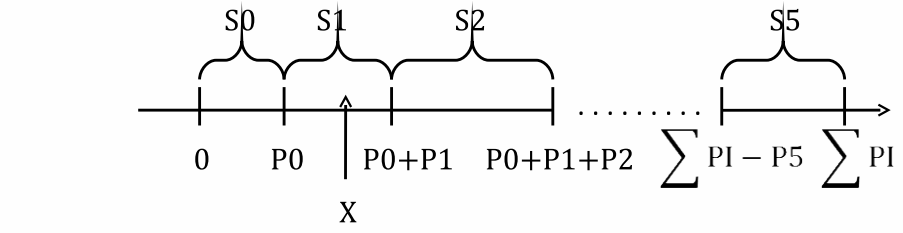

Figure 4.1. Method for determining what sleep stage an individual is in using Basner's Markov model.

One limitation of the sleep structure model is that the noise models only take into account whether an aircraft event occurred and not the level of the noise event. The results from numerous studies, as discussed in Chapter 3 indicate that the degree of disturbance will increase with level. Another problem is that for each model, 35 different coefficients had to be estimated. From the *SAS CATMOD* outputs, included in Basner's report (2006), the standard error of some of the parameters was infinite, or the standard error was very large (e.g. greater than 50). The reason for this high variance in the estimates is that some sleep transitions, such as the transition from Stage 4 to Stage 1 do not occur very often. Therefore the probability of this transition occurring is or is close to zero. An individual most likely will pass through Stage 3 and Stage 2 on the way to Stage 1. Therefore, there was not enough data to

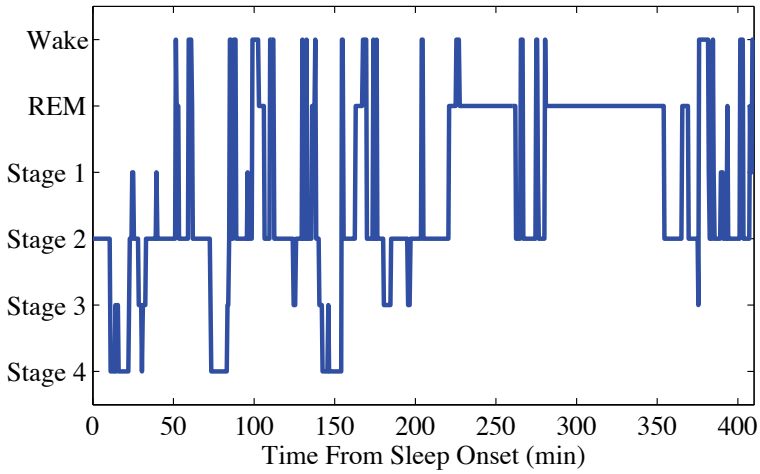

Figure 4.2. Sleep hypnogram, the output of the sleep structure model using the no noise model for one person.

estimate these coefficients. The coefficients that could not be estimated well due to a low probability of the associated sleep stage transition occurring are listed in Table 4.1.

4.2 Modification of Sleep Structure Model

To overcome one limitation of Basner's sleep structure model, a method of adding a noise level dependence to the model was explored. This approach was meant to be a first attempt at adding this dependence. A linear relationship was defined between the noise level of an event ($SELA$) and the model coefficients. The linear models were developed based on the baseline coefficient and the corresponding coefficient in the noise models. It was assumed that for the baseline coefficients the noise level was 30 dB(A) which was the background noise level in the sleep rooms of the laboratory. The noise level for the noise model coefficients was assumed to be 63 dB(A) which is the mean $SELA$ level of the aircraft events used in the laboratory study when

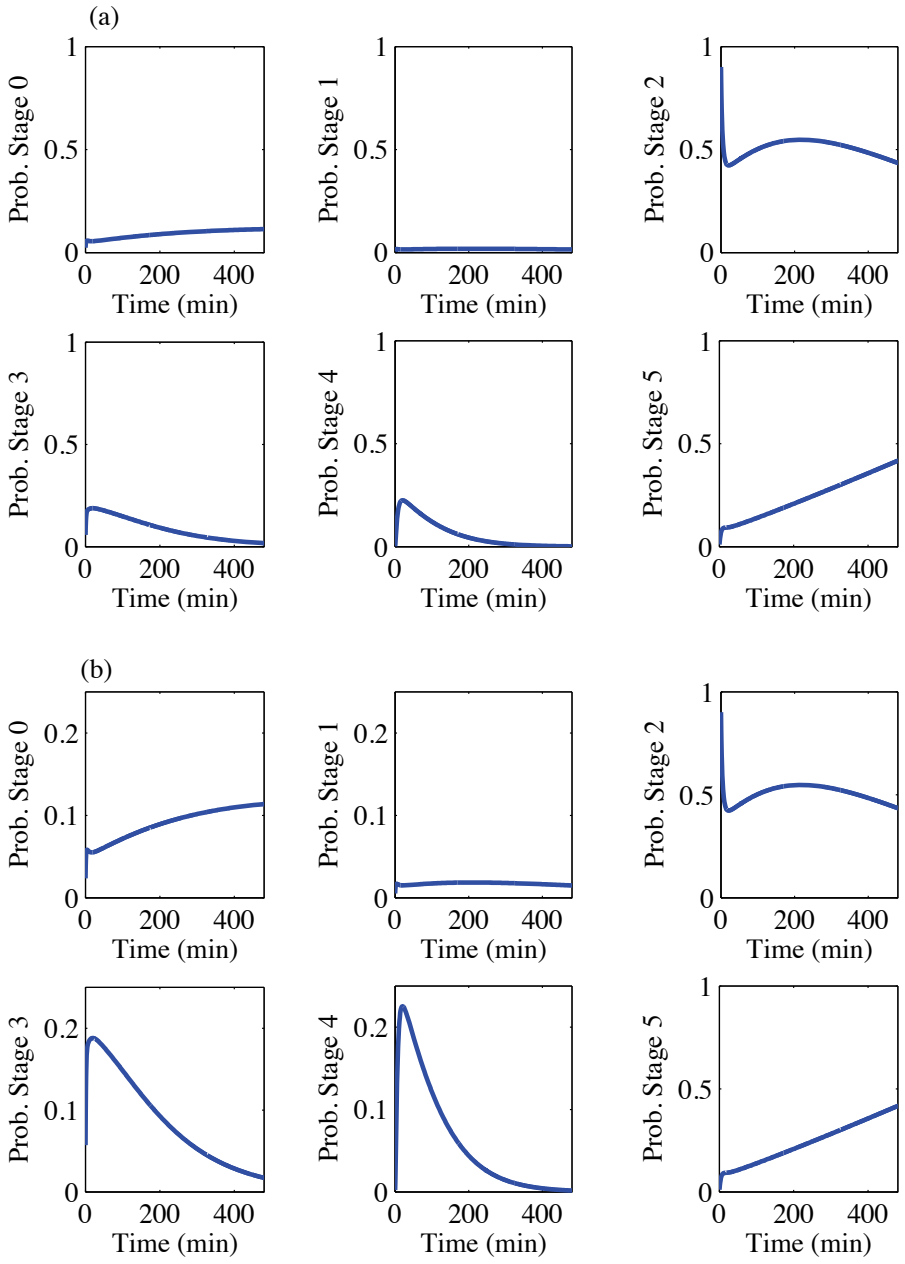

Figure 4.3. (a) Probability of being in a particular sleep stage throughout the night predicted using Basner's baseline model. Stage 5 is REM, Stages 3 and 4 are slow wave sleep, Stage 0 is awake. (b) A close up of the plots for Stage 0, 1, 3, and 4.

Table 4.1. Coefficients of Basner's Markov models that were not estimated well due to a low probability of the transition occurring and thus a lack of observations on which to make a good estimate of the probability.

Model	Coefficients
Baseline	$c(s_4,s_1)$
	$c(s_4,s_5)$
1st Noise Model	$c(s_4,s_1)$
	$c(s_5,s_4)$
	$c(s_3,s_5)$
	$c(s_4,s_5)$
2nd Noise Model	$c(s_3,s_1)$
	$c(s_4,s_2)$
	$c(s_5,s_4)$
	$c(s_3,s_5)$
	$c(s_4,s_5)$
3rd Noise Model	$c(s_4,s_1)$
	$c(s_1,s_4)$
	$c(s_5,s_4)$
	$c(s_3,s_5)$
	$c(s_4,s_5)$

the number of people, number of events, and level of each event was considered. A conversion from L_{Amax} which was used in Basner's study to $SELA$ was performed because most sleep models are based on $SELA$. The method for converting between the two was defined by Pearsons, Barber, Tabachnick, and Fidell (1995), the relation is defined as:

$$SELA = L_{Amax} + 10log_{10}(D_{10}) - 3.7, \tag{4.3}$$

where D_{10} is the duration of the event when it is within 10 dB of the maximum noise level. An average value of D_{10} was assumed based on aircraft recordings and was found to be approximately 9.5 seconds. Therefore 6 dB was added to the L_{Amax} levels to predict the *SELA* values.

The change in coefficients $c(s_i,s_1)$ with noise levels from 53 to 103 in increments of 10 dB for the 4 different models are shown in Figure 4.4. The coefficients are for transitions between Stage 1, s_1 to five sleep stages (s_o, s_1, s_3, s_4, s_5). Recall that s_2 is the reference and therefore $c(s_2, s_1) = 0$. In Figure 4.5 through Figure 4.7 the average transition probabilities for the entire night, for increasing noise levels from 53 to 103 in increments of 10 dB, for all three noise models are shown. For the first noise model, most of the changes in the transition probabilities followed expected trends; the probability of a transition from each sleep stage to Stage Wake increases with noise level. The probability of a transition to deeper stages of sleep, such as Stage 3 and 4 decreases with noise level. There was one unexpected change with noise level; the probability of transitioning from REM sleep to Stage 4 increased with high noise levels in the first noise model. The value of the coefficient $c(s_4, s_5)$ related to this transition was therefore reduced, and it was made equal to the value of the coefficient for the second noise model. For the second and third noise models, in general there is an increase in transition probabilities to lighter stages of sleep with increased noise levels. Some of the unexpected trends, such as the decrease in probability of remaining

in Stage Wake in the second and third noise model, may be due to the fact that most awakenings are brief and therefore individuals will fall back to sleep after the event.

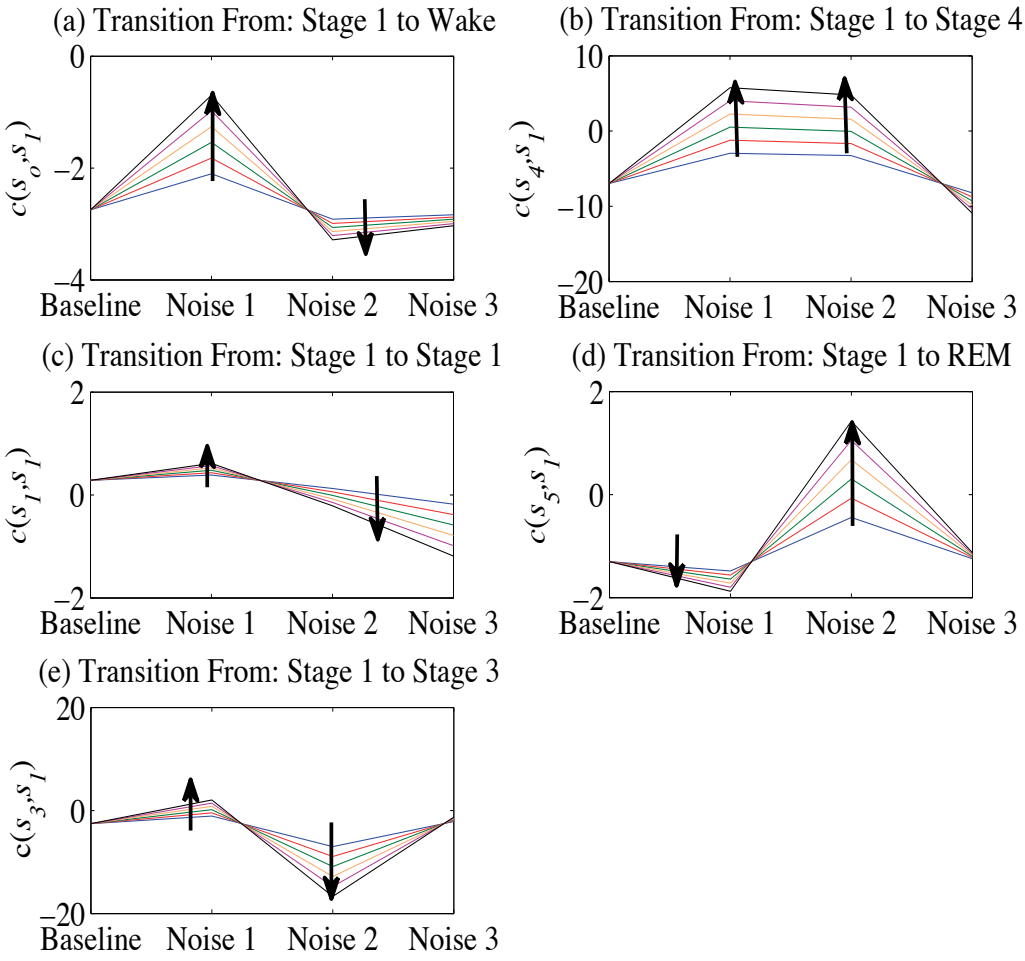

Figure 4.4. Change in coefficients $c(s_i,s_1)$ (i=0, 1, 3, 4, 5) with noise level for transitions from Stage 1 to each sleep stage. Noise 1-First noise model, Noise 2-Second noise model, and Noise 3-Third noise model.

Once the noise level component was added to the model it was desired to determine whether this model would still be a reasonable estimate of the original data of Basner's study. Therefore, a simulated dataset was created using the level dependent version

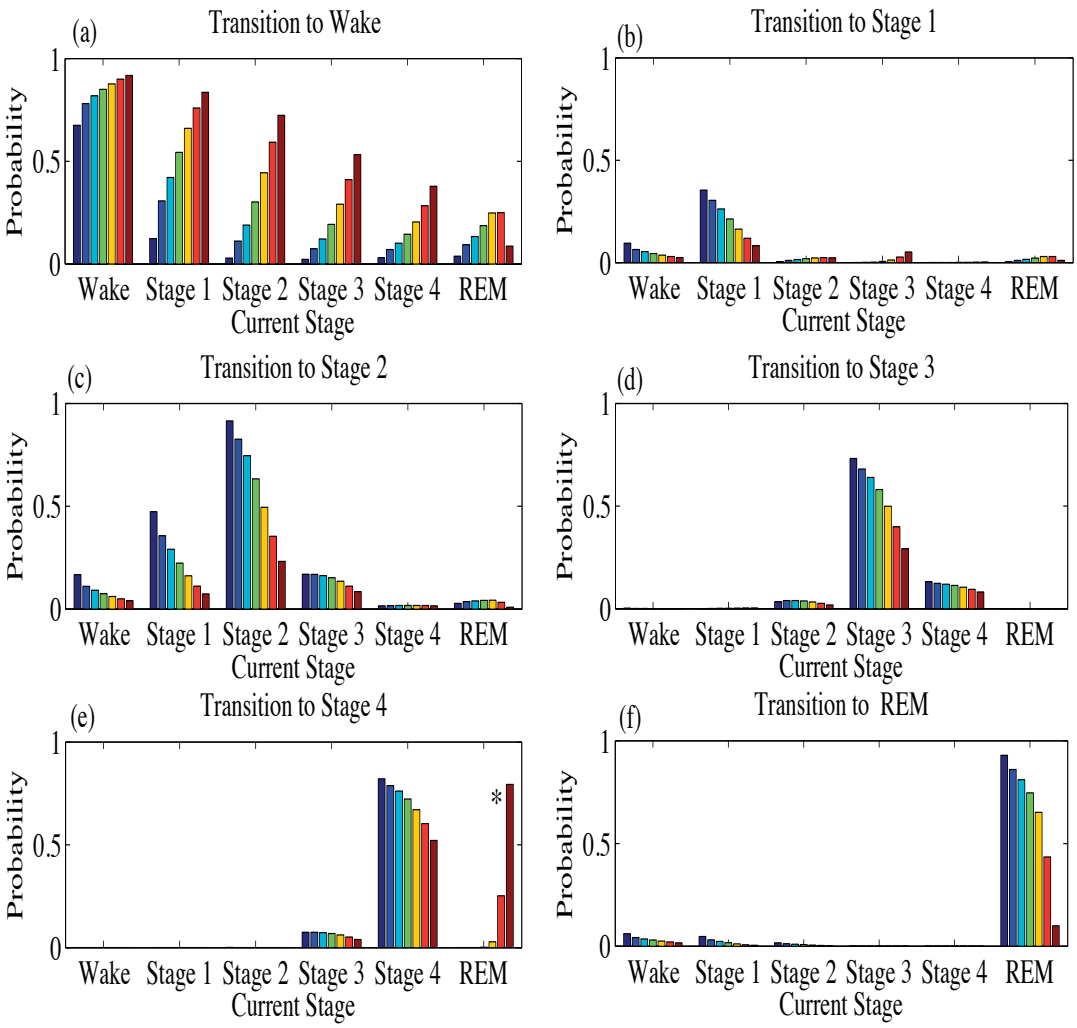

Figure 4.5. Change in the transition probabilities of the first noise model with noise level: (a) to (f) transitions to s_o thru s_5 for each stage. Bars further to the right are results for higher noise levels. The bar all the way to the left is for the baseline model. Levels are $SELA$ = 53, 63, 73, 83, 93, and 103 dB(A). * denotes unlikely scenario.

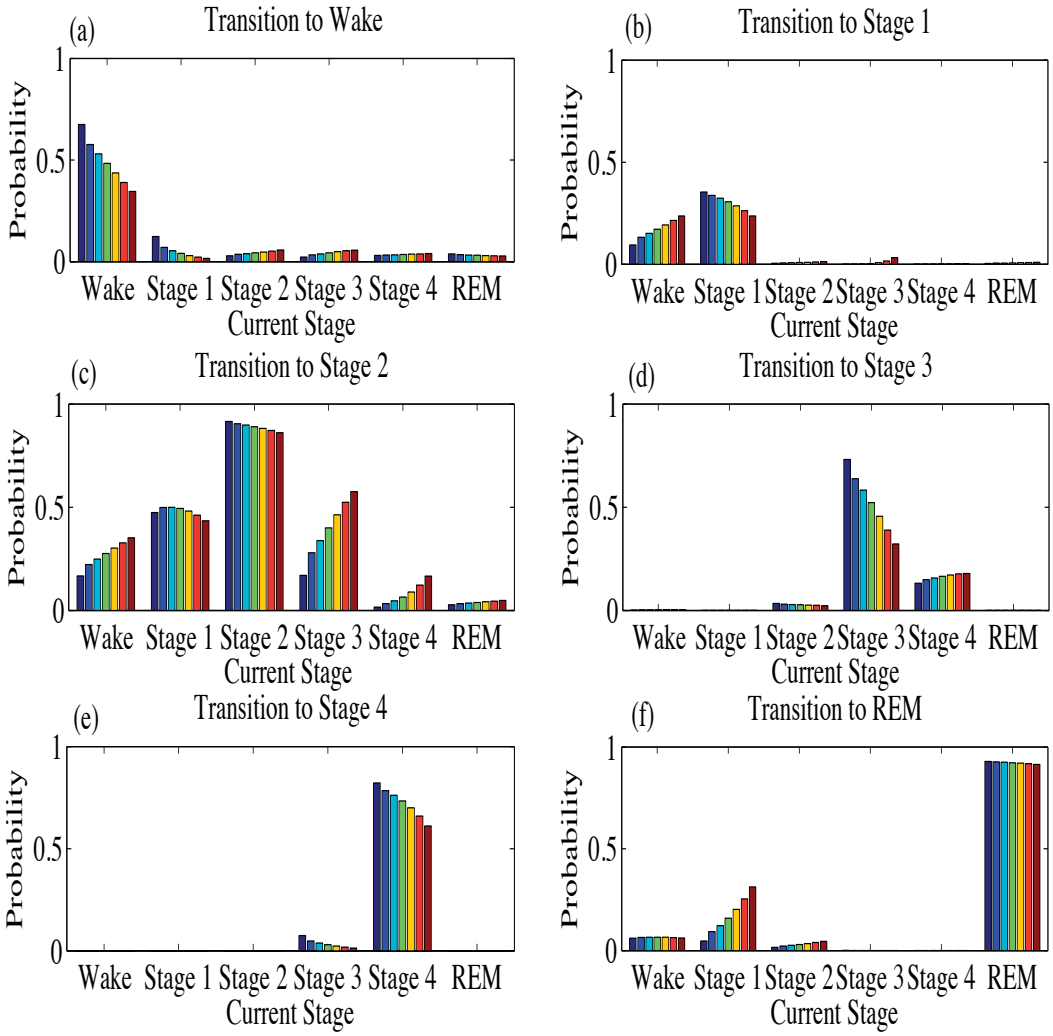

Figure 4.6. Change in the transition probabilities of the second noise model with noise level: (a) to (f) transitions to s_o thru s_5 for each stage. Bars further to the right are results for higher noise levels. The bar all the way to the left is for the baseline model. Levels are $SELA$ = 53, 63, 73, 83, 93, and 103 dB(A).

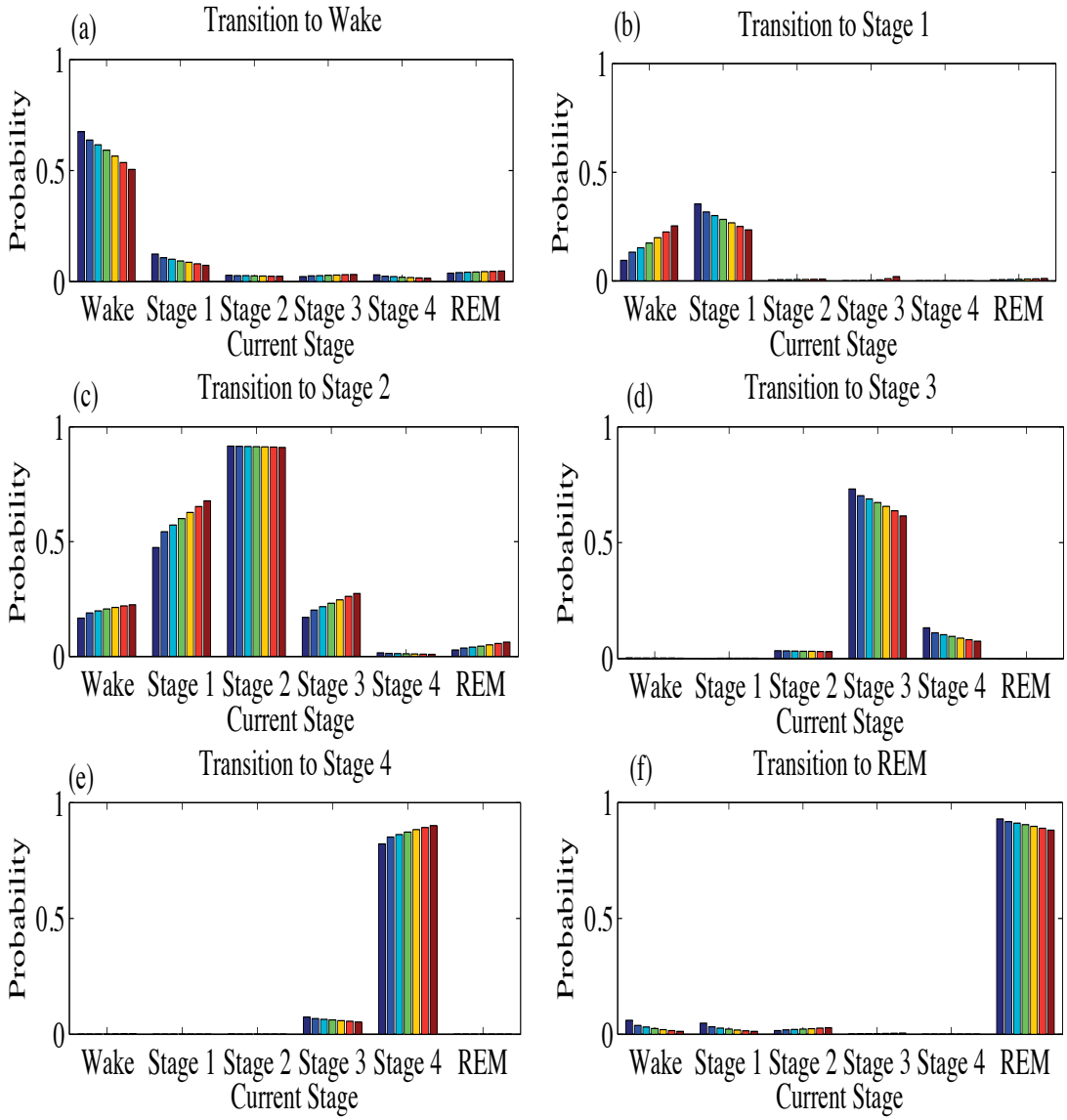

Figure 4.7. Change in the transition probabilities of the third noise model with noise level: (a) to (f) transitions to s_o thru s_5 for each stage. Bars further to the right are results for higher noise levels. The bar all the way to the left is for the baseline model. Levels are $SELA$ = 53, 63, 73, 83, 93, and 103 dB(A).

of Basner's model. This simulation was conducted using the same number of people, same number and timing of aircraft events, and the same noise level of the events. From the simulated dataset the coefficients of Basner's original model, i.e. the model without noise level dependence, was estimated, by using the *mnrfit* command in Matlab. The simulation was performed 40 times, and the mean value and the 5th and 95th percentiles of the estimated coefficient values are shown in Figure 4.8. The largest differences between the original and estimated parameters typically were for the coefficients that were not estimated well in the original model (see Table 4.1). These coefficients are indicated by black boxes in the figure. It is noted though that these coefficients would be difficult to estimate even with a large quantity of data as these transitions do not occur often in sleep, an example being a transition from Stage 1 directly to Stage 4. Also there was more variance in the estimation of parameters when the current stage was Stage 3 and 4 and also for transitions to these stages (Figure 4.8 (b) and (d)).

4.3 Comparison of Markov Model Predictions to Behavioral Awakening US Survey Data

To further validate the modified version of Basner's model, with incorporated noise-level dependence, the model was used to create simulated responses for the same event scenarios as those of the three US surveys conducted by Fidell et al. (1995, 2000). For this simulation the same number of people, events, timing of events, and noise levels as in the original survey data were used. For the simulation, a definition for a behavioral or conscious awakening had to be defined since sleep was measured in the surveys by having subjects press a button when awakened. In one simulation it was assumed that a conscious awakening occurred if the subject was awake for at least two and a half minutes and in the other a conscious awakening was deemed to have occurred if the subject was awake for at least 3 minutes. The awakenings were

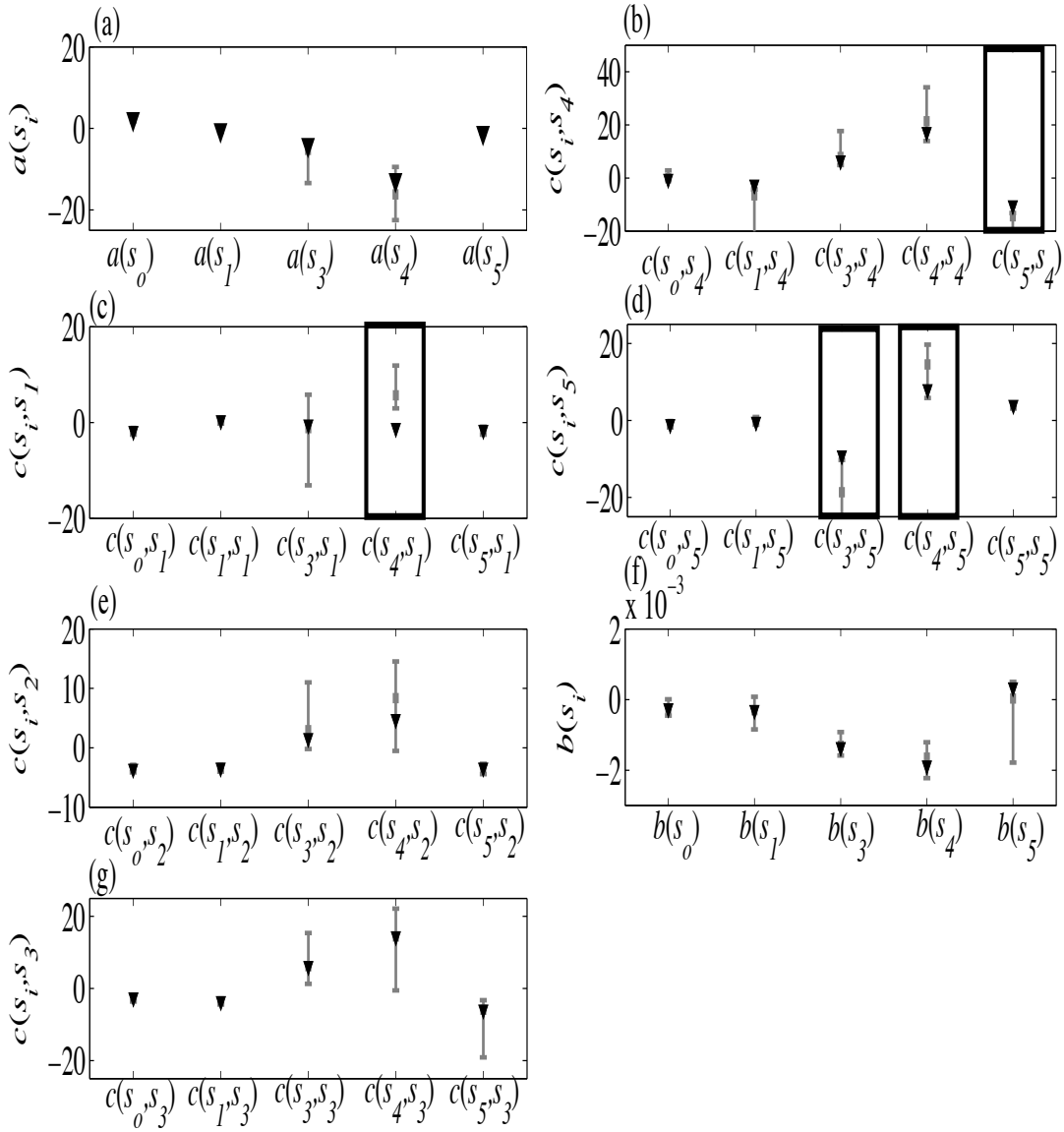

Figure 4.8. Coefficients of the first noise model. Basner's Original model coefficients (black triangles) and the estimated coefficients from the simulated noise-level dependent model (gray squares). Bars show the 5th and 95th percentile of estimates.

required to start within 90 seconds or 3 epochs from the start of the noise event. An example of the outcome for 2 simulations for both conditions are shown in Figure 4.9.

The model over-predicted the number of awakenings when a definition of two and a half minutes was used for conscious awakenings. A better agreement was obtained when a definition of three minutes was used. This demonstrates how comparing model predictions to survey data is highly dependent on the definition of awakening that is used. The Markov model with added noise dependence tracks the Passchier-Vermeer et al. (2002) model predictions at higher *SELA*, but there appears to be less noise level sensitivity in the actual survey data.

4.4 Comparison of Markov Model Predictions to Data from UK Study

While the number of subject nights was limited in the UK Study (Flindell et al., 2000), predictions of sleep stages using Basner's Markov model for the baseline laboratory nights was made. To compare the predictions for baseline non-noise disturbed nights, the data from nine laboratory subjects in the UK study was used. The probability of being in NREM, REM, and Wake states was calculated for each 5 minute block of time. The results are shown along with predictions using the baseline Markov model in Figure 4.10.

The the probability of being in REM, NREM, and Wake stages calculated using Basner's Markov model followed the same trends as the predictions from the 1999 UK data. However the oscillating nature in the 1999 UK data, i.e. the probability of NREM and REM sleep varying every 90 to 100 minutes, is clearly missing in the Markov model predictions. The variation in probability of being in NREM and REM sleep was present in the data used to create Basner's Markov model. The values for the probability of being in REM sleep for his study were extracted from a graph in the report by Basner (2006) and are shown in Figure 4.11. For direct comparison

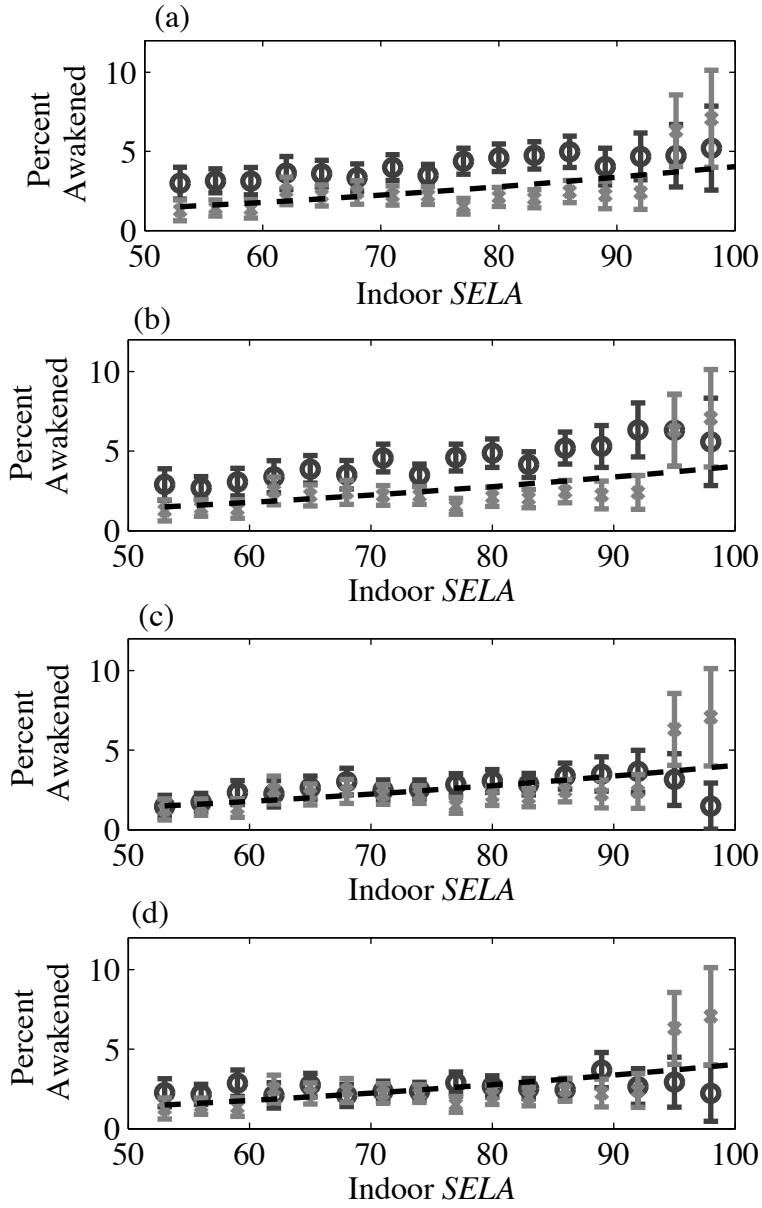

Figure 4.9. The percent awakened in the three US studies (light gray x) of Fidell et. al (1995, 2000) and that predicted by a modified version of Basner's model (dark gray circles) with 95% confidence intervals, the percent awakened predicted by Passchier-Vermeer et al.'s model (2002) is shown by the black dashed line. (a,b) A conscious awakening was defined as lasting at least 2 and half minutes. (c,d) A conscious awakening was defined as lasting at least 3 minutes.

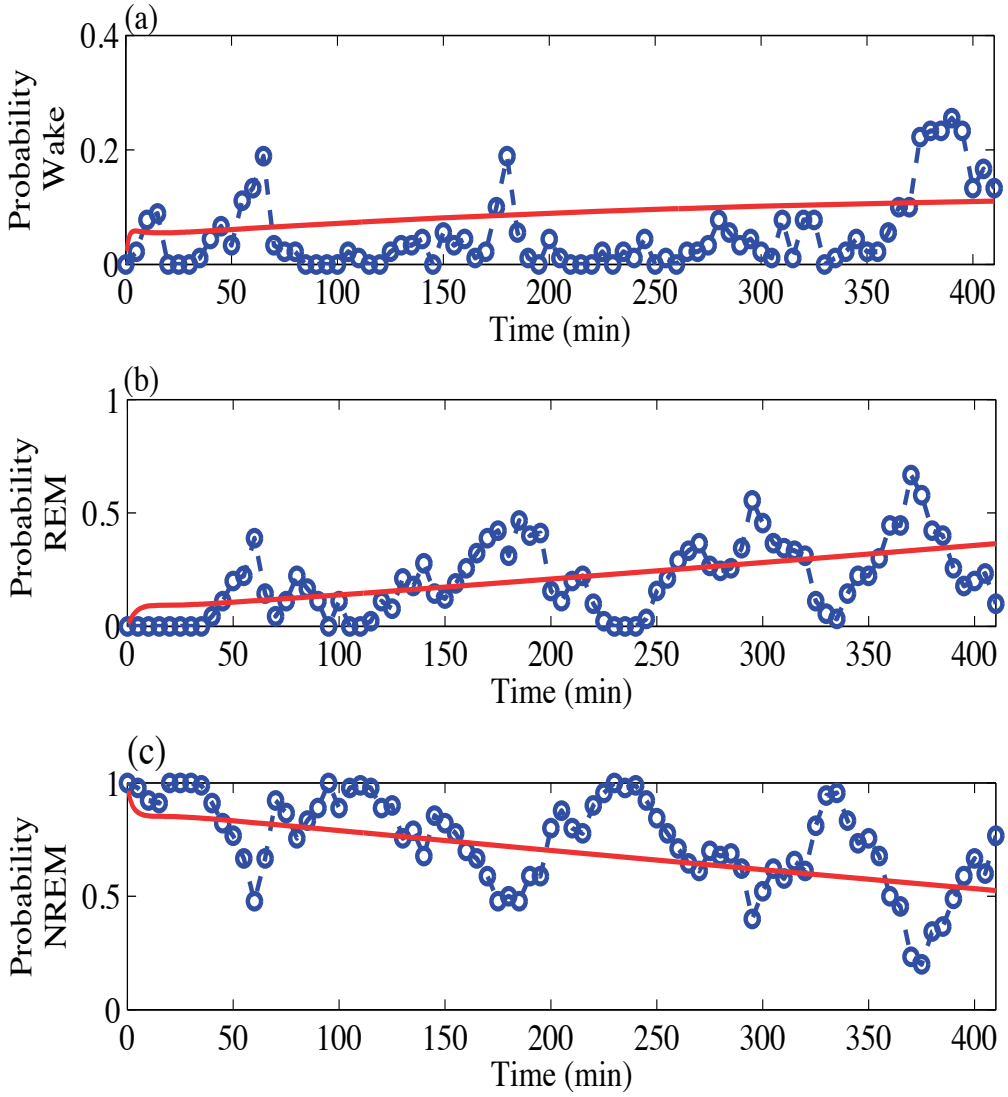

Figure 4.10. Baseline Markov model predictions of the probability of being in Wake, REM, and NREM (red line). The estimated probability of being in these sleep stages calculated using the 1999 UK sleep data (blue circles).

the results from the 1999 UK data are also shown again. The oscillations in Basner's data are less extreme than in the UK data but are clearly present.

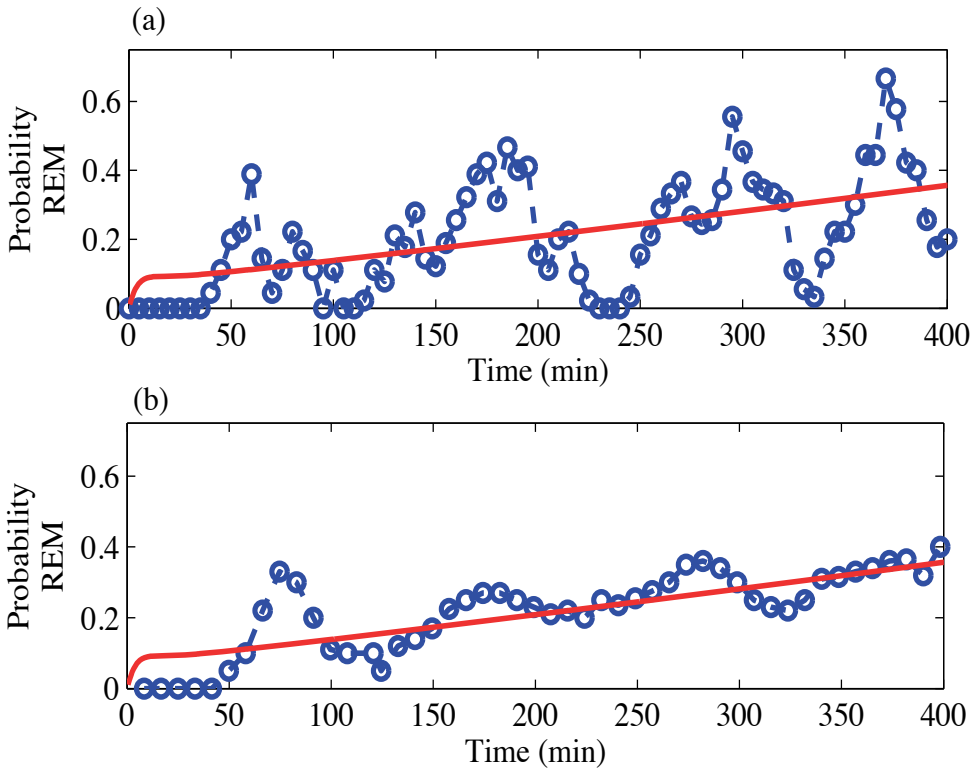

Figure 4.11. Comparison of Markov model predictions for the probability of being in REM (red line), and the probability of being in the same sleep stages calculated using the (a) 1999 UK sleep data (blue circles) and (b) extracted from Basner (2006) (blue circles).

The predicted time spent in each of the six sleep stages and the actual time spent in the sleep stages for non-noise nights in the 1999 UK laboratory study are listed in Table 4.2. The durations are based on the first 410 minutes of sleep. Using the baseline component of Basner's Markov model, simulations of the sleep of 9 people were performed. This was repeated 100 times and the mean of those 100 simulations and the standard deviation of the data are listed in the table. The amount of time

spent in Stage 2 and Stage REM in the 1999 UK study are similar to the predictions. However, in the UK study, more time was spent in Stage 1 and less time in Stage 4 than was predicted from the Markov Baseline model. Possible reasons for the differences found are that the model is based on 128 nights of data while the UK data used only consisted of 9 subject nights. In the UK study all subjects were between 30 to 40 years old. Subjects in Basner's laboratory study ranged from 18 to 65 years old, with a mean age of 38 years old. As individuals age less time is spent in Stage 4, but it is unknown whether the younger subjects in Basner's dataset may have affected the results.

Table 4.2. Mean time spent in each sleep stage for baseline no noise nights. The standard deviation of the data is in parenthesis.

Sleep Stage	1999 U.K. Data (minutes)	Basner Markov Model Predictions (minutes)
Wake	20.7 (15.7)	35.7 (2.9)
Stage 1	45.1 (18.1)	7.3 (1.7)
Stage 2	217.6 (25.7)	210.3 (3.9)
Stage 3	37.6 (12.7)	39.9 (2.9)
Stage 4	5.2 (12.9)	26.9 (1.7)
REM	83.7 (18.1)	90.3 (2.3)

4.5 Conclusions

A Markov model for predicting changes in sleep stages through the night was developed by Basner (2006). One limitation of the model is that it does not predict changes in sleep for noise events of different noise levels. An initial attempt to add a noise level dependence to the model was explored by varying the model coefficients with noise level. Predictions of conscious awakenings obtained using the modified form of Basner's model were found to be similar to the percent awakened found in

the US survey data. Not surprisingly, the results are dependent on the definition of awakening that is used. Although the number of subjects nights of data from the UK study is limited, the probability of being in REM, NREM, and Wake stages calculated based on 9 nights of data were compared to predictions using Basner's Markov model and both followed similar trends. However, there were differences in the actual and predicted time spent in the 5 NREM stages. There are many possible reasons for the differences found. It may be useful to have a model that incorporates age groups, noise sensitivity and other individual characteristics as variables. Although Basner's model represents a significant improvement over awakening models, there are still deficiencies that need to be addressed if a goal is to have a more accurate predictor of sleep structure. One approach would be to gather more data and make coefficients more complicated functions of time and of other variables. Another approach would be to look at more physical models of sleep and adapt those to incorporate the effects of disturbances such as aircraft noise.

5. NON-NOISE DISTURBED SLEEP MODELS

In this chapter sleep models that predict normal, non-noise disturbed sleep patterns, are described. While Markov models and additional simplistic sleep pattern models are reviewed the focus of this chapter is an examination of existing nonlinear dynamic sleep models which can be used to predict the amount of slow wave activity, REM sleep, and awakenings during the night. The attraction of the nonlinear models is the ability to understand at a more fundamental level the dynamic properties of sleep. These models were examined in order to determine a candidate model that could be modified to predict the effect of aircraft noise on sleep. A parameter variation study conducted for several of the nonlinear dynamic models is also described.

5.1 Markov Models

Basner's model is the only Markov model that has been developed to predict the impact of noise on sleep, however several other Markov models have been developed to predict normal sleep patterns. Zung, Naylor, Gianturco, and Wilson (1965) developed a Markov model based on the data from 14 subjects. They developed one model for subjects who were 20 to 29 years old, another for those 30 to 39 years old, and a combined model for those between 20 and 39 years of age. For each age group, there is a transition probability matrix for each half hour of the night. These models do not predict the probability of transitions between the sleep stages that are currently used (e.g. NREM Stages 1 to 4 and REM). These models are based on an earlier definition of sleep stages which were labeled A through E. A indicates lighter sleep while E indicates deeper sleep. These stages were defined by Davis, Davis, Loomis,

Harvey, and Hobart (1937). There is no stage corresponding to REM Sleep. When performing simulations with the model they assigned one sleep stage to each 3 minute interval rather than to each 30 second epoch as Basner did in his Markov model. The probabilities of being in a particular sleep stage during the night are shown in Figure 5.1. The probability of being in a sleep stage as predicted by Basner's Baseline Markov model (2006) is also shown for comparison. The probabilities through time for Zung's model are not smooth functions since there is a different probability matrix used for each 30 minute block of sleep. Zung's model predicts a much greater probability of awakening (Stage A) at the end of the night than what is predicted by Basner's model. Basner's model though was limited to 410 minutes of the sleep period. For Zung's model the probability of being in Stage B is much higher than the probability of being in Stage 1. However, Stage B means there is no alpha activity therefore it includes Stage 1, Stage 2 when there is no sleep spindles, and REM sleep. The prediction for Stage E, or the deepest sleep is much greater at the beginning of the night than predicted by Basner's model. However, this stage incorporates part of Stage 3 as well as Stage 4. Due to differences in sleep stage definitions it is difficult to make comparisons between predictions of Basner's and Zung et al.'s models. However, both follow some similar trends: the probability of deep sleep decreases during the night and lighter sleep increases.

Kemp and Kamphuisen (1986) also developed a Markov model to simulate sleep hypnograms. Their model is based on the data of 23 subjects, 2 nights of data per subject. They determined the number of transitions between sleep stages from Stage s_i to Stage s_j per second during a specific time interval (transition rates). For each sleep stage transition, 32 transition rates, one for each 15 minute interval of the night, was calculated. The average transition rates calculated for the entire night are shown in Table 5.1. For comparison, the average transition rates for Basner's baseline model

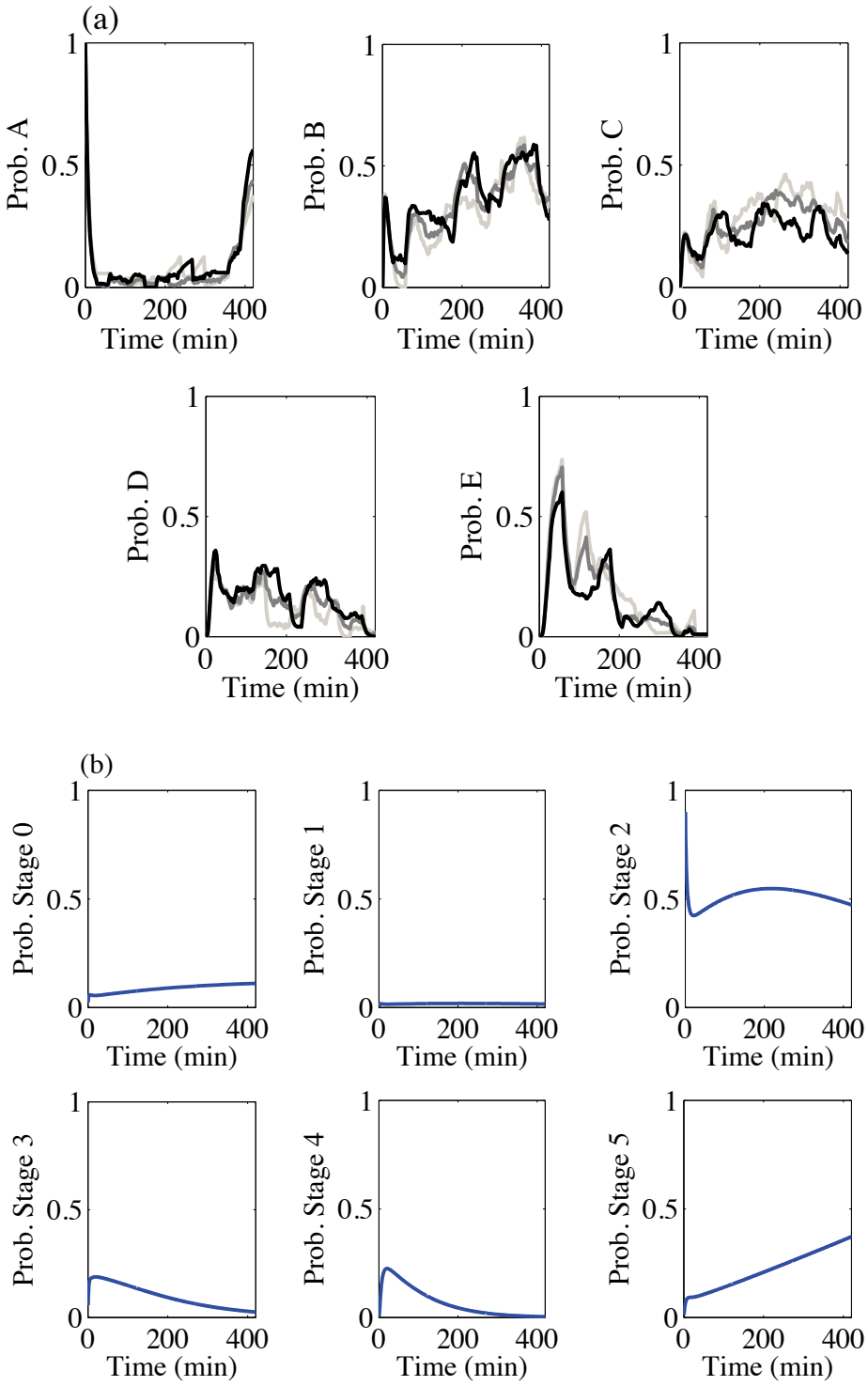

Figure 5.1. (a) Probability of being in a particular sleep stage throughout the night, from Zung et al.'s model: (light gray) model for 20-29 yr olds, (dark gray) model for 30-39 yr olds, and (black) model for 20-39 yr olds. (b) Probability of being in a particular sleep stage throughout the night predicted using Basner's baseline model.

were estimated and are in Table 5.2. The largest difference between the two models is that Basner's model predicts that transitions from Stage 4 to Stage Wake happen more often than transitions from Stage 4 to Stage 2; Kemp and Kamphuisen's model show the opposite. Also for Basner's model, the transition from one of the 6 sleep stages to Stage Wake was either the highest transition rate or the second highest transition rate.

Table 5.1. Average (entire night) transition rates from Stage s_i to Stage s_j for Kemp and Kamphuisen's model (1986): (dark gray) highest transition rate, (light gray) second highest transition rate.

s_i/s_j	0	5	1	2	3	4
0	-	0.000149	0.007771	0.000130	0.00000	0.000000
5	0.000221	-	0.001409	0.000338	0.000000	0.000003
1	0.001363	0.003211	-	0.011243	0.000000	0.000000
2	0.000249	0.000405	0.001069	-	0.001033	0.000000
3	0.000137	0.000026	0.000231	0.005195	-	0.003734
4	0.000028	0.000000	0.000028	0.000198	0.005777	-

Table 5.2. Average (entire night) transition rates from Stage s_i to Stage s_j for Basner's baseline model (2006): (dark gray) highest transition rate, (light gray) second highest transition rate.

s_i/s_j	0	5	1	2	3	4
0	–	0.000179	0.000266	0.000474	0.000007	0.000000
5	0.000266	–	0.000028	0.000184	0.000000	0.000000
1	0.000072	0.000028	–	0.000276	0.000000	0.000000
2	0.000500	0.000281	0.000082	–	0.000568	0.000015
3	0.000059	0.000004	0.000000	0.000471	–	0.000285
4	0.000035	0.000000	0.000000	0.000020	0.000244	–

Yang and Hursch (1973) argued that Markov models like the ones developed by Zung et al. (1965) and Kemp and Kamphuisen (1986) are inadequate for modeling sleep. For a Markov model, the cumulative distribution for the length of time spent

in a given stage should follow an exponential distribution. However, Yang and Hursch (1973) found that their data did not follow this distribution. They instead developed a Semi-Markov model in which the cumulative distribution of transition times can follow any distribution. They assumed that the distribution was independent of the stage that was being transitioned to, it only depended on the stage an individual was currently in. Also they assumed that transitions could only occur between adjacent stages. For example, a transition could be made from Stage 3 to Stage 2 or from Stage 3 to Stage 4. However, a transition can not occur from Stage 3 directly to Stage 1. Due to this assumption the probability of transitioning from Stage 3 to Stage 2 is just 1 minus the probability of transitioning from Stage 3 to Stage 4. These assumptions reduced the number of transition probabilities to 3 (p_{ji} is the probability of transitioning from Stage j to Stage i): p_{12}, p_{34}, p_{23}. They assumed that the transition probabilities were constant over 1 hour. Also the probability p_{12} was determined to be constant throughout the entire night. The transition probabilities they determined for subjects between the ages of 30 to 39 years old are listed in Table 5.3. The probability for the transition p_{34} was only defined in the article up to hour 5.

Table 5.3. The transition probabilities for the Semi-Markov model developed by Yang and Hursch (1973).

Hour	$p_{23} = 1 - p_{21}$	$p_{34} = 1 - p_{32}$	$p_{12} = 1 - p_{10}$
1	0.63	0.51	0.853
2	0.3	0.33	0.853
3	0.4	0.35	0.853
4	0.14	0.28	0.853
5	0.16	0.39	0.853
6	0.1	—	0.853
7	0.04	—	0.853

5.2 Simple Dynamic Models

There are several simple models that have been developed to predict sleep patterns and processes regulating sleep, such as a force that pulls an individual from an awake state to sleep. These models are briefly described.

5.2.1 Sleep Patterning Model

A simple model developed by Lawder (1984) is composed of a line with a negative slope and a triangular waveform which are used to predict when certain sleep stages will occur. When a defined triangular waveform is above the ramp REM sleep is predicted, when the triangular waveform is below the ramp and the ramp exceeds the triangular waveform by 70 arbitrary units, Stages 3/4 is considered to occur, otherwise Stages 1/2 are predicted. The increase in duration spent in REM sleep during the night is predicted by this model as well as the cycling between NREM and REM sleep during the night. The ramp starting height and slope could be changed to predict sleep for different age groups. Lawder (1984), for example, stated that a lower initial value of the ramp and a smaller slope could be used to predict the sleep of children as this would lead to a greater amount of REM sleep. An example of an output of the model is shown in Figure 5.2.

5.2.2 Sleep Package Model

Kobayashi (1994) developed a model which he referred to as the Sleep Package Model. The model can be used to predict the time out of 100 minutes that is occupied by Stage 2, REM, or SWS (slow wave sleep). The amount of REM sleep is determined by the circadian rhythm. The circadian rhythm is the 24-hour variation in biological processes, such as the temperature, of the human body. For this model, the circadian

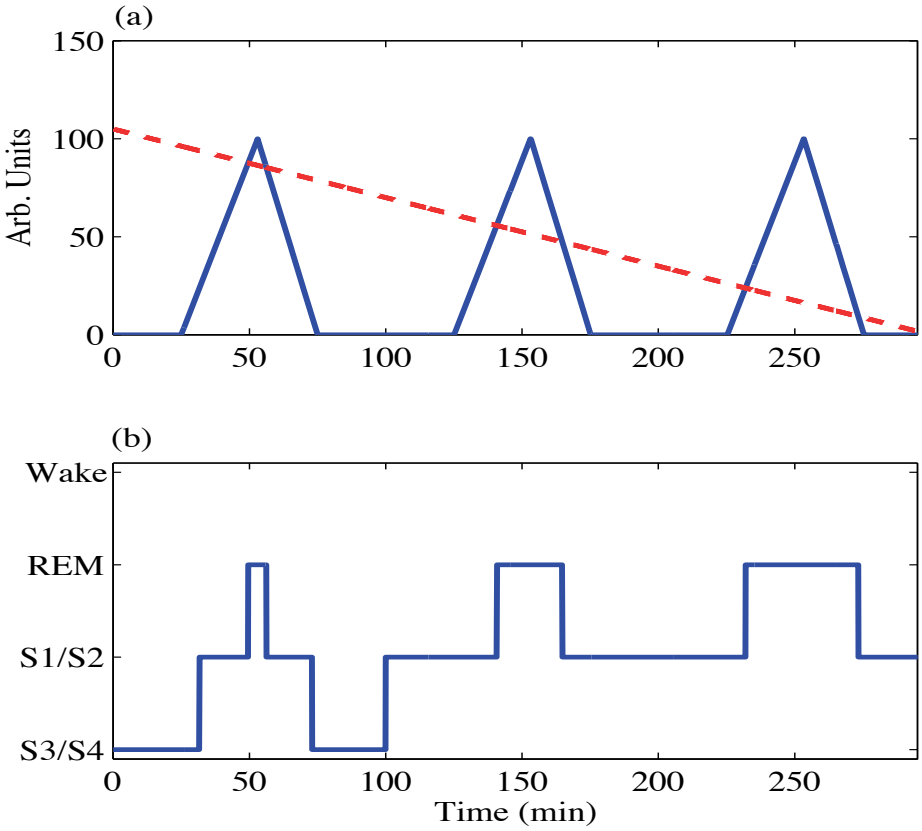

Figure 5.2. Example of the results obtained from one simulation with Lawder's Model (1984). (a) The ramp (red-dotted line) and triangular waveform (blue-solid line) and (b) estimated sleep stages.

rhythm is modeled with a sinusoidal term with a period of 24 hours. The percent of a 100 minute time frame that is occupied by REM sleep is defined as,

$$\%REM = 10sin(24t + \theta) + 40. \tag{5.1}$$

From the results of an experiment they conducted, they found that the total amount of SWS during the night increases with the amount of prior wakefulness

before the sleep period in a logarithmic fashion. The equation for the total amount of SWS during the night is defined by the equation,

$$SWS(Tw) = a\ log(b\ Tw + 1), \tag{5.2}$$

where Tw is the duration of prior wakefulness before the sleep period. The amount of SWS during each 100 minute interval of sleep is based on a linear decreasing function, there is less SWS at the end of the night,

$$SWS = (ct + d)SWS(Tw). \tag{5.3}$$

The amount of Stage 2 sleep is just the difference between 100 minutes and the amount of SWS and REM sleep. None of the values for the coefficients of the model were defined in the paper by Kobayashi (1994). This model like the model developed by Lawder (1984) involves many assumptions including the number of sleep cycles during the night.

5.2.3 Random Walk Sleep Model

Lo, Nunes Amaral, Havlin, Ivanov, Penzel, Peter, and Stanley (2002) developed a model which predicts sleep and wake states. The model is based on 39 nights of data, from 20 subjects. They calculated the cumulative distributions for the durations of sleep states and wake states during the night. They determined that the cumulative distribution for the duration of wake states followed a power law,

$$P(t_w) = t_w^{-\alpha}, \tag{5.4}$$

while the duration of sleep states followed an exponential distribution,

$$P(t_s) = e^{-t_s/\tau}. \tag{5.5}$$

They found that the value of α of the power law did not change with time from sleep onset, but the value of τ in the exponential distribution of Equation (5.5) did. It was determined that the length of Wake states increase toward the end of the night. They also assumed that there is a restoring force which pulls a person back to sleep if they have entered an awake state. However, the strength of this force decreases the longer an individual is awake. Based on these assumptions they developed a random walk model. They decided to use a random walk model because they thought it would account for the random competition between the firing of sleep promoting neurons and sleep inhibiting neurons. When x is less than 0 an individual is considered to be in a sleep state, and the equation for the model is,

$$x(t+1) - x(t) = \epsilon(t), \quad \text{if } -\Delta \leq x(t) \leq 0 \text{ (sleep)}. \tag{5.6}$$

When x is larger than 0, an individual is considered to be in an awake state and the equation for the model is,

$$x(t+1) - x(t) = \frac{-b}{x} + \epsilon(t), \quad \text{if } x(t) > 0 \text{ (wake)}. \tag{5.7}$$

In the Equations (5.6) and (5.7), $\epsilon(t)$ is a Gaussian distributed random variable with zero mean and unit standard deviation. The value of Δ and b can be altered in order to match the cumulative probability distributions for the duration of sleep and wake states. The equation,

$$\alpha = 1/2 + b, \tag{5.8}$$

relates b, which is the term for the restoring force, to α, which is the coefficient in the power distribution. The equation,

$$\tau = \Delta^2, \tag{5.9}$$

relates Δ, which limits the minimum level of x, to τ, which is the coefficient in the exponential distribution. An example of an output simulated using Lo et al.'s model is shown in Figure 5.3. The results are only plotted for 6 hours of sleep because only three different values of Δ were defined for the model, one for each two hours of sleep.

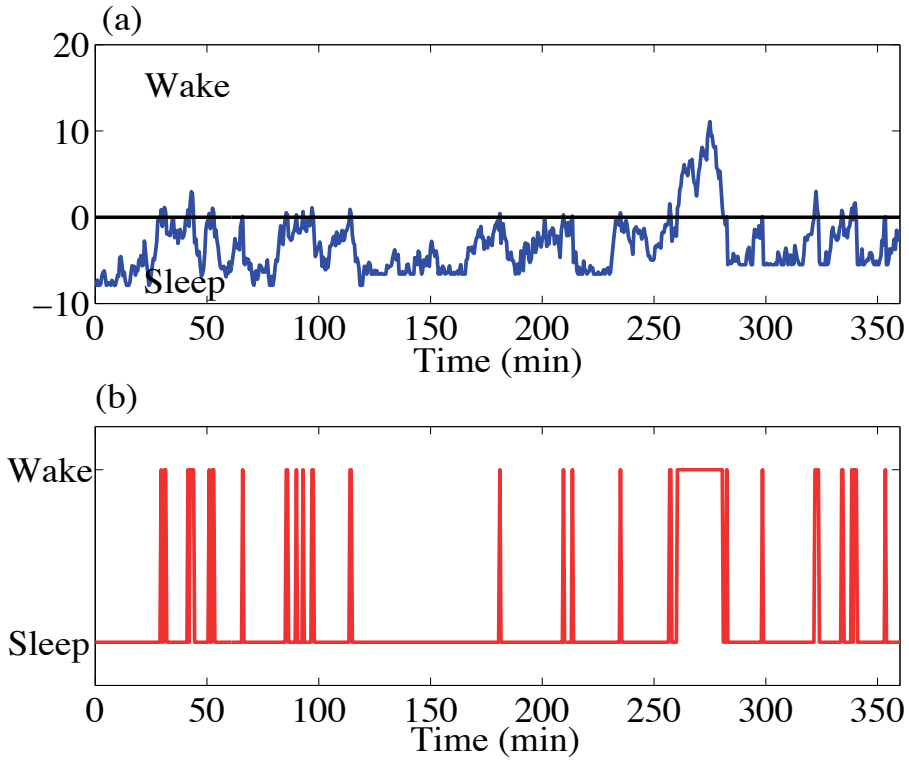

Figure 5.3. Example of the results obtained from one simulation with Lo et al.'s model. (a) Output of model and (b) classification of sleep stages.

To calculate the probability of awakening as predicted by Lo et al.'s model, 1000 simulations were performed. The result is shown along with the probability of being awakened predicted using Basner's baseline model (2006) in Figure 5.4. The model by Lo et al. predicted a lower probability of awakening than Basner's baseline model but by decreasing the values of Δ, a better agreement between the two models was able to be obtained.

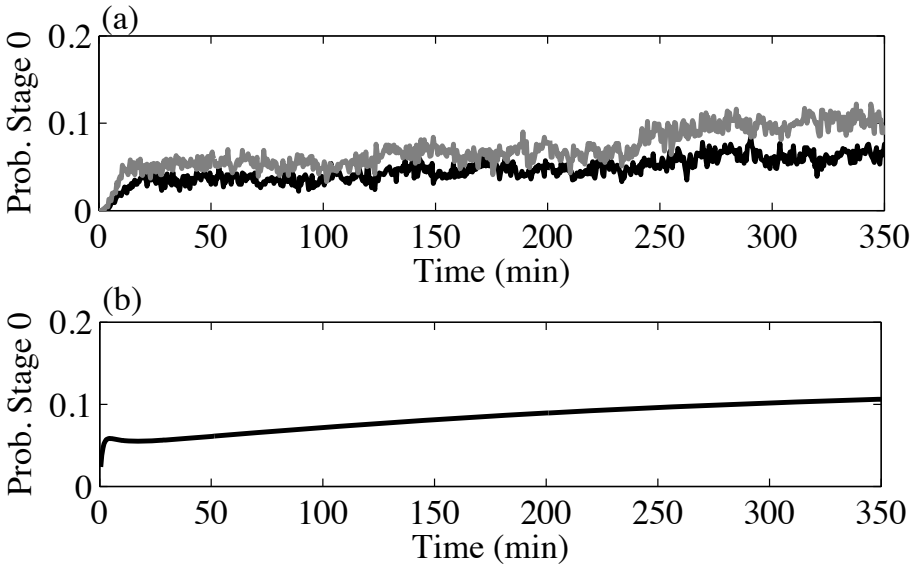

Figure 5.4. (a) Predicted probability of awakening using Lo et al.'s model for (black) original values of Δ and (gray) decreased values of Δ. (b) Predicted probability of awakening using Basner's Baseline Markov model.

5.3 Flip-Flop Sleep-Wake Nonlinear Dynamic Models

There are two primary approaches in modeling the oscillation between sleep and wake states during 24 hour periods and NREM and REM sleep during the night. One approach, defined by Lu, Sherman, Devor, and Saper (2006) involves modeling the control of REM sleep as a flip-flop switch. In their descriptive model there are two

distinct states, one associated with high levels of REM promoting neuron activity and another related to high levels of REM inhibiting neuron activity. Each group of neurons will inhibit the other and thus are self exciting as they will disinhibit and reinforce their own firing rate. The state an individual is in is dependent on the balance of inhibition between the two states (Fort, Bassetti, and Luppi, 2009). A descriptive flip-flop switch model for sleep and wake states has also been developed by Saper, Chou, and Scammell (2001). Two mathematical models based on the concept of the flip-flop switch have been developed and will be described.

5.3.1 Phillips and Robinson's Sleep-Wake Model

Phillips and Robinson (2007) modeled the behavior of neuron activity that leads to sleep and wake states during a 24 hour period. One population of neurons they modeled are monoaminergic (MA) neurons which are found in the brain stem. This group of neurons have a high firing rate during wake states and a lower firing rate during sleep. The second group of neurons are found in the ventrolateral preoptic area (VLPO) and have a high firing rate during sleep and a low firing rate during wake states. The homeostatic and circadian drives act on the VLPO population in the model. The homeostatic drive is an indication of the need for sleep and increases during the day and decreases during the night. The equations for the two neuron populations are,

$$\dot{V_v}\tau_v + V_v = \nu_{vm}Q_m + D_v^o + \Delta D_v, \tag{5.10}$$

and,

$$\dot{V_m}\tau_m + V_m = \nu_{mv}Q_v + D_m^o + \Delta D_m, \tag{5.11}$$

where the subscript v refers to the VLPO neurons and the subscript m refers to the MA neurons. In the equations V is the cell body potential and Q is the mean firing rate of the neurons. The equation for Q_j, j=m or v is:

$$Q_j = \frac{Q_{max}}{1 + exp(-(V_j - \theta)/\sigma)}. \tag{5.12}$$

The circadian (C) and homeostatic (H) terms of the model cause an increase in the VLPO population potential and this is modeled by:

$$D_v^o = \nu_{vc}C + \nu_{vh}H, \tag{5.13}$$

where the equation for the circadian term is,

$$C(t) = sin\omega t + c_o, \tag{5.14}$$

and the homeostatic term is defined by,

$$\chi\dot{H} + H = \mu Q_m. \tag{5.15}$$

The values for the model parameters are in Table 5.4. The behavior of the model follows the concept of sleep neuron activity behaving like a flip-flop circuit. The two populations of neurons are mutually inhibiting and it is the circadian and homeostatic terms that lead to the imbalance in firing and the rapid transitions between the two states. An example an output of the model, that was simulated, is shown in Figure 5.5.

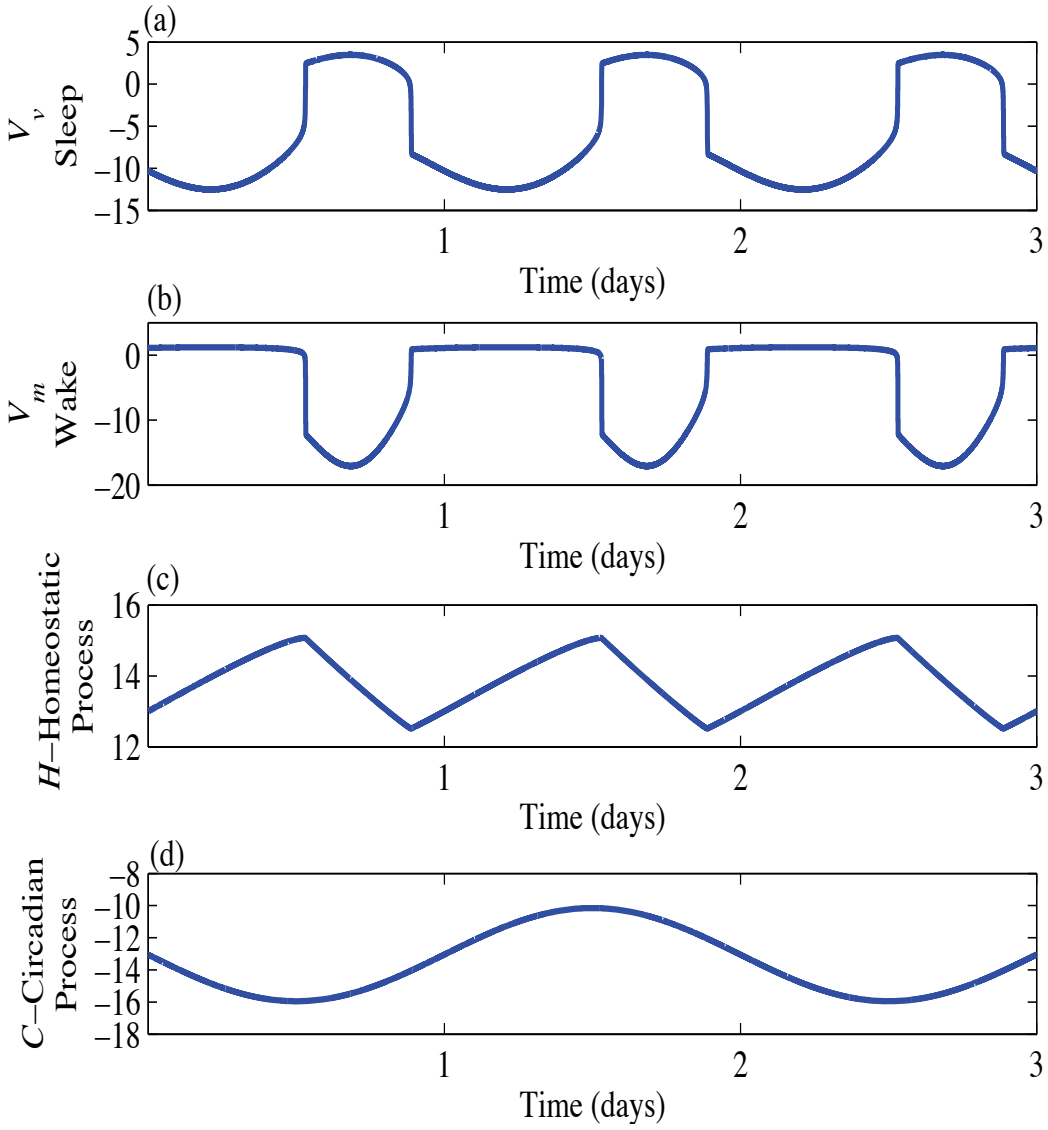

Figure 5.5. An example of an output of Phillips and Robinson's model (2007). (a) V_v the cell potential for VLPO neurons, (b) V_m, the cell potential for MA neurons, (c) the Homeostatic Process and (d) the Circadian Process.

Table 5.4. Values of the model parameters for the Fulcher, Phillips and Robinson sleep model (2008).

Model Parameter	Value
Q_{max}	100 s^{-1}
θ	10 mV
σ	3 mV
A	1.3 mV
ν_{vm}	-2.1 mVs
ν_{mv}	-1.8 mVs
ν_{vh}	1 $mVnM^{-1}$
ν_{vc}	-2.9 mV
μ	4.4 nMs
χ	45 h
τ_m	10 s
τ_v	10 s
c_o	4.5

5.3.2 Rempe, Best, and Terman's Sleep Model

Rempe, Best, and Terman (2010) also developed a sleep model based on the flip-flop concept of sleep regulation. However, unlike the Phillips and Robinson (2007) model they also modeled NREM and REM activity. The basic form of the model equations for wake (x_A, y_A) are,

$$\delta_A \dot{x_A} = f_A(x_A, y_A) - I_V + I_A, \tag{5.16}$$

$$\dot{y_A} = g_A(x_A, y_A), \tag{5.17}$$

and the equations for x_V (sleep promoting activity) are defined in a similar manner,

$$\delta_V \dot{x_V} = f_V(x_V, y_V) - I_A + I_V, \tag{5.18}$$

$$\dot{y_V} = g_V(x_V, y_V), \tag{5.19}$$

where $f(x, y)$ and $g(x, y)$ are defined as,

$$f(x, y) = 3x - x^3 + 2 - y, \tag{5.20}$$

$$g(x, y) = \varepsilon(\gamma H_\infty - y)/\tau(x), \tag{5.21}$$

and H_∞ is a Heaviside function. The aminergic (AMIN) wake promoting neurons are inhibiting the VLPO sleep promoting neurons, as is expected from the flip-flop concept of sleep modeling. As there are numerous equations for this model, the entire set of equations are not listed here but refer to Rempe, Best, and Terman (2010). The form of the equations for the NREM and REM promoting neurons are similar to those listed for wake and sleep, in that the two neuron populations are mutually inhibiting. Circadian and Homeostatic terms in the model largely control the switch from sleep to wake. The switch between NREM and REM sleep is partly controlled through one type of VLPO neuron, the extended eVLPO, which inhibits NREM activity. When the level of eVLPO decreases, NREM sleep is activated. An example of the output of the model simulated using the full model given in Rempe, Best, and Terman (2010) is shown in Figure 5.6.

5.4 Reciprocal Interaction REM Models

McCarley (2007) argued against the flip-flop models for REM sleep regulation. He stated that the model of Lu, Sherman, Devor, and Saper (2006) did not state what the external force is that will lead to an imbalance in REM promoting and REM inhibiting activity which causes the switch, between the two states. Another comment made by McCarley is that transitions from one stage to another are not immediate. It is evident from EEG, and other sleep data, that there are short periods of transitions between sleep states. McCarley instead stated that REM sleep regulation is controlled

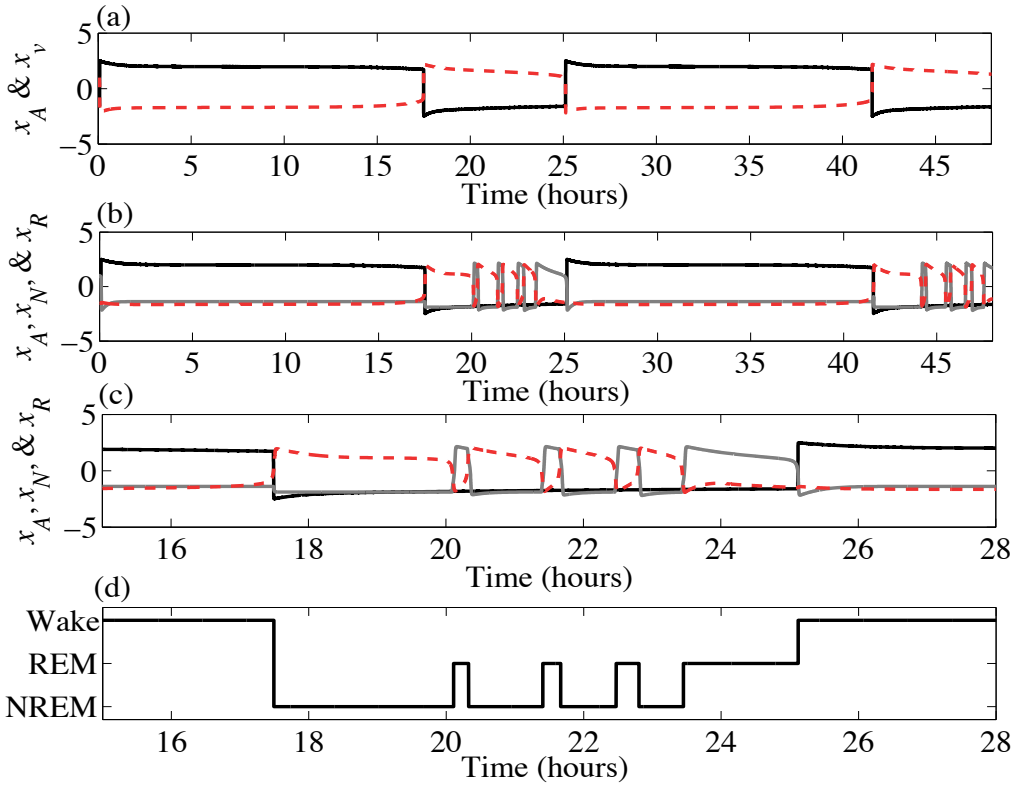

Figure 5.6. An example of the output of Rempe, Best, and Terman's model (2010). (a) Firing rate of aminergic wake promoting x_A (black) and VLPO sleep promoting x_V neurons (red dashed line), (b) firing rate of wake promoting x_A (black), NREM sleep promoting x_N (red dashed line) and REM sleep promoting x_R neuron activity (light gray),(c) firing rate of wake promoting x_A (black), NREM sleep promoting x_N (red dashed line) and REM sleep promoting x_R neuron activity (light gray) between 15 and 28 hours, and (d) scored sleep stages between 15 and 28 hours.

by the reciprocal interaction between REM promoting and REM inhibiting neuron activity. Two models of this reciprocal interaction have been developed and both are described. These models seemed to represent the best approach for modeling REM sleep patterns for normal sleep and have a structure that could be adapted

to incorporate effects of noise disturbance. Therefore they are examined in greater detail than the models that have previously been discussed.

5.4.1 McCarley and Hobson Lotka-Volterra REM Sleep Model

McCarley and Hobson (1971) examined the firing of neurons in the brain during different stages of sleep. The results were used to develop the REM Sleep Reciprocal Interaction Model. To determine which neurons are related to REM sleep they compared the firing rates of different neurons in cats during REM, NREM, and Wake periods. They measured the rate of firing for 69 neurons in 4 different areas; gigantocellular tegmental field (FTG), tegmental fields adjacent to FTG, tegmental reticular nucleus, and the pontine gray matter. They found that firing rates in the FTG cells are greater in REM sleep than in Wake or NREM sleep. This trend was not found in the other cells examined. Therefore, they hypothesized that the FTG cells may excite REM sleep.

Hobson, McCarley, and Wyzinski (1975) further examined individual neuron firings in cats. They found that some LC (locus coeruleus) cells had firing rates that were opposite to those of the FTG cells. Thirteen of 21 LC cells showed a decrease in firing in REM sleep compared to NREM and Wake states. Eight out of the 21 LC cells showed similar trends to those of the FTG cells. It was stated that there must be two types of LC cells. There are LC cells that are related to the excitation of REM sleep and those cells related to the inhibition.

McCarley and Hobson (1975) wanted to model the reciprocal interaction found between some of the LC cells and the FTG cells. They found evidence that the rate of change of activity of the FTG cells is dependent on the current level and is excitatory while the LC cell activity is also dependent on the current level but in an inhibitory fashion. The firing rate of the neurons was non-sinusoidal in behavior, which they

assumed must be due to an interaction between the FTG and LC cells. They decided to model this as a multiplication of the terms representing the FTG and LC cells. The resulting equations they used are known as the Lotka-Volterra equations, X is the level of activity of the FTG or REM promoting (REM-ON) cells and Y is the level of activity of the LC or REM inhibiting (REM-OFF) cells. The two equations of the model are,

$$\dot{X} = aX - bXY, \tag{5.22}$$

$$\dot{Y} = -cY + dXY, \tag{5.23}$$

where a, b, c, and d are positive constants. These equations can also be written as:

$$\dot{X} + \gamma_1 X = 0, \tag{5.24}$$

where $\gamma_1 = (bY - a)$. If $(bY - a) \approx$ constant, then $X \approx e^{-\gamma_1 t}$ and

$$\dot{Y} + \gamma_2 Y = 0, \quad Y = e^{-\gamma_2 t}, \tag{5.25}$$

where $\gamma_2 = (c - dX)$. If $(c - dX) \approx$ constant, then $Y \approx e^{-\gamma_2 t}$.
When γ_1 or γ_2 are less than 0, there is an increase in activity, and when γ_1 or γ_2 are greater than zero there is a decrease in neuron activity. If Y decreases γ_1 becomes negative and X increases, but if X gets too large γ_2 becomes negative and Y increases causing γ_1 to become positive and X decays.

The Lotka-Volterra equations have been extensively studied (Strogatz, 2000), they are often also referred to as Predator-Prey equations. The equilibrium points of the equations can be found by setting the left hand sides of the Equations (5.22) and (5.23) equal to zero. The stability of the equilibrium points can be determined by

calculating the Jacobian J and determining the eigenvalues (λ) for each equilibrium point (Strogatz, 2000),

$$J = \begin{bmatrix} a - bY & -bX \\ dY & -c + dX \end{bmatrix}. \tag{5.26}$$

The equilibrium point at the origin has one positive and one negative eigenvalue,

$$X = 0, \;\; Y = 0, \quad \lambda = a, \; -c, \tag{5.27}$$

and is therefore a saddle point and unstable. The other equilibrium point has two imaginary eigenvalues,

$$X = \frac{c}{d}, \;\; Y = \frac{a}{b}, \quad \lambda = \pm i\sqrt{ca}, \tag{5.28}$$

and is therefore a center. The solution in the phase plane is a set of ellipses. Each elliptical path is neutrally stable. There is a different path for each set of initial conditions.

The dependence of the solution on initial conditions can be more clearly seen by obtaining an intrinsic solution for the Lotka-Volterra equations,

$$\frac{\frac{dY}{dt}}{\frac{dX}{dt}} = \frac{(-c + dX)Y}{(a - bY)X}. \tag{5.29}$$

The solution is,

$$a \; ln(Y) - bY + c \; ln(X) - dX + C(X_o, Y_o) = 0, \tag{5.30}$$

where $C(X_{\mathrm{o}}, Y_{\mathrm{o}})$ is a constant dependent on the initial conditions and is equal to,

$$-a \; ln(Y_o) + bY_o - c \; ln(X_o) + dX_o. \tag{5.31}$$

and ln denotes log_e. When the initial conditions are varied the different solutions in the phase plane can be clearly distinguished. The initial conditions for both X and Y were varied from 0.5 times the original value (X_o=1, Y_o=4.5) to 1.5 times the original value in increments of 0.25 in order to emphasize the differences in the solution paths. The obtained solutions for different initial conditions in the phase plane are shown in Figure 5.7 and in the time domain in Figure 5.8. The initial conditions of the solution clearly have a large effect on the solution both in the magnitude and period of the response.

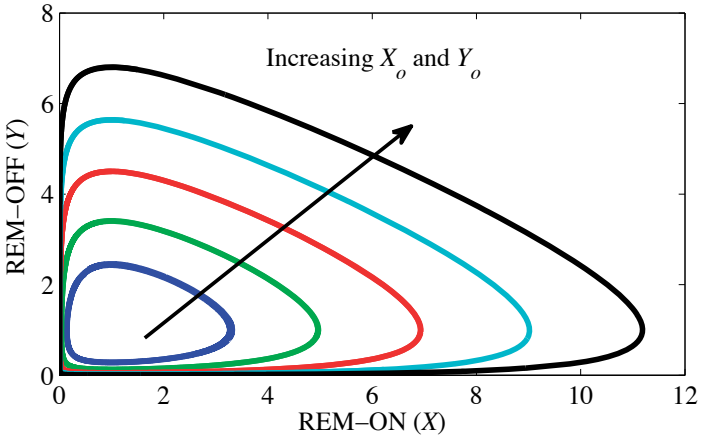

Figure 5.7. Solutions in the phase plane for different initial values of REM-ON (X) and REM-OFF (Y) activity.

The effect of varying the parameters of the model, in addition to varying the initial conditions was also examined. The values for the coefficients in the report by McCarley and Hobson (1975) were used. The coefficients are listed in Table 5.5. The Lotka-Volterra equations can be rescaled, the equation for X becomes,

$$x = (d/c)X, \;\; \dot{x} = a(x - xy), \tag{5.32}$$

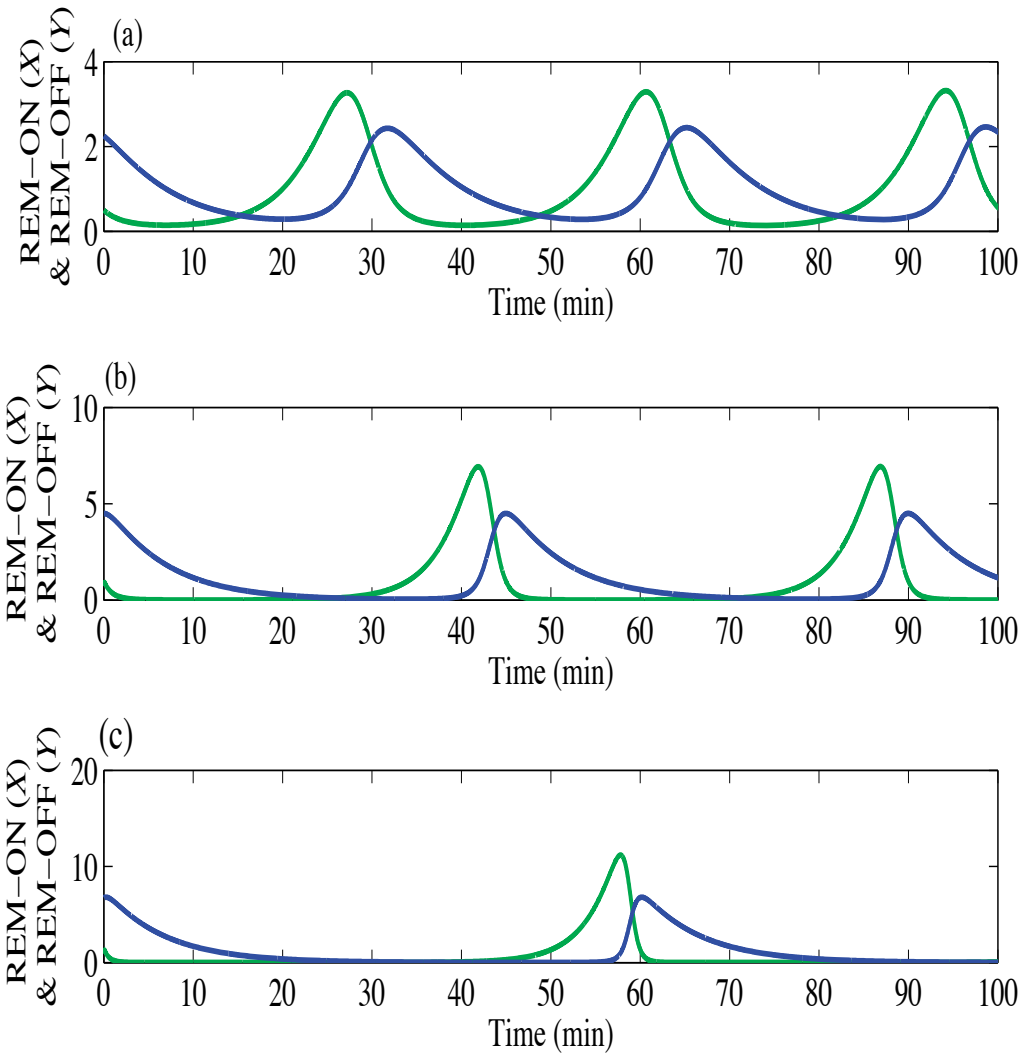

Figure 5.8. REM-ON (X) (green/light gray) and REM-OFF (Y) (blue/black) activity for different initial conditions, (a) 0.5 times the original initial conditions, (b) the original initial conditions, and (c) 1.5 times the original initial conditions.

and the equation for Y becomes,

$$y = (b/a)Y, \;\; \dot{y} = c(-y + xy). \tag{5.33}$$

Therefore, according to McCarley and Massaquoi (1986) the dynamic behavior of the equations is dominated by the a and c terms and b and d just scale the responses. In Table 5.5 the coefficients for a and b, and c and d are equivalent. Despite the ability to simplify the equations, the effect that varying all four coefficients (a, b, c, and d) has on the solution was examined because the intersection of the X and Y curves (affected by b and d) is used to define REM thresholds.

Table 5.5. Coefficients of the REM Reciprocal Interaction model (McCarley and Hobson, 1975).

Coefficient	Original Value
a	0.3029
b	0.3029
c	0.1514
d	0.1514
Xo	1.0
Yo	4.5
Phase	2.3

In the absence of Y, the coefficient a determines the exponential growth of X (REM-ON) activity. An increase in a will increase the growth rate of X. This increase in X will also increase the growth of Y. These changes are shown in Figure 5.9. The result is that when a is increased the number of REM cycles increase and the length of REM sleep during a given cycle decreases. The duration of REM sleep is defined by a threshold. The threshold level is based on the point at which REM-OFF activity intersects REM-ON activity as depicted in Figure 5.10.

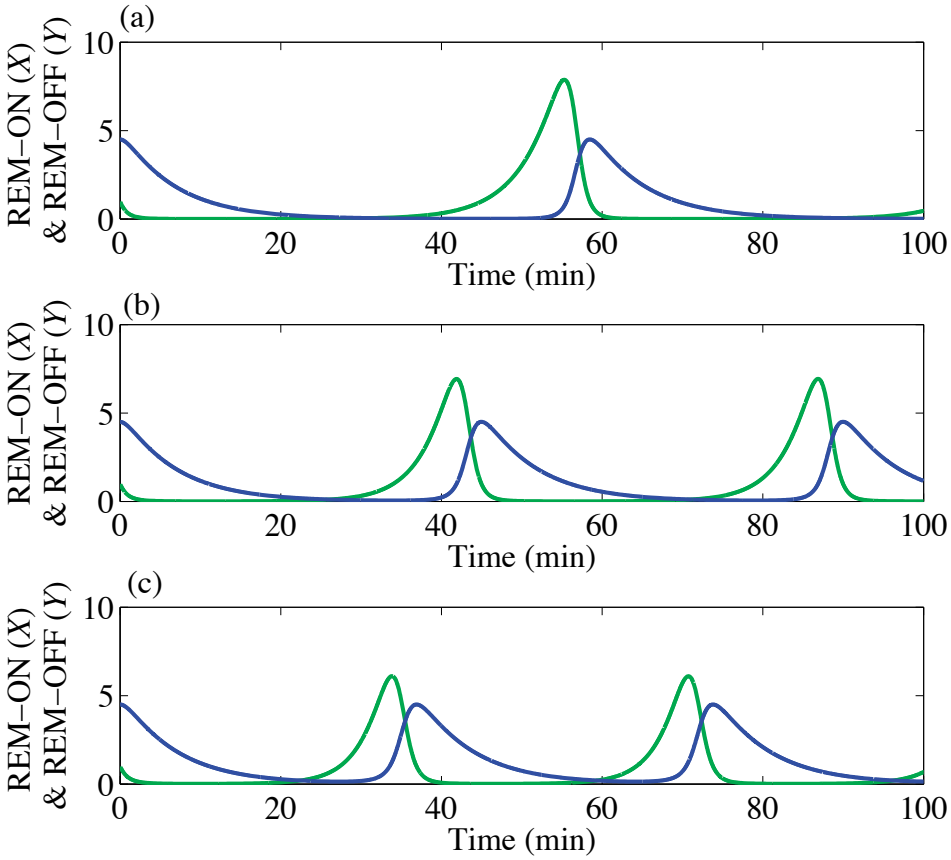

Figure 5.9. Results for different values of a, (a) $a = 0.75$ times the original coefficient, (b) $a =$ the original coefficient value, and (c) $a =$ 1.25 times the original coefficient. REM-ON (X) (green) and REM-OFF (Y) (blue). See Table 5.5 for original values. Note the decrease in the X-Y period with increased a.

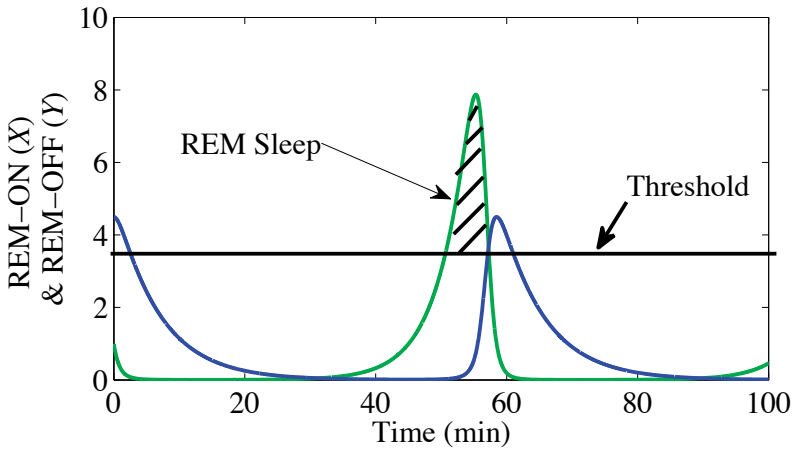

Figure 5.10. Example of how the threshold for REM sleep is determined. REM-ON (X) (green) and REM-OFF (Y) (blue).

The coefficient b determines the inhibiting effect that Y (REM-OFF) cells have on the level of X (REM-ON) activity. When b is increased the rate of increase of X (REM-ON) activity decreases, therefore the first cycle occurs later and the number of REM cycles decreases. Increasing b will also decrease the rate of increase of Y (REM-OFF) activity. The result is that the duration of REM sleep during a given cycle will increase, which is shown in Figure 5.11.

The coefficient c determines the inhibiting effect that the activity of Y (REM-OFF) cells have on themselves. If the value of c is increased, this leads to an increase in the decay rate of Y. The level of Y activity becomes low which is why in Figure 5.12 the X (REM-ON) activity grows to a higher level when c is increased. An increase in the coefficient c also results in an increase in the number of REM cycles and an increase in the duration of REM sleep for one cycle.

The coefficient d determines the excitatory effect of X (REM-ON) cells on Y (REM-OFF) cells. This coefficient affects the rate of growth of the Y (REM-OFF) activity. An increase in d will cause an increase in Y activity which results in a decrease in the level of X (REM-ON) activity, which is shown in Figure 5.13. Increasing d also results in a decrease in the duration of REM sleep for one cycle.

From varying all of the coefficients in the Lotka-Volterra equations, it was found that changing the level of coefficients had an affect on the number of REM cycles during a given period of time. Also the duration of REM sleep during one sleep cycle changed. Coefficients a and d caused a decrease in duration of REM sleep for one cycle, while the coefficients b and c caused an increase. The change in the duration of REM sleep for one sleep cycle when the model coefficients were varied is listed in Table 5.6.

Table 5.6. Duration of REM sleep and period of X in minutes for different coefficient values. (See Table 5.5 for original values of a, b, c, and d).

	Coefficient	0.75 times the Original Value	Original Value	1.25 times the Original Value
REM Duration	a	6.4	5.1	4.3
	b	4.5	5.1	5.5
	c	5.0	5.1	5.2
	d	6.1	5.1	4.4
REM Period	a	58.4	45.0	36.9
	b	38.3	45.0	52.2
	c	55.9	45.0	38.5
	d	45.1	45.0	45.1

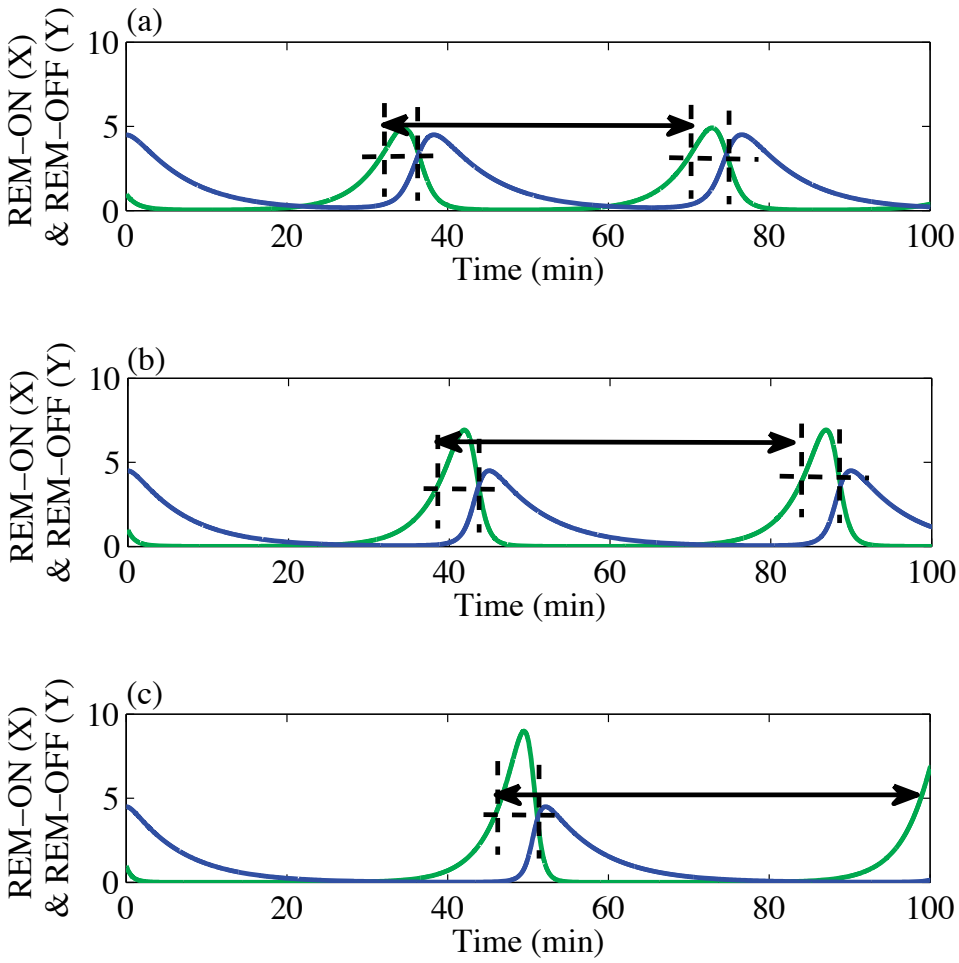

Figure 5.11. Results for different values of b, (a) $b = 0.75$ times the original coefficient, REM duration = 4.5 minutes and REM period = 38.3 minutes, (b) b = the original coefficient value, REM duration = 5.1 minutes and REM period = 45.0 minutes and (c) $b = 1.25$ times the original coefficient, REM duration = 5.5 minutes and REM period = 52.2 minutes. REM-ON (X) (green) and REM-OFF (Y) (blue). See Table 5.5 for original values. Note the increase of the X-Y period with increased b.

5.4.2 REM Limit Cycle Reciprocal Interaction Model (LCRIM)

McCarley and Massaquoi (1986) updated the REM Reciprocal Interaction model. One of the primary reasons for updating the model was that the behavior of the

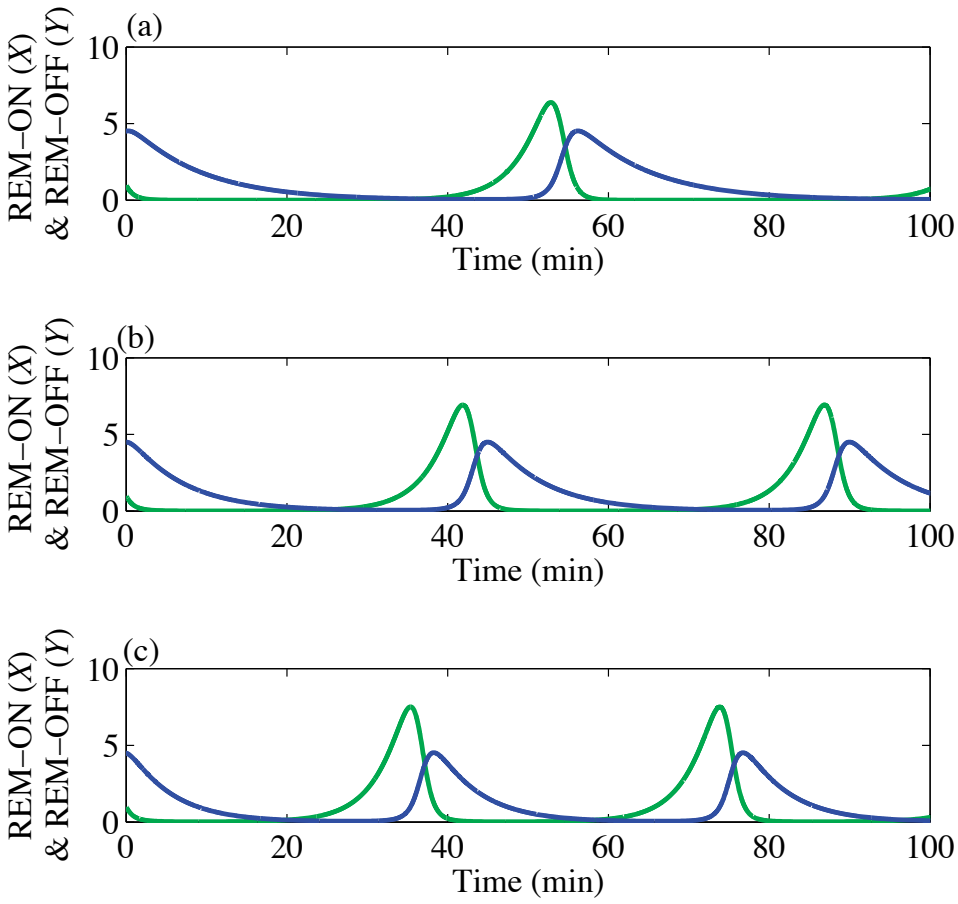

Figure 5.12. Results for different values of c, (a) $c = 0.75$ times the original coefficient, (b) $c =$ the original coefficient value, and (c) $c =$ 1.25 times the original coefficient. REM-ON (X) (green) and REM-OFF (Y) (blue). See Table 5.5 for original values. Note the decrease in the X-Y period with increased c.

Lotka-Volterra model is highly dependent on the initial conditions. They decided to model the reciprocal interaction of REM neuron activity as a limit cycle model. The solutions for a limit cycle model are a group of spirals that all converge to the same path (Strogatz, 2000) unlike the Lotka-Volterra equations. Initial conditions determine whether the limit cycle is approached from the interior or exterior.

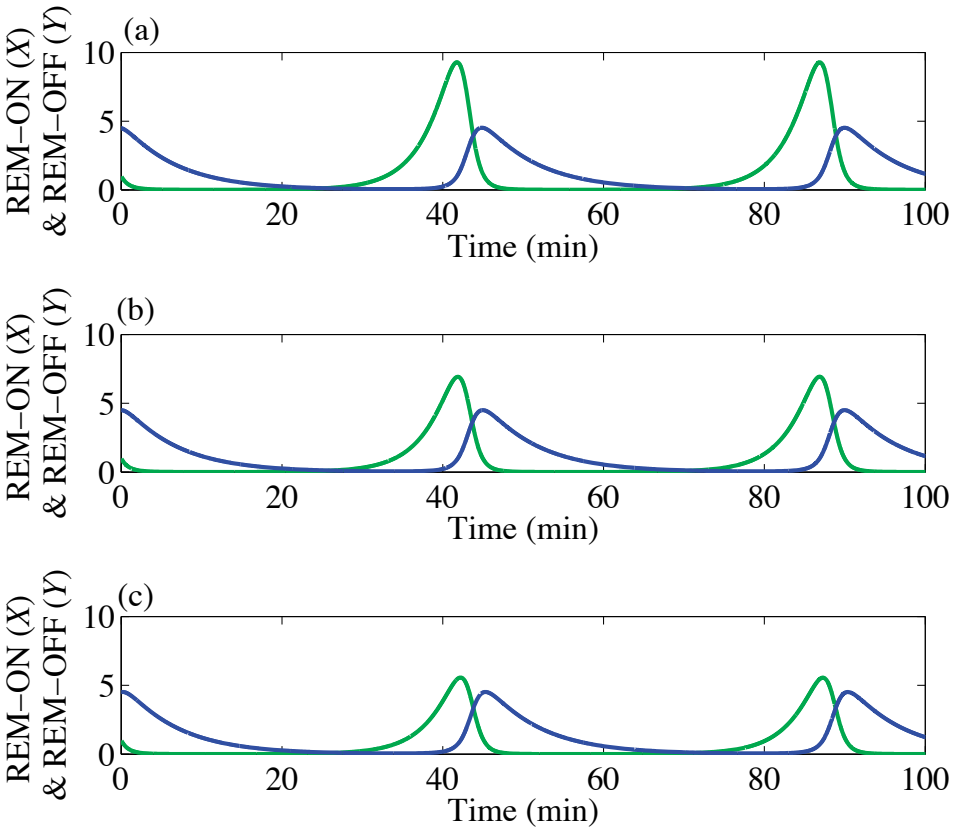

Figure 5.13. Results for different values of d, (a) $d = 0.75$ times the original coefficient, (b) $d =$ the original coefficient value, and (c) $d =$ 1.25 times the original coefficient. REM-ON (X) (green) and REM-OFF (Y) (blue). See Table 5.5 for original values. Note the small change in the X-Y period with increased d.

The difference between the Limit-Cycle model and the Lotka-Volterra model that was previously described is that the coefficients a and b are now functions of the level of X (REM-ON activity) and there are two saturation functions that have been added which limit the growth of X and Y activity. The Limit-Cycle model equations are,

$$\dot{X} = a(X)S_1(X)X - b(X)XY, \tag{5.34}$$

$$\dot{Y} = -cY + d_{circ}S_2(Y)XY, \tag{5.35}$$

$$a(X) = 2 - 1.8\left(1 - \frac{1}{1 + e^{-4(X-0.5)}}\right), \tag{5.36}$$

$$b(X) = \frac{2}{1 + e^{-80(X-0.1)}}, \tag{5.37}$$

$$S_1(X) = 1 - 1.4\left(\frac{1}{1 + e^{-0.8(X-2.5)}}\right) + 0.167, \tag{5.38}$$

$$S_2(Y) = 1 - 1.5\left(\frac{1}{1 + e^{-20(Y-2)}}\right). \tag{5.39}$$

The term d_{circ} in Equation (5.35) accounts for the circadian variation in sleep. It is a sinusoidal function with a period of 24 hours. Each of the coefficients and saturation functions are shown in Figure 5.14. The function $a(X)$ reduces the growth rate of X when the level of X is low. Therefore $a(X)$ decreases the level of X and Y for the first cycle, but it will cause a large increase in level of X and Y for the second cycle because a low level of Y will lead to an increase in the growth of X. The purpose of $b(X)$ is to prevent the level of X activity from decaying to zero. When X is low the second term, *b(X)XY* in Equation (5.34), will also be low and will be less than the first term in the equation. $S_1(X)$ limits the growth of X and $S_2(Y)$ limits the growth of Y.

The effect of the term d_{circ} on the solution was examined. This circadian term affects the growth rate of Y. When the phase is changed so is the number of REM cycles. Also a change in phase will result in each REM period having a different duration. Without d_{circ}, the duration of each REM cycle would be the same. For the results shown in Figure 5.15 (a) the duration of the first REM cycle is 18.7 minutes, the duration of the second cycle was 25.2 minutes, the third cycle was 28.3 minutes, and for the fourth REM cycle the duration was 30.0 minutes.

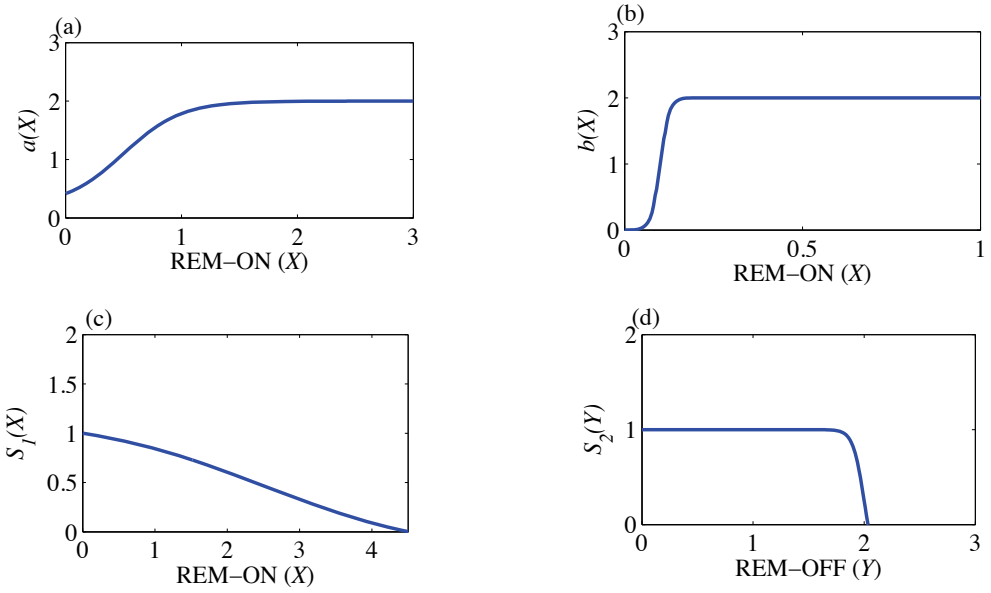

Figure 5.14. Coefficient and saturation functions for the REM Limit Cycle Reciprocal Interaction model; (a) $a(X)$, (b) $b(X)$, (c) $S_1(X)$, and (d) $S_2(X)$.

5.5 Two Process Model of Slow Wave Activity

In addition to models of REM sleep there are also models that have been developed to predict slow wave activity during the night which is related to the depth of sleep. A model developed by Achermann and Borbély (1990) is referred to as the Two Process Model. This model is based on the results of laboratory studies by Borbély, Baumann, Brandeis, Strauch, and Lehmann (1981) in which they measured sleep using polysomnography for two baseline nights and for two recovery nights following 40.5 hours of sleep deprivation. They found that during the recovery night there was a greater need for sleep which resulted in an increase in slow wave activity particularly in the first sleep cycle. Slow wave activity is measured by calculating the power between 0.5 and 4.5 Hz in the EEG signal. They also found that there was an exponential decay in the amount of slow wave activity during the night. These two observations serve as the foundation of the Two Process Model.

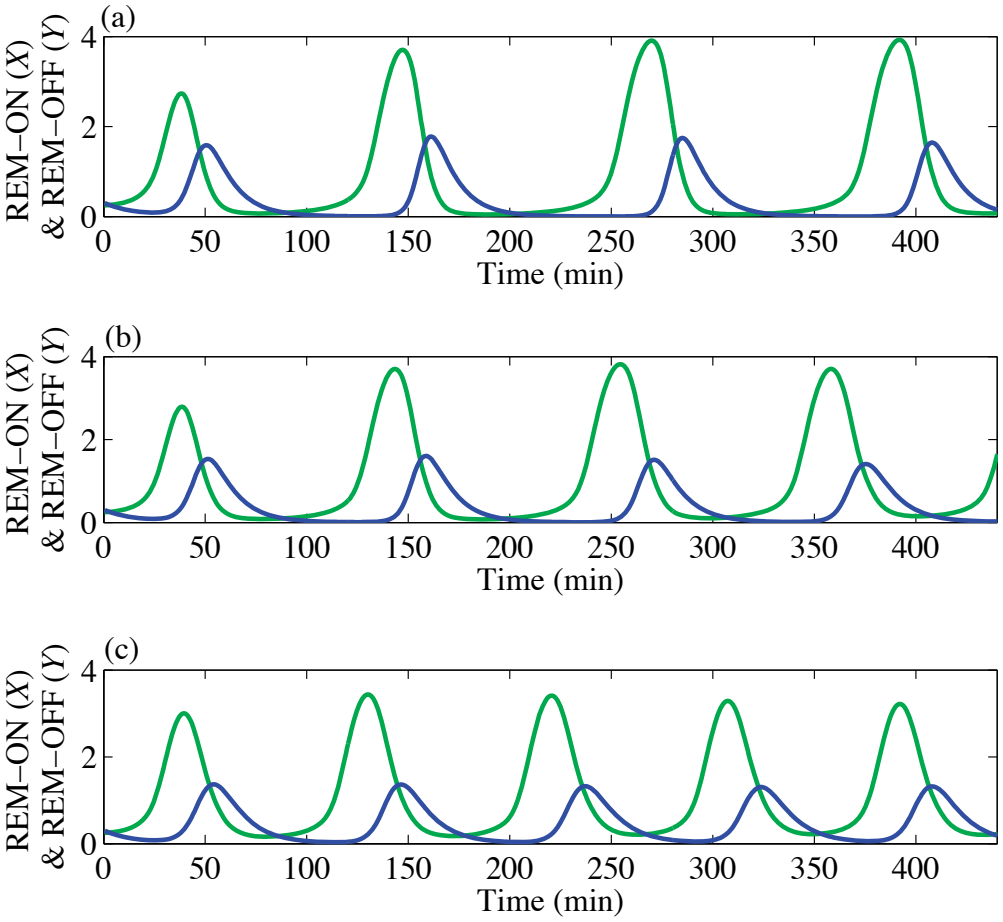

Figure 5.15. Solutions for a different phase of d_{circ}; (a) 0.5 times the original phase, (b) original phase = 2.3, and (c) 1.5 times the original phase. REM-ON (X) (green/light gray) and REM-OFF (Y) (blue/black).

One process accounted for in the model is the Homeostatic process, called Process S, which increases while an individual is awake and decreases during sleep. The longer a person is awake the greater their need for sleep and the greater the level that Process S is at the beginning of the sleep period. The decay of Process S is approximately exponential, but is dependent on the level of slow wave activity (SWA). The equation for Process S is,

$$\dot{S} = -gc\, SWA. \tag{5.40}$$

The model also predicts the amount of slow wave activity (SWA). The level of slow wave activity varies during the night in cycles, it increases when an individual is in Stage 3 or 4 and decreases when the individual is in REM sleep or Stages 1 and 2. The equation for slow wave activity is,

$$\dot{SWA} = rc\, SWA \left(1 - \frac{SWA}{S}\right) - fc\, SWA\, REMT + SWA\, n(t). \tag{5.41}$$

The values for the coefficients of the model are in Table 5.7, and S_o and SWA_o are the values of S and SWA, respectively, at the start of sleep (t=0). In Equation (5.41) *n(t)* is Gaussian random noise with a zero mean and a standard deviation of 0.2. The term $REMT$ refers to a REM trigger. This trigger is equal to 1 during REM sleep and 0 during NREM sleep. The REM trigger causes the level of slow wave activity to increase when REM sleep is not occurring and to decrease when REM sleep is occurring.

An estimate of the timing of REM sleep ($REMT$), that was used for simulations, was obtained from the data of the 1999 UK study (Flindell et al., 2000). The dataset includes information on the sleep stages each subject was in during the night. Therefore, the time when an individual is in REM sleep and not in REM sleep could be determined. The value of $REMT$ was set equal to 1, 12 minutes before REM sleep

Table 5.7. Coefficients of the Two Process Model (Achermann and Borbély, 1990).

Coefficient	Original Value
rc	0.2
fc	0.4
gc	0.008
S_o	0.624
SWA_o	0.007

began in the data so that a decrease in slow wave activity could occur before the onset of REM sleep. This procedure was also done by Achermann and Borbély (1990). Figure 5.16 contains an example of results obtained using Achermann and Borbély's model, using the timing of REM sleep, determined for two different subjects in the UK study. The values of $REMT$ were rescaled in this plot for viewing purposes only.

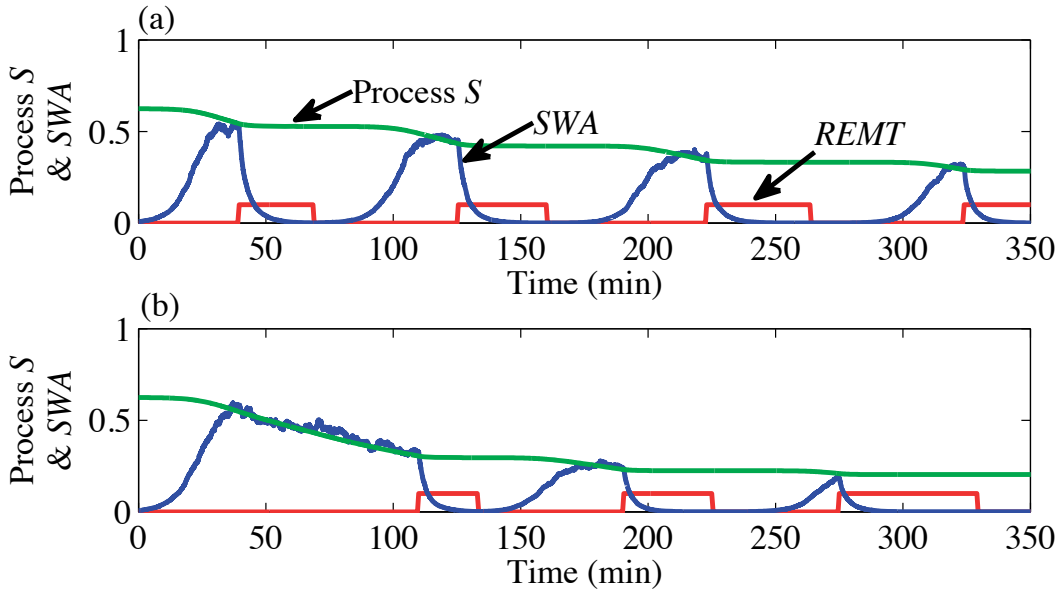

Figure 5.16. Example of results from Achermann and Borbéy's Two Process Model (1990). Process S (Green), slow wave activity (SWA) (Blue), and scaled $REMT$ (Red). (a) Example 1 and (b) Example 2.

In order to further understand the model a parameter variation study was conducted. The term for Gaussian noise (*n(t)* in Equation (5.41)) was not included when results were obtained in order to better demonstrate the effect that each individual coefficient has on the solutions. For the parameter variation study, the nonlinear equations were solved by using the *ode45* solver in Matlab.

In Equation (5.41), rc is the rise constant. The original value was varied from 0.8 times the original value to 1.2 times the original value in increments of 0.1. The slow wave activity obtained for different values of rc is shown in Figure 5.17. When the value of rc is increased the rise time of slow wave activity decreases.

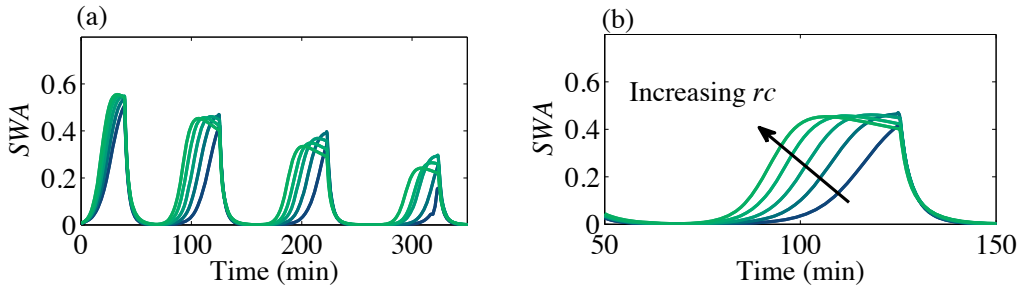

Figure 5.17. Slow wave activity for different values of rc. (a) Slow wave activity for the entire night and (b) slow wave activity between 50 and 150 minutes.

The term fc in Equation (5.41) is called the fall constant. The value of fc was varied from 0.5 times the original value to 1.5 times the original value in increments of 0.25. The effect that fc has on the level of slow wave activity is shown in Figure 5.18. When the value of fc is increased, the rate of fall of slow wave activity increases. Also the minimum level of slow wave activity during the REM period decreases. This decrease in the minimum level results in an increase in rise time for the next NREM sleep cycle. The level of SWA reaches a maximum later and the shape of SWA changes.

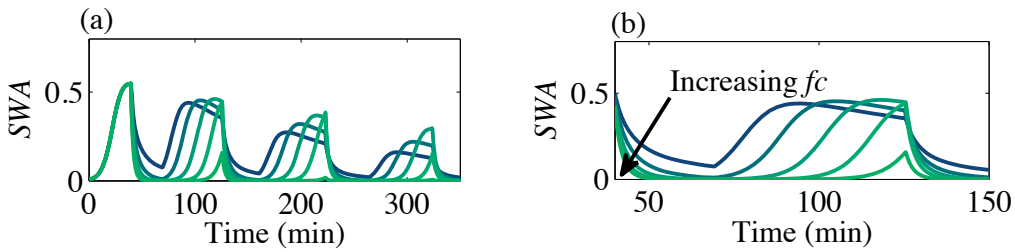

Figure 5.18. Slow wave activity for different values of fc. (a) Slow wave activity for the entire night and (b) slow wave activity between 40 and 150 minutes.

The equation for Process S contains only one coefficient gc, which is referred to as the gain constant. The original value was varied from 0.8 times the original value to 1.2 times the original value in increments of 0.1. When gc is increased it will result in a lower level of Process S and slow wave activity. These changes are shown in Figure 5.19.

The initial values of slow wave activity and Process S were also varied. The initial value of Process S (S_o) was varied from 0.8 times the original value to 1.2 times the original value in increments of 0.1. The initial value of slow wave activity (SWA_o) was varied from 0.5 times the original value to 1.5 times the original value in increments of 0.25. The resulting changes in the solutions are shown in Figure 5.20. Increasing S_o results in a higher level of Process S and slow wave activity for the entire night. Increasing SWA_o results in an earlier increase in SWA for the first sleep cycle, though the change is small. An overview of how each coefficient affects the solution of the model is listed in Table 5.8.

Several variations in the form of the equations for the Two Process Model have been proposed including an extra S term in the SWA equation and the addition of a lower bound for the slow wave activity (Achermann and Borbély, 1992),

$$\dot{SWA} = rc\,SWA\ (S - SWA) - fc\,(SWA - SWA_L)REMT. \tag{5.42}$$

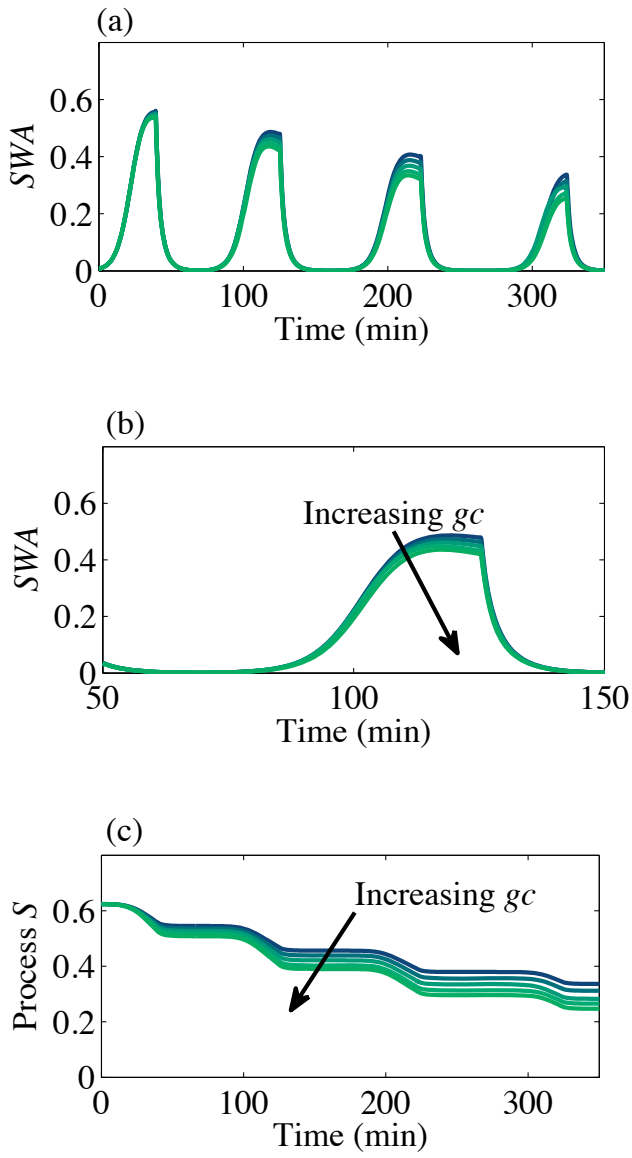

Figure 5.19. Results for different values of gc. (a) Slow wave activity, (b) slow wave activity from 50 and 150 minutes, and (c) Process S.

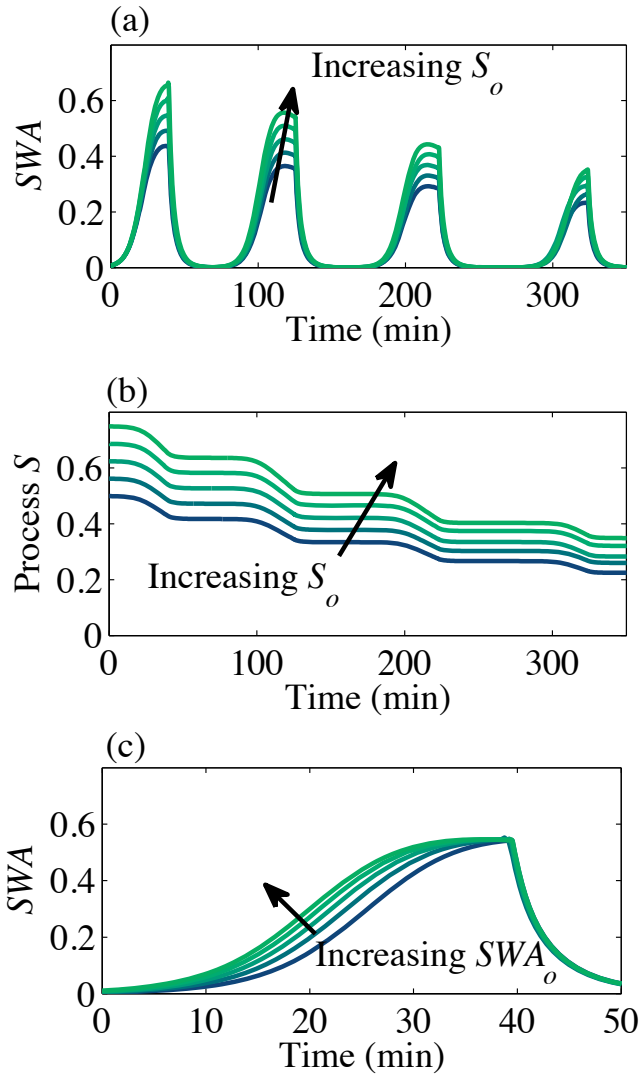

Figure 5.20. (a) Slow wave activity and (b) Process S for different initial values of Process S (S_o). (c) A close-up of slow wave activity between 0 and 50 minutes for different initial values of SWA (SWA_o).

Table 5.8. Effect of an increase in coefficient value on the solution of the Two Process Model.

Coefficient	SWA	Process S
rc	Decrease in rise time	No significant change
fc	Decrease in fall time Increase in rise time	No significant change
gc	Decrease in level	Decrease in level
S_{o}	Increase in level	Increase in level
SWA_{o}	Earlier increase in level for first sleep cycle	No significant change

The additional S term primarily affects the shape of the SWA activity. The changes are shown in Figure 5.21. The SWA_L term acts as a lower asymptote.

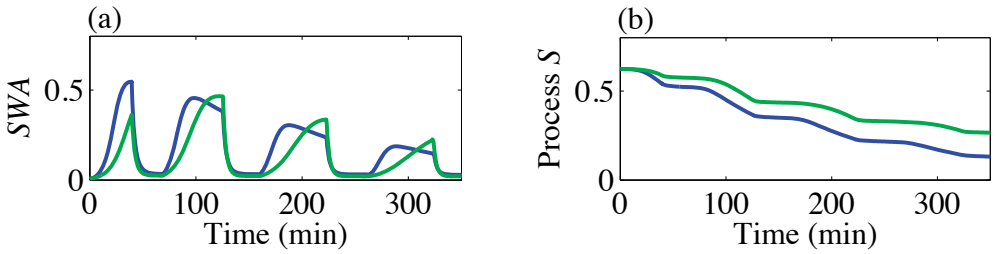

Figure 5.21. Illustration of the effect of the extra S term on the outcome of slow wave activity, without the extra term (blue/black) and with the extra term (green/light gray). (a) SWA and (b) level of Process S for the entire night.

Two other variations in the form of the model have been proposed which includes a different form of the Process S equation (Achermann, Dijk, Brunner, and Borbély, 1993),

$$\dot{SWA} = \frac{rc}{Su}\, SWA\ (S - SWA) - fc\,(SWA - SWA_L)REMT, \tag{5.43}$$

$$\dot{S} = -gc\, SWA + rs(S_u - S). \tag{5.44}$$

An upper asymptote S_u was added to the model. Increasing S_u results in an increase in slow wave activity. Also, for some variations of the Two Process Model, the Gaussian noise term $n(t)$ (which has a zero mean and a standard deviation of 0.18) is applied within the differential equation (Achermann and Borbély, 1990), and in other variations the noise is applied to SWA after solving the differential equations,

$$SWA := SWA(1 + n(t)). \tag{5.45}$$

Due to the slow dynamics of the SWA equation, the noise term causes smaller, lower frequency oscillations when it is within the differential equation. A version of the

model in Achermann, Dijk, Brunner, and Borbély (1993) also has a term for brief awakenings,

$$\dot{SWA} = rc\, SWA\ (S - SWA) - fc\,(SWA - SWA_L)REMT - fcw\,(SWA - SWA_L)w(t), \tag{5.46}$$

where $w(t)$ is equal to one when awake and zero otherwise. A specification of timing and duration of the awakenings used to simulate normal sleep, spontaneous awakenings, was not specified.

5.6 Combined Two Process SWA and Reciprocal Interaction REM Models

In order to predict both REM and slow wave activity, several models have been developed which have combined one of the variants of the Two Process Model and the Reciprocal Interaction REM Model.

5.6.1 REM and Slow Wave Activity LCRIM-Based Integrated Sleep Control Model

Massaquoi and McCarley (1992) developed a model called the LCRIM-based Integrated Sleep Control Model (LCRIM/I). The coefficients of the model are in Table 5.9. The equation for REM-ON (X) activity is the same as in the LCRIM model,

$$\dot{X} = a(X)S_1(X)X - b(X)XY. \tag{5.47}$$

One change was made to the equation for REM-OFF (Y) activity. An excitatory term E was added to the equation,

$$\dot{Y} = -cY + d_{circ}S_2(Y)(X + E)Y. \tag{5.48}$$

The addition of E allows spontaneous awakenings to be predicted. The term E represents neuron activity from the forebrain or brainstem that act as an excitatory input to the REM-OFF neurons. The equation for the excitatory term E is,

$$\dot{E} = N - kE, \tag{5.49}$$

The equation can also be written as,

$$\dot{E} + kE = N. \tag{5.50}$$

This is a first order system and behaves as a low pass filter with a cut-off frequency of k rad/time units. The equation for the frequency response and the cut-off frequency for the filter is defined as,

$$H(\omega) = \frac{1}{j\omega + k}, \tag{5.51}$$

$$\omega_c = k. \tag{5.52}$$

For a step input $N = N_o$ for $t <= 0$ and $N = N_1$ for t >0,

$$E = \frac{1}{k}(N_1 - (N_1 - N_o)e^{-kt}). \tag{5.53}$$

The term N is a Poisson noise process. A Poisson process is one in which the inter-arrival time between pulses T follows an exponential distribution $p(T) = e^{-\gamma T}$ for $T \geq 0$ and $p(T) = 0$ for $T < 0$ which for this model had a mean $(1/\gamma)$ of 1.1. The shape of the pulses were assumed to be square waves and with varied amplitude and duration. The amplitude is uniformly distributed from 1.25 to 25 and the duration is uniformly distributed from 2.7 to 5.4 minutes. E exponentially increases and decreases. The

excitatory term (E) can also be thought of as low pass filtered impulse noise. An example of N and E for 1 pulse are shown in Figure 5.22.

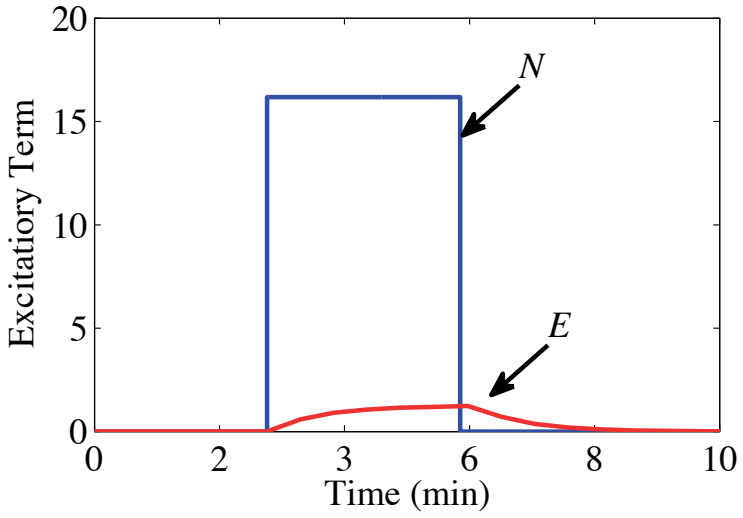

Figure 5.22. An example of the terms for excitation, N and E, ($k = 10$).

The amplitude of the excitatory term E is greatly reduced compared to the level of the noise term N. The form of Equation (5.50) does not allow the cutoff frequency of the lowpass filter and the gain of the filter to be controlled independently. A correction should perhaps be applied to the model to allow the two to be separately defined, e.g.,

$$\dot{E} + kE = kAN. \tag{5.54}$$

where k is the cut-off frequency and A is the gain.

Massaquoi and McCarley (1992) also made a change to the equation for slow wave activity,

$$\dot{SWA} = rc\, SWA(1 - SWA/SWA_{max}) + SWA\, n(t). \tag{5.55}$$

The REM trigger was removed and a dependency on the level of REM-ON (X) behavior through the term $SWA_{\max}$was added,

$$SWA_{max} = max(S(1 - 0.95\ min(X^4 + E/2, 1.0)), 0.05). \tag{5.56}$$

This term also includes a dependence on the excitatory term E, which causes a decrease in the level of SWA. The equation for the homeostatic Process S is of the form,

$$\dot{S} = -gc\ SWA + rs(1 - S), \tag{5.57}$$

Using this model, the time spent in NREM, REM, and Wake states can be determined. Massaquoi and McCarley (1992) classified REM when the level of X (REM-ON) activity exceeded 1.4, Wake is scored when the slow wave activity is below 0.1 and the level of E exceeds 0.5 and the remaining time is classified as NREM sleep. An example of how the outputs of the model could be used to classify sleep states is shown in Figure 5.23. The values for the coefficients of the model are listed in Table 5.9.

The excitatory term E causes a decrease in the slow wave activity and causes an increase in the Y (REM-OFF) activity. This increase in Y can lead to an increase in the duration of NREM periods and a decrease in REM sleep. An example of the outcome for more noise is shown in Figure 5.24 along with the results for the original level. For this example, the amplitude of N was increased by 50% and exactly the same process was used (just scaled). The noise term ($n(t)$) was not included in the SWA equation for this comparision as the desire was to purely observe the effect of E on the model ouput. Increasing the interarrival time or duration of the events will similarly also lead to a greater decrease in slow wave activity and REM-ON activity.

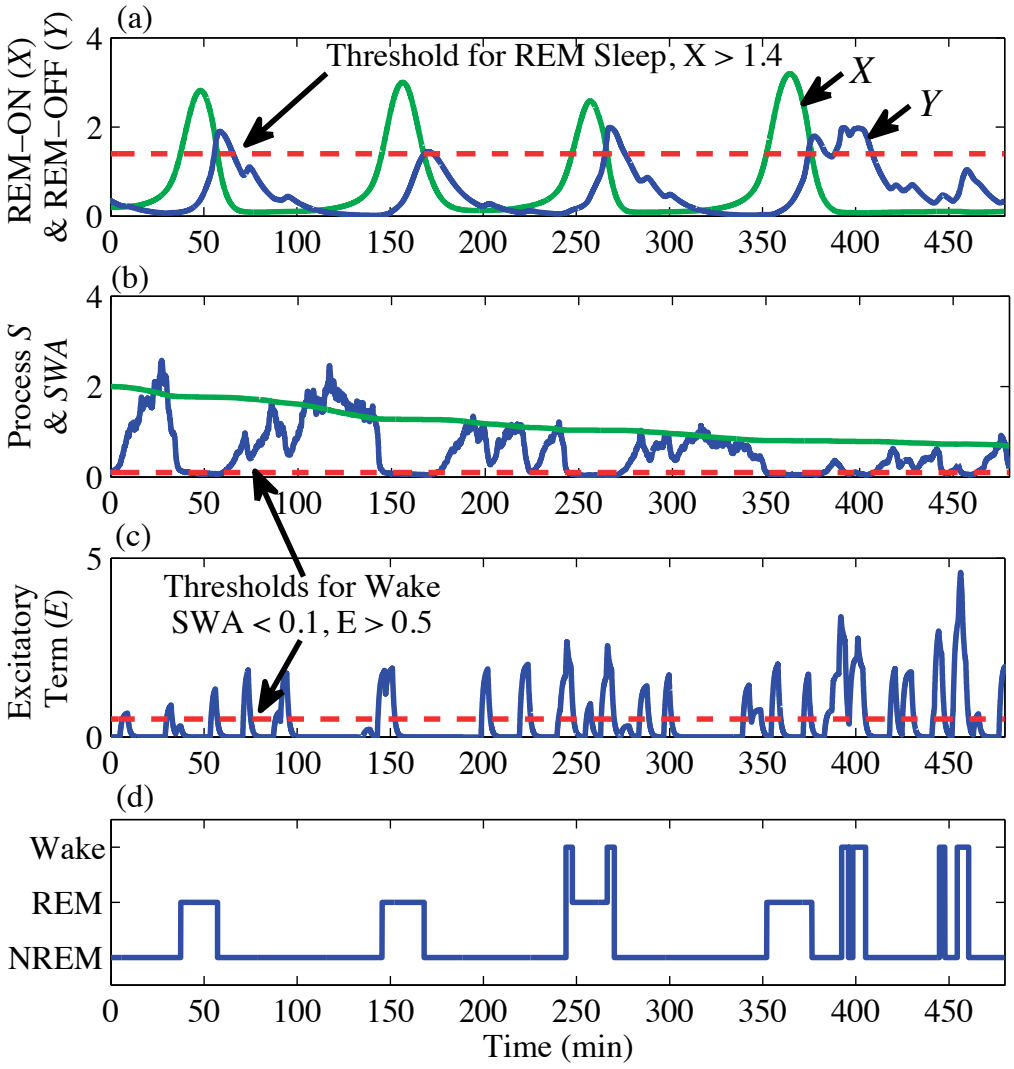

Figure 5.23. An example of using Massaquoi and McCarley's LCRIM/I model (1992) to classify sleep stages, (a) REM-ON (X) (green) and REM-OFF (Y) (blue) activity, (b) Process S and SWA, (c) Excitatory Activity (E), and (d) sleep stages. Thresholds used for scoring sleep stages (red-dashed lines).

Table 5.9. Coefficients of Massaquoi and McCarley's LCRIM/I Model (1992).

Model Parameters	Original Values
c	1
gc	0.05
k	10
rc	3.0
rs	0.005
E_o	0.001
X_o	0.12
Y_o	0.35
S_o	2.0
SWA_o	0.1
N Amplitude	Uniformly distributed between 1.25 and 25
N Duration	Uniformly distributed between 0.25 and 0.5
N Inter-arrival Time	Exponentially distributed with mean of 1.1
n	Uniformly distributed between -10 and 10

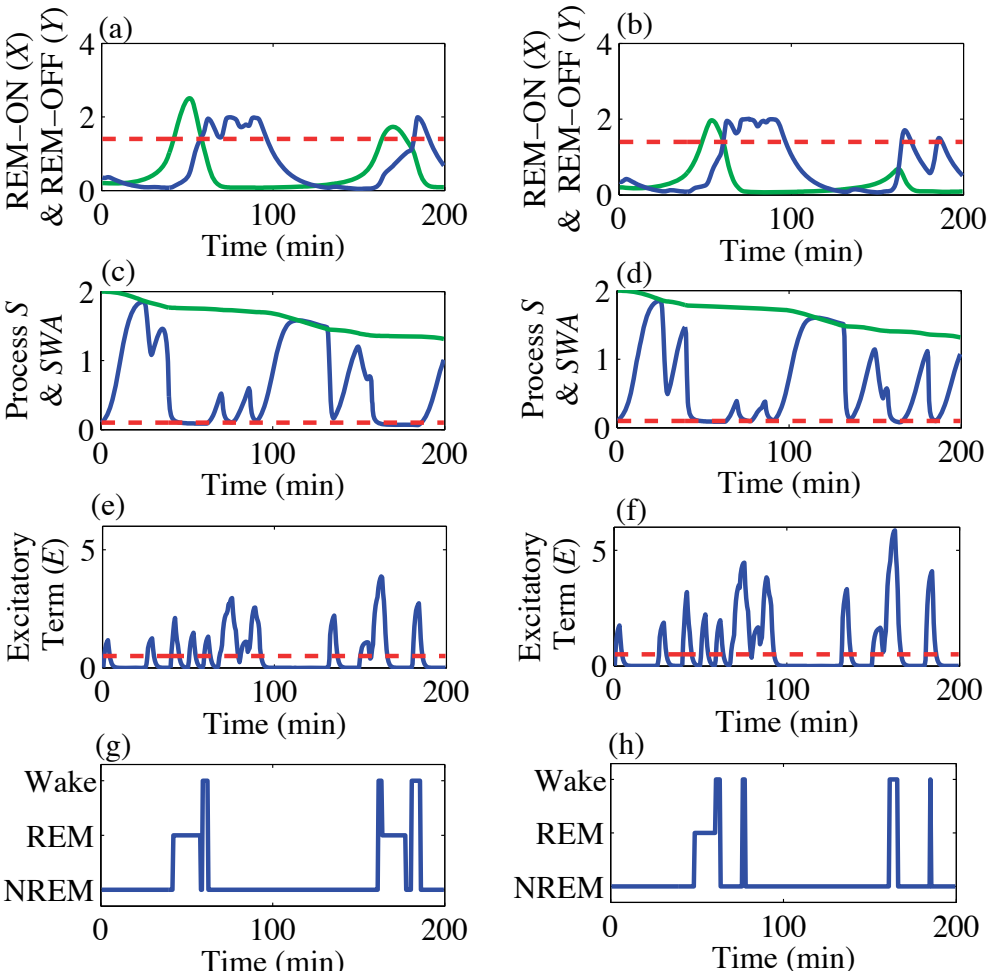

Figure 5.24. The effect of changing the amplitude of N on the level of X (REM-ON) (green), Y (REM-OFF) (blue), and slow wave activity (SWA). (a,c,e,g) variation of amplitudes was based on the original model parameters, (b,d,f,h) amplitudes of N used to obtain E was increased by 50%, (Thresholds used for scoring sleep stages, red-dashed lines).

5.6.2 Acherman and Borbély's Combined REM and Slow Wave Activity Model

Achermann and Borbély (1992) also combined the Two Process Model with the REM Sleep Limit-Cycle Reciprocal Interaction model (LCRIM). They combined the two models by using the value of REM-ON (X) activity to determine when to initiate the REM trigger. When the level of X activity is greater than 1.4, $REMT$ is equal to 1, otherwise it is equal to 0. This model, unlike the Integrated Sleep Control model (LCRIM/I), is a 24 hour model. The main purpose of extending the model to 24 hours is that Achermann and Borbély (1992) also included a model for predicting alertness during the day. The alertness portion of the model, though, will not be discussed further because the emphasis of this research is on predicting sleep. The equations for the REM model are the same as those used in the LCRIM/I model,

$$\dot{X} = a(X)S_1(X)X - b(X)XY, \tag{5.58}$$

$$\dot{Y} = -cY + d_{circ}S_2(Y)(X + E)Y, \tag{5.59}$$

however, the term E is very different. The excitatory term is defined as,

$$E = e + 0.95W. \tag{5.60}$$

where e is defined as,

$$e = 0.39 + 0.3C_{SO} - \frac{0.05}{10.7}(t - t_{SO}) \text{ if } e > 0 \text{ else, } e = 0. \tag{5.61}$$

The term e, in Equation (5.60), has a small effect on the results. This term, is dependent on the value of the circadian oscillator C at sleep onset (C_{SO}) and linearly decreases with time. However this decrease is for only a short time period, until e becomes less than zero, at which point it is reset to 0. Changing the value of C_{SO}

will either slightly increase or slightly decrease the number of ultradian oscillations. The term t_{SO} is the time of sleep onset.

The purpose of E in this model is to turn off the ultradian oscillations. Ultradian oscillations are the oscillations in the slow wave activity, or REM and NREM sleep during the night. When the sleep period has ended W (Wake) is equal to 1, during sleep it is equal to zero. E becomes a large number when W is 1. This high level of E causes an increase in Y (REM-OFF) activity which causes the ultradian oscillations during the night to end.

The final difference between this model and the LCRIM/I model is the circadian oscillator term. In the combined model developed by Massaquoi and McCarley (1992), the circadian dependence was modeled by a sinusoidal term. Achermann and Borbély have modeled the circadian behavior with a set of nonlinear equations dependent on the light intensity I,

$$d_{circ} = 0.975 + do\ C, \tag{5.62}$$

$$\dot{C} = \left(\frac{\pi}{720}\right)\left(C_c + \mu_c\left(C - \frac{4C^3}{3}\right) + B\right), \tag{5.63}$$

$$\dot{C}_c = \left(\frac{\pi}{720}\right)(-C + BC_c), \tag{5.64}$$

$$B = (1 - mC)kI^{1/3}. \tag{5.65}$$

The resulting term C is still oscillatory in nature. The values of all the coefficients of the model are listed in Table 5.10 and an example of an output of the model is shown in Figure 5.25.

5.6.3 Additional Combined REM and Slow Wave Activity Models

Ferrillo, Donadio, De Carli, Garbarino, and Nobili (2007) also developed a combined model for predicting REM sleep and slow wave activity. Unlike the two previously

Table 5.10. Coefficients of Achermann and Borbély's Combined REM and Slow Wave Activity model (1992).

Model Component	Coefficient	Original Value
C and C_c	μ_c	0.26
	m	0.3333
	k	0.018
	I	1000 during day 0 during night
SWA and S	rc	0.283
	fc	0.236
	SWA_L	0.0177
	gc	0.00835
	rs	0.0009167
	n	mean 0 st. dev 0.182
X and Y	c	1
	d_o	0.08

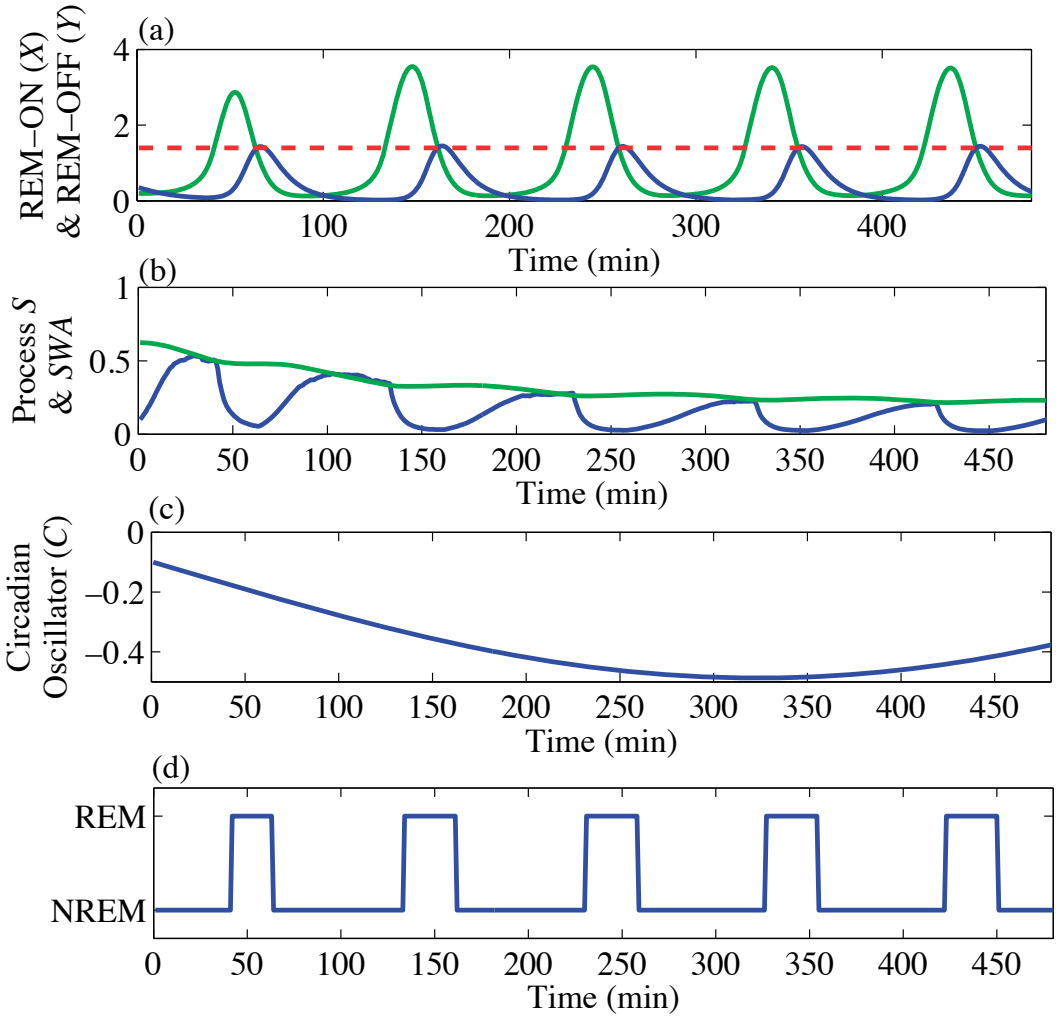

Figure 5.25. An example of the outcome of the combined Limit-Cycle Reciprocal Interaction Model and the Two Process Model by Achermann and Borbély (1992). (a) REM-ON (green) and REM-OFF Activity (blue), (b) Process S (green) and SWA (blue), (c) the circadian oscillator, and (d) scored sleep stages.

discussed combined models, they used the simpler Lotka-Volterra equations to model REM sleep. To predict slow wave activity they used equations that were similar to the Two Process Model. The reason for using the simpler REM model was that Ferrillo et al. (2007) wanted to fit the models to sleep data, which would have been difficult with the saturation functions in the REM model.

Comte, Schatzman, Ravassard, Luppi, and Salin (2006) created a three state model to predict Wake, REM (sometimes termed paradoxical sleep) and slow wave sleep. This model is also based on the simpler Lotka-Volterra REM sleep model. The equation for the change in level of slow wave neuron activity (sw) has a cubic dependence on its current level and is also dependent on the product of the level of Wake neuron firing (w) and REM neuron firing (p). The equations for the model are,

$$\dot{w} = -\alpha_o w + \beta_o wp, \tag{5.66}$$

$$\dot{p} = \alpha_1 p - \beta_1 wp, \tag{5.67}$$

$$\dot{sw} = -\alpha_2 (sw - sw_o)^3 - \beta_2 wp. \tag{5.68}$$

The coefficients for the model are listed in Table 5.11.

Table 5.11. Comte et al.'s model cofficients (2006).

Model Coefficient	Value
α_o	4
α_1	2
α_2	1
β_o	1
β_1	4
β_2	1
SW_o	5.5

In order to define sleep states, the levels of REM, NREM and Wake neuron firing are all normalized so that they are between 0 and 1. Sleep Stages are then assigned based on the highest neuron firing rate. Limitations of this model include the fact that the duration of REM sleep does not increase during the night and also brief arousals during REM and NREM sleep are not predicted. Also *sw* does not provide information on the depth of sleep. An example of an output of the model is shown in Figure 5.26.

Diniz Behn, Brown, Scammell, and Kopell (2007) also developed a model of neuron firing activity during sleep. They used Massaquoi and McCarley's reciprocal interaction concept to model REM sleep regulation, the REM sleep promoting neurons excite the Wake promoting neurons and the Wake promoting neurons inhibit the REM promoting neurons. Their model is more complex than those already mentioned, readers are referred to Diniz Behn, Brown, Scammell, and Kopell (2007) for further details. They not only modeled neuron firing activity, but also the dynamics of neurotransmitters which drive the change in neuron firing rate. An example of the output of the model is shown in Figure 5.27.

5.7 Use of Nonlinear Dynamic Models to Predict Noise-Induced Sleep Disturbance

In Table 5.12 is a summary of the features of the various models discussed. The nonlinear dynamic models were reviewed because it was desired to identify a model that could be altered and used to predict the effect of aircraft noise on sleep structure. The best candidate model that was identified was the LCRIM-based Integrated Sleep Control Model developed by Massaquoi and McCarley (1992). It is the only combined model that could be used to estimate slow wave activity, REM, and spontaneous awakenings.

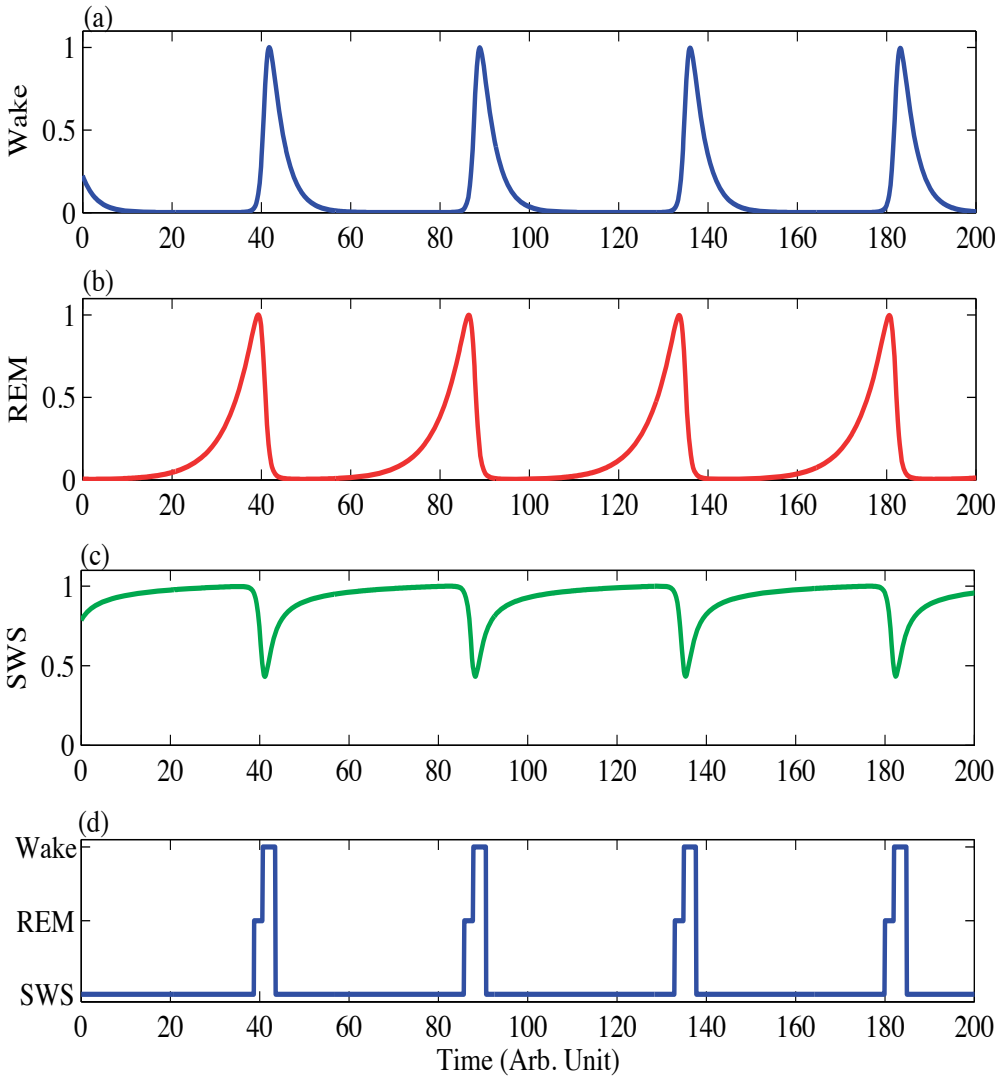

Figure 5.26. An example of the output of Comte et al.'s model (2006). (a) Wake neuron activity (w), (b) REM neuron activity (p), (c) SWS neuron activity (sw), and (d) sleep stages.

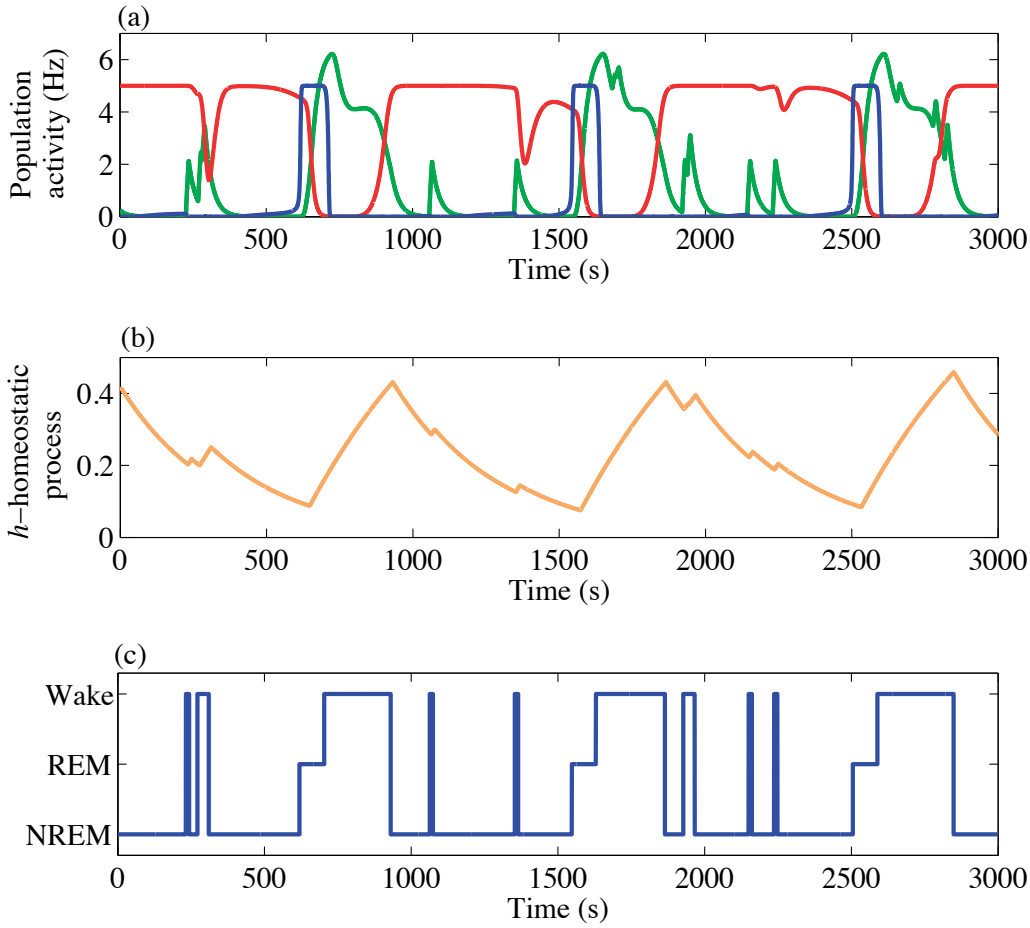

Figure 5.27. An example of the output of Diniz Behn and Booth's model (2010). (a) Firing rate of different neuron populations. Wake promoting neurons locus coeruleus and dorsal raphe (green), sleep promoting neurons VLPO (red), and REM promoting neurons (blue). (b) Homeostatic sleep drive (h) and (c) sleep stages.

Table 5.12. Summary of nonlinear dynamic sleep model structures.

Model	SWA	REM Activity	Brief Awakenings
Two Process Model (1990)	✓		
Lotka-Volterra REM Model (1975)		✓	
REM LCRIM Model (1986)		✓	
Achermann and Borbély's Combined Model (1992)	✓	✓	
Behn and Booths's Sleep Model (2007)		✓	✓
Comte et al.'s Model (2006)		✓	
Ferrillo et al.'s Combined Model (2007)	✓	✓	
Massaquoi and McCarley's LCRIM/I Model (1992)	✓	✓	✓

While the Massaquoi and McCarley model was found to be best candidate model, it is not without its limitations. When examining the model, there does appear to be one immediate problem with the excitatory term. It seems that the excitatory term will never cause awakenings to occur during REM sleep, only during NREM sleep. The reason is that the excitation term increases Y (REM-OFF) which in turn will decrease X (REM-ON) activity. The time-scale of the dynamics of X and Y interplay and mirror the slow-term behavior observed in subjects REM and NREM sleep. However, the level of Y is low when the level of X is high. Therefore changes need to be made to the model in order predict changes in sleep structure that are similar to those found in sleep studies. This limitation and approaches for overcoming it are discussed in more detail in Chapter 7.

5.8 Conclusions

Several models are reported in the sleep literature that predict sleep patterns. The nonlinear dynamic models that have been developed predict spontaneous awakenings, rapid eye movement (REM) sleep, and slow wave activity which is related to the depth of sleep. These models are based on a more physical explanation for changes in sleep, than the Markov models such as the one developed by Basner (2006). Out of all the models that have been reviewed the best candidate model for predicting sleep patterns of individuals exposed to aircraft noise is the LCRIM-based Integrated Sleep Control model by Massaquoi and McCarley (1992). It is the most complete model out of those reviewed. However, changes to the excitatory term (E) in the model will need to be made, both to predict spontaneous awakenings and to model aircraft noise induced awakenings.

6. ARTIFACT REMOVAL AND SLEEP STAGE CLASSIFICATION

This chapter contains a description of some of the methodologies used to remove artifacts from polysomnography data. A description of methods used to automatically detect characteristics that are present in different sleep stages, and the development of an algorithm for automatically classifying sleep stages is presented.

6.1 Overview of EEG Artifacts

An understanding of how the time history and spectrum of the EEG signal may be affected by artifacts is needed to reduce the number of incorrect evaluations. Several artifacts occur in EEG signals. A list of the artifacts that can occur, frequencies they affect, and potential methods for successful removal or significant attenuation of them are listed in Table 6.1. Two types of artifacts; sweating and breathing affect low frequencies. Sweat artifacts appear as high amplitude, low frequency activity. They can be removed by high pass filtering the EEG signal with a cut-off frequency between 0.75 and 1.0 Hz. Breathing artifacts appear as slow waves and are caused by movement of an individual when they are breathing in and out. Breathing artifacts are typically below the lowest frequency of the delta band (0.5 Hz or 1 Hz) (Devuyst, Dutoit, Stenuit, Kerkhofs, and Stanus, 2008), which is the lowest frequency range that is examined. Another artifact that can be easily removed are those caused by interference or from a loose or faulty electrode, these artifacts will appear around 60 Hz and can be removed by using a notch filter. Sweat, breathing, and 60 Hz artifacts though do not occur very often in EEG sleep recordings (Schlögl, Anderer, Barbanoj,

Klösch, Gruber, Lorenzo, Filz, Koivuluoma, Rezek, Roberts, Värri, Rappelsberger, Pfurtscheller, and Dorffner, 1999).

Table 6.1. Artifacts in EEG signals. PCA-Principal Components Analysis, ICA-Independent Components Analysis, Regression-Linear regression using other recorded signals such as ECG and EOG.

Artifact	Frequency Range	Methods for Removal
Breathing	Below 1 Hz	High pass filter
Sweat	Below 1 Hz	High pass filter
EOG Artifact	Primarily Delta Band	Regression, Adaptive filtering, PCA, ICA
ECG Artifact	Maximum energy approx. 15Hz	Regression, Adaptive filtering, PCA, ICA
Muscle Activity	Strongest in high frequencies	Remove epoch from analysis
Movement	Strongest in high frequencies	Remove epoch from analysis
Interference, Loose Electrode	60 Hz	Notch filter

The artifacts that occur more often are caused by body movements and muscle activity, eye movement commonly referred to as an EOG artifact, and heart activity which is referred to as an ECG artifact. ECG artifacts are caused by the heart beat being picked up in the EEG signals because the electrode is located near a vein or artery (Spriggs, 2008). These artifacts will appear as a repetitive spike in the EEG signal occurring about once every minute. An example of an ECG artifact is shown in Figure 6.1. Garcés Correa, Laciar, Patiño, and Valentinuzzi (2007) stated the maximum energy of the ECG artifact is at approximately 15 Hz in the EEG signal.

Eye movement may also be picked up in the EEG signal. It will appear as large amplitude oscillations and will primarily affect the delta frequency band (Inuso, La Foresta, Mammone, and Carlo Morabito, 2007). This artifact most strongly contaminates the frontal EEG channels. The effect on other EEG channels decreases with the square of the distance. The data from the 1999 UK study contains EEG

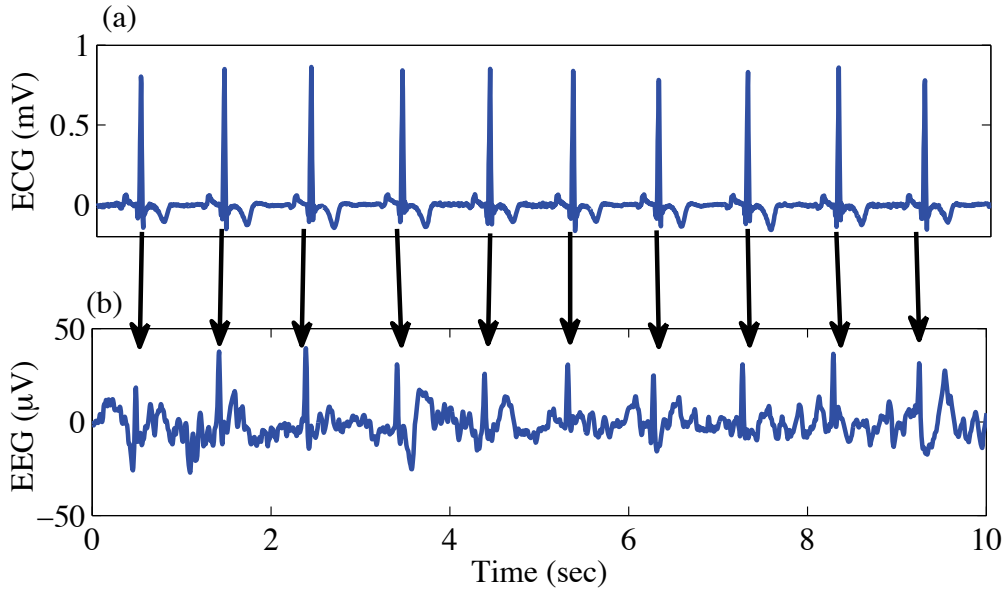

Figure 6.1. (a) The ECG signal and (b) the EEG signal where the heart beats are being picked up in addition to the EEG information.

.

data for the central and occipital channels, therefore eye movement artifacts can still appear but not as strongly. Also between EOG and EEG signals there is bidirectional contamination, therefore while eye movement may contaminate the EEG signal, brain activity may contaminate the EOG signal. This makes it more difficult to remove EOG artifacts from an EEG signal. An example of an EOG artifact is shown in Figure 6.2.

Muscle artifacts may also occur, which are caused by movement of facial and neck muscles. These artifacts affect frequencies primarily above 15 Hz (van de Velde, van Erp, and Cluitmans, 1998). The last type of artifact is caused by whole or partial body movement and will appear as a high amplitude, high frequency component and will affect most channels that are recorded, an example is shown in Figure 6.3.

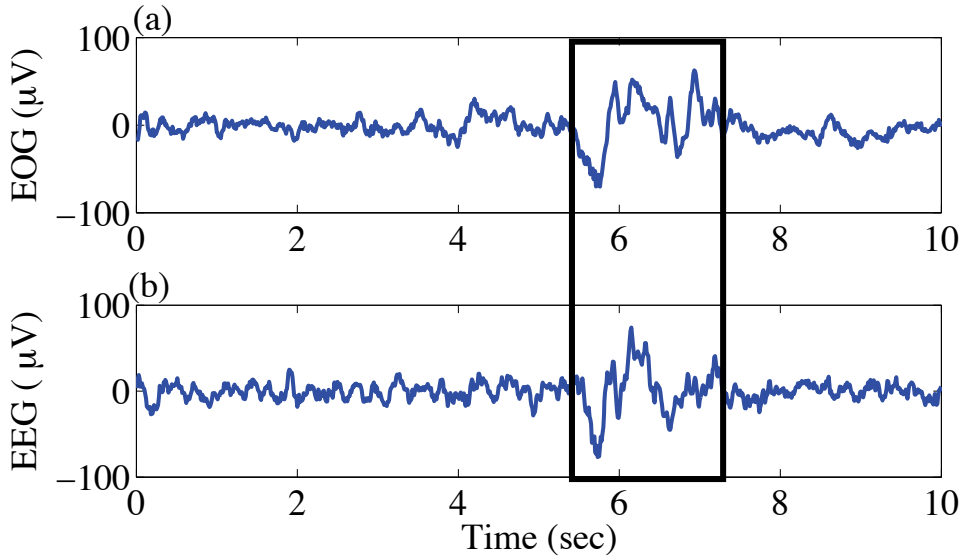

Figure 6.2. An example of an EOG artifact in an EEG signal, (a) EOG and (b) corresponding EEG signal with artifact.

6.2 Description of Artifact Removal Methods

The most common technique for removing artifacts is still through visual scoring. The epochs containing artifacts are identified and removed before conducting further analysis. While this is possible for movement artifacts, other artifacts such as ECG and EOG, can affect many epochs of the data. Eliminating these epochs would result in a large loss of data. Therefore, several methods for removing artifacts from EEG signals have been proposed. The first method is based on a linear regression approach which can be performed either in the frequency or the time domain. This method can only be applied if a reference signal was recorded, i.e. if ECG or EOG activity was recorded. For linear regression it is assumed that the obtained or recorded EEG signal is a linear combination of the actual EEG signal and the artifact signal (Anderer, Roberts, Schlögl, Gruber, Klösch, Herrmann, Rappelsberger, Filz, Barbanoj, Dorffner, and Saletu, 1999). The portion of the signal that contains the artifact can be estimated and subtracted from the EEG signal. One problem with this linear

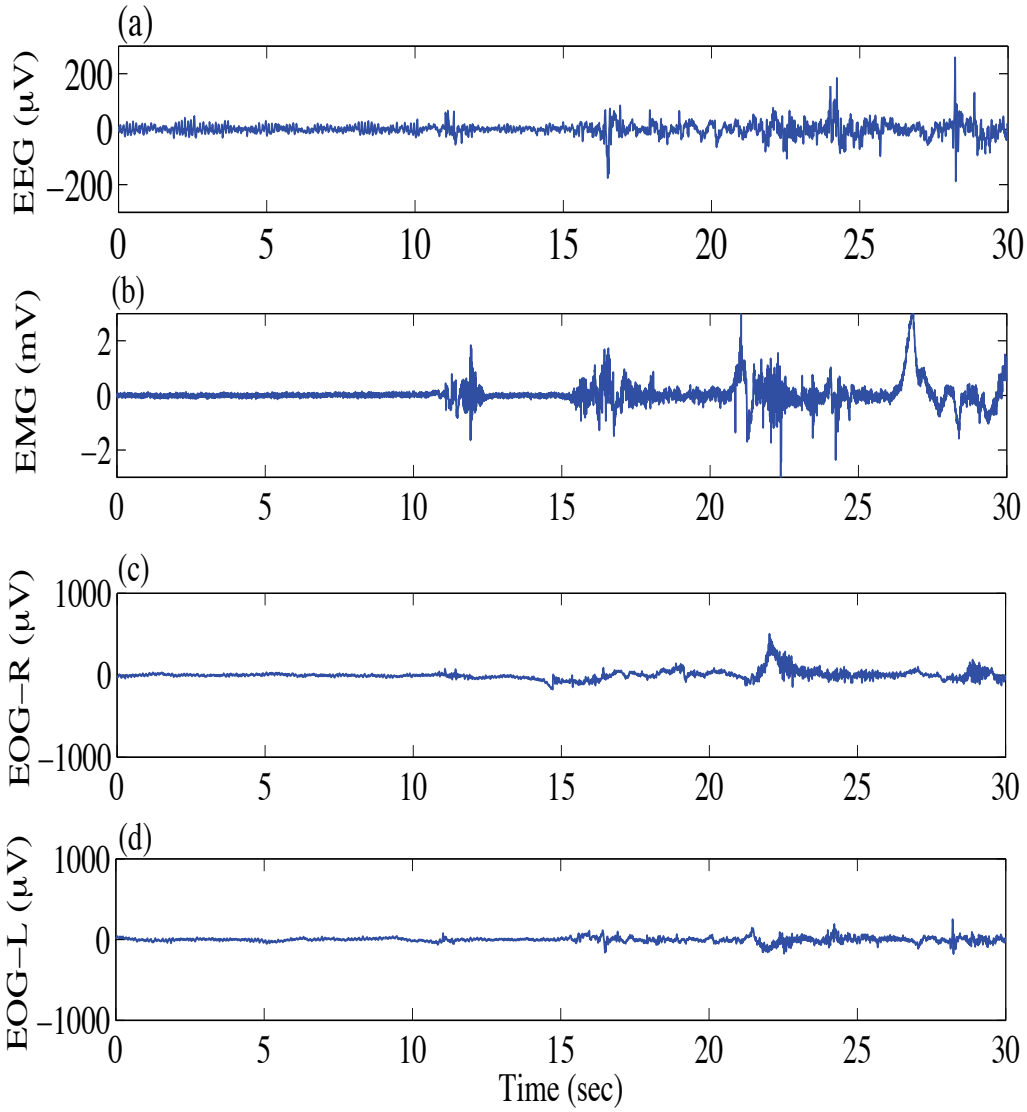

Figure 6.3. An example of a movement artifact in the (a) EEG, (b) EMG, (c) Right EOG, and (d) Left EOG signal.

regression approach is that the EEG signal and the artifact signal may not be aligned in time. Also, the relationship between the two signals may be more complicated than a simple amplification and offset and the bidirectional contamination may result in removal of desired information.

Another method for removing the artifacts that allows for a more complex relationship to exist between the EOG or ECG and the EEG signals is to use an adaptive filter. Most often in the literature, a recursive least squares (RLS) algorithm is used to estimate the filter coefficients (He, Wilson, and Russell, 2004) which defines the relationship between the artifact measurement and the signal affected by the artifact. The input (x) is the artifact signal, either the ECG or the EOG signal. An estimate is made of the ECG or EOG component in the EEG signal ($\hat{y}$). The error e, which is the difference between the recorded EEG signal (y) and the estimate of the ECG or the EOG signal, is the uncontaminated EEG signal. A diagram of the process for removing an ECG artifact is shown in Figure 6.4.

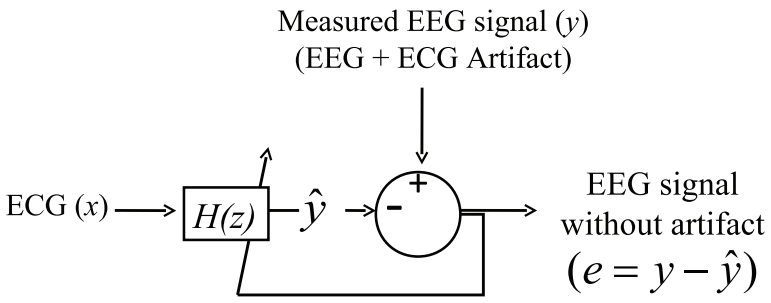

Figure 6.4. A diagram of the process used to remove ECG artifacts from the EEG signal.

For an (RLS) adaptive filter there are two parameters that have to be specified; M which is the filter order and λ which is the forgetting factor. The goal is to estimate the filter coefficients h_k in the equation,

$$\widehat{y}(n) = \sum_{k=0}^{M-1} h_k x(n-k). \tag{6.1}$$

Note this is a M-point finite impulse response filter. The forgetting factor is related to an exponential weighting on the cost function (J), data points in the past have less effect on the estimate of the weighted sum of the magnitude squared error e,

$$e(n) = y(n) - \widehat{y}(n), \tag{6.2}$$

$$\varepsilon = \sum_{k=0}^{n} \lambda^{n-k} |e(k)|^2, \tag{6.3}$$

(Haykin, 1996). At each time step the coefficients of the filter are estimated by updating the previous values. Garcés Correa, Laciar, Patiño, and Valentinuzzi (2007) used an adaptive filter to remove ECG artifacts and found that the maximum energy at 15 Hz due to the artifact was attenuated anywhere from 4 to 50% depending on the subject. Therefore, the effectiveness of adaptive filters at reducing ECG artifacts varies greatly for different subject nights. An example of using adaptive filtering to remove the ECG artifact from an EEG signal of the UK dataset is shown in Figure 6.5. A filter order of 3 and a forgetting factor of 0.9999 was used.

A challenge in using adaptive or regression methods for removing EOG artifacts from EEG data is bidirectional contamination. When a portion of the EOG signal is subtracted from the EEG signal, not only is the artifact removed but so is part of the EEG signal. Several researchers have pre-filtered the EOG signal to reduce the brain wave activity in the recording. Wallstrom, Kass, Miller, Cohn, and Fox (2004) used a

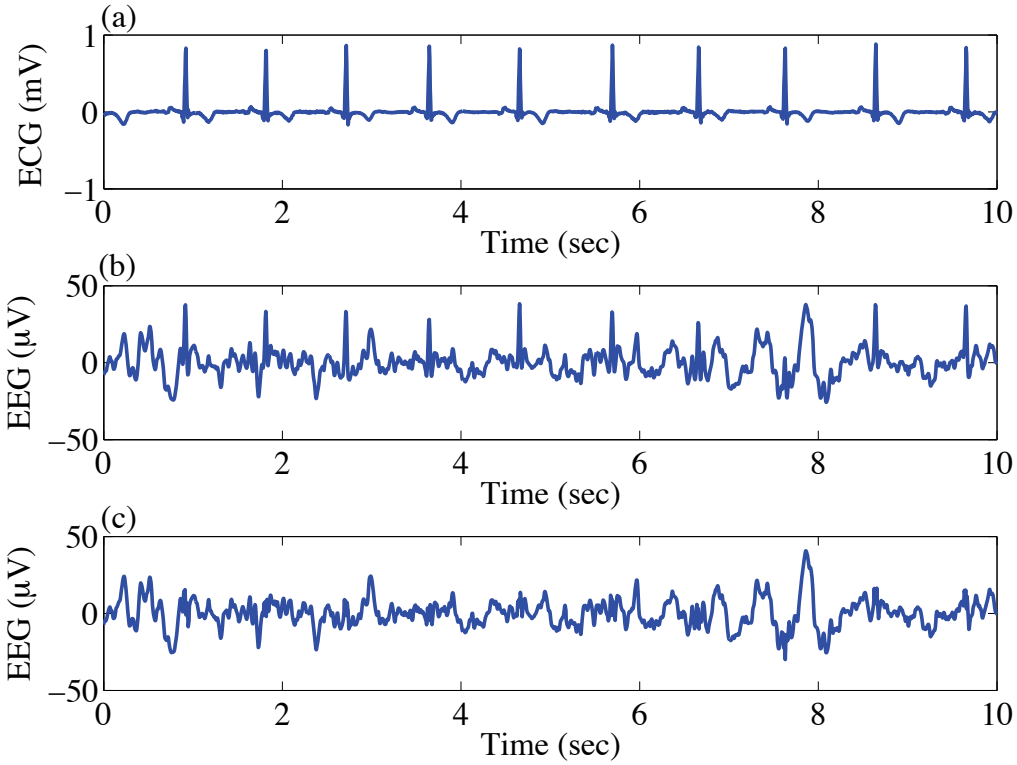

Figure 6.5. An example of an outcome obtained using an RLS adaptive filter to remove ECG artifacts. The (a) ECG, (b) EEG with artifact, and (C) EEG after minimizing artifact signals.

Bayesian adaptive regression spline. They wanted to smooth out the high frequency small amplitude activity (this is due to brain wave activity) of the EOG signal and retain the high frequency large amplitude activity which is more likely to be caused by eye movement. For a spline the signal is divided into segments. For each segment a polynomial is defined to represent the data, the end points of the segments are called knots. A Bayesian adaptive regression spline is a free-knot spline. This means the placement of the knots are determined by the data rather then being placed at fixed locations. More knots are placed in locations where the data has large changes in values (DiMatteo, Genovese, and Kass, 2001). Another challenge with removing

the EOG signal is that at least two channels, vertical and horizontal EOG, have been found to be needed to fully remove artifacts from the signal (Anderer et al., 1999). However, only 1 channel was recorded in the 1999 UK sleep study. Therefore, using adaptive or regression techniques, it may not be possible to remove all of the artifacts caused by ocular motion.

One disadvantage of both adaptive filtering and regression is that a reference signal is needed. While EOG and ECG signals were recorded for the UK sleep study, for some subjects the recordings have poor quality or the electrodes became loose during the night. Two methods that have been used to remove artifacts which do not require a reference electrode are Principal Component Analysis (PCA) and Independent Component Analysis (ICA).

PCA involves finding a matrix that separates the signals into the contributing components. PCA finds components which are uncorrelated. The definition for two random variables (X, Y) being uncorrelated is that the covariance is zero (E is the expected value) and it is assumed that $E[X]$ and $E[Y]$=0:

$$E[XY] = E[X]E[Y] = 0. \tag{6.4}$$

Using PCA, the components can be found through singular value decomposition of the covariance matrix (Sanei and Chambers, 2007).

For ICA analysis it is also assumed that you have N signals which are mixtures of N components (Jung, Makeig, Humphries, Lee, McKeown, Iragui, and Sejnowski, 2000). The goal once again is to find a matrix that will result in the calculation of the individual components. ICA is used to find independent components, which means that unlike PCA in which the results or components can be rotated, the components

of ICA cannot because they would no longer be independent (Stone, 2009). The definition of independence is that:

$$p(x, y) = p_x(x)p_y(y), \tag{6.5}$$

where $p(x, y)$ is the joint probability density function and $p(x)$ and $p(y)$ are each individual probability density functions (DeVore, 2008). For Independent Component Analysis the assumption is also made that the components are non-Gaussian. Vigário, Särelä, Jousmäki, Hämäläinen, and Oja (2000) stated that artifacts tend to be non-Gaussian and therefore this method is more applicable then PCA. The methods used to calculate the Independent components maximize the non-Gaussianity of the components.

A problem with both PCA and ICA is determining which of the components are artifacts. The artifact components are usually determined based on a combination of spectral features, spatial topography, and time domain features. Particularly for spatial topography this requires that a large number of EEG channels were recorded. In studies in which ICA or PCA have been used more than 10 channels of recordings were typically made. However, for the data that was obtained from the 1999 UK study only 4 channels of EEG were recorded for each subject.

The most common method for dealing with muscle and movement artifacts is to eliminate contaminated epochs from the analysis. Brunner, Vasko, Detka, Monahan, Reynolds III, and Kupfer (1996) developed a method to automatically detect muscle artifacts to remove that data from subsequent analysis. They determined the average power in the range of 26.25 and 32.0 Hz for each four second epoch. They then applied a 45 point median filter to smooth the power estimate and multiplied this smoothed power time history by some constant and used this as a threshold for detecting muscle artifacts. When the threshold is exceeded it is assumed that an artifact has occurred.

They found a threshold at 4 times the level of the smoothed average power worked well for identifying artifacts. An example of the use of this method for removing artifacts from an EEG signal in the UK dataset is shown in Figure 6.6.

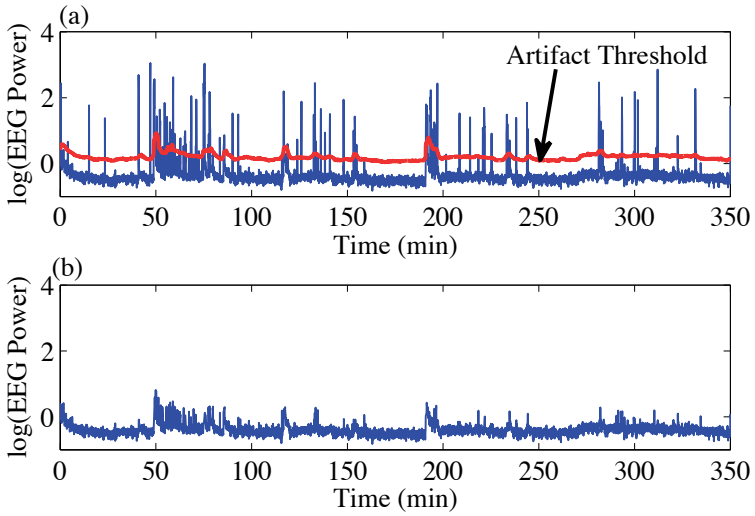

Figure 6.6. An example of the use of Brunner et al.'s (1996) method to remove muscle and movement artifacts. (a) Power between 26.0 and 32.0 Hz of an EEG signal with artifacts present and (b) power after removing epochs which exceeded the threshold.

After examining several artifact removal methods, the best approach for removing artifacts from the EEG data of the 1999 UK Sleep Study was determined to be the use of recursive least squares (RLS) estimated adaptive filters to remove EOG and ECG artifacts. All subject nights of data did have EOG measurements, however not all had ECG recordings that could be used. Therefore, for some EEG signals examined ECG artifacts could not be removed. For the removal of EOG and ECG artifacts a filter order of 3 and a forgetting factor of 0.9999 was used. The method developed by Brunner et al. (1996) was used to identify epochs with muscle and movement activity. For calculations of slow wave activity or power in other frequency bands, segments containing movement artifacts were identified and not used in the analysis.

6.3 Review of Existing Sleep Stage Classification Methods

Many approaches have been developed to extract different features from polysomnography data, such as sleep spindles and rapid eye movements, which are then used to classify sleep stages. Some of these methods for feature detection and sleep stage classification are described.

6.3.1 Slow Wave Sleep Detection

Slow waves are the defining feature of Stage 3 and Stage 4 sleep. They are defined as having a frequency between 0.5 and 2 Hz and having a peak-to-peak amplitude of at least 75 μV. A method that can be used to identify these waves is a peak amplitude detection method similar to an approach used by Kuwahara, Higashi, Mizuki, Matsunari, Tanaka, and Inanaga (1988). This method involves applying a 4th order Butterworth band-pass filter, with cutoff frequencies of 0.5 and 2.0 Hz, to the EEG signal, identifying the zero crossings of the signal and then the peak amplitude between each zero crossing. The peak-to-peak amplitude can then be calculated by taking the magnitude and then adding together adjacent peak amplitudes and then the percent of an epoch that contains slow wave activity, defined by when the peak-to-peak amplitude exceeds 75 μV, can be calculated. An example of the use of this approach for detecting slow wave sleep is shown in Figure 6.7. The percentage of each 30 second epoch, sliding 1 second through time, that contains slow wave sleep, calculated for one subject night in the UK dataset, is shown in Figure 6.8.

6.3.2 Rapid Eye Movement Detection

In order to classify Stage REM, rapid eye movements need to be identified. The primary method used to identify the occurrence of rapid eye movement is to calculate

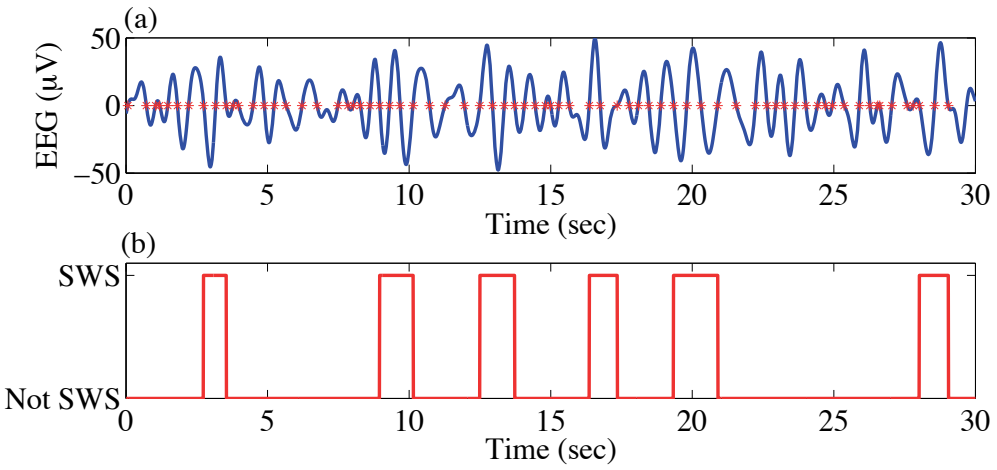

Figure 6.7. An example of slow wave sleep detection. (a) An EEG signal filtered between 0.5 and 2.0 Hz (blue) and zero crossings (red x) and (b) detected slow wave sleep.

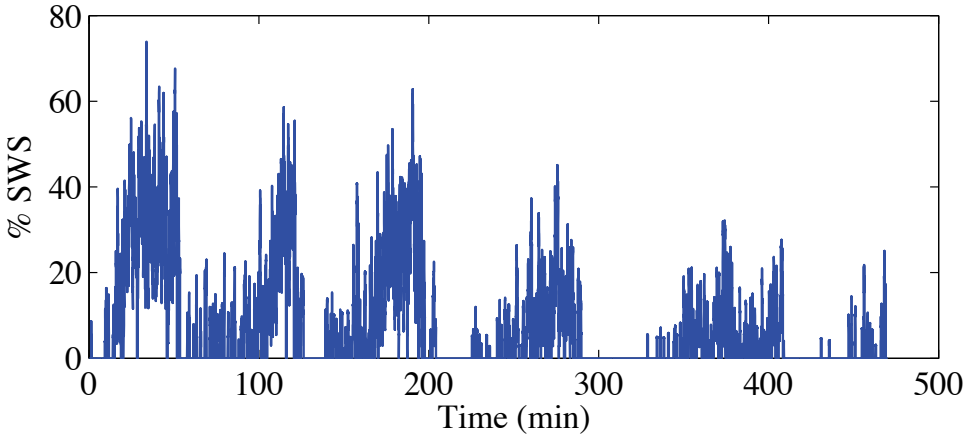

Figure 6.8. The percent of each epoch containing slow wave sleep (SWS).

the correlation of the right EOG and left EOG channel. The standard placement of the EOG electrodes is to have one electrode placed outside and above the corner of one eye, and the other electrode placed outside and below the corner of the other eye. Therefore, when an eye movement occurs one of the measurements will have

a negative value while the other will have a positive value and therefore the two channels will be negatively correlated.

In most of the methods developed to detect rapid eye movements the EOG signals have been filtered to retain only energy below 5 Hz before further analysis. Agarwal and Gotman (2001) applied a 6th order low-pass filter with a cutoff frequency of 5 Hz to the EOG signals. Gopal and Haddad (1981) used a low pass Butterworth filter of order 3 with a cutoff frequency of 6.5 Hz. Agarwal, Takeuchi, Laroche, and Gotman (2005) used a 4th order Butterworth bandpass filter with cutoff frequencies of 1 and 5 Hz, Boukadoum and Ktonas (1986) stated that most REM movements are between 200 ms and 1 second in duration, which would correspond to a frequency range of 1 to 5 Hz, while Smith, Cronin, and Karacan (1971) used a slightly smaller frequency range than the other researchers for their detection of REM; they only examined activity between 1 to 3 Hz.

In addition to filtering the EOG signals and calculating the correlation between the EOG channels, a few additional methods have been used. Hatzilabrou, Greenberg, Sclabassi, Carroll, Guthrie, and Scher (1994) used a method of matched filtering for detecting rapid eye movements. They created a template of the shape of a rapid eye movement and then calculated the cross-correlation between the template and the EOG signal. Virkkala, Hasan, Värri, Himanen, and Härmä (2007) also used cross-correlation to identify rapid eye movements. They bandpass filtered the EOG signals with a passband between 0.5 to 6 Hz and 1 to 6 Hz. The difference in the cross-correlation results of the 0.5 to 6 Hz band and the 1 to 6 Hz band was used to separate slow eye movements from rapid eye movements.

McPartland, Kupfer, and Foster (1973) used an 11 point moving average filter in order to smooth the EOG signals before extracting additional features to identify rapid eye movements including: requiring the two channels to be negatively corre-

lated, the events on each channel to occur within 100 ms of each other and have a minimum amplitude of 25 μV. Smith, Cronin, and Karacan (1971) also set minimum requirements for the amplitude of the EOG signals. They required that the maximum amplitude of a rapid eye movement must be greater than or equal to 50 μV in one EOG channel and greater than 30 μV in the other channel. Gopal and Haddad (1981) derived a method to automatically detect rapid eye movements in infants. In one method used they calculated the average of the first derivative of the slope for the segment of the EOG signal between the local minimum and maximum value. A rapid eye movement was considered to occur if the slope was between 0.33 to 0.66 mV/s. Agarwal, Takeuchi, Laroche, and Gotman (2005) also examined the slope of the EOG signals. They calculated the deflection angle, the angle of the peak of the eye movement, to determine if the eye movement was a rapid or a slow eye movement.

The primary methods found in the literature for detecting rapid eye movements only utilize EOG activity below 5 Hz, calculate the correlation between the left and right EOG channels and set a minimum threshold for EOG activity. Therefore, this was the approach taken to identify rapid eye movements in the 1999 UK sleep study EOG data. A 4th order Butterworth bandpass filter was used with cutoff frequencies of 0.5 and 5 Hz. The correlation between the two EOG channels was calculated and if the correlation was below -0.2 a rapid eye movement was considered to occur. This threshold for the correlation was used by Agarwal, Takeuchi, Laroche, and Gotman (2005). A minimum amplitude threshold of 25 μV was used. This minimum threshold as well as the cutoff frequencies of the bandpass filter were determined after visually identifying and extracting over 1000 examples of rapid eye movement and then analyzing the frequency content and maximum amplitudes. An example of the cumulative sum of power in every 0.25 Hz frequency block is shown in Figure 6.9 for all samples of rapid eye movements that were extracted, and it can be seen

that a significant amount of power of the EOG signal is below 1 Hz which was the reason for defining a lower cutoff of 0.5 Hz, compared to other researchers who set the lower threshold at 1 Hz. An example of the correlation between the filtered left and right EOG channels calculated for one subject night is shown in Figure 6.10. The oscillations between REM and NREM sleep can be identified from the correlation between EOG channels. Eye movements that occur during Stage Wake may also be identified using this method. By also using other characteristics, including amplitude of the EMG signal and power in the alpha frequency band of the EEG signals, these eye movements can often be distinguished from the rapid eye movements which occur during REM sleep.

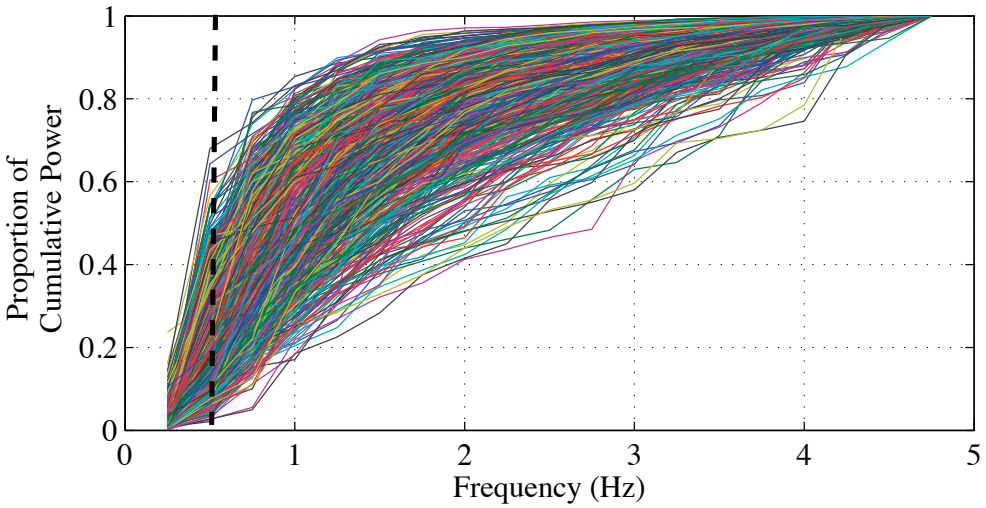

Figure 6.9. Cumulative power of 1,166 samples of rapid eye movement (black-dash line is at 0.5 Hz).

6.3.3 Sleep Spindle Detection

Sleep spindles were defined by Rechtschaffen, Hauri, and Zeitlin (1966) as short bursts of activity between 12 and 14 Hz (sigma band). These bursts of activity must last at

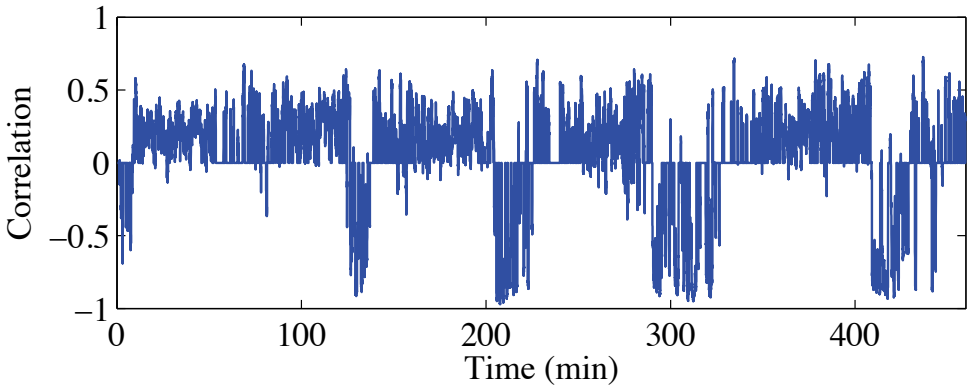

Figure 6.10. Correlation between right and left EOG Channels for one subject night in 1999 UK study.

least 0.5 seconds. However, the frequency range for sleep spindles has been expanded and in automatic detection methods activity as low as 11 Hz and as high as 16 Hz has been considered. Two methods have been primarily used to detect sleep spindles, one approach is to detect sigma activity exceeding a set amplitude threshold while the second approach is to use autoregressive modeling to detect sigma activity.

Devuyst, Dutoit, Didier, Meers, Stanus, Stenuit, and Kerkhofs (2006) applied a bandpass filter to their EEG signals, the filter had cutoff frequencies of 11.5 and 15 Hz. If a defined amplitude threshold was exceeded for more than 0.5 seconds then a sleep spindle was considered to occur. Their threshold was defined as:

$$threshold = \mu + K\sigma, \tag{6.6}$$

where μ is the mean amplitude of the filtered EEG signal and σ is the standard deviation. They found that a value of K equal to 2 provided the best sensitivity and specificity for identifying sleep spindles. This approach allows the threshold for detecting sleep spindles to be set separately for each subject which is different from a

method used by Schimcek, Zeitlhofer, Anderer, and Saletu (1994) in which a minimum peak to peak amplitude of 25 μV was used for identifying spindles.

Dang-Vu, McKinney, Buxton, Solet, and Ellenbogen (2010) automatically identified sleep spindles in their analysis of the relationship between the number of sleep spindles and the probability of awakening to a noise event. Like Devuyst et al. (2006) they also used a variable threshold. To calculate sleep spindles they bandpass filtered the central EEG channels using an FIR filter with cutoff frequencies of 11 and 15 Hz. They then calculated the rms (root-mean-square) power of the filtered EEG signal for each 0.25 second segment of the signal. They assumed that a sleep spindle occurred when the rms power was above the 87th percentile of activity within the sigma band. They also required that the peak-to-peak amplitude of the sigma activity was between 10 and 100 μV and that the duration of the sleep spindle was at least 0.5 seconds. In many algorithms a minimum duration for sleep spindles is defined however Ray, Fogel, Smith, and Peters (2010) also defined a maximum duration. The criteria they defined were that spindles had to have a minimum duration of 0.5 seconds, maximum duration of 3 seconds and an interval of at least 0.1 seconds between spindles.

Olbrich and Achermann (2008) and Venkatakrishnan, Sangeetha, and Sukanesh (2008) used autoregressive (AR) modeling to identify sleep spindles. An autoregressive model is defined as (Haykin, 1996),

$$y_n = \sum_{k=1}^{M} a_k y_{n-k} + \varepsilon_n, \tag{6.7}$$

where ε_n is white noise or can be thought of as an error term. It is called an autoregressive model because the value y_n is a combination of past values. The transfer function of an AR model is defined as,

$$H(z) = \frac{1}{\sum_{n=0}^{M} a_n z^{-n}}. \tag{6.8}$$

As can be seen from the transfer function, AR models are all pole models. Where the the poles z_m are defined as,

$$z_m = r_m e^{i\theta_m}, \quad m = 1, 2, ...M \tag{6.9}$$

the decay rate is defined as,

$$\gamma_m = -ln(r_m)/\Delta, \tag{6.10}$$

and the frequency of that component is:

$$f_m = \theta_m/(2\pi\Delta). \tag{6.11}$$

Olbrich and Achermann (2008) examined the use of an AR(M=8) model and a AR(M=4) model. They noted that the AR(8) model resulted in frequencies being identified that are not found in oscillatory events like sleep spindles during the night. The coefficients of the AR model were calculated using the Burg Algorithm (Olbrich and Achermann, 2005) and the frequencies and the decay associated with the poles were calculated. The decays of the AR model components were used as an indicator for whether a sleep spindle could be occurring. From Equation (6.10), the higher the value of r_m the lower the damping of a particular frequency component. Therefore, if a sleep spindle was occurring it would be expected that the damping coefficient for a frequency between 11.5 and 16 Hz would be low and the value of $r_m$would be high. Olbrich and Achermann (2008) set a threshold for detecting sleep spindles, if the value of r_m was greater then 0.95 and the frequency was within the sigma frequency band, then it was assumed that the occurrence of a sleep spindle was probable. The duration of a potential sleep spindle was defined by the duration that r_m was greater than 0.9.

In order to characterize sleep spindles a similar approach to that of Olbrich and Achermann (2008) was used. The EEG signal was segmented into 1 second segments. An AR(4) model was used and the coefficients were calculated by using *arburg* in Matlab. The frequency component with the lowest decay rate was then found. If the frequency was within the sigma frequency band then the occurrence of a sleep spindle was considered probable. The frequency with the lowest decay rate calculated for each 1 second segment of an EEG signal for an entire night is shown in Figure 6.11. Periods in which the dominant frequency was within the sigma frequency band can be seen to correspond to periods of Stage 2 sleep.

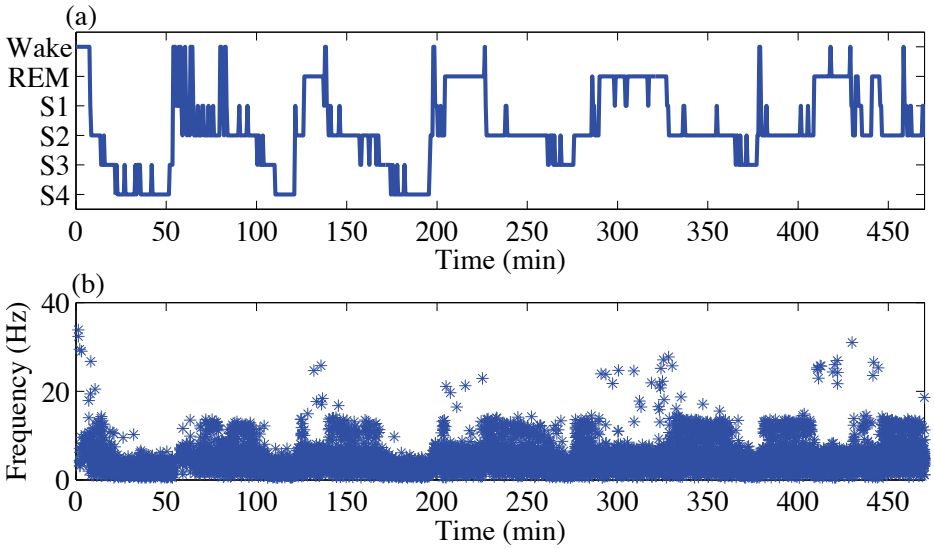

Figure 6.11. (a) Scored sleep stages for one subject night from the 1999 UK Dataset and (b) the frequency with lowest decay rate calculated using an AR(4) model.

An example of identifying a sleep spindle in a single brief 20 second segment of EEG data is shown in Figure 6.12.

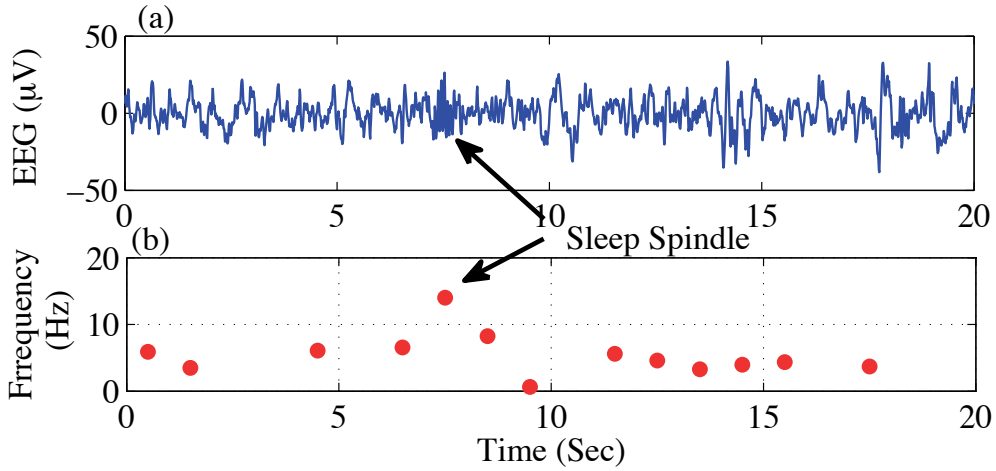

Figure 6.12. (a) EEG Segment and (b) the frequency with lowest decay rate for each 1 second segment determined from an adaptive AR(4) model.

6.3.4 Additional Features

Additional features of EEG signals that are sometimes identified as part of sleep stage classification algorithms include K-complexes and Vertex Waves. A K-complex is defined as a sharp negative deflection followed by a positive deflection that lasts at least 0.5 seconds. They occur during Stage 2 sleep and may or may not be followed by a sleep spindle. The peak-to-peak amplitude of a K-complex should be greater than 75 μV. To identify K-complexes, Devuyst, Dutoit, Stenuit, and Kerkhofs (2010) extracted several features of the wave including the peak-to-peak amplitude and the second derivative of the waveform in order to obtain an estimate of the sharpness of the negative component of the wave.

Bremer, Smith, and Karacan (1970) also examined different features that could be used to classify K-complexes. They found that an interval of 2 seconds typically occurred between K-complexes and that the maximum amplitude of the EEG signal both before and after a K-complex should not exceed 50 μV. They stated that requiring an interval of low EEG activity before and after a K-complex was a way

to distinguish K-complexes from bursts of delta activity. Bankman, Sigillito, Wise, and Smith (1992) also attempted to automatically classify K-complexes. They stated that when visually detecting K-complexes the distinction between them and Delta waves is the sharpness of the waveform, therefore possible measures to help separate the two include the rise time, or the slope of the signal.

Vertex Waves have also been detected as part of sleep stage classification algorithms and are a key feature of Stage 1 sleep. Exarchos, Tzallas, Fotiadis, Konitsiotis, and Giannopoulos (2006) and Da Rosa, Kemp, Paiva, Lopes da Silva, and Kamphuisen (1991) defined Vertex Waves as having a duration between 70 and 200 milliseconds. The amplitude of Vertex Waves are typically greater than 100 μV and should not exceed 250 μV.

While the ability to identify K-complexes and Vertex Waves was examined, Stage 1 sleep was not estimated separately as part of the sleep stage classification algorithm that was developed as it is a transitory stage and it won't be estimated as part of the developed nonlinear model described in Chapter 7. K-complexes often have very similar features as slow wave sleep, therefore epochs which had nonzero slow wave activity calculated using the peak-to-peak amplitude detection approach often also provided an indication of whether a K-complex occurred. Therefore, K-complexes were not identified separately.

6.4 Sleep Stage Classification Algorithm

There were two methods for automatically classifying sleep stages which were identified in the sleep literature. One approach is to use some type of classifier. Becq, Charbonnier, Chapotot, Buguet, Bourdon, and Baconnier (2005) for example examined the use of linear and quadratic classifiers, k nearest neighbors, Parzen kernels and neural networks to classify sleep stages. Others have developed a set of rules,

a series of (if-then statements) in their code, to identify sleep stages (Agarwal and Gotman, 2001). As sleep stages are traditionally scored visually based on a set of rules/criteria the second approach was used. A list of key features of each sleep stage and methods to identify these characteristics are listed in Table 6.2.

Table 6.2. Key features of sleep stages and characteristics of polysomnography data that were extracted.

Sleep Stage	Key Features	Extraction Method
REM	Fast Eye Movements Low EMG	Correlation between EOG channels Amplitude of EMG Power in different Frequency Bands Peak-to-Peak Amplitude Detection AR(4) Modeling
Stage Wake	Alpha waves (8-12 Hz), Movement, High EMG	
Stage 2	Sleep Spindles (12-14 Hz), K-complexes, Theta activity (4-8 Hz)	
Stage 3/4	Low freq. activity (0.5-2 Hz), $> 75\ \mu V$ Peak to Peak amplitude for > 20 % of epoch	

In addition to features already described including the use of AR modeling to identify sleep spindles, the calculation of the correlation between left and right EOG channels to identify rapid eye movements, and peak-to-peak amplitude detection for identifying slow wave sleep, the power in several EEG frequency bands including delta, theta, alpha, sigma, and gamma was also calculated. To calculate the power in each frequency band, the EEG signals were band-passed filtered using 4th order Butterworth filters and the total power within each 30 second segment, sliding one second through time was calculated. An example of the percent of the total power in several frequency bands for one subject night is shown in Figure 6.13.

The mean and standard deviation of the power in each frequency band during each of the 6 sleep stages was also calculated using all 76 subject nights of data in the UK dataset, the results are shown in Figure 6.14. The Delta_1 frequency band refers

to power between 0.5 to 2 Hz, while the entire Delta frequency band ranges from 0.5 to 4.5 Hz. The mean and standard deviation for the ratio of alpha to theta is shown in Figure 6.15 (a). The mean and standard deviation for the the average percentile of the EMG amplitude is shown in Figure 6.15 (b). The mean and standard deviation of the percent of a 30 second epoch occupied by slow wave sleep calculated using the peak-to-peak amplitude detection method described earlier, are shown in Figure 6.15 (c). The mean values shown were useful in determing thresholds to use in the sleep stage classification algorithm.

The standard method for scoring sleep stages is to assign a stage to each 30 second epoch or block of time. However, it was desired to create a more continuous method for scoring sleep stages. Therefore while sleep stages were still scored for 30 second segments a sliding window of 1 second was used. Thus for each 30 second interval there are 30 classifications, one for each 1 second interval derived from a 30 second period around that time. To compare the results to 30 second sleep stages, the probability of being in each stage for each 30 second epoch was calculated and then the 30 second sleep stage was assigned according to which stage had the highest probability of occurrence. The 4 main steps of the algorithm are shown in Figure 6.16.

To classify the sleep stages for each 1 second (center of 30 second window), a set of rules were developed, which are shown in Figure 6.17. First of all, if the 30 seconds of data contained a movement artifact for 20% or more of the 30 second segment or it contained alpha activity in greater than 50% of the epoch, then the sleep stage was classfied as wake. If the segment did not contain an artifact or high alpha activity then the next step was to seperate segments according to whether it contained eye movement, which was classified according to whether the correlation of the two filtered EOG channels was less than -0.2. If the segment did not contain

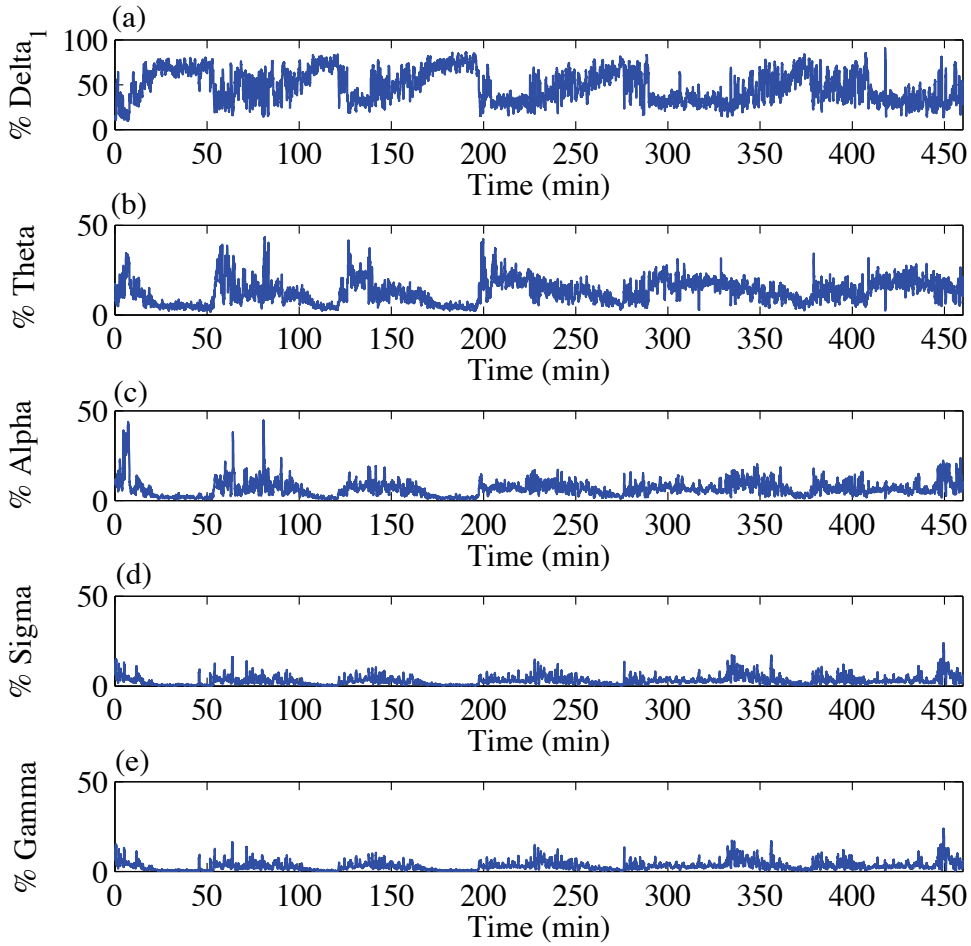

Figure 6.13. Percentage of the total power in an EEG signal in the (a) Delta$_1$ band, (b) Theta band, (c) Alpha band, (d) Sigma band, and (e) Gamma frequency bands.

eye movement then the sleep stage was either Stage 3/4, Stage 2 or Wake. Stage 3/4 was identified according to the amount of delta power and whether the percentage of slow wave sleep identified (using the peak-to-peak amplitude detection method) was greater then 15 %. The sleep stage was classified as Stage 2 if the amount of slow wave sleep was greater than zero and if sleep spindles occured. When rapid eye

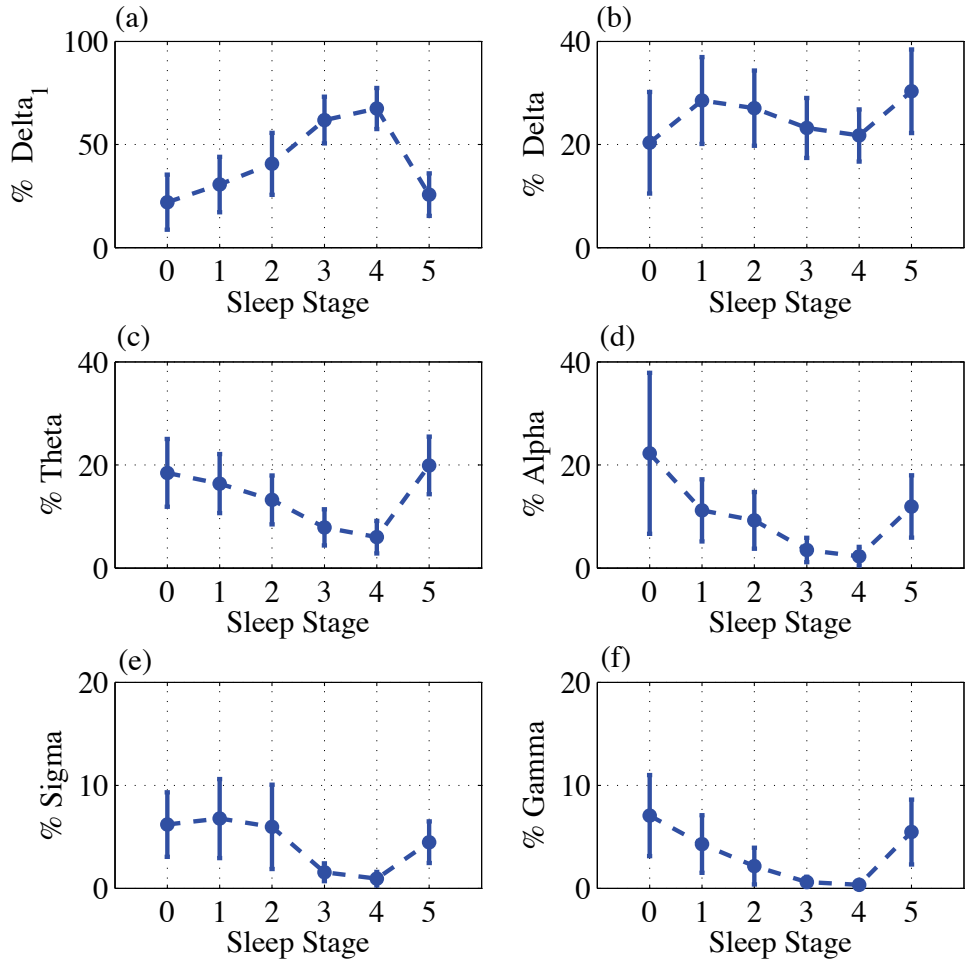

Figure 6.14. Average percentage of power for 76 subject nights in each of the frequency bands for sleep stages Wake (0), NREM Stages 1 through 4, and REM sleep (5).

movement was identified, if the EMG activity was greater than the 85th percentile or the power in the alpha frequency band was greater than the power in the theta frequency band by a factor of 1.5 then the segment was categorized as Stage Wake otherwise it was classified as Stage REM. An example of the probability of being in each sleep stage through the night calculated using the developed algorithm for one subject night is shown in Figure 6.18.

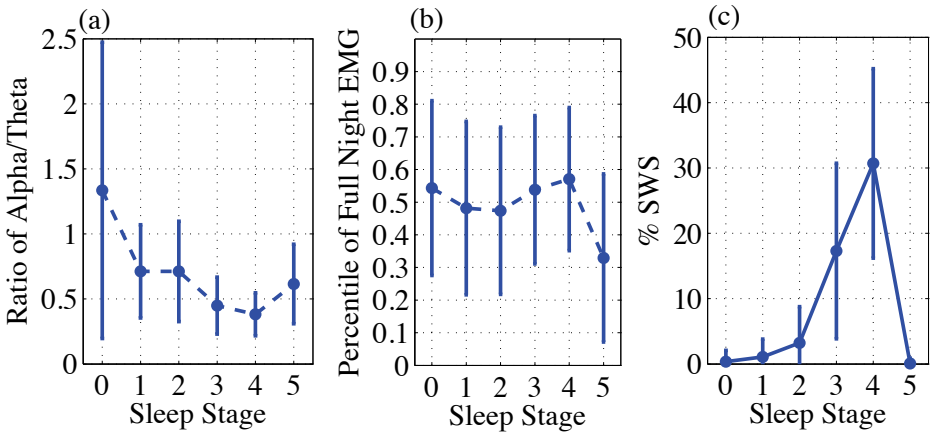

Figure 6.15. The average (a) ratio of power in the alpha frequency band to the power in the theta frequency band, (b) percentile of the EMG and (c) percent of an epoch occupied by slow wave sleep (SWS) for 76 subject nights for sleep stages Wake (0), NREM Stages 1 through 4 and REM sleep (5).

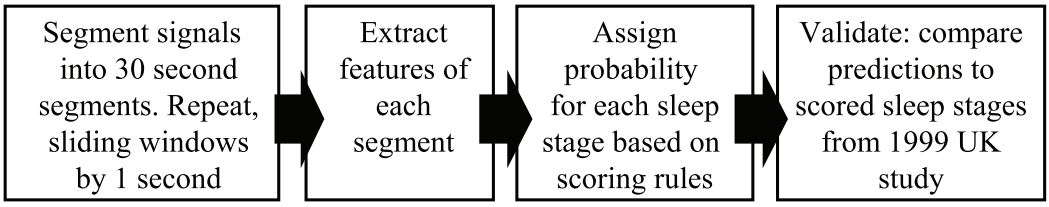

Figure 6.16. Steps used in developing sleep stage classification algorithm.

The estimated 30 second sleep stages and the original stages for one subject night from the 1999 UK dataset are shown in Figure 6.19. The mean agreement between original and estimated sleep stages was 0.70. This was found by calculating the proportion of sleep stages correctly identified for each subject night and then taking the average of all scores. The minimum agreement for one subject night was 0.51 and the maximum agreement was 0.83. The specificity and sensitivity were also calculated

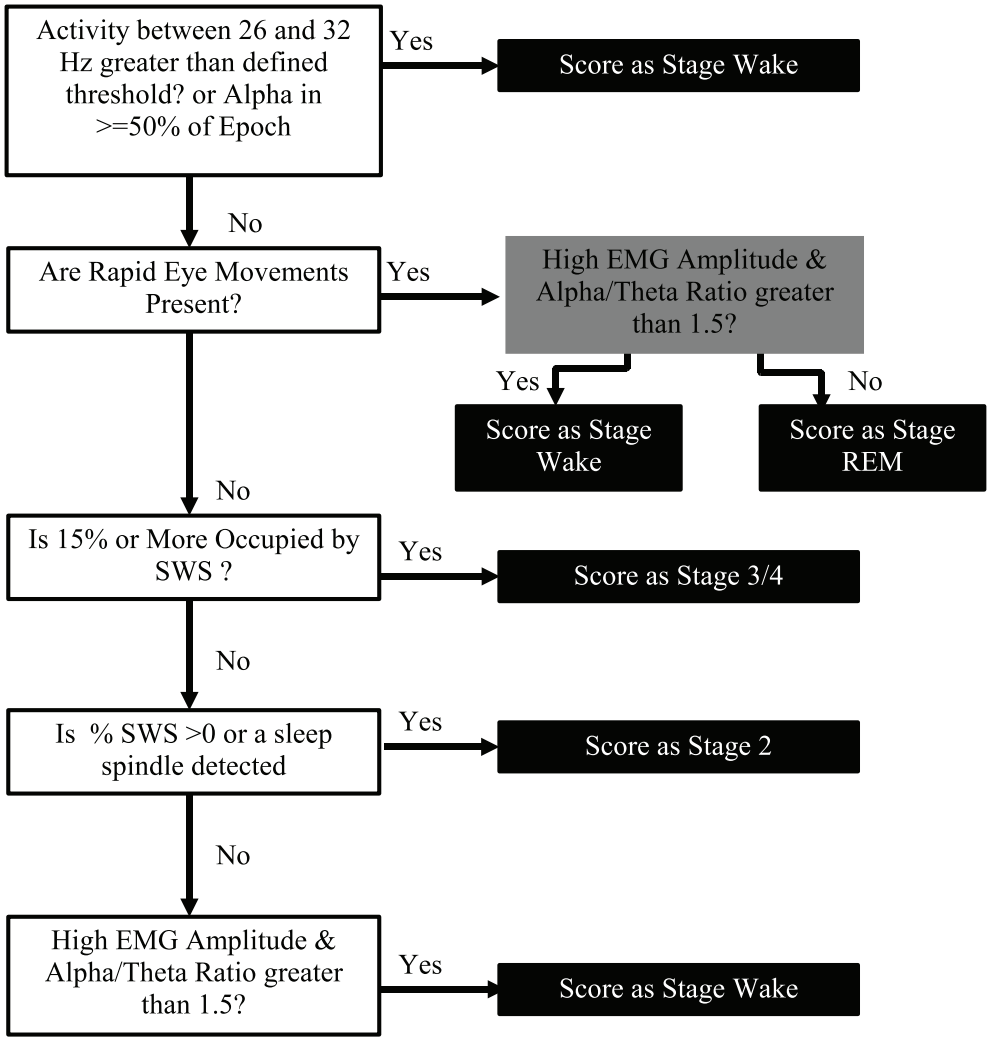

Figure 6.17. Rules used in scoring sleep stages.

for each sleep stage. The sensitivity is a measure of how well a sleep stage can be identified, while the specificity is related to how well the lack of a certain sleep stage can be identified. Both sensitivity and specificity would be equal to 1 if the sleep stage algorithm was correct in identifying each sleep stage. A reasonable specificity

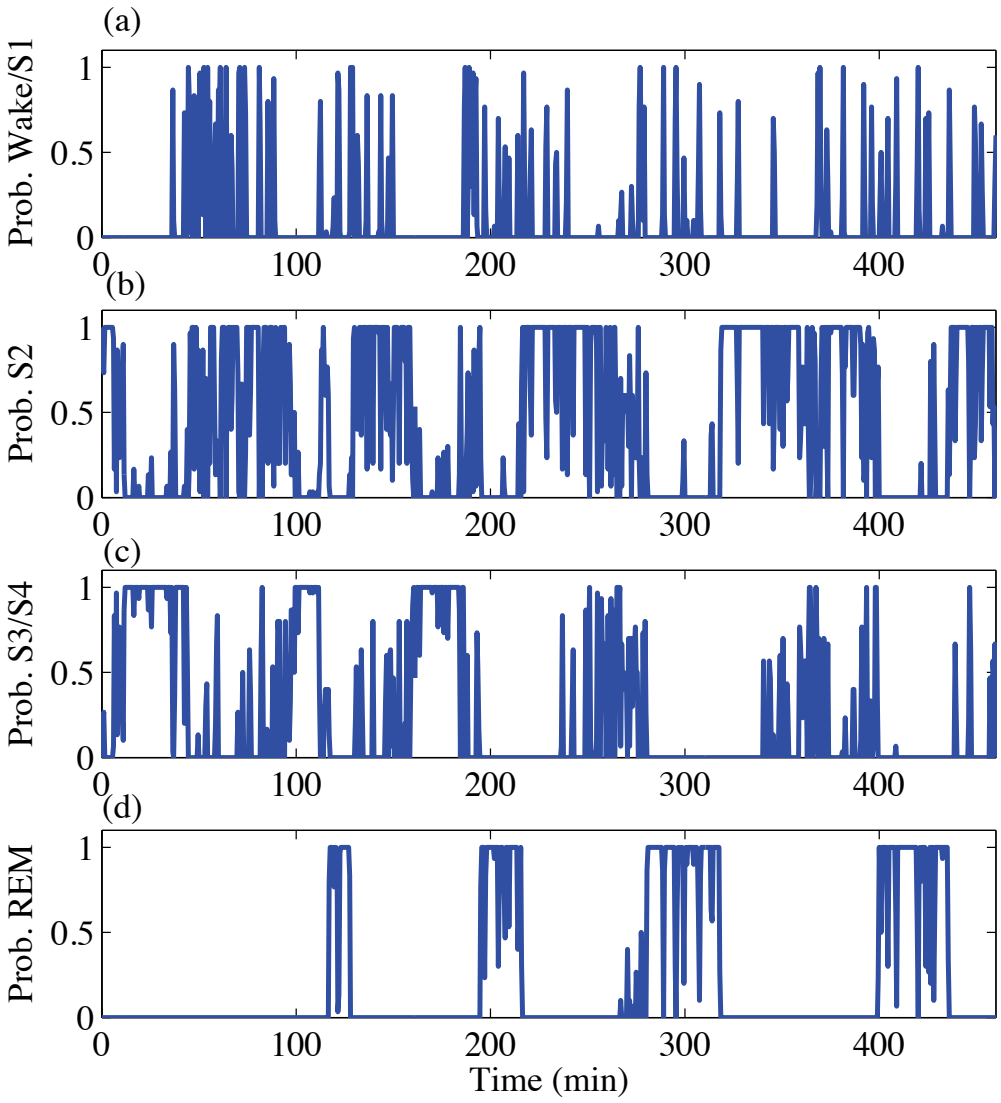

Figure 6.18. Probability of being in (a) Stage Wake/S1, (b) Stage 2, (c) Stage 3/4 and (d) REM calculated using the developed algorithm.

and sensitivity similar to other sleep stage classification approaches were obtained for Stage 2, Stage 3/4 and Stage REM (Agarwal and Gotman, 2001). The results are listed in Table 6.3. However, a low sensitivity was obtained for Stage Wake/1. Part of the reason for the low sensitivity is that Stage 1 sleep was not identified separately

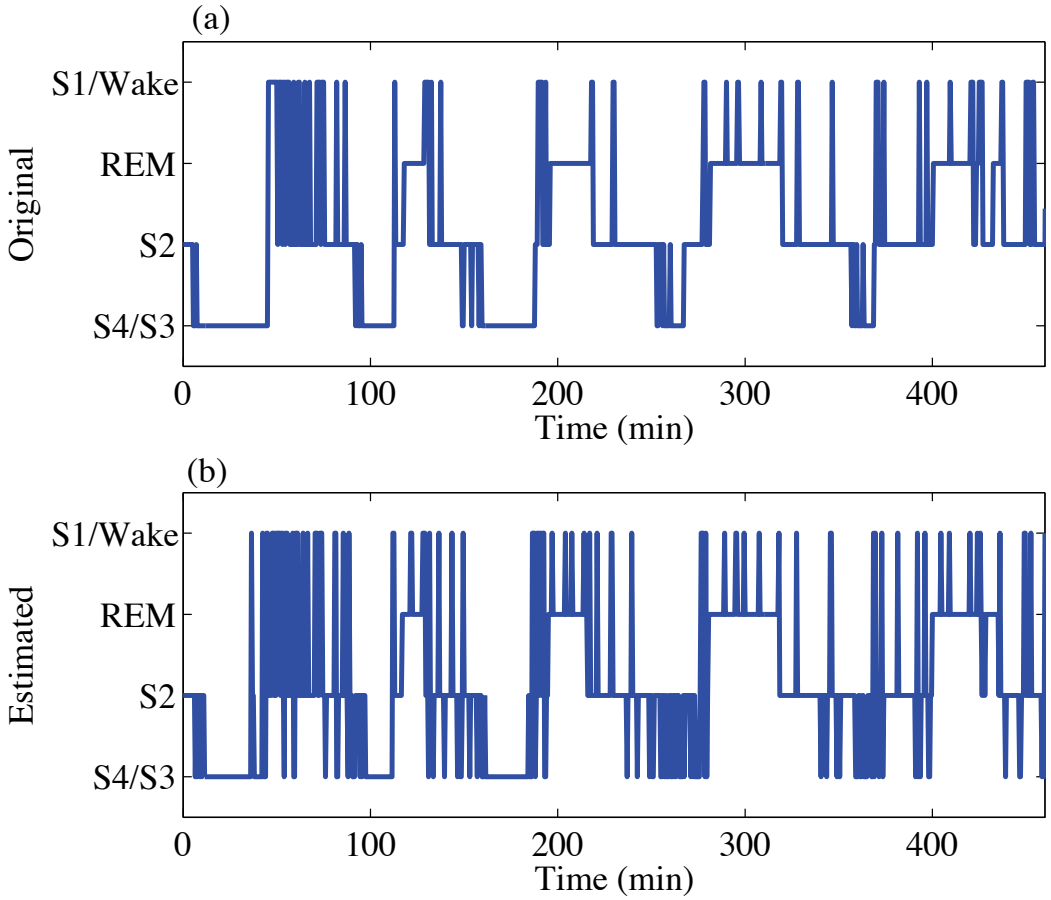

Figure 6.19. (a) Original Sleep Stages from the UK dataset and (b) sleep stages scored using the developed algorithm.

because it is just a transient stage and is often grouped with Stage Wake in noise induced sleep literature (Basner, Buess, Elmenhorst, Gerlich, Luks, MaaB, Mawet, Müller, Müller, Plath, Quehl, Samel, Schulze, Vejvoda, and Wenzel, 2004), another reason is that awakenings and transitions to Stage Wake and Stage 1 are brief. If the sensitivity is calculated considering a period of plus or minus 1 minute about the current epoch then the sensitivity for classifying Stage Wake/1 is greatly improved, the resulting sensitivity was 0.66.

Table 6.3. Sensitivity and Specificity for identifying sleep stages.

Sleep Stage	Specificity	Sensitivity
Wake/1	0.92	0.21
Stage 2	0.66	0.85
Stage 3/4	0.97	0.48
REM	0.95	0.74

6.5 Conclusions

Methods for processing the polysomnography data that was obtained as part of the UK dataset were reviewed. To remove artifacts, movement artifacts were identified based on power in the gamma EEG frequency band and a recursive least squares adaptive filtering approach was used to remove both EOG and ECG artifacts. To identify characteristics of different sleep stages various methods including AR modeling, calculation of power in different frequency bands, and correlation of the EOG signals was used. Based on these characteristics a sleep stage classification algorithm was developed in which sleep stages were assigned based on Tp seconds of data centered on each 1 second of the dataset. Here $Tp = 30$ seconds was used. The data in each 1 second interval contributed to 30 windows of data, each of which results in a classification. The probability of being in a sleep stage can be calculated from these 30 results. The time intervals Tp can be varied. Small Tp intervals will produce highly variable results while intervals that are too large will produce oversmoothed sleep stage plots. The choice of 30 seconds was used to be consistent with visual scoring and the sliding window was used to remove sensitivity to the starting point of the window. The contribution made, was to build on previous people's automatic sleep stage classification algorithms, combining and refining their approaches and to introduce the sliding window and window size flexibility to provide a more continuous assessment of changes in sleep stages during the night.

7. NONLINEAR SLEEP MODEL DEVELOPMENT AND PARAMETER ESTIMATION

After reviewing the literature on sleep models, the Massaquoi and McCarley nonlinear dynamic model was found to be the best candidate for altering so it could be used to predict the effect of aircraft noise on sleep. However, the model has slow dynamics which makes it difficult to predict brief awakenings including those that occur due to noise. To overcome this limitation additional components were introduced into the models. These components include an additional excitation term which has a dependence on noise level and a model that predicts faster dynamics during a REM period. The parameter values for the modified model were estimated using the 1999 UK study data. This required developing parameter estimation methods and also methods to process the polysomnography data to produce signals that are closely related to the E, $n(t)$, X, Y, SWA and S of the original Massaquoi and McCarley model. Similarly, parameters in the new fast REM part of the model had to be estimated from signals derived from the sleep study data. A method to determine whether a person is in Tonic or Phasic REM sleep, based on the occurrence of Rapid Eye Movement was also developed. The results of simulations using the model will also be presented later in this chapter.

7.1 Limitations of Massaquoi and McCarley Model

Before determining how to add a noise level dependence to the Massaquoi and McCarley model, simulations were conducted using the original model to determine if it could be used to predict trends in sleep stages similar to those observed with other

models. The values of the coefficients of the model, used in the simulations, are listed in Table 7.1 and the equations were provided in Chapter 5 (Equations (5.47), (5.48), (5.49), (5.55), (5.56), (5.57)) . One hundred simulations were performed using the model. The variability in the predictions for each simulation was due to the impulsive excitation term E (filtered square waves) where each impulse has a random arrival time, height, and duration (Massaquoi and McCarley, 1992). The probability of being in NREM, REM and Wake stages was calculated and the results were compared to predictions using Basner's Baseline Markov model (2006). The results are shown in Figure 7.1. The Massaquoi and McCarley model predicted a higher probability of being in NREM sleep than Basner's model, and lower probability of being awake or in REM sleep. In order to improve the predictions of the model the value of c (in Equation (5.48)), which controls the rate of decay of Y (REM-OFF) activity, was increased by 40%. A better agreement was obtained between the predicted probabilities.

Table 7.1. Coefficients of Massaquoi and McCarley's LCRIM/I Model (1992).

Model Parameters	Original Values
c	1
gc	0.05
k	10
rc	3.0
rs	0.005
E_o	0.001
X_o	0.12
Y_o	0.35
S_o	2.0
SWA_o	0.1
N Amplitude	Uniformly distributed between 1.25 and 25
N Duration	Uniformly distributed between 0.25 and 0.5
N Inter-arrival Time	Exponentially distributed with mean of 1.1
$n(t)$	Uniformly distributed between -10 and 10

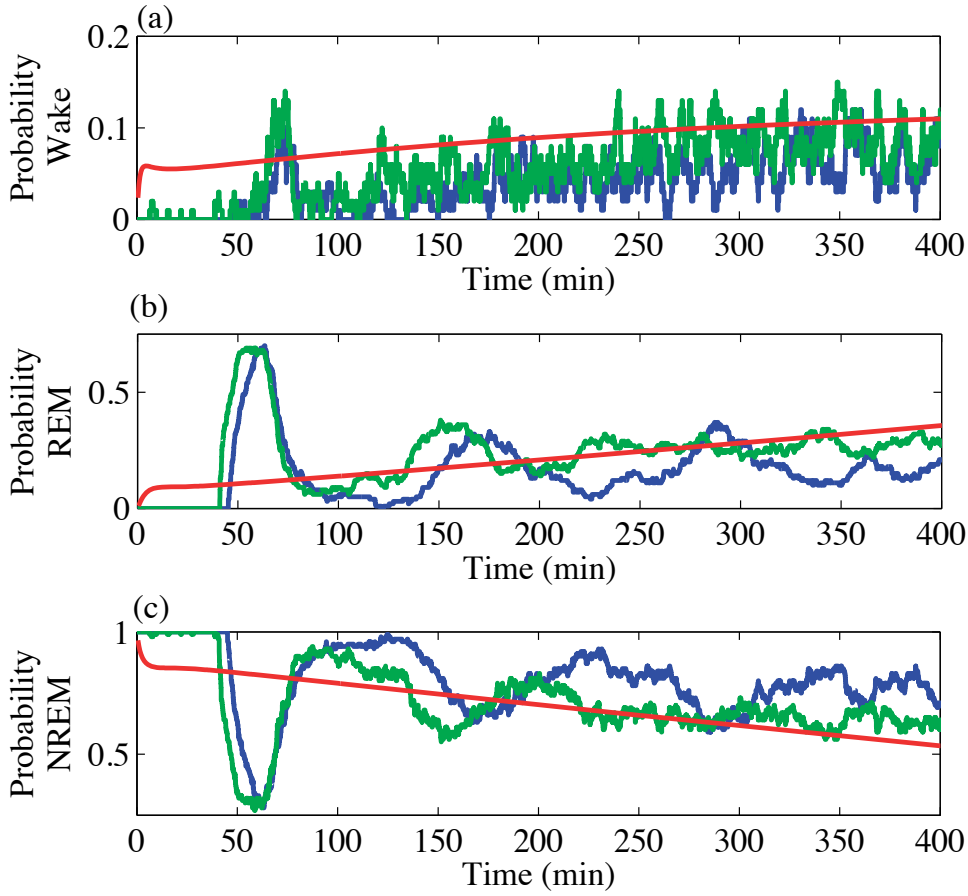

Figure 7.1. Probability of being in Wake, REM, and NREM sleep predicted using the original parameters of the Massaquoi and McCarley model (blue), with the parameter c increased by 40% (green) and with Basner's Markov model (red).

Another difference between the predictions of the two models is that the Massaquoi and McCarley model predictions have oscillations in the probability of being in NREM and REM sleep which Basner's Markov model does not. These ultradian oscillations are partly due to the assumption when performing the simulations that everyone falls asleep at the same time. In one set of simulations it was assumed that everyone retired at the same time (11:00 pm), and in another set of simulations the time to fall asleep was varied randomly for each simulation according to a normal distribution which had a mean start time of 11:00 pm and a standard deviation of 30 minutes. One hundred simulations were conducted using Basner's Markov model (Equation (4.1)) and the Massaquoi and McCarley model (Equations (5.47), (5.48), (5.49), (5.55), (5.56), (5.57)). The results are shown in Figure 7.2. The ultradian cycles in the predictions of the Massaquoi and McCarley model were smoothed out when the sleep onset time was varied and the predictions were more similar to those of Basner's Markov model but with a less pronounced increase in REM towards the end of the night.

While the overall trends in sleep stage predictions between the two models are in agreement, the Massaquoi and McCarley model is not without limitations. One limitation of the model is that awakenings or transitions to lighter sleep are not predicted by the model during a REM sleep period. A transition from REM to Wake and then back to REM cannot occur. In Figure 7.3, an example of a REM period and transitions from REM sleep to Stage Wake and Stage 1 during that period for one night of sleep, from the UK dataset, is shown. The Massaquoi and McCarley model in its current form cannot predict awakenings during REM sleep because the level of X (REM-ON) activity does not oscillate during a REM period. The level of Y (REM-OFF) neuron activity is low when X (REM-ON) activity is high and will not cause a large change in the level of X when an excitation occurs. An alternative

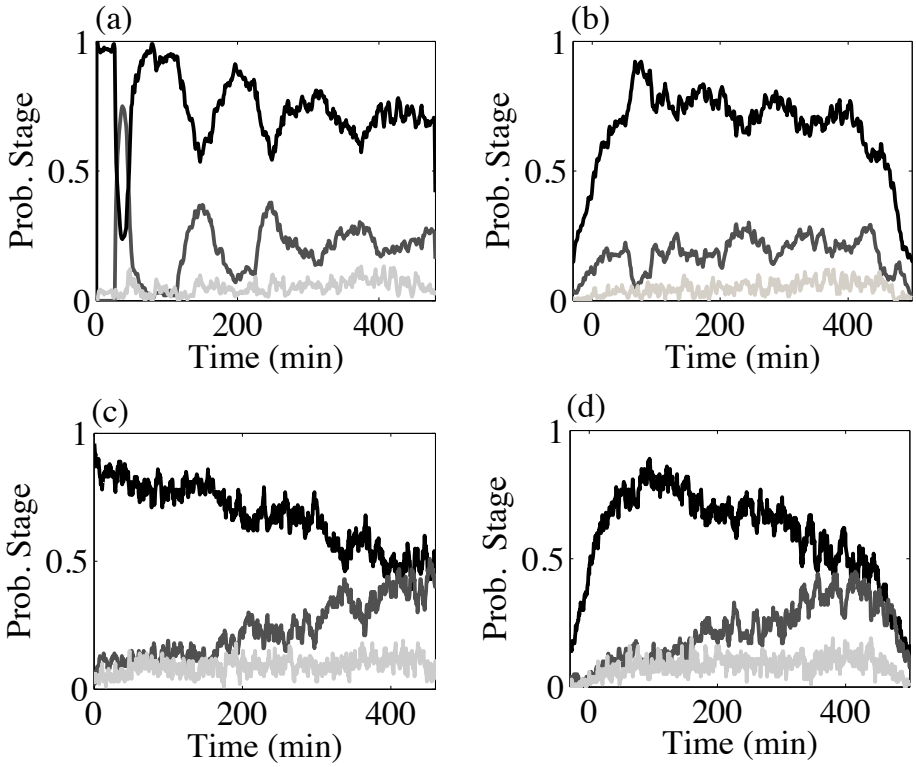

Figure 7.2. Probability of being in Wake (light gray), REM (dark gray), and NREM sleep (black) predicted using, (a) and (b) the Massaquoi and McCarley model and (c) and (d) Basner's Markov model. (a) and (c) All individuals retired at 11:00 pm and (b) and (d) Gaussian variation in sleep onset was assumed. Results based on 100 simulations.

sleep stage scoring rule could be used in which an awakening is considered to occur if the excitation term is greater than a certain value, instead of always scoring the stage as REM when X is greater than 1.4. This type of approach was taken by Comte, Schatzman, Ravassard, Luppi, and Salin (2006) when scoring sleep stages using their model. However, an inadequacy of this approach is that an awakening will not play a more dynamic role in the sleep process and whether an individual awakens during REM sleep has been found to depend on ongoing brain activity and whether an individual is in Phasic or Tonic REM sleep (Ermis, Krakow, and Voss, 2010).

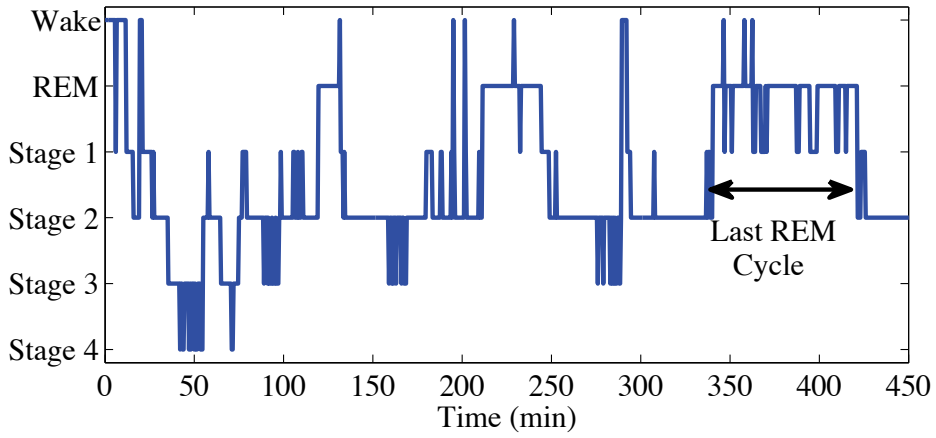

Figure 7.3. Example of a REM sleep period and the change in sleep stages within that period.

The second limitation of the Massaquoi and McCarley model is that it has slow dynamics. While the model can predict the slow ultradian 90-100 minute oscillation between NREM and REM sleep, it cannot be used to adequately predict brief awak-

enings. To emphasize the slow dynamics, the equations of the REM sleep portion of the model can be rewritten where the equation for REM promoting (X) activity is,

$$\dot{X} + \omega_{c1} X = 0, \tag{7.1}$$

$$\omega_{c1} = b(X)Y - a(X)S_1(X). \tag{7.2}$$

The equation for REM inhibiting (Y) activity can also be rewritten as,

$$\dot{Y} + \omega_{c2} Y = 0, \tag{7.3}$$

$$\omega_{c2} = c - d_{circ} S_2(Y)(X + E). \tag{7.4}$$

Both equations have the form of a low pass filter with time varying cutoff frequencies. In Figure 7.4 the variations in the two frequencies are shown. The majority of the behavior of the model is on the order of hours not seconds. Dynamics on a timescale of several seconds are needed to predict awakenings during REM periods.

In order to further examine the use of the Massaquoi and McCarley model for predicting brief awakenings, simulations were conducted in which excitation events ($N(t)$) were of equal spacing, amplitude, and duration. The duration of the impulses was one minute, which is approximately the duration of an aircraft event, the amplitude of the impulses was varied in increments of 1, from 1 to 10. For these simulations the following equation was used for E,

$$\dot{E} + kE = kN, \tag{7.5}$$

where k was equal to 10, which is the value in the original Massaquoi and McCarley model. The duration spent in NREM, REM, and Wake states were calculated for each

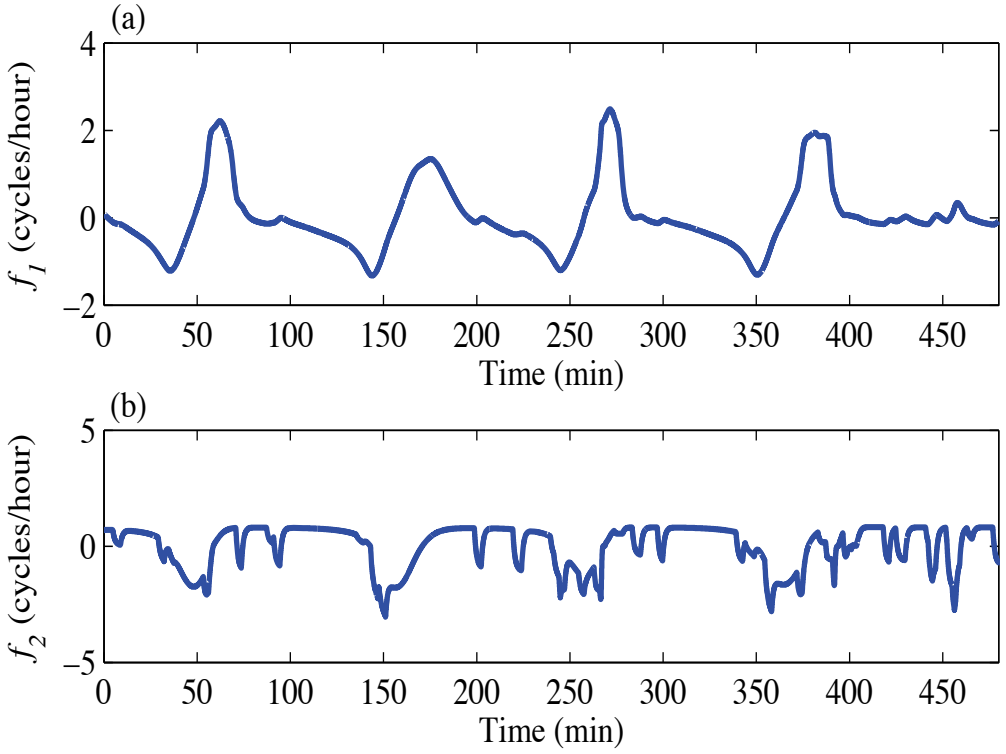

Figure 7.4. The time varying frequencies of the Massaquoi and McCarley model. (a) X model and (b) Y model.

simulation. In Figure 7.5 the results of two simulations, with low (E_{max}=2.4) and high excitation levels (E_{max}=6.0) for 16 events are shown. The number of REM sleep periods and the level of slow wave activity were found to decrease as the amplitude of the events were increased. However, due to the sleep stage scoring thresholds of the original model, the number of predicted awakenings did not increase when the amplitude of the impulses was increased. In Figure 7.6 the duration of REM, NREM, and Wake stages for various amplitudes of the excitation parameter ($N(t)$) are shown.

Simulations were also conducted for 64 events of varying amplitudes. The results are shown for low amplitudes (E_{max}=1.8) and high amplitudes (E_{max}=3.6) in Figure 7.7 and the duration of REM, NREM and Wake stages for various amplitudes of the excitation parameter are shown in Figure 7.8. As the amplitude of the noise events was increased, the NREM and REM sleep cycles during the night disappeared and there was still not a large increase in the number of predicted awakenings.

The addition of an excitation term to the equation for X (REM-ON) activity was examined to determine if more variations in the level of activity and an increase in the prediction of awakenings could be obtained without destroying the slow ultradian cycling. One approach was to use the following equation,

$$\dot{X} = a(X)S_1(X)X - b(X)XY - EX. \tag{7.6}$$

The term EX was added rather than just E alone in order to prevent the level of X from becoming negative. The results for a simulation using this approach is shown in Figure 7.9. The addition of the E term caused a decay in REM-ON (X) activity which caused the ultradian cyclic behavior to end. Therefore, another approach in which a saturation function ($f(X)$) was added was also examined, the equation for which is,

$$\dot{X} = a(X)S_1(X)X - b(X)XY - f(X)EX. \tag{7.7}$$

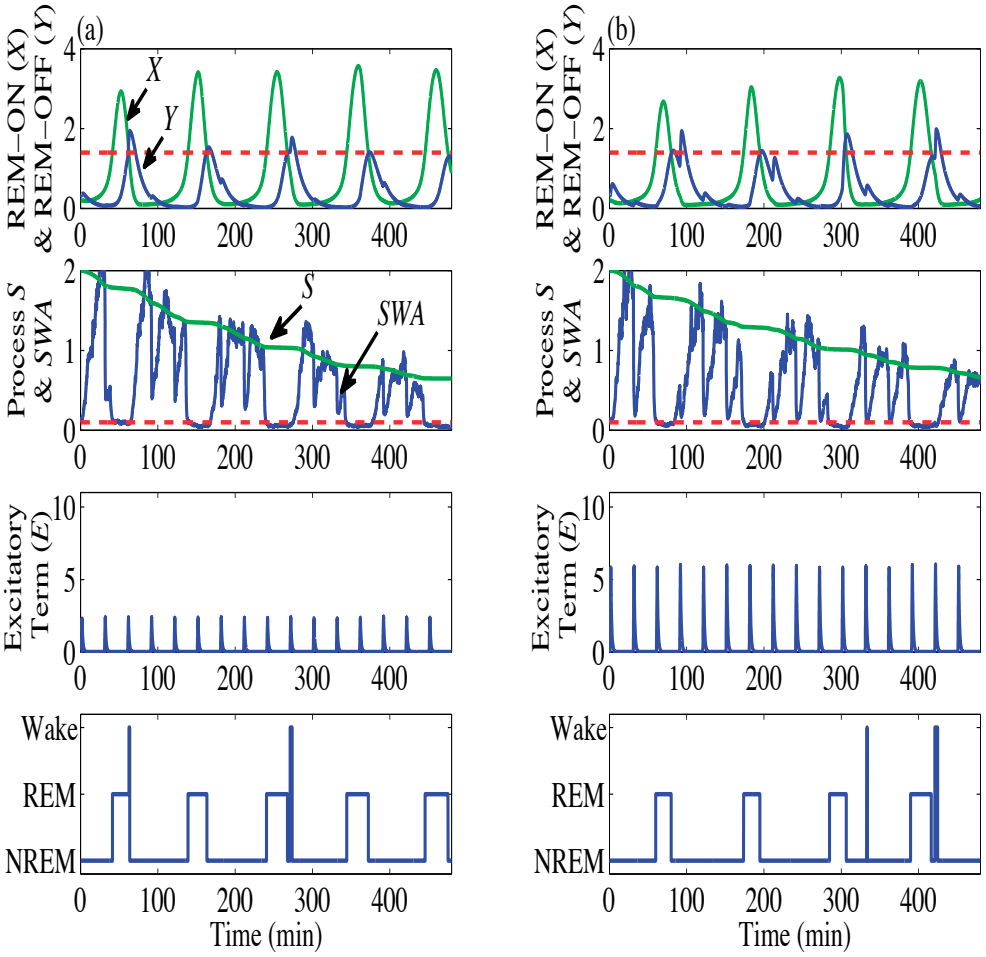

Figure 7.5. Massaquoi and McCarley model predictions for 16 events of 1 minute duration occurring during the night. (a) Low amplitude (E_{max}=2.4, N_{max}=4) and (b) high amplitude (E_{max}=6.0, N_{max}=10) impulses.

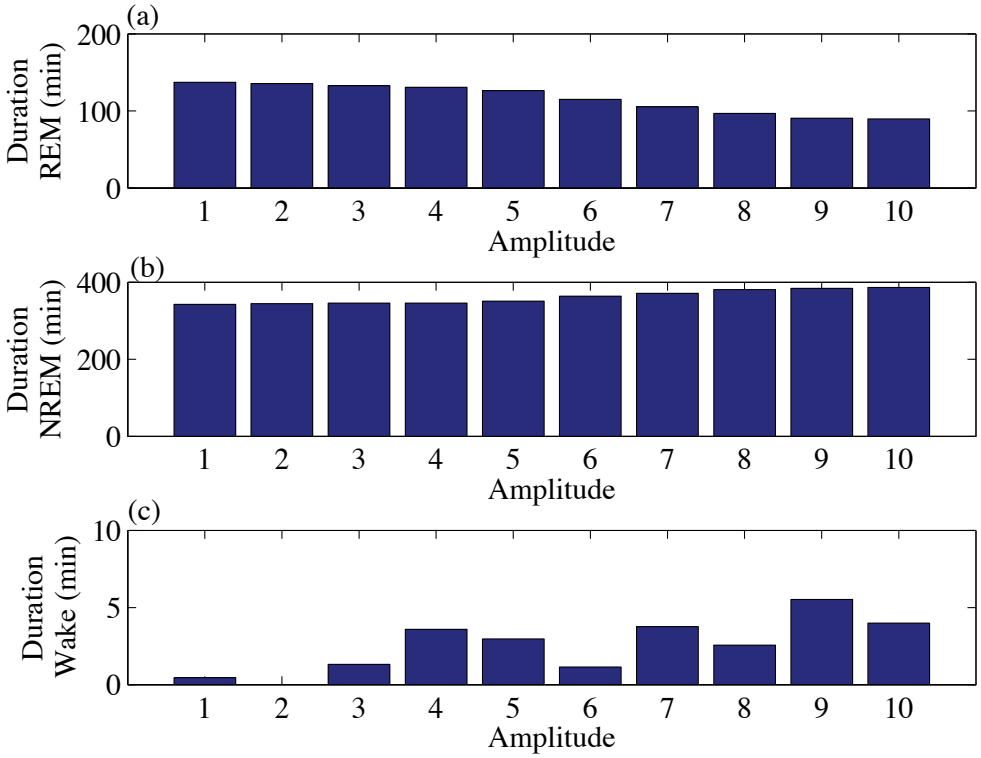

Figure 7.6. The duration of REM, NREM and Wake stages predicted using the Massaquoi and McCarley model for nights with 16 events of different amplitudes of $N(t)$. The duration of the impulses in $N(t)$ was 1 minute and spacing between impulses was 30 minutes.

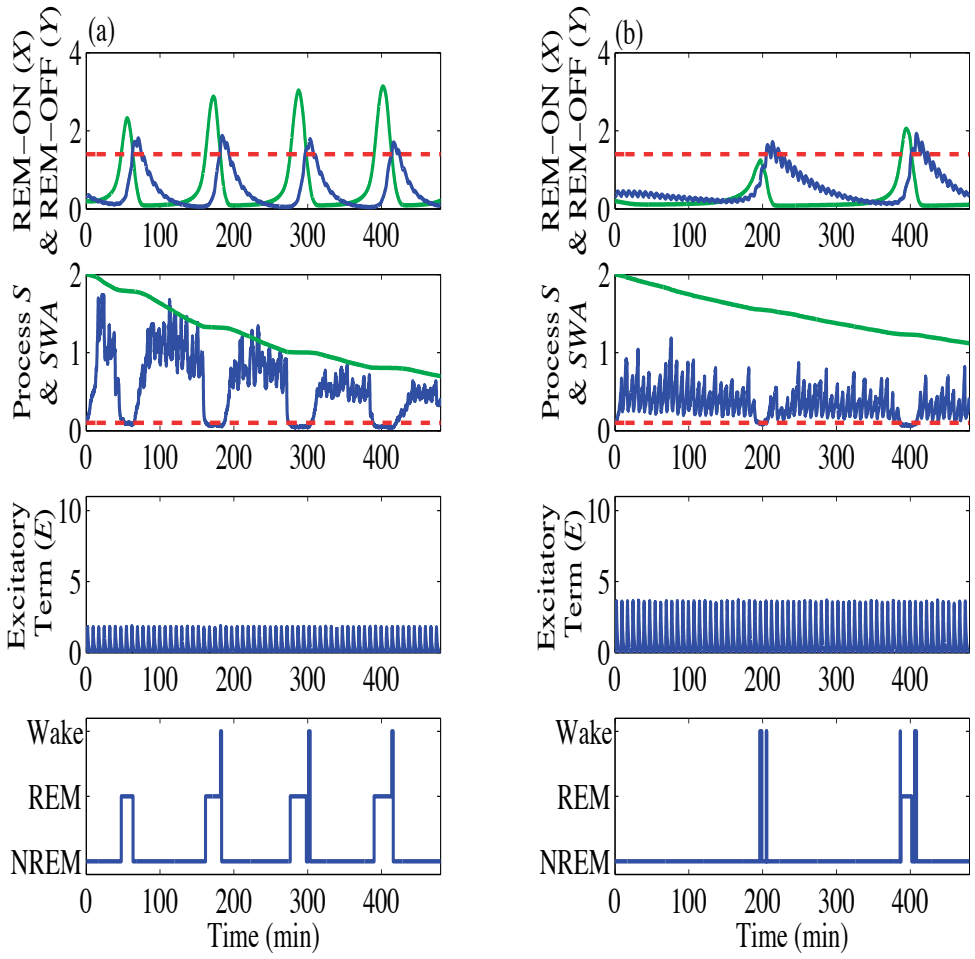

Figure 7.7. Massaquoi and McCarley model predictions for 64 events of 1 minute duration occurring during the night. (a) Low amplitude (E_{max}=1.8, N_{max}=3) and (b) high amplitude (E_{max}=3.6, N_{max}=7) impulses.

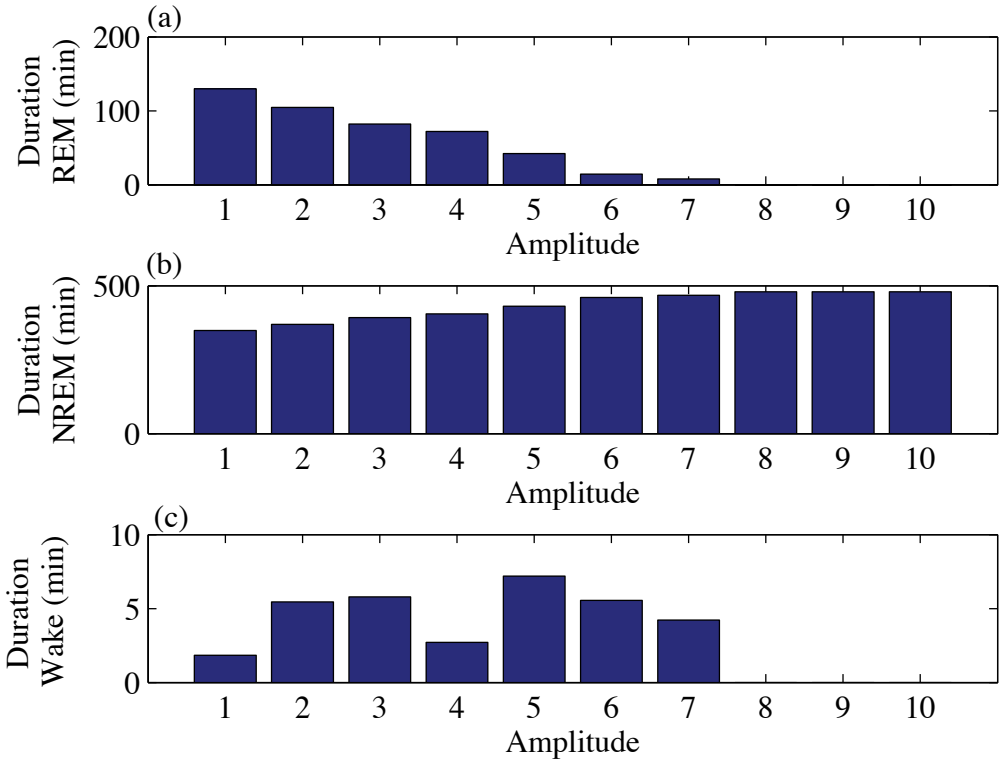

Figure 7.8. The duration of REM, NREM and Wake stages predicted using the Massaquoi and McCarley model for nights with 64 events of different amplitudes of $N(t)$. The duration of the impulses in $N(t)$ was 1 minute and spacing between impulses was 7.5 minutes.

In Figure 7.10 the saturation function is shown. The form of the saturation function was chosen so the excitation term only affected X when the level of X was high. The results for a simulation conducted with the added saturation function are shown in Figure 7.11, where the labels A and B, in the Figure, indicate the decay in the X activity due to the addition of the excitation term to the REM-ON (X) equation. While awakenings were predicted during the REM periods this behavior is still not fast enough for predicting awakenings during sleep, which can be as brief as 15 seconds. Also not all simulations using this approach resulted in desirable results, such as the example shown in Figure 7.12, in which the X and Y activity no longer appears cyclic.

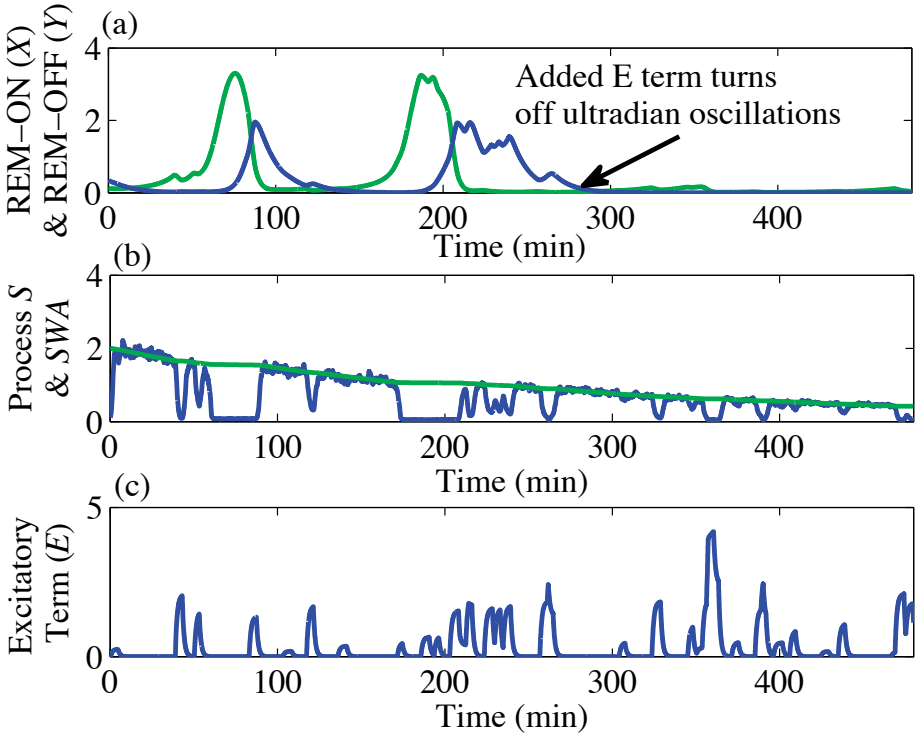

Figure 7.9. Prediction of the Massaquoi and McCarley model when an excitation term (EX) was introduced in the REM-ON (X) equation.

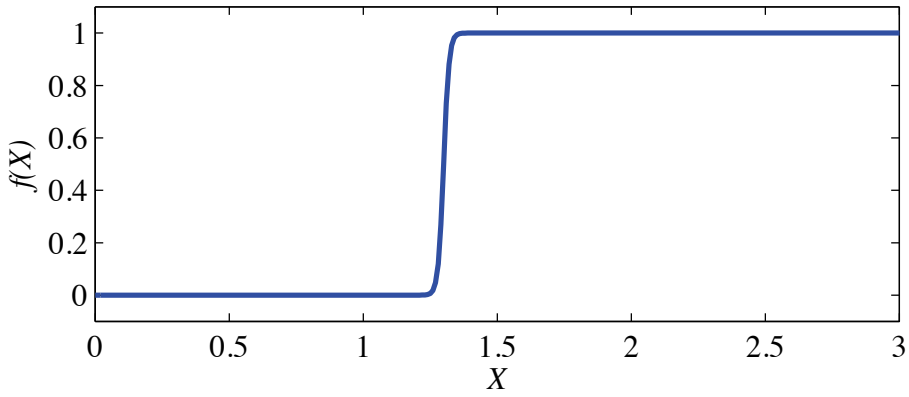

Figure 7.10. Saturation function $f(X)$ used in Equation (7.7) to turn on E effects only when $X > 1.3$.

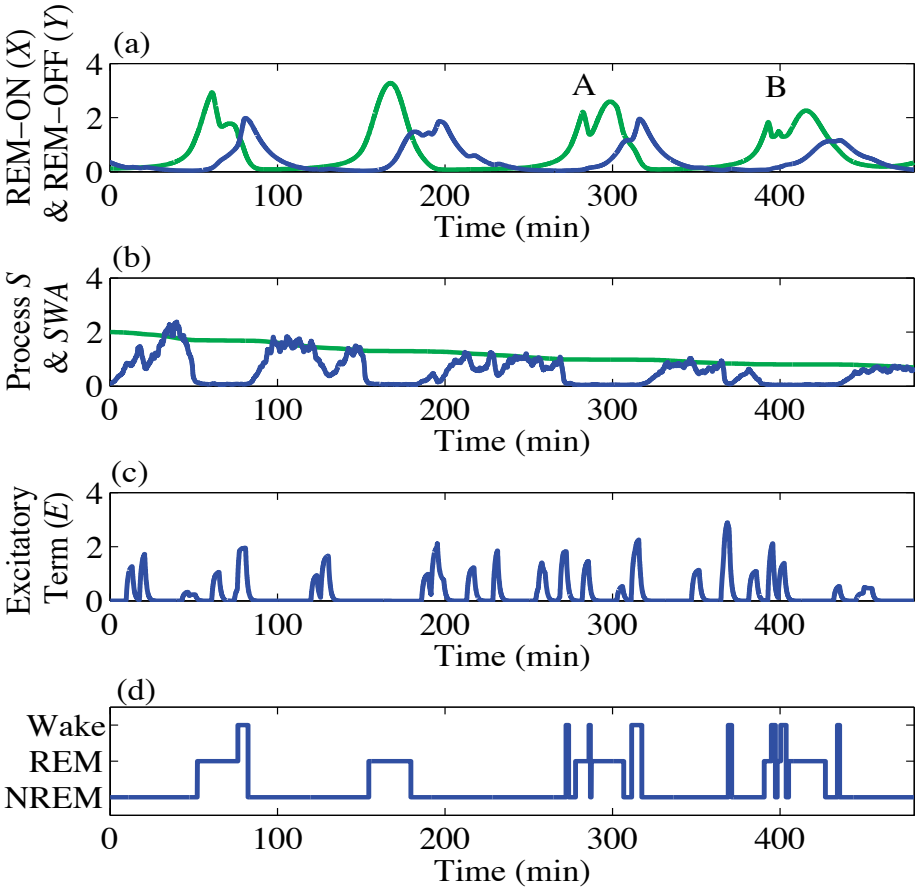

Figure 7.11. Prediction of the Massaquoi and McCarley model when an excitation term with a saturation function was added to the REM-ON (X) equation. A and B mark times when there are awakenings during the REM sleep period. (a) X (green) and Y (blue); (b) Process S (green) and SWA (blue); (c) excitatory term (E) (filtered rectangular pulses with uniformly distributed amplitudes and durations and exponentially distributed arrival times); and (d) sleep stage classification.

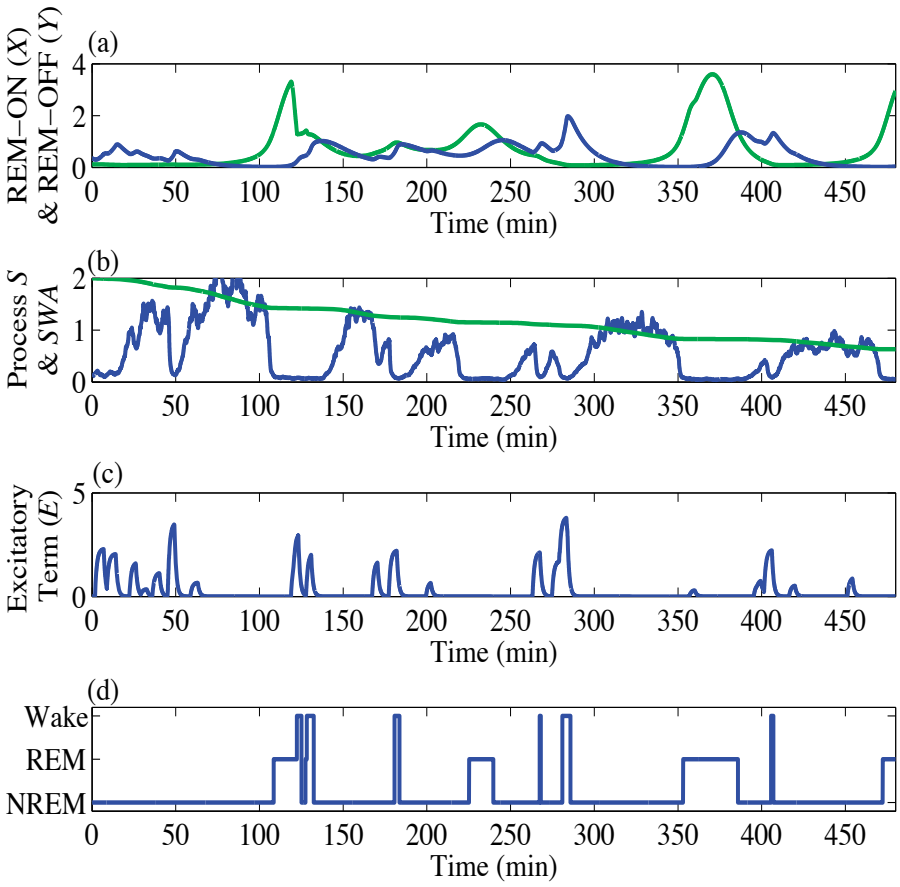

Figure 7.12. Prediction of the Massaquoi and McCarley model when an excitation term with a saturation function was added to the REM-ON (X) equation. Less desirable changes in sleep were obtained. (a) X (green) and Y (blue); (b) Process S (green) and SWA (blue); (c) excitatory term (E) (filtered rectangular pulses with uniformly distributed amplitudes and durations and exponentially distributed arrival times); and (d) sleep stage classification.

The only approach that did result in fast oscillations in REM-ON (X) activity was when a band-passed noise or sinusoidal noise term, denoted by (q) in Equation (7.8) was added to the X equation,

$$\dot{X} = a(X)S_1(X)X - b(X)XY + qX. \tag{7.8}$$

An example of the results obtained using this approach is shown in Figure 7.13. The example results shown in Figure 7.13 (a) is for when q is equal to a sinusoidal term with an amplitude of 40 and 4 oscillations per minute. For results shown in Figure 7.13 (b) q is uniformly distributed band passed noise with frequencies of oscillation between 1 and 4 per minute and has an amplitudes between -50 and 50. While fast oscillations were predicted, the impulsive, random occurrence of awakenings during REM periods was not.

7.2 Altering Ultradian Oscillator-Slow REM Model

Based on the limitations of the Massaquoi and McCarley model, it was determined that slow and fast activity during REM sleep needed to be modeled separately. Therefore, instead of trying to manipulate the REM-ON and REM-OFF equations to obtain oscillations in activity that could lead to awakenings using scoring rules, the REM-ON and REM-OFF equations would be used for just controlling the ultradian cycling.

Having a slow term whose only role is to control the ultradian oscillations in the model is not a new concept, Achermann, Beersma, and Borbély (1990) used a Van der pol oscillator with the two-process model to control the ultradian oscillations between NREM and REM sleep, which was defined by the equation,

$$\ddot{X} = a(b - X^2)\dot{X} - wX. \tag{7.9}$$

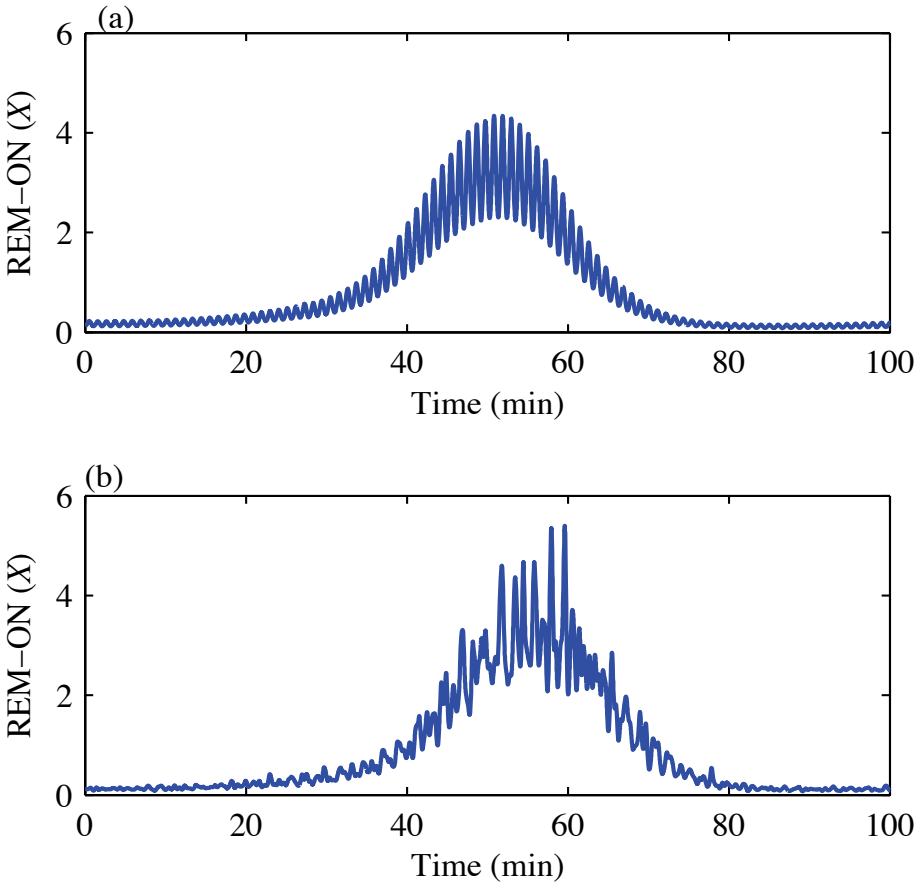

Figure 7.13. REM-ON activity (X) with (a) added sinusoidal noise with frequency of 4 oscillations per minute and amplitude of 40. (b) Added uniformly distributed (between -50 and 50) band-passed noise between frequencies of 1 and 4 oscillations per minute.

Wever (1980) used two coupled nonlinear oscillators one for circadian and one for ultradian oscillations. The form of his equations are,

$$\ddot{y} + \varepsilon_1(y^2 - y^{-2} - a_1)\dot{y} + {\omega_1}^2(y + g_1 y^2) = {\omega_1}^2(c_1(\ddot{x} + \dot{x} + x)), \tag{7.10}$$

and

$$\ddot{x} + \varepsilon_2(x^2 - x^{-2} - a_2)\dot{x} + {\omega_2}^2(x + g_2 x^2) = {\omega_2}^2(c_2(\ddot{y} + \dot{y} + y)). \tag{7.11}$$

The excitation term E in the REM-OFF equation of the Massaquoi and McCarley REM model though will remain in the slow REM model. If the maximum amplitude of the excitation is limited the loss of NREM-REM cycling will not occur as in the the simulations in the previous sections. The reason for keeping the E term in a slow REM model is that several researchers have found that the duration of sleep cycles is affected by awakenings. Foret, Touron, Clodoré, and Bouard (1990) examined the effect of forced awakenings on the duration of NREM sleep during one sleep cycle. They interrupted sleep one time a night, for 3 nights. The time of the interruption varied per test night and occurred at either 1:30, 3:30, or 5:30 am. The duration of the interruption was 10 minutes. To calculate the effect of the interruption on the NREM-REM timing they calculated what they called the inter-REM interval which was the time between the start of one REM period until the start of the next period, however the 10 minute interruption time was not included when calculating the inter-REM interval duration. They found that compared to a baseline night, the interruption caused a decrease in cycle duration if it occurred in the first half of the cycle but it caused an increase in cycle duration if the interruption occurred in the second half of the cycle.

Massaquoi and McCarley (1990) compared predictions using their model to the data from the study conducted by Foret, Touron, Clodoré, and Bouard (1990). They

applied excitations at various locations during a sleep cycle. Each pulse in the E term in the model had a duration of one unit or 10.7 minutes. They examined the effect of different amplitudes of excitation on the duration of a sleep cycle. They found that the strength of the excitation does have an effect on the change in cycle length. A strong excitation will result in a linear relationship between the time an excitation occurs and the change in cycle duration. However, they found that moderate or weak pulses have more of a curvilinear relationship.

7.3 Fast REM Model

The development of a fast REM sleep model is based on the notion that during REM sleep the probability of awakening to a noise event is dependent on ongoing brain activity and, in particular, whether an individual is in Tonic or Phasic REM sleep. The Tonic and Phasic activity in the UK dataset was examined and used to develop the model.

7.3.1 REM Density Calculation

While it might not be well understood yet what exactly is causing the variation in stimulus response during REM sleep, what is clear is that response to auditory stimuli cannot be assumed to be constant during this stage. Results from Wehrle et al. (2007) indicate that a noise stimulus will be processed differently depending on whether an individual is in Tonic or Phasic REM sleep, and this in turn affects whether they awaken.

In order to evaluate the timing and duration of Phasic and Tonic REM sleep in the data from the 1999 UK study, the density of rapid eye movements was calculated. To calculate the density of rapid eye movements first the left and right EOG channels

were bandpass filtered between 0.5 and 5 Hz by using a 4th order Butterworth filter. The beginning and end of each REM period was identified. Within the defined REM period the two EOG channels were segmented into 30 second segments. The correlation between the two channels was calculated and then the process was repeated moving in 1 second increments through time. If the correlation of the two channels was below -0.2, rapid eye movements were considered to occur. A second method was also used to identify rapid eye movement which was similar to an approach used by Agarwal, Takeuchi, Laroche, and Gotman (2005). The inverse or negative of the left EOG channel was multiplied by the Right EOG channel and then amplitudes greater than 625 μV^2 were identified. A 2 second segment of both the right and left EOG channel was obtained around each peak. The correlation between the 2 seconds of the left and the 2 seconds of the right EOG channels was calculated. If the correlation was below -0.2 and the peaks of the two channels were within 100 ms of one another, then rapid eye movement was considered to occur. Then, for each 30 second segment, the proportion of the segment that was occupied by rapid eye movement was calculated in order to obtain a measure of REM density. The measure of REM density was again calculated for 30 second segments, moving 1 second in time. The results for one REM period are shown in Figure 7.14. The REM Indicator is an indicator of Phasic and Tonic REM activity, it is equal to 1 when the REM density is greater than zero and Phasic REM sleep is occurring, and is equal to zero when Tonic REM sleep is occurring. Tonic REM periods of less than 15 seconds duration were set equal to Phasic REM sleep though, this approach has been used by others (Ermis, Krakow, and Voss, 2010) to define Tonic and Phasic REM sleep.

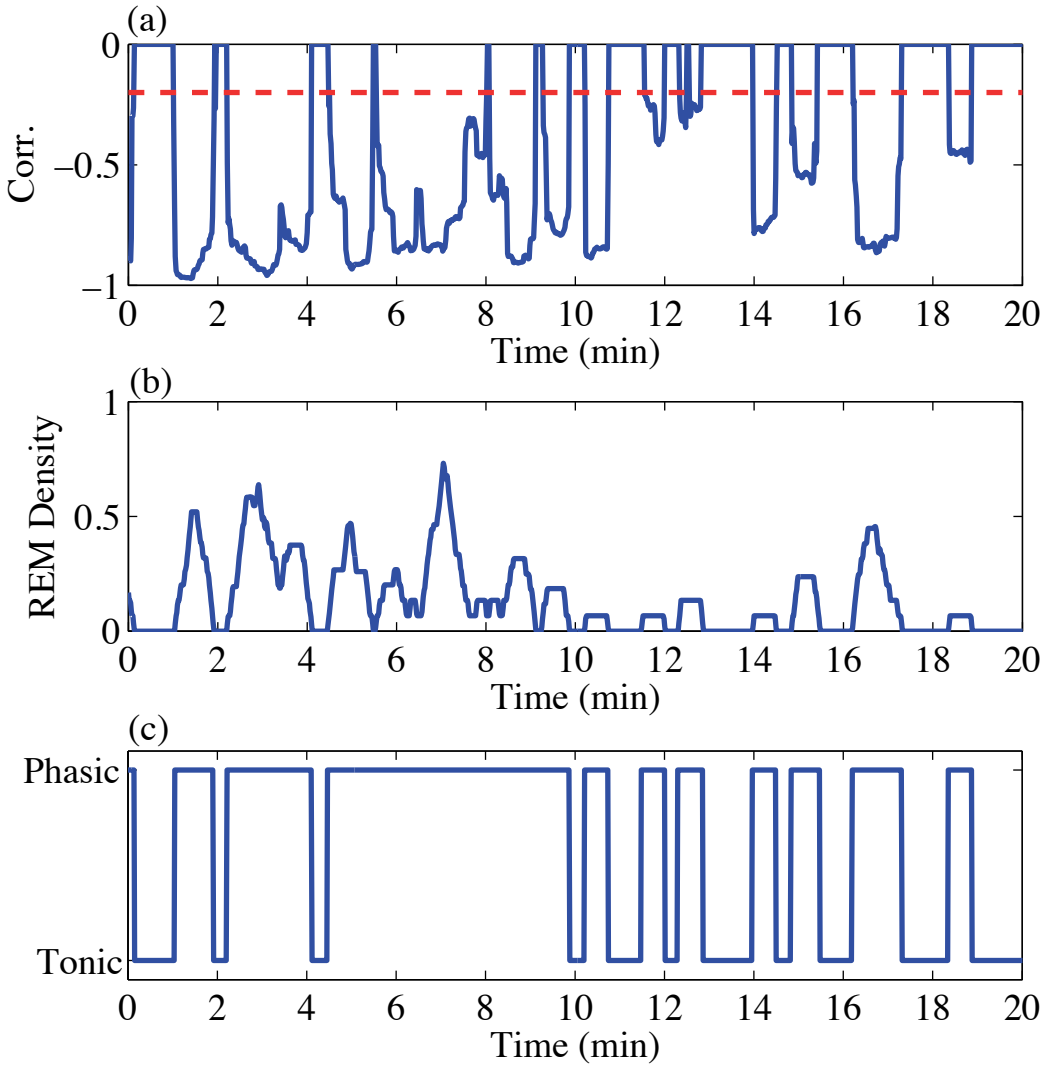

Figure 7.14. An example of rapid eye movement activity. (a) 30 second correlation between right and left EOG signals and the -0.2 threshold used (red dashed line), (b) REM density measurement-proportion of the 30 second epoch occupied by rapid eye movement activity, and (c) an indicator of Phasic and Tonic REM sleep.

7.3.2 Form of Fast REM Model

A few researchers have tried to identify/model the process that causes the occurrence of rapid eye movements. Trammell and Ktonas (2003) stated that the occurrence of rapid eye movements may not be due to a random process. One method they used to determine if the process that caused rapid eye movement bursts was deterministic or stochastic was the correlation dimension. They calculated the correlation dimension using the inter-REM periods or the time between rapid eye movements and found values near 2. This indicated to Trammell and Ktonas (2003) that a low order non-linear process may explain the intervals between rapid eye movements. Boukadoum and Ktonas (1988) analyzed the probability density function of inter-REM intervals between rapid eye movements. They categorized inter-REM periods according to two criteria: (1) the time between rapid eye movements within a burst, (a burst is defined if the inter-REM period is less than 2 seconds), and (2) inter-REM period between isolated bursts of rapid eye movement. From the estimated probability density function they concluded that two separate processes may be involved in the occurrence of rapid eye movements, one process controlling the brief bursts of activity and another controlling the longer intervals between rapid eye movements. They stated that the inter-REM intervals cannot be predicted by using an exponential distribution.

After examining the occurrence of Phasic and Tonic REM sleep in the UK data, it seemed that the oscillation between the two states, along with the change to awake states during REM sleep could be modeled using a Duffing equation with the harmonic excitation in a region in which chaotic response behavior is possible. The form of the Duffing equation with up to a 5th order stiffness term was examined (Li and Moon, 1990). This equation has the form,

$$\ddot{x} + \delta\dot{x} + \beta_5 x^5 + \beta_4 x^4 + \beta_3 x^3 + \beta_2 x^2 + \beta_1 x + \beta_o = A cos(\omega t); \qquad (7.12)$$

which can also be written as,

$$\ddot{x} + \delta\dot{x} + \beta(x-\alpha_1)(x-\alpha_2)(x-\alpha_3)(x-\alpha_4)(x-\alpha_5) = Acos(\omega t); \tag{7.13}$$

If the unforced case is considered the corresponding set of first order differential equations are,

$$\dot{x} = y, \tag{7.14}$$

$$\dot{y} = -\delta y - \beta_5 x^5 - \beta_4 x^4 - \beta_3 x^3 - \beta_2 x^2 - \beta_1 x - \beta_o. \tag{7.15}$$

There are 5 equilibrium points and they occur when,

$$y = 0, \tag{7.16}$$

$$\beta_5 x^5 + \beta_4 x^4 + \beta_3 x^3 + \beta_2 x^2 + \beta_1 x + \beta_o = 0. \tag{7.17}$$

The Duffing equation (usually with only a 3rd order polynomial rather than the 5th order shown here) has been used to model the behavior of an elastic beam which is clamped vertically above magnets of fixed position. The entire system consisting of the beam and the magnets are shaken horizontally. When the system is shaken with a low amplitude the beam will oscillate about one of the magnets which are stable equilibrium points. If the system is shaken with a large enough sinusoidal force, in certain frequency and amplitude regions the beam will jump chaotically from magnet to magnet (Moon and Holmes, 1979). This is illustrated in Figure 7.15 for a third order nonlinearity and in Figure 7.16 for a fifth order nonlinearity.

For the Duffing equation with a 5th order stiffness term, three of the equilibrium points are stable, the other two equilibrium points are saddle points and are unstable. For the fast REM model, two of the stable points were considered to be Tonic and Phasic REM sleep. The third stable point represents Stage 1/Wake. As research

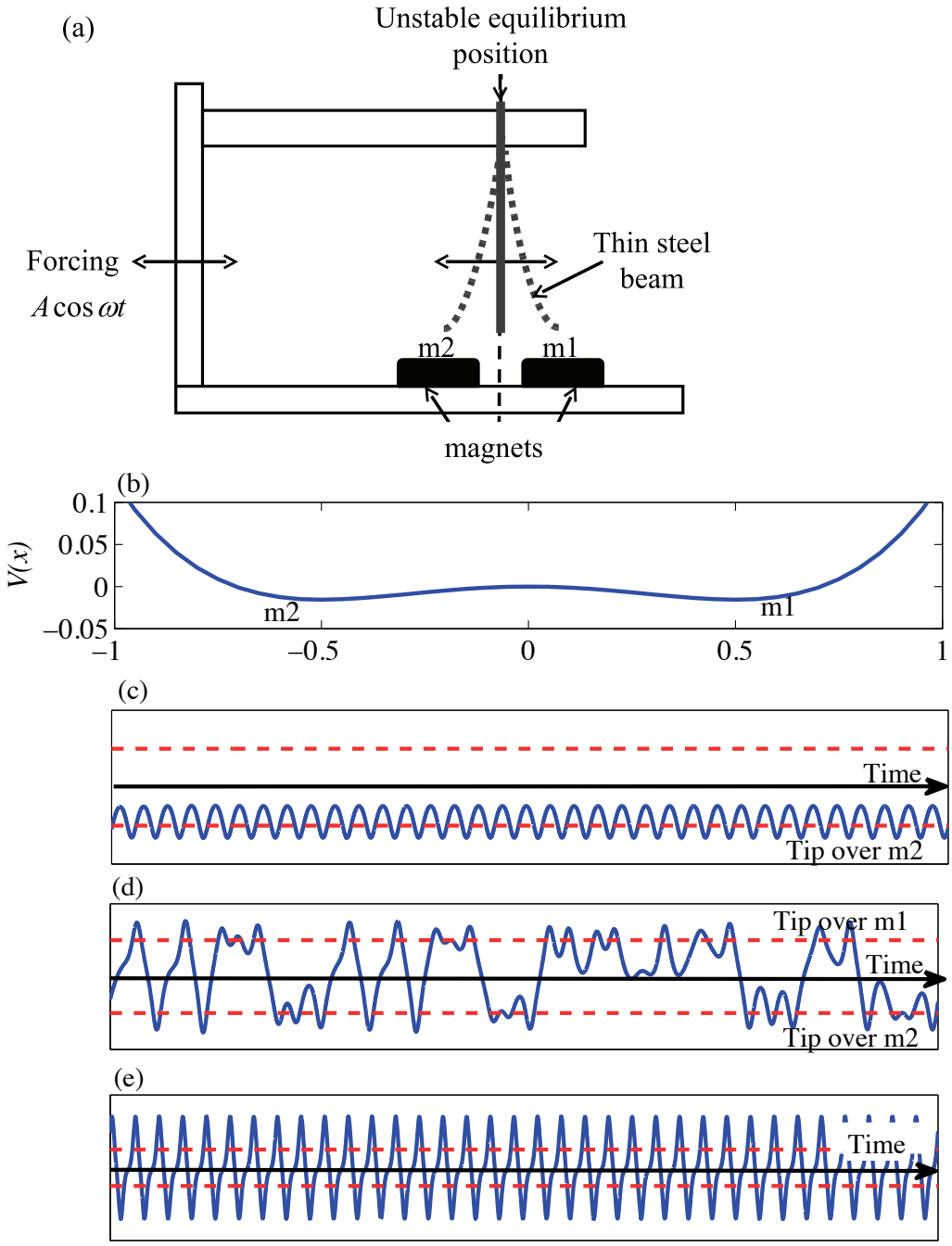

Figure 7.15. A Duffing oscillator with two stable points at 0.5 and -0.5 and one unstable point at 0, $\delta = 0.06$ and $\omega = 2\pi(0.1)$. (a) Beam analogy, (b) potential function, (c) oscillations about one stable equilibrium (A=0.01), (d) chaotic jumps between equilibrium (A=0.4), and (e) periodic oscillations about both stable equilibria (A=0.6).

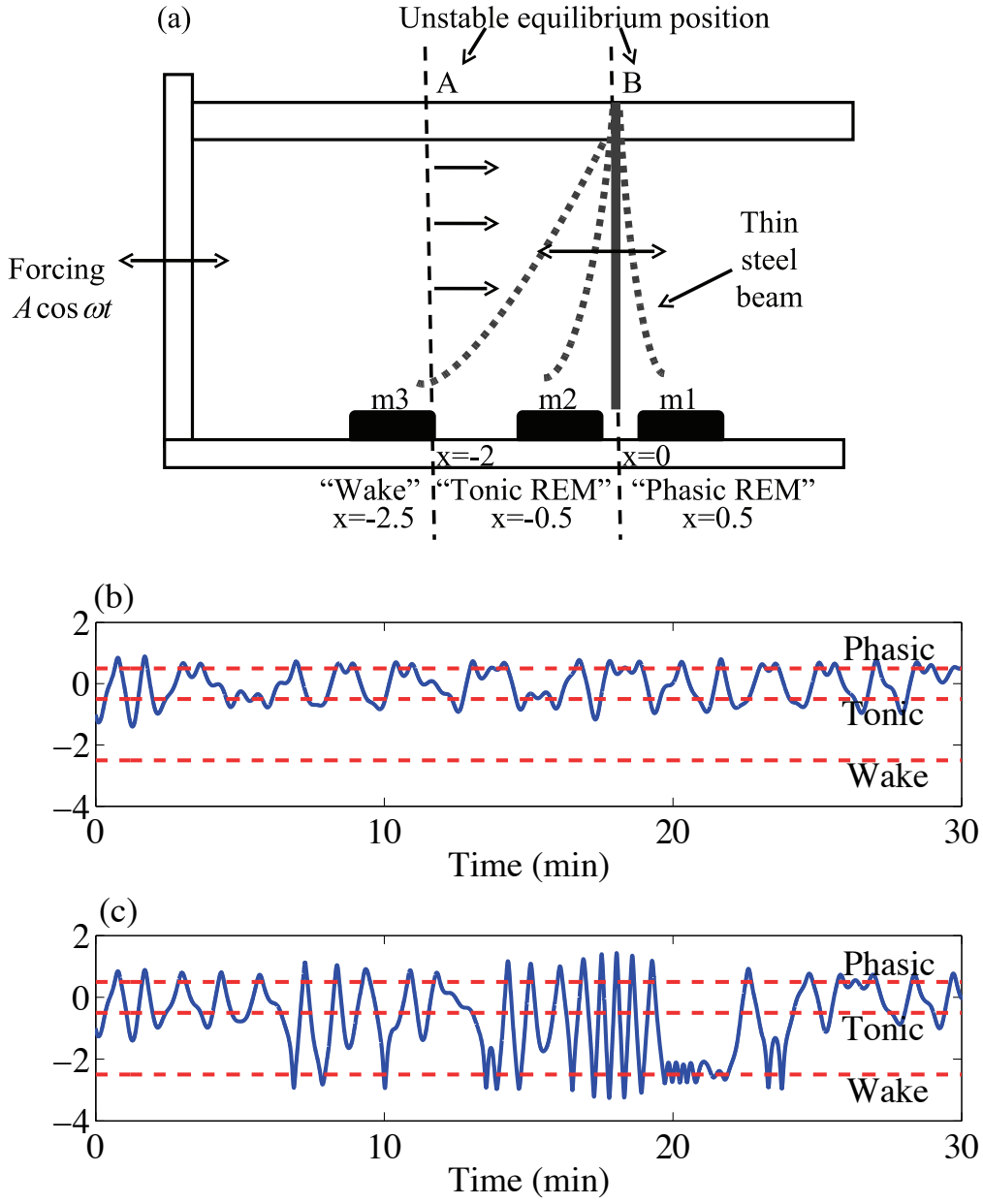

Figure 7.16. (a) REM period model beam analogy. A Duffing oscillator with 3 stable and 2 unstable equilibrium positions, ($\delta = 0.06$, $\omega = 2\pi(0.3)$, A=0.5) (b) $w(t)$=0, (c) 8 evenly spaced events of 1 minute, $-2 + \gamma w(t)$=-0.6 when events were occurring.

on auditory awakening thresholds have indicated that an individual is more likely to awaken during Tonic than Phasic REM sleep, the awakening stable point was positioned closer to the stable point representing Tonic REM sleep. Also as awakenings are less likely to occur than Phasic or Tonic REM sleep during a REM sleep period, the distance between the Tonic and Wake stable point was greater than the distance between the Tonic and Phasic stable point. The positions of the equilibrium points for the baseline no-noise conditions are listed in Table 7.2. The phase plane and position of the equilibrium points for the fast REM model is shown in Figure 7.17, where, $\delta = 0.06$.

Table 7.2. Positions of the equilibrium points for the baseline fast REM sleep model.

Equilibrium Point	Position
Phasic REM sleep	0.5
Tonic REM sleep	-0.5
Wake	-2.5
Unstable Point Between Tonic and Phasic	0
Unstable Point Between Wake and Tonic	-2

To simulate awakenings due to noise events the position of the saddle point between the Wake stable point and Tonic stable point was allowed to vary and it moved closer to the Tonic stable point when an excitation term occurred. The equation for the model is,

$$\ddot{x} + \delta\dot{x} + (x + 2.5)(x - (-2 + \gamma w(t)))(x + 0.5)(x)(x - 0.5) = Acos(\omega t). \qquad (7.18)$$

where, $(-2 + \gamma w(t))$, is the unstable saddle point which moves when an excitation occurs. Here $w(t)$ is an excitation, a different naming convention then the slow model

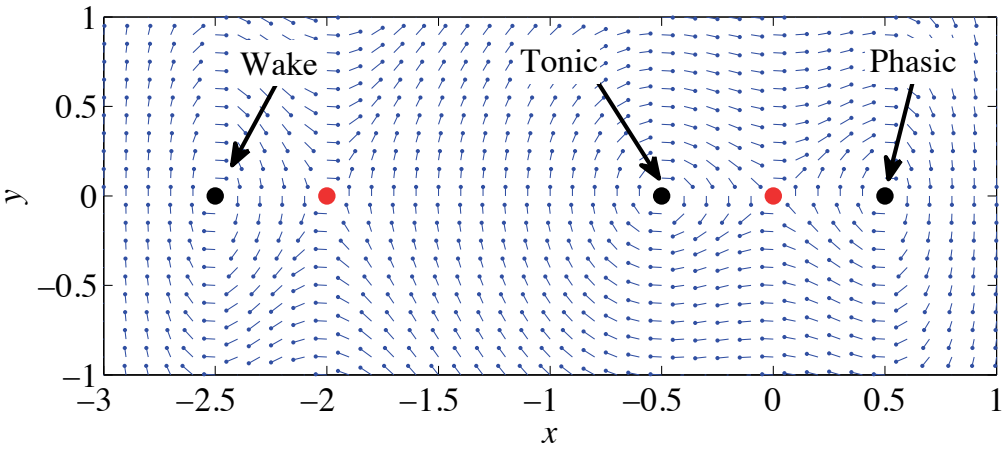

Figure 7.17. Phase plane for Duffing equation. Unstable equilibrium points (red/light gray), stable equilibrium points (black) ($\delta = 0.06$, $\omega = 2\pi(0.3)$, A=0.5), $y = \dot{x}$.

in which the excitations are labeled as (E) is used as the two may or may not have the same form.

The term $\gamma w(t)$ is always positive so this impulsive excitation, which models brain activity pushes the unstable equilibrium position at $x = -2.0$ toward the "Tonic" equilibrium position at $x = -0.5$ making it easier for the beam to move to the Wake equilibrium position at $x = -2.5$. In Figure 7.16 (b) $w(t) = 0$ and the unstable equilibrium point is at -2.0 and in Figure 7.16 (c) there were 8 evenly spaced events of 1 minute with $(-2+\gamma w(t))$=-0.6 when events were occurring and equal to -2 when events were not occurring $(w(t) = 0)$. By moving the unstable equilibrium point the likelihood of transitioning to an awake state increases as the noise level increases. In Figure 7.18 the potential function of the Duffing equation is shown for different positions of the unstable point between Wake (m3) and Tonic REM (m2); in Figure 7.18 (a) the potential function when the unstable point is at -2.0 is shown, if the beam is close to m1 (Phasic REM) and m2 (Tonic REM) it would be difficult to jump out of the well at lower amplitudes of excitation to reach m3 (Wake). In Figure 7.18 (b) the unstable point is at -1.5 and you can see that escape from the m1-m2 region to m3 would be easier and in Figure 7.18 (c) when the unstable point is at -1.0 it would be very easy to escape from the m1-m2 region to m3 and it would be difficult to escape the m3 region to return to the m1-m2 region.

An example of the output of the model with awakenings is shown in Figure 7.19. Here the unstable equilibrium point is defined as $-2 + \gamma N(t)$ and $N(t)$ is a series of impulses of duration 1 minute and are spaced 5 minutes apart. To classify sleep states, a set of thresholds were defined. If the value of x is greater than 0 then Phasic REM sleep occurs and if the value of x is less than zero then Tonic REM sleep is occurring. However, there are exceptions used in order to eliminate very brief sleep stage changes. If the peak value, when the signal is above zero, is never greater than

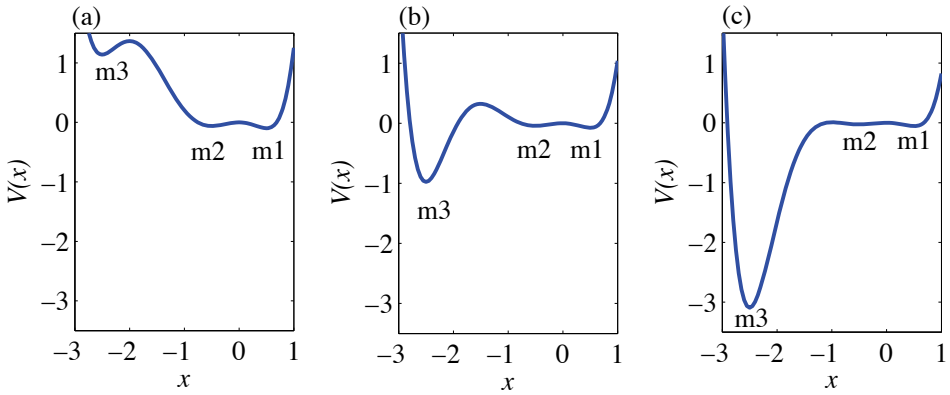

Figure 7.18. The potential function for the 5th order stiffness Duffing equation for different positions of the unstable equilibrium point between Wake and Tonic REM sleep, (a) -2.0, (b) -1.5, and (c) -1.0. m1, m2, m3 represent the magnet locations in the beam system analogy corresponding to "Phasic REM","Tonic REM" and "Wake" respectively.

0.25, i.e. it never approaches the Phasic stable equilibrium point, which is at 0.5, then the activity above zero was set equal to the previous classified state, a similar approach was taken when activity is below zero but the minimum never approaches the Tonic stable equilibrium or Wake stable equilibrium point. Wake states are classified if the level of x is below -2.0 during an excitation. An example of scoring REM sleep stages using these rules is shown in Figure 7.19.

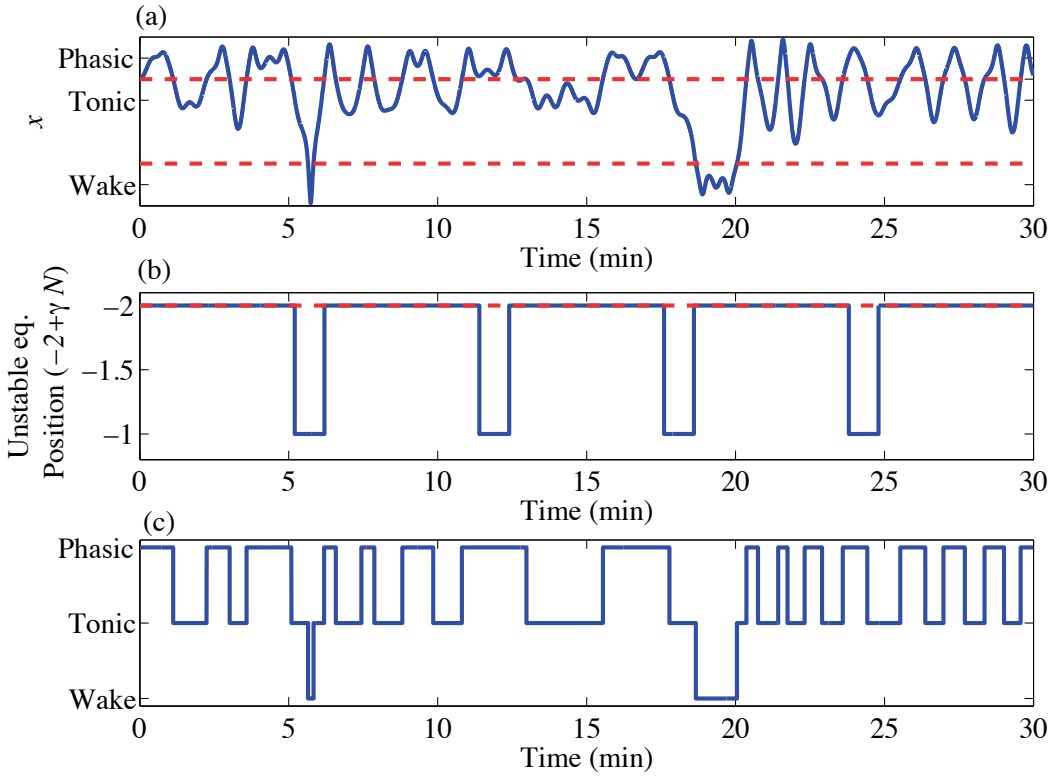

Figure 7.19. (a) Solution of the Duffing equation, oscillations are about 3 stable equilibria, (red-dashed line) thresholds used to assign sleep stages. (b) Unstable equilibrium position $(-2 + \gamma N)$ and (c) classified sleep stages. The driving frequency $\omega = 2\pi(0.3)$, $\delta = 0.06$ and the amplitude (A) was 0.5.

In order to determine the remaining parameters of the Duffing equation, simulations were completed in which the frequency (ω) and the amplitude of the driving

force (A) were varied in order to match the percentage of time spent in Tonic and Phasic sleep and the inter-arrival time between Phasic activity as calculated based on the 1999 UK data. For these simulations the location of the stable and unstable points and the damping (δ) which was set equal to 0.06, remained constant. The damping was set at a low enough value so that chaotic behavior could be obtained, and it was not varied for the simulations as changing the amplitude and the damping would have similar effects. The initial conditions were randomized for each trial between -0.5 and 0.5, and the drive frequency and amplitude were systematically varied. One hundred simulations were conducted for each combination of parameters. A reasonable agreement was found when the drive frequency was set equal to 0.3 Hz and the amplitude of excitation was set equal to 0.5, the results are shown in Figure 7.20. The time t, also had to be scaled after each solution was obtained to match values, t for the solutions was set equal to $(1/5)t$ to obtain agreement between the simulated and actual values.

Simulations using the fast REM model for different numbers, level, and duration of excitations ($w(t) = N(t)$) were completed. For each combination of parameters, 25 simulations were completed, the initial conditions were varied for each simulation. The average proportion of a REM period classified as Wake based on the simulation results is shown in Figure 7.21 and the average proportion of a REM period classified as Tonic and Phasic REM sleep is shown in Figure 7.22. The proportion of the REM period classified as Wake increased with both excitation level and duration of the event, while the proportion spent in Tonic and Phasic REM sleep both decreased. The proportion of the REM period classified as Wake also increased with the number of events. The probability of awakening to a noise event is shown in Figure 7.21, and it increases with the duration of an event and the excitation level. From the simulations it was found that an impulse that moved the unstable equilibrium point

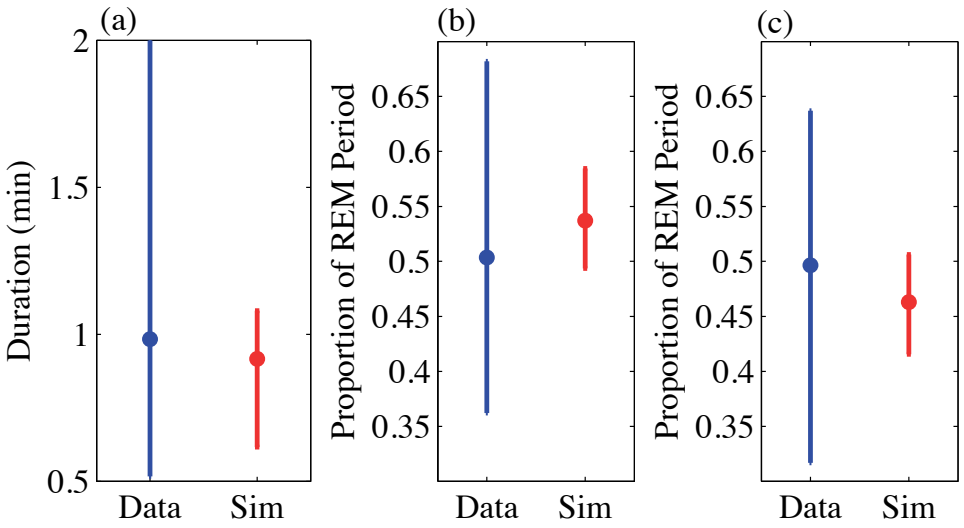

Figure 7.20. Statistics of Tonic and Phasic REM sleep for simulations (red) and survey data (blue). (a) Inter-arrival time of Phasic activity, (b) proportion of REM period (without awakenings) occupied by Tonic REM sleep and (c) proportion of REM period (without awakenings) occupied by Phasic REM sleep.

to -1.6 will start to cause transitions to Stage Wake. The baseline position of the unstable equilibrium between Wake and Tonic was set at -2 because at this location the probability of moving to the Wake state without an excitation term is essentially zero.

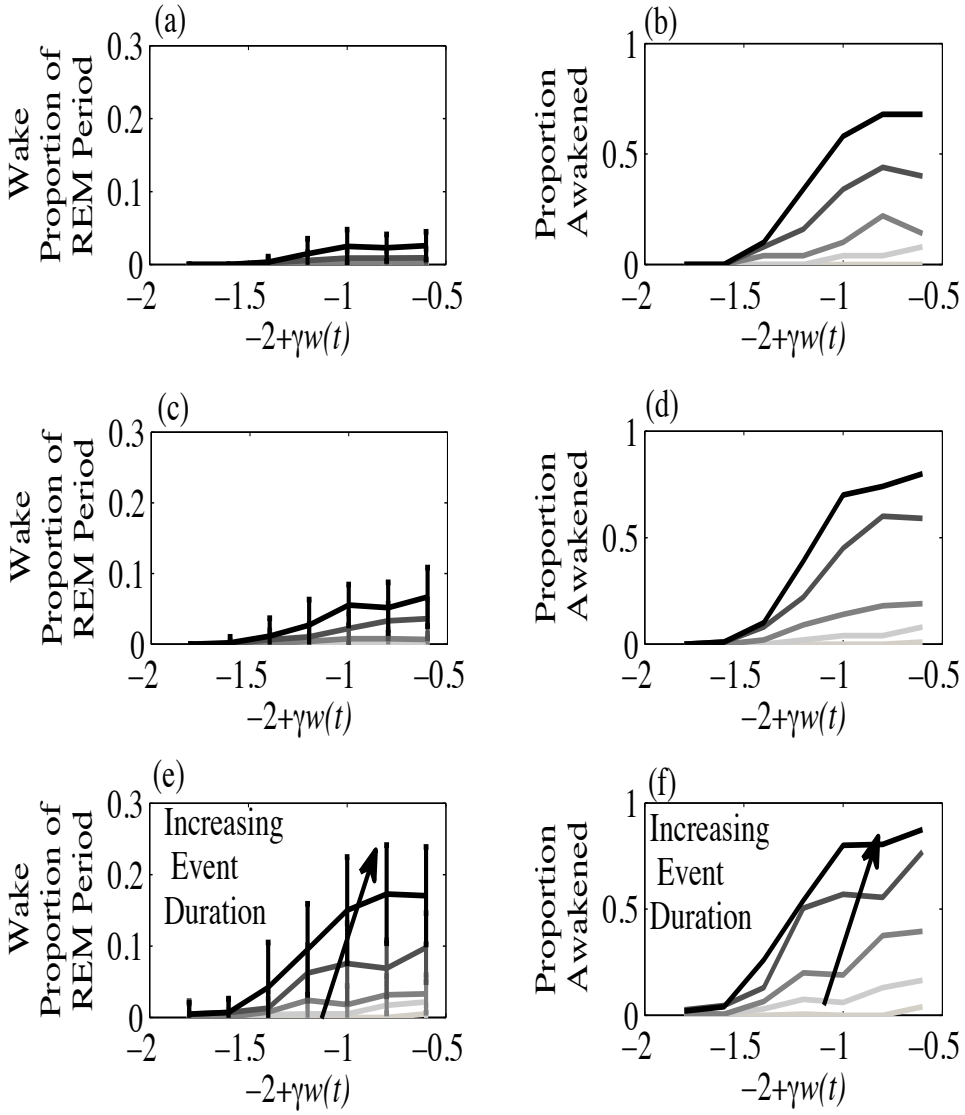

Figure 7.21. Proportion of the REM period defined as awake for (a) 2, (c) 4, and (e) 8 events as a function of level. Probability of awakening to, (b) 2, (d) 4, and (f) 8 noise events as a function of level.

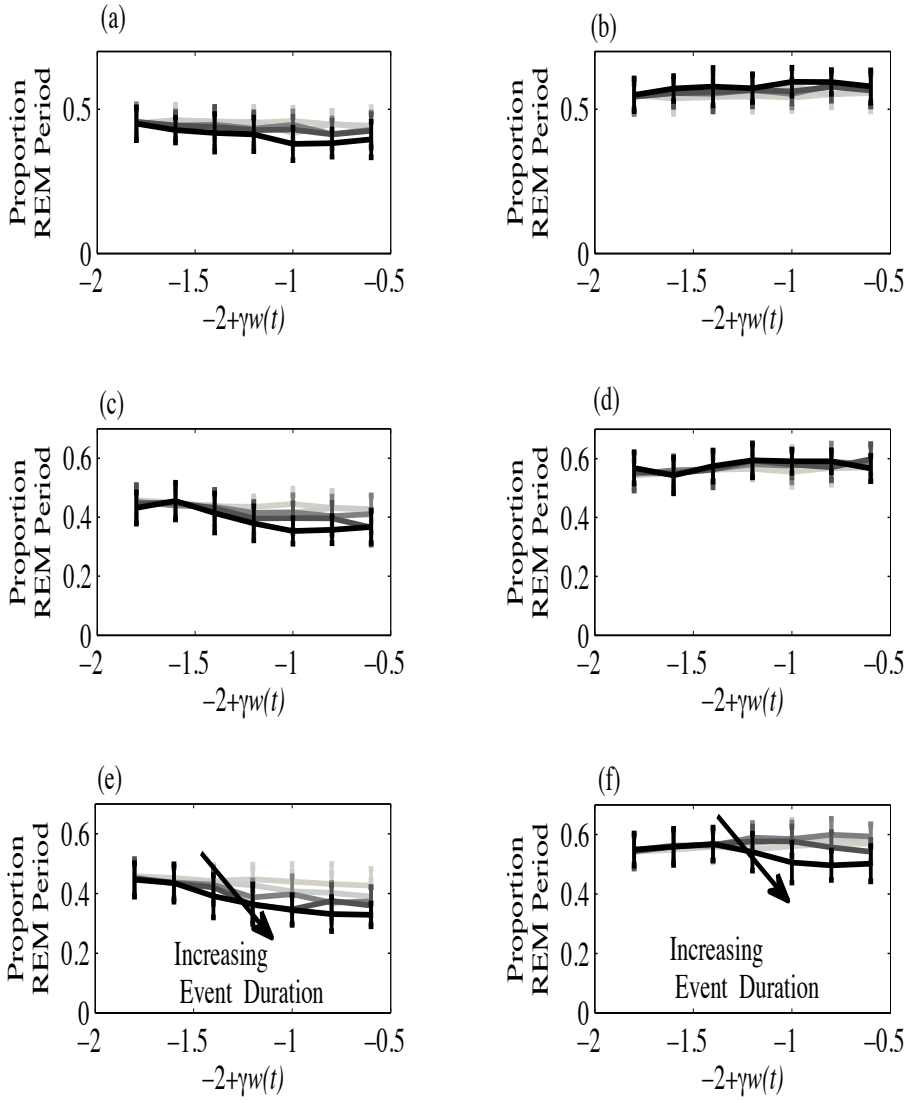

Figure 7.22. Proportion of the REM period defined as Phasic REM sleep for (a) 2, (c) 4, and (e) 8 events as a function of level. Proportion of the REM period defined as Tonic REM sleep for (b) 2, (d) 4, and (f) 8 events as a function of level.

Based on simulations and the classification of Tonic and Phasic REM sleep in the UK dataset, the Duffing equation appears to predict the behavior of fast REM activity. The use of a Duffing type equation for modeling brain activity does have support in the sleep literature. There have been many models developed for neuron bursting activity. Phasic REM sleep can be thought of bursting activity. One of the most commonly used models is the Hodgkin-Huxley model. This is a model of the behavior of 3 channels through a neuron membrane: sodium, potassium and a leakage channel (Gerstner and Kistler (1996); Izhikevich (2004)). Either a constant current or a short current pulse is applied as input to the model and the output is the voltage potential which may contain a spike.

A simplification of the Hodgkin-Huxley equations was made, that model is called the Fitz-Hugh Nagumo model and consists of the following two equations (Gerstner and Kistler, 1996),

$$\dot{x} = x - \frac{1}{3}x^3 - y, \tag{7.19}$$

$$\dot{y} = a + bx - cy. \tag{7.20}$$

The two equations can be combined to create a second order differential equation by solving Equation (7.19) for y,

$$y = x - \frac{1}{3}x^3 - \dot{x}, \tag{7.21}$$

taking the derivative,

$$\dot{y} = \dot{x} - \dot{x}x^2 - \ddot{x}, \tag{7.22}$$

and substituting them into Equation (7.20). The equation that is obtained is:

$$\ddot{x} + (1-c)\left(\frac{1}{1-c}x^2 - 1\right)\dot{x} + (b-c)x + c\frac{1}{3}x^3 + a = 0, \tag{7.23}$$

which with an applied sinusoidal force can be written as,

$$\ddot{x} + p(kx^2 - 1)\dot{x} + \omega_o^2 x + \beta x^3 = a_o + Acos(\omega t). \tag{7.24}$$

This equation has the same form as the Duffing Van der Pol equation. If k is zero then the equation has the form of a Duffing oscillator. Curtco, Sakata, Marguet, Itskov, and Harris (2009) modeled neuron activity in the auditory cortex when urethane-anesthetized rats were exposed to auditory stimuli using the Fitz-Hugh Nagumo equations, though the form of the Fitz-Hugh Nagumo model they used was slightly different, in that the model had an x^2 term in addition to the x and x^3 in Equation (7.19).

In addition to neuron bursting models, Zeeman (1976) discussed how there are different scales at which to model brain activity. He described small-scale theory as consisting of models of individual neurons, synapses, and nerve impulses. Large-scale models are models of the end result like thinking and responding. He stated that what is needed is a model of medium-scale behavior. The medium-scale model he believes could be something like the Duffing oscillator because it has the oscillatory behavior found in neurons and he stated that it would be expected that some neuron activity would be stable and some would not.

The Duffing equation has also been used to model epileptic seizures as well as visual evoked responses. Stevenson, Mesbah, Boylan, Colditz, and Boashash (2010) wanted to create a model of newborns EEG activity including seizure activity. The model developed consisted of a Duffing oscillator driven by Gaussian noise for the

background EEG and a Duffing oscillator driven by impulsive noise to simulate the seizure activity. The two signals output from the models were added in order to obtain a simulated newborn's EEG signal. Srebro (1995) used a Duffing equation to model visual evoked potentials observed in EEG data. The visual stimulus that was used consisted of a checkerboard pattern that was shown at intervals. Srebro (1995) was mostly interested in modeling the response of the system to impulsive perturbations and matching the increase and subsequent decay of the response to the individual evoked potentials that were observed in experiments. They found that the result with the Duffing oscillator was a better match to the evoked potentials then what would be predicted by using a linear stiffness.

7.4 Model Parameter Estimation

Now that a fast REM sleep model has been developed and the fast dynamic behavior limitations of the Massaquoi and McCarley model have been overcome, the parameters of the different components of the sleep model needed to be estimated using the 1999 UK data. The methods used and the values of the estimated parameters for the different components of the model are described.

7.4.1 The Homeostatic Process S Model

The term S in the Massaquoi and McCarley model represents the need for sleep and decreases through the night. While there have been several variations in the equation for this term, in its most basic form S is an exponentially decaying function (Achermann and Borbély, 1990) of the form:

$$S = S_o e^{-g_c t}, \tag{7.25}$$

where the parameter gc controls the decay rate. While there is no direct measurement of Process S, it can be estimated from the decay of slow wave activity (SWA). Process S is an upper bound on the level of slow wave activity. To estimate the initial value of S and the decay rate, first SWA during the night was calculated. Slow wave activity was calculated in a manner similar to that used by Ferrillo, Donadio, De Carli, Garbarino, and Nobili (2007). The EEG signals, from the 1999 UK study were segmented into 30 second segments of sleep. This segmentation was repeated moving through the signal in 1 second increments. Using the segment average ($pWelch$ in Matlab) the power spectral density was calculated. The 30 second segment was further segmented into 4 second segments with 75% overlap. The total power between 0.5 and 4.5 Hz was calculated from the estimated power spectral density. To smooth the result further, a moving average filter was used in which the averaging was performed over three minute segments (Achermann, Dijk, Brunner, and Borbély, 1993). The smoothed SWA estimate was then normalized by the mean of the SWA activity for the entire night. This normalization was also done by Achermann, Dijk, Brunner, and Borbély (1993).

Once the SWA estimate was smoothed and normalized then the 95th percentile of SWA during each NREM period was calculated. Before performing this calculation, though, first the boundaries of each REM period during the night had to be calculated. To calculate these limits the original scored sleep stages from the 1999 UK study for each subject were used. First, all stages scored as REM sleep during the night were identified. Then, if there were less than 15 minutes duration of NREM sleep or Wake between scored REM stages, the REM and intervening NREM stages were considered to be in the same REM period. REM periods that were less than 5 minutes in duration were ignored because REM periods should be greater than 5 minutes in

duration (Achermann, Dijk, Brunner, and Borbély, 1993). An example of the scored sleep stages during the night and the defined REM periods are shown in Figure 7.23.

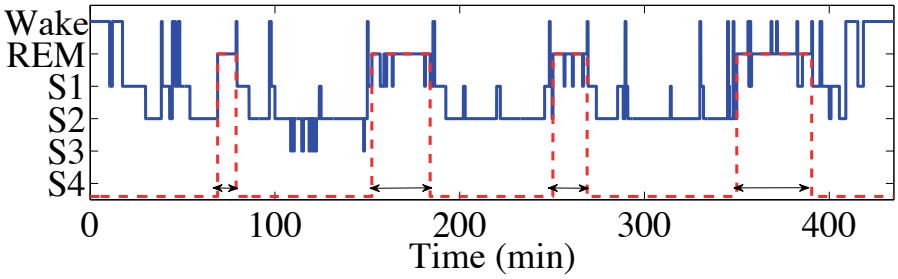

Figure 7.23. An example of Sleep Stages (blue) and identified REM periods (red dashed line).

The 95th percentile of SWA levels for each intervening NREM period was then calculated and the time of these points was determined. The 95th percentile rather than the maximum level was used to reduce the likelihood that the point was associated with an artifact. An exponential function was then fitted to the set of points. An example of the estimated slow wave activity and the values used to to estimate the exponential function are shown in Figure 7.24. The mean and standard deviation for both the decay parameter gc and the amplitude at the start of the night (S_o) estimated from the data are listed in Table 7.3.

The data from the 1999 UK study that was used to estimate the model parameters comes from measurements of subjects between the ages of 30 and 40. Dijk, Beersma, and van den Hoofdakker (1989) calculated the decay rate of Process S for two different age groups, 20-28 and 42-56. They found a decay rate of -0.225 units/hour for the younger group and -0.155 units/hour for the middle age group. The results listed in Table 7.3 need to be scaled by 60 minutes/10.7 minutes, due to differences in time scaling, however when rescaled the resulting decay rate based on the data from the UK study is -0.1794 units/hour which is in-between the results found for the two age

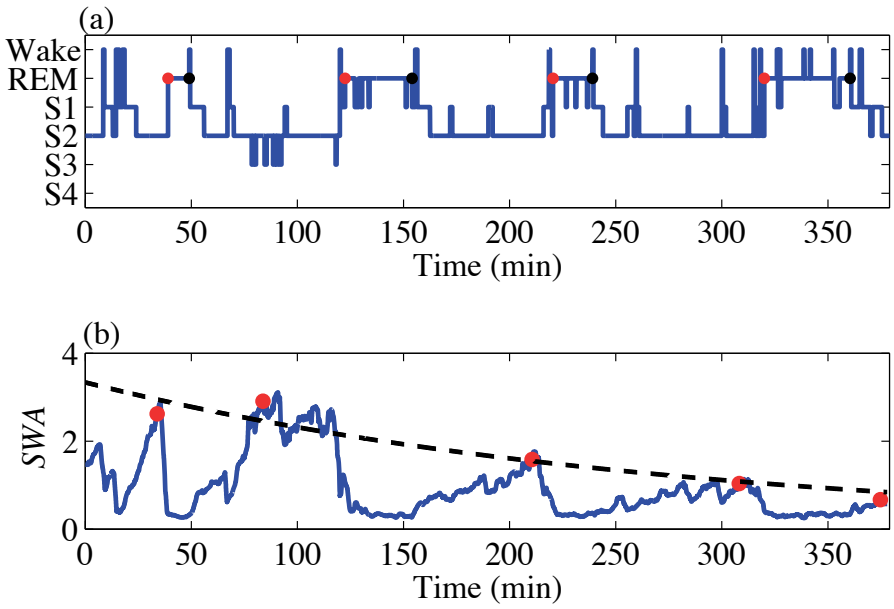

Figure 7.24. (a) Sleep Stages. The start of each REM period is indicated by a red dot and the end of each REM period is marked by a black dot. (b) Estimated SWA (blue), 95th percentile of SWA for each NREM period (red dot) and the estimated Homeostatic Process S (black-dashed line).

groups by Dijk, Beersma, and van den Hoofdakker (1989). This gives an indication of how the coefficients of Process S need to be varied in order to account for different age groups.

7.4.2 Slow Wave Activity

The model for slow wave activity that is being used is not the model in Massaquoi and McCarley (1992). The model in Achermann, Dijk, Brunner, and Borbély (1993) is being used. The primary reason for this is that this model of SWA has separate terms for controlling (1) the fall of SWA due to the onset of REM sleep and awakenings and (2) the rise of the slow wave activity. The equations for the slow wave model are,

$$\dot{S} = -gc\, SWA \tag{7.26}$$

and

$$\begin{aligned} S\dot{W}A = rc\, SWA\ (S - SWA) - fc\,(SWA - SWA_L)REMT - \\ fcw\,(SWA - SWA_L)E. \end{aligned} \tag{7.27}$$

The parameters in the slow wave activity equation were estimated using the 1999 UK data. The initial value of slow wave activity ($SWAo$), was determined by first identifying the onset of sleep, which is the first occurrence of Stage 2, and then calculating the mean of the slow wave activity for the first minute of sleep. The method Achermann, Dijk, Brunner, and Borbély (1993) used to estimate SWA_L was used. They set the parameter SWA_L, which is the lower bound for the level of slow wave activity, equal to a value that is five percent lower than the lowest value of slow wave activity observed during periods of REM sleep. The mean values and standard

deviation for these two coefficients, estimated using the 1999 UK data, are listed in Table 7.3.

To calculate the rise parameter (rc), the first 30 minutes of the slow wave activity was extracted. The maximum value for the segment of SWA was calculated and only the portion of the segment between the first point and the maximum value was used to calculate rc. An example of SWA for one subject and the portion used to calculate rc is shown in Figure 7.25 (a).

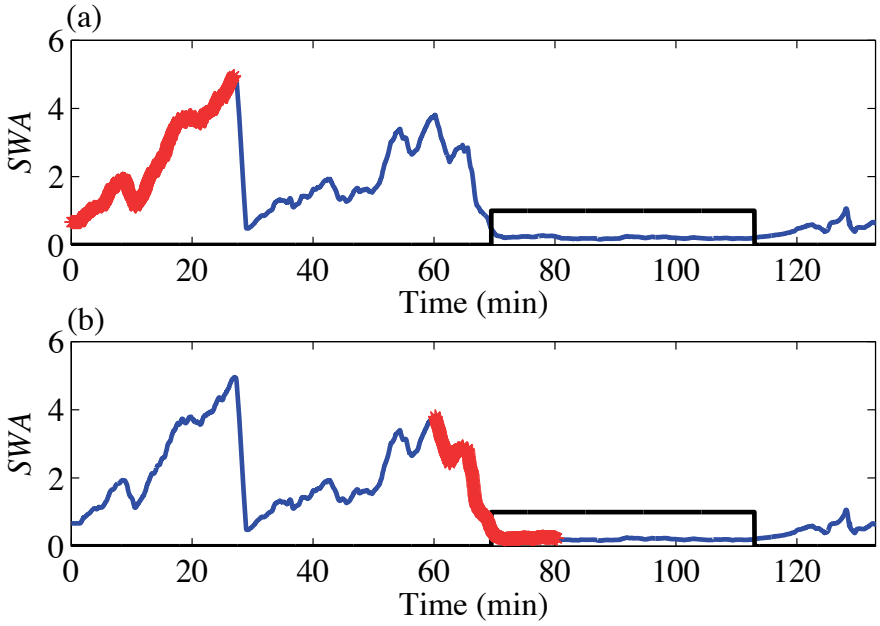

Figure 7.25. SWA activity (blue), REM periods (black) and (a) portion of segment used to calculate rc (red) and (b) portion of segment used to calculate fc (red).

To calculate rc, a continuous time system identification approach/least squares approach was used (Doughty, Davies, and Bajaj, 2002). When SWA is increasing in level the second term in Equation (7.27), $REMT$, is equal to zero. Therefore the equation is,

$$\dot{SWA} = rc\, SWA\ (S - SWA)\,. \tag{7.28}$$

The value of $S\dot{W}A$ was calculated by taking the derivative of the segment of SWA. Taking the derivative of a signal can increase high frequency components therefore the derivative was also low pass filtered. The value of S used was based on the estimated value of S.

To calculate the fall parameter (fc), 15 minutes of the slow wave activity before each REM period plus the slow wave activity within the first quarter of each REM period was extracted. The maximum value of SWA for the segment was calculated and only the portion of the segment between the maximum value and the last data point was used to calculate fc. An example of SWA and the portion used to calculate fc are shown in Figure 7.25 (b).

The value of fc can be calculated in a similar manner as rc in which the equation,

$$S\dot{W}A - rc\,SWA\ (S - SWA) = -fc\,(SWA - SWA_L), \tag{7.29}$$

is solved for fc. The model parameters rc and fc were calculated in order to obtain an estimate of the rise and fall of slow wave activity and to verify that the values in the literature are also applicable to the UK data. However, real slow wave activity is more variable than the slow wave activity simulated by using the model due to awakenings and other ongoing activity, therefore, for all subject nights of data a reasonable single rise and fall constant could not be calculated. As the mean values for rc and fc for all subject nights was similar to the mean values reported in the literature, the mean values were used in the combined model, but it should be noted that they actually vary by subject and also probably by situation and are perhaps better characterized by a distribution.

To estimate the characteristics that define the noise ($n(t)$) in the model Achermann, Dijk, Brunner, and Borbély (1993) calculated the difference between a smooth version of the slow wave activity and that of an unsmoothed version of the slow

wave activity. The SWA activity within each 3 minute block of time was averaged to obtain the smoothed SWA_S. The noise time histories can be estimated for each subject-night by using,

$$n = \frac{SWA - SWA_S}{SWA_S}, \tag{7.30}$$

where SWA is the unsmoothed version of slow wave activity and SWA_S is the smoothed version of the slow wave activity. An example of the original SWA, the smoothed SWA and the noise term n, that was calculated for one subject night using the UK dataset is shown in Figure 7.26. A distribution of the amplitude of the noise is shown in Figure 7.27. A Gaussian function was fit to this distribution data and is shown for comparison. There appeared to be a skewness in the distribution of $n(t)$. A possible reason for this skew, maybe, is that while most large artifacts in the data were removed perhaps smaller movement artifacts were not. To examine if this is the reason for the positive skew, the mean, standard deviation, skewness, and kurtosis for $n(t)$ were calculated when only portions of the data were considered. The noise ($n(t)$) data for each subject night was sorted and the lower and upper 0.5% of the data was eliminated. The statistics of n were then calculated through time using a sliding 30 minute segment. This procedure was repeated eliminating larger protions of the lowest and highest values in the dataset up to an elimination of 5% (the upper and lower 2.5%) of the data. The results for one subject night are shown in Figure 7.28. When portions of the data were removed, as expected, kurtosis is reduced but a skew in the data is still prevelant. This is also clearly seen in the data, Figure 7.26 (a). The results for all subjects indicate a skewness in the data, the results of which are shown in Figure 7.29. Therefore in the model to simulate n a skewed Gaussian distribution was used based on the parameters in Table 7.3.

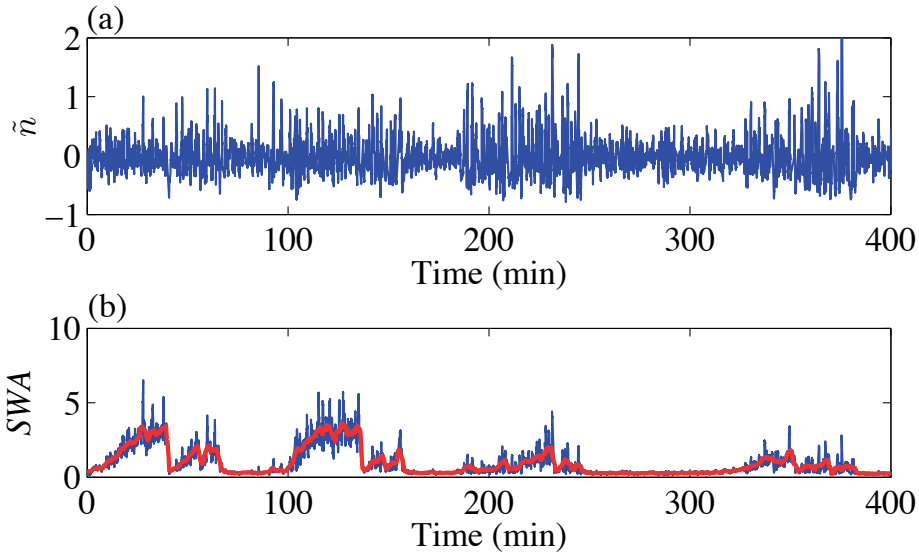

Figure 7.26. (a) Estimated noise term $n(\tilde{t})$, (b) the original SWA (blue), and smoothed SWA (red).

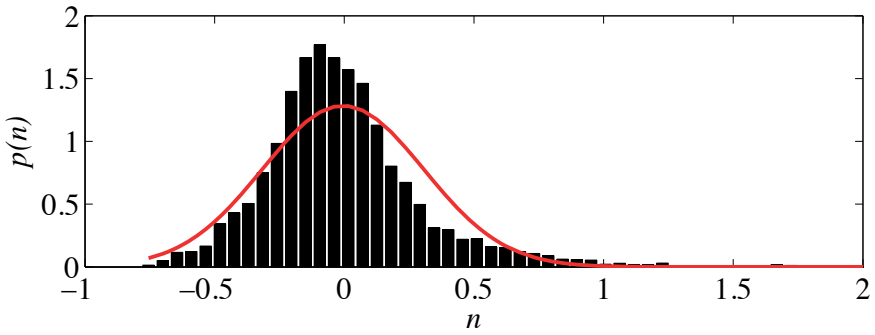

Figure 7.27. Probability density function of $n(t)$ (black) and Gaussian distribution resulting from a fit to the data (red).

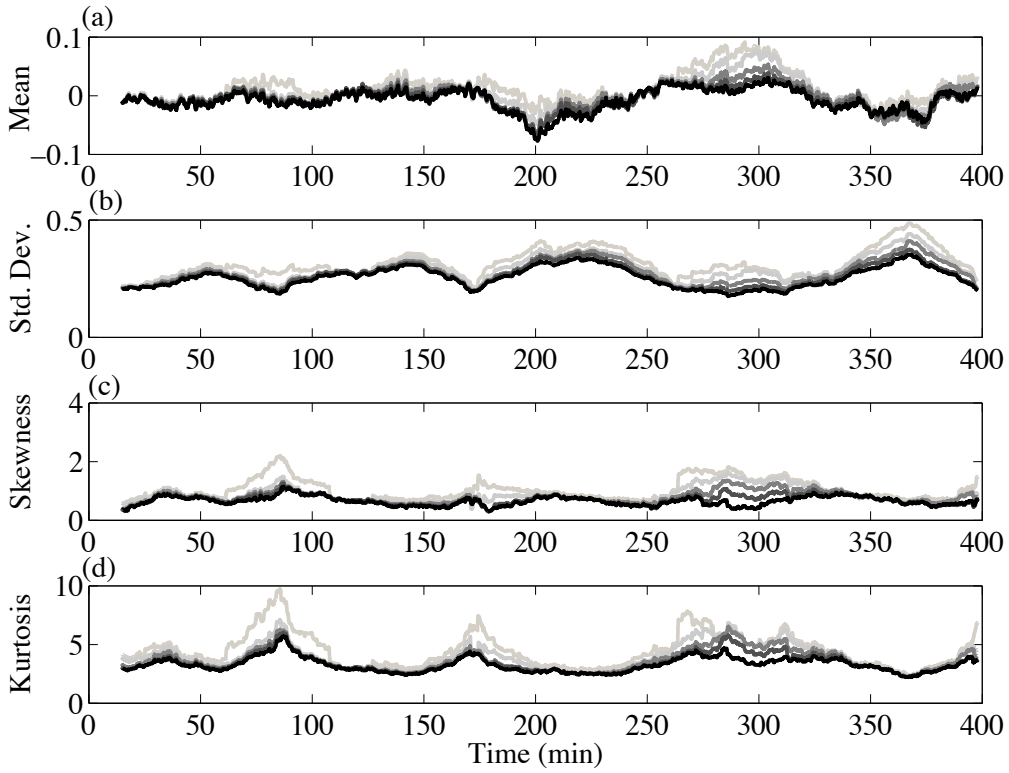

Figure 7.28. Statistics of $n(t)$ with tails of the distribution removed. Gray to black results from eliminating 1% to 5% of the tails of the distribution of $n(t)$ before calculating the statistics for each 30 minute segment.

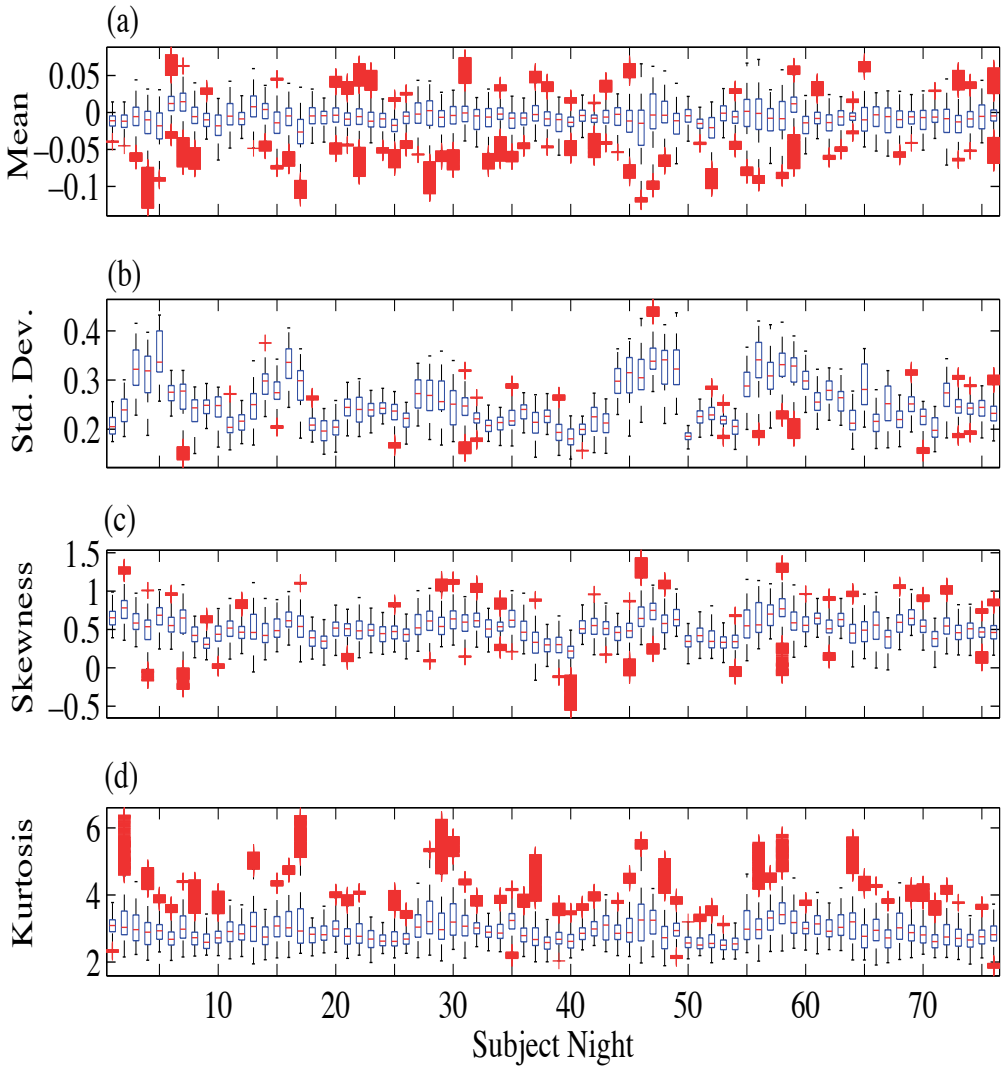

Figure 7.29. Range of values for the (a) mean, (b) standard deviation, (c) skewness, and (d) kurtosis for all subjects based on statistics calculated from each moving 30 minute segment of the estimated random noise term $n(t)$. The results are shown as a boxplot: red line median, edge of each box is the lower and upper quartile, the red plus signs are outliers.

The last parameter of the SWA model is the fall in slow wave activity due to noise events (fcw). Achermann, Dijk, Brunner, and Borbély (1993) considered the rate of fall in slow wave activity when awakenings occur to be four times faster than the rate when a REM period occurs. However, they assumed that the wake term was never larger than 1 in their model. A value for E other than 1 was used, and this will be discussed in the following section. The value for fcw that was chosen was 2 times the value of fc.

Table 7.3. Coefficients of the SWA model estimated from data taken from 76 subject nights of the 1999 UK study. Mean and standard deviation of these estimates, based on the data, and original values from Achermann, Dijk, Brunner, and Borbély (1993).

Coefficient	Mean (std. dev)	Original Values
gc	0.03 (0.01)	0.0893
fc	2.1 (1.0)	2.5252
rc	0.4 (0.1)	0.5368
S_o	3.7 (0.7)	3.138
SWA_o	0.8 (0.3)	0.468
SWA_L	0.17 (0.04)	0.1
$nt - mean$	-0.017 (0.005)	0
$nt - std$	0.25 (0.04)	0.182
$nt - skew$	0.5 (0.1)	0
$nt - kurtosis$	3.0 (0.2)	3

7.4.3 The Wake Term

The characteristics of the excitation term E, that can lead to spontaneous non-noise induced awakenings, was calculated by using the data from no noise laboratory nights in the UK study. It was decided to use the power in the gamma band of the EEG signal (activity between 25 and 35 Hz) to represent this term. The calculation of activity in the different frequency bands of the EEG signal were described in Section

6.4. It is noted that this band contains both movement activity and EEG activity, however, as movements are an indicator of awakenings this was considered acceptable activity to include in the Wake term. The time between the occurrence of these pulses or the inter-arrival time was calculated. An example of the gamma activity and the definition of duration, amplitude and inter-arrival time are shown in Figure 7.30 and the distributions of these parameters are shown in Figure 7.31. The distribution for the inter-arrival time appears to be exponential. The mean value for the inter-arrival time was 6.1 minutes. The value used by Massaquoi and McCarley (1992) in their model was 11.8 minutes, therefore, the inter-arrival time found in the UK dataset was half the value of the original model.

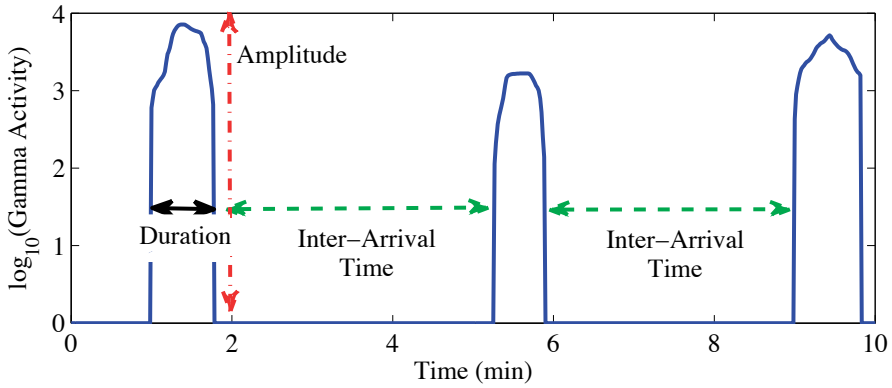

Figure 7.30. An example of gamma activity, arrows indicate inter-arrival time, duration and amplitude of the excitations.

The values for the duration of $N(t)$ ranged from 3 seconds to 1.2 minutes, with a mean of 0.5 minutes and a standard deviation of 0.2 minutes. The minimum and maximum values for the duration of $N(t)$ used in the original Massaquoi and McCarley model were 2.7 minutes and 5.4 minutes. This range is obviously too high and does not allow brief awakenings to be predicted. The amplitude of $N(t)$ is difficult to determine based on the gamma activity. There is not a direct relationship between the level of the impulses in the model and the level of gamma activity. However, the current

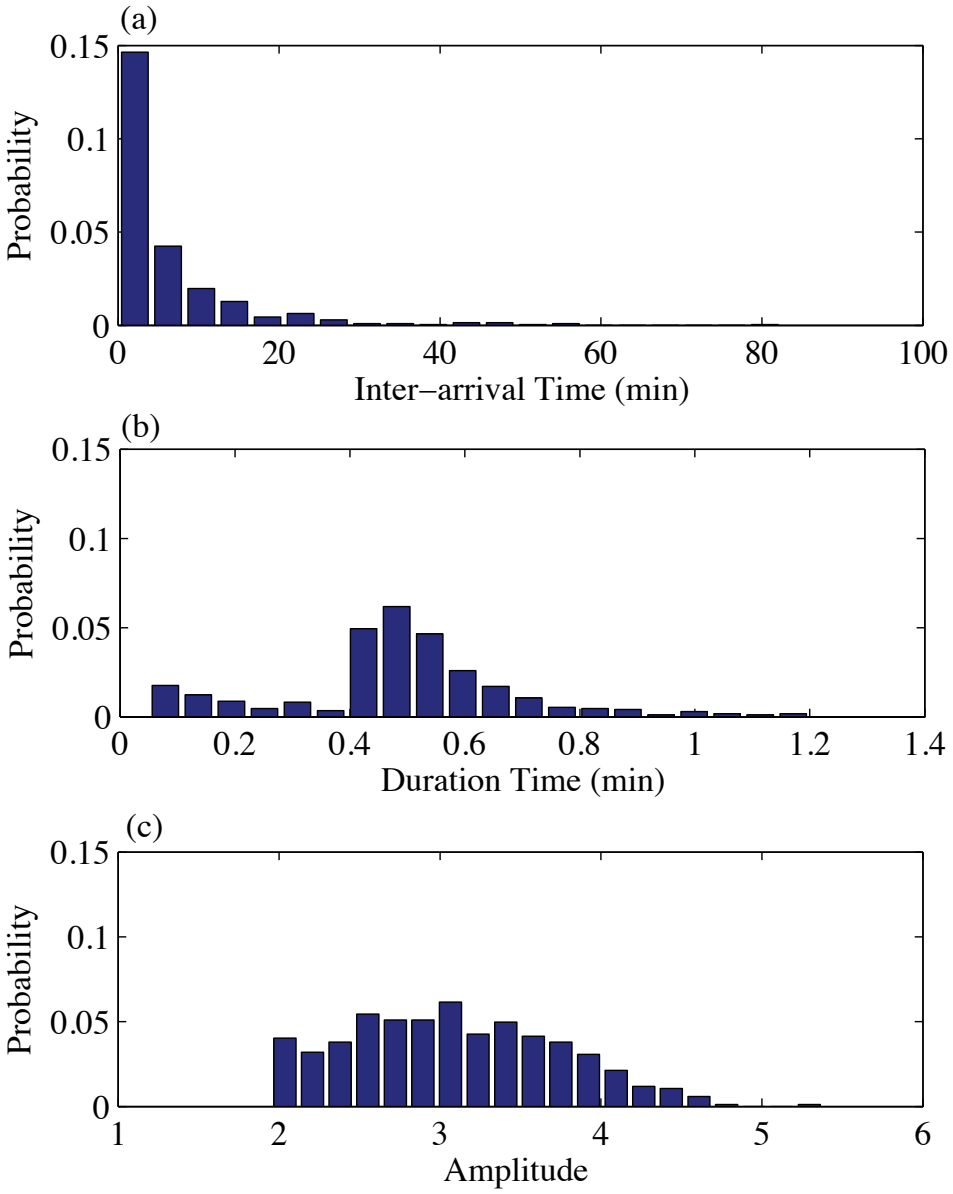

Figure 7.31. (a) Distribution of inter-arrival times between estimated $N(t)$, (b) distribution of the duration of $N(t)$, and (c) distribution of the amplitude of $N(t)$ in the UK dataset.

approach used to estimate the amplitude was to take the log based 10 of the power in the gamma band. The minimum value obtained was 2.0, the maximum value was 5.4, the mean was 3.1, and the standard deviation of the data was 0.65. A summary of the parameters for the spontaneous wake model are in Table 7.4. To model $N(t)$ for spontaneous awakenings, the duration and amplitude was defined by Gaussian distributions based on the statistics that were calculated and the inter-arrival time was defined by an exponential distribution.

Table 7.4. Estimated values for the statistics of the impulsive excitation ($N(t)$) that leads to the spontaneous wake model based on the UK dataset and original values from Massaquoi and McCarley (1992).

Coefficient	Estimated Value	Original Values
mean inter-arrival time	6.1 minutes	11.8 minutes
minimum duration	3 seconds	2.7 minutes
maximum duration	1.2 minutes	5.4 minutes
mean duration	0.5 minutes	4.0 minutes

7.4.4 Slow REM Sleep

The Massaquoi and McCarley model (1992) contains two equations for defining REM sleep, one representing REM-ON or REM promoting neuron activity (X) and one representing REM-OFF or REM inhibiting neuron activity (Y) (see Equations (5.47) and (5.48)). The difficulty in estimating the parameters of the REM model is that the UK dataset can be used to estimate the timing of REM sleep but not REM neuron activity.

Ferrillo, Donadio, De Carli, Garbarino, and Nobili (2007) tried to estimate the parameters of the REM sleep model based on data. They calculated the parameters for the Lotka-Volterra REM model by using a stochastic search of parameters and

minimizing the difference between slow wave activity from their dataset and the slow wave activity that was predicted. One problem with their parameter estimation method is that they calculated only one set of parameters for the model, i.e. they assumed that the duration of successive REM periods are the same.

From the UK dataset, the mean duration of REM and NREM sleep were calculated for the first 4 REM periods based on 76 subject nights of data. The results are shown in Figure 7.32. The mean duration of REM sleep does increase during the night while the duration of NREM sleep decreases. Therefore, the assumptions made by Ferrillo, Donadio, De Carli, Garbarino, and Nobili (2007) in estimating the parameters of their model may be incorrect.

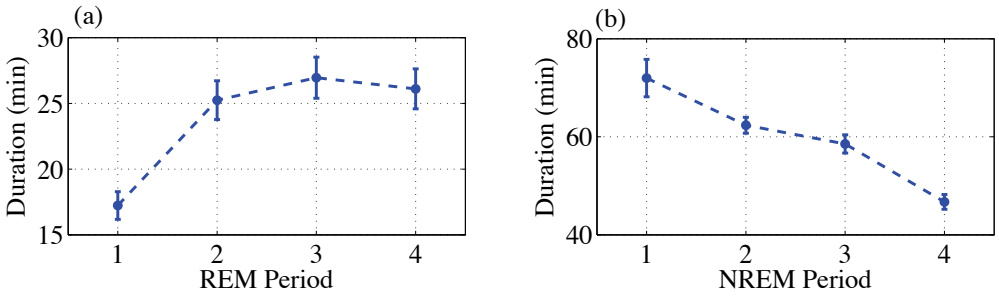

Figure 7.32. (a) REM sleep duration and (b) NREM sleep duration. Mean values and ± one standard deviation of the estimated mean, estimated from the 1999 UK study.

A different approach than that of Ferrillo et al. (2007) was used to estimate the REM model parameters. The parameters were estimated separately for each REM period. Signals for REM-ON and REM-OFF activity were created based on the timing of REM sleep in the UK data. The equations for the simplified REM model were used and these are:

$$\dot{X} = aX - bXY, \tag{7.31}$$

$$\dot{Y} = -cY + dXY. \tag{7.32}$$

If an assumption is made that c and d are equal and a and b are equal, which is a necessary step in order to create REM-ON and REM-OFF signals, then the equations are,

$$\dot{X} + aX(Y - 1) = 0, \tag{7.33}$$

and

$$\dot{Y} + cY(1 - X) = 0. \tag{7.34}$$

When Y is varying slowly compared to X the solution is approximately of the form,

$$X = e^{-a(Y-1)t}, \tag{7.35}$$

and when X is varying slowly compared to Y then Y is approximately,

$$Y = e^{-c(1-X)t}. \tag{7.36}$$

Therefore, Y grows when X is greater than 1 and decays when X is less than 1, and X grows when Y is less than 1 and decays when Y is greater than 1. The value of X was set equal to one at the start of the REM period and at the end of the REM period. The value of Y was set equal to 1 when X is at a maximum and it reaches its maximum level at the end of the REM period. Based on these values, an exponential function was used to create the rise and decay of each signal and where the exponential functions join the transition was smoothed by rounding out the slope of the signals. An example of the signals generated with this approach is shown in Figure 7.33 (a) and the smoothed signals are shown in Figure 7.33 (b).

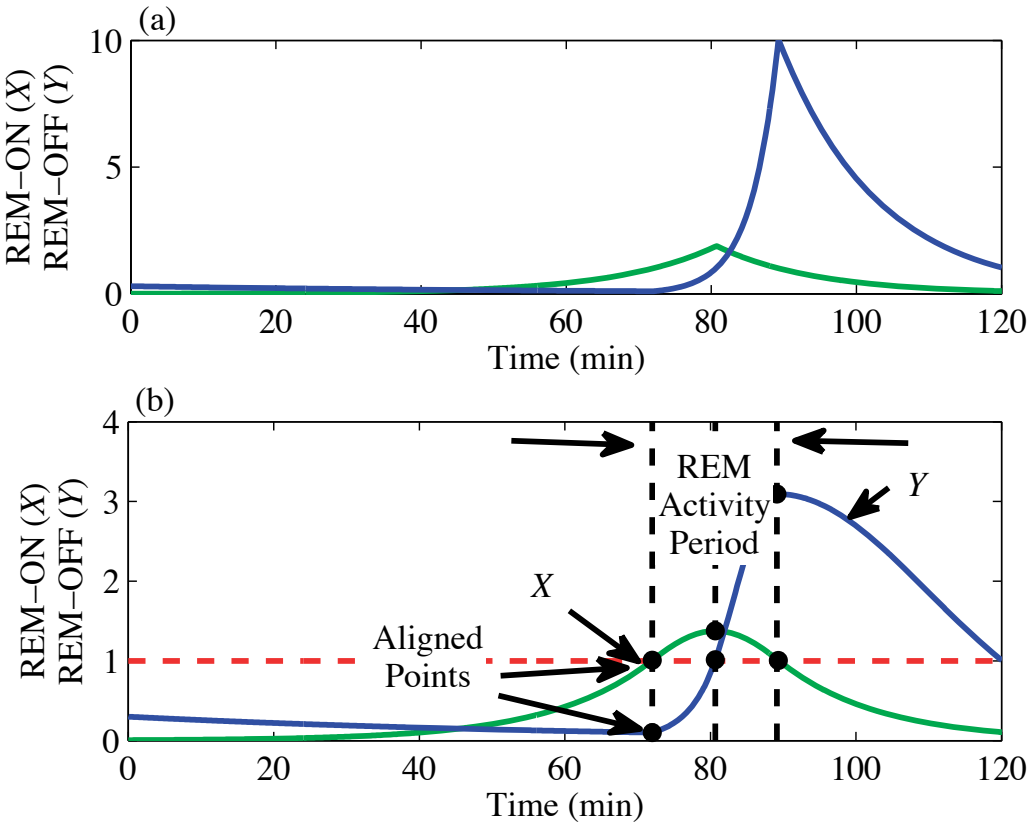

Figure 7.33. An example of creating REM-ON (X) and REM-OFF (Y) signals based on the timing of REM sleep periods in the 1999 UK study data and Equations (7.33) and (7.34).

To estimate the parameters of the X and Y model the derivative of both of the constructed signals were calculated and then the following two linear equations in parameters (a and b, and c and d):

$$\frac{\dot{X}}{X} = a - bY, \tag{7.37}$$

$$\frac{\dot{Y}}{Y} = -c + dX, \tag{7.38}$$

were fitted to the data. An example of the estimated linear relationships for REM-ON and REM-OFF activity are shown in Figure 7.34.

Using the estimated parameters, the REM-ON and REM-OFF activity was then calculated by solving Equations (7.31) and (7.32) using *ode45* in Matlab. Based on the obtained solution, the value for the coefficient a was altered in order to align the calculated REM-ON activity (when X is greater than 1) with the actual start of REM sleep in the survey data. Similarly the value for c was altered, if needed, in order to better match the duration of the calculated REM activity and the duration of REM sleep in the UK data. The coefficients, a and c, were increased or decreased until the error between the duration and start time of actual and simulated REM sleep, was less than 2 minutes. However, sometimes a low error value could not be obtained due to brief or long REM periods. The error for these values for all REM periods in the UK dataset are shown in Figure 7.35. The duration of NREM sleep is the duration prior to the start of a REM period, therefore it is related to the start time of each REM period. An example of the agreement between a created signal for REM-ON activity and the REM-ON activity, calculated using the estimated parameters, is shown in Figure 7.36. The interest was in matching the start and end of each REM signal, when the REM-ON signal is greater than 1.

The estimated coefficients are plotted against the duration of a REM sleep period in Figure 7.37. The coefficients, c and d, decreased with REM duration. The decrease in c with REM duration is partly due to the fact that it was systematically altered so that the duration of the simulated REM sleep period matched the values derived from the UK dataset. The estimated coefficients are plotted against the duration of NREM sleep in Figure 7.38. The decrease in a with NREM sleep duration is again partly due to the fact that it was altered so that there was agreement between the simulated and actual start time of each REM sleep period.

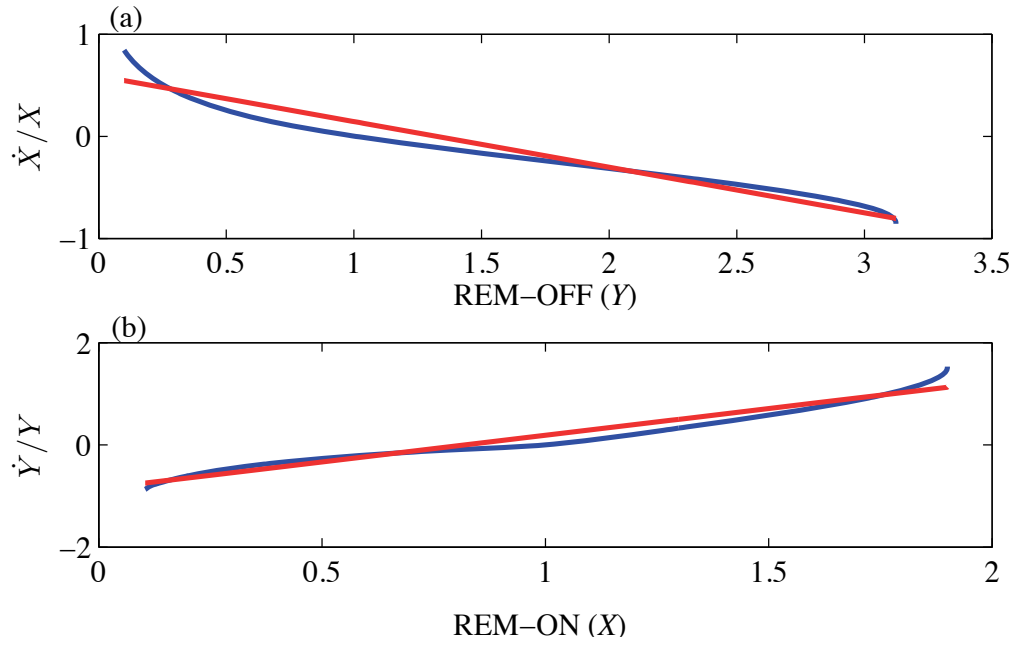

Figure 7.34. An example of the fitting of REM sleep model parameters of (a) the REM-ON model and (b) the REM-OFF model. Blue line is based on created signals and the red line is the linear model using the estimated parameters.

The mean and standard deviation of the estimated coefficients for the first four REM periods were also calculated and are shown in Figure 7.39. The coefficients a and b show similar increasing trends while coefficients c and d both show similar decreasing trends during the night. The change in all parameters though during the night was small. Therefore, for the slow REM model, only a and b were varied with time. The variations are modeled in a similar manner to that in the original Massaquoi and McCarley model, i.e., with a sinusoidal term which has a period of 24 hours. The equation for which is,

$$dc = 1.55 + 0.8sin(0.0467t + 4). \tag{7.39}$$

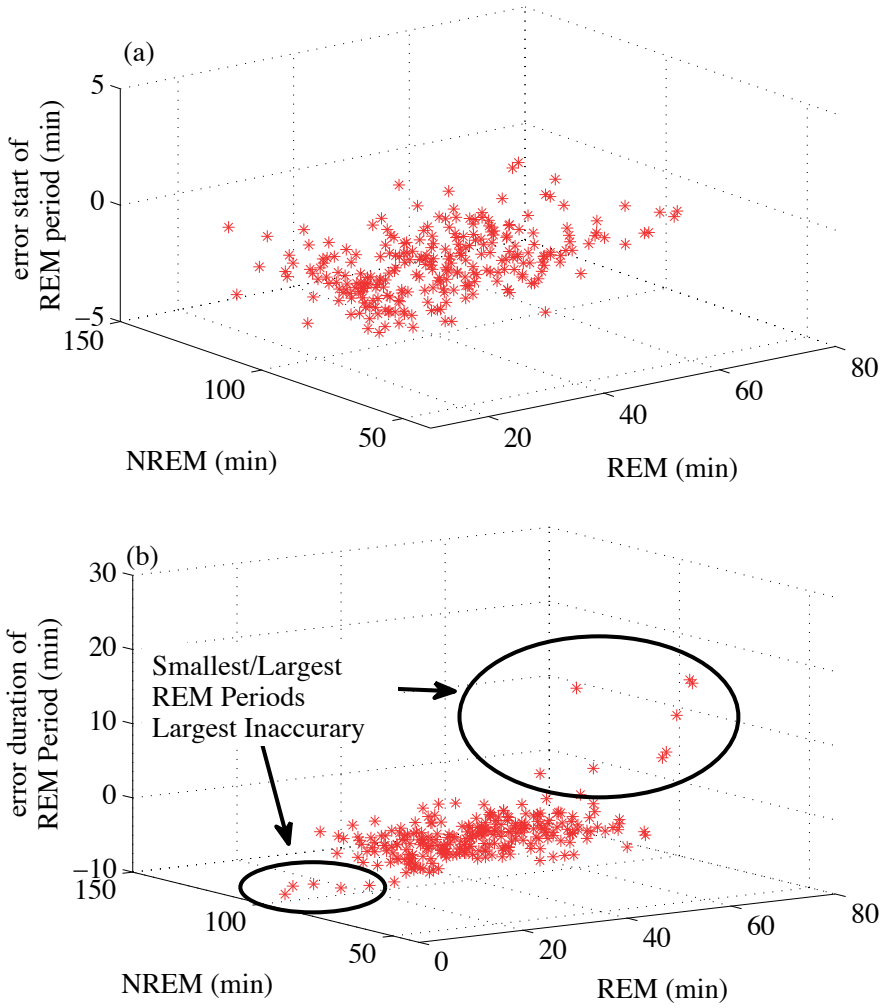

Figure 7.35. (a) Error between the estimated start time of each REM sleep period and the value derived from the UK dataset. (b) Error between the estimated duration of the REM sleep period and the value derived from the UK study data. The NREM duration is for the NREM period just before the REM period.

Note again that in the Massaquoi and McCarley model time is measured in units and 1 unit is equal to 10.7 minutes.

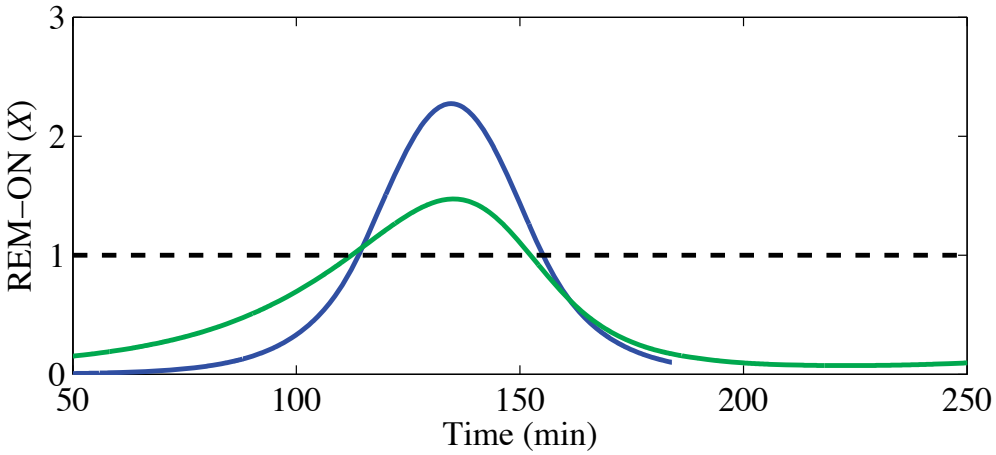

Figure 7.36. The created REM signal based on data and a simplified REM model (Equations 7.31 and 7.32) (blue/dark gray) and the simulated REM signal (green/light gray) using model parameters obtained from a linear fit to the study data.

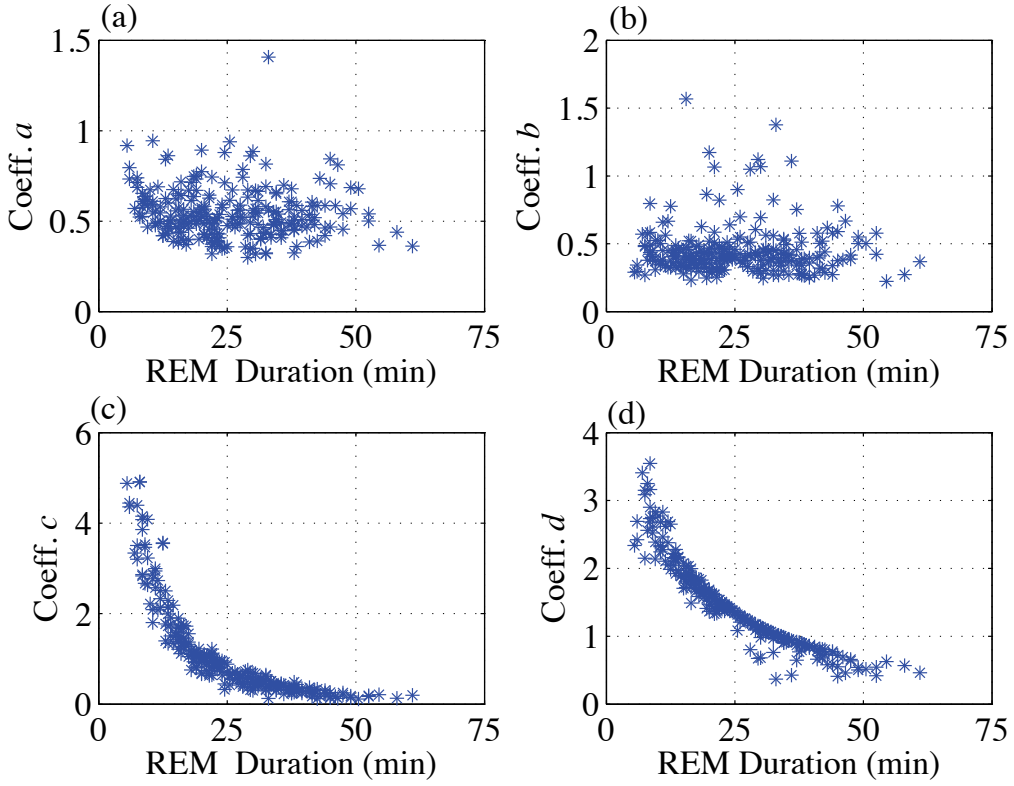

Figure 7.37. Estimated parameters of slow REM model versus the duration of REM sleep.

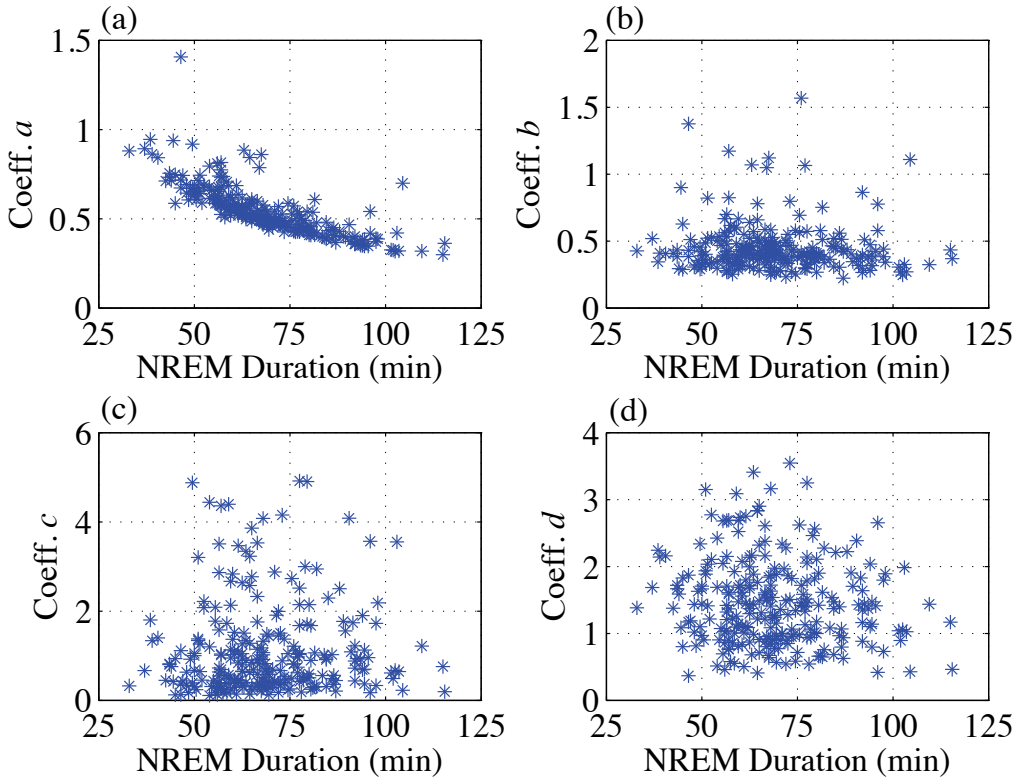

Figure 7.38. Estimated parameters of the slow REM model versus the duration of the NREM sleep period prior to the REM period.

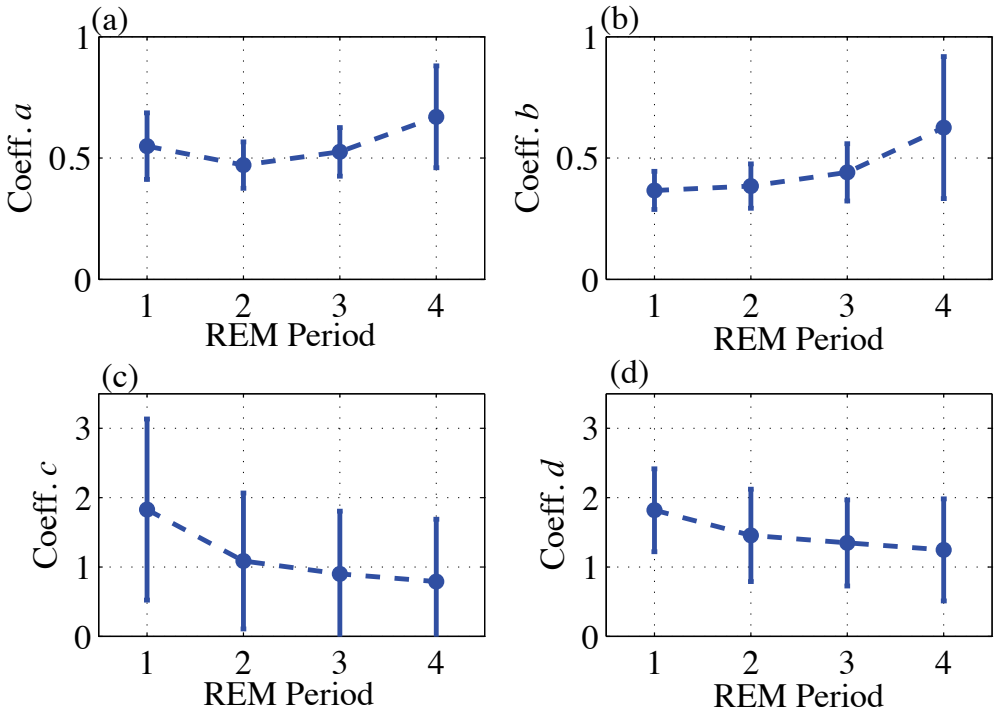

Figure 7.39. Mean and standard deviation of the estimated REM model parameters for each REM period.

7.5 Overview of The Model So Far

The complete nonlinear model is the result of all issues addressed and noted in this chapter and what follows in this and the following sections. So far, to recap, the SWA, S, the slow REM (X, Y) model and the fast REM model have been described. These models contain an impulsive term based on $N(t)$. $N(t)$ is a series of square pulses whose amplitudes and durations are Gaussian distributed, and the inter-arrival time has an exponential distribution. The parameters of these models have been estimated based on the data from the UK study. The following issues, though, still need to be resolved.

1. The desire is to have a model that results in the prediction of sleep stages. To calculate different stages, thresholds based on the level of SWA need to be assigned.

2. How should a noise event impact the sleep model? One possibility is to increase the number of excitations $N(t)$ and this will be a function of the L_{Amax} of the noise event.

These issues will be addressed in the following sections.

7.6 Thresholds for Scoring Sleep Stages

The output of the model being developed includes REM sleep, slow wave activity and awakenings. However, it is desired to also estimate different NREM stages (i.e. Stage 2 and Stage 3/4). In order to determine at what level to set the thresholds for this classification, first the mean, minimum and maximum level of SWA activity associated with Stage 3/4, Stage 2, and Stage 1/Wake were calculated for the 76 subject nights of the UK study. The results are listed in Table 7.5. Based on these levels a set of scoring rules were developed and are as follows:

1. Stage 3/4 was scored if SWA was greater than 2.75.

2. Stage Wake/1 was scored if SWA was less then 0.3.

3. Stage Wake/1 was scored if SWA was less than 1 and E was greater than 0.5.

4. At all other times when REM sleep was not occurring, stages were scored as Stage 2 sleep.

To evaluate the accuracy of these thresholds, simulations of slow wave activity for each subject night of data from the 1999 UK study, were completed using the model

parameters estimated in the previous sections, and the timing of REM sleep. The gamma activity for each subject was used to create the impulsive excitation term E. The fast REM model was not used for these simulations as the focus was on setting thresholds for scoring NREM sleep. Based on the thresholds and simulated levels of SWA, sleep stages were assigned to each 30 second epoch. The agreement between the actual scored sleep stages in the UK dataset and the simulated sleep stages was calculated. The agreement was defined as the fraction of all stages that were correctly identified. The overall agreement statistics are listed in Table 7.6 and the mean and standard deviation of the fraction of correctly identifying stages for each sleep stage is listed in Table 7.7. An example of the simulation that yielded the highest agreement is shown in Figure 7.40, and the simulation that had the lowest agreement is shown in Figure 7.41.

Table 7.5. Statistics of slow wave activity during different sleep stages for 76 subject nights in the 1999 UK dataset.

Sleep Stage	Mean (std. dev of data)	Min.	Max.
Stage Wake/1	0.42 (0.14)	0.14	1.24
Stage 2	1.06 (0.21)	0.67	1.53
Stage 3/4	3.41 (0.52)	1.86	5.08

Table 7.6. Overall statistics of the fraction of times there was agreement in sleep stage classification between scoring of the original data and automated scoring of simulated data for each of 76 subject nights.

mean	0.66
std. dev	0.07
max	0.79
min	0.43

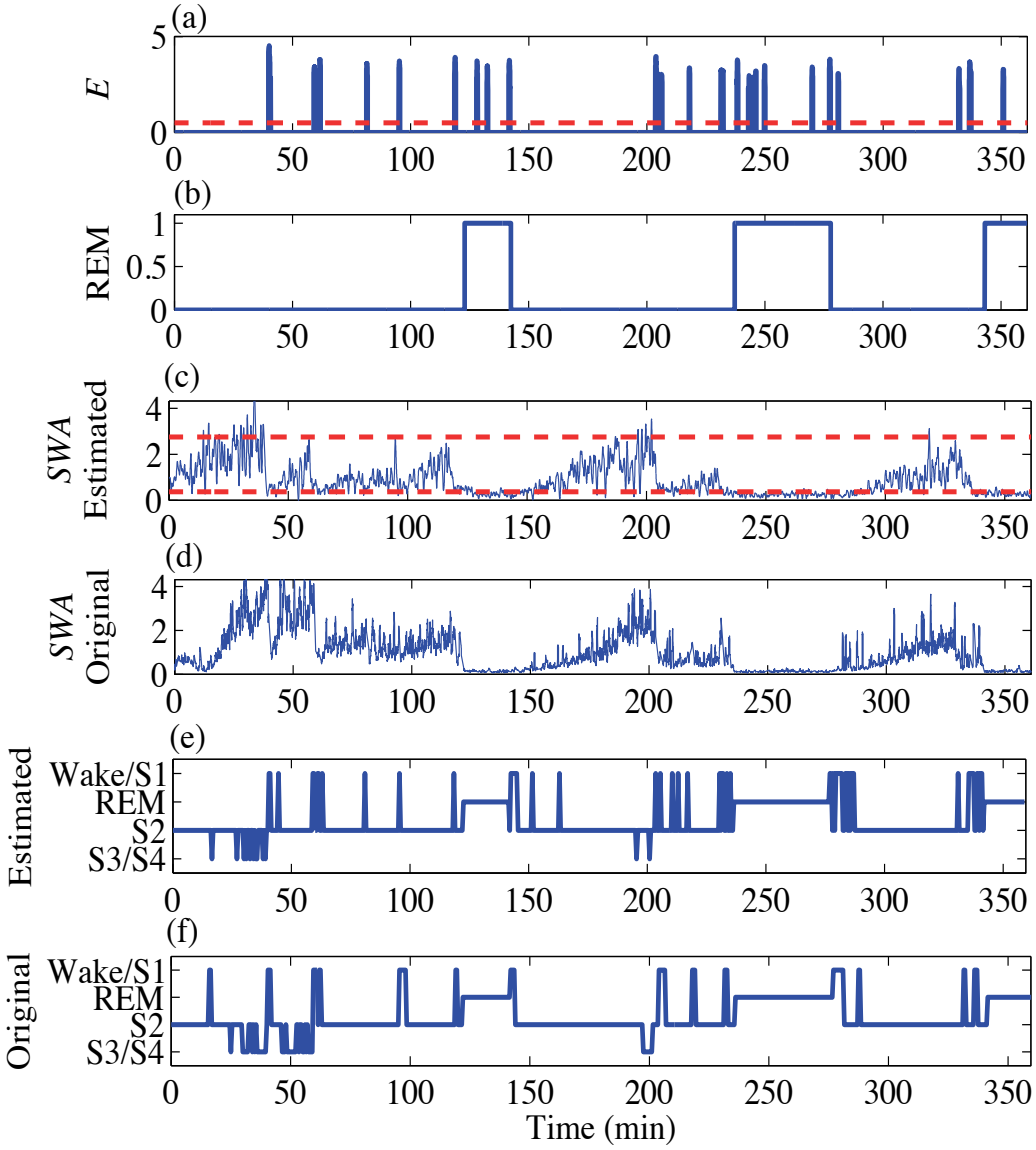

Figure 7.40. Best agreement between simulated and actual slow wave activity for one subject night of the 1999 UK dataset, thresholds used for scoring sleep stages (red-dashed lines).

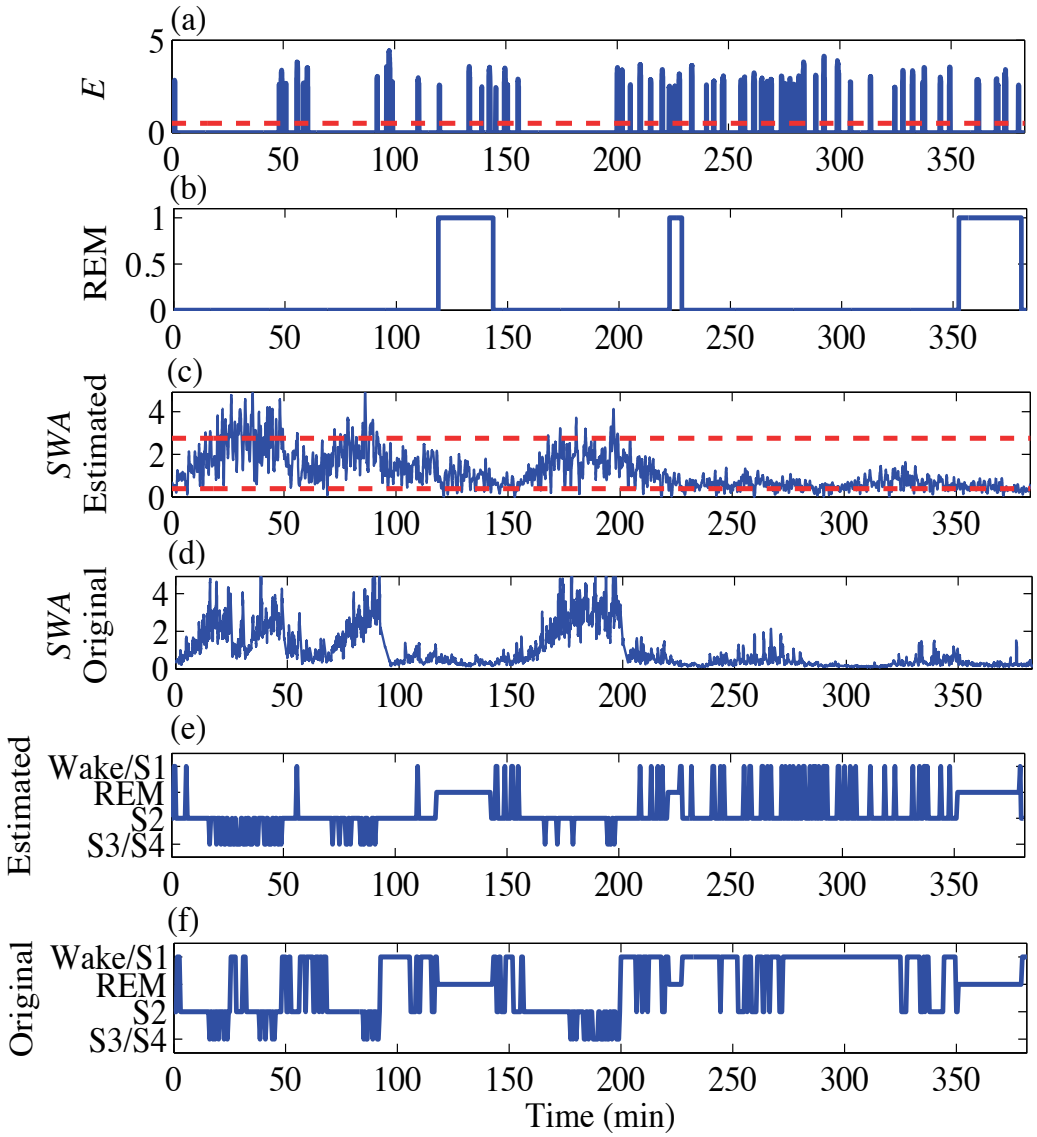

Figure 7.41. Worst agreement between simulated and actual slow wave activity for one subject night of the 1999 UK dataset, thresholds used for scoring sleep stages (red-dashed lines).

Table 7.7. Statistics of the fraction of times that there was agreement in sleep stage classification between scoring of the original data and automated scoring of simulated data for each of the 76 subject nights, for each sleep stage.

Sleep Stage	Mean (std)
Wake/S1	0.43 (0.17)
Stage 2	0.73 (0.09)
Stage 3/4	0.51 (0.29)

7.7 Adding Noise Dependence to Model

As discussed $N(t)$ is impulsive noise. The inter-arrival time of $N(t)$ is exponentially distributed and the amplitude and duration are both defined based on Gaussian distributions. The $N(t)$ term is low-pass filtered to obtain E which is used in the slow wave model and as mentioned in Section 7.3, is rescaled and also used in the fast REM model. Some of the examples shown for the fast REM model have used scaled versions of $N(t)$ (square impulses), not E. A diagram of the use of the impulsive terms is shown in Figure 7.42. The concept for introducing noise into the model was to create an excitation term for spontaneous (non-noise related excitations) and one for aircraft noise related excitations. The two components, both non-noise induced and noise induced excitations, are summed together and then fed into other parts of the model.

In order to determine how to add a noise level dependence to the nonlinear dynamic model, the amplitude of E from the UK data, was examined when noise events of different maximum levels occurred. Characteristics of E including the duration and amplitude of the events were examined, for every aircraft event that occurred during sleep Stage 2. Due to the limited amount of data, only two noise groups were examined: events which had a noise level below 50 dB(A) and events that had a maximum level greater than 50 dB(A). A small difference in amplitude of E was found,

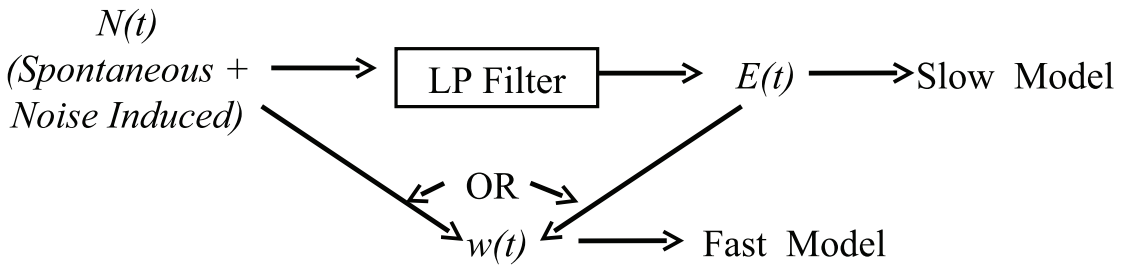

Figure 7.42. Diagram of impulsive noise as used in nonlinear dynamic model.

however, the primary difference was in the number of events that elicited additional impulses. Therefore, when modeling the effect of noise on sleep a linear relationship between the percentage of the population that will have a response to the noise event and the Indoor L_{Amax} of an event was created. The equation used is,

$$fraction\ \ responding = 0.0084 L_{Amax} - 0.1256. \tag{7.40}$$

Only L_{Amax} levels above 35 dB(A) cause a change in the fraction responding. Researchers have found from studies on aircraft noise and sleep that aircraft events with a L_{Amax} level below 35 dB(A) do not increase the probability of awakening (Basner, Buess, Elmenhorst, Gerlich, Luks, MaaB, Mawet, Müller, Müller, Plath, Quehl, Samel, Schulze, Vejvoda, and Wenzel, 2004). The percent increase in response with noise level was added based on existing awakening models (see Chapter 3 for more information) because the data from the UK study was limited and could not be used to create a reliable dose response relationship. The duration and height of $N(t)$ is assigned randomly based on normal distributions with mean and standard deviation as

defined in Table 7.8. Perhaps with more data, a variation in amplitude and duration with noise level will be identified and can be added to the model.

7.8 Combined Model

The components of the nonlinear dynamic model that was developed include a fast and a slow REM model, a SWA activity model, and impulsive excitations $N(t)$ for both spontaneous and noise induced awakenings. To simulate the sleep pattern of a person for a single night the following steps are performed:

1. The spontaneous excitation term $N(t)$ is generated based on an exponential inter-arrival time and Gaussian duration and amplitude distributions and is low-pass filtered to obtain $E(t)$.

2. If aircraft noise is present, the additional noise excitation term is generated and then the spontaneous and noise-induced excitation terms are summed together.

3. Both noise and spontaneous excitation terms are scaled to generate $w(t)$ for the fast REM model.

4. The excitation term $E(t)$, that includes both spontaneous and noise induced activity is fed into the slow REM activity model. The output of the slow REM model is REM-ON and REM-OFF activity which is used to generate a REM sleep indicator which is equal to 1 when the level of REM-ON X activity is above a level of 1. This REM indicator defines the REM periods.

5. The REM indicator that is generated is used to signal when to model fast REM activity. The term $w(t)$ is fed into the fast REM model in order to predict transitions to Stage Wake during a REM period.

6. The REM indicator and excitation term ($E(t)$) are fed into the Slow Wave Activity Model. For the SWA model, the rise and fall terms for the slow wave activity (fc, rc), and the mean, standard deviation, and skewness of the noise term ($n(t)$) are not varied for each simulation (one person night). The other parameters are varied according to Gaussian distributions, the mean and standard deviations of which are listed in Table 7.8.

7. Based on the SWA, REM-Indicator, excitation terms, and fast REM model, sleep stages are assigned for each 1 second. In order to compare predicted sleep stages though to other existing models, the probability of being in each sleep stage for each 30 second epoch is calculated from the 1-second sliding sleep stage classification and then a sleep stage is assigned according to the highest probability.

In Table 7.8 is a list of the model parameters and the values used in the simulations. An example of the individual output components of the combined model are shown in Figure 7.43. An example of sleep stages calculated from a simulation with and without aircraft noise is shown in Figure 7.44. For the simulation with aircraft events, there were 32 evenly spaced events with an L_{Amax} of 60 dB(A). Note the additional awakenings that occur during the REM sleep period.

The predictions of the nonlinear model were compared to those of Basner's Baseline Markov model (2006). Six hundred simulations, each simulation contains a different choice of random variables for parameters that are described by distributions, for baseline conditions without aircraft noise events were completed using the nonlinear model. The probability of being in each sleep stage was calculated. For these simulations the threshold used to assign Stage 3/4 was lowered to 2 instead of 2.75. The reason is that perhaps the properties of $N(t)$ are more time varying, with less excitations occurring during Stage 3/4, this should be explored in the future. The results

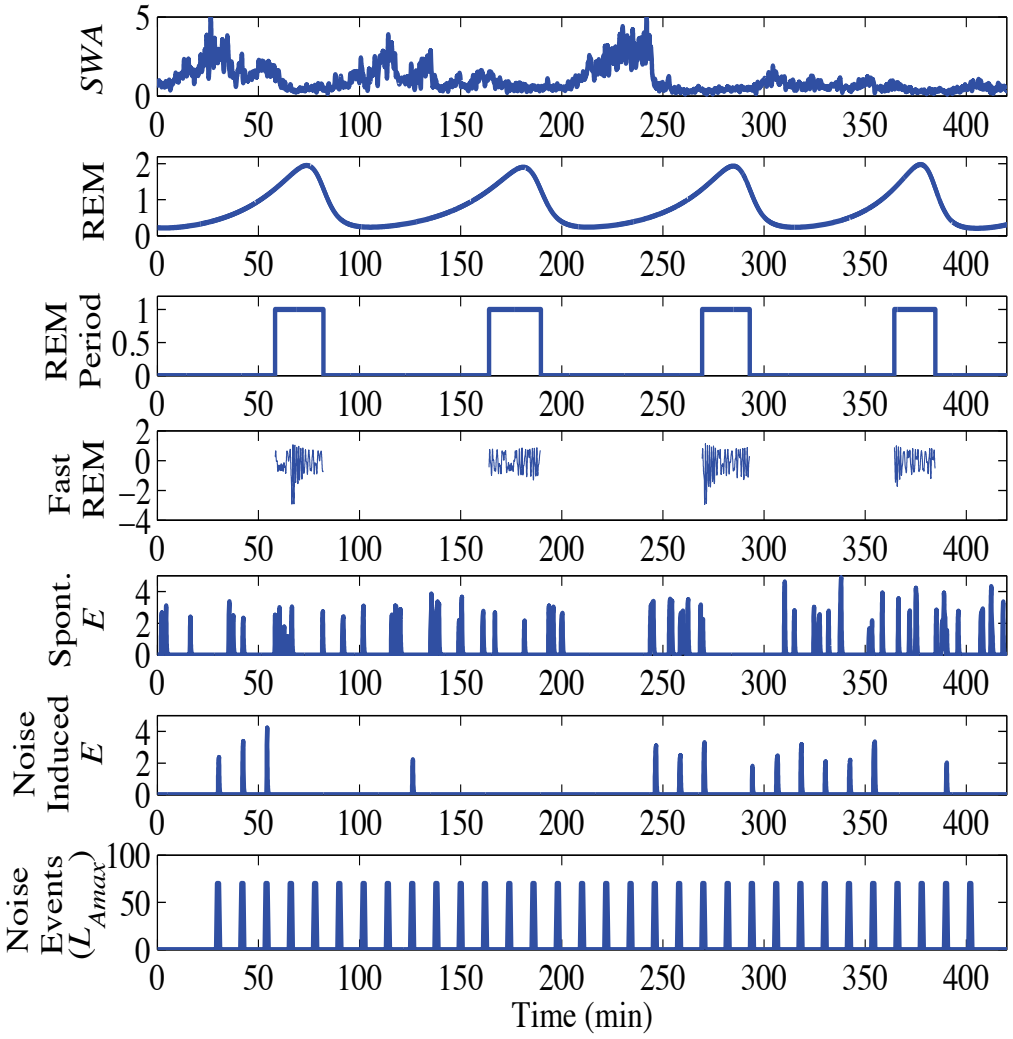

Figure 7.43. Example of the parameters for the developed nonlinear sleep model, which include slow wave activity (SWA), REM which is the X or REM-ON activity, REM sleep period indicator, Fast REM model and the spontaneous and noise induced excitation terms.

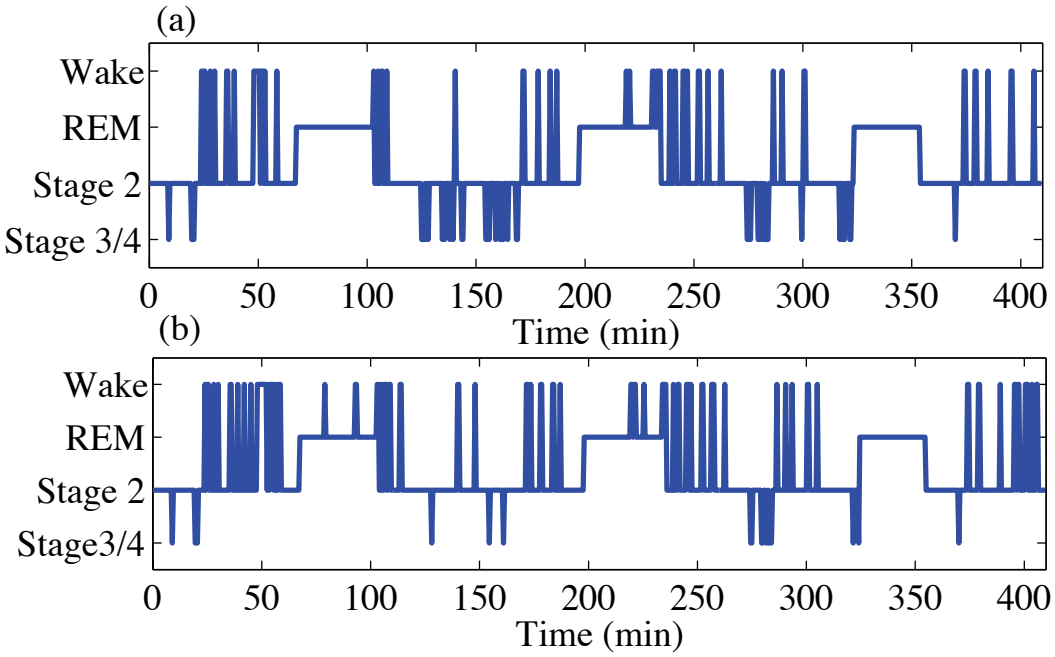

Figure 7.44. Sleep stages calculated using the developed nonlinear model. (a) No aircraft events, and (b) 32 events of an L_{Amax} of 60 dB(A).

Table 7.8. Parameters of the nonlinear model. *Parameters varied according to a Gaussian distribution, + parameters varied according to a uniform distribution, and x parameter varied according to an exponential distribution.

SWA		Slow REM		Fast REM		Excitations	
$^*S_o$	mean 3.75 std. dev 0.67	$^*a$	mean 0.47 std. dev 0.1	ω	2 π (0.3)	N	^{x}mean inter-arr 6.1 min
$^*SWA_o$	mean 0.78 std. dev 0.29	$^*b$	mean 0.41 std. dev 0.1	A	0.5		*dur.-mean 0.5 min
$^*gc$	mean 0.03 std. dev 0.01	$^*c$	mean 1.4 std. dev 0.15	δ	0.06		*dur.-std. dev 0.2 min
SWA_L	0.2	$^*d$	mean 1.83 std. dev 0.15	^+x_o	min -1.0 max 1.0		*amp.- mean 3.0
fc	2.0	e	0.05	^+y_o	min -1.0 max 1.0		*amp.-std. dev 0.65
fcw	4.0	^+X_o	min 0.15 max 0.3				amp.-max 5.0
rc	0.4	^+Y_o	min 0.5 max 3.0				
$n(t)$	mean 0 std. dev 0.2 skewness 0.53						

are shown in Figure 7.45. Similar predictions for time spent in Stage Wake/Stage 1 were obtained from both of the models. The Markov model did, however, predict a higher probability of being in Stage 3/4 at the start of the night and the increase in the probability of being in REM sleep toward the end of night was greater for that model. However, the subjects in the UK study did have less Stage 3/4 sleep than those in Basner's study which might explain some of the difference in predicted probabilities. Note that the nonlinear model has been tuned to the UK study data and the Basner model to data from a laboratory study (Basner et al., 2004).

Simulations with the nonlinear model were also conducted for scenarios with 16 and 32 noise events of different noise levels. For each simulation, the noise events

were all of the same level. Fifty simulations were conducted for each noise level which ranged from 40 to 90 dB(A), L_{Amax}. The increase in the predicted probability of being awakened with noise level is shown in Figure 7.46 and the change in duration spent in the Slow Wave, REM, and Wake states is shown in Figure 7.47. Fifty simulations for each condition were also completed using Basner's Markov model with added noise level dependence (see Chapter 4). The probability of awakening predicted by the nonlinear model did increase with noise level. Also an increase in duration spent in Stage Wake and a reduction in time spent in Stage 3/4 was found, and the changes were greater for nights when there were 32 events than for nights with only 16 events. The change in REM sleep was less predicable in that it did not vary with noise level. The results for the probability of awakening is in agreement with the modified version of Basner's Markov model. The nonlinear model does predict a higher duration spent awake and a greater reduction in slow wave sleep. However, in Basner's laboratory study (Basner and Samel, 2005) when subjects were exposed to 32 noise events at an L_{Amax} of 70 dB a reduction in Slow Wave Sleep of 10.7 minutes was found, the prediction of the nonlinear model is a reduction of 10 minutes. Also an increase in duration of time spent awake of 11.4 minutes, for the same number and level of events, was found in Basner's Laboratory study while the nonlinear model predicts 12.6 minutes. It is not clear whether the the nonlinear dynamic model needs to be altered to predict less change in sleep stage duration or if the altered version of Basner's Markov model needs to be modified further to predict a larger change in duration, perhaps both modifications are needed.

7.9 Conclusions

The Massaquoi and McCarley sleep model had two primary limitations: it had slow dynamics and could not predict brief awakenings during the night and it could not

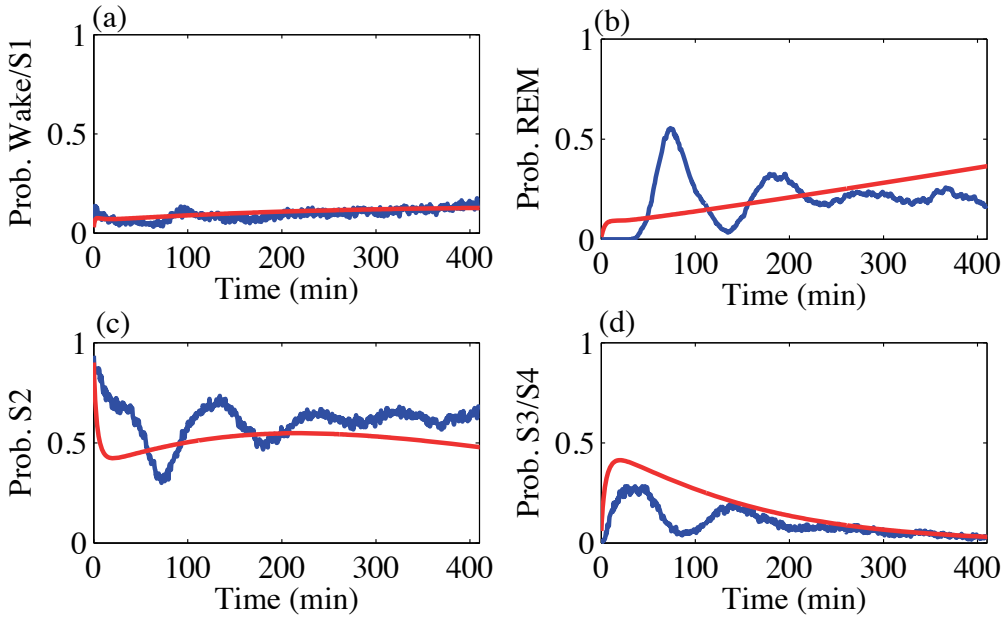

Figure 7.45. Probability of being in each sleep stage predicted for a baseline no noise night using the developed nonlinear model (blue) and Basner's Markov model (red): (a) Wake/S1, (b) REM, (c) S2, (d) S3/S4 Stages.

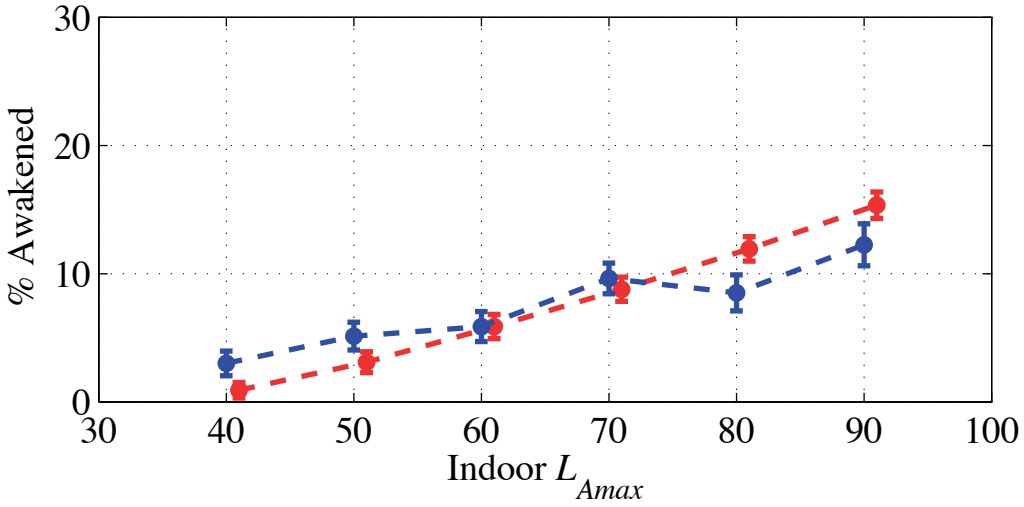

Figure 7.46. Percent awakened predicted with the nonlinear dynamic model developed in this research (blue/dark gray) and the modified version of Basner's Markov model (red/light gray).

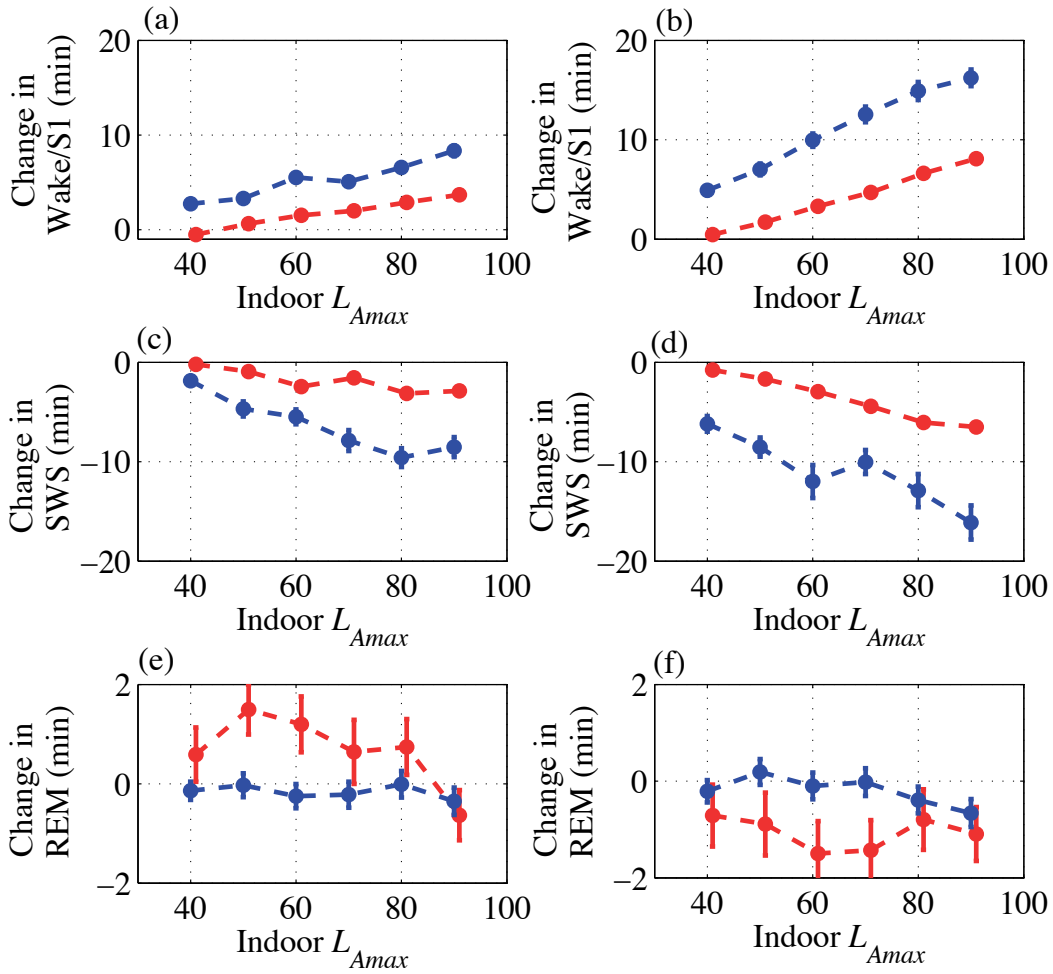

Figure 7.47. Change in duration of Wake/S1, SWS, and REM sleep for (a,c,e) 16 evenly spaced events and (b,d,f) 32 evenly spaced events. The nonlinear dynamic model predictions are shown in blue/dark gray and the predictions from the modified version of Basner's Markov model are shown in red/light gray.

predict awakenings during REM sleep. To overcome these challenges a modified version of the Massaquoi and McCarley sleep model was developed. With this model it is possible to predict spontaneous and noise induced awakenings, slow wave activity and fast and slow REM sleep. The parameters of the developed model were estimated using the data from the 1999 UK data. The predictions of changes in sleep stage duration and increase in probability of awakening for events of different noise levels, using the developed nonlinear model, was found to be similar to other sleep models.

8. NOISE MODEL COMPARISONS FOR AIRPORT OPERATIONS

Data on flight operations from two US airports, aircraft and flight tracks, were obtained. This was used as input to noise prediction software so that noise levels inside houses could be estimated for each aircraft event. By using this information, it is possible to compare sleep disturbance model predictions for different models and for different flight operation scenarios. Comparisons of both awakening model predictions and changes in sleep stages predicted using Basner's Markov model and the nonlinear dynamic sleep model developed in this research are described in this Chapter.

8.1 Airport Noise Modeling

Flight operations data were obtained for two US airports. The airports will be referred to as Airport A and Airport B. The data included the arrival and departure flight paths and the timing of aircraft events, whether they occurred during the day, evening, or night. The specific time of each flight operation was obtained for one of the airports. Information on type of aircraft and distance the aircraft was traveling was also obtained.

A list of aircraft responsible for approximately 90 percent of the operations at each airport was made, to reduce the amount of computation. This was not felt to be a significant problem because a few aircraft made up the majority of operations. By having a smaller number of aircraft it was feasible to calculate the noise for these aircraft on many different flight paths. For Airport A there were 3 runways, 89 arrival and 80 departure flight paths. For Airport B there were 4 runways, 44 arrival and 76 departure flight paths. The primary aircraft for Airport A are given in Table 8.1 and

the primary aircraft for Airport B are listed in Table 8.2. The departure standard, in both tables, refers to how far an aircraft is traveling. The higher the departure standard the farther the aircraft is traveling. In general an aircraft that is flying farther will be heavier at takeoff due to a greater amount of fuel and it will take longer for the aircraft to reach higher altitudes. Therefore, for the same aircraft, as the departure standard increases so do the noise levels on the ground.

Table 8.1. Aircraft at Airport A.

INM Aircraft ID	Description	Departure Standards
757PW	Boeing 757-200/PW2037	1, 2, 3, 4
757RR	Boeing 757-200/RB211-535E4	1, 2, 3, 4
7373B2	Boeing 737-300/CFM56-3B-2	1, 2, 3, 4
737300	Boeing 737-300/CFM56-3B-1	1, 2, 3, 4
737700	Boeing 737-700/CFM56-7B24	1, 2, 3, 4
747400	Boeing 747-400/PW4056	1, 2, 3, 4, 5
767300	Boeing 767-300/PW4060	1, 2, 3, 4
A300-622R	Airbus A300-622R/PW4158	1, 2, 3, 4
BEC190	Beech 1900	1
CL601	CL601/CF34-3A	1
CNA560	Cessna 560 Citation V	1
EMB145	Embraer 145 ER/Allison AE3007	1
EMB170	Embraer EMB-170	1
FAL20	FALCON 20/CF700-2D-2	1
MD11GE	MD-11/CF6-80C2D1F	1, 2
MD82	MD-82/JT8D-217A	1, 2
SD360	SD360	1

For the consolidated list of aircraft, the L_{Amax} and *SELA* noise levels for single event operations on every flight path were calculated by using the Federal Aviation Administration's Integrated Noise Model (INM) (FAA, 2007). The grid size used for the calculations was 0.1 by 0.1 nautical mile. Different flight operation scenarios were created based on the single event data and then sleep disturbance was predicted using

Table 8.2. Aircraft at Airport B.

INM Aircraft ID	Description	Departure Standards
757PW	Boeing 757-200/PW2037	1, 2, 3, 4, 5
757RR	Boeing 757-200/RB211-535E4	1, 2, 3, 4
767CF6	Boeing 767-200/CF6-80A	1, 2, 3, 4, 5, 6
737300	Boeing 737-300/CFM56-3B-1	1, 2, 3, 4
737400	Boeing 737-400/CFM56-3C-1	1, 2, 3, 4
737500	Boeing 737-500/CFM56-3C-1	1, 2, 3, 4
737700	Boeing 737-700/CFM56-7B24	1, 2, 3, 4
737800	Boeing 737-800/CFM56-7B26	1, 2, 3, 4
747400	Boeing 747-400/PW4056	1, 2, 4, 7
767300	Boeing 767-300/PW4060	1, 2, 3, 4, 5, 6, 7
777200	Boeing 777-200ER/GE90-90B	1, 2, 3, 4, 7
A319-131	Airbus A319-131/V2522-A5	1, 2, 3, 4
A320-232	Airbus A320-232/V2527-A5	1, 2, 3, 4
A321-232	Airbus A321-232/IAE V2530-A5	1, 2, 3, 4
A340-211	Airbus A340-211/CFM 56-5C2	1, 2, 3, 4, 5, 6, 7
CL600	CL600/ALF502L	1
CLREGJ	Canadair Regional Jet	1
DHC8	DASH 8-100/PW121	1
EMB14L	Embraer 145 LR / Allison AE3007A1	1
EMB120	Embraer 120 ER Pratt and Whitney PW118	1
MD82	MD-82/JT8D-217A	1, 2, 3, 4
MD83	MD-83/JT8D-219	1, 2, 3, 4
SF340	SF340B/CT7-9B	1

different models including the ANSI sleep model, Basner's Markov Model, and the nonlinear dynamic model developed in this research.

8.2 Awakening Model Comparisons

A baseline scenario for Airport A and Airport B was created. The scenario for Airport A had 150 operations and the scenario for Airport B had 281 operations. These numbers were the same for all the different scenarios investigated at each airport.

The aircraft and flight paths used were assigned randomly after calculating usage statistics for both airports. The percentage of the population awakened at least once for the airport scenarios was predicted using the ANSI standard method, however no time dependence was used, and different dose-response relationships were used (see Chapter 3) in order to compare models in a more comprehensive manner. Also as the sleep models are based on indoor noise levels and INM only predicts outdoor levels, for all simulations an outdoor to indoor noise attenuation of 25 dB(A) was used. In the future, it would be desirable to improve the outdoor-to-indoor prediction using characteristics of typical houses, window opening habits, house orientation, etc. This 25 dB(A) level of attenuation is similar to the reduction in noise level found in numerous studies (WHO, 2009).

The results for the baseline scenario for Airport A is shown in Figure 8.1 (a,b,c) for predictions calculated using the the ANSI (2008), FICAN (1997), and Basner et al. (2004) awakenings models. The results in Figure 8.1 (d,e,f) are percent awakened at least once predictions for a scenario in which 25 of the 150 operations were assigned to the third cross runway. For comparison, the 40 and 55 dB(A) $L_{night,outside}$ contours are shown. According to the WHO Night Noise Guidelines for Europe (2009) an $L_{night,outside}$ of 40 dB(A) should not be exceeded in order to prevent adverse health effects caused by noise. However, as this contour encompasses a large area and it would be difficult to reduce noise levels below this level, reducing nighttime noise to levels below an $L_{night,outside}$ of 55 dB(A) is the target goal. The ANSI standard model was found to predict the lowest percent awakened at least once. This is due to the fact that the model is based on behavioral awakening data. This low prediction (compared to that of other models) is particularly noticeable for the scenario in which there were 25 events on the cross runway.

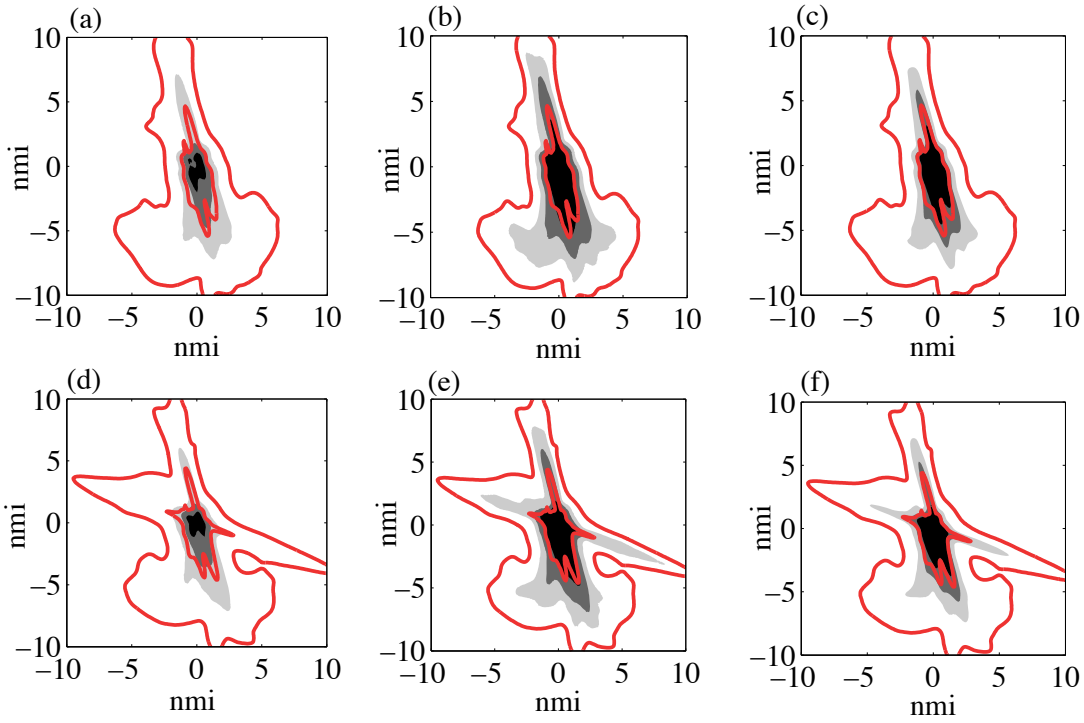

Figure 8.1. Gray-scale shading indicates percent awakened at least once. Black to dark gray 75%, dark gray to light gray 50%, and light gray to white 25%. (a,b,c) Scenario 1 and (d,e,f) Scenario 2 for Airport A. (a,d) ANSI, (b,e) FICAN and (c,f) Basner et al. model. Red contours are the 40 and 55 dB(A) $L_{night,outside}$ contours.

The number of people predicted to be awakened in communities surrounding Airport A and Airport B was also calculated. Population data was obtained from the US census and the number of people living within each 0.1 by 0.1 nautical mile block was calculated. The number of people in each block was then multiplied by the percent awakened at least once predicted using Basner et al.'s dose-response model. In Figure 8.2, the number of people living in each block for both Airport A and Airport B are shown and in Figure 8.3 the number of people predicted to be awakened at least once is shown. For comparison the $L_{night,outside}$ 40 to 55 dB(A) contours are also plotted. People living outside the WHO guideline of 55 dB(A) are clearly still awakened, this is especially noticeable at Airport B which has a larger population of people living near the airport. Awakenings occurred out to the 40 dB(A) contour.

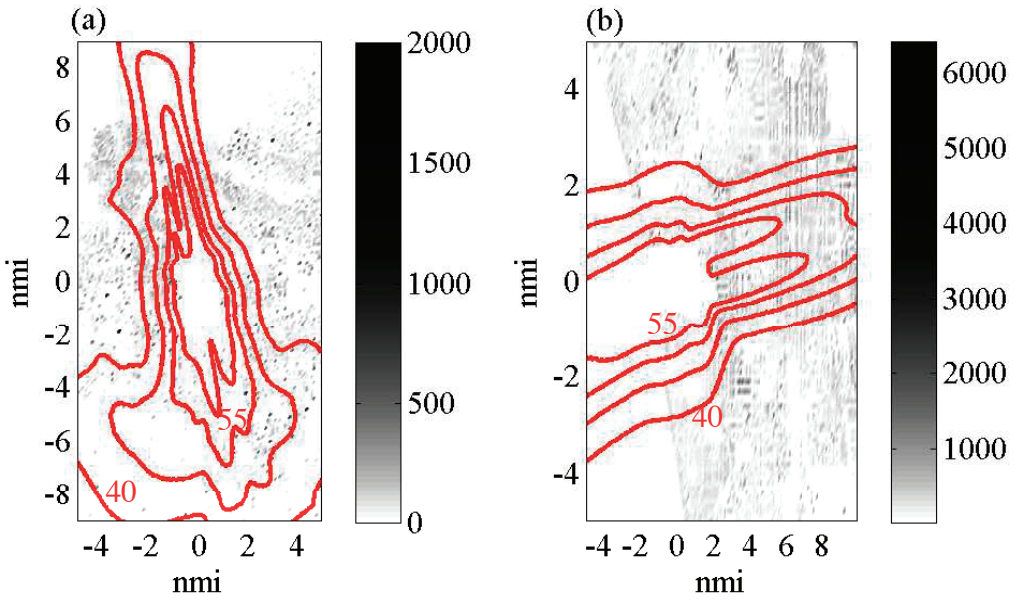

Figure 8.2. Population distribution living around the Airports. (a) Airport A and (b) Airport B. Red contours are the 40 to 55 dB(A) $L_{night,outside}$ contours.

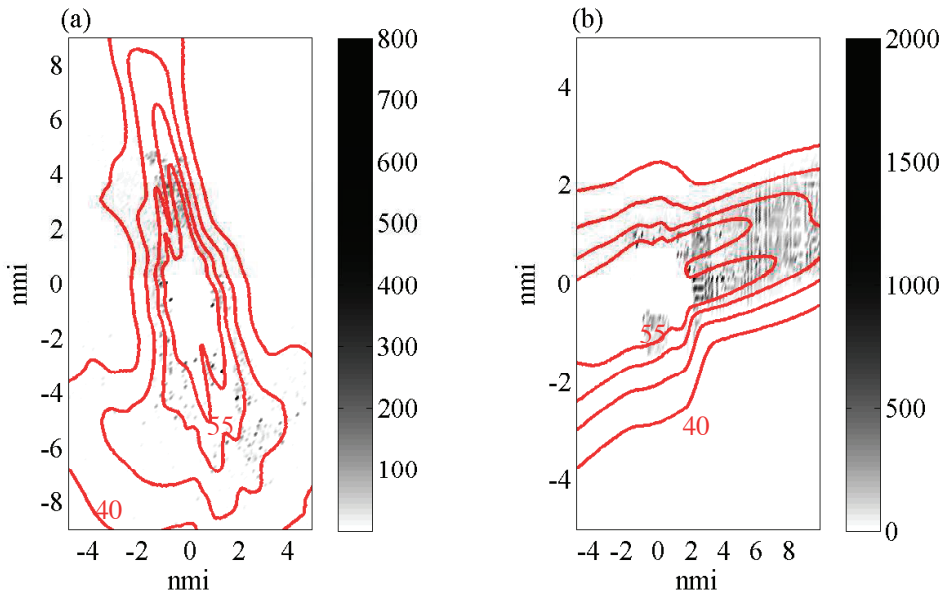

Figure 8.3. Number of people awakened at least once around the Airports, predicted using Basner et al.'s awakening model. (a) Airport A and (b) Airport B. Red contours are the 40 to 55 dB(A) $L_{night,outside}$ contours.

8.3 Sleep Disturbance Comparisons for Different Time Scenarios

Sleep disturbance predictions for different distributions of aircraft events during the night were also examined. Comparisons of sleep disturbance predictions made using the ANSI standard model with time dependence, a modified version of Basner's Markov model and the nonlinear dynamic model developed in this research are discussed.

8.3.1 Addition of Quadratic Dependence on Noise Level to Markov Model

In Chapter 4, a linear dependence on noise level was added to Basner et al.'s Markov model. For this analysis it was decided to add a quadratic dependence on level in order to better match Basner et al.'s dose-response awakening model. The equation for Basner et al.'s (2004) dose-response model is,

$$\%Awake = (1.894e^{-3})L_{Amax}^2 + (4.008e^{-2})L_{Amax} - 3.3243. \tag{8.1}$$

To determine how to change the coefficient values in the Markov model in order to obtain this same relationship, simulations of the same person nights as in Basner's study were completed. Events were evenly spaced throughout the night and the model coefficients, all denoted by a generic coefficient name c were varied for each simulation according to the following:

$$\begin{aligned} c = NoNoisemodelCoeff + \\ (NoiseModelCoeff - NoNoiseModelCoeff)mult, \end{aligned} \tag{8.2}$$

where $mult$ is a multiplier. The coefficients associated with a dependence on time t were not varied with noise level. The time dependence needed to stay as close to the original model as possible, as the focus was on comparing predictions for

different time scenarios, and the change in coefficients made for different noise levels are based on assumptions and not actual data. The relationship between the predicted percent awakened and different values of the multiplier *mult* are shown in Figure 8.4. The value of the multiplier was then compared to the L_{Amax} level (determined from Basner's dose-response relationship) that was associated with the same percent awake, this is shown in Figure 8.4.

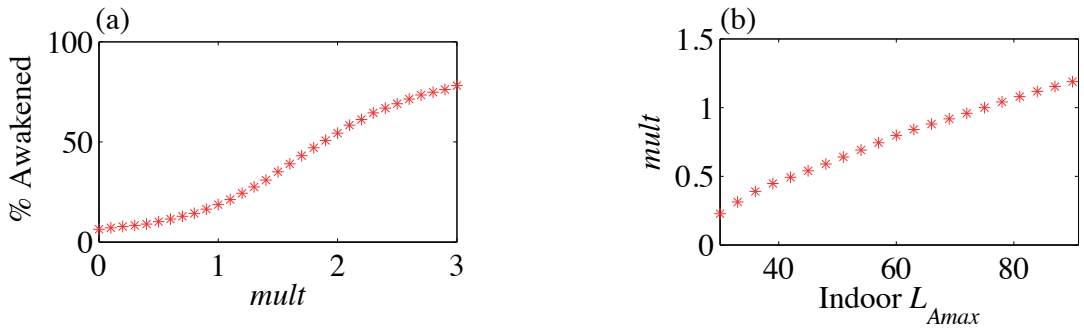

Figure 8.4. (a) Percent awakened predicted when using Basner's Markov model for different values of the multiplier. (b) The relationship between L_{Amax} and the multiplier, based on Basner's field dose-response relationship.

The data, shown in Figure 8.4 (b), was fit with a quadratic function, and the obtained equation was:

$$mult = (-8.1508e^{-5})L_{Amax}^2 + (2.5274e^{-2})L_{Amax} - 0.4321. \tag{8.3}$$

To verify that this change in the Markov Model coefficient values resulted in the desired percent awakened dose-response curve, a simulation was performed using the coefficients with the added noise level dependence. Simulations of 50 person nights with 32 evenly spaced noise events for each L_{Amax} noise level from 35 to 90 dB(A) in increments of 5 dB(A) were completed. The percent awakened was calculated for each noise level based on the simulated dataset. This simulation process was than repeated

100 times and the mean was calculated and variation of the results examined. The results from this verification are shown in Figure 8.5.

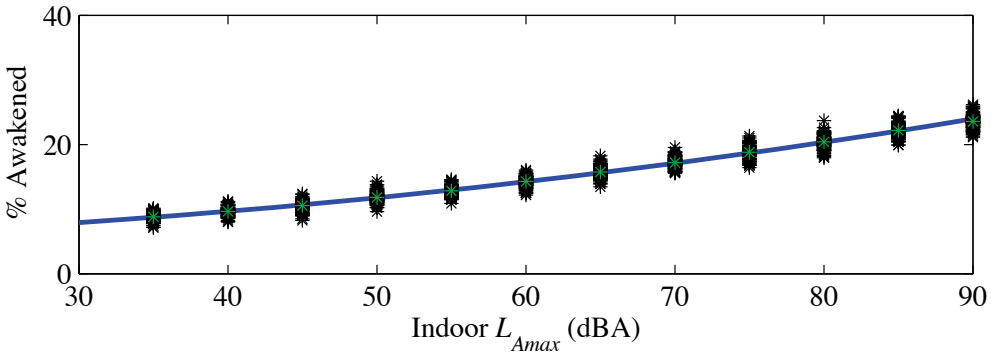

Figure 8.5. The obtained relationship between L_{Amax} and the percent awakened using the modified version of Basner's Markov model. Basner et al.'s (2004) dose-response curve is shown in blue,the mean of the simulated results in (green/light gray), and the results of 100 simulations in black.

The equation for the probability of sleep stage transitions with the added quadratic dependence on noise level has the form:

$$p(s_i|s_j) = \frac{e^X}{\sum_{i=0}^{5} e^X}, \tag{8.4}$$

where

$$\begin{aligned} X = A(s_i) + A_{N1}(s_i)L_{Amax} + A_{N2}(s_i)L_{Amax}^2 + Bt + C(s_i, s_j) \\ + C_{N1}(s_i, s_j)L_{Amax} + C_{N2}(s_i, s_j)L_{Amax}^2. \end{aligned} \tag{8.5}$$

8.3.2 Time-Dependent Model Comparisons

Sleep disturbance, using different models, was predicted for 6 nighttime operation scenarios. The distributions of aircraft events are shown in Figure 8.6. These time scenarios were chosen in order to determine the largest difference in sleep disturbance predictions that might be expected with various scenarios.

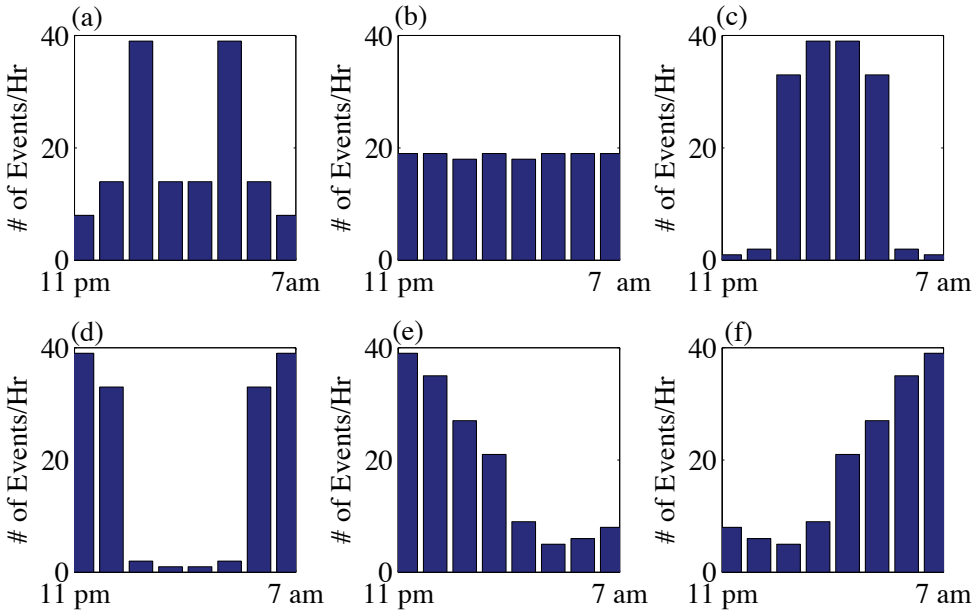

Figure 8.6. The occurrence of events for six nighttime scenarios that were examined. Each bar represents the number of events during an hour of the night. There are eight bars per scenario representing each hour from 11 pm to 7 am. (a) Peak in operations in two hours in the middle of the night, (b) an even distribution, (c) most events in the middle of the night, (d) a U-shaped distribution, (e) most events at the beginning of the night, and (f) most events occurring at the end of the night.

The average number of awakenings for the six scenarios was calculated using the ANSI standard model with time dependence. The results are shown in Figure 8.7. The ANSI standard has a time dependence which results in events at the beginning

of the night having the lowest probability of causing an awakening and events at the end of the night having the highest probability of causing an awakening. Scenarios 1, 2, 3 in which most of the events are in the middle of the night all caused similar number of awakenings.

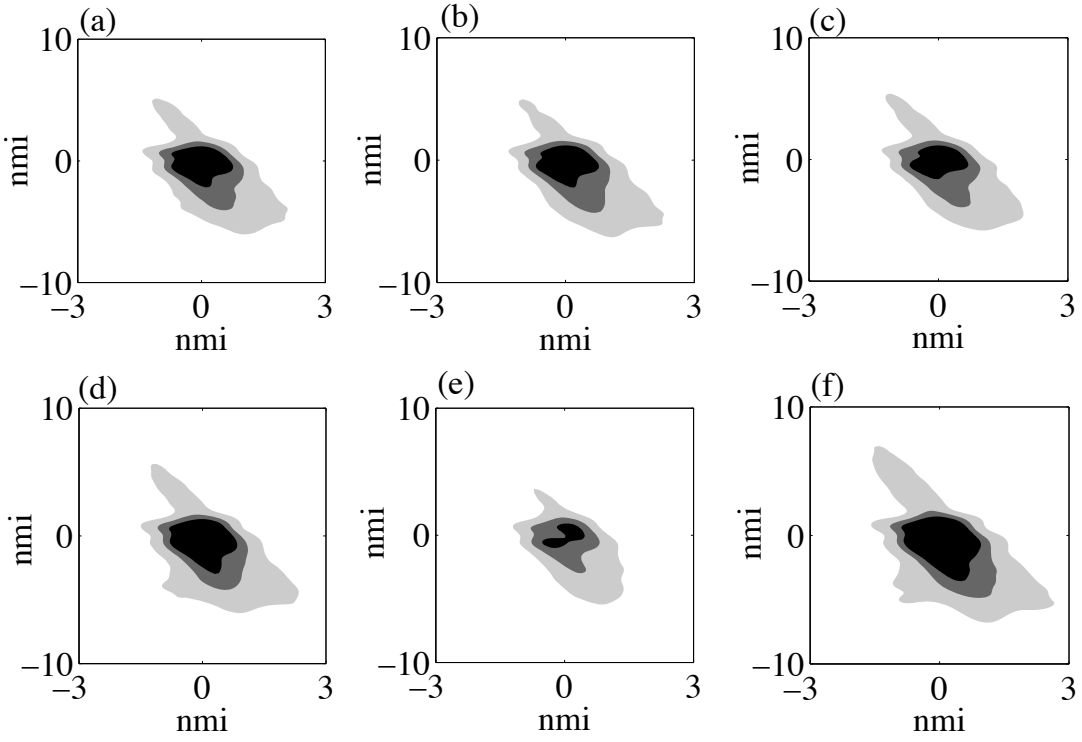

Figure 8.7. Average number of awakenings for the 6 time scenarios predicted using the ANSI standard model with time dependence. Black to dark gray 1.5, dark gray to light gray 1.0 and light gray to white 0.5 awakenings. (a) Peak in operations in two hours in the middle of the night, (b) an even distribution, (c) most events in the middle of the night, (d) a U-shaped distribution, (e) most events at the beginning of the night, and (f) most events occurring at the end of the night.

Using Basner's Markov model with the added quadratic dependence on noise level described earlier in this chapter, the average number of awakenings in 50 simulations at each grid point was calculated for the six time scenarios. The results are shown in

Figure 8.8. The awakenings that are calculated are EEG, not behavioral awakenings, they must occur within 90 seconds or three epoch of the start of the aircraft event and the minimum duration of an awakening is 30 seconds. The results are opposite to those of the ANSI standard model, more awakenings were predicted when most events were at the beginning of the night. This difference in predictions is partly due to the time dependent coefficients of the Markov model. While the baseline no-noise model predicts an increase in awakenings, the time dependence coefficients of the first and second noise models are negative. This decrease in awakening response to events with time is supported by other models (Brink, Lercher, Eisenmann, and Schierz, 2008). In addition, more spontaneous awakenings tend to occur at the end of the night and therefore more noise-induced and spontaneous awakenings may be jointly occurring. In Figure 8.9, the results for the beginning of the night and end of the night scenarios for both Basner's Markov model and the ANSI Standard model with time dependence are shown. The differences in percent awakened do appear small for the two time scenarios. However, when the number of people living within each contour are calculated the difference is more substantial, these results are given in Table 8.3.

Table 8.3. Number of people within awakening contours for Airport A, with 150 events during the night.

Average Number of Awakenings Per Night	Basner Beginning of the Night	Basner End of the Night	ANSI Beginning of the Night	ANSI End of the Night
0.5 Awakenings	40,276	35,514	14,302	39,531
1.0 Awakenings	27,281	11,772	2,790	7,657
1.5 Awakenings	17,288	6,513	10	4,829

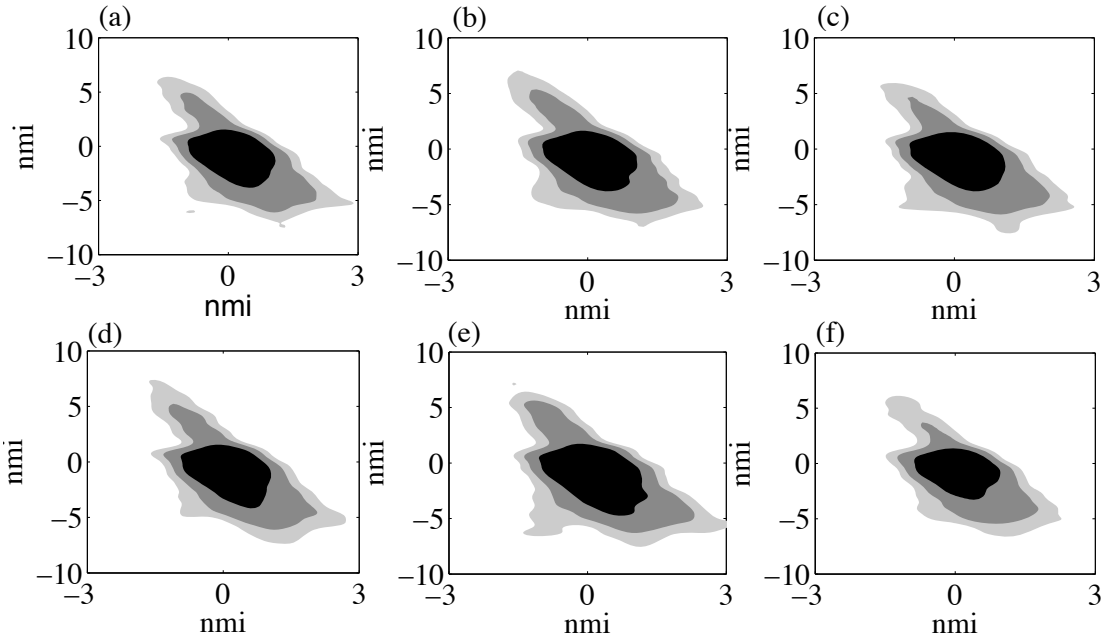

Figure 8.8. Average number of awakenings for the 6 time scenarios predicted using Basner's Markov model with added quadratic dependence on noise level. Black to dark gray 1.5, dark gray to light gray 1.0, and light gray to white 0.5 awakenings. (a) Peak in operations in two hours in the middle of the night, (b) an even distribution, (c) most events in the middle of the night, (d) a U-shaped distribution, (e) most events at the beginning of the night, and (f) most events occurring at the end of the night.

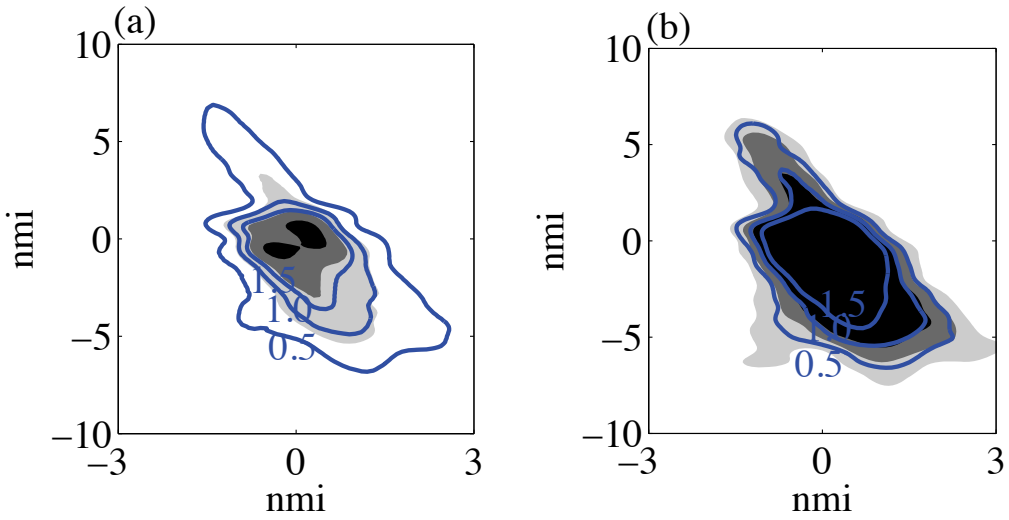

Figure 8.9. Average number of awakenings for the beginning of the night (black to dark gray 1.5, dark gray to light gray 1.0 and light gray to white 0.5 awakenings) and end of the night (blue contours) for (a) the ANSI standard model with time dependence and (b) Basner's Markov model with added quadratic dependence on noise level.

As the the use of $L_{night,\ outside}$ is advocated by WHO, contours for the scenario in which most events occurred at the beginning of the night calculated using Basner's Markov model and the $L_{night,outside}$ contours is shown in Figure 8.10. In addition to the WHO guidelines, recommendations have also been made based on the acceptable number of awakenings per night such that 0.5 (Schrenkenberg, Meis, Kahl, Peschel, and Eikmann, 2010) or 1.0 (Basner, Samel, and Isermann, 2006) additional awakening on average should be prevented in order to protect communities from the adverse effects of nighttime noise. Both limits, based on number of average awakenings, were found to be more protective than the WHO Guideline of $L_{night,outside}$=55 dB(A).

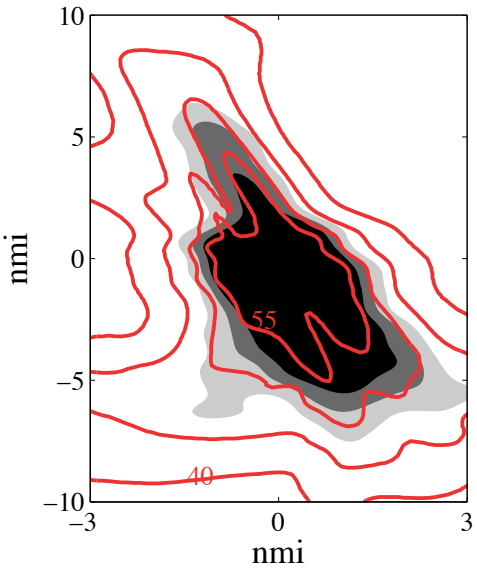

Figure 8.10. Predictions of the average number of awakenings using Basner's Markov model with added quadratic dependence on noise level for the scenario in which most events are at the beginning of the night (black to dark gray 1.5, dark gray to light gray 1.0 and light gray to white 0.5 awakenings) and the $L_{night,outside}$ contours (red).

The change in duration of sleep stages predicted using the modified version of Basner's Markov model was also examined. The Sleep Quality Index (SQI) (Basner,

2006) was calculated based on the duration of time spent in the different sleep stages. The SQI is defined as,

$$SQI = 0.657\ S2 + 0.840\ REM + 0.879\ S3 + S4, \tag{8.6}$$

where $S2$, $S3$, $S4$, andREM are the duration of these stages in minutes. The equation for SQI linearly weights the duration spent in different stages of sleep. The highest weighting is for the duration spent in Stage 4 sleep and lowest is for Stage 2 sleep. Time spent in Stage 1 and Wake are not included in the equation as they are not restorative. A lower value of the SQI corresponds with worse sleep as REM, $S3$, and $S4$ in the equation would have lower durations. The SQI values for the 6 nighttime operation scenarios are shown in Figure 8.11. The scenario in which most events were at the beginning of the night resulted in the lowest SQI values due to a greater reduction in Stage 3 and 4 sleep. The reduction in Stage 3 and 4 sleep and the increase in Stage Wake for the 6 time scenarios are also shown in Figures 8.12 and 8.13, respectively.

Due to increased computational complexity of the developed nonlinear model, full contours for the six scenarios were not able to be generated with the model in time for inclusion in this thesis. However, simulations for the six different scenarios for a few grid points was completed. For each of these grid points, 50 simulations were completed for each noise scenario. For each simulation a different set of random parameters were selected as described in Chapter 7. For two grid points, the average number of additional awakenings calculated by taking the difference between the number of awakenings occurring when noise events are present and the number that would occur at the same time spontaneously without noise present, are shown in Figure 8.14.

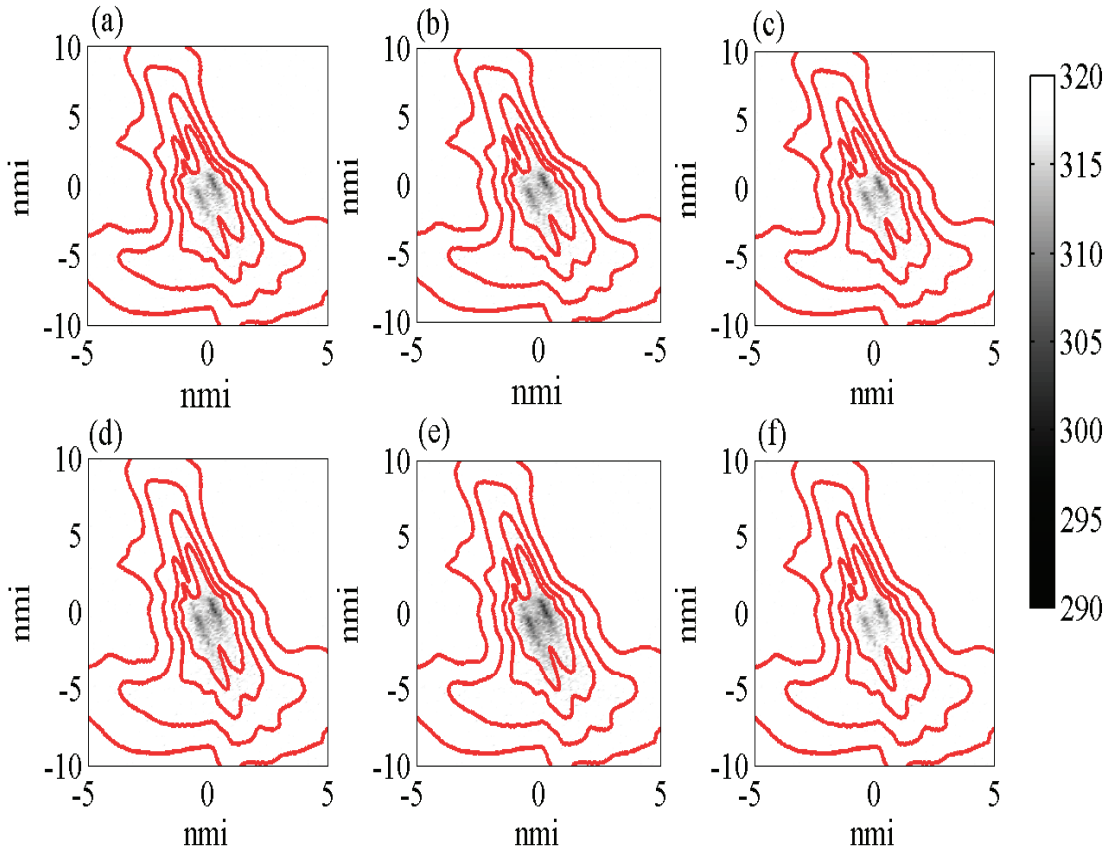

Figure 8.11. *SQI* predictions for the 6 nighttime flight operation scenarios. (a) Peak in operations in two hours in the middle of the night, (b) an even distribution, (c) most events in the middle of the night, (d) a U-shaped distribution, (e) most events at the beginning of the night, and (f) most events occurring at the end of the night. Red contours are the 40 to 55 dB(A) $L_{night,outside}$ contours.

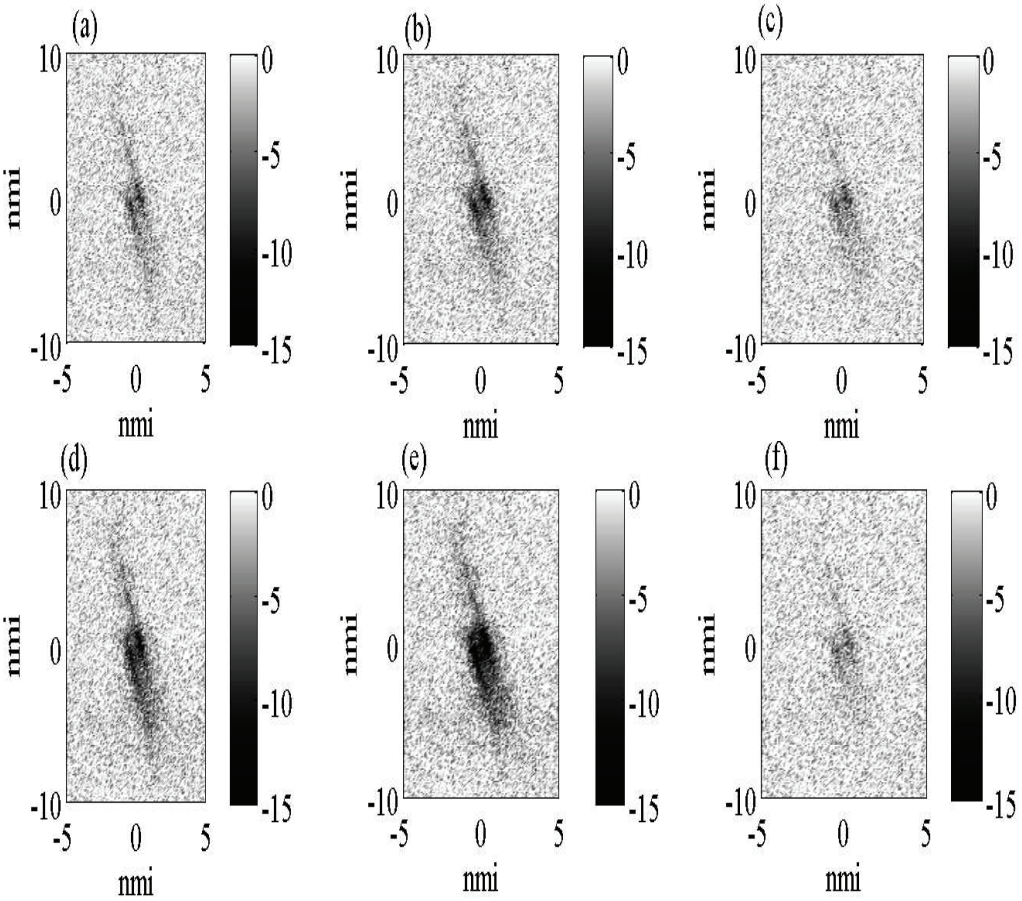

Figure 8.12. Reduction in time spent (minutes) in slow wave sleep for the 6 nighttime flight operation scenarios. (a) Peak in operations in two hours in the middle of the night, (b) an even distribution, (c) most events in the middle of the night, (d) a U-shaped distribution, (e) most events at the beginning of the night, and (f) most events occurring at the end of the night.

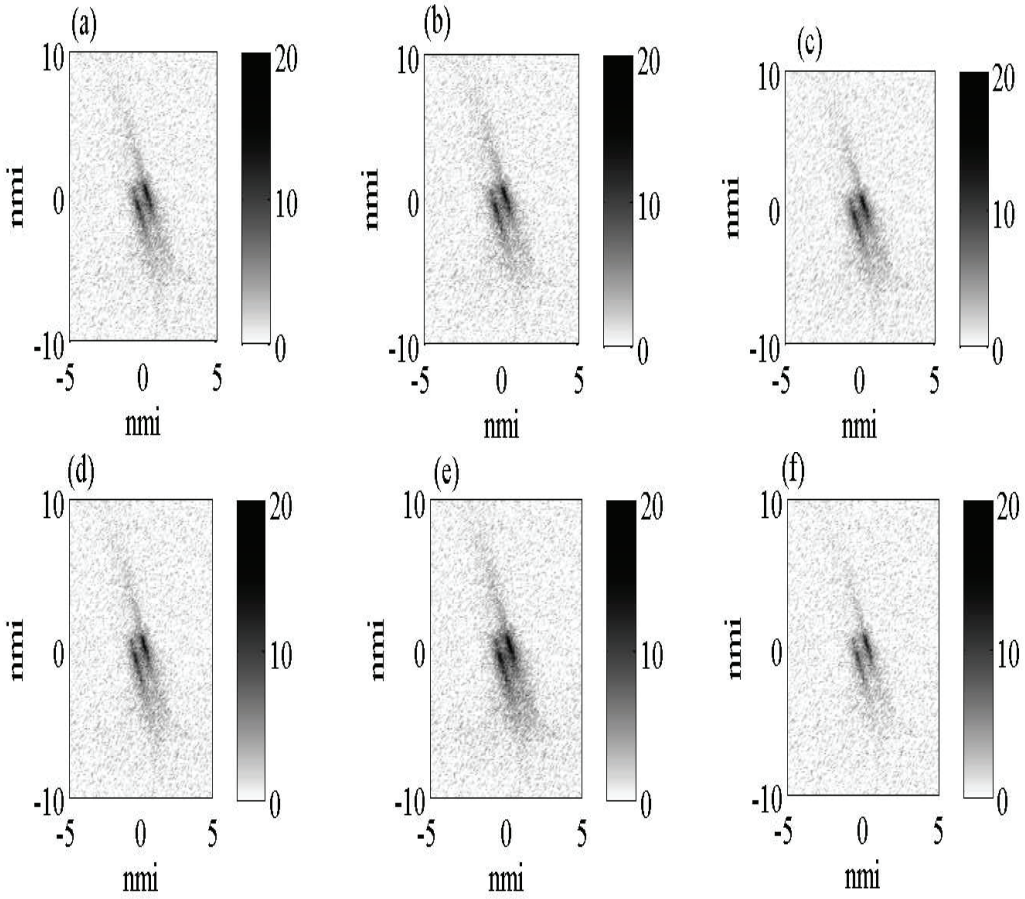

Figure 8.13. Increase in time spent (minutes) in Wake for the 6 night-time flight operation scenarios. (a) Peak in operations in two hours in the middle of the night, (b) an even distribution, (c) most events in the middle of the night, (d) a U-shaped distribution, (e) most events at the beginning of the night, and (f) most events occurring at the end of the night.

As with modified version of Basner's Markov model a greater number of additional awakenings occurred when most of the events were at the beginning of the night than when most events were at the end of the night. The change in sleep stage durations, compared to nights without aircraft events, for the two grid points is shown in Figure 8.15. The change in sleep stage durations did not vary greatly between the six scenarios. The largest difference occurred between the scenario when most of the events were at the end of the night and the scenario in which most events were at the beginning of the night. When most events were at the beginning of the night, there was a greater reduction in slow wave sleep. However, unlike with the modified version of Basner's Markov model predictions, there was not a greater increase in Stage Wake. A possible reason for this result is that the events at the end of the night, for the nonlinear dynamic model, might have caused a greater reduction in slow wave activity than when the events were at the beginning of the night, which might have increased the duration spent awake due to both spontaneous and noise excitations.

8.4 Conclusions

Sleep disturbance in communities was predicted for realistic airport operations scenarios. Models based on behavioral awakenings were found to predict a low number of awakenings compared to those based on polysomnography data and may, particularly, under-predict the impact of nighttime noise on communities for scenarios in which there are only a few events on a runway or flight-path. For different distributions of aircraft events during the night, the ANSI standard model predicted opposite results, in terms of the average number of awakenings, when compared to predictions from Basner's Markov model with added quadratic dependence on noise level and the nonlinear model developed in this research. A possible explanation for this result

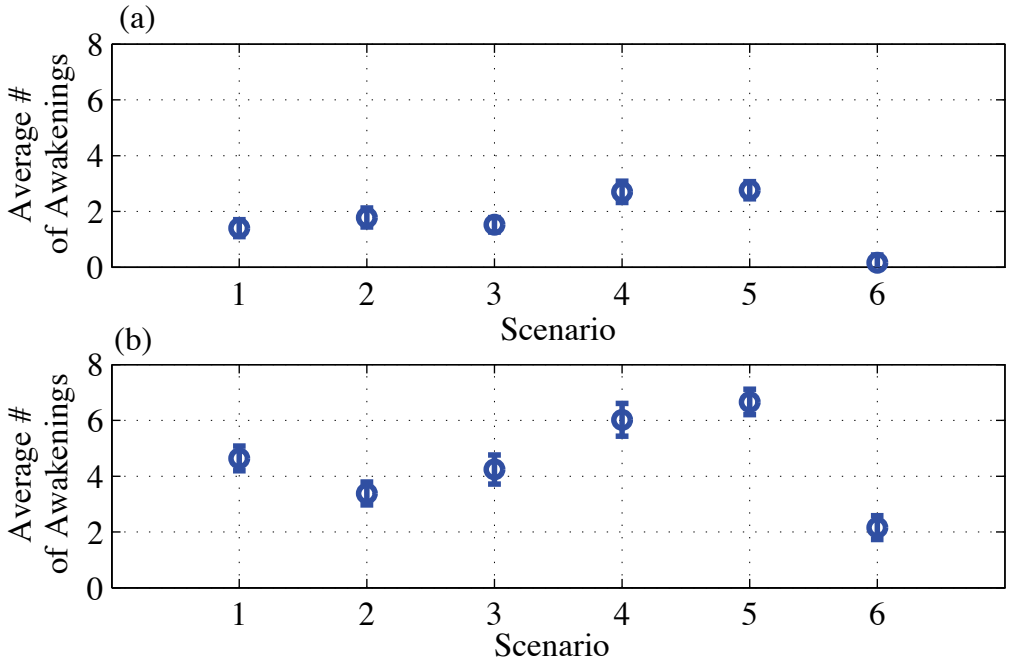

Figure 8.14. Average number of awakenings for 6 flight operation scenarios predicted using the nonlinear dynamic model for (a) grid point at (-1 nmi, 5 nmi) and (b) grid point at (1 nmi, -4 nmi). The scenarios are: (1) Peak in operations in two hours in the middle of the night, (2) an even distribution, (3) most events in the middle of the night, (4) a U-shaped distribution, (5) most events at the beginning of the night, and (6) most events occurring at the end of the night.

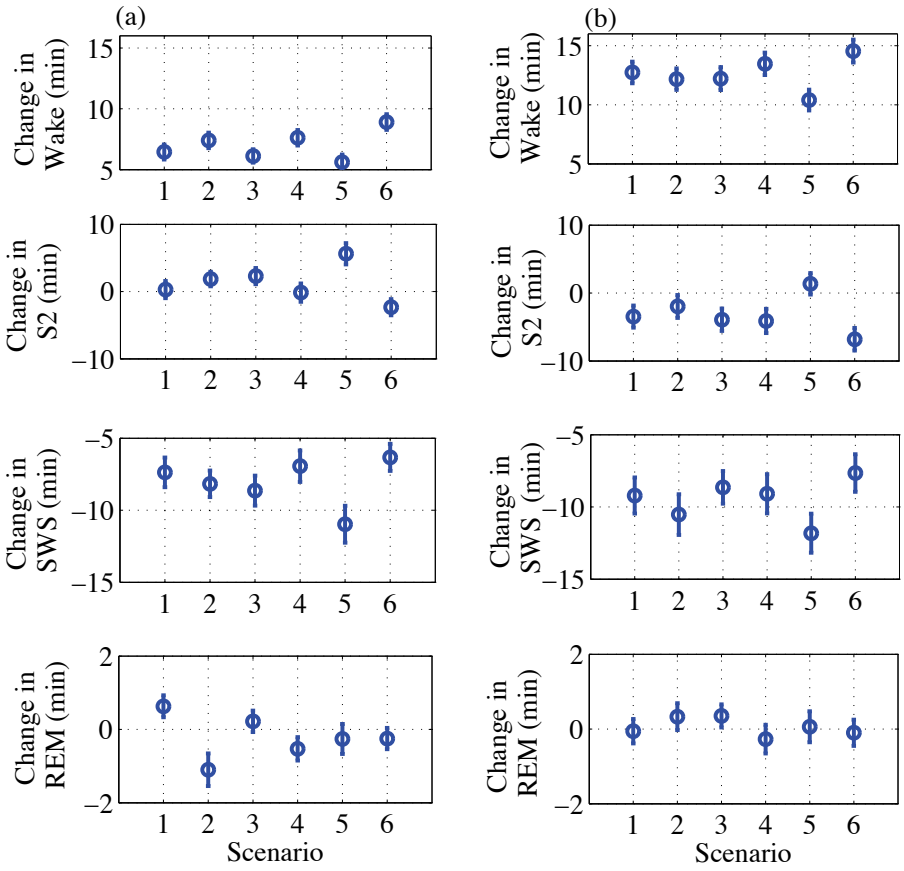

Figure 8.15. Change in sleep stage durations for the 6 flight operation scenarios predicted using the nonlinear dynamic model for (a) grid point at (-1 nmi, 5 nmi) and (b) grid point at (1 nmi, -4 nmi). The scenarios are: (1) Peak in operations in two hours in the middle of the night, (2) an even distribution, (3) most events in the middle of the night, (4) a U-shaped distribution, (5) most events at the beginning of the night, and (6) most events occurring at the end of the night.

is that the ANSI standard model does not take into account the difference between normal and noise disturbed sleep. Also, while the differences in disturbance between more events at the the beginning and more events at the end of the night scenarios appeared small for predictions calculated using both the ANSI standard model and the modified version of Basner's Markov model when translated into the number of people impacted differences were quite large for the two scenarios. Therefore, the number of people awakened by noise as well as contour size should be considered when evaluating sleep disturbance in communities.

While similar trends were found in the number of additional awakenings and the reduction in slow wave sleep calculated using the nonlinear dynamic model and the modified version of Basner's Markov model, there were differences in the predicted total duration of being awake due to noise events. For the Markov Model a noise event impacts the model predictions for 3 epochs, while for the nonlinear model the noise events can impact the predictions of sleep for a longer duration. This difference and its impact on predictions needs to be examined further. In addition, methods for increasing the computation speed of the nonlinear dynamic model need to be examined so that, in the future, it can be used to predict sleep disturbance contours.

9. SUMMARY, OUTCOMES AND RECOMMENDATIONS FOR FUTURE WORK

Nighttime aircraft noise can disturb sleep in communities, causing a decrease in rapid eye movement and slow wave sleep and an increase in the number of awakenings and time spent awake. These changes in sleep may lead to both next day and long term health effects. There have been several models developed to predict noise induced sleep disturbance. Most of the models, however, are limited because they only predict the number of awakenings and not a change in sleep structure which may be important when relating noise-induced sleep disturbance to potential health effects. A Markov model which can be used to predict changes in sleep structure has been developed by Basner (2006). However, the model does not have a noise level dependence and it has many coefficients which makes it difficult to validate due to a large amount of data being needed to produce estimates of the model parameters.

Nonlinear dynamic models have been developed to predict normal, non-noise induced sleep patterns. This type of model was examined to determine if it could be used to predict noise induced sleep disturbance. The nonlinear models have limitations: they cannot predict awakenings during REM sleep or brief awakenings during both NREM and REM sleep as observed in data from sleep studies. Approaches to modifying a nonlinear dynamic model in order to be able to predict this type of behavior was examined. This resulted in the development of a model that could predict slow wave, and slow and fast REM activity.

9.1 Outcomes of This Research

To determine how to introduce faster dynamics into the Massaquoi and McCarley model, first a sleep stage classification algorithm was developed. This algorithm includes methods for removing artifacts and for identifying specific features of polysomnography data including rapid eye movement and sleep spindles. Based on the extracted features, a sleep stage classification algorithm in which sleep stages are classified for each 1 second in time was developed. The standard method for scoring sleep is to assign a sleep stage to each 30 second epoch. The algorithm that was developed provides a more continuous evaluation of sleep stages than this standard method. While in this research 30 second epochs were used at 1 second intervals (sliding through the data), the algorithm is flexible so that shorter or longer epochs could be used and the amount of overlap of segments changed.

To predict brief awakenings during REM sleep using the Massaquoi and McCarley model (1992), a fast REM activity model was added. The occurrence of rapid eye movements, identified using the sleep stage classification algorithm, was used to classify when an individual was awake, in Tonic REM or in Phasic REM sleep. Based on this classification, the fast REM activity was modeled by using a Duffing equation with a 5th order stiffness term, undergoing periodic excitations in a region where chaotic responses are occurring. The Duffing system has 3 stable and 2 unstable equilibrium positions. When responses were in the regions of the stable equilibria sleep was classified as being in Stage Wake, Phasic REM, or Tonic REM. The unstable equilibrium position between Wake and Tonic stable equilbria is a function of the impulsive excitation in the sleep model.

To introduce aircraft noise into the model, extra impulsive excitations were added. The probability of having a non-zero excitation response to a noise event increased from its no-noise/external stimulus level with the maximum A-weighted Sound Pres-

sure Level (L_{Amax}) of the noise event. The complete nonlinear model has 5 components: fast and slow REM sleep, slow wave activity and spontaneous and aircraft-noise induced excitation models. The parameters of this model were estimated by using the 1999 UK sleep study data (Flindell et al., 2000). This model can predict similar durations of sleep stages for baseline non-noise nights as other existing sleep stage models.

To compare predictions of noise induced sleep disturbance for different models, two approaches for adding a noise level dependence to Basner's Markov model were examined. The coefficients of the three noise models were made a function of the maximum A-weighted indoor noise level during a noise event. Both a linear and quadratic dependence on noise level were examined. By using the modified version of Basner's Markov Model, with a quadratic dependence on noise level, and the nonlinear model developed in this research, changes in sleep structure were predicted for different airport noise scenarios. Both models predicted an increase in awakenings with noise level, and a decrease in time spent in slow wave sleep. However, the magnitude of these changes varied between the two models. A further refinement of the model parameters used in the nonlinear model, and further examination of the coefficients of the Markov model is still needed.

It should be noted that Basner's model was tuned using the data the he had available, the data from the DLR laboratory study. The model developed in this research was tuned to the 1999 UK study, a relatively small dataset. Therefore some differences may be due to the unique conditions in the two studies. There is clearly a need with both models to have data from more studies to make the models more generally applicable. Having emphasized the differences between the Markov and nonlinear model predictions in terms of absolute levels it should be noted that while tuned with different study data, the trends predicted agree very well with each other,

perhaps evidence that they are predicting more generally observable trends in sleep behavior.

In summary, the nonlinear dynamic model developed in this research with further refinement can be a useful tool for predicting sleep disturbance in communities around airports. One of the advantages of this type of model is that model coefficients can be related to specific physiological processes and unlike Markov models which require a large amount of data to estimate the large number of model parameters, the parameters of the nonlinear model can be estimated using data for each subject night. This perhaps will allow sleep disturbance to be able to be predicted for different subgroups of the populations such as children, elderly, and individuals with preexisting sleep problems, by estimating and using a different set of model parameters for each group.

9.2 Recommendations for Future Work

There are many areas in which research on the development of sleep disturbance models should be conducted. Suggested areas of future research are provided below.

1. *Further validation of the nonlinear model.* The nonlinear dynamic sleep model was developed based on one dataset the 1999 UK sleep study. This model should be further validated by estimating parameters using additional sleep datasets. In addition, further work should be done on validating and defining the thresholds used to score sleep stages.

2. *Incorporate additional noise characteristics into the model.* Only the maximum indoor noise level was considered in the model. However, researchers examining the effects of noise on sleep have found that the rise time of the event as well as spectral characteristics of the sound affect whether an individual will be awakened. The incorporation of these characteristics into the model through modification of the excitation term should be explored.

3. *Examine use of the model for predicting sleep in different subgroups of the population.* An advantage of the nonlinear dynamic model is that the parameters can be changed on a more intuitive basis than those of Markov sleep models. For example, as individuals age the depth of sleep lightens therefore the decay parameters for slow wave activity can be altered to reflect these changes. In addition, individuals with sleep apnea have more awakenings during the night which could potentially be modeled by increasing the rate of the excitation term. An examination of how to change the model parameters in order to predict sleep in different populations should be examined.

4. *Improve predictions of indoor noise levels.* For the airport noise simulations that were conducted, outdoor noise levels, L_{Amax} and $SELA$, were predicted and an outdoor to indoor noise attenuation of 25 dB(A) was assumed. However, one-third octave band levels can be predicted using noise prediction software, though it is computationally intensive. By using sound transmission software and housing construction data, house transfer filters could be developed and perhaps a better prediction of indoor noise levels could be obtained. Effects of house orientation and window opening would be interesting issues to explore in communities around airports and this would be possible with improved sound transmission models.

5. *Perform simulations of surveys around airports.* There are very few large aircraft noise and sleep field studies and so there is a limited number of datasets that can be used to further validate the developed models. As part of designing a future survey, simulations of the outcomes of different survey designs together with predictions of sleep disturbance from existing models for current airport operations should be completed. This will enable researchers/survey designers to determine if the resulting datasets would provide robust estimates of the parameters of existing sleep models.

LIST OF REFERENCES

LIST OF REFERENCES

P. Achermann and A. A. Borbély. Simulation of human sleep: ultradian dynamics of electroencephalographic slow-wave activity. *Journal of Biological Rhythms*, 5(2): 141–157, 1990.

P. Achermann and A. A. Borbély. Combining different models of sleep regulation. *Journal of Sleep Research*, 1:144–147, 1992.

P. Achermann, D. G. M. Beersma, and A. A. Borbély. The two-process model: Ultradian dynamics of sleep. In *Sleep 90': proceedings of the tenth European Congress on Sleep Research*, Strasbourg, France, May 1990.

P. Achermann, D. J. Dijk, D. P. Brunner, and A. A. Borbély. A model of human sleep homeostasis based on EEG slow-wave activity: Quantitative comparison of data and simulations. *Brain Research Bulletin*, 31(1-2):97–113, 1993.

R. Agarwal and J. Gotman. Computer-assisted sleep staging. *IEEE Transactions on Biomedical Engineering*, 48(12):1412–1423, 2001.

R. Agarwal, T. Takeuchi, S. Laroche, and J. Gotman. Detection of rapid-eye movement in sleep studies. *IEEE Transactions on Biomedical Engineering*, 52(8):1390–1396, 2005.

T. Åkerstedt and M. Gillberg. Subjective and objective sleepiness in the active individual. *International Journal of Neuroscience*, 52:29–37, 1990.

P. Anderer, S. Roberts, A. Schlögl, G. Gruber, G. Klösch, W. Herrmann, P. Rappelsberger, O. Filz, M. J. Barbanoj, G. Dorffner, and B. Saletu. Artifact processing in computerized analysis of sleep EEG - A review. *Neuropsychobiology*, 40(3):150–157, 1999.

G. S. Anderson and N. Miller. A pragmatic re-analysis of sleep disturbance data. In *Noise-Con 2005*, Minneapolis, Minnesota, Oct. 2005.

G. S. Anderson and N. Miller. Alternative analysis of sleep-awakening data. *Noise Control Engineering Journal*, 55(2):224–245, 2007.

ANSI. S12.9-2008, Quantities and procedures for description and measurement of environmental sound - Part 6: Methods for estimation of awakenings associated with outdoor noise events heard in homes. American National Standards Institute, 2008.

I. Bankman, V. G. Sigillito, R. A. Wise, and P. L. Smith. Feature-based detection of the K-Complex using neural networks. *IEEE Transactions on Biomedical Engineering*, 39(12):1305–1310, 1992.

M. Basner. Markov state transition models for the prediction of changes in sleep structure induced by aircraft noise. Technical report, German Aerospace Center (DLR), Institute of Aerospace Medicine, Cologne, Germany, 2006.

M. Basner. Nocturnal aircraft noise exposure increases objectively assessed daytime sleepiness. *Somnologie*, 12:110–117, 2008.

M. Basner. Arousal threshold determination in 1862: Kohlschütters measurements on the firmness of sleep. *Sleep Medicine*, 11:417–422, 2010.

M. Basner and A. Samel. Nocturnal aircraft noise effects. *Noise & Health*, 6(22): 83–93, 2004.

M. Basner and A. Samel. Effects of nocturnal aircraft noise on sleep structure. *Somnologie*, 9:84–95, 2005.

M. Basner, H. Buess, D. Elmenhorst, A. Gerlich, N. Luks, H. MaaB, L. Mawet, E. W. Müller, U. Müller, G. Plath, J. Quehl, A. Samel, M. Schulze, M. Vejvoda, and J. Wenzel. Effects of nocturnal aircraft noise, Volume 1, Executive Summary. Technical report, German Aerospace Center (DLR), Institute of Aerospace Medicine, Cologne, Germany, 2004.

M. Basner, A. Samel, and U. Isermann. Aircraft noise effects on sleep: Application of the results of a large polysomnographic field study. *Journal of the Acoustical Society of America*, 119(5):2772–2784, 2006.

M. Basner, E. M. Elmenhorst, H. Maass, U. Müller, J. Quehl, and M. Vejvoda. Single and combined effects of air, road and rail traffic noise on sleep. In *9th International Congress on Noise as a Public Health Problem (ICBEN)*, Foxwoods, Ct., July 2008a.

M. Basner, C. Glatz, B. Griefahn, T. Penzel, and A. Samel. Aircraft noise: Effects on macro- and microstructure of sleep. *Sleep Medicine*, 9:382–387, 2008b.

M. Basner, U. Müller, E. M. Elmenhorst, G. Kluge, and B. Griefahn. Aircraft noise effects on sleep: a systematic comparison of EEG awakenings and automatically detected cardiac activations. *Physiological Measurement*, 29:1089–1103, 2008c.

G. Becq, S. Charbonnier, F. Chapotot, A. Buguet, L. Bourdon, and P. Baconnier. Comparison between five classifiers for automatic scoring of human sleep recordings. *Studies in Computational Intelligence*, 4:113–127, 2005.

M. Bonnet and D. L. Arand. EEG arousal norms by age. *Journal of Clinical Sleep Medicine*, 3(3):271–274, 2007.

M. Bonnet, D. Carley, M. Carkskadon, P. Easton, C. Guilleminault, R. Harper, B. Hayes, M. Hirshkowitz, P. Ktonas, S. Keenan, M. Pressman, T. Roehrs, J. Smith, J. Walsh, S. Weber, and P. Westbrook. EEG arousals: Scoring rules and examples. *Sleep*, 15(2):173–184, 1992.

A. A. Borbély, F. Baumann, D. Brandeis, I. Strauch, and D. Lehmann. Sleep deprivation: effect on sleep stages and EEG power density in man. *Electroencephalography and Clinical Neurophysiology*, 51:483–495, 1981.

J. Born and H. L. Fehm. The neuroendocrine recovery function of sleep. *Noise & Health*, 2(7):25–37, 2000.

A. M. Boukadoum and P. Y. Ktonas. EOG-based recording and automated detection of sleep rapid eye movements: A critical review and some recommendations. *Psychophysiology*, 23(5):598–611, 1986.

A. M. Boukadoum and P. Y. Ktonas. Non-random patterns of REM occurrences during REM sleep in normal human subjects: an automated second-order study using Markovian modeling. *Electroencephalography and Clinical Neurophysiology*, 70(5):404–416, 1988.

G. Bremer, J. R. Smith, and I. Karacan. Automatic detection of the K-complex in sleep electroencephalograms. *IEEE Transactions on Bio-Medical Engineering*, 17 (4):314–323, 1970.

M. Brink and M. Basner. Determination of awakening probabilities in night time noise effects research. In *Proceedings of Euronoise 2009*, Edinburgh, Scotland, Oct. 2009.

M. Brink, C. H. Müller, and C. Schierz. Contact-free measurement of heart rate, respiration rate, and body movements during sleep. *Behavior Research Methods*, 38 (3):511–521, 2006.

M. Brink, P. Lercher, A. Eisenmann, and C. Schierz. Influence of slope of rise and event order of aircraft noise events on high resolution actimetry parameters. *Somnologie*, 12:118–128, 2008.

D. Bruck, M. Ball, I. Thomas, and V. Rouillard. How does the pitch and pattern of a signal affect auditory arousal thresholds? *Journal of Sleep Research*, 18:196–203, 2009.

D. P. Brunner, R. C. Vasko, C. S. Detka, J. P. Monahan, C. F. Reynolds III, and D. J. Kupfer. Muscle artifacts in the sleep EEG: Automated detection and effect on all-night EEG power spectra. *Journal of Sleep Research*, 5:155–164, 1996.

M. A. Carskadon and W. C. Dement. Normal human sleep: an overview. In M. H. Kryer, T. Roth, and W. C. Dement, editors, *Principles and Practice of Sleep Medicine*. Elsevier, Philadelphia, Pennsylvania, 4th edition, 2005.

N. Carter, R. Henderson, S. Lal, M. Hart, S. Booth, and S. Hunyor. Cardiovascular and autonomic response to environmental noise during sleep in night shift workers. *Sleep*, 25(4):444–451, 2002.

N. L. Carter, S. N. Hunyor, G. Crawford, D. Kelly, and A. J. M. Smith. Environmental noise and sleep, a study of arousals, cardiac arrhythmia, and urinary catecholamines. *Sleep*, 17(4):298–307, 1994.

A. Coenen. Subconscious stimulus processing recognition and processing during sleep. *Psyche*, 16(2):90–97, 2010.

J. C. Comte, M. Schatzman, P. Ravassard, P. H. Luppi, and P. A. Salin. A three states sleep-waking model. *Chaos, Solitons, Fractals*, 29:808–815, 2006.

C. Curtco, S. Sakata, S. Marguet, V. Itskov, and K. D. Harris. A simple model of cortical dynamics explains variability and state dependence of sensory response in urethane-anesthetized auditory cortex. *The Journal of Neuroscience*, 29(34):10600–10612, 2009.

M. Czisch, T. C. Wetter, C. Kaufmann, T. Pollmächer, F. Holsboer, and D. P. Auer. Altered processing of acoustic stimuli during sleep: Reduced auditory activation and visual deactivation detected by a combined fMRI/EEG study. *NeuroImage*, 16:251–258, 2002.

A. C. Da Rosa, B. Kemp, T. Paiva, F. H. Lopes da Silva, and H. A. Kamphuisen. A model-based detector of vertex waves and K-complexes in sleep electroencephalogram. *Electroencephalography and Clinical Neurophysiology*, 78(1):71–79, 1991.

T. T. Dang-Vu, S. M. McKinney, O. M. Buxton, J. M. Solet, and J. M. Ellenbogen. Spontaneous brain rhythms predict sleep stability in the face of noise. *Current Biology*, 20(15):R626–R627, 2010.

H. Davis, P. A. Davis, A. L. Loomis, E. N. Harvey, and G. Hobart. Changes in human brain potentials during the onset of sleep. *Science*, 86(2237):448–450, 1937.

J. L. DeVore. *Probability and Statistics*. Thomson, Belmont, California, 7th edition, 2008.

S. Devuyst, T. Dutoit, J. F. Didier, F. Meers, E. Stanus, P. Stenuit, and M. Kerkhofs. Automatic sleep spindle detection in patients with sleep disorders. In *Proceedings of the 28th IEEE EMBS Annual International Conference*, New York City, Aug.-Sept.3 2006.

S. Devuyst, T. Dutoit, P. Stenuit, M. Kerkhofs, and E. Stanus. Removal of ECG artifacts from EEG using a modified Independent Component Analysis approach. In *Proceedings of the 30th Annual International IEEE EMBS Conference*, Vancouver, British Columbia, Canada, Aug. 2008.

S. Devuyst, T. Dutoit, P. Stenuit, and M. Kerkhofs. Automatic K-complexes detection in sleep EEG recordings using likelihood thresholds. In *Proceedings of the 32nd Annual International Conference of the IEEE EMBS*, Buenos Aires, Argentina, Aug. 31-Sept. 4 2010.

J. Di Nisi, A. Muzet, J. Ehrhart, and J. P. Libert. Comparison of cardiovascular responses to noise during waking and sleeping in humans. *Sleep*, 13(2):108–120, 1990.

D. J. Dijk, D. G. M. Beersma, and R. H. van den Hoofdakker. All night spectral analysis of EEG sleep in young adult and middle-aged male subjects. *Neurobiology of Aging*, 10(6):677–682, 1989.

I. DiMatteo, C. R. Genovese, and R. E. Kass. Bayesian curve-fitting with free-knot splines. *Biometrika*, 88(4):1055–1071, 2001.

C. G. Diniz Behn and V. Booth. Simulating microinjection experiments in a novel model of the rat sleep-wake regulatory network. *Journal of Neurophysiology*, 103: 1937–1953, 2010.

C. G. Diniz Behn, E. N. Brown, T. E. Scammell, and N. J. Kopell. Mathematical model of network dynamics governing mouse sleep-wake behavior. *Journal of Neurophysiology*, 97:3828–3840, 2007.

J. B. Dixon, L. M. Schachter, and P. E. O'Brien. Polysomnography before and after weight loss in obese patients with severe sleep apnea. *International Journal of Obesity*, 29:1048–1054, 2005.

M. Domjan, J. W. Grau, and M. A. Krause. *The Principles of Learning and Behavior*. Wadsworth, Belmont, California, 2010.

DORA. Aircraft noise and sleep disturbance: final report. Technical Report DORA report no. 8008, Directorate of Operational Research and Analysis, Civil Aviation Authority, U.K., 1980.

T. A. Doughty, P. Davies, and A. K. Bajaj. A comparison of three techniques using steady state data to identify non-linear modal behavior of an externally excited cantilever beam. *Journal of Sound and Vibration*, 249(4):785–813, 2002.

M. Ekstedt, T. Åkerstedt, and M. Söderström. Microarousals during sleep are associated with increased levels of lipids, cortisol, and blood pressure. *Psychosomatic Medicine*, 66:925–931, 2004.

E. M. Elmenhorst and M. Basner. Fluglärmwirkungen band 5 leistung. Technical report, German Aerospace Center (DLR), Institute of Aerospace Medicine, Cologne, Germany, 2008.

U. Ermis, K. Krakow, and U. Voss. Arousal thresholds during human tonic and phasic REM sleep. *Journal of Sleep Research*, 19:400–406, 2010.

T. P. Exarchos, A. T. Tzallas, D. I. Fotiadis, S. Konitsiotis, and S. Giannopoulos. EEG transient event detection and classification using association rules. *IEEE Transactions on Information Technology in Biomedicine*, 10(3):451–457, 2006.

FAA. *Integrated Noise Model (INM) Version 7.0 User's Guide*. Federal Aviation Administration, 2007.

F. Ferrillo, S. Donadio, F. De Carli, S. Garbarino, and L. Nobili. A model-based approach to homeostatic and ultradian aspects of nocturnal sleep structure in narcolepsy. *Sleep*, 30(2):157–165, 2007.

FICAN. Effects of aviation noise on awakenings from sleep, 1997. URL http:\\www.fican.org/pdf/Effects_AviationNoise_Sleep.pdf.

FICON. Federal agency review of selected airport noise analysis issues, 1992. URL http://www.fican.org/pdf/nai-8-92.pdf.

S. Fidell, K. Pearsons, B. Tabachnick, R. Howe, L. Silvati, and D. S. Barber. Field study of noise-induced sleep disturbance. *Journal of the Acoustical Society of America*, 98(2):1025–1033, 1995.

S. Fidell, K. Pearsons, B. G. Tabachnick, and R. Howe. Effects on sleep disturbance of changes in aircraft noise near three airports. *Journal of the Acoustical Society of America*, 107(5):2535–2547, 2000.

J. M. Fields, R. G. De Jong, T. Gjestland, I. H. Flindell, R. F. S. Job, S. Kurra, P. Lercher, M. Vallet, T. Yano, R. Guski, U. Felscher-suhr, and R. Schumer. Standardized general-purpose noise reaction questions for community noise surveys research and a recommendation. *Journal of Sound and Vibration*, 242(4):641–679, 2001.

L. S. Finegold and B. Elias. A predictive model of noise induced awakenings from transportation noise sources. In *Proceedings of Internoise 2002*, Dearborn, Michigan, Aug. 2002.

L. S. Finegold, C. S. Harris, and H. E. von Gierke. Community annoyance and sleep disturbance: Updated criteria for assessing the impacts of general transportation noise on people. *Noise Control Engineering Journal*, 42(1):25–30, 1994.

R. S. Fisher and S. Cordova. EEG for beginners. In G. L. Krauss and R. S. Fisher, editors, *The John Hopkins Atlas of Digital EEG: An Interactive Training Guide*, pages 11–76. The John Hopkins University Press, Baltimore, Maryland, 2006.

I. H. Flindell, A. J. Bullmore, K. A. Robertson, N. A. Wright, C. Turner, C. L. Birch, M. Jiggins, B. F. Berry, M. Davison, and N. Dix. Aircraft noise and sleep, 1999 UK trial methodology study. Technical report, ISVR Consultancy Services, Institute of Sound and Vibration Research, University of Southampton, UK, 2000.

J. Foret, N. Touron, O. Clodoré, Benoit, and G. Bouard. Modification of sleep structure by brief forced awakenings at different times of the night. *Electroencephalography and Clinical Neurophysiology*, 75:141–147, 1990.

P. Fort, C. L. Bassetti, and P. H. Luppi. Alternating vigilance states: new insights regarding neuronal networks and mechanisms. *European Journal of Neuroscience*, 29:1741–1753, 2009.

D. J. Frey, P. Badia, and K. P. Wright Jr. Inter- and intra-individual variability in performance near the circadian nadir during sleep deprivation. *Journal of Sleep Research*, 13:305–315, 2004.

B. D. Fulcher, A. J. K. Phillips, and P. A. Robinson. Modeling the impact of impulsive stimuli on sleep-wake dynamics. *Physical Review E*, 78:051920, 2008.

K. H. Fuller, W. F. Waters, P. Binks, and T. Anderson. Generalized anxiety and sleep architecture: A polysomnographic investigation. *Sleep*, 20(5):370–376, 1997.

A. Garcés Correa, E. Laciar, H. D. Patiño, and M. E. Valentinuzzi. Artifact removal from EEG signals using adaptive filters in cascade. In *In Proceedings of the 16th Argentine Bioengineering Congress and the 5th Conference of Clinical Engineering*, 2007.

W. Gerstner and W. Kistler. *Spiking Neuron Model*. Cambridge University Press, New York, 1996.

I. S. Gopal and G. G. Haddad. Automatic detection of eye movements in REM sleep using the electrooculogram. *American Journal of Physiology*, 241(3):R217–21, 1981.

D. J. Gottlieb, N. M. Punjabi, A. B. Bewman, H. E. Resnick, S. Redline, C. M. Baldwin, and F. J. Nieto. Association of sleep time with diabetes mellitus and impaired glucose tolerance. *Archives of Internal Medicine*, 165:863–868, 2005.

J. M. A. Graham, S. A. Janssen, J. Vos, and H. M. E. Miedema. Habitual traffic noise at home reduces cardiac parasympathetic tone during sleep. *International Journal of Psychophysiology*, 72:179–186, 2009.

B. Griefahn. Long-term exposure to noise-aspects of adaptation, habituation and compensation. *Waking and Sleeping*, 1:383–386, 1977.

B. Griefahn and A. Muzet. Noise-induced sleep disturbances and their effects on health. *Journal of Sound and Vibration*, 59(1):99–106, 1978.

B. Griefahn, A. Schuemer-Kohrs, R. Schuemer, U. Moehler, and P. Mehnert. Physiological, subjective, and behavioural responses during sleep to noise from rail and road traffic. *Noise & Health*, 3(9):59–71, 2000.

B. Griefahn, A. Marks, and S. Robens. Noise emitted from road, rail, and air traffic and their effects on sleep. *Journal of Sound and Vibration*, 295:129–140, 2006.

B. Griefahn, P. Bröde, A. Marks, and M. Basner. Autonomic arousals related to traffic noise during sleep. *Sleep*, 31(4):569–577, 2008a.

B. Griefahn, S. Robens, P. Bröde, and M. Basner. The sleep disturbance index-a measure for structural alterations of sleep due to environmental influences. In *Proceedings of the 9th International Congress on Noise as a Public Health Problem (ICBEN)*, Foxwoods, Connecticut, July 2008b.

C. Guilleminault and R. Stoohs. Arousals increased respiratory efforts, blood pressure and obstructive sleep apnoea. *Journal of Sleep Research*, 4(Supplement 1): 117–124, 1995.

C. Guilleminault, V. C. Abad, P. Philip, and R. Stoohs. The effect of CNS activation versus EEG arousal during sleep on heart rate response and daytime tests. *Clinical Neurophysiology*, 117:731–739, 2006.

A. S. Haralabidis, K. Dimakopoulou, F. Vigna-Taglianti, M. Giampaolo, A. Borgini, M. L. Dudley, G. Pershagen, G. Bluhm, D. Houthuijs, W. Babisch, M. Velonakis, K. Katsouyanni, and L. Jarup. Acute effects of night-time noise exposure on blood pressure in populations living near airports. *European Heart Journal*, 29:658–664, 2008.

N. Hatzilabrou, N. Greenberg, R. J. Sclabassi, T. Carroll, R. D. Guthrie, and M. S. Scher. A comparison of conventional and matched filtering techniques for rapid eye movement detection of the newborn. *IEEE Transactions on Biomedical Engineering*, 41(10):990–995, 1994.

S. Haykin. *Adaptive Filter Theory*. Prentice Hall, Upper Saddle River, New Jersey, 3rd edition, 1996.

P. He, G. Wilson, and C. Russell. Removal of ocular artifacts from electroencephalogram by adaptive filtering. *Medical and Biological Engineering and Computing*, 42: 407–412, 2004.

J. A. Hobson, R. W. McCarley, and P. W. Wyzinski. Sleep cycle oscillation: reciprocal discharge by two brainstem neuronal groups. *Science*, 189:55–58, 1975.

A. Huss, A. Spoerri, M. Egger, and M. Röösli. Aircraft noise, air pollution, and mortality from myocardial infarction. *Epidemiology*, 21(6):829–836, 2010.

C. Iber, S. Redline, A. M. Kaplan Gilpin, S. F. Quan, L. Zhang, D. G. Gottlieb, D. Rapoport, H. Resnick, M. Sanders, and P. Smith. Polysomnography performed in the unattended home versus the attended laboratory setting, Sleep Heart Health Study Methodology. *Sleep*, 27(3):536–540, 2004.

G. Inuso, F. La Foresta, N. Mammone, and F. Carlo Morabito. Wavelet-ICA methodology for efficient artifact removal from electroencephalographic recordings. In *Proceedings of International Joint Conference on Neural Networks*, Orlando, Florida, Aug. 2007.

H. Ising and M. Ising. Chronic cortisol increases in the first half of the night caused by road traffic noise. *Noise & Health*, 4(16):13–21, 2002.

E. B. Issa and X. Wang. Altered neural responses to sounds in primate primary auditory cortex during slow-wave sleep. *The Journal of Neuroscience*, 31(8):2965–2973, 2011.

E. M. Izhikevich. Which model to use for cortical spiking neurons? *IEEE Transactions on Neural Networks*, 15(5):1063–1070, 2004.

L. Jarup, W. Babisch, D. Houthuijs, G. Pershagen, K. Katsouyanni, E. Cadum, M. L. Dudley, P. Savigny, I. Seiffert, W. Swart, O. Brugelmans, G. Bluhm, J. Selander, A. Haralabidis, K. Dimakopolou, P. Sourtzi, M. Velonakis, and F. Vigna-Taglianti. Hypertension and exposure to noise near airports: the HYENA study. *Environmental Health Perspective*, 116(3):329–333, 2008.

M. W. Johns. A new method for measuring daytime sleepiness: The Epworth Sleepiness Scale. *Sleep*, 14(6):540–545, 1991.

T. P. Jung, S. Makeig, C. Humphries, T. W. Lee, M. J. McKeown, V. Iragui, and T. J. Sejnowski. Removing electroencephalographic artifacts by blind source separation. *Psychophysiology*, 37:163–178, 2000.

A. Kales and J. Kales. Evaluation, diagnosis, and treatment of clinical conditions related to sleep. *Journal of the American Medical Association*, 213(13):2229–2235, 1970.

B. Kemp and H. A. Kamphuisen. Simulation of human hypnograms using a Markov chain model. *Sleep*, 9(3):405–414, 1986.

T. Kobayashi. Sleep Package Model. *Computers and Industrial Engineering*, 27: 385–388, 1994.

M. Kuroiwa, P. Xin, S. Suzuki, Y. Saszawa, and T. Kawada. Habituation of sleep to road traffic noise observed not by polygraphy but by perception. *Journal of Sound and Vibration*, 250(1):101–106, 2002.

H. Kuwahara, H. Higashi, Y. Mizuki, S. Matsunari, M. Tanaka, and K. Inanaga. Automatic real-time analysis of human sleep stages by an interval histogram method. *Electroencephalography and Clinical Neurophysiology*, 70:220–229, 1988.

R. E. Lawder. A proposed mathematical model for sleep patterning. *Journal of Biomedical Engineering*, 6:63–69, 1984.

T. E. LeVere, R. T. Bartus, and F. D. Hart. The relation between time of presentation and the sleep disturbing effects of nocturnally occurring jet aircraft flyovers. Technical Report NASA/ CR-2036, National Aeronautics and Space Administration, Washington, D. C., 1972.

T. E. LeVere, R. T. Bartus, G. W. Morlock, and F. D. Hart. Arousal from sleep: Responsiveness to different auditory frequencies equated for loudness. *Physiological Psychology*, 10(3):53–57, 1973.

T. E. LeVere, G. W. Morlock, L. P. Thomas, and F. Hart. Arousal from sleep: The differential effect of frequencies equated for loudness. *Physiological Psychology*, 12 (4):573–582, 1974.

T. E. Levere, N. Davis, J. Mills, E. H. Berger, and W. F. Reiter. Arousal from sleep: The effects of the rise-time of auditory stimuli. *Physiological Psychology*, 4 (2):213–218, 1976.

G. X. Li and F. C. Moon. Criteria for chaos of a three-well potential oscillator with homoclinic and heteroclinic orbits. *Journal of Sound and Vibration*, 136(1):17–34, 1990.

R. R. Llinas and D. Pare. Of dreaming and wakefulness. *Neuroscience*, 44(3):521–535, 1991.

C. C. Lo, L. A. Nunes Amaral, S. Havlin, P. C. Ivanov, T. Penzel, J. H. Peter, and H. E. Stanley. Dynamics of sleep-wake transitions during sleep. *Europhysics Letters*, 57(5):625–631, 2002.

J. S. Loredo, S. Ancoli-Israel, and J. E. Dimsdale. Sleep quality and blood pressure dipping in obstructive sleep apnea. *American Journal of Hypertension*, 14(9):887–892, 2001.

J. S. Loredo, R. Nelesen, S. Ancoli-Israel, and J. E. Dimsdale. Sleep quality and blood pressure dipping in normal adults. *Sleep*, 27(6):1097–1103, 2004.

J. Lu, D. Sherman, M. Devor, and C. B. Saper. A putative flip-flop switch for control of REM sleep. *Nature*, 44(1):589–594, 2006.

J. S. Lukas. Effects of aircraft noise on human sleep. *American Industrial Hygiene Association Journal*, 33(5):298–303, 1972.

G. Luz, D. Nykaza, C. Stewart, and L. Pater. Use of actimeters to determine awakenings by sounds of large guns. *Noise Control Engineering Journal*, 56(3): 211–217, 2008.

H. MaaB and M. Basner. Effects of nocturnal aircraft noise: Volume 3 stress hormones. Technical report, German Aerospace Center (DLR), Institute of Aerospace Medicine, 2006.

A. Marks and B. Griefahn. Railway noise - its effects on sleep, mood, subjective sleep quality, and performance. *Somnologie*, 9:68–75, 2005.

A. Marks and B. Griefahn. Associations between noise sensitivity and sleep, subjectively evaluated sleep quality, annoyance, and performance after exposure to nocturnal traffic noise. *Noise & Health*, 9:1–7, 2007.

A. Marks, B. Griefahn, and M. Basner. Event-related awakenings caused by nocturnal transportation noise. *Noise Control Engineering Journal*, 56(1):52–62, 2008.

S. Massaquoi and R. McCarley. Resetting the REM sleep oscillator. In *Sleep 90': proceedings of the tenth European Congress on Sleep Research*, Strasbourg, France, May 1990.

S. G. Massaquoi and R. W. McCarley. Extension of the limit cycle reciprocal interaction model of REM cycle control. An integrated sleep control model. *Journal of Sleep Research*, 1:138–143, 1992.

R. W. McCarley. Neurobiology of REM and NREM sleep. *Sleep Medicine*, 8:302–330, 2007.

R. W. McCarley and J. A. Hobson. Single neuron activity in cat gigantocellular tegmental field: Selectivity of discharge in desynchronized sleep. *Science*, 174:1250–1252, 1971.

R. W. McCarley and J. A. Hobson. Neuronal excitability modulation over the sleep cycle: A structure and mathematical model. *Science*, 189:58–60, 1975.

R. W. McCarley and S. G. Massaquoi. A limit cycle mathematical model of the REM sleep oscillator system. *American Journal of Physiology- Regulatory, Integrative, and Comparative Physiology*, 251:1011–1029, 1986.

R. J. McPartland, D. J. Kupfer, and F. G. Foster. Rapid eye movement analyzer. *Electroencephalography and Clinical Neurophysiology*, 34(3):317–320, 1973.

W. C. Meecham and H. G. Smith. Effects of jet aircraft noise on mental hospital admissions. *British Journal of Audiology*, 11(3):81–85, 1977.

H. M. E. Miedema and C. G. M. Oudshoorn. Annoyance from transportation noise: Relationships with exposure metrics DNL and DENL and their confidence intervals. *Environmental Health Perspectives*, 109(4):409–416, 2001.

H. M. E. Miedema, W. Passchier-Vermeer, and H. Vos. Elements for a position paper on night-time transportation noise and sleep disturbance. Technical Report TNO report 2002-59, TNO, Delft, Nederland, 2002.

F. C. Moon and P. J. Holmes. A magnetoelastic strange attractor. *Journal of Sound and Vibration*, 65(2):275–296, 1979.

NIH. National sleep disorders research plan. Technical report, National Institute of Health, 2003. URL http://www.nhlbi.nih.gov/health/prof/sleep/res_plan/sleep-rplan.pdf.

E. Öhrström. Effects of low levels of road traffic noise during the night: A laboratory study on number of events, maximum noise levels, and noise sensitivity. *Journal of Sound and Vibration*, 179(4):603–615, 1995.

E. Öhrström and M. Björkman. Effects of noise-disturbed sleep-A laboratory study on habituation and subjective noise sensitivity. *Journal of Sound and Vibration*, 122 (2):277–290, 1988.

E. Öhrström, E. Hadzibajramovic, M. Holmes, and H. Svensson. Effects of road traffic noise on sleep: studies on children and adults. *Journal of Environmental Psychology*, 26:116–126, 2006.

E. Olbrich and P. Achermann. Analysis of oscillatory patterns in the human sleep EEG using a novel detection algorithm. *Journal of Sleep Research*, 14:337–346, 2005.

E. Olbrich and P. Achermann. Analysis of the temporal organization of sleep spindles in the human sleep EEG using a phenomenological modeling approach. *Journal of Biological Physiology*, 34:341–349, 2008.

J. B. Ollerhead, C. J. Jones, R. E. Cadoux, A. Woodley, B. J. Atkinson, J. A. Horne, F. Pankhurst, L. Reyner, K. I. Hume, F. Van, I. D. Watson, A. Diamond, P. Egger, D. Holmes, and J. McKean. Report of a field study of aircraft noise and sleep disturbance. Technical report, Department of Safety, Environment, and Engineering, Civil Aviation Authority, UK, 1992.

I. Oswald, A. M. Taylor, and M. Treisman. Discriminative responses to stimulation during human sleep. *Brain*, 83:440–453, 1960.

W. Passchier-Vermeer, H. Vos, J. H. M. Steenbekkers, F. D. van der Ploeg, and K. Froothuis-Oudshoorn. Sleep disturbance and aircraft noise exposure: Exposure-effect relationships. Technical report, TNO, Leiden, the Netherlands, 2002.

K. S. Pearsons, D. S. Barber, B. G. Tabachnick, and S. Fidell. Predicting noise-induced sleep disturbance. *Journal of the Acoustical Society of America*, 97(1): 331–338, 1995.

A. J. K. Phillips and P. A. Robinson. A quantitative model of sleep-wake dynamics based on the physiology of the brainstem ascending arousal system. *Journal of Biological Rhythms*, 22(2):167–179, 2007.

A. J. K. Phillips and P. A. Robinson. Sleep deprivation in a quantitative physiologically based model of the ascending arousal system. *Journal of Theoretical Biology*, 255:413–423, 2008.

C. M. Portas, K. Karakow, P. Allen, O. Josephs, J. L. Armony, and C. D. Frith. Auditory processing across the sleep-wake cycle: simultaneous EEG and fMRI monitoring in humans. *Neuron*, 28(3):991–999, 2000.

J. Quehl and M. Basner. Annoyance from nocturnal aircraft noise exposure: Laboratory and field-specific dose-response curves. *Journal of Environmental Psychology*, 26(2):127–140, 2006.

L. B. Ray, S. M. Fogel, C. T. Smith, and K. R. Peters. Validating an automated sleep spindle detection algorithm using an individualized approach. *Journal of Sleep Research*, 19(2):374–378, 2010.

A. Rechtschaffen, P. Hauri, and M. Zeitlin. Auditory awakening thresholds in REM and NREM sleep stages. *Perceptual and Motor Skills*, 22(3):927–942, 1966.

A. Rechtschaffen, A. Kales, R. J. Berger, W. C. Dement, A. Jacobson, L. C. Johnson, M. Jouvet, L. J. Monroe, I. Oswald, H. P. Roffwarg, B. Roth, and R. D. Walter. *A Manual of Standardized Terminology, Techniques and Scoring System for Sleep Stages of Human Subjects*. Public Health Service, Washington, D. C., 1968.

M. J. Rempe, J. Best, and D. Terman. A mathematical model of the sleep/wake cycle. *Journal of Mathematical Biology*, 60(5):615–644, 2010.

A. Sadeh, R. Gruber, and A. Raviv. Sleep, neurobehavioral functions, and behavior problems in school-age children. *Child Development*, 73(2):405–417, 2002.

M. Sallinen, J. Kaartinen, and H. Lyytine. Processing of auditory stimuli during tonic and phasic periods of REM sleep as revealed by event-related brain potentials. *Journal of Sleep Research*, 5(4):220–228, 1996.

S. Sanei and J. A. Chambers. *EEG Signal Processing*. John Wiley & Sons, West Sussex, England, 2007.

C. B. Saper, T. C. Chou, and T. E. Scammell. The sleep switch: Hypothalamic control of sleep and wakefulness. *TRENDS in Neurosciences*, 24(12):726–731, 2001.

M. Saremi, J. Grenéche, A. Bonnefond, O. Rohmer, A. Eschenlauer, and P. Tassi. Effects of nocturnal railway noise on sleep fragmentation in young and middle-aged subjects as a function of type of train and sound level. *International Journal of Psychophysiology*, 70(3):184–191, 2008.

S. A. Schapkin, M. Falkenstein, A. Marks, and B. Griefahn. After effects of noise-induced sleep disturbances on inhibitory functions. *Life Sciences*, 78(10):1135–1142, 2006.

P. Schimcek, J. Zeitlhofer, P. Anderer, and B. Saletu. Automatic sleep spindle detection procedure: aspects of reliability and validity. *Clinical Electroencephalography*, 25:26–29, 1994.

A. Schlögl, P. Anderer, M. J. Barbanoj, G. Klösch, G. Gruber, J. L. Lorenzo, O. Filz, M. Koivuluoma, I. Rezek, S. J. Roberts, A. Värri, P. Rappelsberger, G. Pfurtscheller, and G. Dorffner. Artifact processing of the sleep EEG in the SIESTA Project. In *Proceedings of the EMBEC*, pages 1644–1645, Edinburgh, Scotland, 1999.

D. Schreckenberg, G. Thomann, and M. Basner. FFI and FNI-two effect based aircraft noise indices at Frankfurt Airport. In *Proceedings of Euronoise 2009*, Edinburgh, Scotland, Oct. 2009.

D. Schrenkenberg, M. Meis, C. Kahl, C. Peschel, and T. Eikmann. Aircraft noise and quality of life around Frankfurt Airport. *International Journal of Environmental Research and Public Health*, 7(9):3382–3405, 2010.

T. J. Schultz. Synthesis of social surveys on noise annoyance. *Journal of the Acoustical Society of America*, 64:377–405, 1978.

J. M. Seigl. Normal human sleep: an overview. In M. H. Kryer, T. Roth, and W. C. Dement, editors, *Principles and Practice of Sleep Medicine*. Elsevier, Philadelphia, Pennsylvania, 4th edition, 2005.

M. H. Silber, S. Ancoli-Israel, M. H. Bonnet, S. Chokroverty, M. M. Grigg-Damberger, M. Hirshkowitz, S. Kapen, S. A. Keenan, M. H. Kryger, T. Penzel, M. R. Pressman, and C. Iber. The visual scoring of sleep in adults. *Journal of Clinical Sleep Medicine*, 3(2):121–135, 2007.

A. Skånberg and E. Öhrström. Sleep disturbances from road traffic noise: A comparison between laboratory and field settings. *Journal of Sound and Vibration*, 290 (1-2):3–16, 2006.

J. R. Smith, M. J. Cronin, and I. Karacan. A multichannel hybrid system for rapid eye movement detection (REM detection). *Computers and Biomedical Research*, 4 (3):275–290, 1971.

M. Sørensen, M. Hvidberg, Z. J. Andersen, R. B. Nordsborg, K. G. Lillelund, J. Jakobsen, A. Tjønneland, K. Overvad, and O. Raaschou-Nielsen. Road traffic noise and stroke: a prospective cohort study. *European Heart Journal*, 32(6):737–744, 2011.

K. Spiegel, R. Leproult, and E. Van Cauter. Impact of sleep debt on metabolic and endocrine function. *The Lancet*, 354:1435–1439, 1999.

K. Spiegel, E. Tasali, P. Penev, and E. Van Cauter. Brief communication: Sleep curtailment in healthy young men is associated with decreased leptin levels, elevated ghrelin levels, and increased hunger and appetite. *Annals of Internal Medicine*, 141 (11):846–850, 2004.

M. Spreng. Noise induced nocturnal cortisol secretion and tolerable overhead flights. *Noise & Health*, 6(22):35–47, 2004.

W. H. Spriggs. *Essentials of Polysomnography: A Training Guide and Reference for Sleep Technicians*. Sleep Ed, LLC, Carrollton, Texas, 2008.

R. Srebro. The Duffing oscillator: a model for the neuronal groups comprising the transient evoked potential. *Electroencephalography and Clinical Neurophysiology*, 96: 561–573, 1995.

S. A. Stansfeld and M. P. Matheson. Noise pollution: non-auditory effects on health. *British Medical Bulletin*, 68:243–257, 2003.

S. A. Stansfeld, C. Clark, R. M. Cameron, T. Alfred, J. Head, M. M. Haines, I. van Kamp, E. van Kempen, and I. Lopez-Barrio. Aircraft and road traffic noise exposure and children's mental health. *Journal of Environmental Psychology*, 29:203–207, 2009.

N. J. Stevenson, M. Mesbah, G. B. Boylan, P. B. Colditz, and B. Boashash. Nonlinear model of newborn EEG. *Annals of Biomedical Engineering*, 38(9):3010–3021, 2010.

J. V. Stone. Independent component analysis: an introduction. *TRENDS in Cognitive Sciences*, 6(2):203–207, 2009.

S. H. Strogatz. *Nonlinear Dynamics and Chaos, With Applications to Physics, Biology, Chemistry, and Engineering*. Westview Press, Cambridge, Massachusetts, 2000.

S. Taheri, L. Lin, D. Austin, T. Young, and E. Mignot. Short sleep duration is associated with reduced Leptin, elevated Ghrelin, and increased Body Mass Index. *Public Library of Science Medicine*, 1(3):210–217, 2004.

E. Tasali, R. Leproult, D. A. Ehrmann, and E. Van Cauter. Slow-wave sleep and the risk of type 2 diabetes in humans. *Proceedings of the National Academy of Science*, 105(3):1044–1049, 2008.

G. J. Thiessen. Disturbance of sleep by noise. *Journal of the Acoustical Society of America*, 64(1):216–222, 1978.

J. Trammell and P. Ktonas. A simple nonlinear deterministic process may generate the timing of rapid eye movements during human REM sleep. In *Proceedings of the 1st International IEEE EMBS Conference on Neural Engineering*, Capri Island, Italy, Oct. 2003.

M. Vallet, J. M. Gagneux, V. Blanchet, B. Favre, and G. Labiale. Long term sleep disturbance due to traffic noise. *Journal of Sound and Vibration*, 90(2):173–191, 1983.

M. van de Velde, G. van Erp, and P. J. M. Cluitmans. Detection of muscle artifact in the normal human awake EEG. *Electroencephalography and Clinical Neurophysiology*, 107(2):149–158, 1998.

P. Venkatakrishnan, S. Sangeetha, and R. Sukanesh. Detection of sleep spindles from electroencephalogram (EEG) signals using auto-recursive (AR) model. In *First International Conference on Emerging Trends in Engineering and Technology*, July 2008.

R. Vigário, J. Särelä, V. Jousmäki, M. Hämäläinen, and E. Oja. Independent Component Approach to the analysis of EEG and MEG recordings. *IEEE Transactions on Biomedical Engineering*, 47(5):589–593, 2000.

J. Virkkala, J. Hasan, A. Värri, S.-L. Himanen, and M. Härmä. The use of two-channel electro-oculography in automatic detection of unintentional sleep onset. *Journal of Neuroscience Methods*, 163(1):137–144, 2007.

G. L. Wallstrom, R. E. Kass, A. Miller, J. F. Cohn, and N. A. Fox. Automatic correction of ocular artifacts in the EEG: a comparison of regression-based and component-based methods. *International Journal of Psychophysiology*, 53:105–119, 2004.

R. Wehrle, C. Kaufmann, T. C. Wetter, F. Holsboer, D. P. Auer, T. Pollmächer, and M. Czisch. Functional microstates within human REM sleep: first evidence from fMRI of a thalamocortical network specific for phasic REM periods. *European Journal of Neuroscience*, 25:863–871, 2007.

R. A. Wever. Mathematical models of circadian one and multi-oscillator systems. In G. A. Carpenter, editor, *Lectures on Mathematics in the Life Sciences Volume 19. Some Mathematical Questions in Biology, Circadian rhythms*. American Mathematical Society, Providence, Rhode Island, 1980.

WHO. Night noise guidelines for Europe. Technical report, 2009. URL http://www.euro.who.int/__data/assets/pdf_file/0017/43316/E92845.pdf.

R. T. Wilkinson and K. B. Campbell. Effects of traffic noise on quality of sleep: Assessment by EEG, subjective report, or performance the next day. *Journal of the Acoustical Society of America*, 75(2):468–475, 1984.

R. L. Williams, I. Karacan, and C. J. Hursch. *Electroencephalography (EEG) of human sleep: Clinical applications*. Wiley, New York, 1974.

M. C. K. Yang and C. J. Hursch. The use of a Semi-Markov model for describing sleep patterns. *Biometrics*, 29(4):667–676, 1973.

E. C. Zeeman. Brain modelling. *Lecture Notes in Mathematics*, 525:367–372, 1976.

H. Zeplin, C. S. McDonald, and G. K. Zammit. Effects of age on auditory awakening thresholds. *Journal of Gerontology*, 39(3):294–300, 1984.

W. K. Zung, T. H. Naylor, D. T. Gianturco, and W. P. Wilson. Computer simulation of sleep EEG patterns with a markov chain model. *Recent Advances in Biological Psychiatry*, 8:335–355, 1965.

APPENDICES

Appendix A. Noise Metrics

The following are noise metrics that were used in this report.

Cumulative Metrics:

1. Day Night Average Sound Pressure Level (DNL or L_{dn}):

$$DNL = 10log_{10}\left[\frac{1}{24}\left(\int_{7:00}^{22:00}\frac{{p_A}^2}{{p_o}^2}dt + 10\int_{22:00}^{7:00}\frac{{p_A}^2}{{p_o}^2}dt\right)\right], \tag{A.1}$$

   p_A is the A-weighted sound pressure level.

2. L_{night}:

$$L_{night} = 10log_{10}\left[\frac{1}{8}\left(\int_{23:00}^{7:00}\frac{{p_A}^2}{{p_o}^2}dt\right)\right]. \tag{A.2}$$

Single Event Metrics:

1. L_{Amax}: Maximum A-weighted noise level.

2. $SELA$: Sound Exposure Level:

$$SELA = 10log_{10}\left(\int_{t_1}^{t_2}\frac{{p_A}^2}{{p_o}^2}dt\right), \tag{A.3}$$

   where t_1 and t_2 are defined in Figure A.1.

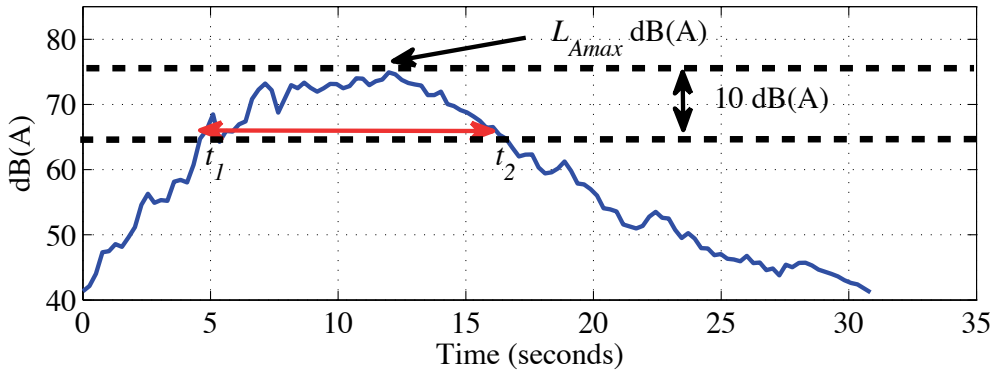

Figure A.1. A-weighted noise level (dB(A)) of aircraft noise event. The maximum noise level (L_{Amax}) and the portion of the sound used to calculate the Sound Exposure Level ($SELA$) (red arrow) are indicated.

Appendix B. Laboratory and Field Studies

This appendix contains tables which list the survey data available for laboratory and field studies on the effects of aircraft noise on sleep.

Table B.1. Laboratory studies-sleep measurements.

Study	# of People	am/pm Surveys	Behav. Awake	Acti-metry	Motility-Other	Polysom-nography
Basner et al. (2004)	128	X		X		X
Basner et al. (2008)	72	X		X		X
Carter et al. (1994)	9					X
Carter et al. (2002)	9					X
Dinisi et al. (1990)	20				X	X
Flindell et al. (2000)	9	X		X		X
Levere et al. (1972)	6					X (EEG)
Levere & Davis (1977)	12	X				X (EEG, EOG)
Lukas & Kryter (1970)	6		X			X (EEG, EOG)
Lukas et al. (1971)	12	X	X			X
Lukas & Dobbs (1972)	8	X	X			X
Marks et al. (2008)	24	X				X

Table B.2. Laboratory studies-additional measurements.

Study	# of People	ECG	Blood Pressure	Hormone Levels, etc	Sleepiness (Objective)	Performance
Basner et al. (2004)	128	X		X	PST (24)	X
Basner et al. (2008)	72	X		X		X
Carter et al. (1994)	9	X		X		
Carter et al. (2002)	9	X	X			
Dinisi et al. (1990)	20	X				
Flindell et al. (2000)	9	X			MSLT	X
Levere et al. (1972)	6					X
Levere & Davis (1977)	12					
Lukas & Kryter (1970)	6					
Lukas et al. (1971)	12					
Lukas & Dobbs (1972)	8					
Marks et al. (2008)	24	X				X

Table B.3. Field studies-sleep measurements.

Study	Location	# of People	Social Survey	am/pm Survey	Behav. Awake	Acti-metry
Basner et al. (2004)	Cologne-Bonn	64		X		X
Borksy (1976)	JFK	1500	X			
Brink et al. (2008)	Zurich	60		X		
DORA (1980)	Heathrow Gatwick	4153	X			
Fidell & Jones (1975)	LAX	1417	X			
Fidell et al. (1995)	Castle Air Force Base LAX	85		X	X	
Fidell et al. (2000)	Stapleton Denver	77		X	X	X
Fidell et al. (2000)	DeKalb-Peachtree	22		X	X	X
Flindell et al. (2000)	Manchester	18		X		X
Haral-abidis et al. (2008)	Athens Arlanda Heathrow Malpensa	140	X			
Ollerhead et al. (1992) Hume et al. (2003)	Heathrow Gatwick Stansted Manchester	400-Act. 46-Poly. 1636-Social Survey	X			X
Passchier-Vermeer et al. (2002)	Schiphol	418		X	X	X

Table B.4. Field studies-additional sleep measurements.

Study	Motility-Other	Polysomnography	ECG	Blood Pressure	Hormone Levels, etc	Performance
Basner et al. (2004)		X	X		X	X
Borksy (1976)						
Brink et al. (2008)	X					
DORA (1980)						
Fidell & Jones (1975)						
Fidell et al. (1995)						
Fidell et al. (2000)						
Fidell et al. (2000)						
Flindell et al. (2000)		X	X			X
Haral-abidis et al. (2008)				X		
Ollerhead et al. (1992) Hume et al. (2003)		X				
Passchier-Vermeer et al. (2002)						X

Table B.5. Field studies-noise measurements.

Surveys	Metrics-# of Locations	Measurement of Outdoor Noise	Measurement of Indoor Noise	Noise Metrics
Basner et al. (2004)	64	X	X	A-weighted time histories
Borksy (1976)	1500			
Brink et al. (2008)	60		X	
DORA (1980)	29	X		L_{Aeq}, L_{Amax}, *SELA*, "number above" and "level exceeded"
Fidell & Jones (1975)	3	X		L_{dn}
Fidell et al. (1995)	45	X	X	A-weighted time histories, L_{Amax}, *SELA*
Fidell et al. (2000)	38	X	X	A-weighted time histories, L_{Amax}, *SELA*
Fidell et al. (2000)	12	X	X	A-weighted time histories, L_{Amax}, *SELA*
Flindell et al. (2000)	18	X	X	1-sec A-weighted time histories
Haralabidis et al. (2008)	140		X	A-weighted time histories
Ollerhead et al. (1992) Hume et al. (2003)	8	X		L_{Amax}, *SELA*, Hourly L_{Aeq}
Passchier-Vermeer et al. (2002)	418	X	X	1 sec A-weighted time histories

Table B.6. Field studies-additional noise measurements.

Surveys	Noise Recordings (e.g. .wav)	Flight Operations Data
Basner et al. (2004)	X	
Borksy (1976)		Distance from airport
Brink et al. (2008)	Played recordings in each subject's home	
DORA (1980)		Flight paths, Location of surveyed areas
Fidell & Jones (1975)		
Fidell et al. (1995)		
Fidell et al. (2000)		
Fidell et al. (2000)		
Flindell et al. (2000)	10 sec .wav recordings for 4 locations	List of aircraft by time of arrival and departure
Haralabidis et al. (2008)	X	
Ollerhead et al. (1992) Hume et al. (2003)		Maps indicating flight paths and study locations
Passchier-Vermeer et al. (2002)		Obtained data from flight track monitoring system indicating aircraft noise events

Appendix C. Coefficients of Basner's Markov Model

Table C.1. Coefficients for Basner's Four Markov Models (2006).

Coefficient/s_j	s_i	Baseline	Noise 1	Noise 2	Noise 3
Intercept	0	1.2144	2.3013	0.7674	0.9691
	1	-0.4702	-0.4125	-0.4415	-0.3739
	3	-3.6542	-4.0295	-3.8388	-3.8809
	4	-6.2984	-12.6277	-14.1409	-5.0150
	5	-1.3717	-1.0818	-1.6914	-2.2264
S1	0	-2.7472	-1.8124	-2.9919	-2.8770
	1	0.2838	0.4352	0.0584	-0.3877
	3	-2.5433	-0.4452	-9.0011	-1.9712
	4	-6.9807	-1.1678	-1.6087	-8.7818
	5	-1.3017	-1.5643	-0.0583	-1.2233
S2	0	-4.8576	-3.5524	-3.8725	-4.6710
	1	-4.6860	-3.3554	-4.2785	-4.7750
	3	0.8986	1.6156	0.8650	1.2007
	4	0.2586	4.8135	6.9155	-3.3496
	5	-3.0316	-3.3679	-2.1935	-1.9309
S3	0	-3.4514	-2.4651	-2.9214	-3.2425
	1	-6.7253	-3.6566	-4.7870	-4.9466
	3	5.7615	5.9772	4.9008	5.8730
	4	6.5807	12.6037	12.5687	4.9879
	5	-3.8353	-4.9858	-5.2357	-2.6269
S4	0	-0.7784	-0.4093	-1.0691	-0.5785
	1	-3.5858	-2.5576	-3.5520	-9.9189
	3	6.5302	6.5707	5.6143	6.9644
	4	11.5460	17.2381	17.5938	10.6345
	5	-3.0085	-10.3476	-10.8294	-8.2248
REM	0	-1.0655	-0.9722	-0.8380	-1.0694
	1	-1.2599	-0.3825	-1.2592	-1.5366
	3	-2.0445	-9.1235	-8.4853	-8.2782
	4	-6.1652	8.0627	-1.0821	-6.7936
	5	4.5398	3.9654	4.6170	4.9946
Transition	0	0.000452	-0.00025	-0.00004	0.000401
	1	-0.00026	-0.00030	-0.0013	0.000277
	3	-0.00147	-0.00135	-0.00125	-0.00190
	4	-0.00273	-0.00187	-0.00150	-0.00285
	5	0.000869	0.000337	0.000822	0.000896

Appendix D. Model Parameters Estimated for Each Subject

The model coefficient values listed in the following tables were calculated for 76 subject nights from the 1999 UK sleep study (Flindell et al., 2000). The methods used to calculate these coefficients are discussed in Chapter 7. For the slow REM sleep model, the coefficients were not calculated if the REM period defined in the original dataset was less than 5 minutes in duration or if the NREM period before or after a REM period was less than 15 minutes. Also the coefficients of the slow REM model were not calculated if the duration of the prior NREM period or the duration of the REM period was considered an outlier, which was defined as:

$$Lower\ Outliers < 25th\ percentile - 1.5(75th\ percentile - 25th\ percentile), \quad \text{(D.1)}$$

$$Upper\ Outliers > 75th\ percentile + 1.5(75th\ percentile - 25th\ percentile), \quad \text{(D.2)}$$

here the 75th and 25th percentiles were calculated based on all NREM or REM periods during the night for all 76 subject nights. The subject nights for which the coefficients were not calculated are indicated by gray/blank entries in the following tables.

Table D.1. Estimated parameters for Process S and SWA models for field subjects 1 through 12 in the 1999 UK study.

Subject	Night	S_o	gc	SWA_L	rc	fc	SWA_o
1	2	3.3365	0.0391	0.2384	0.1064	4.1062	1.5094
1	4	4.1180	0.0497	0.1725	0.2324	1.4241	1.0915
2	1	3.3673	0.0248	0.1094	0.4977	3.2499	0.8288
2	3	3.7074	0.0304	0.1411	0.3090	1.1422	1.1137
2	4	3.5105	0.0307	0.1501	0.3532	3.0706	0.9375
3	3	3.8628	0.0306	0.2220	0.2636	1.0852	0.9697
3	4	2.8551	0.0265	0.1641	0.8013	1.9962	0.5251
6	1	4.3358	0.0442	0.1103	0.2309	1.7047	1.0080
6	2	4.0398	0.0441	0.1010	0.2930	2.1427	1.1029
6	3	5.4750	0.0544	0.1075	0.1779	2.5459	1.1783
8	4	2.9164	0.0240	0.2467	0.3148	1.1791	0.9923
9	1	4.2406	0.0350	0.1879	0.2398	1.0777	0.9125
9	3	5.8348	0.0461	0.1513	0.2348	1.4101	0.6386
9	4	4.9060	0.0410	0.1532	0.3571	1.7851	0.6713
10	0	3.0004	0.0155	0.1751	0.5186	2.3834	0.7325
10	1	3.3971	0.0251	0.1691	0.3169	4.6552	1.0097
10	3	3.0035	0.0175	0.1817	0.4090	2.8392	0.8222
12	0	2.6382	0.0084	0.2029	0.6562	1.7541	0.6065
12	1	3.5689	0.0268	0.2300	0.2968	1.9174	0.6616
12	2	3.6195	0.0290	0.2220	0.3064	2.4094	0.6035
12	3	3.2195	0.0272	0.2102	0.3388	0.8993	0.8086
12	4	3.2789	0.0346	0.2216	0.5200	1.6621	0.6518

Table D.2. Estimated parameters for Process S and SWA Models for field subjects 13 through 18 in the 1999 UK study.

Subject	Night	S_o	gc	SWA_L	rc	fc	SWA_o
13	1	3.6619	0.0391	0.2099	0.3742	2.3962	0.9962
13	2	3.2038	0.0368	0.2127	0.6463	1.4571	1.0797
13	3	3.6877	0.0396	0.1749	0.4544	2.6606	0.9135
13	4	3.6919	0.0384	0.2346	0.3296	1.7203	0.8148
14	0	3.1813	0.0191	0.2252	0.5168	1.3479	0.4149
14	1	3.6535	0.0378	0.2081	0.3027	2.4437	0.4495
14	3	3.4100	0.0349	0.1948	0.4929	3.1263	0.4518
14	4	3.5922	0.0260	0.2182	0.4196	1.3223	0.3784
15	0	4.0728	0.0448	0.1920	0.2650	1.6454	0.8416
15	1	3.4671	0.0380	0.1849	0.4188	0.8472	0.8556
15	2	5.1299	0.0526	0.1491	0.2146	2.2660	1.0116
15	3	3.5554	0.0316	0.1909	0.3501	2.1493	0.8968
15	4	2.8822	0.0237	0.2099	0.3902	2.8141	0.9586
16	2	3.7999	0.0511	0.1885	0.3281	2.4172	0.6750
16	3	2.5900	0.0132	0.2515	0.4534	2.3607	0.7207
16	4	4.1062	0.0329	0.2400	0.4131	1.1499	0.6461
17	2	3.1666	0.0085	0.1984	0.6205	2.5602	0.1973
17	4	3.5993	0.0111	0.1903	0.2904	1.8888	0.7340
18	0	3.9134	0.0293	0.1481	0.5266	0.9661	0.3428
18	1	4.0829	0.0277	0.1769	0.4777	1.5498	0.6446
18	3	3.8975	0.0259	0.1720	0.5255	1.1675	1.3014

Table D.3. Estimated parameters to define the random noise term $n(t)$ for field subjects 1 through 12 in the 1999 UK study.

Subject	Night	mean	std. dev	skew	kurtosis
1	2	-0.0137	0.2052	0.6424	3.1467
1	4	-0.0162	0.2376	0.7350	3.2077
2	1	-0.0249	0.3184	0.5866	3.0170
2	3	-0.0233	0.3076	0.5346	3.0197
2	4	-0.0270	0.3529	0.6954	3.0037
3	3	-0.0155	0.2619	0.6994	3.0650
3	4	-0.0183	0.2516	0.5569	3.1028
6	1	-0.0148	0.2358	0.4925	2.8902
6	2	-0.0163	0.2421	0.3801	2.7713
6	3	-0.0169	0.2414	0.4245	2.7671
8	4	-0.0131	0.2039	0.5482	3.0342
9	1	-0.0159	0.2125	0.4902	2.9049
9	3	-0.0153	0.2424	0.5413	3.0465
9	4	-0.0221	0.2908	0.4896	2.8882
10	0	-0.0166	0.2699	0.4735	3.0702
10	1	-0.0217	0.3305	0.5821	3.0052
10	3	-0.0231	0.2896	0.5359	2.9910
12	0	-0.0115	0.1989	0.4082	2.9315
12	1	-0.0126	0.2057	0.3081	2.8874
12	2	-0.0109	0.1999	0.4820	3.0699
12	3	-0.0127	0.2363	0.4677	2.8805
12	4	-0.0152	0.2335	0.5244	3.0019

Table D.4. Estimated parameters to define the random noise term $n(t)$ for field subjects 13 through 18 in the 1999 UK study.

Subject	Night	mean	std. dev	skew	kurtosis
13	1	-0.0150	0.2333	0.4922	2.7396
13	2	-0.0126	0.2398	0.4638	2.7454
13	3	-0.0147	0.2262	0.4192	2.6815
13	4	-0.0117	0.2101	0.4216	2.7749
14	0	-0.0194	0.2653	0.6029	3.1969
14	1	-0.0188	0.2689	0.5385	3.2537
14	3	-0.0176	0.2690	0.6065	3.2100
14	4	-0.0171	0.2430	0.6088	3.3874
15	0	-0.0176	0.2389	0.5988	3.2506
15	1	-0.0148	0.2298	0.6067	2.9735
15	2	-0.0165	0.2028	0.5076	3.0437
15	3	-0.0144	0.2079	0.5460	2.9984
15	4	-0.0181	0.2209	0.6691	3.2496
16	2	-0.0152	0.2316	0.4356	2.7253
16	3	-0.0094	0.2039	0.3273	2.8323
16	4	-0.0110	0.2145	0.2778	2.7091
17	2	-0.0123	0.1875	0.3502	2.8473
17	4	-0.0113	0.1788	0.2057	2.7489
18	0	-0.0129	0.2000	0.4971	2.8332
18	1	-0.0187	0.2207	0.5803	3.1554
18	3	-0.0132	0.2158	0.5883	3.1180

Table D.5. Estimated Slow REM parameters for the 1st REM period for field subjects 1 through 12 in the 1999 UK study.

Subject	Night	a	b	c	d
1	2	0.9449	0.3452	1.8029	2.2423
1	4	0.4772	0.3628	0.4370	1.0013
2	1				
2	3				
2	4	0.5625	0.3310	0.5577	1.2185
3	3				
3	4				
6	1	0.6171	0.3082	2.6341	2.1381
6	2	0.7395	0.2693	3.5046	2.1494
6	3	0.5880	0.5230	3.2306	2.8342
8	4	0.6009	0.3204	1.7271	1.9237
9	1	0.5630	0.2888	0.9491	1.4708
9	3	0.4375	0.3988	1.6747	1.8993
9	4	0.4624	0.2723	0.2468	0.7767
10	0	0.5033	0.2472	1.0223	1.4101
10	1	0.7957	0.2963	4.4418	2.4240
10	3				
12	0	0.5003	0.2333	1.4639	1.4902
12	1	0.5599	0.3768	0.4808	1.1372
12	2	0.4742	0.3416	0.3624	0.8917
12	3	0.4671	0.3713	4.0835	2.3865
12	4				

Table D.6. Estimated Slow REM parameters for the 1st REM period for field subjects 13 through 18 in the 1999 UK study.

Subject	Night	a	b	c	d
13	1	0.8421	0.4053	1.3973	2.1578
13	2	0.3383	0.4697	2.9938	2.9428
13	3	0.6519	0.4009	1.3782	1.9353
13	4	0.5565	0.4542	1.5234	2.0760
14	0	0.4277	0.3275	1.0295	1.5120
14	1	0.5209	0.3732	0.8963	1.4355
14	3	0.6248	0.3588	1.7732	2.0457
14	4	0.4921	0.3768	0.9242	1.5152
15	0				
15	1	0.4890	0.4508	2.9965	2.4623
15	2	0.4987	0.3260	2.5135	2.0515
15	3	0.4328	0.3804	0.5348	1.0644
15	4				
16	2	0.5231	0.5728	4.9164	3.2492
16	3	0.5326	0.5202	1.2638	1.9961
16	4	0.6534	0.4220	2.8619	2.6845
17	2	0.4584	0.3948	2.1441	2.1096
17	4	0.4532	0.2789	0.3634	0.8962
18	0	0.4601	0.3255	1.6773	1.7843
18	1	0.4294	0.2975	0.9734	1.4024
18	3	0.5304	0.4369	1.0966	1.8001

Table D.7. Estimated Slow REM parameters for the 2nd REM period for field subjects 1 through 12 in the 1999 UK study.

Subject	Night	a	b	c	d
1	2	0.4639	0.3865	0.5274	1.0631
1	4	0.5053	0.3594	1.9105	1.9666
2	1	0.4896	0.4300	0.8211	1.4968
2	3	0.4815	0.3023	0.5093	1.0836
2	4	0.4277	0.2928	1.0524	1.4569
3	3	0.3494	0.2807	0.6846	1.1034
3	4	0.4522	0.2536	1.0486	1.3399
6	1	0.4283	0.4861	3.2037	3.1510
6	2	0.3507	0.3839	0.9261	1.3689
6	3	0.6365	0.3903	1.0005	1.7083
8	4	0.5400	0.3777	4.9061	2.5620
9	1				
9	3	0.4857	0.2791	0.3239	0.9093
9	4	0.3462	0.3166	0.6968	1.1381
10	0	0.3200	0.2705	0.6440	1.0248
10	1	0.3870	0.3070	0.9110	1.3715
10	3	0.4808	0.4389	0.4637	0.9781
12	0	0.3189	0.3230	1.2159	1.4351
12	1				
12	2	0.4674	0.3754	0.2581	0.7168
12	3				
12	4				

Table D.8. Estimated Slow REM parameters for the 2nd REM period for field subjects 13 through 18 in the 1999 UK study.

Subject	Night	a	b	c	d
13	1	0.5208	0.4153	0.6243	1.2152
13	2				
13	3	0.5909	0.3677	2.7721	2.3193
13	4	0.5863	0.3894	0.2723	0.8640
14	0	0.4264	0.3666	0.5073	1.0169
14	1	0.4901	0.4151	0.5836	1.1526
14	3	0.4566	0.4687	0.8856	1.5078
14	4	0.4850	0.4171	0.6355	1.2381
15	0	0.4898	0.5628	2.7293	2.6201
15	1	0.5081	0.2515	0.2453	0.8591
15	2	0.5007	0.4217	0.1873	0.5431
15	3	0.4853	0.3430	0.3609	0.9168
15	4	0.3844	0.3957	0.3694	0.7949
16	2	0.5862	0.2872	0.1222	0.8035
16	3	0.7002	0.3297	0.1092	0.5507
16	4	0.5370	0.4100	0.7989	1.4283
17	2	0.5171	0.3613	1.2800	1.7625
17	4	0.3584	0.3965	0.8833	1.3490
18	0	0.4221	0.4101	0.5928	1.1745
18	1	0.3666	0.2230	0.2092	0.6277
18	3	0.5499	0.3413	0.3794	1.0031

Table D.9. Estimated Slow REM parameters for the 3rd REM period for field subjects 1 through 12 in the 1999 UK study.

Subject	Night	a	b	c	d
1	2	0.5024	0.3216	1.1445	1.5797
1	4	0.4838	0.5494	0.6685	1.2813
2	1	0.5188	0.3152	0.2316	0.8083
2	3	0.4390	0.5583	0.4880	0.9656
2	4	0.4011	0.4044	1.7710	1.9035
3	3	0.4550	0.3972	4.6822	2.9365
3	4				
6	1	0.7139	0.4861	3.2037	3.1510
6	2	0.4969	0.4907	1.1780	3.1510
6	3	0.5158	0.5850	0.9091	1.6064
8	4	0.4733	0.4081	1.4409	1.8836
9	1				
9	3	0.3599	0.2662	0.4348	0.8829
9	4	0.4198	0.3390	0.3032	0.7564
10	0	0.5402	0.5777	0.1713	0.4179
10	1	0.3928	0.4597	0.9503	1.4718
10	3	0.6591	0.4520	0.1129	0.4489
12	0	0.4552	0.3867	0.2471	0.6599
12	1	0.4861	0.4889	1.9929	2.2783
12	2	0.4854	0.3978	0.6604	1.2595
12	3				
12	4				

Table D.10. Estimated Slow REM parameters for the 3rd REM period for field subjects 13 through 18 in the 1999 UK study.

Subject	Night	a	b	c	d
13	1	0.5238	0.4283	1.0469	1.7118
13	2	0.6365	0.4470	3.4673	2.7505
13	3	0.4666	0.3557	0.7078	1.2666
13	4	0.5455	0.4493	2.3287	2.3778
14	0	0.5051	0.4106	0.2837	0.7724
14	1	0.5639	0.4553	0.3234	0.8716
14	3	0.6588	0.5353	0.3121	0.9028
14	4				
15	0	0.6721	0.4306	0.3627	1.1717
15	1	0.3238	0.2679	0.4875	0.8953
15	2	0.5598	0.4507	0.3937	1.0072
15	3	0.5276	0.6923	0.4838	0.9810
15	4	0.5040	0.4025	0.8526	1.4848
16	2	0.3968	0.3456	1.5555	1.7050
16	3	0.4699	0.4098	2.1466	2.1424
16	4	0.4970	0.2984	0.3987	0.9866
17	2	0.5683	0.5020	0.1770	0.5425
17	4	0.5104	0.4287	0.6854	1.3078
18	0	0.5262	0.4634	0.9469	1.6672
18	1	0.3623	0.3685	0.1945	0.4621
18	3	0.4293	0.3853	0.8116	1.4171

Table D.11. Estimated Slow REM parameters for the 4th REM period for field subjects 1 through 12 in the 1999 UK study.

Subject	Night	a	b	c	d
1	2	0.5365	0.5782	0.2852	0.6619
1	4	1.5974	1.3901	0.1178	0.2581
2	1	0.6074	0.7519	0.3061	0.6471
2	3	1.4069	1.3761	0.1261	0.3670
2	4	0.8437	0.7795	0.1388	0.4083
3	3	0.8604	1.1212	0.3128	0.6724
3	4				
6	1	0.6818	0.3391	0.1062	0.5235
6	2	0.5887	0.3292	0.4522	1.2172
6	3	0.7326	0.3834	0.8000	1.6670
8	4	0.5739	0.6394	0.6444	1.3707
9	1				
9	3	0.3905	0.4391	0.3334	0.7305
9	4	0.5724	1.5681	1.2130	1.7177
10	0				
10	1	0.5912	0.4784	0.7260	1.4171
10	3	0.8150	0.8238	0.3115	0.7617
12	0	0.7859	1.0489	0.3869	0.8025
12	1	0.6698	0.3620	0.1179	0.5445
12	2	0.5553	0.6585	2.5723	2.8309
12	3	0.7427	0.5116	0.4340	1.1898
12	4				

Table D.12. Estimated Slow REM parameters for the 4th REM period for field subjects 13 through 18 in the 1999 UK study.

Subject	Night	a	b	c	d
13	1	0.5669	0.4338	1.0256	1.6158
13	2	0.6722	0.6984	0.5466	1.2074
13	3	0.4981	0.5578	3.3427	3.3730
13	4	0.6880	0.4682	0.1152	0.4618
14	0	0.8844	1.0687	0.2996	0.6810
14	1	0.6790	0.5767	0.2644	0.7689
14	3	0.6432	0.3055	0.6329	1.4333
14	4				
15	0	0.5792	0.6659	2.1312	2.6890
15	1	0.4194	0.7760	3.5629	2.6521
15	2	0.7735	1.1726	0.6910	1.3673
15	3	0.8922	0.5190	0.6672	1.6873
15	4				
16	2	1.1560	1.1883	0.1378	0.1548
16	3	0.5448	0.4312	0.4498	1.0866
16	4				
17	2	0.6413	0.5223	1.2624	2.0347
17	4	0.5594	0.3957	0.2866	0.8331
18	0	0.8106	0.6671	0.1257	0.4598
18	1				
18	3	0.5416	0.4163	0.2068	0.6370

Table D.13. Estimated parameters for Process S and SWA Models for laboratory subjects in the 1999 UK study.

Subject	Night	S_o	gc	SWA_L	rc	fc	SWA_o
19	0	4.4617	0.0388	0.1322	0.2723	2.7529	0.7880
19	1	4.1486	0.0416	0.1389	0.5287	2.3165	0.6207
19	2	4.4169	0.0377	0.1574	0.3119	1.8867	0.7717
20	1	3.7485	0.0301	0.1414	0.2021	1.2187	0.7005
20	2	4.4947	0.0510	0.1266	0.3502	1.9782	0.6344
20	3	4.5684	0.0447	0.1118	0.3991	0.9658	1.0292
22	0	3.6723	0.0302	0.1618	0.2413	0.8112	0.8331
22	1	2.7767	0.0224	0.1888	0.5033	0.6205	1.0756
22	2	2.9903	0.0215	0.1799	0.4356	3.9335	0.5538
22	3	3.3267	0.0247	0.1887	0.2465	0.5896	1.4638
22	4	3.2060	0.0299	0.1781	0.3031	1.4033	1.1598
23	0	4.3522	0.0437	0.1360	0.2274	1.5741	0.5255
23	1	3.6144	0.0427	0.1253	0.5919	3.0516	0.5897
23	2	3.5923	0.0458	0.1170	0.4904	3.2262	0.9388
23	3	3.9107	0.0403	0.1123	0.4474	0.7768	0.7866
23	4	4.2102	0.0408	0.0962	0.4243	5.2869	0.1287
24	1	3.7697	0.0262	0.1946	0.3005	1.2354	0.9240
24	2	3.6909	0.0287	0.1616	0.3345	1.2877	0.7526
24	3	3.5164	0.0242	0.1131	0.1927	2.1170	1.0128
24	4	3.3937	0.0310	0.1446	0.3861	2.5985	0.7584
25	0	4.4544	0.0408	0.1317	0.3577	3.0195	0.5270
25	1	5.5164	0.0423	0.1339	0.3528	1.8326	0.3762
25	3	4.1590	0.0326	0.1568	0.3428	1.7633	0.5745
25	4	4.6178	0.0388	0.1379	0.3817	4.4222	0.5808
26	0	4.1647	0.0367	0.2180	0.3898	1.8732	0.8575
26	1	3.5370	0.0251	0.1832	0.5734	2.5480	0.2611
26	2	3.5335	0.0148	0.2155	0.4978	3.5402	0.6858
26	3	3.0433	0.0285	0.2277	0.5752	1.0266	0.5940
26	4	3.3089	0.0247	0.1842	0.8444	3.5710	0.5459
27	0	3.7023	0.0310	0.1469	0.1939	2.1031	1.3816
27	1	4.2429	0.0291	0.1901	0.5101	2.4893	0.3781
27	2	3.6894	0.0174	0.1578	0.7144	3.8975	0.6864
27	3	2.2853	0.0092	0.1519	0.5768	1.3976	1.3098

Table D.14. Estimated parameters to define the random noise term $n(t)$ for laboratory subjects in the 1999 UK study.

Subject	Night	mean	std. dev	skew	kurtosis
19	0	-0.0230	0.2976	0.4820	2.9347
19	1	-0.0238	0.3001	0.4651	3.0426
19	2	-0.0223	0.3166	0.7243	3.4013
20	1	-0.0248	0.3499	0.7557	3.2273
20	2	-0.0208	0.3163	0.6404	2.9809
20	3	-0.0282	0.3209	0.7196	3.2341
22	0	-0.0102	0.1855	0.3313	2.5732
22	1	-0.0122	0.2177	0.4288	2.6868
22	2	-0.0139	0.2222	0.3567	2.7088
22	3	-0.0089	0.2127	0.3329	2.5741
22	4	-0.0126	0.1957	0.3300	2.6127
23	0	-0.0230	0.2794	0.6314	3.2467
23	1	-0.0270	0.3284	0.6696	3.2777
23	2	-0.0264	0.3022	0.7096	3.3291
23	3	-0.0269	0.3437	0.7923	3.4239
23	4	-0.0259	0.3180	0.6423	3.3163
24	1	-0.0215	0.2784	0.5800	3.2364
24	2	-0.0209	0.2496	0.7014	3.3164
24	3	-0.0246	0.2742	0.5689	3.1053
24	4	-0.0183	0.2503	0.6000	3.1454
25	0	-0.0153	0.2173	0.4594	3.1641
25	1	-0.0179	0.2804	0.4747	2.9093
25	3	-0.0153	0.2127	0.5792	3.0931
25	4	-0.0148	0.2390	0.4520	2.9289
26	0	-0.0138	0.2104	0.6281	3.2015
26	1	-0.0168	0.2368	0.6540	3.1220
26	2	-0.0135	0.2158	0.5218	2.8605
26	3	-0.0119	0.1976	0.3841	2.7699
26	4	-0.0180	0.2549	0.5501	2.9491
27	0	-0.0156	0.2358	0.4369	2.8233
27	1	-0.0206	0.2284	0.4893	2.7561
27	2	-0.0200	0.2304	0.4844	2.8232
27	3	-0.0157	0.2285	0.4956	2.8772

Table D.15. Estimated Slow REM parameters for the 1st REM period for laboratory subjects in the 1999 UK study.

Subject	Night	a	b	c	d
19	0				
19	1	0.4251	0.2834	4.9021	2.2987
19	2	0.3810	0.3050	1.0263	1.3982
20	1	0.6702	0.3544	0.9204	1.6302
20	2	0.7062	0.5900	0.1642	0.5507
20	3	0.6909	0.4573	0.3386	1.0201
22	0	0.6138	0.3478	1.1979	1.6893
22	1	0.9176	0.2900	4.8776	2.3368
22	2	0.7329	0.3431	4.3607	2.6913
22	3	0.4388	0.2721	0.1291	0.5678
22	4	0.7147	0.2939	0.7556	1.5869
23	0	0.4287	0.4356	2.5031	2.2213
23	1				
23	2	0.6862	0.4797	4.3969	3.0872
23	3	0.4092	0.5104	1.0667	1.6152
23	4	0.6191	0.3796	2.6691	2.5219
24	1	0.3248	0.3053	0.6152	1.0414
24	2				
24	3	0.3725	0.3171	1.0875	1.4275
24	4	0.3869	0.3413	2.1844	1.8916
25	0	0.5445	0.3723	2.8765	2.3358
25	1	0.4892	0.4575	1.4841	1.9746
25	3	0.4685	0.3327	1.5071	1.8612
25	4	0.6223	0.2788	1.5787	1.7070
26	0	0.3708	0.3830	1.7241	1.7961
26	1	0.4198	0.3258	3.5515	1.9850
26	2				
26	3	0.4386	0.3382	1.7017	1.8136
26	4				
27	0	0.6900	0.3382	2.0799	2.1056
27	1				
27	2	0.5655	0.3170	1.3695	1.7208
27	3	0.7115	0.4085	0.4487	1.3780

Table D.16. Estimated Slow REM parameters for the 2nd REM period for laboratory subjects in the 1999 UK study.

Subject	Night	a	b	c	d
19	0	0.4803	0.5197	0.3091	0.6831
19	1	0.3598	0.3574	1.1256	1.4724
19	2	0.3997	0.3644	0.5559	1.0828
20	1	0.4260	0.2717	0.3975	0.9515
20	2	0.7553	0.4345	0.8170	1.7184
20	3	0.5803	0.3985	0.3900	1.0402
22	0	0.4607	0.4267	1.3724	1.8195
22	1	0.3668	0.5099	0.9374	1.4428
22	2	0.5261	0.7963	4.1544	3.5468
22	3	0.3817	0.4728	1.9004	2.0365
22	4	0.4082	0.4221	0.4460	0.9360
23	0	0.6101	0.4355	2.8321	2.7324
23	1	0.3572	0.2965	0.7228	1.1619
23	2	0.6739	0.5253	2.2173	2.7709
23	3	0.6715	0.3244	1.0515	1.6653
23	4	0.5010	0.4570	1.7549	2.1579
24	1	0.4336	0.4467	2.2907	2.2103
24	2	0.5105	0.3927	1.3382	1.8843
24	3	0.4776	0.3814	2.9425	2.2768
24	4	0.4261	0.3919	1.1084	1.5847
25	0	0.4851	0.4419	1.0678	1.7222
25	1	0.5728	0.3633	1.0387	1.5875
25	3	0.4326	0.4155	0.8186	1.4586
25	4	0.3923	0.3724	1.7375	1.8288
26	0	0.4667	0.2680	0.2915	0.8435
26	1	0.4088	0.2678	0.5056	1.0000
26	2	0.3176	0.2458	0.6736	1.0591
26	3	0.4307	0.3001	0.6203	1.1292
26	4	0.2989	0.4336	0.7549	1.1672
27	0	0.4469	0.3773	0.4208	0.9390
27	1	0.4478	0.4120	0.4503	0.9404
27	2				
27	3	0.5702	0.5707	3.3406	3.4079

Table D.17. Estimated Slow REM parameters for the 3rd REM period for laboratory subjects in the 1999 UK study.

Subject	Night	a	b	c	d
19	0	0.6687	0.4552	0.3896	1.1010
19	1	0.4728	0.3570	0.3457	0.8511
19	2	0.4754	0.4595	0.6974	1.3590
20	1	0.3470	0.4226	0.9595	1.4112
20	2	0.5526	0.3769	1.1329	1.6898
20	3	0.5821	0.5023	0.2380	0.7116
22	0				
22	1	0.6749	0.3394	1.3436	1.8864
22	2	0.8796	0.4257	0.3223	1.3819
22	3	0.6144	0.4661	0.4351	1.0741
22	4	0.5689	0.4450	0.4569	1.1015
23	0	0.5458	0.3444	0.4666	1.1157
23	1	0.4042	0.4423	0.5583	1.0675
23	2	0.6268	0.3094	0.6703	1.4387
23	3	0.4075	0.3986	0.8956	1.4221
23	4	0.5821	0.4232	1.0106	1.6091
24	1	0.5238	0.2789	0.2633	0.8962
24	2	0.5222	0.5068	0.5811	1.2142
24	3	0.5527	0.5264	0.6560	1.2955
24	4	0.5049	0.3868	0.3160	0.8776
25	0	0.5605	0.3765	0.5711	1.2564
25	1	0.4855	0.3871	0.4313	0.9964
25	3	0.5264	0.3732	0.6560	1.2955
25	4	0.4878	0.4818	0.8249	1.5370
26	0				
26	1				
26	2	0.6989	1.1090	0.2242	0.4263
26	3	0.4499	0.5123	0.3603	0.7970
26	4	0.6328	0.6036	0.4991	1.0923
27	0	0.5763	0.5844	4.0785	3.1609
27	1	0.5280	0.4658	1.5061	2.1693
27	2				
27	3	0.7172	0.3840	1.1155	1.8699

Table D.18. Estimated Slow REM parameters for the 4th REM period for laboratory subjects in the 1999 UK study.

Subject	Night	a	b	c	d
19	0				
19	1				
19	2	0.6152	0.5341	0.6383	1.3189
20	1	0.5484	0.3193	1.1088	1.5594
20	2	0.5387	0.4948	0.3856	0.9102
20	3	0.7437	0.8210	0.6442	1.4124
22	0	0.6091	0.5014	2.0878	2.6806
22	1	0.5382	1.0653	0.7443	1.3323
22	2	0.6858	0.5499	0.1414	0.5037
22	3	0.5855	0.3806	0.1708	0.6939
22	4	0.7367	0.6174	0.1708	0.5800
23	0	0.5867	0.5784	0.2321	0.5851
23	1				
23	2	0.3950	0.4652	1.0138	1.5328
23	3	0.6093	0.4891	3.8592	2.9005
23	4	0.5175	0.3944	0.8351	1.4474
24	1	0.4008	0.8642	1.2226	1.6379
24	2	0.6070	0.3593	0.2406	0.9023
24	3	0.6052	0.3211	0.1749	0.8150
24	4	0.5982	0.4042	3.5296	2.6082
25	0	0.4848	0.4690	0.9139	1.6335
25	1	0.4930	0.3682	0.3855	0.9550
25	3	0.5087	0.4269	0.4168	0.9627
25	4	0.6791	0.5020	0.115	0.5144
26	0	0.9384	0.8990	0.4220	1.0837
26	1				
26	2				
26	3	0.6516	0.4208	0.3062	0.9689
26	4				
27	0	0.7471	0.6266	0.9356	1.8275
27	1	0.6651	0.5636	0.3960	1.0266
27	2	0.8620	0.4098	1.3385	2.1424
27	3	0.4858	0.4788	1.3242	1.8655

Appendix E. Range for Nonlinear Model Parameters Estimated for Each Subject

Table E.1. Range of estimated parameter values for Process S and SWA Models for all field subject nights in the 1999 UK study.

	Range min to max
S_o	2.5900 to 5.8348
gc	0.0084 to 0.0544
SWA_L	0.1010 to 0.2515
rc	0.1064 to 0.8013
fc	0.8472 to 4.6552
SWA_o	0.1973 to 1.5094

Table E.2. Range of estimated parameter values for $n(t)$ for all field subject nights in the 1999 UK study.

	Range min to max
mean	-0.0094 to -0.0270
standard deviation	0.1788 to 0.3529
skew	0.2057 to 0.7350
kurtosis	2.6815 to 3.3874

Table E.3. Range of estimated parameter values for the Slow REM model for all field subject nights in the 1999 UK study.

REM Period	a min to max	b min to max	c min to max	d min to max
1	0.3383 to 0.9449	0.2333 to 0.5728	0.2468 to 4.9164	0.7767 to 3.2492
2	0.3189 to 0.7002	0.2230 to 0.5628	0.1092 to 4.9061	0.5431 to 3.1510
3	0.3238 to 0.7139	0.2662 to 0.6923	0.1129 to 4.6822	0.4179 to 3.1510
4	0.3905 to 1.5974	0.3055 to 1.5681	0.1062 to 3.5629	0.1548 to 3.3730

Table E.4. Range of estimated parameter values for Process S and SWA Models for all laboratory subject nights in the 1999 UK study.

	Range min to max
S_o	2.2853 to 5.5164
gc	0.0092 to 0.0510
SWA_L	0.0962 to 0.2277
rc	0.1927 to 0.8444
fc	0.5896 to 5.2869
SWA_o	0.1287 to 1.4638

Table E.5. Range of estimated parameter values for $n(t)$ for all laboratory subject nights in the 1999 UK study.

	Range min to max
mean	-0.0089 to -0.0282
standard deviation	0.1788 to 0.3529
skew	0.2057 to 0.7923
kurtosis	2.5732 to 3.4239

Table E.6. Range of estimated parameter values for the Slow REM model for all laboratory subject nights in the 1999 UK study.

REM Period	a min to max	b min to max	c min to max	d min to max
1	0.3248 to 0.9176	0.2721 to 0.5900	0.1291 to 4.9021	0.5507 to 3.0872
2	0.2986 to 0.7553	0.2458 to 0.7963	0.2915 to 4.1544	0.6831 to 3.5468
3	0.3470 to 0.8796	0.2789 to 1.1090	0.2242 to 4.0785	0.4263 to 3.1609
4	0.3950 to 0.9384	0.3193 to 1.0653	0.1115 to 3.8592	0.5037 to 2.9005

Appendix F. Equations and Coefficients of Nonlinear Dynamic Models

F.1 Massaquoi and McCarley Model

The Massaquoi and McCarley model (1992) has 4 main components. The first part of the model is the reciprocal interaction REM model. The equation for REM promoting neuron activity is,

$$\dot{X} = a(X)S_1(X)X - b(X)XY, \tag{F.1}$$

and the equation for REM inhibiting neuron activity is,

$$\dot{Y} = -cY + d_{circ}S_2(Y)(X + E)Y, \tag{F.2}$$

where,

$$d_{circ} = 0.975(1 + 0.125sin(0.0467 + 2.3)), \tag{F.3}$$

and E is defined in Equation F.11. The equations for the coefficients of the REM model are,

$$a(X) = 2 - 1.8\left(1 - \frac{1}{1 + e^{-4(X-0.5)}}\right), \tag{F.4}$$

$$b(X) = \frac{2}{1 + e^{-80(X-0.1)}}, \tag{F.5}$$

$$S_1(X) = 1 - 1.4\left(\frac{1}{1 + e^{-0.8(X-2.5)}}\right) + 0.167, \tag{F.6}$$

$$S_2(Y) = 1 - 1.5\left(\frac{1}{1 + e^{-20(Y-2)}}\right). \tag{F.7}$$

The equations for the Process S and SWA models are:

$$\dot{SWA} = rc\, SWA(1 - SWA/SWA_{max}) + SWA\, n(t), \tag{F.8}$$

and

$$\dot{S} = -gc\, SWA + rs(1 - S), \tag{F.9}$$

where SWA_{max} is defined as,

$$SWA_{max} = max(S(1 - 0.95\ min(X^4 + E/2, 1.0)), 0.05), \tag{F.10}$$

and $n(t)$ is a uniformly distributed random noise signal. The excitation term E in the above equations is filtered Poisson noise (N) which has an exponentially distributed arrival time, and uniformly distributed amplitude and duration, the equation for E is,

$$\dot{E} = N - kE. \tag{F.11}$$

Sleep stages during the night are scored according to the following rules:

1. If X >1.4 score as stage REM,
2. If SWA <0.1 and E >0.5 score as Wake,
3. Else score as NREM sleep.

The values of the model parameters are in Table F.1. An example of the output of the model is shown in Figure F.1.

F.2 The Nonlinear Model Developed as Part of This Research.

The following are the equations for the modified version of the Massaquoi and McCarley model that was developed as part of this research. The equations used for the slow wave activity model are,

$$\dot{S} = -gc\, SWA, \tag{F.12}$$

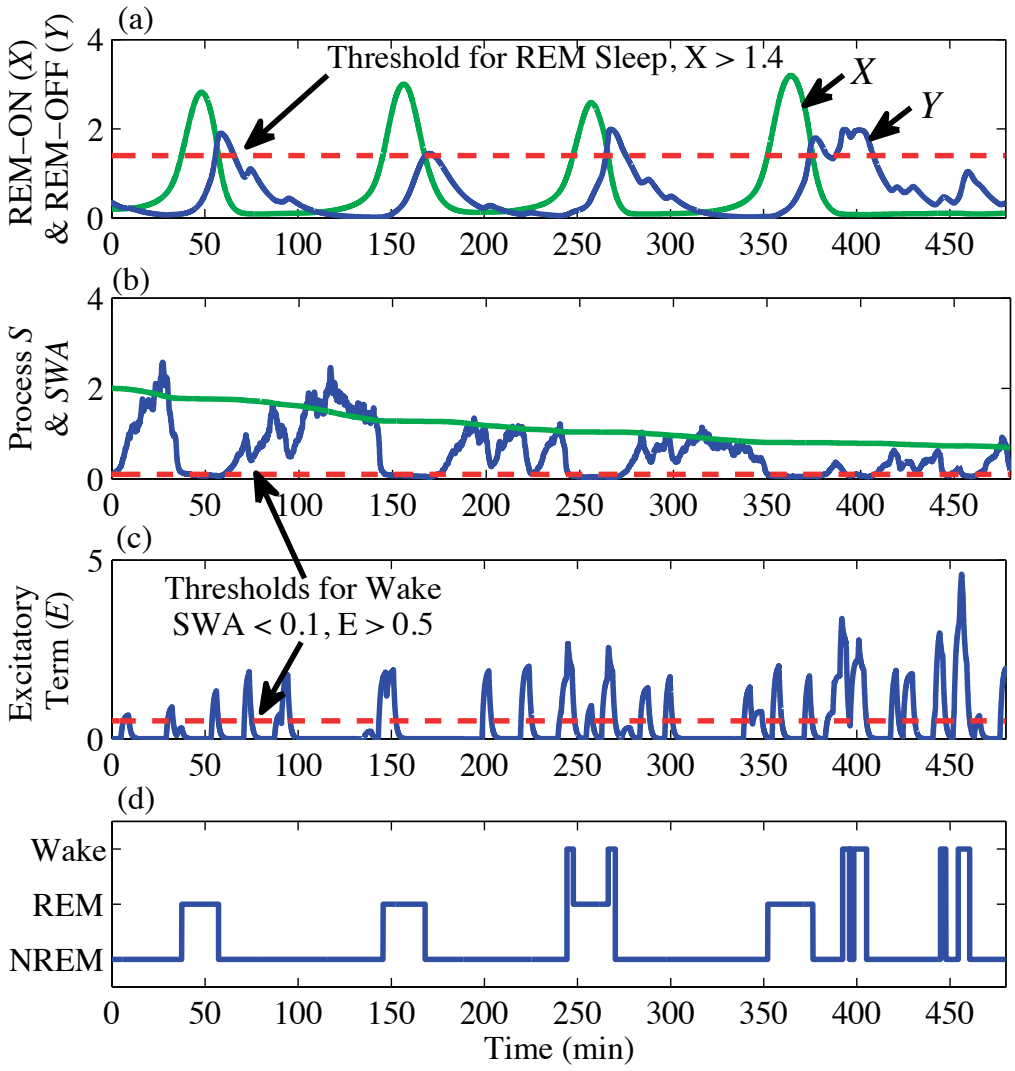

Figure F.1. An example of using Massaquoi and McCarley's LCRIM/I model to classify sleep stages, (a) REM-ON (X) (green) and REM-OFF(X) (blue) activity, (b) Process S (green) and SWA (blue), (c) Excitatory activity E, and (d) sleep stages. Thresholds used for scoring sleep stages (red-dashed lines).

and

$$\dot{SWA} = rc\, SWA\ (S - SWA) - fc\,(SWA - SWA_L)REMT - fcw\,(SWA - SWA_L)E, \tag{F.13}$$

Table F.1. Coefficients of Massaquoi and McCarley's LCRIM/I Model (1992).

Model Parameters	Original Values
c	1
gc	0.05
k	10
rc	3.0
rs	0.005
E_o	0.001
X_o	0.12
Y_o	0.35
S_o	2.0
SWA_o	0.1
N Amplitude	Uniformly distributed between 1.25 and 25
N Duration	Uniformly distributed between 0.25 and 0.5
N Inter-arrival Time	Exponentially distributed with mean of 1.1
$n(t)$	Uniformly distributed between -10 and 10

and

$$SWA = SWA(1 + n(t)). \tag{F.14}$$

The equations for the Slow REM model are similar to those of the Massaquoi and McCarley model but without the saturation functions. The equation for REM promoting neuron activity is thus,

$$\dot{X} = (aX - bXY)dc, \tag{F.15}$$

where dc is a sinusoidal term with a period of 24 hours,

$$dc = 1.55 + 0.8sin(0.0467t + 4), \tag{F.16}$$

where t is measured in units rather than seconds with 1 unit equal to 10.7 minutes. The equation for the REM inhibiting neuron activity is,

$$\dot{Y} = -cY + d(X + eE)Y. \tag{F.17}$$

The equation for the fast REM model is,

$$\ddot{x} + \delta\dot{x} + (x + 2.5)(x - (-2 + \gamma w(t)))(x + 0.5)(x)(x - 0.5) = Acos(\omega t), \tag{F.18}$$

where $w(t)$ in the equation is typically the excitation term $E(t)$. An example of the output of the model when noise events are occurring is shown in Figure F.2. The model parameter values are listed in Table F.2. The following rules were used for assigning NREM sleep stages:

1. If SWA >2.0 score as Stage 3/4,
2. If SWA <0.3 score as Stage Wake/1 ,
3. If SWA <1 and E >0.5 score as Stage Wake/1,
4. All other times when REM sleep is not occurring are scored as Stage 2 sleep.

The following rules were used to assign REM sleep stages according to the value of x of the fast REM model:

1. If x >0 score as Phasic REM sleep,
2. If x <-2 and an excitation is occurring score as Wake,
3. All other times are scored as Tonic REM sleep.

REM sleep periods were defined by the level of REM promoting activity X in the slow REM model. When X is greater than 1, REM sleep periods was considered to be occurring.

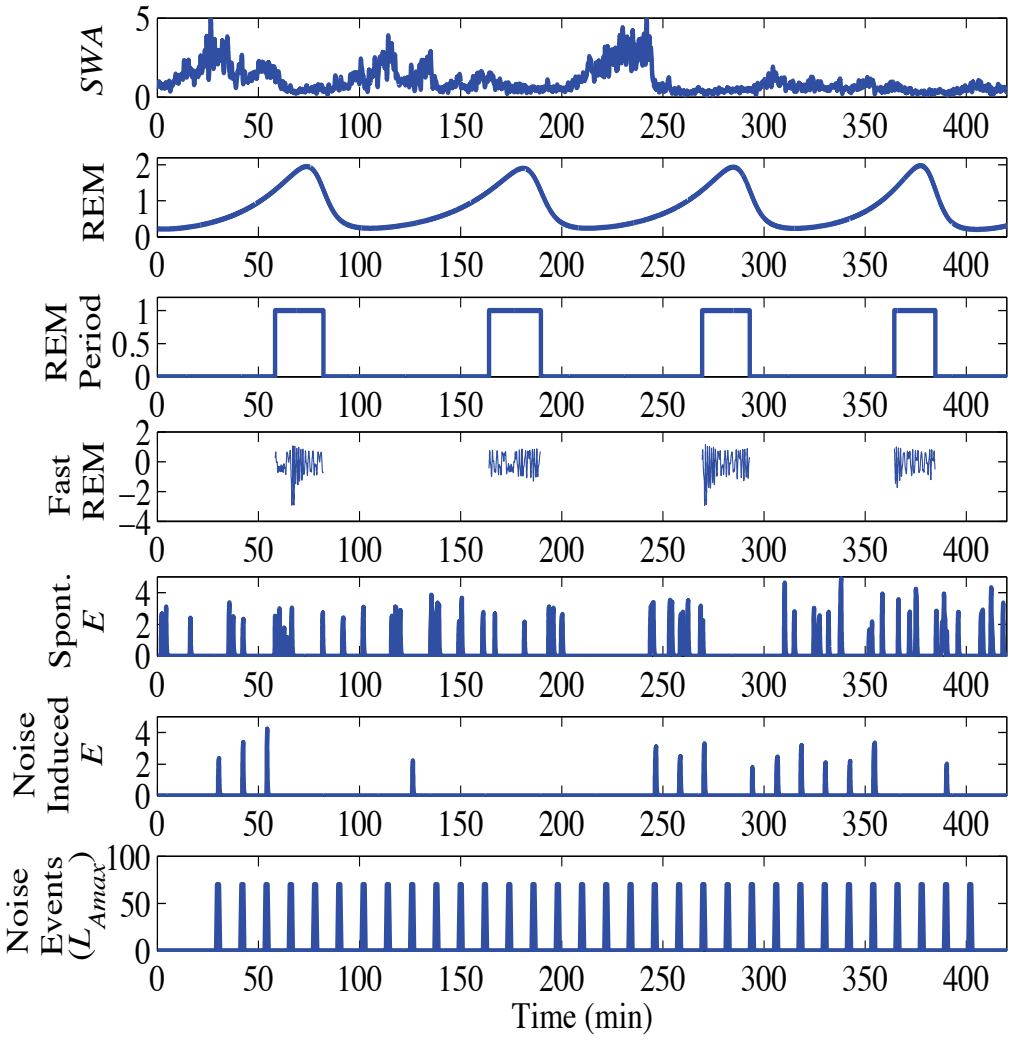

Figure F.2. An example of the parameters for the developed nonlinear sleep model, which include slow wave activity (SWA), REM, REM sleep period indicator, fast REM model and the spontaneous and noise induced excitation terms.

Table F.2. Parameters of the nonlinear model. *Parameters varied according to a Gaussian distribution and + parameters varied according to a uniform distribution, x parameter varied with an exponential distribution.

SWA		Slow REM		Fast REM		Excitations	
$*S_o$	mean 3.75 std. dev 0.67	$*a$	mean 0.47 std. dev 0.1	ω	2 π (0.3)	N	^{x}mean inter-arr 6.1 min
$*SWA_o$	mean 0.78 std. dev 0.29	$*b$	mean 0.41 std. dev 0.1	A	0.5		*dur.-mean 0.5 min
$*gc$	mean 0.03 std. dev 0.01	$*c$	mean 1.4 std. dev 0.15	δ	0.06		*dur.-std. dev 0.2 min
SWA_L	0.2	$*d$	mean 1.83 std. dev 0.15	^+x_o	min -1.0 max 1.0		*amp.- mean 3.0
fc	2.0	e	0.05	^+y_o	min -1.0 max 1.0		*amp.-std. dev 0.65
fcw	4.0	^+X_o	min 0.15 max 0.3				amp.-max 5.0
rc	0.4	^+Y_o	min 0.5 max 3.0				
$n(t)$	mean 0 std. dev 0.2 skewness 0.53						

Appendix G. Code for Nonlinear Dynamic Model

The following is the Matlab program for the nonlinear dynamic sleep model that was developed as part of this research. The components of the model are the slow and fast REM model, slow wave activity model, and spontaneous and aircraft noise induced excitation terms. Based on these components sleep stages are predicted. In Table G.1 is a list of subroutines in this program and the functions they call.

Table G.1. Subroutines of the nonlinear dynamic model.

Subroutine Name	Is Called By	Makes Calls to
Input_Parameters	Model_Main	None
Create_Aircraft Input	Model_Main	None
Generate_Random_Input_Variables	Model_Main	None
Create_Spontaneous	Model_Main	None
Create_Aircraft_Awakenings	Model_Main	None
E_Calc	Model_Main	None
REM_Calc	Model_Main	None
Create_REM_INPUT	Model_Main	None
SWA_Calc	Model_Main	None
NREM_Sleep_Stage_Classify	Model_Main	None
Fast_REM_Main	Model_Main	calc_tonic_phasic_int Phasic_Tonic_Calc
Phasic_Tonic_Calc	Fast_REM_Main	None
calc_tonic_phasic_int	Fast_REM_Main	None
Calc_30_Sec_Stages	Model_Main	None

The following are the inputs to the model:

1. optionN: which is used if a noise scenario is being run,
2. position: the x,y grid position,
3. LAMAX: the maximum noise levels of sound events during the night. This term is a vector and its length is equal to the length of the number of events during the night,
4. Numpeople: is the number of people to simulate for each location point,
5. Timing: the time of each noise event during the night in minutes.

An example of an input to the model is the following if the events were of all the same noise level during the night,

```
optionN={'Noise'};%%Run for noise events
position=[0 0];%%X,Y position
LAMAX=40*ones(1,16);%%LAMAX and timing must be equal in length
Numpeople=50;%%Number of people at grid point
Timing=30:24:402;%%Time of events in minutes
```

Function Model_Main: This is the main code for the nonlinear dynamic model.

```
%%%-------------------------------------------------------------------------%%
%%%-------------------------------------------------------------------------%%
%%%Function Model_Main
%%%Main code for the nonlinear dynamic sleep model
%%%Note 1 Unit in the model is equal to 10.7 minutes
%%%
%%%Input:  LAMAX-noise level for each nighttime event
%%%        Timing-timing of aircraft events in minutes
%%%        Numpeople-number of people at a location point
%%%        optionN: is used if a noise scenario is being run
%%%        position: x,y location for grid point
%%%-------------------------------------------------------------------------%%
%%%-------------------------------------------------------------------------%%
function Model_Main(LAMAX,Timing,Numpeople,optionN,position)
warning off;
len=48;
Fs=640;

[Data]=Input_Parameters;%%Obtain model parameter values

if strcmp(optionN,'Noise')
  %%Run simulation once for baseline conditions and once for
  %%Noise event conditions
  Repeat=2;

  %%Create aircraft noise input
  [Events]=Create_Aircraft_Input(Data,LAMAX,Numpeople);
else
  Repeat=1;
end

for ink=1:Numpeople
  display(ink)
  time=0:1/Fs:len;
```

```
%%Relationship between NREM excitation amplitude
%%and fast REM sleep excitation amplitude
REM=[.5 1.45];
NREM=[.5 5];
pr=polyfit(NREM,REM,1);

%%Spontaneous awakenings
[Nt,NtREM]=Create_Spontaneous(Fs,len,Data,pr);

%%Limit amplitude of REM and NREM excitation terms
if max(NtREM)>1.45
  I=find(NtREM>1.45);
  NtREM(I)=1.45;
end
if max(Nt)>5
  I=find(Nt>5);
  Nt(I)=5;
end

[Data,nt,initRx,initRy]=Generate_Random_Input_Variables(Data,len,Fs);

for ii=1:Repeat
  tic
  if strcmp(optionN,'Noise') && ii==2
    %%Create excitation term (N(t)) for
    %%noise-induced awakenings
    [aircraftREM aircraft]=...
    Create_Aircraft_Awakenings(Data,Timing,len,Fs,pr,ink,Events);

    %%Add spontaneous and noise-induced excitation terms
    Nt=Nt+aircraft;
    NtREM=NtREM+aircraftREM;

    if max(NtREM)>1.45
      I=find(NtREM>1.45);
      NtREM(I)=1.45;
    end
    if max(Nt)>5
      I=find(Nt>5);
      Nt(I)=5;
    end
  end

  %%Low-pass filter N(t) to obtain E(t)
  [T,Wake]=E_Calc(Nt,Fs,len);
  [T,WakeREM]=E_Calc(NtREM,Fs,len);

  %%Calculate REM promoting (X) and
  %%REM inhibiting activity (Y)
  [T,X]=REM_Calc(Data,Wake,Fs,len);
  REM=X(:,1);%%REM-ON activity
```

```
  %%Create REM sleep indicator (REMT)
  [REM_NEW,st_new,ff_new]=Create_REM_INPUT(REM,Fs,len);
  toc

  %%Calculate SWA activity
  tic
  [T,X]=SWA_Calc(Data,REM_NEW,Wake,Fs,len);
  SWA=X(:,1).*(1+nt(1:length(X(:,1))))';
  toc

  %%Assign 1 second NREM sleep stages based on SWA and E(t)
  Est_Stage=zeros(1,960);
  tic
  [Est_Stage]=NREM_Sleep_Stage_Classify(Est_Stage,SWA,Wake,REM_NEW);

  %%Calculate Fast REM activity and assign 1 second REM sleep stages
  [Est_Stage]=Fast_REM_Main(Est_Stage,initRx,initRy,Fs,st_new,ff_new,WakeREM);

  %%Calculate 30 second sleep stages
  [tempstage,tempstage30plot]=Calc_30_Sec_Stages(Est_Stage);
  toc

  %%Calculate duration of each sleep stage
  for jj=1:4
    I=find(tempstage(1:960)==jj);
    dur_stage(jj,ink,ii)=length(I)/2;
  end

  %%Calculate percent of events individual awakened
  %%to during the night
  if strcmp(optionN,'Noise')
    perawake1=0;
    for jj=1:length(Timing)
      I=find(tempstage(Timing(jj)*2:Timing(jj)*2+3)==1);
      if length(I)>0 && tempstage(Timing(jj)*2-1)~=1
        perawake1=perawake1+1;
      end
    end
    perawake(ink,ii)=perawake1/length(Timing);
  end
  Full_Stages(1:length(tempstage30plot),ink,ii)=tempstage30plot';
end

%%Calculate difference in sleep stage duration
%%and probability of awakening at the time of noise events
%%for (1) baseline no-noise nights and (2)
%%nights with aircraft noise exposure
if strcmp(optionN,'Noise') && ii==2
  change(1:4,ink)=dur_stage(:,ink,2)-dur_stage(:,ink,1);
  changeperawake(ink)=(perawake(ink,2)-perawake(ink,1))
end
```

```
end

%%Save data
if strcmp(optionN,'Noise')
total_awake(1)=...
sum(perawake(1:Numpeople,1)*length(Timing))/(Numpeople*length(Timing));
total_awake(2)=...
sum(perawake(1:Numpeople,2)*length(Timing))/(Numpeople*length(Timing));
totalchangeper=mean(changeperawake)';
totalchangedur(1:4)= mean(change');
save(['Ntotal_awake_LAmax' num2str(LAMAX(1)) ...
'NumEvents' num2str(length(Timing)) 'Numpeop' num2str(Numpeople) ...
'position' num2str(position(1)) '_' num2str(position(2)) '.mat'],'total_awake')
save(['Ntotalchangeper_LAmax' num2str(LAMAX(1)) ....
'NumEvents' num2str(length(Timing)) 'Numpeop' num2str(Numpeople)...
'position' num2str(position(1)) '_' num2str(position(2)) '.mat'],'totalchangeper')
save(['Ntotalchangedur_LAmax' num2str(LAMAX(1)) ...
'NumEvents' num2str(length(Timing)) 'Numpeop' num2str(Numpeople)...
'position' num2str(position(1)) '_' num2str(position(2)) '.mat'],'totalchangedur')
save(['Ntotal_awake_LAmax' num2str(LAMAX(1)) ...
'NumEvents' num2str(length(Timing)) 'Numpeop' num2str(Numpeople)...
'position' num2str(position(1)) '_' num2str(position(2)) '.mat'],'total_awake')
save(['Nchange_LAmax' num2str(LAMAX(1)) ...
'NumEvents' num2str(length(Timing)) 'Numpeop' num2str(Numpeople) ...
'position' num2str(position(1)) '_' num2str(position(2)) '.mat'],'change')
save(['Nchangeperawake_LAmax' num2str(LAMAX(1)) ...
'NumEvents' num2str(length(Timing)) 'Numpeop' num2str(Numpeople)...
'position' num2str(position(1)) '_' num2str(position(2)) '.mat'],'changeperawake')
end

save(['NFull_Stages_LAmax' num2str(LAMAX(1)) ...
'NumEvents' num2str(length(Timing)) 'Numpeop' num2str(Numpeople)...
'position' num2str(position(1)) '_' num2str(position(2)) '.mat'],'Full_Stages')
%%%-------------------------------------------------------------------------%%
%%%-------------------------------------------------------------------------%%
```

Function Input_Parameters: This function contains the values for the parameters of the model.

```
%%%-------------------------------------------------------------------------%%
%%%-------------------------------------------------------------------------%%
%%%Function Input_Parameters
%%%Contains values of most model inputs-these values are based on the 1999
%%%UK data
%%%
%%%Output: Data-contains model parameters used
%%%-------------------------------------------------------------------------%%
%%%-------------------------------------------------------------------------%%
function [Data]=Input_Parameters
```

```
%%Noise n(t) model parameters
Data.ntmean=0;
Data.ntstd=0.20;
Data.ntskew=0.5269;
Data.ntkurtosis=3;

%%wt/E model parameters
%%divide by 10.7 to convert parameters from
%%minutes to units
Data.wtintarr=6.1/10.7;
Data.wtstddur=0.20/10.7;
Data.wtmeandur=0.5/10.7;
Data.wtmindur=0.05/10.7;

Data.wtminamp=0.5;
Data.wtmaxamp=5.0;
Data.wtmeanamp=3.0;
Data.wtstdamp=0.65;

%%Slow REM model parameters
Data.amean=0.47;
Data.astd=0.1;
Data.bmean=0.41;
Data.bstd=0.1;
Data.cmean=1.4;
Data.cstd=0.15;
Data.dmean=1.83;
Data.dstd=0.15;
Data.yomin=0.5;
Data.yomax=3;
Data.xomin=0.15;
Data.xomax=0.3;

%%SWA model parameters
Data.SWAL=0.2;
Data.fc=2.0;
Data.rc=0.4;
Data.fcw=2*Data.fc;
Data.Somean=3.75;
Data.Sostd=0.67;
Data.Somin=2.3;
Data.Somax=5.8;
Data.gcmax=0.05;
Data.gcmin=0.008;
Data.gcstd=0.011;
Data.gcmean=0.0320;
Data.SWAomin=0.13;
Data.SWAomax=1.51;
Data.SWAomean=0.78;
Data.SWAostd=0.29;
%%%-------------------------------------------------------------------------%%
```

```
%%%-------------------------------------------------------------------------%%
```

Function Generate_Random_Input_Variables: The following program is used to generate all model parameters for one person night based on uniform and Gaussian distributions.

```
%%%-------------------------------------------------------------------------%%
%%%-------------------------------------------------------------------------%%
%%%Function Generate_Random_Input_Variables
%%%Code for generating all random inputs to the model
%%%
%%%Input:  Data-contains model parameters used
%%%        len-length of night that is being simulated
%%%        Fs-sampling rate
%%%
%%%Output: Data-contains model parameter values for subject
%%%        nt-noise term applied to SWA
%%%        initRx-initial xo values for fast REM model
%%%        initRy-initial yo values for fast REM model
%%%-------------------------------------------------------------------------%%
%%%-------------------------------------------------------------------------%%
function [Data,nt,initRx,initRy]=Generate_Random_Input_Variables(Data,len,Fs)

%%Minimum and maximum values are used to
%%limit current range of parameters
%%note: acceptable range of parameters will be
%%further explored in the future

%%SWA and Process S model parameters
Data.SWAo=normrnd(Data.SWAomean,Data.SWAostd,1,1);
if Data.SWAo<Data.SWAomin
  Data.SWAo=Data.SWAomin;
elseif Data.SWAo>Data.SWAomax
  Data.SWAo=Data.SWAomax;
end

Data.So=normrnd(Data.Somean,Data.Sostd,1,1);
if Data.So<Data.Somin
  Data.So=Data.Somin;
elseif Data.So>Data.Somax
  Data.So=Data.Somax;
end

Data.gc=normrnd(Data.gcmean,Data.gcstd,1,1);
if Data.gc<Data.gcmin
  Data.gc=Data.gcmin;
elseif Data.gc>Data.gcmax
  Data.gc=Data.gcmax;
```

```
end

%%More restrictive on range for
%%slow REM sleep models as certain
%%combinations of a,b,c,d will result
%%in no REM cycling

%%Slow REM sleep model parameters
Data.a=normrnd(Data.amean,Data.astd,1,1);
if Data.a<Data.amean-Data.astd
  Data.a=Data.amean-Data.astd;
elseif Data.a>Data.amean+Data.astd
  Data.a=Data.amean+Data.astd;
end

Data.b=normrnd(Data.bmean,Data.bstd,1,1);
if Data.b<Data.bmean-Data.bstd
  Data.b=Data.bmean-Data.bstd;
elseif Data.b>Data.bmean+Data.bstd
  Data.b=Data.bmean+Data.bstd;
end

Data.c=normrnd(Data.cmean,Data.cstd,1,1);
if Data.c<Data.cmean-Data.cstd
  Data.c=Data.cmean-Data.cstd;
elseif Data.c>Data.cmean+Data.cstd
  Data.c=Data.cmean+Data.cstd;
end

Data.d=normrnd(Data.dmean,Data.dstd,1,1);
if Data.d<Data.dmean-Data.dstd
  Data.d=Data.dmean-Data.dstd;
elseif Data.d>Data.dmean+Data.dstd
  Data.d=Data.dmean+Data.dstd;
end

%%Slow and Fast REM sleep model initial conditions
Data.yo=Data.yomin+(Data.yomax-Data.yomin)*rand(1,1);
Data.xo=Data.xomin+(Data.xomax-Data.xomin)*rand(1,1);
initRx=-1+2*rand(1,10);
initRy=-1+2*rand(1,10);

%%Random noise term n(t)
cc=pearsrnd(Data.ntmean,Data.ntstd,Data.ntskew,Data.ntkurtosis, 1,len*Fs);
[b,a]=butter(3,10/(Fs/2));
nt=filter(b,a,cc);
nt=nt*(max(cc)/max(nt));
%%%-------------------------------------------------------------------------%%
%%%-------------------------------------------------------------------------%%
```

Function Create_Aircraft_Input: The following program is used to generate a matrix which contains, for each person and aircraft event, the amplitude of the associated excitation based on the maximum noise level of the event.

```
%%%-------------------------------------------------------------------------%%
%%%-------------------------------------------------------------------------%%
%%%Function Create_Aircraft_Input
%%%Code for assigning excitation values for aircraft events
%%%for every subject
%%%
%%%Input:  Data-contains model parameters used
%%%        LAMAX-noise level for each nighttime event
%%%        Numpeople-number of people at location point
%%%
%%%Output: Events-amplitudes of excitation N for all subjects for all
%%%        aircraft events during the night
%%%-------------------------------------------------------------------------%%
%%%-------------------------------------------------------------------------%%

function [Events]=Create_Aircraft_Input(Data,LAMAX,Numpeople)

%%linear relationship between noise level and
%%fraction responding
Noise=[35 80];%%Lamax level
per=[.17 .55];%%percent nonzero response(above baseline)
p=polyfit(Noise,per,1);

%%Cycle through for each noise event
for ii=1:length(LAMAX)
  %%These are nonzero responses hence value not zero
  rel=p(1)*LAMAX(ii)+p(2);
  val = normrnd(Data.wtmeanamp,Data.wtstdamp,floor(Numpeople*rel),1);
  I=find(val<Data.wtminamp);

  %%Limit range of excitations
  if length(I)>0
    val(I)=val;
  end

  I=find(val>Data.wtmaxamp);
  if length(I)>0
    val(I)=Data.wtmaxamp;
  end

  %%Nonzero and zero aircraft responses
  Total=[val(:); zeros(Numpeople,1)];
  Total=Total(1:Numpeople);
  rr=randperm(Numpeople);
  for jj=1:length(rr)
```

```
    Events(jj,ii)=Total(rr(jj));
  end
end
%%%-------------------------------------------------------------------------%%
%%%-------------------------------------------------------------------------%%
```

Function Create_Spontaneous: The following program is used to generate $N(t)$ for spontaneous awakenings for one subject night.

```
%%%-------------------------------------------------------------------------%%
%%%-------------------------------------------------------------------------%%
%%%Function Create_Spontaneous
%%%Code for generating spontaneous excitations N(t)
%%%
%%%Input:  Fs-sampling rate
%%%        len-length of night that is being simulated
%%%        Data-contains model parameters used
%%%        pr-relationship between noise amplitudes during slow and
%%%        fast models
%%%
%%%Output: Nt-amplitudes of excitation N(t) for slow models
%%%        NtREM-amplitudes of excitation N(t) for fast REM model
%%%
%%%-------------------------------------------------------------------------%%
%%%-------------------------------------------------------------------------%%
function [Nt,NtREM]=Create_Spontaneous(Fs,len,Data,pr)

delta=1/Fs;
time=0:delta:len;
Nt=zeros(1,1.1*len*Fs);
NtREM=zeros(1,1.1*len*Fs);

%%Create vectors of amplitudes and durations
Amp=normrnd(Data.wtmeanamp,Data.wtstdamp,1,length(time)*1.1);
I=find(Amp < Data.wtminamp);
Amp(I)=Data.wtminamp;

duration=normrnd(Data.wtmeandur,Data.wtstddur,1,length(time)*1.1);
I=find(duration < Data.wtmindur);
duration(I)=Data.wtmindur;

%%Time between pulses are exponentially distributed
int_arr=exprnd(Data.wtintarr,1,length(time)*1.1);
total_dur=0;
ii=1;

%%Create N(t) for slow models
%%Assuming inter-arrival time is between the start of each pulse
while (total_dur <len)
```

```
  beg=round(sum(int_arr(1:ii))/delta);
  if beg==0
    beg=1;
  end
  fin=beg+round(duration(ii)/delta);
  Nt(beg:fin)=Nt(beg:fin)+Amp(ii).*ones(1,round(duration(ii)/delta)+1);

  %%Create N(t) for fast models
  Aramp=pr(1)*Amp(ii)+pr(2);
  NtREM(beg:fin)=NtREM(beg:fin)+Aramp.*ones(1,round(duration(ii)/delta)+1);
  ii=ii+1;
  total_dur=sum(int_arr(1:ii))+duration(ii);
end
%%%-------------------------------------------------------------------------%%
%%%-------------------------------------------------------------------------%%
```

Function Create_Aircraft_Awakenings: The following program is used to generate $N(t)$ for aircraft noise events.

```
%%%-------------------------------------------------------------------------%%
%%%-------------------------------------------------------------------------%%
%%%Function Create_Aircraft_Awakenings
%%%Code for creating excitations N(t) associated with the occurrence
%%%of aircraft events
%%%
%%%Input:  Data-contains model parameters used
%%%        Timing-timing of aircraft events in minutes
%%%        len-length of night that is being simulated
%%%        Fs-sampling rate
%%%        pr-relationship between noise amplitudes during slow and
%%%        fast models
%%%        ink-subject number
%%%        Events-amplitudes of excitation N(t) for all subjects for all
%%%        events during the night
%%%
%%%Output: aircraftREM-amplitudes of excitation N(t) for fast REM model for
%%%        aircraft events
%%%        aircraft-amplitudes of excitation N(t) for slow models
%%%        aircraft events
%%%-------------------------------------------------------------------------%%
%%%-------------------------------------------------------------------------%%
function [aircraftREM aircraft]=Create_Aircraft_Awakenings(Data,Timing,...
len,Fs,pr,ink,Events)
aircraft=zeros(1,1.1*len*Fs);
aircraftREM=zeros(1,1.1*len*Fs);

for ii=1:length(Timing)
  if Events(ink,ii)>0
    dur=normrnd(Data.wtmeandur,Data.wtstddur,1,1);
```

```
    if dur<Data.wtmindur
      dur(1)= Data.wtmindur;
    end

    %%Create N(t) for slow models
    beg=round((Timing(ii)/10.7)*Fs);
    fin=beg+round(dur*Fs);
    aircraft(beg:fin)=aircraft(beg:fin)+Events(ink,ii).*ones(1,round(dur*Fs)+1);

    %%Create N(t) for fast models
    Aramp=pr(1)*Events(ink,ii)+pr(2);
    aircraftREM(beg:fin)=aircraftREM(beg:fin)+Aramp.*ones(1,round(dur*Fs)+1);
    end
  end
%%%-------------------------------------------------------------------------%%
%%%-------------------------------------------------------------------------%%
```

Function E_Calc: The following program is used to generate $E(t)$ by low pass filtering $N(t)$, which is the summation of the aircraft noise induced and spontaneous excitation terms.

```
%%%-------------------------------------------------------------------------%%
%%%-------------------------------------------------------------------------%%
%%%Function E_Calc
%%%Code for low-pass filtering the excitation term N(t)
%%%
%%%Input:  Wake-this is the Poisson Noise (N(t))
%%%        Fs-sampling rate
%%%        len-length of night that is being simulated
%%%
%%%Output: T-time
%%%        X-low pass filtered noise process E(t)
%%%-------------------------------------------------------------------------%%
%%%-------------------------------------------------------------------------%%
function [T,X]=E_Calc(Wake,Fs,len)
options = odeset('RelTol',1e-6);
[T,X]=ode45(@(t,x) fun(t,x,Wake,Fs),1/Fs:1/Fs:len,[.001],options);
end

function dxdt=fun(t,x,Wt,Fs)
dxdt=zeros(1,1);
time=(0:1:(length(Wt)-1))/Fs;
w=interp1(time,Wt,t);
dxdt(1)=(64)*w-(64)*x(1);%%Lowpass below 10 seconds
end
%%%-------------------------------------------------------------------------%%
%%%-------------------------------------------------------------------------%%
```

Function REM_Calc: The following program is used to calculate the slow REM activity, both X REM promoting activity and Y REM inhibiting activity.

```
%%%-------------------------------------------------------------------------%%
%%%-------------------------------------------------------------------------%%
%%%Function REM_Calc
%%%Code for calculating slow REM activity-based on the Massaquoi and
%%%McCarley model.
%%%
%%%Reference:S. G. Massaquoi and R. W. McCarley. Extension of the limit
%%%cycle reciprocal interaction model of REM cycle control. An integrated
%%%sleep control model, 1:138-143,1992.
%%%
%%%Input:  REM_Param-data for REM model
%%%        Wake-excitation term E(t)
%%%        Fs-sampling rate
%%%        len-length of night that is being simulated
%%%
%%%Output: T-time
%%%        X-slow REM model
%%%-------------------------------------------------------------------------%%
%%%-------------------------------------------------------------------------%%
function [T,X]=REM_Calc(REM_Param,Wake,Fs,len)
options = odeset('RelTol',1e-6);
[T,X]=ode45(@(t,x) fun(t,x,REM_Param,Wake,Fs),1/Fs:1/Fs:len,...
[REM_Param.xo REM_Param.yo],options );
end

function dxdt=fun(t,x,REM_Param,Wake,Fs)
dxdt=zeros(2,1);
time=(0:1:(length(Wake)-1))/Fs;
w=interp1(time,Wake,t);

dc2=(1.55+0.8*sin(.0467*t+4));%%24 hour circadian variation
dc=1;

%%REM-ON (X)
dxdt(1)=REM_Param.a*x(1)*dc2-x(1)*x(2)*REM_Param.b*dc2;

%%REM-OFF (Y)
dxdt(2)=-x(2)*REM_Param.c*dc+dc*(x(1)+(0.25/max(Wake))*w)*x(2)*REM_Param.d;
end
%%%-------------------------------------------------------------------------%%
%%%-------------------------------------------------------------------------%%
```

Function Create_REM_INPUT: The following program is used to calculate the start and end of each REM period based on the level of X, REM-promoting activity, from the slow REM model.

```
%%%-------------------------------------------------------------------------%%
%%%-------------------------------------------------------------------------%%
%%%Function Create_REM_INPUT
%%%Program for determining the beginning and end of each REM period
%%%based on the level of slow REM activity
%%%%
%%%Input:  REM-slow REM model activity
%%%        Fs-sampling rate
%%%        len-length of night that is being simulated
%%%
%%%Output: st_new-start of each REM period
%%%        ff_new-end of each REM period
%%%        REM_NEW-REM-indicator, 1 during REM sleep and zero during NREM
%%%        sleep
%%%-------------------------------------------------------------------------%%
%%%-------------------------------------------------------------------------%%
function [REM_NEW,st_new,ff_new]=Create_REM_INPUT(REM,Fs,len)
ii=1;
if max(REM)<1.5
  valgreat=.5*(max(REM)-min(REM));
else
  valgreat=1;
end

%%Calculate Multipliers
tempShift=REM;
Ind=find(tempShift>=valgreat);
st(ii)=Ind(1);
tempShift=tempShift(Ind(1):length(tempShift));
Ind=find(tempShift<valgreat);
maxval=max(tempShift(1:Ind(1)));
ff(ii)=Ind(1)+st(ii);
sc(ii)=1.5/maxval;
tempShift=tempShift(Ind(1):length(tempShift));
Ind=find(tempShift>=valgreat);

while(ff(ii)<len*Fs && length(Ind)>0)
  ii=ii+1;
  st(ii)=Ind(1)+ff(ii-1);
  tempShift=tempShift(Ind(1):length(tempShift));
  Ind=find(tempShift<valgreat);
 if length(Ind)>0
   maxval=max(tempShift(1:Ind(1)));
   ff(ii)=Ind(1)+st(ii);
   sc(ii)=1.5/maxval;
```

```
   tempShift=tempShift(Ind(1):length(tempShift));
else
  ff(ii)=len*Fs ;
  maxval=max(tempShift(1:length(tempShift)));
  sc(ii)=1.5/maxval;
end
  Ind=find(tempShift>=valgreat);
end

%%Cycle through and find start points for the scaled REM signal
REM_NEW=zeros(1,length(REM));
for ii=1:length(st)
  if ii==1
    temp=REM(1:ff(1)+(st(2)-ff(1))/2)*sc(ii);
    Ind=find(temp>=1);
    REM_NEW(Ind)=1;
    st_new(ii)=Ind(1);
    ff_new(ii)=Ind(length(Ind));
  elseif ii<length(st)
    temp=REM(ff(ii-1)+(st(ii)-ff(ii-1))/2:ff(ii)+(st(ii+1)-ff(ii))/2)*sc(ii);
    Ind=find(temp>=1);
    REM_NEW(round(Ind+ff(ii-1)+(st(ii)-ff(ii-1))/2-1))=1;
    st_new(ii)=round(Ind(1)+ff(ii-1)+(st(ii)-ff(ii-1))/2-1);
    ff_new(ii)=round(Ind(length(Ind))+ff(ii-1)+(st(ii)-ff(ii-1))/2-1);
  else
    temp=REM(ff(ii-1)+(st(ii)-ff(ii-1))/2:length(REM))*sc(ii);
    Ind=find(temp>=1);
    REM_NEW(round(Ind+ff(ii-1)+(st(ii)-ff(ii-1))/2-1))=1;
    st_new(ii)=round(Ind(1)+ff(ii-1)+(st(ii)-ff(ii-1))/2-1);
    ff_new(ii)=round(Ind(length(Ind))+ff(ii-1)+(st(ii)-ff(ii-1))/2-1);
  end
end
%%%-------------------------------------------------------------------------%%
%%%-------------------------------------------------------------------------%%
```

Function SWA_Calc: The following program is used to calculate the slow wave activity (SWA) and Process S.

```
%%%-------------------------------------------------------------------------%%
%%%-------------------------------------------------------------------------%%
%%%Function SWA_Calc
%%%Program for calculating slow wave activity based on Achermann et al.'s
%%%model
%%%
%%%Reference: P. Achermann, D. J. Dijk, D. P. Brunner and A. A. Borbly.  A
%%%model of human sleep homeostasis based on EEG slow-wave activity:
%%%Quantitative comparison of data and simulations. Brain Research
%%%Bulletin. 31: 97-113, 1993.
%%%
```

```
%%%Input:  Param-model parameters
%%%        REM-indicator of REM periods
%%%        Wake-aircraft and spontaneous excitations, E(t)
%%%        Fs-sampling rate
%%%        len-length of night that is being simulated
%%%
%%%
%%%Output: T-time vector
%%%        X-SWA and Process S
%%%
%%%-------------------------------------------------------------------------%%
%%%-------------------------------------------------------------------------%%
function [T,X]=SWA_Calc(Param,REM,Wake,Fs,len)
options = odeset('RelTol',1e-6);
[T,X]=ode45(@(t,x) fun(t,x,Param,REM,Wake,Fs),1/Fs:1/Fs:len,...
[Param.SWAo  Param.So],options);
end

function dxdt = fun(t,x,Param,REM,Wake,Fs)
dxdt=zeros(2,1);
timew=(0:1:(length(Wake)-1))/Fs;
timeR=(0:1:(length(REM)-1))/Fs;
w=interp1(timew,Wake,t);
R=interp1(timeR,REM,t);

%%dxdt(1) and x(1) is for SWA (slow wave activity)
%%dxdt(2) and x(2) is for process S
dxdt(1)=(Param.rc)*x(1)*x(2)*(1-x(1)/x(2))-(Param.fc)*(x(1)-Param.SWAL)*R...
-(x(1)-Param.SWAL)*(Param.fcw)*w;
dxdt(2)=-Param.gc*x(1);
end
%%%-------------------------------------------------------------------------%%
%%%-------------------------------------------------------------------------%%
```

Function NREM_Sleep_Stage_Classify: The following program is used to classify NREM sleep stages based on the level of SWA and the excitation term E.

```
%%%-------------------------------------------------------------------------%%
%%%-------------------------------------------------------------------------%%
%%%Function NREM_Sleep_Stage_Classify
%%%Program for calculating NREM sleep stages based on SWA activity
%%%and excitation values
%%%
%%%Input:  Est_Stage-empty vector for sleep stage assignment
%%%        SWA-Slow wave activity
%%%        Wake-excitation term
%%%        REM-NEW-indicator of REM periods
%%%
%%%Output: Est_Stage-assigned NREM sleep stages
```

```
%%%-------------------------------------------------------------------------%%
%%%-------------------------------------------------------------------------%%
function [Est_Stage]=NREM_Sleep_Stage_Classify(Est_Stage,SWA,Wake,REM_NEW)

for ii=1:length(SWA)
  if REM_NEW(ii)==0
    if SWA(ii)>=2.0
      Est_Stage(ii)=3;%%Stage 3/4
    elseif SWA(ii)<1.0 && Wake(ii)>=.5
      Est_Stage(ii)=1;%%Stage Wake/S1
    elseif SWA(ii)<0.3
      Est_Stage(ii)=1;%%Stage Wake/S1
    else
      Est_Stage(ii)=2;%%Stage 2
    end
  else
    Est_Stage(ii)=5;%%Temporary place holder
  end
end
%%%-------------------------------------------------------------------------%%
%%%-------------------------------------------------------------------------%%
```

Function Fast_REM_Main: The following program is the main program for calculating fast REM activity.

```
%%%-------------------------------------------------------------------------%%
%%%-------------------------------------------------------------------------%%
%%%Function Fast_REM_Main
%%%Program for calculating fast REM activity
%%%
%%%
%%%Input:  Est_Stage-vector containing sleep stages
%%%        initRx-initial xo values for fast REM model
%%%        initRy-initial yo values for fast REM model
%%%        Fs-sampling rate
%%%        st_new-start of each REM period
%%%        ff_new-end of each REM period
%%%        WakeREM-excitation term for fast REM model
%%%
%%%Output: Est_Stage-assigned sleep stages
%%%-------------------------------------------------------------------------%%
%%%-------------------------------------------------------------------------%%
function [Est_Stage]=Fast_REM_Main...
(Est_Stage,initRx,initRy,Fs,st_new,ff_new,WakeREM)

%%Moving unstable equilibrium position
Eq_Wake=2-(WakeREM);

%%Cycle through for each REM period
```

```
for ii=1:length(st_new)
  Wake_Seg=Eq_Wake(st_new(ii):ff_new(ii));

  %%t of fast REM model is on a different scale
  t=0:1/Fs:(ff_new(ii)-st_new(ii))/Fs;
  tnew=0:1/(10.7*Fs*5):(ff_new(ii)-st_new(ii))/Fs;
  Wake_Seg_sp = spline(t,Wake_Seg,tnew);

  lenT=(ff_new(ii)-st_new(ii)+1)/Fs*10.7*5;
  initREM(1)=initRx(ii);
  initREM(2)=initRy(ii);

  delta=.06;
  w=0.3*2*pi;
  A=0.50;

  %%Calculate Duffing oscillator solution
  [T,X]=Phasic_Tonic_Calc(delta,w,Wake_Seg_sp,A,Fs,lenT-1,initREM);

  %%Initial assignment of REM sleep stages
  %%1-Tonic, 0-Phasic, -1-Wake
  X=X(:,1);
  REM_Stage=0;
  I=find(X>=0);
  REM_Stage(I)=1;
  I=find(X<0 & X>-2);
  REM_Stage(I)=0;
  I=find(X<=-2);
  for jj=1:length(I)
    if Wake_Seg_sp(I(jj))<1.9
      REM_Stage(I(jj))=-1;
    else
      REM_Stage(I(jj))=0;
    end
  end

  [st, ff]=calc_tonic_phasic_int(REM_Stage);
  REM_Stage_New=REM_Stage;

  %%Correction for Tonic REM
  if st(1)~=0 && ff(1)~=0
    for jj=1:length(ff)
      if min(X(st(jj):ff(jj)))>=-.25
        REM_Stage_New(st(jj):ff(jj))=1;
      end
    end
  end
  [st, ff]=calc_tonic_phasic_int(REM_Stage_New);

  %%Tonic REM period less than 15 seconds is equal to previous stage
  if st(1)~=0 && ff(1)~=0
   for jj=1:length(ff)
```

```
    if ff(jj)-st(jj)<.25*5*Fs && st(jj)>1
      REM_Stage_New(st(jj):ff(jj))=REM_Stage_New(st(jj)-1);
    end
  end
end

%%Correct for Phasic period in which max is not near 0.5
TempREM_Phasic=ones(1,length(REM_Stage_New));
I=find(REM_Stage_New==1);
TempREM_Phasic(I)=zeros(1,length(I));
[st, ff]=calc_tonic_phasic_int(TempREM_Phasic);
if st(1)~=0 && ff(1)~=0
  for jj=1:length(ff)
    if max(X(st(jj):ff(jj)))<.25
      REM_Stage_New(st(jj):ff(jj))=0;
    end
  end
end

%%Correct if awakening started during noise event-find its end
tempEvents=ones(1,length(REM_Stage_New));
I=find(Wake_Seg_sp<1.9);
tempEvents(I)=zeros(1,length(I));
[stN, ffN]=calc_tonic_phasic_int(tempEvents);

if ffN(1)~=0 && ffN(length(ffN))<length(X)
  for jj=1:length(ffN)
    if X(ffN(jj))<-2 && X(ffN(jj)+1)<-2
      I=find(X(ffN(jj):length(X))>-2);
      if length(I)~=0
        REM_Stage_New(ffN(jj):ffN(jj)-1+I(1))=-1;
      end
    end
  end
end

%%Determine sleep stage- five points for every one point in slow models.
stageREM=[-1 0 1];
REM_StageFinal=0;
for jj=1:length(X)/(5*10.7)
  for kk=1:3
    I=length(find(REM_Stage_New((jj-1)*5*10.7+1:jj*5*10.7)==stageREM(kk)));
    perseg(kk)=I/length(REM_Stage_New((jj-1)*5*10.7+1:jj*5*10.7));
  end
  I=find(perseg==max(perseg));
  REM_StageFinal(jj)=stageREM(I(1));
  if REM_StageFinal(jj)==-1
    Est_Stage(st_new(ii)+jj-1)=1;%%Stage Wake/S1
  else
    Est_Stage(st_new(ii)+jj-1)=5;%%Stage REM
  end
end
```

```
end
%%%-------------------------------------------------------------------------%%
%%%-------------------------------------------------------------------------%%
```

Function Phasic_Tonic_Calc: The following program is used to calculate the fast REM activity based on the Duffing model with the 5th order stiffness term.

```
%%%-------------------------------------------------------------------------%%
%%%-------------------------------------------------------------------------%%
%%%Function Phasic_Tonic_Calc
%%%Program for Duffings system with a 5th order stiffness term
%%%
%%%Reference:G. X. Li and F. C. Moon.  Criteria for chaos of a three-well
%%%potential oscillator with homoclinic and heteroclinic orbits. Journal
%%%of Sound and Vibration. 136(1): 17-34, 1990.
%%%
%%%Input:  delta-damping
%%%        w-drive frequency
%%%        Wake-spontaneous and aircraft excitations
%%%        A-drive amplitude
%%%        Fs-sampling rate
%%%        len-length of night that is being simulated
%%%        init-inital conditions
%%%
%%%Output: X-fast REM model
%%%-------------------------------------------------------------------------%%
%%%-------------------------------------------------------------------------%%
function [T,X]=Phasic_Tonic_Calc(delta,w,Wake,A,Fs,len,init)
options = odeset('RelTol',1e-6);
[T,X]=ode45(@(t,X) fun(t,X,delta,w,Wake,A,Fs),1/Fs:1/Fs:len,init,options);
end

function dxdt=fun(t,X,delta,w,Wake,A,Fs)
time=(0:1:(length(Wake)-1))/Fs;
m=interp1(time,Wake,t);
dxdt=zeros(2,1);

dxdt(1)=X(2);
dxdt(2)=-1*((X(1)-0.5)*(X(1)-0))*(X(1)+0.5)*(X(1)+m)*(X(1)+2.5)...
-delta*X(2)+A*cos(w*t);
end
%%%-------------------------------------------------------------------------%%
%%%-------------------------------------------------------------------------%%
```

Function Phasic_Tonic_Calc: The following program is used to calculate the inter-arrival times of Phasic or Tonic REM sleep.

```
%%%-------------------------------------------------------------------------%%
%%%-------------------------------------------------------------------------%%
%%%Function Phasic_Tonic_Calc
%%%Program for determing start and end points of certain activity, for
%%%example calculating the inter-arrival time of phasic activity
%%%
%%%Input:  REM_Dens-fast REM model sleep stages
%%%
%%%Output: st-start
%%%        ff-end
%%%-------------------------------------------------------------------------%%
%%%-------------------------------------------------------------------------%%
function [st, ff]=calc_tonic_phasic_int(REM_Dens)
st=0;
ff=0;
ink(1:2)=1;%%ink(1) start, %%ink(2)=fin
for kk=1:length(REM_Dens)
  if REM_Dens(kk)==0 && kk <length(REM_Dens)
    if kk==1
      st(ink(1))=kk;
      ink(1)=ink(1)+1;
    elseif REM_Dens(kk-1)~=0
      st(ink(1))=kk;
      ink(1)=ink(1)+1;
    end
    if REM_Dens(kk+1)~=0
      ff(ink(2))=kk;
      ink(2)=ink(2)+1;
   end
  elseif REM_Dens(kk)==0 && kk ==length(REM_Dens)
   if REM_Dens(kk-1)~=0
     st(ink(1))=kk;
     ff(ink(2))=kk;
     ink(1)=ink(1)+1;
     ink(2)=ink(2)+1;
   else
     ff(ink(2))=kk;
     ink(2)=ink(2)+1;
     end
  end
end
%%%-------------------------------------------------------------------------%%
%%%-------------------------------------------------------------------------%%
```

Function Calc_30_Sec_Stages: The following program is used to calculate 30 second sleep stages.

```
%%%-------------------------------------------------------------------------%%
%%%-------------------------------------------------------------------------%%
```

```
%%%Function Calc_30_Sec_Stages
%%%Program for calculating 30 second sleep stages
%%%
%%%Input:  Est_Stage-1 second sleep stages
%%%
%%%Output: tempstage-30 second sleep stages
%%%        tempstage30plot-30 second sleep stages for plotting
%%%-------------------------------------------------------------------------%%
%%%-------------------------------------------------------------------------%%
function [tempstage,tempstage30plot]=Calc_30_Sec_Stages(Est_Stage)
val=[1 2 3 5];

tempstage=0;
tempstage30plot=0;
for ii=1:length(Est_Stage)/(30)
  for kk=1:length(val)
    I=find(Est_Stage((ii-1)*30+1:ii*30-1)==val(kk));
    per(ii,kk)=length(I)/(30);
  end

  maxval=max(per(ii,:));
  I=find(per(ii,:)==maxval);
  tempstage(ii)=I(1);

  if tempstage(ii)==4
    tempstage30plot(ii)=3;
  elseif tempstage(ii)==3
    tempstage30plot(ii)=1;
  elseif tempstage(ii)==2
    tempstage30plot(ii)=2;
  elseif tempstage(ii)==1
    tempstage30plot(ii)=4;
  end
end
%%%-------------------------------------------------------------------------%%
%%%-------------------------------------------------------------------------%%
```

Appendix H. Code for Feature Extraction and Sleep Stage Scoring

The following is the Matlab program used for extracting different features of the polysomnography data and for scoring sleep stages. The first part of the program extracts characteristics such as the occurrence of movement artifacts, level of EMG activity, correlation of EOG channels, power in EEG frequency bands, and the frequency with the lowest decay rate identified using Auto-Regressive modeling. An example of some of the features that were extracted for one subject night is shown in Figure H.1. Sleep stages are assigned for each second based on the extracted features using a classification algorithm that was developed and the probability of being in different sleep stages was calculated for each 30 seconds of scored sleep stages, an example for one subject night is shown in Figure H.2. An overview of the subroutines of the program is in Table H.1.

Table H.1. Subroutines of the feature extraction code and sleep stage scoring algorithm.

Subroutine Name	Is Called By	Makes Calls to
Movement_Artifacts_Threshold	Main_Feature_Calc	None
Dominant_Band_AR	Main_Feature_Calc	None
Calc_Correlation	Main_Feature_Calc	None
RLS_Calc	Main_Feature_Calc	None
Amplitude_Time_Exceeded	Main_Feature_Calc	None
Per_Power	Main_Feature_Calc	None
Power_Welch	Main_Feature_Calc	None
Classify_Stage	None	Calc_REM_Periods
Calc_REM_Periods	Classify_Stage	None

Function Main_Feature_Calc: This is the main program for extracting features of polysomnography data for later use. The data is saved and then imported into the separate sleep stage classification program.

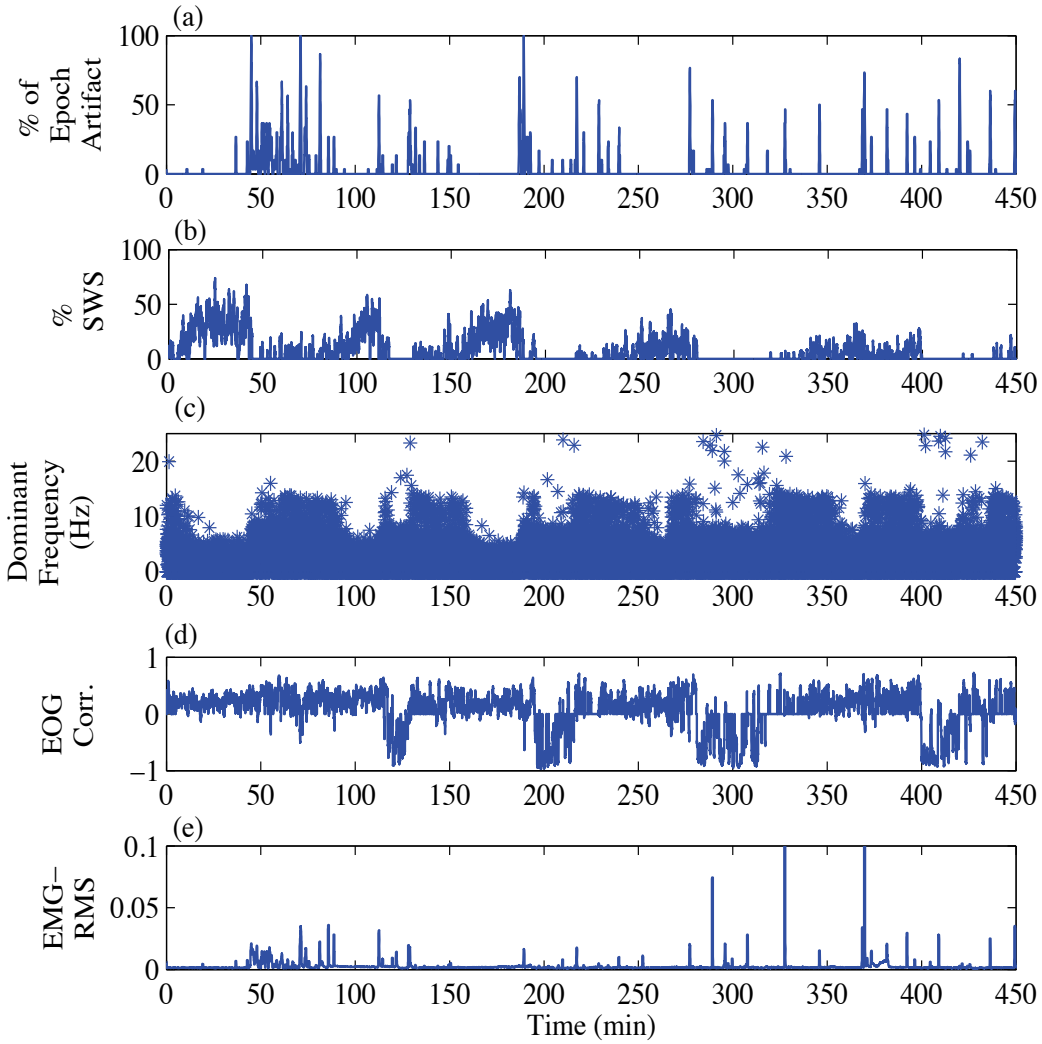

Figure H.1. An example of some of the characteristics that are extracted including; (a) the percent of an epoch occupied by movement artifacts, (b) the percent of an epoch occupied by Slow Wave Sleep (SWS), (c) the frequency that has the lowest decay rate identified using an AR(4) model, (d) correlation between the right and left EOG channels, and (e) the root-mean-square (RMS) of the EMG activity for each epoch.

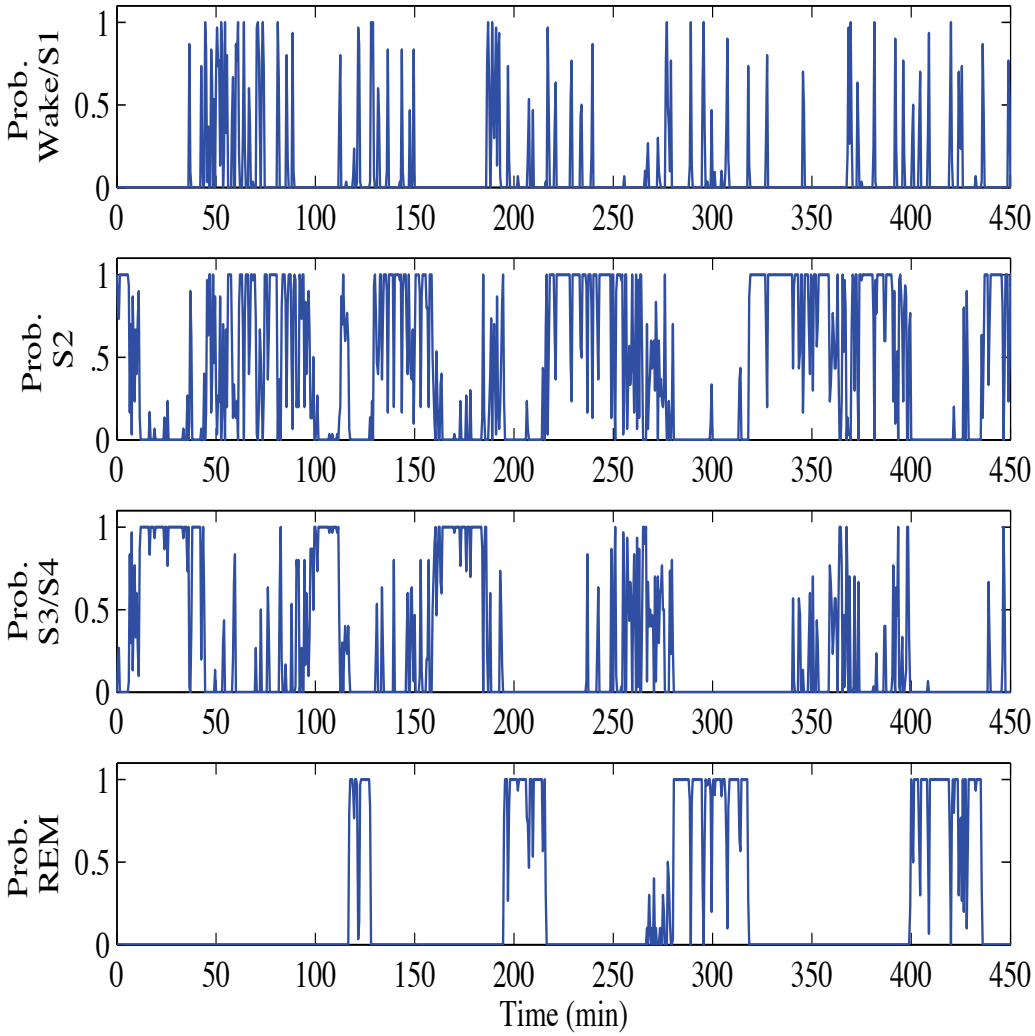

Figure H.2. Probability of being in Stage Wake/S1, Stage 2, Stage 3/4, and REM sleep calculated using the developed sleep stage scoring algorithm.

```
%%%-------------------------------------------------------------------------%%
%%%-------------------------------------------------------------------------%%
%%%Function Main_Feature_Calc
%%%Main code for extracting and saving signal characteristics for later
%%%analysis
%%%Input:  subject_num-subject number
%%%        night_num-night number
%%%        Seg_Len-length of moving signal (i.e. usually 15 or 30 seconds)
%%%        inc_Len-length of increment in time (i.e. usually 1 for 1 second)
%%%        Fs-sampling rate
%%%        correct_option-'correct' if EKG and EOG artifact corrections
%%%        are going to be applied to the EEG data
%%%        EKG_File-indicates whether the EKG file is usuable or not for
%%%        correction, equal to 0 if it is fine to use, 1 if it contains
%%%        artifacts
%%%
%%%Output: The data is saved as .mat files within this
%%%        program
%%%-------------------------------------------------------------------------%%
%%%-------------------------------------------------------------------------%%
function Main_Feature_Calc...
(subject_num, night_num,Seg_Len,inc_Len,Fs,correct_option,EKG_File)

%%Read in the Physiological Data from 1999 UK dataset
choice={'C4-A1','C3-A2','EMG','EOG-L','EOG-R','EKG','Stages'};
[Signals, Stages, Missing_Data]=Load_Signals(subject_num,night_num,choice);

%%For EOG and EKG Corrections
lambda = .9999; %%Forgetting Factor
delta = .01; %%Initial Value
M=3;%%Filter Order

%%Indentify movement artifacts
%%ART indicates whether a 1 second epoch was above the threshold (1 there
%%is an artifact and 0 there is not an artifact.)
%%Cycle through twice for both EEG channels
for ii=1:2
  [ART_Thres(:,ii),ART_Thres_onesec(:,ii)]...
  =Movement_Artifacts_Threshold(Signals(:,ii),Fs,inc_Len);
end

%%Frequency Bands
bandHigh= [ 2 4.5 4.5 8 12 16 25  35 45 15 14 45];
bandlow=  [.5 2  .5  4.5 8 12 16  25 35 11 12 .5];

%%Save AR Model for every increment
Band=[.5 45];
Size=1;
for jj=1:2
  [Damp_AR(:,jj) Freq_AR(:,jj)]=Dominant_Band_AR...
  (Signals(:,jj),Band,floor(length(Signals(:,1))/(Fs)),Size,inc_Len,Fs);
```

```
end

%%Incase I want to run for multiple segment lengths
for ink=1:length(Seg_Len)
  %%Preallocate Space
  SWS=zeros((length(ART_Thres(:,1)))-Seg_Len,2);
  ART=zeros((length(ART_Thres(:,1)))-Seg_Len,2);
  Pow=zeros((length(ART_Thres(:,1)))-Seg_Len,length(bandHigh),2);
  Pow_Welch=zeros((length(ART_Thres(:,1)))-Seg_Len,length(bandHigh),2);
  EOG_Corr=zeros((length(ART_Thres(:,1)))-Seg_Len,1);
  maxEOG=zeros((length(ART_Thres(:,1)))-Seg_Len,2);
  EMG_RMS=zeros((length(ART_Thres(:,1)))-Seg_Len,1);
  K_Complex=zeros((length(ART_Thres(:,1)))-Seg_Len,30,1);
  inc=1;
 for kk=1:(length(ART_Thres(:,1)))-Seg_Len
   display(kk)
   for jj=1:2%%Cycle twice for both EEG channels
    Seg=Signals((kk-1)*inc_Len*Fs+1:(kk-1)*inc_Len*Fs+Seg_Len(ink)*Fs,jj);
    ART(kk,jj)=sum(ART_Thres((kk-1)*1+1:(kk-1)*1+Seg_Len(ink),jj));
    EKG=Signals((kk-1)*inc_Len*Fs+1:(kk-1)*inc_Len*Fs+Seg_Len*Fs,6);
    EOGL=Signals((kk-1)*inc_Len*Fs+1:(kk-1)*inc_Len*Fs+Seg_Len*Fs,4);
    EOGR=Signals((kk-1)*inc_Len*Fs+1:(kk-1)*inc_Len*Fs+Seg_Len*Fs,5);
    EMG=Signals((kk-1)*inc_Len*Fs+1:(kk-1)*inc_Len*Fs+Seg_Len*Fs,3);

    if jj==1;%%Don't need this step for both cycles through
      Band=[.5 5];
      Thresholds=[25 250];
      %%Calculate EOG_Corr
      [EOG_Corr(kk) maxEOG(kk,1:2)]=Calc_Correlation...
      (EOGL,EOGR,Thresholds,Band,Fs);
      %%Calculate EMG RMS
      EMG_RMS(kk)=sqrt(mean(abs(EMG).^2));
    end

    %%If the EEG signal is going to be corrected for EKG and EOG artifacts
    if strcmp(correct_option,'correct')
    %%if EKG signal is usuable && low amount of movement artifacts
       if EKG_File==0 && ART(kk,jj)<15
         %%For EKG Correction
         %%Determine if segment contains EKG
         [CC]=...
         Calc_Correlation(Seg,EKG,[0 1.1*max([max(Seg) max(EKG)])],[.5 40],Fs);

         if abs(CC)>=.2 %%If EEG and EKG are Correlated
           %%EKG input signal measured in mV, EEG is measured in micro volts
           u=EKG*1000;
           d=Seg;%%Contaminated/desired EEG signal
           %%use RLS to correct EEG signal
           %%"Fixed Signal" is the output error of RLS
           [Seg,w,h]=RLS_Calc(lambda,M,u,d,delta);
         end
       end
```

```
        %%For EOG Correction
        %%Determine if segment contains eye mvmts
        %%if eye Movement && low amount of EEG artifacts
        if EOG_Corr(kk)<=-.2 && ART(kk,jj)<15
          Band=[.5 5];
          Thresholds=[25 250];

          %%Corr between EEG and EOGL
          [CCL]=Calc_Correlation(EOGL,Seg,Thresholds,Band,Fs);
          %%Corr between EEG and EOGR
          [CCR]=Calc_Correlation(EOGR,Seg,Thresholds,Band,Fs);

           %%Determine if EEG and EOG signals are correlated
           if abs(CCL)>=abs(CCR) && abs(CCL)>=.2%%Use Signal most correlated
             u=EOGL;%%input signal
             d=Seg;%%Contaminated/desired EEG signal
             %%"Fixed Signal" is the output error of RLS
             [Seg,w,h]=RLS(lambda,M,u,d,delta);
           elseif abs(CCR)>=.2
             u=EOGR;%%input signal
             d=Seg;%%Contaminated desired EEG signal
             [Seg,w,h]=RLS_Calc(lambda,M,u,d,delta);
           end
        end
    end

    %%Detect SWS
    Threshold_SWS=[75 250];
    [DataSWS]=Amplitude_Time_Exceeded(Seg,Threshold_SWS,[.5 2],Fs);
    SWS(kk,jj)=sum(DataSWS.Time_Above)/DataSWS.Total_Time;

    %%Power for segment
    [Pow(kk,1:length(bandHigh),jj)]=Per_Power(Seg,bandHigh,bandlow,Fs);

    %%Power using Welch Method
    Band=[.5 45];
    [Pow_Welch(kk,1:length(bandHigh),jj)]=...
    Power_Welch(Seg,bandHigh,bandlow,Band,Fs);
    end
  end
end


%%Save files
save(['Seg_Len_' num2str(Seg_Len(1)) 's' num2str(subject_num) '_n' ...
num2str(night_num) '_Damp_ARburg.mat'],'Damp_AR')
save(['Seg_Len_' num2str(Seg_Len(1)) 's' num2str(subject_num) '_n'...
num2str(night_num) '_Freq_ARburg.mat'],'Freq_AR')
save(['Seg_Len_' num2str(Seg_Len(ink)) 's' num2str(subject_num) '_n'...
num2str(night_num) '_SWS.mat'],'SWS')
save(['Seg_Len_' num2str(Seg_Len(ink)) 's' num2str(subject_num) '_n' ...
```

```
num2str(night_num) '_EOG_Corr.mat'],'EOG_Corr')
save(['Seg_Len_' num2str(Seg_Len(ink)) 's' num2str(subject_num) '_n'...
num2str(night_num) '_ART.mat'],'ART')
save(['Seg_Len_' num2str(Seg_Len(ink)) 's' num2str(subject_num) '_n' ...
num2str(night_num) '_EMG_RMS.mat'],'EMG_RMS')
save(['Seg_Len_' num2str(Seg_Len(ink)) 's' num2str(subject_num) '_n'...
num2str(night_num) '_Pow.mat'],'Pow')
save(['Seg_Len_' num2str(Seg_Len(ink)) 's' num2str(subject_num) '_n'...
num2str(night_num) '_Pow_Welch.mat'],'Pow_Welch')
save(['Seg_Len_' num2str(Seg_Len(ink)) 's' num2str(subject_num) '_n'...
num2str(night_num) '_maxEOG.mat'],'maxEOG')
save(['Seg_Len_' num2str(Seg_Len(ink)) 's' num2str(subject_num) '_n'...
num2str(night_num) '_ART_Thres.mat'],'ART_Thres')
save(['Seg_Len_' num2str(Seg_Len(ink)) 's' num2str(subject_num) '_n'...
num2str(night_num) '_ART_Thres_onesec.mat'],'ART_Thres_onesec')
end
%%%-------------------------------------------------------------------------%%
%%%-------------------------------------------------------------------------%%
```

Function Movement_Artifacts_Threshold: This program is used to identify when movement artifacts are occurring based on activity in the gamma frequency band of the EEG signal.

```
%%%-------------------------------------------------------------------------%%
%%%-------------------------------------------------------------------------%%
%%%Function Movement_Artifacts_Threshold
%%%Code for calculating thresholds which are used to identify movement
%%%artifacts.  The method used is based on the work of Brunner et al.
%%%
%%%Reference: D. P. Brunner, R. C. Vasko, C. S. Detka, J. P. Monahan, C. F.
%%%Reynolds III and D. J. Kupfer.  Muscle artifacts in the sleep EEG:
%%%Automated detection and effect on all-night EEG power spectra.  J. Sleep
%%%Res. 5: 155-164, 1996.
%%%
%%%Input:  Signal-typically the EEG channel
%%%        Fs-is the sampling frequency
%%%        inc_Len-size of increment in time (i.e. usually 1 for 1 second)
%%%
%%%Output: ART-indicator of artifacts, 1 if there is an artifact and 0 if
%%%        there is not an artifact
%%%        ART_Thres_re-threshold used for defining artifacts
%%%-------------------------------------------------------------------------%%
%%%-------------------------------------------------------------------------%%
function [ART,ART_Thres_re]=Movement_Artifacts_Threshold(Signal,Fs,inc_Len)

%%Consider only activity from 26 to 32 Hz
[b,a]=butter(4,[26 32]./(Fs/2),'bandpass');
Filt_Signal=filtfilt(b,a,Signal);
```

```
%%Calculate average power every 4 seconds
meanval=zeros(1,length(Signal)/(4*Fs));

for ii=1:length(Signal)/(4*Fs)
  meanval(ii)=mean(abs(Filt_Signal((ii-1)*4*Fs+1:ii*4*Fs)).^2);
end

pow_smooth=medfilt1(meanval,45); %%Brunner smoothed out the spectrum for the
                                 %%threshold using the
                                 %%surrounding three minutes
                                 %%three minutes divided by 4 second epochs
                                 %%is 45 points

ART_Thres_4sec=pow_smooth.*4;%%Brunner found that 4* the smoothed threshold
                             %%provided the best results

%%Resample threshold
len=length(Signal)/(inc_Len*Fs)-(4/inc_Len);
t=(0:1:length(ART_Thres_4sec)-1)*4;
tnew=(0:1:(len-1))*inc_Len;
ART_Thres_re=spline(t,ART_Thres_4sec,tnew);

%%Cycle through signal and and determine if the mean of the
%%signal is above the smoothed out threshold
for ii=1:length(ART_Thres_re)
  meanval(ii)=mean(abs(Filt_Signal((ii-1)*inc_Len*Fs+1:ii*inc_Len*Fs)).^2);
  if meanval(ii)> ART_Thres_re(ii)
    ART(ii)=1;
  else
    ART(ii)=0;
  end
end
end
%%%-------------------------------------------------------------------------%%
%%%-------------------------------------------------------------------------%%
```

Function Dominant_Band_AR: This program is used to determine the frequency with the lowest decay rate using an AR model.

```
%%%-------------------------------------------------------------------------%%
%%%-------------------------------------------------------------------------%%
%%%Function Dominant_Band_AR
%%%Code for calculating the frequencies that have the least damping
%%%identified using an AR model. The approach is based on Olbrich and
%%%Achermann.
%%%
%%%Reference: E. Olbrich and P. Achermann. Analysis of the temporal
%%%organization of sleep spindles in the human sleep EEG using a
```

```
%%%phenomenological modeling approach. Journal of Biological Physiology,
%%%34:341349, 2008.
%%%
%%%Input:  Signal-the EEG signal
%%%        Band-frequency band limits for filtering
%%%        Seg_Len-length of signal being used
%%%        Size-length of sub-segment
%%%        inc_Len-length of increment in time (i.e. usually 1 for 1 second)
%%%        Fs-the sampling frequency
%%%
%%%Output: max_freq-frequency associated with the minimum damping
%%%        max_damp-minimum damping value.
%%%-------------------------------------------------------------------------%%
%%%-------------------------------------------------------------------------%%

function [max_damp,max_freq]=Dominant_Band_AR(Signal,Band,Seg_Len,Size,inc_Len,Fs)
[b,a]=butter(4,[Band(1) Band(2)]./(Fs/2),'bandpass');
Seg=filtfilt(b,a,Signal);

N=4;%%Order of AR filter

%%preallocate space
max_damp=zeros((Seg_Len/inc_Len)-Size,1);
max_freq=zeros((Seg_Len/inc_Len)-Size,1);

%%Determine frequency and damping
for ii=1:floor(Seg_Len/inc_Len)-Size
  [a,e]=arburg(Seg((ii-1)*Fs*inc_Len+1:(ii-1)*Fs*inc_Len+1+Fs*Size),N);
  damping=abs(roots(a));
  freq=rad2deg(abs(angle(roots(a))))*(Fs/2)/180;

  %%find maximum value
  maxval=max(damping);
  I=0;
  I=find(damping==maxval);
  if length(I)>1
    I2=find(freq(I)>=.5 & freq(I)<45);
    if length(I2)>0
      freqval=min(freq(I(I2)));
    else
      freqval=min(freq(I));
    end
  else
    freqval=freq(I(1));
  end
  if freqval>=Band(1) &&  freqval<Band(2)
    max_damp(ii)=maxval;
    max_freq(ii)=freqval;
  else
    max_damp(ii)=0;
    max_freq(ii)=0;
  end
```

```
end
%%%-------------------------------------------------------------------------%%
%%%-------------------------------------------------------------------------%%
```

Function RLS_Calc: This program is used to create a Recursive Least Squares Filter (RLS) for removing eye movement and ECG artifacts from EEG data.

```
%%%-------------------------------------------------------------------------%%
%%%-------------------------------------------------------------------------%%
%%%Function RLS_Calc
%%%Code for Recursive Least Squares Filter
%%%
%%%Reference: S. Haykin Adaptive Filter Theory. Prentice Hall, Upper Saddle
%%%River, New Jersey, 3rd edition, 1996.
%%%
%%%Input:  Lambda=forgetting factor
%%%        M = filter order
%%%        x=input signal (ECG or EOG)
%%%        d=desired signal (contaminated EEG)
%%%        delta=initial value
%%%
%%%Output: e = error estimate (corrected signal)
%%%        h = filter coefficients
%%%-------------------------------------------------------------------------%%
%%%-------------------------------------------------------------------------%%
function [e,w,h]=RLS_Calc(lambda,M,x,d,delta)
w=zeros(M,1);
P=eye(M)/delta;

x=x(:);
d=d(:);
len=length(x);

%%error vector
e=d;

for ii=M:len
  x_est=x(ii:-1:ii-M+1);
  k=P*x_est/(lambda+x_est'*P*x_est);
  e(ii)=d(ii)-w'*x_est;
  w=w+k*conj(e(ii));
  h(:,ii)=w;
  P=lambda^(-1)*P-lambda^(-1)*k*x_est'*P;
end
%%%-------------------------------------------------------------------------%%
%%%-------------------------------------------------------------------------%%
```

Function Calc_Correlation: This program is used to calculate the correlation between two signals.

```
%%%-------------------------------------------------------------------------%%
%%%-------------------------------------------------------------------------%%
%%%Function Calc_Correlation
%%%Code for calculating the correlation between two signals
%%%
%%%Input:  Seg1-Signal 1
%%%        Seg2-Signal 2
%%%        Thresholds-minimum and maximum amplitude of signal
%%%        primarily used for EOG to eliminate artifacts
%%%        Band-frequency band limits
%%%        Fs-the sampling frequency
%%%
%%%Output: CC-correlation of the two channels
%%%-------------------------------------------------------------------------%%
%%%-------------------------------------------------------------------------%%
function [CC,maxval]=Calc_Correlation(Seg1,Seg2,Thresholds,Band,Fs)

if Band(1)~=0
   [b,a]=butter(4,[Band(1) Band(2)]./(Fs/2),'bandpass');
   temp1=filtfilt(b,a,Seg1);
   temp2=filtfilt(b,a,Seg2);
else
  [b,a]=butter(4,Band(2)./(Fs/2),'low');
  temp1=filtfilt(b,a,EOGL);
  temp2=filtfilt(b,a,EOGR);
end

maxval(1)=max(abs(temp1));
maxval(2)=max(abs(temp2));

if maxval(1)<Thresholds(2) && maxval(2)<Thresholds(2) && ...
maxval(1)>Thresholds(1) && maxval(2)>Thresholds(1)
 C=corrcoef(temp1,temp2);
 CC=C(1,2);
else
 CC=0;
end
%%%-------------------------------------------------------------------------%%
%%%-------------------------------------------------------------------------%%
```

Function Amplitude_Time_Exceeded: This program is used to calculate the percent of each epoch occupied by slow wave sleep.

```
%%%-------------------------------------------------------------------------%%
%%%-------------------------------------------------------------------------%%
%%%Function Amplitude_Time_Exceeded
%%%Code for calculating peak to peak amplitude critera
%%%
%%%Reference: H. Kuwahara, H. Higashi, Y. Mizuki, S. Matsunari, M. Tanaka,
%%%and K. Inanaga.  Automatic real-time analysis of human sleep stages by
%%%an interval histogram method. Electroencephalography and Clinical
%%%Neurophysiology, 70: 220-229,1988.
%%%
%%%Input:  Signal-either the EOG, EEG, or EMG signal
%%%        Thresholds-vector containing the minimum and maxmium amplitude
%%%        Band-frequency band limits
%%%        Fs-sampling frequency
%%%
%%%Output: Data.Time_Above-time the signal is within the specified thresholds
%%%        Data.Total_Time-total time of segment
%%%        Data.Range-maximum value of signal between zero crossings
%%%        Data.Duration-duration of the signal between zero crossings
%%%        Data.Start_Time-start time of each zero crossing
%%%        Data.End_Time-end time of each zero crossing
%%%-------------------------------------------------------------------------%%
%%%-------------------------------------------------------------------------%%
function [Data]= Amplitude_Time_Exceeded(Signal,Thresholds,Band,Fs)
[b,a]=butter(4,[Band(1) Band(2)]./(Fs/2),'bandpass');
Seg=filtfilt(b,a,Signal);

greater=[];
greater=find(Seg>=0);%%Find values greater then 0

incpos=1;
crossingpos=[];
incneg=1;
crossingneg=[];

%%Find all zero crossings
for ii=1:length(greater)
  if (greater(ii)-1)>0 && (greater(ii)+1)<length(Seg)
    if Seg(greater(ii)-1)<0 && Seg(greater(ii)+1)>0 %%make sure it is a crossing
      crossingpos(incpos)=greater(ii);
      incpos=incpos+1;
    end
    if Seg(greater(ii)+1)<0 && Seg(greater(ii)-1)>0
      crossingneg(incneg)=greater(ii);
      incneg=incneg+1;
    end
  end
end

%%Find the start, end, range, and duration for each crossing
ink=1;
if crossingpos(1)<crossingneg(1)
```

```
  lenval= length(crossingpos)-1;
else
  lenval= length(crossingneg)-1;
end
for ii=1:lenval
  if crossingpos(1)<crossingneg(1)
    temp=abs(Seg(crossingpos(ii):crossingneg(ii)));
    Data.Range(ink)=max(abs(Seg(crossingpos(ii):crossingneg(ii))));
    Data.Duration(ink)=(crossingneg(ii)-crossingpos(ii))/Fs;
    Data.Start_Time(ink)=crossingpos(ii)/Fs;
    Data.End_Time(ink)=crossingneg(ii)/Fs;
    ind=[];
    ind=find(temp==Data.Range(ink));
    Data.Max_Time(ink)=(ind(1)-1)/Fs;
    ink=ink+1;

    temp=abs(Seg(crossingneg(ii):crossingpos(ii+1)));
    Data.Range(ink)=max(abs(Seg(crossingneg(ii):crossingpos(ii+1))));
    Data.Duration(ink)=(crossingpos(ii+1)-crossingneg(ii))/Fs;
    Data.Start_Time(ink)=crossingneg(ii)/Fs;
    Data.End_Time(ink)=crossingpos(ii+1)/Fs;
    ind=[];
    ind=find(temp==Data.Range(ink));
    Data.Max_Time(ink)=(ind(1)-1)/Fs;
    ink=ink+1;
  else
    temp=abs(Seg(crossingneg(ii):crossingpos(ii)));
    Data.Range(ink)=max(abs(Seg(crossingneg(ii):crossingpos(ii))));
    Data.Duration(ink)=(crossingpos(ii)-crossingneg(ii))/Fs;
    Data.Start_Time(ink)=crossingneg(ii)/Fs;
    Data.End_Time(ink)=crossingpos(ii)/Fs;
    ind=[];
    ind=find(temp==Data.Range(ink));
    Data.Max_Time(ink)=(ind(1)-1)/Fs;
    ink=ink+1;

    temp=abs(Seg(crossingpos(ii):crossingneg(ii+1)));
    Data.Range(ink)=max(abs(Seg(crossingpos(ii):crossingneg(ii+1))));
    Data.Duration(ink)=(crossingneg(ii+1)-crossingpos(ii))/Fs;
    Data.Start_Time(ink)=crossingpos(ii)/Fs;
    Data.End_Time(ink)=crossingneg(ii+1)/Fs;
    ind=[];
    ind=find(temp==Data.Range(ink));
    Data.Max_Time(ink)=(ind(1)-1)/Fs;
    ink=ink+1;
  end
end
ii=length(crossingpos);
if crossingpos(1)<crossingneg(1)  && length(crossingneg)==length(crossingpos)
  temp=abs(Seg(crossingpos(ii):crossingneg(ii)));
  tempSign=Seg(crossingpos(ii):crossingneg(ii));
  Data.Range(ink)=max(abs(Seg(crossingpos(ii):crossingneg(ii))));
```

```
  Data.Duration(ink)=(crossingneg(ii)-crossingpos(ii))/Fs;
  Data.Start_Time(ink)=crossingpos(ii)/Fs;
  Data.End_Time(ink)=crossingneg(ii)/Fs;
  ind=[];
  ind=find(temp==Data.Range(ink));
  Data.Max_Time(ink)=(ind(1)-1)/Fs;
  Data.Range_Sign(ink)=tempSign(ind(1));
elseif length(crossingneg)==length(crossingpos)
  temp=abs(Seg(crossingneg(ii):crossingpos(ii)));
  tempSign=Seg(crossingneg(ii):crossingpos(ii));
  Data.Range(ink)=max(abs(Seg(crossingneg(ii):crossingpos(ii))));
  Data.Duration(ink)=(crossingpos(ii)-crossingneg(ii))/Fs;
  Data.Start_Time(ink)=crossingneg(ii)/Fs;
  Data.End_Time(ink)=crossingpos(ii)/Fs;
  ind=[];
  ind=find(temp==Data.Range(ink));
  Data.Max_Time(ink)=(ind(1)-1)/Fs;
  Data.Range_Sign(ink)=tempSign(ind(1));
end

%%Determine time when peak to peak amplitude is greater than the threshold
Data.Total_Time=sum(Data.Duration);
Data.Time_Above=zeros(1,length(Data.Range));
for ii=1:length(Data.Range)-1
  if (Data.Range(ii)+Data.Range(ii+1))>=Thresholds(1) &&...
   (Data.Range(ii)+Data.Range(ii+1))<=Thresholds(2)
   %%Make sure that half of wave is not contributing to the entire peak to
   %%peak amplitude
   if Data.Range(ii)>=Thresholds(1)*.25 && Data.Range(ii+1)>=Thresholds(1)*.25
     if (Data.Duration(ii)+Data.Duration(ii+1))>=1/Band(2) &&...
      (Data.Duration(ii)+Data.Duration(ii+1))<=1/Band(1)
       Data.Time_Above(ii)=Data.Duration(ii);
       Data.Time_Above(ii+1)=Data.Duration(ii+1);
     end
   end
  end
end
%%%-------------------------------------------------------------------------%%
%%%-------------------------------------------------------------------------%%
```

Function Per_Power: This program is used to calculate the root-mean-square value for the power in each frequency band.

```
%%%-------------------------------------------------------------------------%%
%%%-------------------------------------------------------------------------%%
%%%Function: Per_Power
%%%Code for calculating RMS values for each frequency band
%%%
%%%Input:  EEG-EEG segment
```

```
%%%        BandHigh-upper frequency band limit
%%%        BandLow-lower frequency band limit
%%%        Fs-sampling frequency
%%%
%%%Output: pow-RMS value for each of the specified frequency bands
%%%-------------------------------------------------------------------------%%
%%%-------------------------------------------------------------------------%%
function [pow]=Per_Power(EEG,bandHigh,bandlow,Fs)
pow=zeros(1,length(bandlow));
for ii=1:length(bandlow) %%Cycle through and calculate
  [b,a]=butter(4,[bandlow(ii) bandHigh(ii)]./(Fs/2),'bandpass');
  temp=filtfilt(b,a,EEG);
  pow(ii)=sqrt(mean(abs(temp).^2));
end
end
%%%-------------------------------------------------------------------------%%
%%%-------------------------------------------------------------------------%%
```

Function Power_Welch: This program is used to calculate power in each frequency band.

```
%%%-------------------------------------------------------------------------%%
%%%-------------------------------------------------------------------------%%
%%%Function: Power_Welch
%%%Code for calculating power spectral density
%%%
%%%Reference: F. Ferrillo, S. Donadio, F. De Carli, S. Gabarino, and
%%%L. Nobili. A model-based approach to homeostatic and ultradian
%%%aspects of nocturnal sleep structure in narcolepsy.
%%%Sleep, 30(2):157165, 2007.
%%%
%%%Input:  EEG-EEG segment
%%%        BandHigh-upper frequency band limits
%%%        BandLow-lower frequency band limits
%%%        Band-cutoff frequencies for filter
%%%        Fs-sampling frequency
%%%
%%%Output: Pow-power for each of the specified frequency bands
%%%-------------------------------------------------------------------------%%
%%%-------------------------------------------------------------------------%%
function [Pow]=Power_Welch(EEG,bandHigh,bandlow,Band,Fs)

%%Method is Similar to Ferrillo et al.  Calculate PSD using
%%Welch method.

%%Filter EEG
[b,a]=butter(4,[Band(1)  Band(2)]./(Fs/2),'bandpass');
EEG_filt=filtfilt(b,a,EEG);
```

```
%%Calculate power spectra using the Welch method
%%Use 4 second segments, apply hamming window
%%Use 75% overlap
%%Sum power in each frequency band
window=4*Fs;
noverlap=.75*window;
nfft=2^(nextpow2(8*window));
[Sxx,f] = pwelch(EEG_filt,window,noverlap,nfft,Fs,'onesided');

%%Calculate power in each frequency Band
for ii=1:length(bandHigh)
  start=find(f>=bandlow(ii));
  fin=find(f<bandHigh(ii));
  Pow(ii)=sum(Sxx(start(1):fin(length(fin))));
end
%%%-------------------------------------------------------------------------%%
%%%-------------------------------------------------------------------------%%
```

Function Calc_REM_Periods: This program is used to identify the start and end of each REM period.

```
%%%-------------------------------------------------------------------------%%
%%%-------------------------------------------------------------------------%%
%%%Function Calc_REM_Periods
%%%Code for calculating potential REM sleep periods as part of
%%%sleep stage classification algorithm
%%%
%%%Input:  Stages-sleep stages
%%%        inc_len-sliding increment used
%%%
%%%Output: start-start of each potential REM period
%%%        fin-end of each potential REM period
%%%-------------------------------------------------------------------------%%
%%%-------------------------------------------------------------------------%%
function [start,fin]=Calc_REM_Periods(Stages,inc_len)

%%Find start and finish for each REM period
starti=[];
fini=[];
starti=0;
fini=0;
I=find(Stages==5);
starti(1)=I(1);
ink=1;

for kk=2:length(I);
  durStage=length(find(Stages(I(kk-1):I(kk))<5));
  %%definition need greater then 15 minutes
  if durStage>15*floor(60/inc_len)%
```

```
    fini(ink)=I(kk-1);
    ink=ink+1;
    starti(ink)=I(kk);
  end
end

%%Can happen if REM sleep period is at end of night
if length(starti)>length(fini)
  fini(length(starti))=I(length(I));
end

%%Eliminate very brief REM sleep periods
start=[];
fin=[];
ink=1;
for kk=1:length(starti)
  lenREM=length(find(Stages(starti(kk):fini(kk))==5));
  if lenREM>=1*floor(60/inc_len) && fini(kk)-starti(kk)>=2.0*floor(60/inc_len)
    start(ink)=starti(kk);
    fin(ink)=fini(kk);
    ink=ink+1;
  end
end
%%%-------------------------------------------------------------------------%%
%%%-------------------------------------------------------------------------%%
```

Function Classify_Stage: This program is used to automatically classify sleep stages.

```
%%%-------------------------------------------------------------------------%%
%%%-------------------------------------------------------------------------%%
%%%Classify_Stage
%%%Code for automatically classifying sleep stages
%%%
%%%Input:  ART-artifact signal
%%%        SWS-percent of epoch occupied by SWS
%%%        EOG_Corr-correlation between left and right EOG channels
%%%        EMG-RMS-root mean square of EMG activity
%%%        Freq-AR-dominant frequency in the EEG signal
%%%        Alpha-power in the alpha frequency band
%%%        Delta-power in the delta frequency band
%%%        Sigma-power in the sigma frequency band
%%%        Theta-power in the theta frequency band
%%%        Seg-Size-size of segment that sleep stages are being scored
%%%        for
%%%        inc_len-sliding increment used
%%%
%%%Output: Est_Stage-sleep stages for each time increment
%%%        Per_Stage-probility of sleep stage
%%%        Hyp-hypnogram for plotting
%%%        Count_AR-percent of epoch dominated by each frequency
```

```
%%%-------------------------------------------------------------------------%%
%%%-------------------------------------------------------------------------%%

function [Est_Stage,Per_Stage,Hyp,Count_AR]=Classify_Stage...
(ART,SWS,EOG_Corr,EMG_RMS,Freq_AR,Alpha,Delta,Sigma,Theta,Seg_Size,inc_len)
I=find(EMG_RMS>0);
a=sort(EMG_RMS(I));
per_85=a(round(.85*length(a)));%%Most EMG_RMS is below 85 percentile
Est_Stage=85.*ones(1,length(SWS));
ink=1;
Est_Stage(1)=2;
jj=1;
Count_AR=0;

for ii=2:length(Alpha)
  bandHigh= [ 4.5 8 12 16 25  35 ];
  bandlow=  [ .5 4.5 8 12 16  25 ];

  for jj=1:length(bandlow)
    tempFreq_Ar=Freq_AR(ii:ii+floor(Seg_Size/inc_len)-1);
    I=find(tempFreq_Ar>=bandlow(jj) & tempFreq_Ar< bandHigh(jj));
    if length(I)~=0
      Count_AR(ii,jj)=length(I)/Seg_Size;
    else
      Count_AR(ii,jj)=0;
    end
  end
  Count_AR(ii,:)=Count_AR(ii,:)./sum(Count_AR(ii,:));

  if  ART(ii,1)>=5 || Count_AR(ii,3)>=.5
    Est_Stage(ii)=0;

  %%If there is not an artifact
  else
    if EOG_Corr(ii)>-.2 %%no eye movements
    %%.15 is from 2 standard deviations for Stage 2 sleep
      if (SWS(ii)>=.15 || Delta(ii)>=0.7 )
        Est_Stage(ii)=3;
      elseif (SWS(ii)>=.05 && SWS(ii)<.15 ) || (Count_AR(ii,4)>=1/Seg_Size )
        if Est_Stage(ii-1)==3 && Delta(ii)>=0.65 ...
        && Count_AR(ii,4)<=1/Seg_Size && Sigma(ii)<=1/Seg_Size
          Est_Stage(ii)=3;
        else
          Est_Stage(ii)=2;
        end
      else
        if Alpha(ii)/Theta(ii) >=1.5
          Est_Stage(ii)=0;
        elseif Est_Stage(ii-1)==5
          if EMG_RMS(ii)<=per_85 && SWS(ii)<=1/Seg_Size && Delta(ii)<0.45
            Est_Stage(ii)=5;
          else
```

```
            Est_Stage(ii)=0;
          end
        else
          Est_Stage(ii)=2;
        end
      end
    %%Eye Movement
    elseif EOG_Corr(ii)<=-.2
     if EMG_RMS(ii)<=per_85  &&  (Alpha(ii)/Theta(ii))< 1.5 && Delta(ii)<0.45
        Est_Stage(ii)=5;
     else
       Est_Stage(ii)=0;
     end
    end
  end
end

%%Get rid of brief eye movements (single eye movements
%%with no other activity around it)
for ii=floor(61/inc_len):length(Est_Stage)-floor(60/inc_len)
   I=find(Est_Stage(ii-floor(60/inc_len):ii+floor(60/inc_len))==5);
   if length(I)<floor(3/inc_len) && Est_Stage(ii)==5
     Est_Stage(ii)=0;
   end
end

%%Correction for rapid eye movements at the beginning of the
%%night
I=find(Est_Stage(1:30*floor(60/inc_len))==5);
for ii=1:length(I)
  if Est_Stage(I(ii)-1)==0
    Est_Stage(I(ii))=0;
  else
    Est_Stage(I(ii))=2;
  end
end

%%Correct for Stage 2 sleep during REM periods
[start,fin]=Calc_REM_Periods(Est_Stage,inc_len);
ink=1;

for ii=1:length(start)
  for jj=start(ii):fin(ii)
    if Est_Stage(jj)==2  && SWS(jj)<2/30 && Count_AR(jj,4)<=.05
      Est_Stage(jj)=5;
    elseif Est_Stage(jj)==2 && Est_Stage(jj-1)==0  && Alpha(ii)/Theta(ii) >=1.5
      Est_Stage(jj)=0;
    elseif Est_Stage(jj)==2 && Est_Stage(jj-1)==0 && Count_AR(jj,3)>Count_AR(jj,2)
      Est_Stage(jj)=0;
    end
  end
end
```

```
%%Get rid of eye movements not between end points
for ii=1:length(start)
    if ii==1
      I=find(Est_Stage(1:start(ii)-1)==5);
      Est_Stage(I)=0;
    elseif ii<=length(start)
      I=find(Est_Stage(fin(ii-1)+1:start(ii)-1)==5);
      Est_Stage(fin(ii-1)+I)=zeros(1,length(I));
    end
end
if fin(length(fin))+1<length(Est_Stage)
  I=find(Est_Stage(fin(length(fin))+1:length(Est_Stage))==5);
  Est_Stage(fin(length(fin))+I)=0;
end

val=[0 2 3 5];
%%Calc_30 second sleep stages
for ii=1:length(Est_Stage)/floor(30/inc_len)
  for jj=1:length(val)
    Per_Stage(ii,jj)=...
    length(find(Est_Stage((ii-1)*floor(30/inc_len)+1:ii*floor(30/inc_len))...
    ==val(jj)))/floor(30/inc_len);
  end

  maxval=max(Per_Stage(ii,:));
  ind=find(Per_Stage(ii,:)==maxval);
  if length(ind)>1
    if ii~=1
      Hyp(ii)=Hyp(ii-1);
    else
      Hyp(ii)=val(ind(1));
    end
  elseif length(ind)==1
     Hyp(ii)=val(ind(1));
  end
end
%%%-------------------------------------------------------------------------%%
%%%-------------------------------------------------------------------------%%
```

MODELING AIRCRAFT NOISE INDUCED SLEEP DISTURBANCE

(Volume 2)

Sponsored by
FAA/NASA/Transport Canada/DOD/EPA PARTNER Center of Excellence

HL 2012-4

Submitted by: Sarah McGuire, Graduate Research Assistant
Patricia Davies, Principal Investigator

Approved by: Patricia Davies, Director
Ray W. Herrick Laboratories

DECEMBER 2013

7. NONLINEAR SLEEP MODEL DEVELOPMENT AND PARAMETER ESTIMATION

After reviewing the literature on sleep models, the Massaquoi and McCarley nonlinear dynamic model was found to be the best candidate for altering so it could be used to predict the effect of aircraft noise on sleep. However, the model has slow dynamics which makes it difficult to predict brief awakenings including those that occur due to noise. To overcome this limitation additional components were introduced into the models. These components include an additional excitation term which has a dependence on noise level and a model that predicts faster dynamics during a REM period. The parameter values for the modified model were estimated using the 1999 UK study data. This required developing parameter estimation methods and also methods to process the polysomnography data to produce signals that are closely related to the E, $n(t)$, X, Y, SWA and S of the original Massaquoi and McCarley model. Similarly, parameters in the new fast REM part of the model had to be estimated from signals derived from the sleep study data. A method to determine whether a person is in Tonic or Phasic REM sleep, based on the occurrence of Rapid Eye Movement was also developed. The results of simulations using the model will also be presented later in this chapter.

7.1 Limitations of Massaquoi and McCarley Model

Before determining how to add a noise level dependence to the Massaquoi and McCarley model, simulations were conducted using the original model to determine if it could be used to predict trends in sleep stages similar to those observed with other

models. The values of the coefficients of the model, used in the simulations, are listed in Table 7.1 and the equations were provided in Chapter 5 (Equations (5.47), (5.48), (5.49), (5.55), (5.56), (5.57)) . One hundred simulations were performed using the model. The variability in the predictions for each simulation was due to the impulsive excitation term E (filtered square waves) where each impulse has a random arrival time, height, and duration (Massaquoi and McCarley, 1992). The probability of being in NREM, REM and Wake stages was calculated and the results were compared to predictions using Basner's Baseline Markov model (2006). The results are shown in Figure 7.1. The Massaquoi and McCarley model predicted a higher probability of being in NREM sleep than Basner's model, and lower probability of being awake or in REM sleep. In order to improve the predictions of the model the value of c (in Equation (5.48)), which controls the rate of decay of Y (REM-OFF) activity, was increased by 40%. A better agreement was obtained between the predicted probabilities.

Table 7.1. Coefficients of Massaquoi and McCarley's LCRIM/I Model (1992).

Model Parameters	Original Values
c	1
gc	0.05
k	10
rc	3.0
rs	0.005
E_o	0.001
X_o	0.12
Y_o	0.35
S_o	2.0
SWA_o	0.1
N Amplitude	Uniformly distributed between 1.25 and 25
N Duration	Uniformly distributed between 0.25 and 0.5
N Inter-arrival Time	Exponentially distributed with mean of 1.1
$n(t)$	Uniformly distributed between -10 and 10

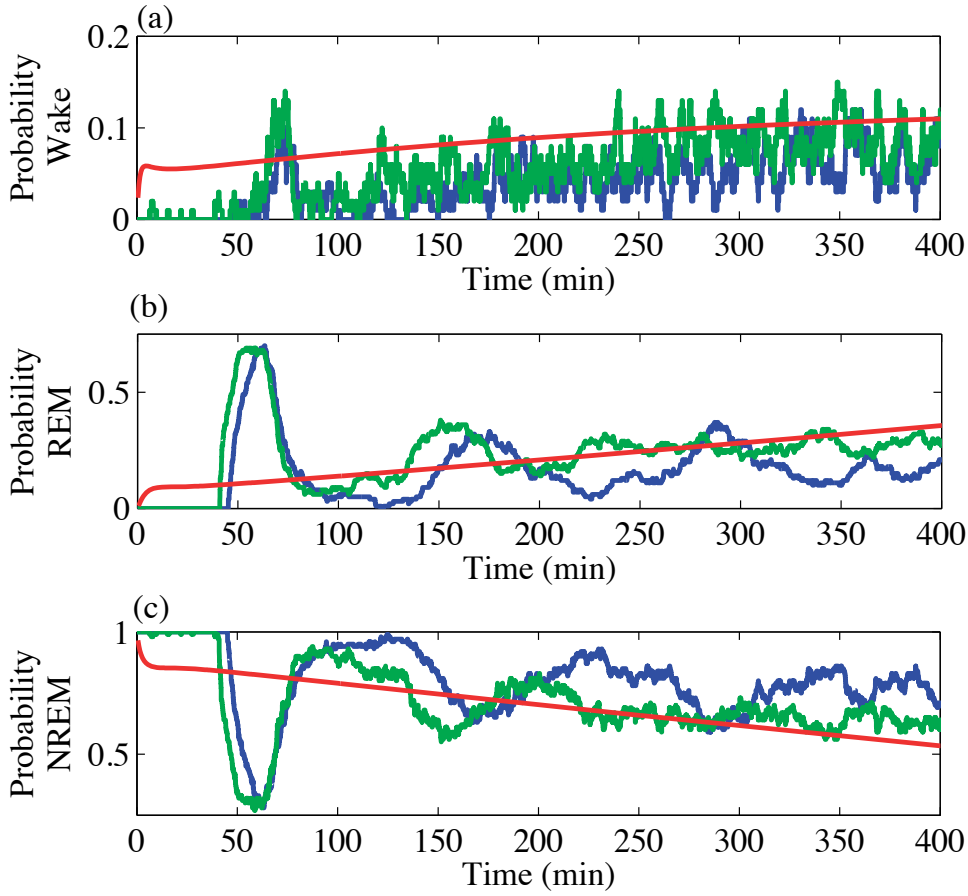

Figure 7.1. Probability of being in Wake, REM, and NREM sleep predicted using the original parameters of the Massaquoi and McCarley model (blue), with the parameter c increased by 40% (green) and with Basner's Markov model (red).

Another difference between the predictions of the two models is that the Massaquoi and McCarley model predictions have oscillations in the probability of being in NREM and REM sleep which Basner's Markov model does not. These ultradian oscillations are partly due to the assumption when performing the simulations that everyone falls asleep at the same time. In one set of simulations it was assumed that everyone retired at the same time (11:00 pm), and in another set of simulations the time to fall asleep was varied randomly for each simulation according to a normal distribution which had a mean start time of 11:00 pm and a standard deviation of 30 minutes. One hundred simulations were conducted using Basner's Markov model (Equation (4.1)) and the Massaquoi and McCarley model (Equations (5.47), (5.48), (5.49), (5.55), (5.56), (5.57)). The results are shown in Figure 7.2. The ultradian cycles in the predictions of the Massaquoi and McCarley model were smoothed out when the sleep onset time was varied and the predictions were more similar to those of Basner's Markov model but with a less pronounced increase in REM towards the end of the night.

While the overall trends in sleep stage predictions between the two models are in agreement, the Massaquoi and McCarley model is not without limitations. One limitation of the model is that awakenings or transitions to lighter sleep are not predicted by the model during a REM sleep period. A transition from REM to Wake and then back to REM cannot occur. In Figure 7.3, an example of a REM period and transitions from REM sleep to Stage Wake and Stage 1 during that period for one night of sleep, from the UK dataset, is shown. The Massaquoi and McCarley model in its current form cannot predict awakenings during REM sleep because the level of X (REM-ON) activity does not oscillate during a REM period. The level of Y (REM-OFF) neuron activity is low when X (REM-ON) activity is high and will not cause a large change in the level of X when an excitation occurs. An alternative

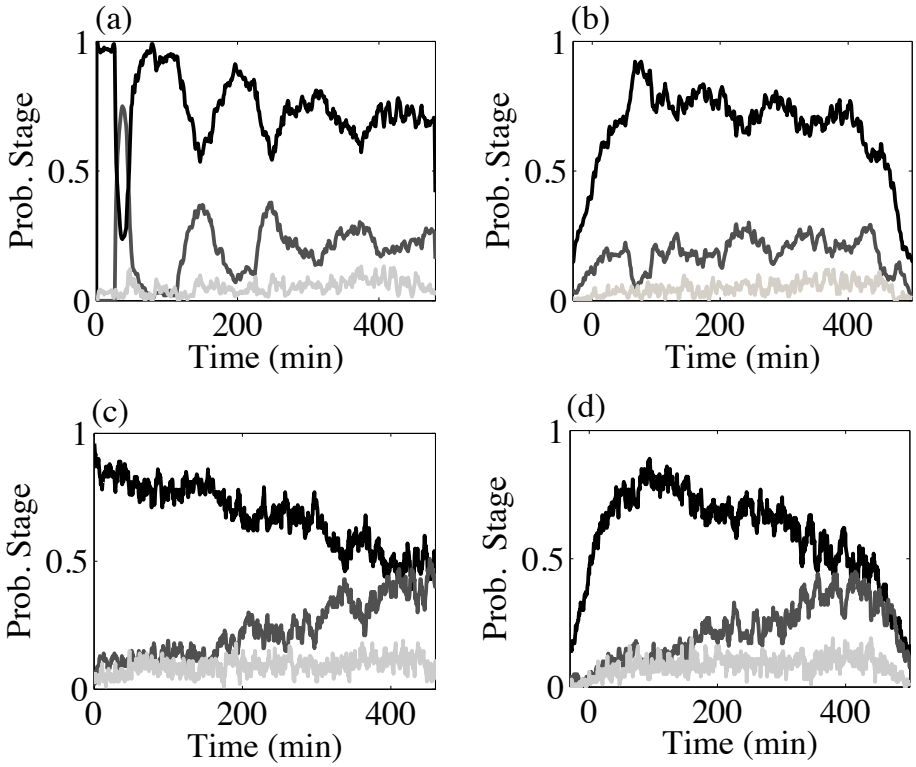

Figure 7.2. Probability of being in Wake (light gray), REM (dark gray), and NREM sleep (black) predicted using, (a) and (b) the Massaquoi and McCarley model and (c) and (d) Basner's Markov model. (a) and (c) All individuals retired at 11:00 pm and (b) and (d) Gaussian variation in sleep onset was assumed. Results based on 100 simulations.

sleep stage scoring rule could be used in which an awakening is considered to occur if the excitation term is greater than a certain value, instead of always scoring the stage as REM when X is greater than 1.4. This type of approach was taken by Comte, Schatzman, Ravassard, Luppi, and Salin (2006) when scoring sleep stages using their model. However, an inadequacy of this approach is that an awakening will not play a more dynamic role in the sleep process and whether an individual awakens during REM sleep has been found to depend on ongoing brain activity and whether an individual is in Phasic or Tonic REM sleep (Ermis, Krakow, and Voss, 2010).

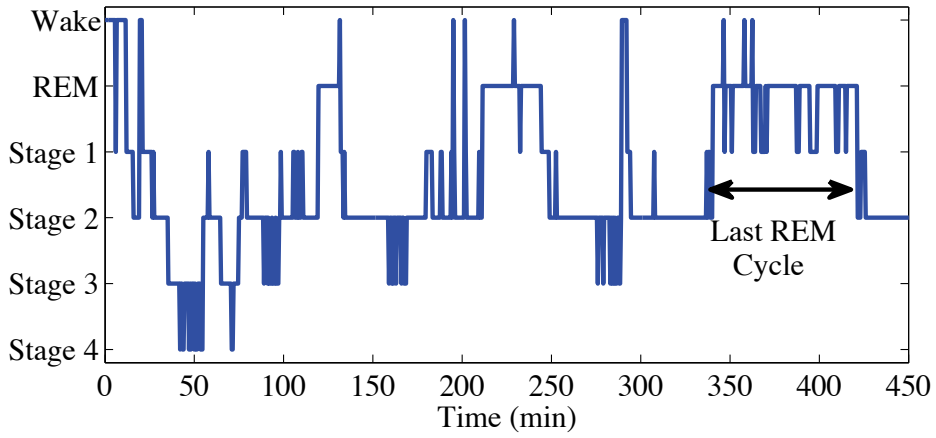

Figure 7.3. Example of a REM sleep period and the change in sleep stages within that period.

The second limitation of the Massaquoi and McCarley model is that it has slow dynamics. While the model can predict the slow ultradian 90-100 minute oscillation between NREM and REM sleep, it cannot be used to adequately predict brief awak-

enings. To emphasize the slow dynamics, the equations of the REM sleep portion of the model can be rewritten where the equation for REM promoting (X) activity is,

$$\dot{X} + \omega_{c1} X = 0, \tag{7.1}$$

$$\omega_{c1} = b(X)Y - a(X)S_1(X). \tag{7.2}$$

The equation for REM inhibiting (Y) activity can also be rewritten as,

$$\dot{Y} + \omega_{c2} Y = 0, \tag{7.3}$$

$$\omega_{c2} = c - d_{circ} S_2(Y)(X + E). \tag{7.4}$$

Both equations have the form of a low pass filter with time varying cutoff frequencies. In Figure 7.4 the variations in the two frequencies are shown. The majority of the behavior of the model is on the order of hours not seconds. Dynamics on a timescale of several seconds are needed to predict awakenings during REM periods.

In order to further examine the use of the Massaquoi and McCarley model for predicting brief awakenings, simulations were conducted in which excitation events ($N(t)$) were of equal spacing, amplitude, and duration. The duration of the impulses was one minute, which is approximately the duration of an aircraft event, the amplitude of the impulses was varied in increments of 1, from 1 to 10. For these simulations the following equation was used for E,

$$\dot{E} + kE = kN, \tag{7.5}$$

where k was equal to 10, which is the value in the original Massaquoi and McCarley model. The duration spent in NREM, REM, and Wake states were calculated for each

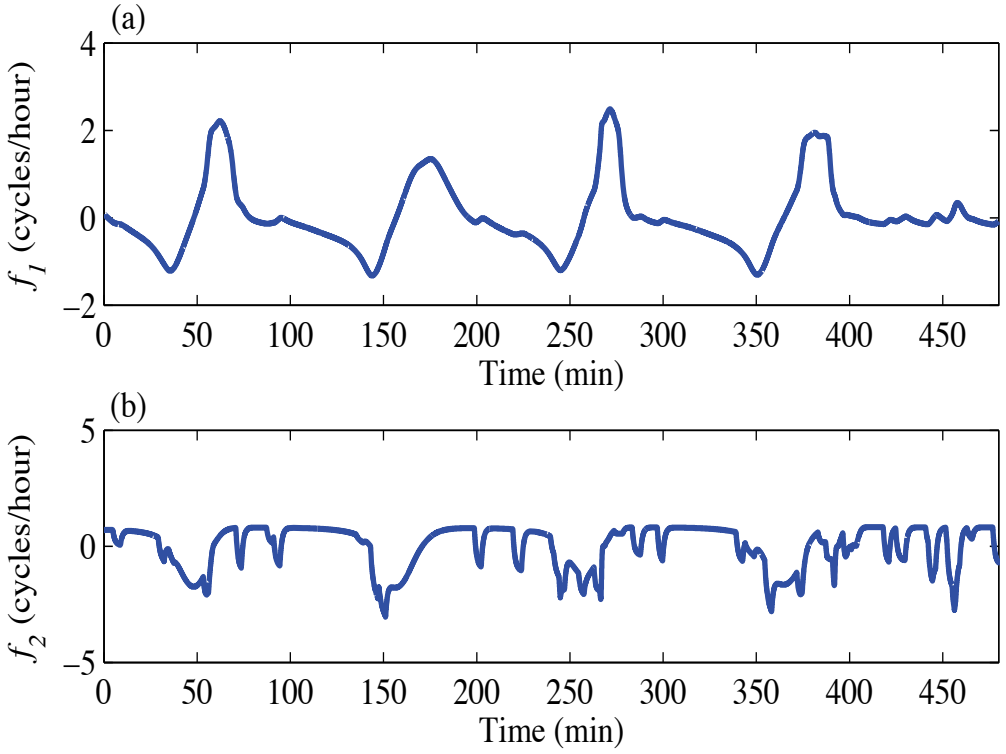

Figure 7.4. The time varying frequencies of the Massaquoi and McCarley model. (a) X model and (b) Y model.

simulation. In Figure 7.5 the results of two simulations, with low (E_{max}=2.4) and high excitation levels (E_{max}=6.0) for 16 events are shown. The number of REM sleep periods and the level of slow wave activity were found to decrease as the amplitude of the events were increased. However, due to the sleep stage scoring thresholds of the original model, the number of predicted awakenings did not increase when the amplitude of the impulses was increased. In Figure 7.6 the duration of REM, NREM, and Wake stages for various amplitudes of the excitation parameter ($N(t)$) are shown.

Simulations were also conducted for 64 events of varying amplitudes. The results are shown for low amplitudes (E_{max}=1.8) and high amplitudes (E_{max}=3.6) in Figure 7.7 and the duration of REM, NREM and Wake stages for various amplitudes of the excitation parameter are shown in Figure 7.8. As the amplitude of the noise events was increased, the NREM and REM sleep cycles during the night disappeared and there was still not a large increase in the number of predicted awakenings.

The addition of an excitation term to the equation for X (REM-ON) activity was examined to determine if more variations in the level of activity and an increase in the prediction of awakenings could be obtained without destroying the slow ultradian cycling. One approach was to use the following equation,

$$\dot{X} = a(X)S_1(X)X - b(X)XY - EX. \tag{7.6}$$

The term EX was added rather than just E alone in order to prevent the level of X from becoming negative. The results for a simulation using this approach is shown in Figure 7.9. The addition of the E term caused a decay in REM-ON (X) activity which caused the ultradian cyclic behavior to end. Therefore, another approach in which a saturation function ($f(X)$) was added was also examined, the equation for which is,

$$\dot{X} = a(X)S_1(X)X - b(X)XY - f(X)EX. \tag{7.7}$$

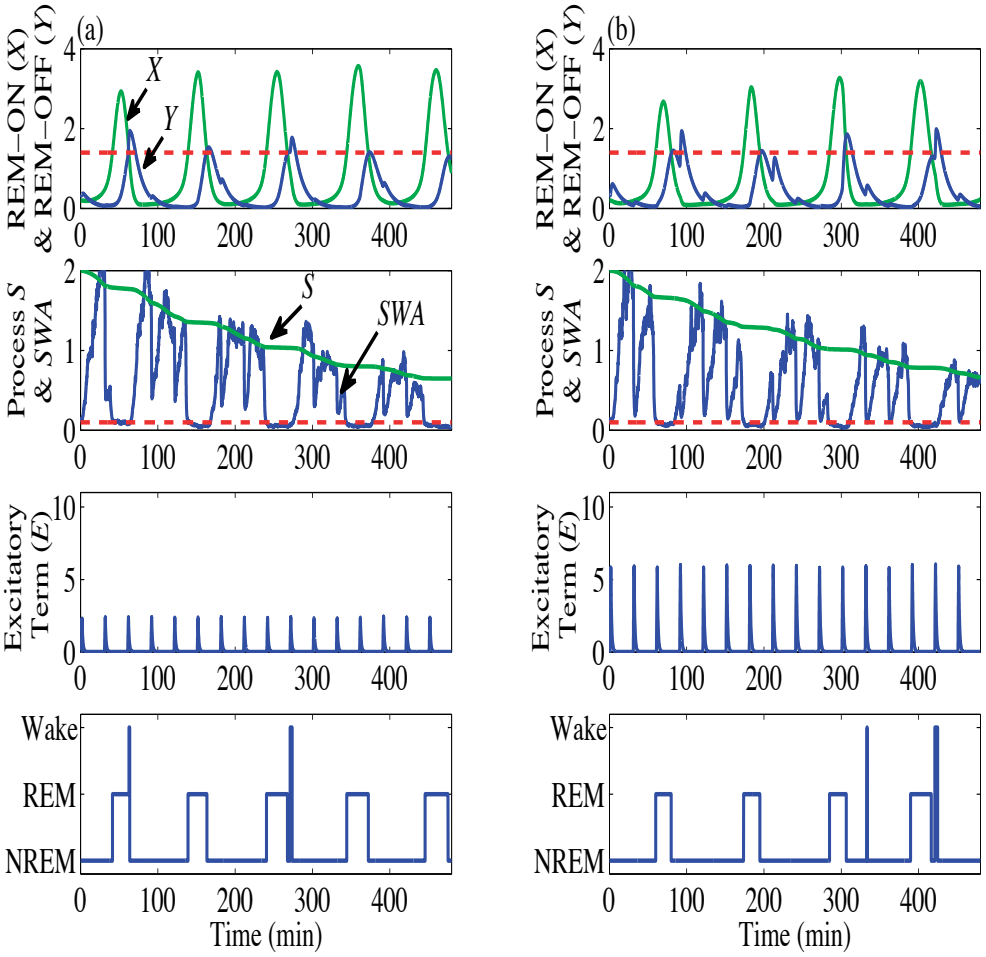

Figure 7.5. Massaquoi and McCarley model predictions for 16 events of 1 minute duration occurring during the night. (a) Low amplitude (E_{max}=2.4, N_{max}=4) and (b) high amplitude (E_{max}=6.0, N_{max}=10) impulses.

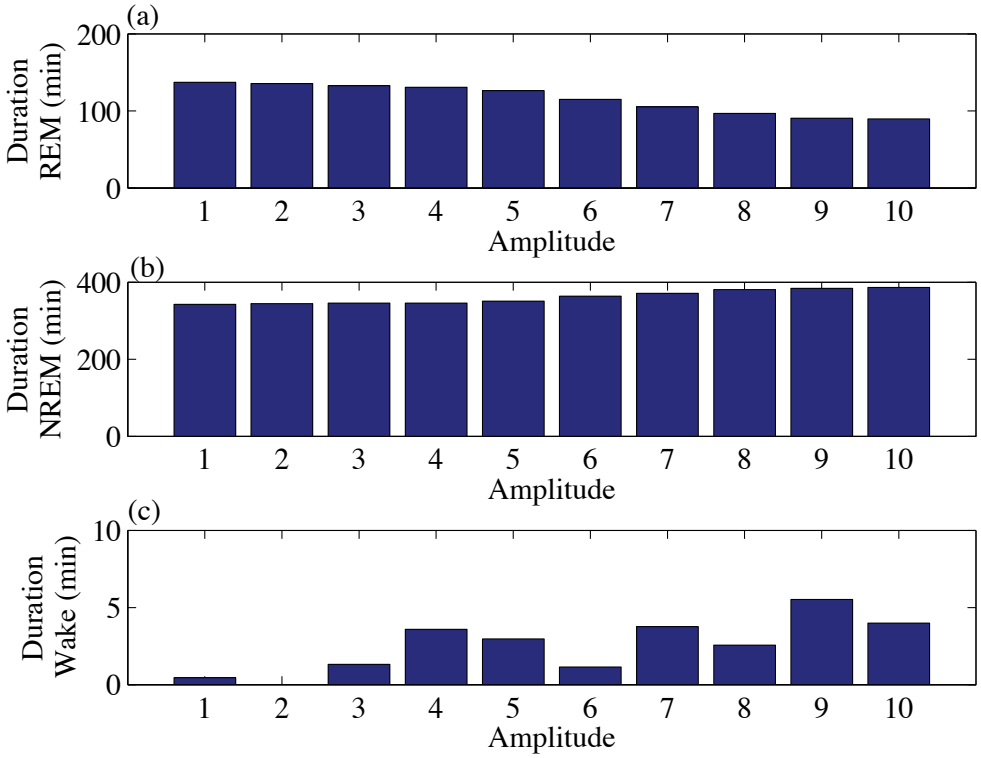

Figure 7.6. The duration of REM, NREM and Wake stages predicted using the Massaquoi and McCarley model for nights with 16 events of different amplitudes of $N(t)$. The duration of the impulses in $N(t)$ was 1 minute and spacing between impulses was 30 minutes.

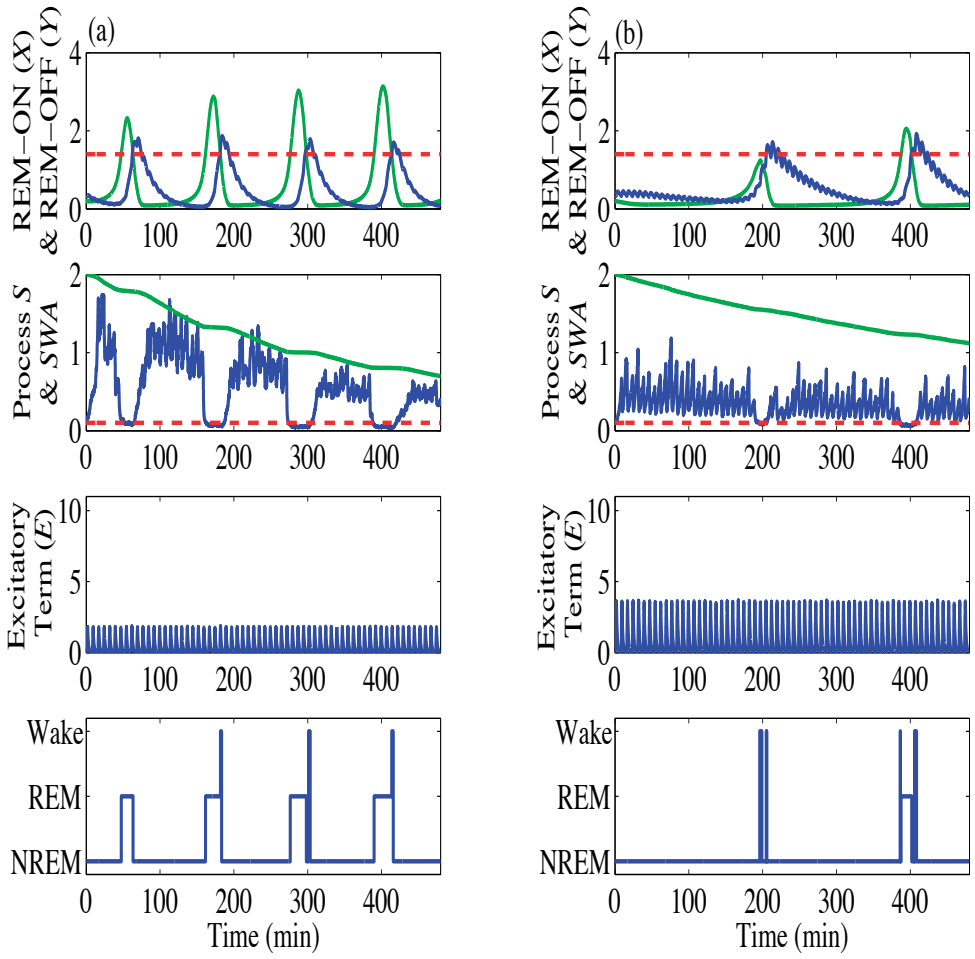

Figure 7.7. Massaquoi and McCarley model predictions for 64 events of 1 minute duration occurring during the night. (a) Low amplitude (E_{max}=1.8, N_{max}=3) and (b) high amplitude (E_{max}=3.6, N_{max}=7) impulses.

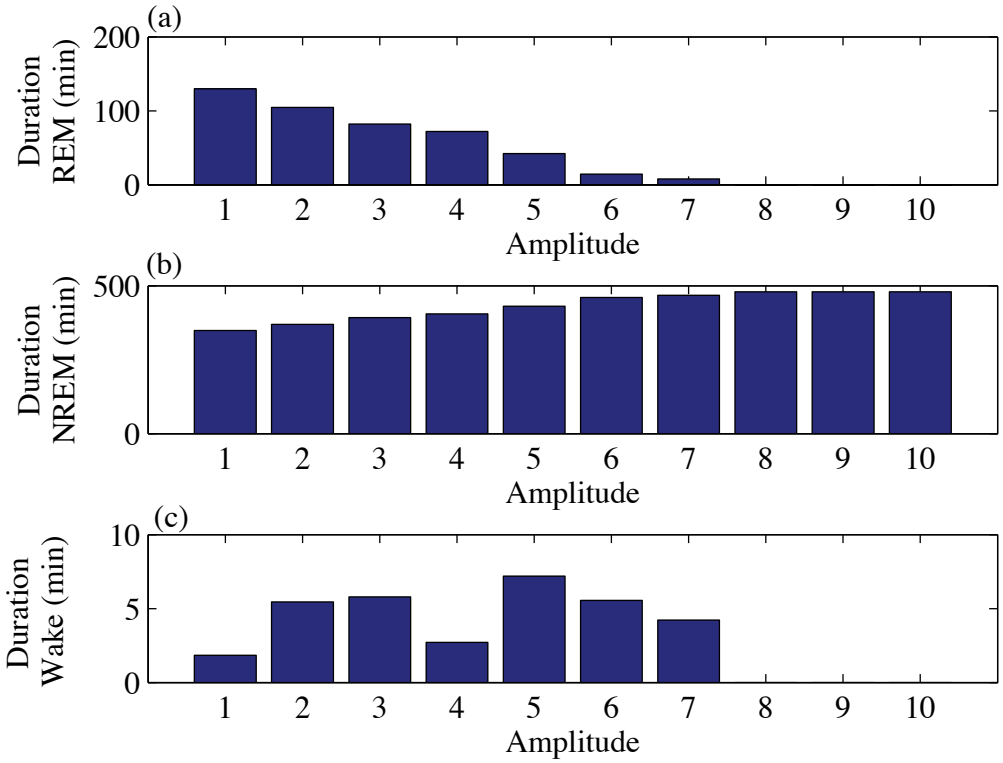

Figure 7.8. The duration of REM, NREM and Wake stages predicted using the Massaquoi and McCarley model for nights with 64 events of different amplitudes of $N(t)$. The duration of the impulses in $N(t)$ was 1 minute and spacing between impulses was 7.5 minutes.

In Figure 7.10 the saturation function is shown. The form of the saturation function was chosen so the excitation term only affected X when the level of X was high. The results for a simulation conducted with the added saturation function are shown in Figure 7.11, where the labels A and B, in the Figure, indicate the decay in the X activity due to the addition of the excitation term to the REM-ON (X) equation. While awakenings were predicted during the REM periods this behavior is still not fast enough for predicting awakenings during sleep, which can be as brief as 15 seconds. Also not all simulations using this approach resulted in desirable results, such as the example shown in Figure 7.12, in which the X and Y activity no longer appears cyclic.

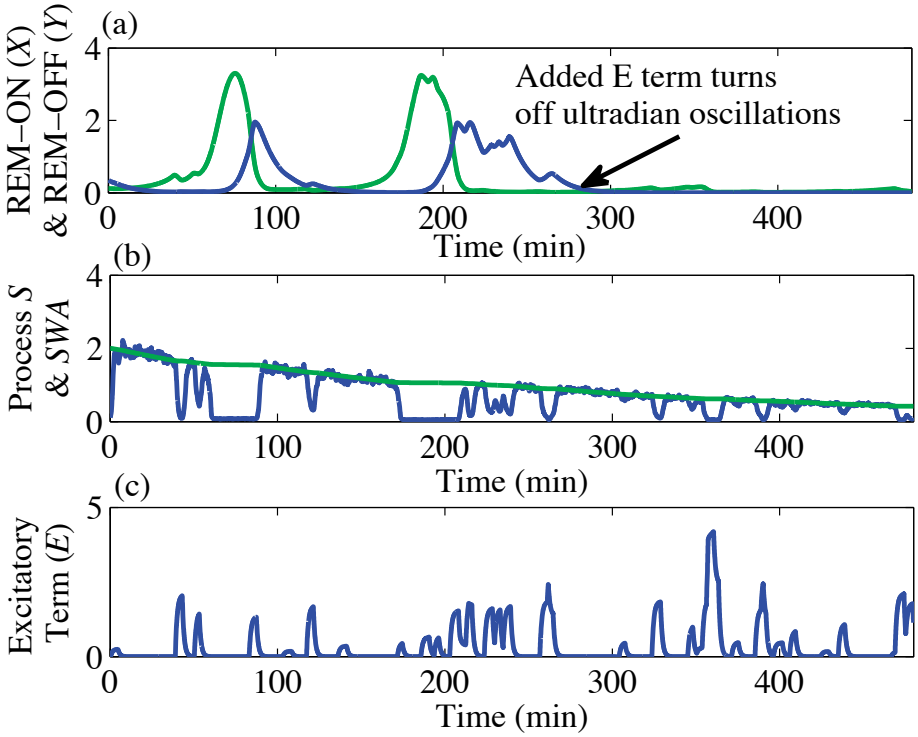

Figure 7.9. Prediction of the Massaquoi and McCarley model when an excitation term (EX) was introduced in the REM-ON (X) equation.

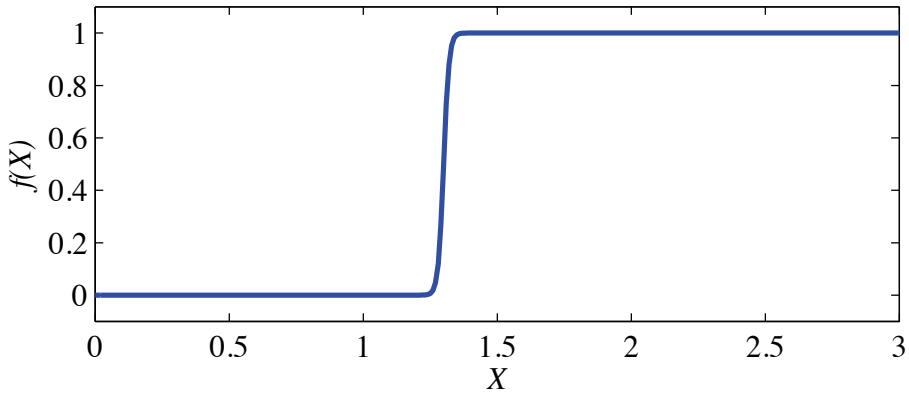

Figure 7.10. Saturation function $f(X)$ used in Equation (7.7) to turn on E effects only when $X > 1.3$.

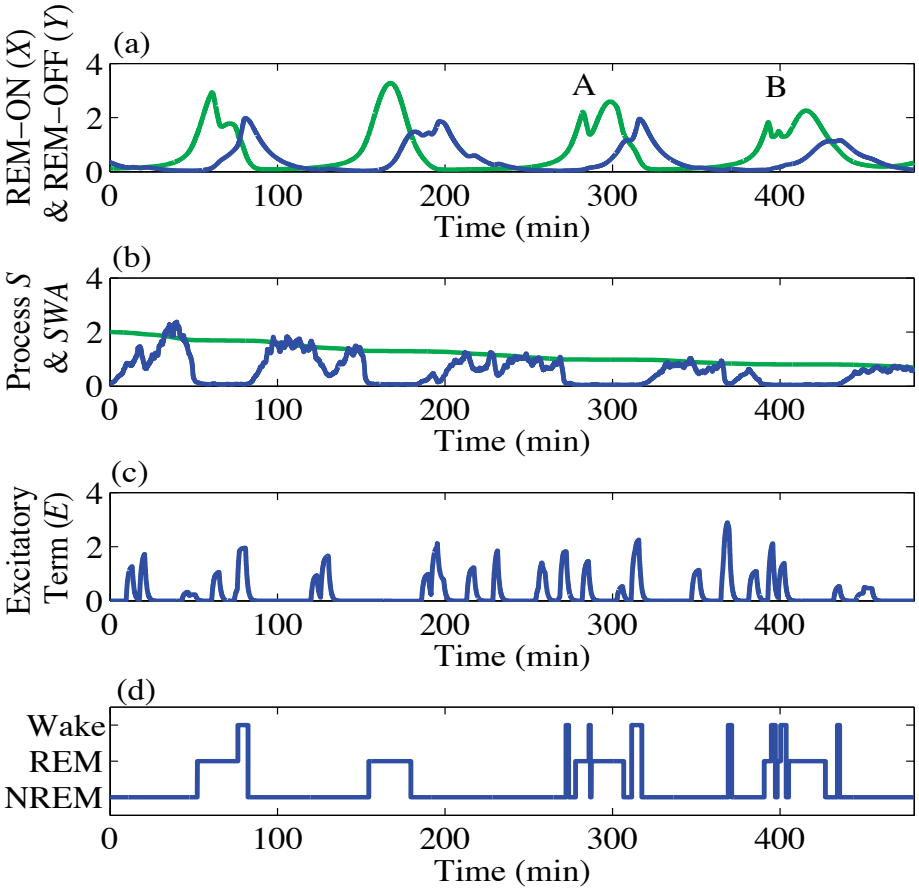

Figure 7.11. Prediction of the Massaquoi and McCarley model when an excitation term with a saturation function was added to the REM-ON (X) equation. A and B mark times when there are awakenings during the REM sleep period. (a) X (green) and Y (blue); (b) Process S (green) and SWA (blue); (c) excitatory term (E) (filtered rectangular pulses with uniformly distributed amplitudes and durations and exponentially distributed arrival times); and (d) sleep stage classification.

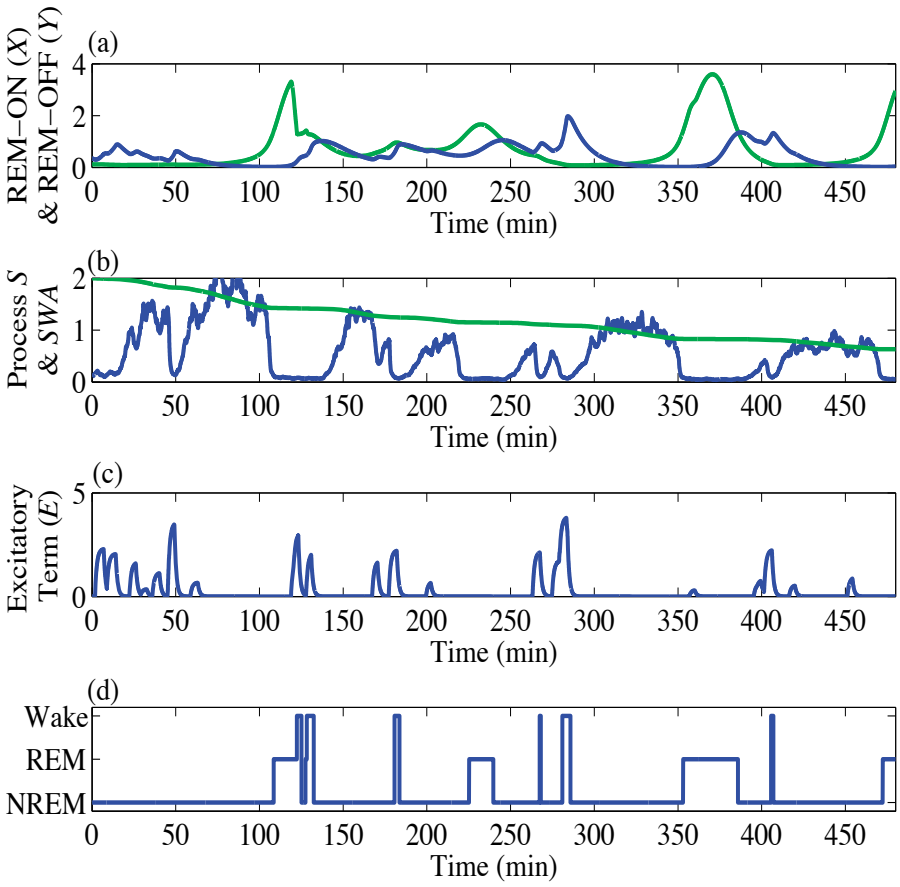

Figure 7.12. Prediction of the Massaquoi and McCarley model when an excitation term with a saturation function was added to the REM-ON (X) equation. Less desirable changes in sleep were obtained. (a) X (green) and Y (blue); (b) Process S (green) and SWA (blue); (c) excitatory term (E) (filtered rectangular pulses with uniformly distributed amplitudes and durations and exponentially distributed arrival times); and (d) sleep stage classification.

The only approach that did result in fast oscillations in REM-ON (X) activity was when a band-passed noise or sinusoidal noise term, denoted by (q) in Equation (7.8) was added to the X equation,

$$\dot{X} = a(X)S_1(X)X - b(X)XY + qX. \tag{7.8}$$

An example of the results obtained using this approach is shown in Figure 7.13. The example results shown in Figure 7.13 (a) is for when q is equal to a sinusoidal term with an amplitude of 40 and 4 oscillations per minute. For results shown in Figure 7.13 (b) q is uniformly distributed band passed noise with frequencies of oscillation between 1 and 4 per minute and has an amplitudes between -50 and 50. While fast oscillations were predicted, the impulsive, random occurrence of awakenings during REM periods was not.

7.2 Altering Ultradian Oscillator-Slow REM Model

Based on the limitations of the Massaquoi and McCarley model, it was determined that slow and fast activity during REM sleep needed to be modeled separately. Therefore, instead of trying to manipulate the REM-ON and REM-OFF equations to obtain oscillations in activity that could lead to awakenings using scoring rules, the REM-ON and REM-OFF equations would be used for just controlling the ultradian cycling.

Having a slow term whose only role is to control the ultradian oscillations in the model is not a new concept, Achermann, Beersma, and Borbély (1990) used a Van der pol oscillator with the two-process model to control the ultradian oscillations between NREM and REM sleep, which was defined by the equation,

$$\ddot{X} = a(b - X^2)\dot{X} - wX. \tag{7.9}$$

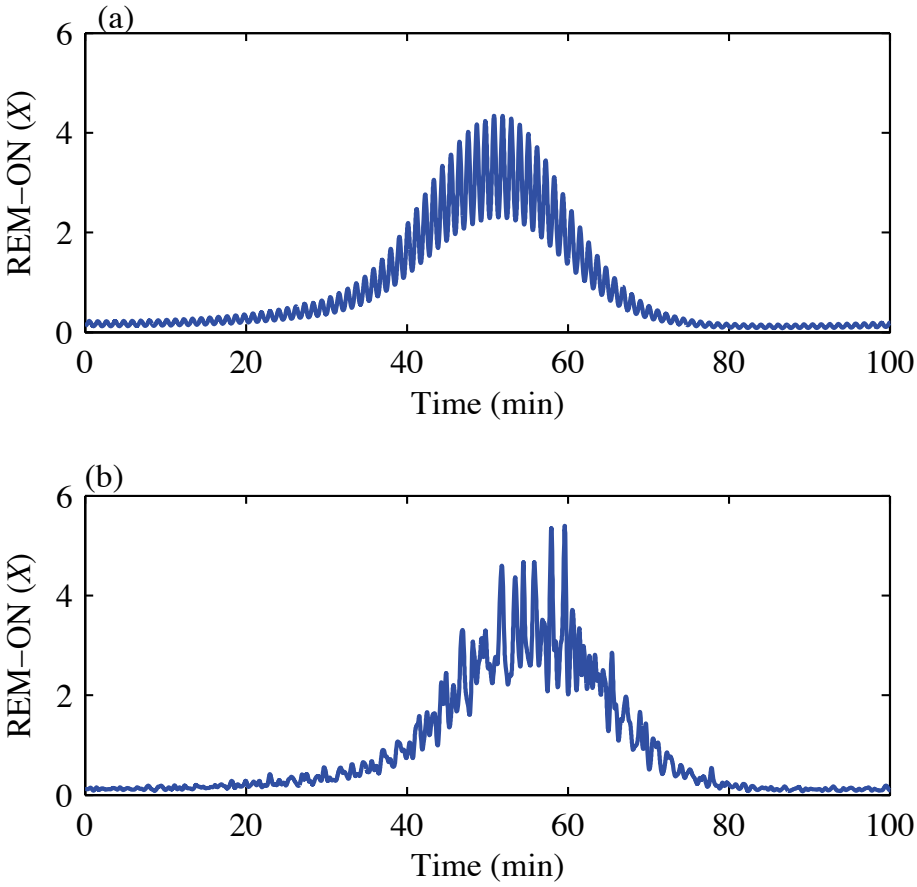

Figure 7.13. REM-ON activity (X) with (a) added sinusoidal noise with frequency of 4 oscillations per minute and amplitude of 40. (b) Added uniformly distributed (between -50 and 50) band-passed noise between frequencies of 1 and 4 oscillations per minute.

Wever (1980) used two coupled nonlinear oscillators one for circadian and one for ultradian oscillations. The form of his equations are,

$$\ddot{y} + \varepsilon_1(y^2 - y^{-2} - a_1)\dot{y} + {\omega_1}^2(y + g_1 y^2) = {\omega_1}^2(c_1(\ddot{x} + \dot{x} + x)), \tag{7.10}$$

and

$$\ddot{x} + \varepsilon_2(x^2 - x^{-2} - a_2)\dot{x} + {\omega_2}^2(x + g_2 x^2) = {\omega_2}^2(c_2(\ddot{y} + \dot{y} + y)). \tag{7.11}$$

The excitation term E in the REM-OFF equation of the Massaquoi and McCarley REM model though will remain in the slow REM model. If the maximum amplitude of the excitation is limited the loss of NREM-REM cycling will not occur as in the the simulations in the previous sections. The reason for keeping the E term in a slow REM model is that several researchers have found that the duration of sleep cycles is affected by awakenings. Foret, Touron, Clodoré, and Bouard (1990) examined the effect of forced awakenings on the duration of NREM sleep during one sleep cycle. They interrupted sleep one time a night, for 3 nights. The time of the interruption varied per test night and occurred at either 1:30, 3:30, or 5:30 am. The duration of the interruption was 10 minutes. To calculate the effect of the interruption on the NREM-REM timing they calculated what they called the inter-REM interval which was the time between the start of one REM period until the start of the next period, however the 10 minute interruption time was not included when calculating the inter-REM interval duration. They found that compared to a baseline night, the interruption caused a decrease in cycle duration if it occurred in the first half of the cycle but it caused an increase in cycle duration if the interruption occurred in the second half of the cycle.

Massaquoi and McCarley (1990) compared predictions using their model to the data from the study conducted by Foret, Touron, Clodoré, and Bouard (1990). They

applied excitations at various locations during a sleep cycle. Each pulse in the E term in the model had a duration of one unit or 10.7 minutes. They examined the effect of different amplitudes of excitation on the duration of a sleep cycle. They found that the strength of the excitation does have an effect on the change in cycle length. A strong excitation will result in a linear relationship between the time an excitation occurs and the change in cycle duration. However, they found that moderate or weak pulses have more of a curvilinear relationship.

7.3 Fast REM Model

The development of a fast REM sleep model is based on the notion that during REM sleep the probability of awakening to a noise event is dependent on ongoing brain activity and, in particular, whether an individual is in Tonic or Phasic REM sleep. The Tonic and Phasic activity in the UK dataset was examined and used to develop the model.

7.3.1 REM Density Calculation

While it might not be well understood yet what exactly is causing the variation in stimulus response during REM sleep, what is clear is that response to auditory stimuli cannot be assumed to be constant during this stage. Results from Wehrle et al. (2007) indicate that a noise stimulus will be processed differently depending on whether an individual is in Tonic or Phasic REM sleep, and this in turn affects whether they awaken.

In order to evaluate the timing and duration of Phasic and Tonic REM sleep in the data from the 1999 UK study, the density of rapid eye movements was calculated. To calculate the density of rapid eye movements first the left and right EOG channels

were bandpass filtered between 0.5 and 5 Hz by using a 4th order Butterworth filter. The beginning and end of each REM period was identified. Within the defined REM period the two EOG channels were segmented into 30 second segments. The correlation between the two channels was calculated and then the process was repeated moving in 1 second increments through time. If the correlation of the two channels was below -0.2, rapid eye movements were considered to occur. A second method was also used to identify rapid eye movement which was similar to an approach used by Agarwal, Takeuchi, Laroche, and Gotman (2005). The inverse or negative of the left EOG channel was multiplied by the Right EOG channel and then amplitudes greater than 625 μV^2 were identified. A 2 second segment of both the right and left EOG channel was obtained around each peak. The correlation between the 2 seconds of the left and the 2 seconds of the right EOG channels was calculated. If the correlation was below -0.2 and the peaks of the two channels were within 100 ms of one another, then rapid eye movement was considered to occur. Then, for each 30 second segment, the proportion of the segment that was occupied by rapid eye movement was calculated in order to obtain a measure of REM density. The measure of REM density was again calculated for 30 second segments, moving 1 second in time. The results for one REM period are shown in Figure 7.14. The REM Indicator is an indicator of Phasic and Tonic REM activity, it is equal to 1 when the REM density is greater than zero and Phasic REM sleep is occurring, and is equal to zero when Tonic REM sleep is occurring. Tonic REM periods of less than 15 seconds duration were set equal to Phasic REM sleep though, this approach has been used by others (Ermis, Krakow, and Voss, 2010) to define Tonic and Phasic REM sleep.

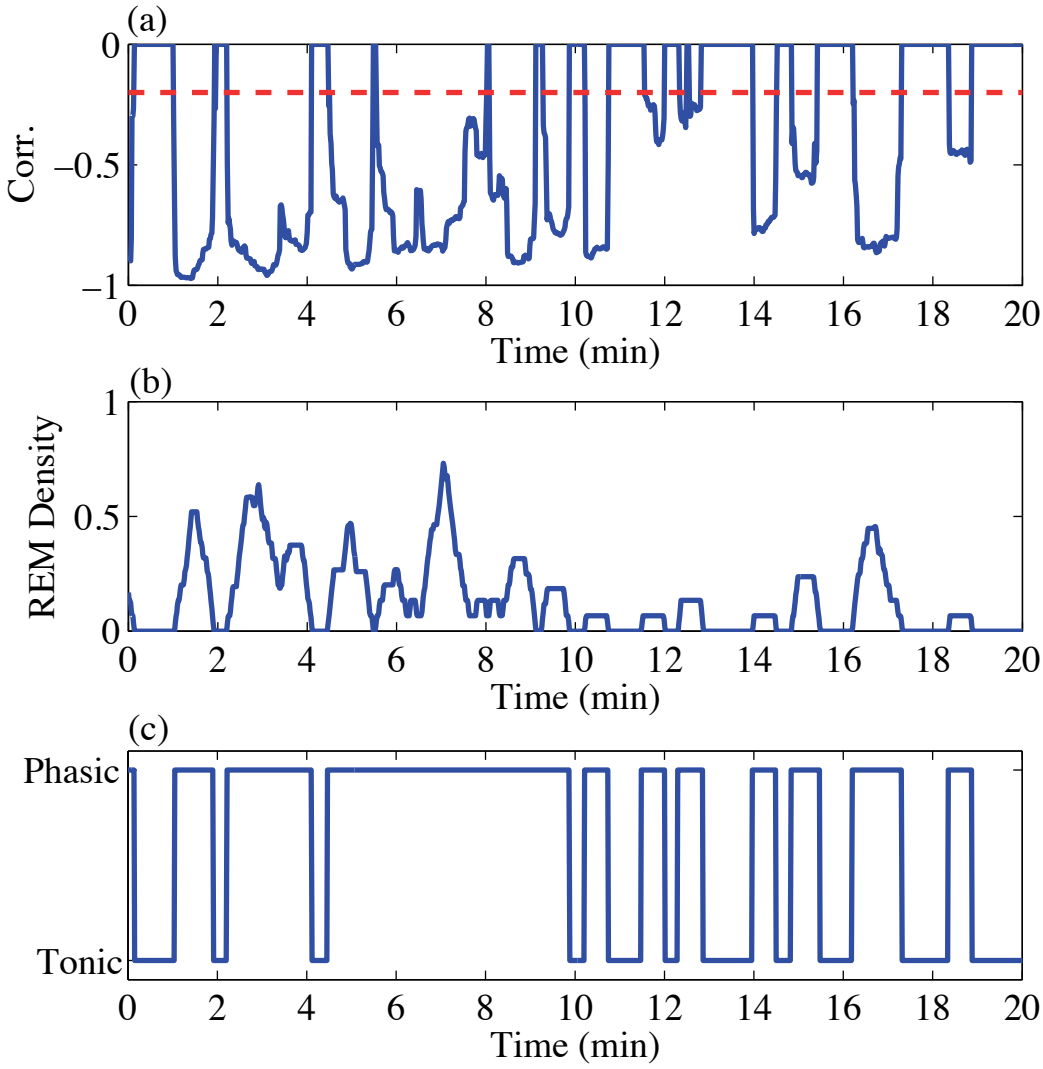

Figure 7.14. An example of rapid eye movement activity. (a) 30 second correlation between right and left EOG signals and the -0.2 threshold used (red dashed line), (b) REM density measurement-proportion of the 30 second epoch occupied by rapid eye movement activity, and (c) an indicator of Phasic and Tonic REM sleep.

7.3.2 Form of Fast REM Model

A few researchers have tried to identify/model the process that causes the occurrence of rapid eye movements. Trammell and Ktonas (2003) stated that the occurrence of rapid eye movements may not be due to a random process. One method they used to determine if the process that caused rapid eye movement bursts was deterministic or stochastic was the correlation dimension. They calculated the correlation dimension using the inter-REM periods or the time between rapid eye movements and found values near 2. This indicated to Trammell and Ktonas (2003) that a low order non-linear process may explain the intervals between rapid eye movements. Boukadoum and Ktonas (1988) analyzed the probability density function of inter-REM intervals between rapid eye movements. They categorized inter-REM periods according to two criteria: (1) the time between rapid eye movements within a burst, (a burst is defined if the inter-REM period is less than 2 seconds), and (2) inter-REM period between isolated bursts of rapid eye movement. From the estimated probability density function they concluded that two separate processes may be involved in the occurrence of rapid eye movements, one process controlling the brief bursts of activity and another controlling the longer intervals between rapid eye movements. They stated that the inter-REM intervals cannot be predicted by using an exponential distribution.

After examining the occurrence of Phasic and Tonic REM sleep in the UK data, it seemed that the oscillation between the two states, along with the change to awake states during REM sleep could be modeled using a Duffing equation with the harmonic excitation in a region in which chaotic response behavior is possible. The form of the Duffing equation with up to a 5th order stiffness term was examined (Li and Moon, 1990). This equation has the form,

$$\ddot{x} + \delta\dot{x} + \beta_5 x^5 + \beta_4 x^4 + \beta_3 x^3 + \beta_2 x^2 + \beta_1 x + \beta_o = A cos(\omega t); \qquad (7.12)$$

which can also be written as,

$$\ddot{x} + \delta\dot{x} + \beta(x-\alpha_1)(x-\alpha_2)(x-\alpha_3)(x-\alpha_4)(x-\alpha_5) = Acos(\omega t); \tag{7.13}$$

If the unforced case is considered the corresponding set of first order differential equations are,

$$\dot{x} = y, \tag{7.14}$$

$$\dot{y} = -\delta y - \beta_5 x^5 - \beta_4 x^4 - \beta_3 x^3 - \beta_2 x^2 - \beta_1 x - \beta_o. \tag{7.15}$$

There are 5 equilibrium points and they occur when,

$$y = 0, \tag{7.16}$$

$$\beta_5 x^5 + \beta_4 x^4 + \beta_3 x^3 + \beta_2 x^2 + \beta_1 x + \beta_o = 0. \tag{7.17}$$

The Duffing equation (usually with only a 3rd order polynomial rather than the 5th order shown here) has been used to model the behavior of an elastic beam which is clamped vertically above magnets of fixed position. The entire system consisting of the beam and the magnets are shaken horizontally. When the system is shaken with a low amplitude the beam will oscillate about one of the magnets which are stable equilibrium points. If the system is shaken with a large enough sinusoidal force, in certain frequency and amplitude regions the beam will jump chaotically from magnet to magnet (Moon and Holmes, 1979). This is illustrated in Figure 7.15 for a third order nonlinearity and in Figure 7.16 for a fifth order nonlinearity.

For the Duffing equation with a 5th order stiffness term, three of the equilibrium points are stable, the other two equilibrium points are saddle points and are unstable. For the fast REM model, two of the stable points were considered to be Tonic and Phasic REM sleep. The third stable point represents Stage 1/Wake. As research

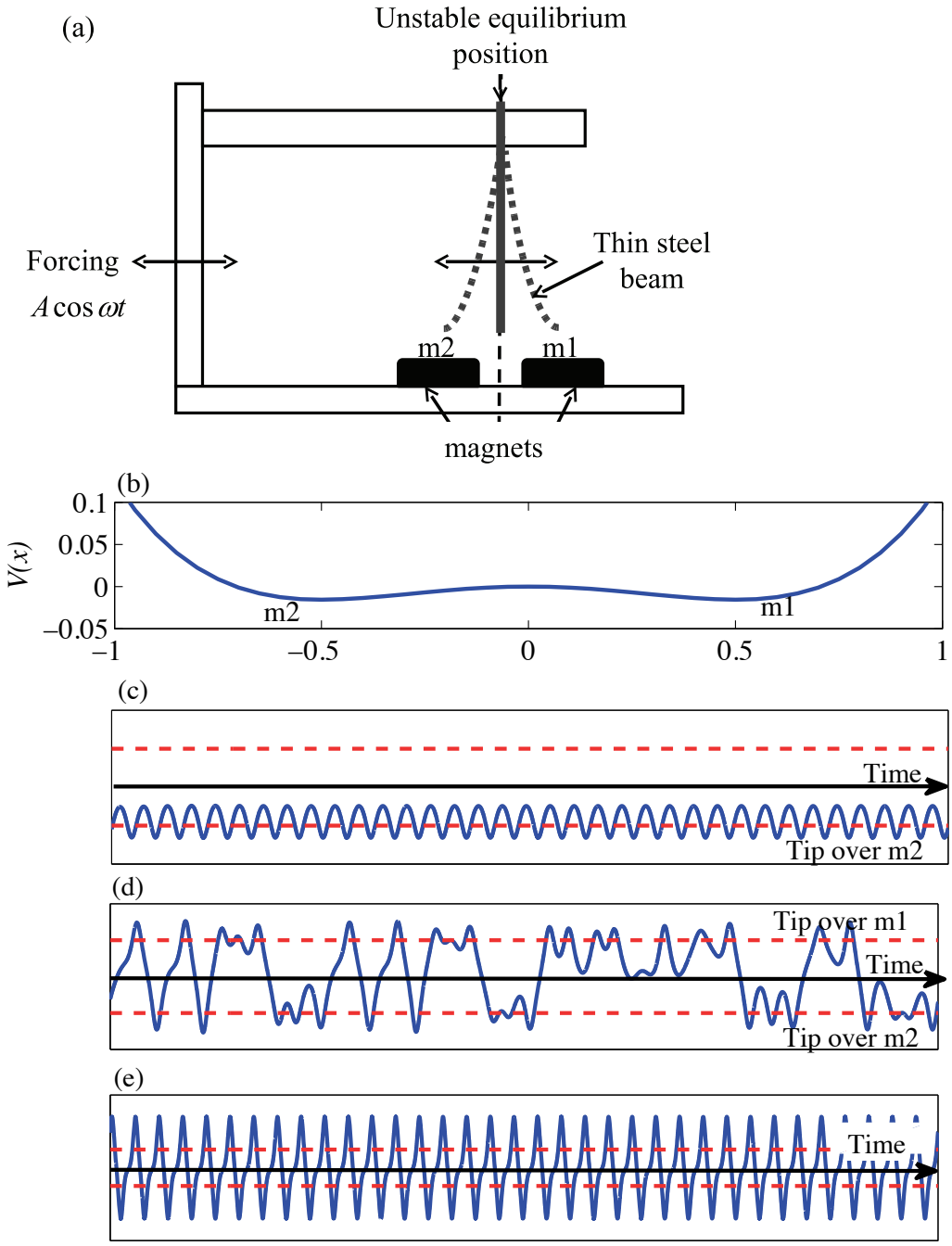

Figure 7.15. A Duffing oscillator with two stable points at 0.5 and -0.5 and one unstable point at 0, $\delta = 0.06$ and $\omega = 2\pi(0.1)$. (a) Beam analogy, (b) potential function, (c) oscillations about one stable equilibrium (A=0.01), (d) chaotic jumps between equilibrium (A=0.4), and (e) periodic oscillations about both stable equilibria (A=0.6).

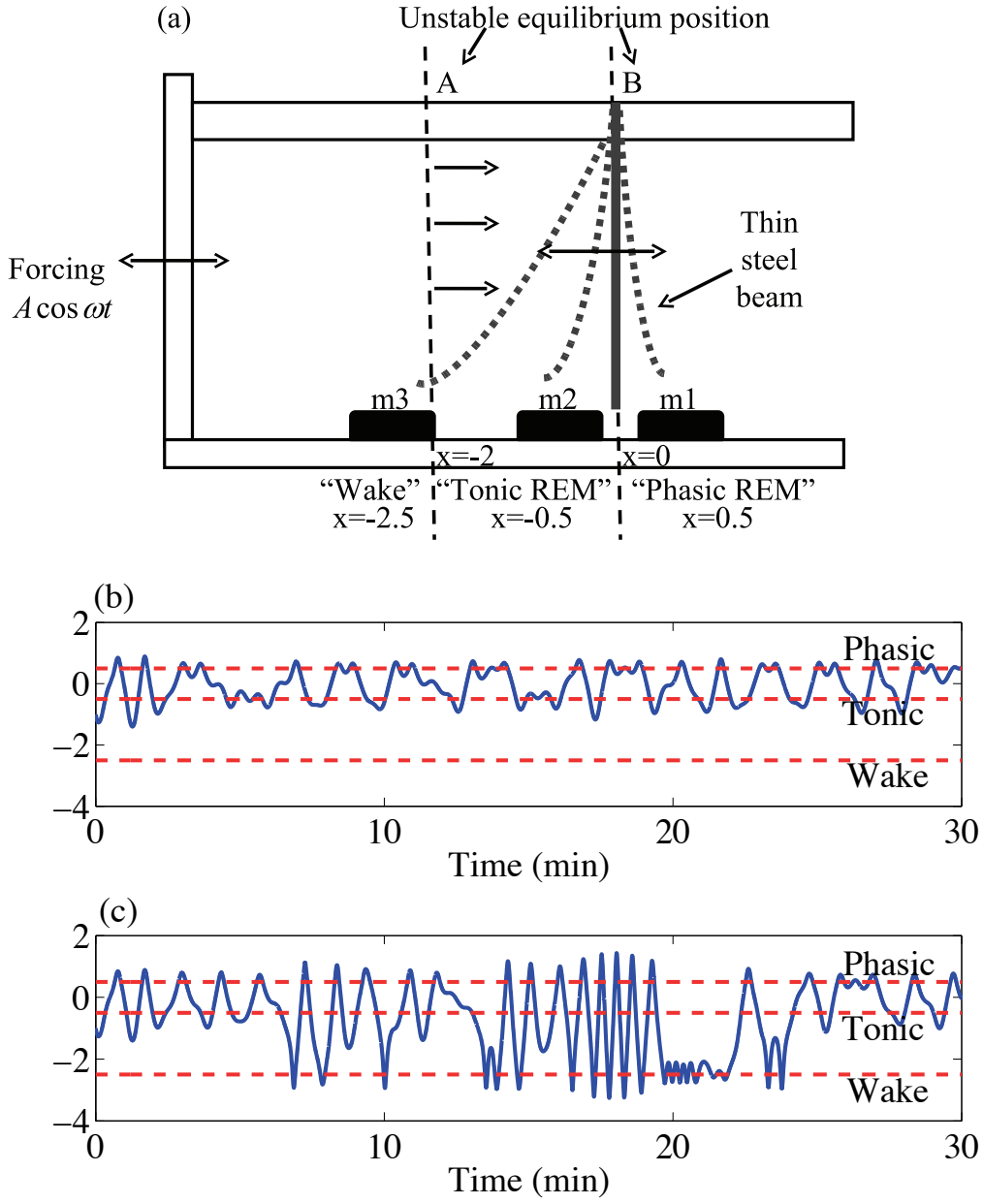

Figure 7.16. (a) REM period model beam analogy. A Duffing oscillator with 3 stable and 2 unstable equilibrium positions, ($\delta = 0.06$, $\omega = 2\pi(0.3)$, A=0.5) (b) $w(t)$=0, (c) 8 evenly spaced events of 1 minute, $-2 + \gamma w(t)$=-0.6 when events were occurring.

on auditory awakening thresholds have indicated that an individual is more likely to awaken during Tonic than Phasic REM sleep, the awakening stable point was positioned closer to the stable point representing Tonic REM sleep. Also as awakenings are less likely to occur than Phasic or Tonic REM sleep during a REM sleep period, the distance between the Tonic and Wake stable point was greater than the distance between the Tonic and Phasic stable point. The positions of the equilibrium points for the baseline no-noise conditions are listed in Table 7.2. The phase plane and position of the equilibrium points for the fast REM model is shown in Figure 7.17, where, $\delta = 0.06$.

Table 7.2. Positions of the equilibrium points for the baseline fast REM sleep model.

Equilibrium Point	Position
Phasic REM sleep	0.5
Tonic REM sleep	-0.5
Wake	-2.5
Unstable Point Between Tonic and Phasic	0
Unstable Point Between Wake and Tonic	-2

To simulate awakenings due to noise events the position of the saddle point between the Wake stable point and Tonic stable point was allowed to vary and it moved closer to the Tonic stable point when an excitation term occurred. The equation for the model is,

$$\ddot{x} + \delta\dot{x} + (x + 2.5)(x - (-2 + \gamma w(t)))(x + 0.5)(x)(x - 0.5) = Acos(\omega t). \qquad (7.18)$$

where, $(-2 + \gamma w(t))$, is the unstable saddle point which moves when an excitation occurs. Here $w(t)$ is an excitation, a different naming convention then the slow model

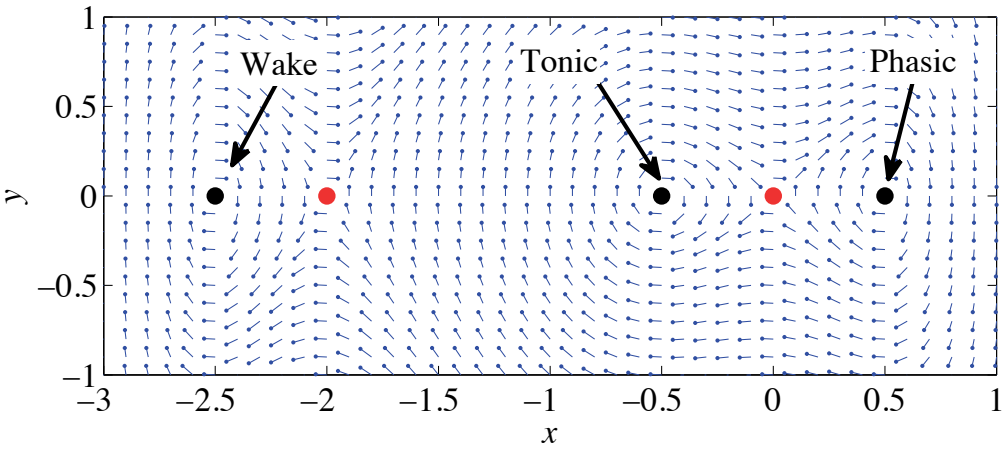

Figure 7.17. Phase plane for Duffing equation. Unstable equilibrium points (red/light gray), stable equilibrium points (black) ($\delta = 0.06$, $\omega = 2\pi(0.3)$, A=0.5), $y = \dot{x}$.

in which the excitations are labeled as (E) is used as the two may or may not have the same form.

The term $\gamma w(t)$ is always positive so this impulsive excitation, which models brain activity pushes the unstable equilibrium position at $x = -2.0$ toward the "Tonic" equilibrium position at $x = -0.5$ making it easier for the beam to move to the Wake equilibrium position at $x = -2.5$. In Figure 7.16 (b) $w(t) = 0$ and the unstable equilibrium point is at -2.0 and in Figure 7.16 (c) there were 8 evenly spaced events of 1 minute with $(-2+\gamma w(t))$=-0.6 when events were occurring and equal to -2 when events were not occurring $(w(t) = 0)$. By moving the unstable equilibrium point the likelihood of transitioning to an awake state increases as the noise level increases. In Figure 7.18 the potential function of the Duffing equation is shown for different positions of the unstable point between Wake (m3) and Tonic REM (m2); in Figure 7.18 (a) the potential function when the unstable point is at -2.0 is shown, if the beam is close to m1 (Phasic REM) and m2 (Tonic REM) it would be difficult to jump out of the well at lower amplitudes of excitation to reach m3 (Wake). In Figure 7.18 (b) the unstable point is at -1.5 and you can see that escape from the m1-m2 region to m3 would be easier and in Figure 7.18 (c) when the unstable point is at -1.0 it would be very easy to escape from the m1-m2 region to m3 and it would be difficult to escape the m3 region to return to the m1-m2 region.

An example of the output of the model with awakenings is shown in Figure 7.19. Here the unstable equilibrium point is defined as $-2 + \gamma N(t)$ and $N(t)$ is a series of impulses of duration 1 minute and are spaced 5 minutes apart. To classify sleep states, a set of thresholds were defined. If the value of x is greater than 0 then Phasic REM sleep occurs and if the value of x is less than zero then Tonic REM sleep is occurring. However, there are exceptions used in order to eliminate very brief sleep stage changes. If the peak value, when the signal is above zero, is never greater than

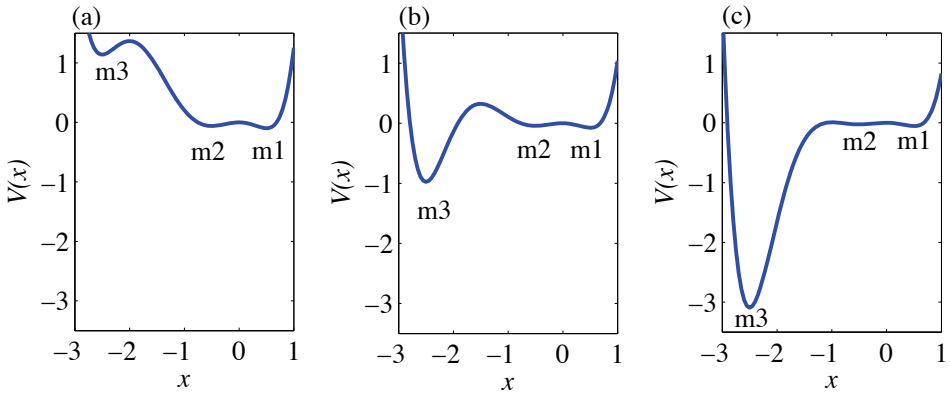

Figure 7.18. The potential function for the 5th order stiffness Duffing equation for different positions of the unstable equilibrium point between Wake and Tonic REM sleep, (a) -2.0, (b) -1.5, and (c) -1.0. m1, m2, m3 represent the magnet locations in the beam system analogy corresponding to "Phasic REM","Tonic REM" and "Wake" respectively.

0.25, i.e. it never approaches the Phasic stable equilibrium point, which is at 0.5, then the activity above zero was set equal to the previous classified state, a similar approach was taken when activity is below zero but the minimum never approaches the Tonic stable equilibrium or Wake stable equilibrium point. Wake states are classified if the level of x is below -2.0 during an excitation. An example of scoring REM sleep stages using these rules is shown in Figure 7.19.

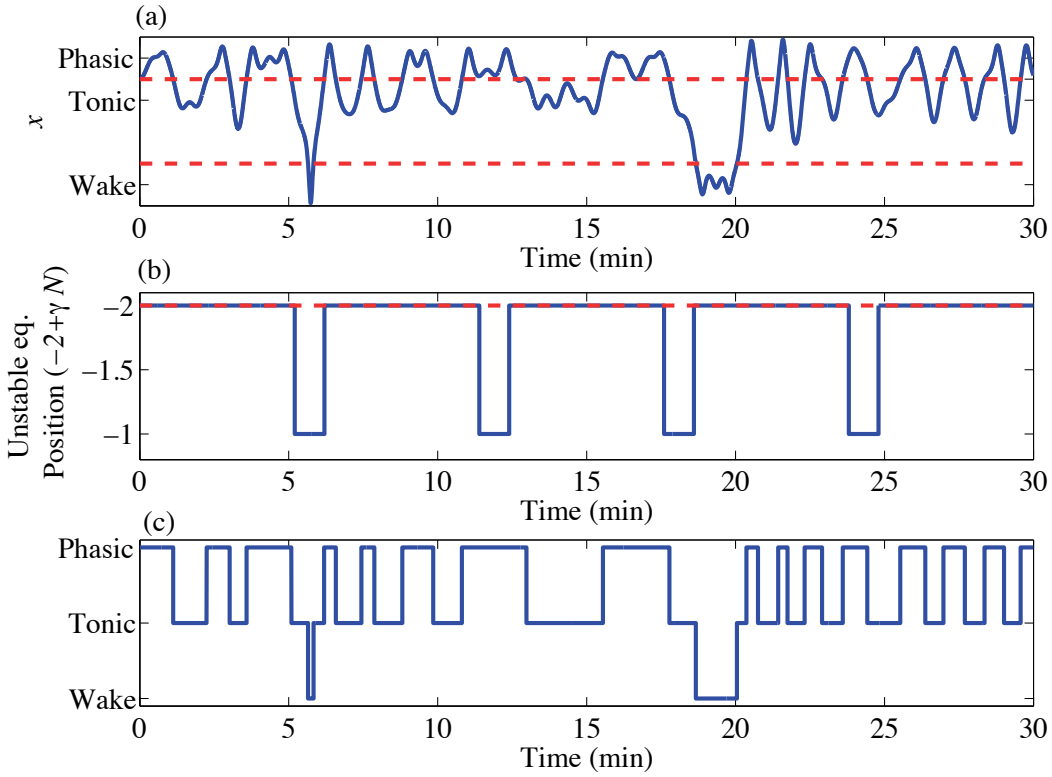

Figure 7.19. (a) Solution of the Duffing equation, oscillations are about 3 stable equilibria, (red-dashed line) thresholds used to assign sleep stages. (b) Unstable equilibrium position $(-2 + \gamma N)$ and (c) classified sleep stages. The driving frequency $\omega = 2\pi(0.3)$, $\delta = 0.06$ and the amplitude (A) was 0.5.

In order to determine the remaining parameters of the Duffing equation, simulations were completed in which the frequency (ω) and the amplitude of the driving

force (A) were varied in order to match the percentage of time spent in Tonic and Phasic sleep and the inter-arrival time between Phasic activity as calculated based on the 1999 UK data. For these simulations the location of the stable and unstable points and the damping (δ) which was set equal to 0.06, remained constant. The damping was set at a low enough value so that chaotic behavior could be obtained, and it was not varied for the simulations as changing the amplitude and the damping would have similar effects. The initial conditions were randomized for each trial between -0.5 and 0.5, and the drive frequency and amplitude were systematically varied. One hundred simulations were conducted for each combination of parameters. A reasonable agreement was found when the drive frequency was set equal to 0.3 Hz and the amplitude of excitation was set equal to 0.5, the results are shown in Figure 7.20. The time t, also had to be scaled after each solution was obtained to match values, t for the solutions was set equal to $(1/5)t$ to obtain agreement between the simulated and actual values.

Simulations using the fast REM model for different numbers, level, and duration of excitations ($w(t) = N(t)$) were completed. For each combination of parameters, 25 simulations were completed, the initial conditions were varied for each simulation. The average proportion of a REM period classified as Wake based on the simulation results is shown in Figure 7.21 and the average proportion of a REM period classified as Tonic and Phasic REM sleep is shown in Figure 7.22. The proportion of the REM period classified as Wake increased with both excitation level and duration of the event, while the proportion spent in Tonic and Phasic REM sleep both decreased. The proportion of the REM period classified as Wake also increased with the number of events. The probability of awakening to a noise event is shown in Figure 7.21, and it increases with the duration of an event and the excitation level. From the simulations it was found that an impulse that moved the unstable equilibrium point

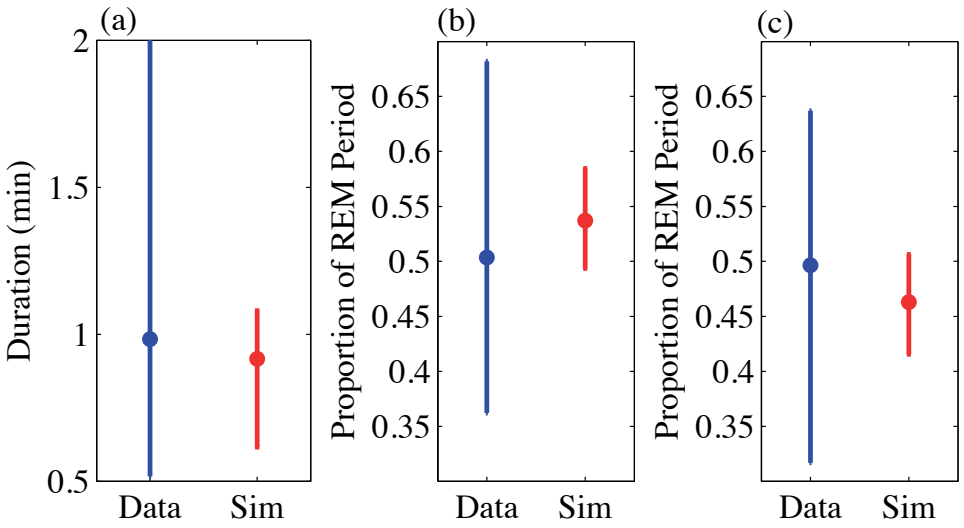

Figure 7.20. Statistics of Tonic and Phasic REM sleep for simulations (red) and survey data (blue). (a) Inter-arrival time of Phasic activity, (b) proportion of REM period (without awakenings) occupied by Tonic REM sleep and (c) proportion of REM period (without awakenings) occupied by Phasic REM sleep.

to -1.6 will start to cause transitions to Stage Wake. The baseline position of the unstable equilibrium between Wake and Tonic was set at -2 because at this location the probability of moving to the Wake state without an excitation term is essentially zero.

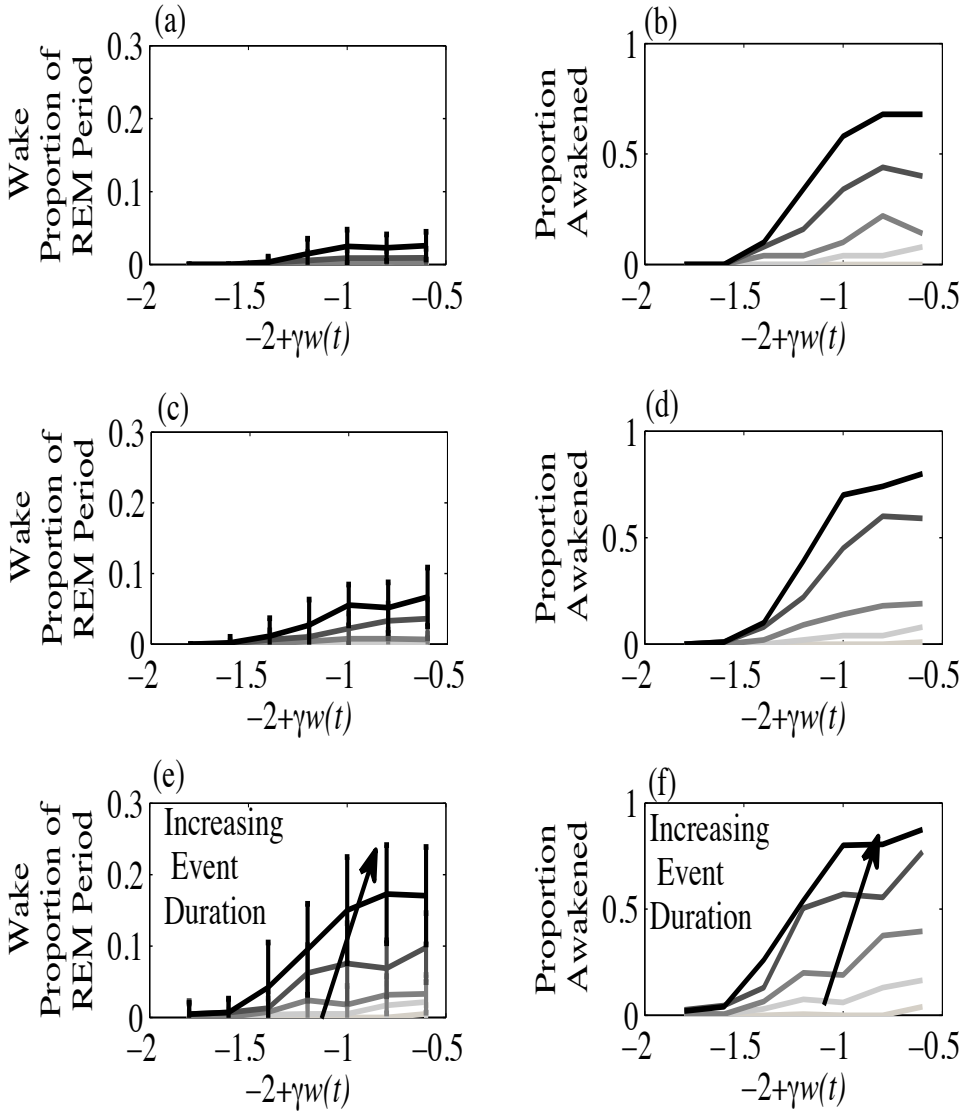

Figure 7.21. Proportion of the REM period defined as awake for (a) 2, (c) 4, and (e) 8 events as a function of level. Probability of awakening to, (b) 2, (d) 4, and (f) 8 noise events as a function of level.

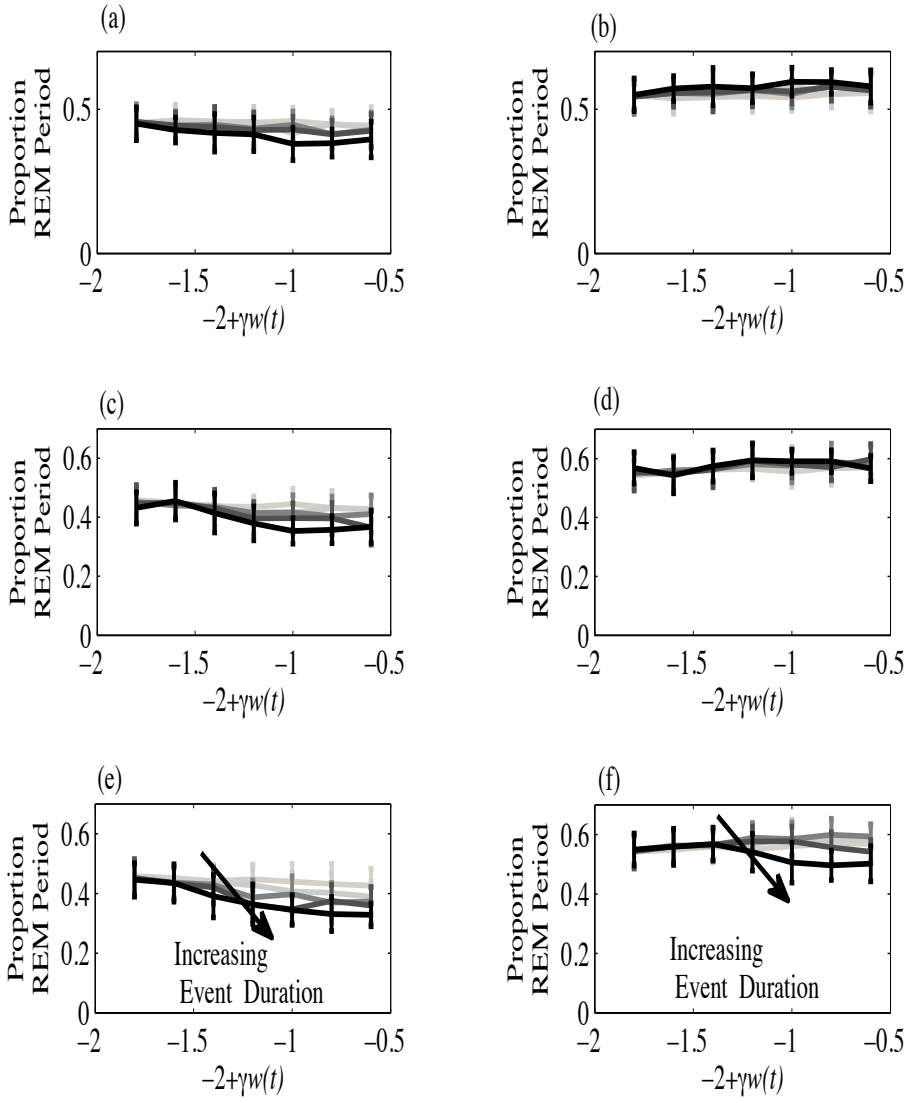

Figure 7.22. Proportion of the REM period defined as Phasic REM sleep for (a) 2, (c) 4, and (e) 8 events as a function of level. Proportion of the REM period defined as Tonic REM sleep for (b) 2, (d) 4, and (f) 8 events as a function of level.

Based on simulations and the classification of Tonic and Phasic REM sleep in the UK dataset, the Duffing equation appears to predict the behavior of fast REM activity. The use of a Duffing type equation for modeling brain activity does have support in the sleep literature. There have been many models developed for neuron bursting activity. Phasic REM sleep can be thought of bursting activity. One of the most commonly used models is the Hodgkin-Huxley model. This is a model of the behavior of 3 channels through a neuron membrane: sodium, potassium and a leakage channel (Gerstner and Kistler (1996); Izhikevich (2004)). Either a constant current or a short current pulse is applied as input to the model and the output is the voltage potential which may contain a spike.

A simplification of the Hodgkin-Huxley equations was made, that model is called the Fitz-Hugh Nagumo model and consists of the following two equations (Gerstner and Kistler, 1996),

$$\dot{x} = x - \frac{1}{3}x^3 - y, \tag{7.19}$$

$$\dot{y} = a + bx - cy. \tag{7.20}$$

The two equations can be combined to create a second order differential equation by solving Equation (7.19) for y,

$$y = x - \frac{1}{3}x^3 - \dot{x}, \tag{7.21}$$

taking the derivative,

$$\dot{y} = \dot{x} - \dot{x}x^2 - \ddot{x}, \tag{7.22}$$

and substituting them into Equation (7.20). The equation that is obtained is:

$$\ddot{x} + (1-c)\left(\frac{1}{1-c}x^2 - 1\right)\dot{x} + (b-c)x + c\frac{1}{3}x^3 + a = 0, \tag{7.23}$$

which with an applied sinusoidal force can be written as,

$$\ddot{x} + p(kx^2 - 1)\dot{x} + \omega_o^2 x + \beta x^3 = a_o + Acos(\omega t). \tag{7.24}$$

This equation has the same form as the Duffing Van der Pol equation. If k is zero then the equation has the form of a Duffing oscillator. Curtco, Sakata, Marguet, Itskov, and Harris (2009) modeled neuron activity in the auditory cortex when urethane-anesthetized rats were exposed to auditory stimuli using the Fitz-Hugh Nagumo equations, though the form of the Fitz-Hugh Nagumo model they used was slightly different, in that the model had an x^2 term in addition to the x and x^3 in Equation (7.19).

In addition to neuron bursting models, Zeeman (1976) discussed how there are different scales at which to model brain activity. He described small-scale theory as consisting of models of individual neurons, synapses, and nerve impulses. Large-scale models are models of the end result like thinking and responding. He stated that what is needed is a model of medium-scale behavior. The medium-scale model he believes could be something like the Duffing oscillator because it has the oscillatory behavior found in neurons and he stated that it would be expected that some neuron activity would be stable and some would not.

The Duffing equation has also been used to model epileptic seizures as well as visual evoked responses. Stevenson, Mesbah, Boylan, Colditz, and Boashash (2010) wanted to create a model of newborns EEG activity including seizure activity. The model developed consisted of a Duffing oscillator driven by Gaussian noise for the

background EEG and a Duffing oscillator driven by impulsive noise to simulate the seizure activity. The two signals output from the models were added in order to obtain a simulated newborn's EEG signal. Srebro (1995) used a Duffing equation to model visual evoked potentials observed in EEG data. The visual stimulus that was used consisted of a checkerboard pattern that was shown at intervals. Srebro (1995) was mostly interested in modeling the response of the system to impulsive perturbations and matching the increase and subsequent decay of the response to the individual evoked potentials that were observed in experiments. They found that the result with the Duffing oscillator was a better match to the evoked potentials then what would be predicted by using a linear stiffness.

7.4 Model Parameter Estimation

Now that a fast REM sleep model has been developed and the fast dynamic behavior limitations of the Massaquoi and McCarley model have been overcome, the parameters of the different components of the sleep model needed to be estimated using the 1999 UK data. The methods used and the values of the estimated parameters for the different components of the model are described.

7.4.1 The Homeostatic Process S Model

The term S in the Massaquoi and McCarley model represents the need for sleep and decreases through the night. While there have been several variations in the equation for this term, in its most basic form S is an exponentially decaying function (Achermann and Borbély, 1990) of the form:

$$S = S_o e^{-g_c t}, \tag{7.25}$$

where the parameter gc controls the decay rate. While there is no direct measurement of Process S, it can be estimated from the decay of slow wave activity (SWA). Process S is an upper bound on the level of slow wave activity. To estimate the initial value of S and the decay rate, first SWA during the night was calculated. Slow wave activity was calculated in a manner similar to that used by Ferrillo, Donadio, De Carli, Garbarino, and Nobili (2007). The EEG signals, from the 1999 UK study were segmented into 30 second segments of sleep. This segmentation was repeated moving through the signal in 1 second increments. Using the segment average ($pWelch$ in Matlab) the power spectral density was calculated. The 30 second segment was further segmented into 4 second segments with 75% overlap. The total power between 0.5 and 4.5 Hz was calculated from the estimated power spectral density. To smooth the result further, a moving average filter was used in which the averaging was performed over three minute segments (Achermann, Dijk, Brunner, and Borbély, 1993). The smoothed SWA estimate was then normalized by the mean of the SWA activity for the entire night. This normalization was also done by Achermann, Dijk, Brunner, and Borbély (1993).

Once the SWA estimate was smoothed and normalized then the 95th percentile of SWA during each NREM period was calculated. Before performing this calculation, though, first the boundaries of each REM period during the night had to be calculated. To calculate these limits the original scored sleep stages from the 1999 UK study for each subject were used. First, all stages scored as REM sleep during the night were identified. Then, if there were less than 15 minutes duration of NREM sleep or Wake between scored REM stages, the REM and intervening NREM stages were considered to be in the same REM period. REM periods that were less than 5 minutes in duration were ignored because REM periods should be greater than 5 minutes in

duration (Achermann, Dijk, Brunner, and Borbély, 1993). An example of the scored sleep stages during the night and the defined REM periods are shown in Figure 7.23.

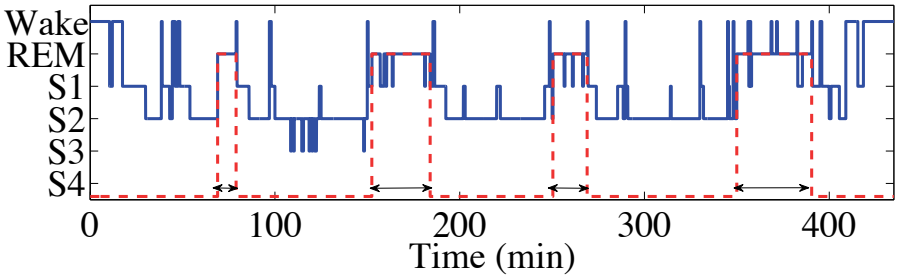

Figure 7.23. An example of Sleep Stages (blue) and identified REM periods (red dashed line).

The 95th percentile of SWA levels for each intervening NREM period was then calculated and the time of these points was determined. The 95th percentile rather than the maximum level was used to reduce the likelihood that the point was associated with an artifact. An exponential function was then fitted to the set of points. An example of the estimated slow wave activity and the values used to to estimate the exponential function are shown in Figure 7.24. The mean and standard deviation for both the decay parameter gc and the amplitude at the start of the night (S_o) estimated from the data are listed in Table 7.3.

The data from the 1999 UK study that was used to estimate the model parameters comes from measurements of subjects between the ages of 30 and 40. Dijk, Beersma, and van den Hoofdakker (1989) calculated the decay rate of Process S for two different age groups, 20-28 and 42-56. They found a decay rate of -0.225 units/hour for the younger group and -0.155 units/hour for the middle age group. The results listed in Table 7.3 need to be scaled by 60 minutes/10.7 minutes, due to differences in time scaling, however when rescaled the resulting decay rate based on the data from the UK study is -0.1794 units/hour which is in-between the results found for the two age

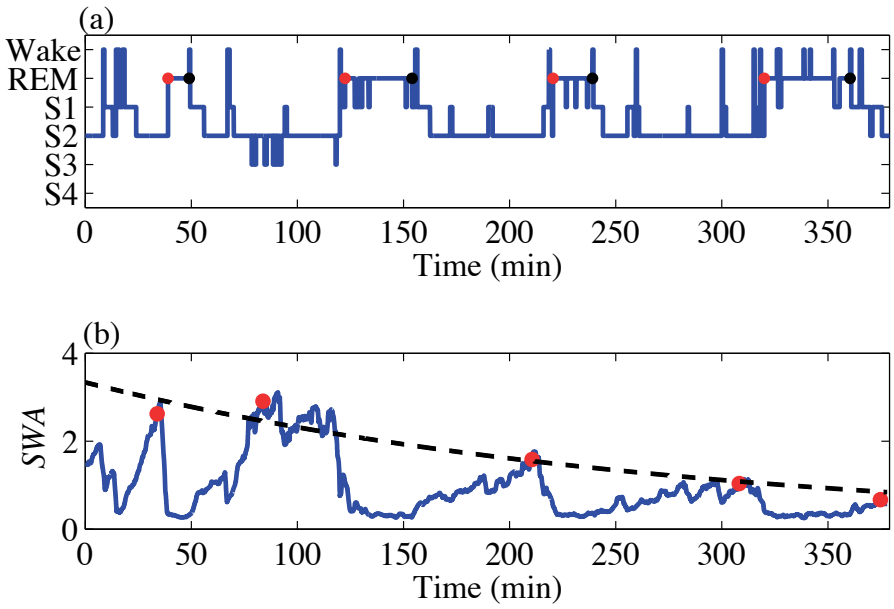

Figure 7.24. (a) Sleep Stages. The start of each REM period is indicated by a red dot and the end of each REM period is marked by a black dot. (b) Estimated SWA (blue), 95th percentile of SWA for each NREM period (red dot) and the estimated Homeostatic Process S (black-dashed line).

groups by Dijk, Beersma, and van den Hoofdakker (1989). This gives an indication of how the coefficients of Process S need to be varied in order to account for different age groups.

7.4.2 Slow Wave Activity

The model for slow wave activity that is being used is not the model in Massaquoi and McCarley (1992). The model in Achermann, Dijk, Brunner, and Borbély (1993) is being used. The primary reason for this is that this model of SWA has separate terms for controlling (1) the fall of SWA due to the onset of REM sleep and awakenings and (2) the rise of the slow wave activity. The equations for the slow wave model are,

$$\dot{S} = -gc\, SWA \tag{7.26}$$

and

$$\begin{aligned} S\dot{W}A = rc\, SWA\ (S - SWA) - fc\,(SWA - SWA_L)REMT - \\ fcw\,(SWA - SWA_L)E. \end{aligned} \tag{7.27}$$

The parameters in the slow wave activity equation were estimated using the 1999 UK data. The initial value of slow wave activity ($SWAo$), was determined by first identifying the onset of sleep, which is the first occurrence of Stage 2, and then calculating the mean of the slow wave activity for the first minute of sleep. The method Achermann, Dijk, Brunner, and Borbély (1993) used to estimate SWA_L was used. They set the parameter SWA_L, which is the lower bound for the level of slow wave activity, equal to a value that is five percent lower than the lowest value of slow wave activity observed during periods of REM sleep. The mean values and standard

deviation for these two coefficients, estimated using the 1999 UK data, are listed in Table 7.3.

To calculate the rise parameter (rc), the first 30 minutes of the slow wave activity was extracted. The maximum value for the segment of SWA was calculated and only the portion of the segment between the first point and the maximum value was used to calculate rc. An example of SWA for one subject and the portion used to calculate rc is shown in Figure 7.25 (a).

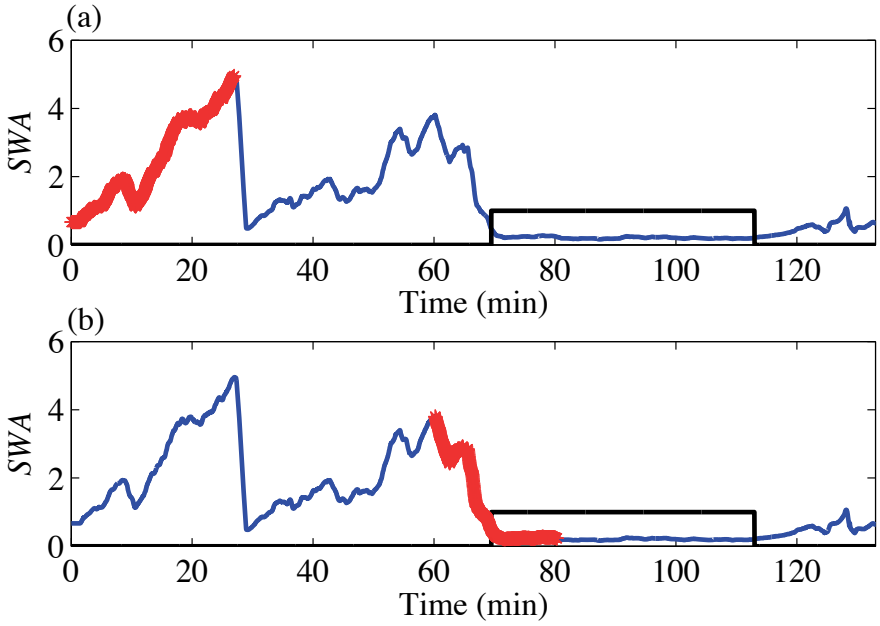

Figure 7.25. SWA activity (blue), REM periods (black) and (a) portion of segment used to calculate rc (red) and (b) portion of segment used to calculate fc (red).

To calculate rc, a continuous time system identification approach/least squares approach was used (Doughty, Davies, and Bajaj, 2002). When SWA is increasing in level the second term in Equation (7.27), $REMT$, is equal to zero. Therefore the equation is,

$$\dot{SWA} = rc\, SWA\ (S - SWA)\,. \tag{7.28}$$

The value of $S\dot{W}A$ was calculated by taking the derivative of the segment of SWA. Taking the derivative of a signal can increase high frequency components therefore the derivative was also low pass filtered. The value of S used was based on the estimated value of S.

To calculate the fall parameter (fc), 15 minutes of the slow wave activity before each REM period plus the slow wave activity within the first quarter of each REM period was extracted. The maximum value of SWA for the segment was calculated and only the portion of the segment between the maximum value and the last data point was used to calculate fc. An example of SWA and the portion used to calculate fc are shown in Figure 7.25 (b).

The value of fc can be calculated in a similar manner as rc in which the equation,

$$S\dot{W}A - rc\,SWA\ (S - SWA) = -fc\,(SWA - SWA_L), \tag{7.29}$$

is solved for fc. The model parameters rc and fc were calculated in order to obtain an estimate of the rise and fall of slow wave activity and to verify that the values in the literature are also applicable to the UK data. However, real slow wave activity is more variable than the slow wave activity simulated by using the model due to awakenings and other ongoing activity, therefore, for all subject nights of data a reasonable single rise and fall constant could not be calculated. As the mean values for rc and fc for all subject nights was similar to the mean values reported in the literature, the mean values were used in the combined model, but it should be noted that they actually vary by subject and also probably by situation and are perhaps better characterized by a distribution.

To estimate the characteristics that define the noise ($n(t)$) in the model Achermann, Dijk, Brunner, and Borbély (1993) calculated the difference between a smooth version of the slow wave activity and that of an unsmoothed version of the slow

wave activity. The SWA activity within each 3 minute block of time was averaged to obtain the smoothed SWA_S. The noise time histories can be estimated for each subject-night by using,

$$n = \frac{SWA - SWA_S}{SWA_S}, \tag{7.30}$$

where SWA is the unsmoothed version of slow wave activity and SWA_S is the smoothed version of the slow wave activity. An example of the original SWA, the smoothed SWA and the noise term n, that was calculated for one subject night using the UK dataset is shown in Figure 7.26. A distribution of the amplitude of the noise is shown in Figure 7.27. A Gaussian function was fit to this distribution data and is shown for comparison. There appeared to be a skewness in the distribution of $n(t)$. A possible reason for this skew, maybe, is that while most large artifacts in the data were removed perhaps smaller movement artifacts were not. To examine if this is the reason for the positive skew, the mean, standard deviation, skewness, and kurtosis for $n(t)$ were calculated when only portions of the data were considered. The noise ($n(t)$) data for each subject night was sorted and the lower and upper 0.5% of the data was eliminated. The statistics of n were then calculated through time using a sliding 30 minute segment. This procedure was repeated eliminating larger protions of the lowest and highest values in the dataset up to an elimination of 5% (the upper and lower 2.5%) of the data. The results for one subject night are shown in Figure 7.28. When portions of the data were removed, as expected, kurtosis is reduced but a skew in the data is still prevelant. This is also clearly seen in the data, Figure 7.26 (a). The results for all subjects indicate a skewness in the data, the results of which are shown in Figure 7.29. Therefore in the model to simulate n a skewed Gaussian distribution was used based on the parameters in Table 7.3.

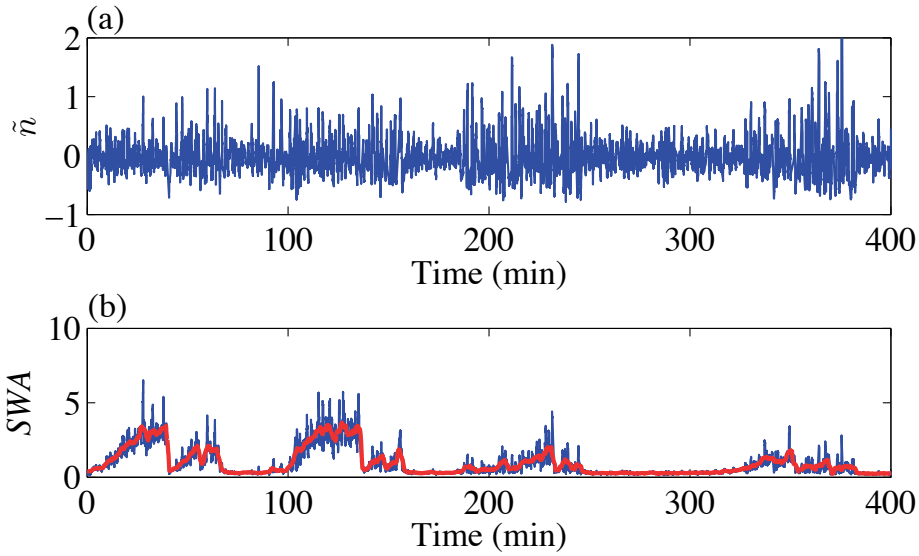

Figure 7.26. (a) Estimated noise term $n(\tilde{t})$, (b) the original SWA (blue), and smoothed SWA (red).

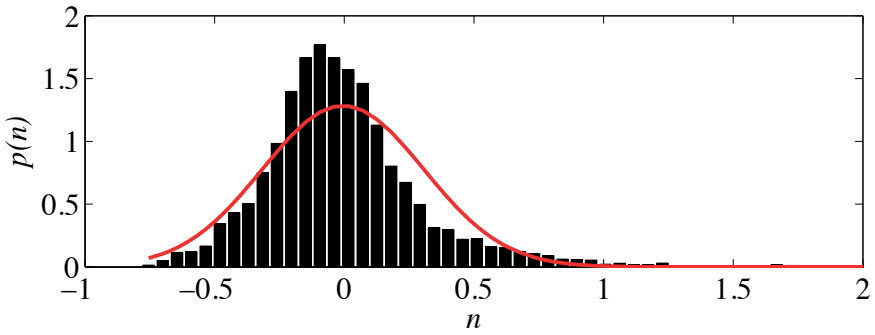

Figure 7.27. Probability density function of $n(t)$ (black) and Gaussian distribution resulting from a fit to the data (red).

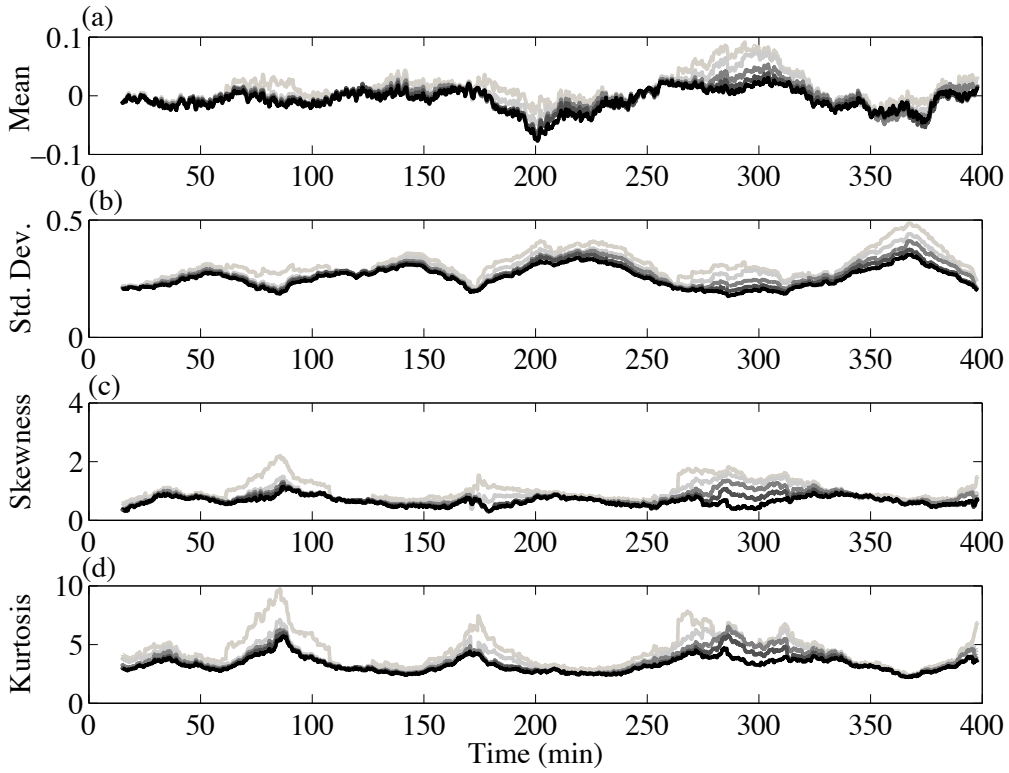

Figure 7.28. Statistics of $n(t)$ with tails of the distribution removed. Gray to black results from eliminating 1% to 5% of the tails of the distribution of $n(t)$ before calculating the statistics for each 30 minute segment.

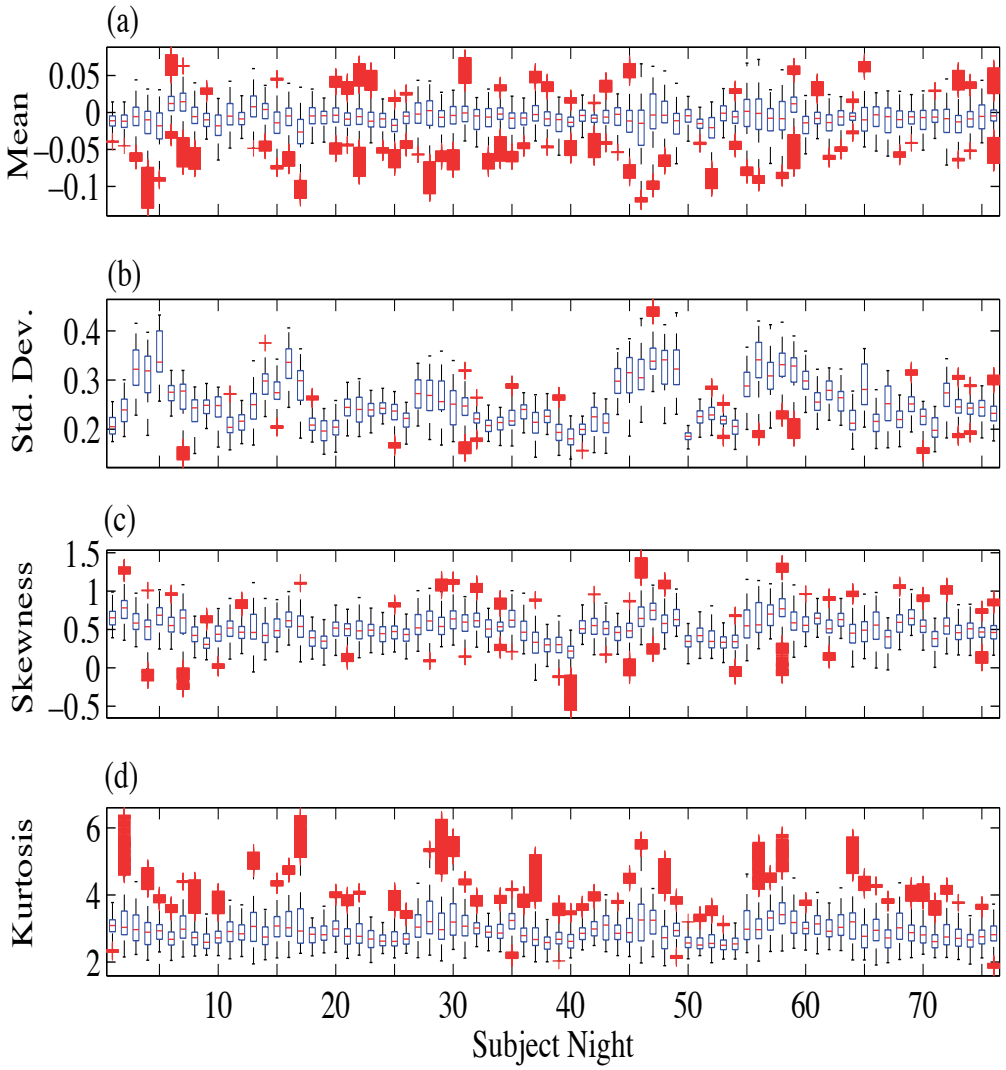

Figure 7.29. Range of values for the (a) mean, (b) standard deviation, (c) skewness, and (d) kurtosis for all subjects based on statistics calculated from each moving 30 minute segment of the estimated random noise term $n(t)$. The results are shown as a boxplot: red line median, edge of each box is the lower and upper quartile, the red plus signs are outliers.

The last parameter of the SWA model is the fall in slow wave activity due to noise events (fcw). Achermann, Dijk, Brunner, and Borbély (1993) considered the rate of fall in slow wave activity when awakenings occur to be four times faster than the rate when a REM period occurs. However, they assumed that the wake term was never larger than 1 in their model. A value for E other than 1 was used, and this will be discussed in the following section. The value for fcw that was chosen was 2 times the value of fc.

Table 7.3. Coefficients of the SWA model estimated from data taken from 76 subject nights of the 1999 UK study. Mean and standard deviation of these estimates, based on the data, and original values from Achermann, Dijk, Brunner, and Borbély (1993).

Coefficient	Mean (std. dev)	Original Values
gc	0.03 (0.01)	0.0893
fc	2.1 (1.0)	2.5252
rc	0.4 (0.1)	0.5368
S_o	3.7 (0.7)	3.138
SWA_o	0.8 (0.3)	0.468
SWA_L	0.17 (0.04)	0.1
$nt - mean$	-0.017 (0.005)	0
$nt - std$	0.25 (0.04)	0.182
$nt - skew$	0.5 (0.1)	0
$nt - kurtosis$	3.0 (0.2)	3

7.4.3 The Wake Term

The characteristics of the excitation term E, that can lead to spontaneous non-noise induced awakenings, was calculated by using the data from no noise laboratory nights in the UK study. It was decided to use the power in the gamma band of the EEG signal (activity between 25 and 35 Hz) to represent this term. The calculation of activity in the different frequency bands of the EEG signal were described in Section

6.4. It is noted that this band contains both movement activity and EEG activity, however, as movements are an indicator of awakenings this was considered acceptable activity to include in the Wake term. The time between the occurrence of these pulses or the inter-arrival time was calculated. An example of the gamma activity and the definition of duration, amplitude and inter-arrival time are shown in Figure 7.30 and the distributions of these parameters are shown in Figure 7.31. The distribution for the inter-arrival time appears to be exponential. The mean value for the inter-arrival time was 6.1 minutes. The value used by Massaquoi and McCarley (1992) in their model was 11.8 minutes, therefore, the inter-arrival time found in the UK dataset was half the value of the original model.

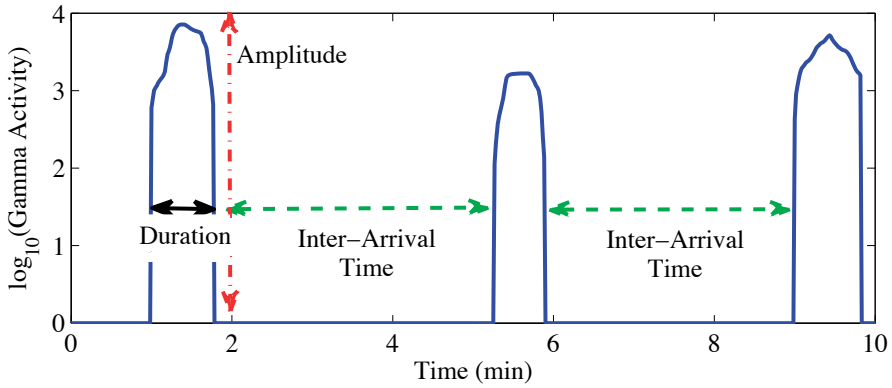

Figure 7.30. An example of gamma activity, arrows indicate inter-arrival time, duration and amplitude of the excitations.

The values for the duration of $N(t)$ ranged from 3 seconds to 1.2 minutes, with a mean of 0.5 minutes and a standard deviation of 0.2 minutes. The minimum and maximum values for the duration of $N(t)$ used in the original Massaquoi and McCarley model were 2.7 minutes and 5.4 minutes. This range is obviously too high and does not allow brief awakenings to be predicted. The amplitude of $N(t)$ is difficult to determine based on the gamma activity. There is not a direct relationship between the level of the impulses in the model and the level of gamma activity. However, the current

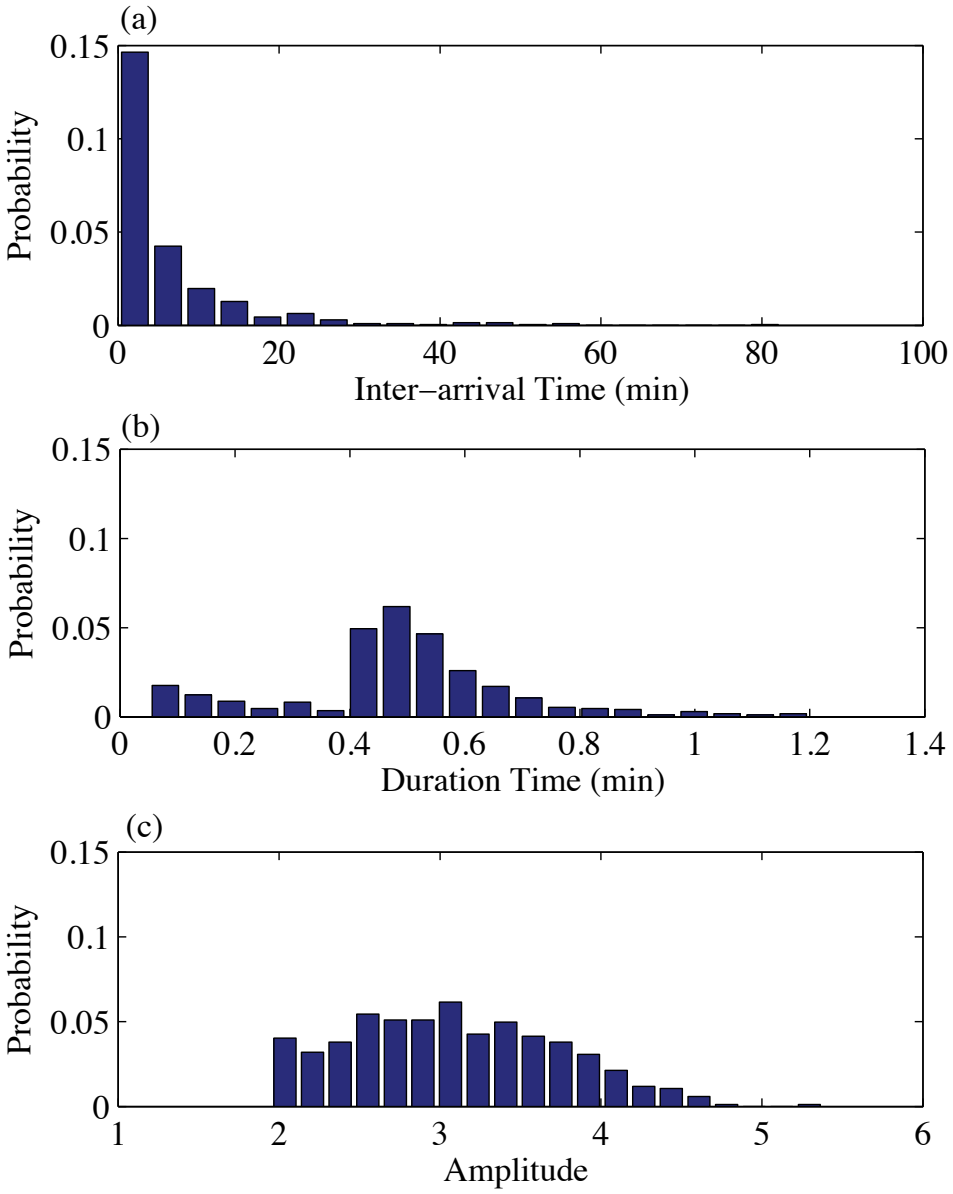

Figure 7.31. (a) Distribution of inter-arrival times between estimated $N(t)$, (b) distribution of the duration of $N(t)$, and (c) distribution of the amplitude of $N(t)$ in the UK dataset.

approach used to estimate the amplitude was to take the log based 10 of the power in the gamma band. The minimum value obtained was 2.0, the maximum value was 5.4, the mean was 3.1, and the standard deviation of the data was 0.65. A summary of the parameters for the spontaneous wake model are in Table 7.4. To model $N(t)$ for spontaneous awakenings, the duration and amplitude was defined by Gaussian distributions based on the statistics that were calculated and the inter-arrival time was defined by an exponential distribution.

Table 7.4. Estimated values for the statistics of the impulsive excitation ($N(t)$) that leads to the spontaneous wake model based on the UK dataset and original values from Massaquoi and McCarley (1992).

Coefficient	Estimated Value	Original Values
mean inter-arrival time	6.1 minutes	11.8 minutes
minimum duration	3 seconds	2.7 minutes
maximum duration	1.2 minutes	5.4 minutes
mean duration	0.5 minutes	4.0 minutes

7.4.4 Slow REM Sleep

The Massaquoi and McCarley model (1992) contains two equations for defining REM sleep, one representing REM-ON or REM promoting neuron activity (X) and one representing REM-OFF or REM inhibiting neuron activity (Y) (see Equations (5.47) and (5.48)). The difficulty in estimating the parameters of the REM model is that the UK dataset can be used to estimate the timing of REM sleep but not REM neuron activity.

Ferrillo, Donadio, De Carli, Garbarino, and Nobili (2007) tried to estimate the parameters of the REM sleep model based on data. They calculated the parameters for the Lotka-Volterra REM model by using a stochastic search of parameters and

minimizing the difference between slow wave activity from their dataset and the slow wave activity that was predicted. One problem with their parameter estimation method is that they calculated only one set of parameters for the model, i.e. they assumed that the duration of successive REM periods are the same.

From the UK dataset, the mean duration of REM and NREM sleep were calculated for the first 4 REM periods based on 76 subject nights of data. The results are shown in Figure 7.32. The mean duration of REM sleep does increase during the night while the duration of NREM sleep decreases. Therefore, the assumptions made by Ferrillo, Donadio, De Carli, Garbarino, and Nobili (2007) in estimating the parameters of their model may be incorrect.

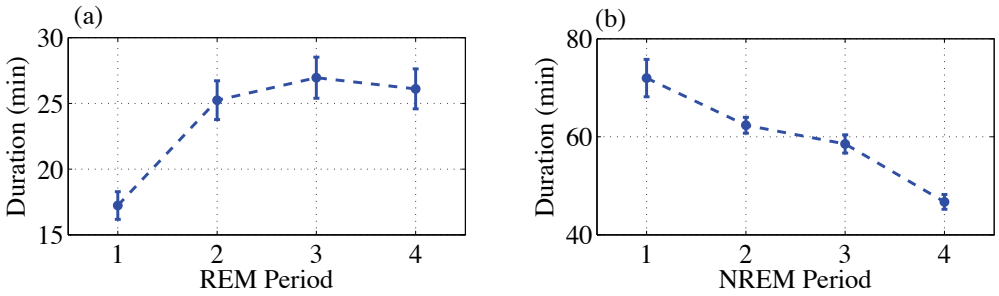

Figure 7.32. (a) REM sleep duration and (b) NREM sleep duration. Mean values and ± one standard deviation of the estimated mean, estimated from the 1999 UK study.

A different approach than that of Ferrillo et al. (2007) was used to estimate the REM model parameters. The parameters were estimated separately for each REM period. Signals for REM-ON and REM-OFF activity were created based on the timing of REM sleep in the UK data. The equations for the simplified REM model were used and these are:

$$\dot{X} = aX - bXY, \tag{7.31}$$

$$\dot{Y} = -cY + dXY. \tag{7.32}$$

If an assumption is made that c and d are equal and a and b are equal, which is a necessary step in order to create REM-ON and REM-OFF signals, then the equations are,

$$\dot{X} + aX(Y - 1) = 0, \tag{7.33}$$

and

$$\dot{Y} + cY(1 - X) = 0. \tag{7.34}$$

When Y is varying slowly compared to X the solution is approximately of the form,

$$X = e^{-a(Y-1)t}, \tag{7.35}$$

and when X is varying slowly compared to Y then Y is approximately,

$$Y = e^{-c(1-X)t}. \tag{7.36}$$

Therefore, Y grows when X is greater than 1 and decays when X is less than 1, and X grows when Y is less than 1 and decays when Y is greater than 1. The value of X was set equal to one at the start of the REM period and at the end of the REM period. The value of Y was set equal to 1 when X is at a maximum and it reaches its maximum level at the end of the REM period. Based on these values, an exponential function was used to create the rise and decay of each signal and where the exponential functions join the transition was smoothed by rounding out the slope of the signals. An example of the signals generated with this approach is shown in Figure 7.33 (a) and the smoothed signals are shown in Figure 7.33 (b).

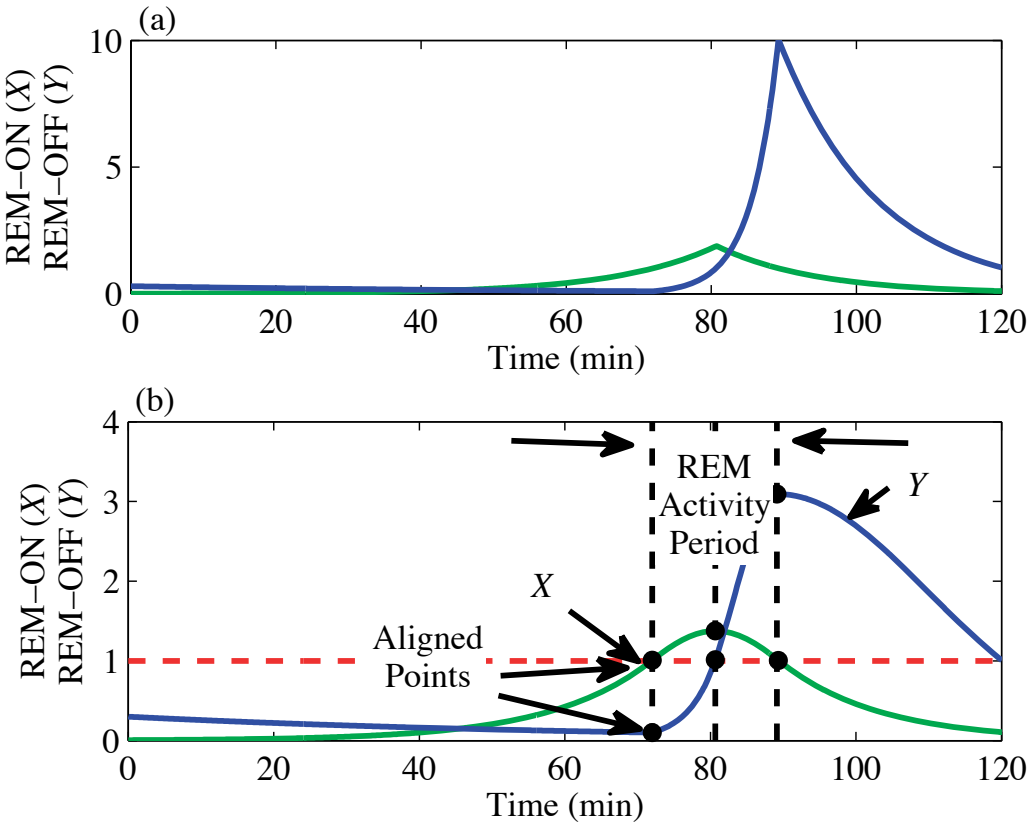

Figure 7.33. An example of creating REM-ON (X) and REM-OFF (Y) signals based on the timing of REM sleep periods in the 1999 UK study data and Equations (7.33) and (7.34).

To estimate the parameters of the X and Y model the derivative of both of the constructed signals were calculated and then the following two linear equations in parameters (a and b, and c and d):

$$\frac{\dot{X}}{X} = a - bY, \tag{7.37}$$

$$\frac{\dot{Y}}{Y} = -c + dX, \tag{7.38}$$

were fitted to the data. An example of the estimated linear relationships for REM-ON and REM-OFF activity are shown in Figure 7.34.

Using the estimated parameters, the REM-ON and REM-OFF activity was then calculated by solving Equations (7.31) and (7.32) using *ode45* in Matlab. Based on the obtained solution, the value for the coefficient a was altered in order to align the calculated REM-ON activity (when X is greater than 1) with the actual start of REM sleep in the survey data. Similarly the value for c was altered, if needed, in order to better match the duration of the calculated REM activity and the duration of REM sleep in the UK data. The coefficients, a and c, were increased or decreased until the error between the duration and start time of actual and simulated REM sleep, was less than 2 minutes. However, sometimes a low error value could not be obtained due to brief or long REM periods. The error for these values for all REM periods in the UK dataset are shown in Figure 7.35. The duration of NREM sleep is the duration prior to the start of a REM period, therefore it is related to the start time of each REM period. An example of the agreement between a created signal for REM-ON activity and the REM-ON activity, calculated using the estimated parameters, is shown in Figure 7.36. The interest was in matching the start and end of each REM signal, when the REM-ON signal is greater than 1.

The estimated coefficients are plotted against the duration of a REM sleep period in Figure 7.37. The coefficients, c and d, decreased with REM duration. The decrease in c with REM duration is partly due to the fact that it was systematically altered so that the duration of the simulated REM sleep period matched the values derived from the UK dataset. The estimated coefficients are plotted against the duration of NREM sleep in Figure 7.38. The decrease in a with NREM sleep duration is again partly due to the fact that it was altered so that there was agreement between the simulated and actual start time of each REM sleep period.

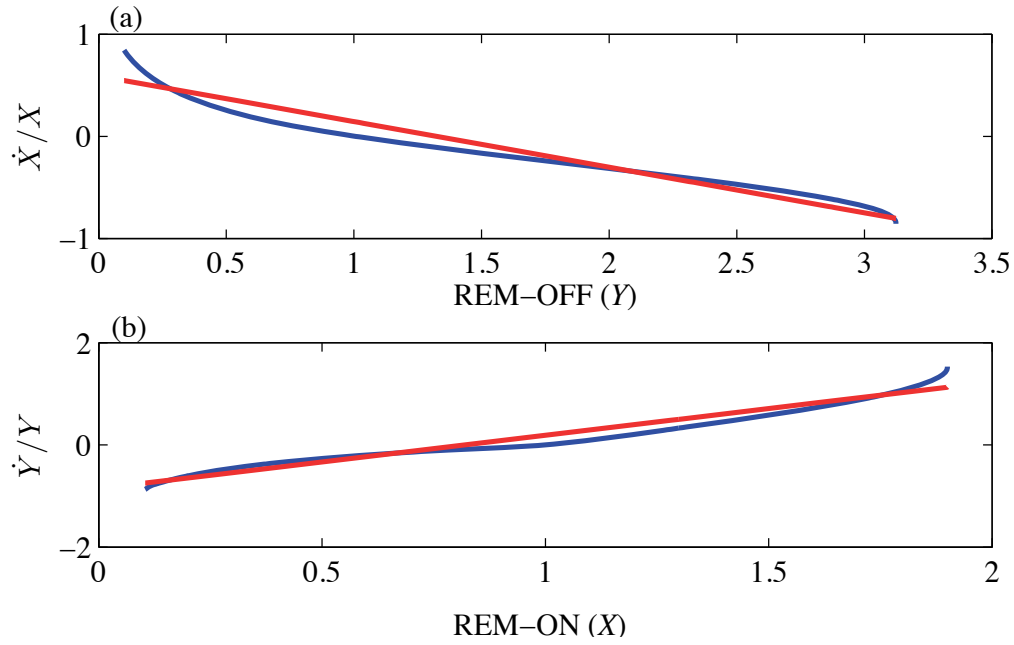

Figure 7.34. An example of the fitting of REM sleep model parameters of (a) the REM-ON model and (b) the REM-OFF model. Blue line is based on created signals and the red line is the linear model using the estimated parameters.

The mean and standard deviation of the estimated coefficients for the first four REM periods were also calculated and are shown in Figure 7.39. The coefficients a and b show similar increasing trends while coefficients c and d both show similar decreasing trends during the night. The change in all parameters though during the night was small. Therefore, for the slow REM model, only a and b were varied with time. The variations are modeled in a similar manner to that in the original Massaquoi and McCarley model, i.e., with a sinusoidal term which has a period of 24 hours. The equation for which is,

$$dc = 1.55 + 0.8sin(0.0467t + 4). \tag{7.39}$$

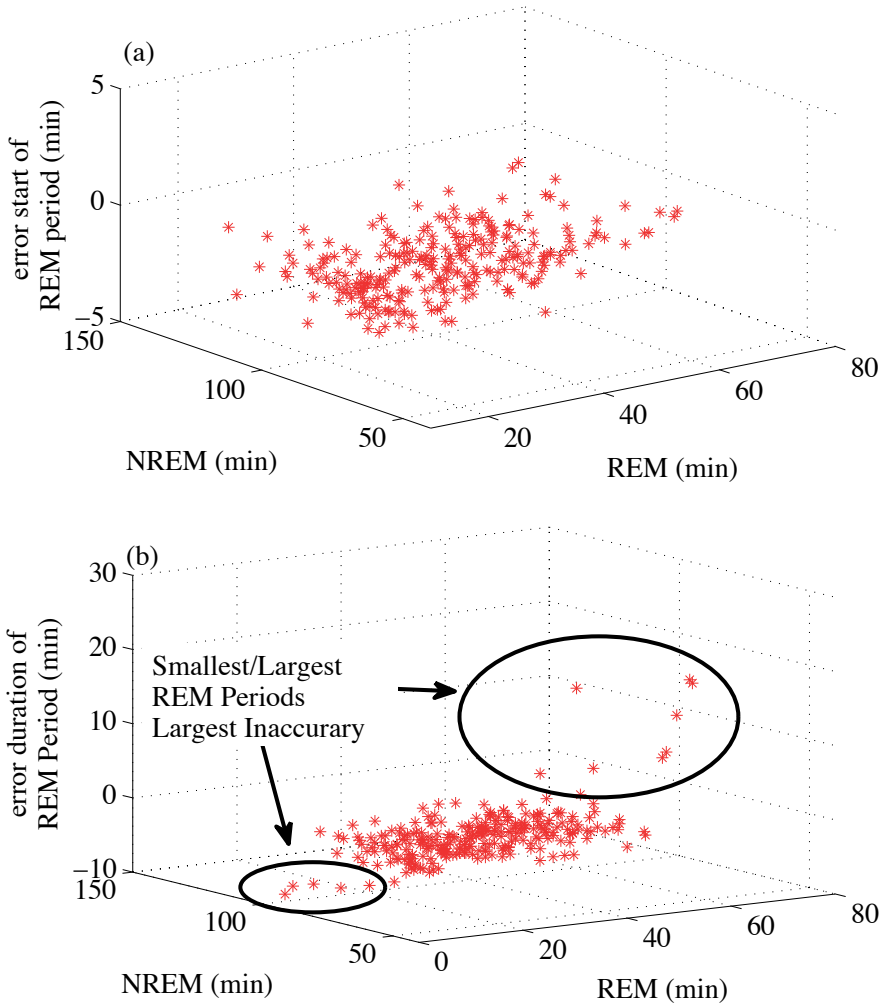

Figure 7.35. (a) Error between the estimated start time of each REM sleep period and the value derived from the UK dataset. (b) Error between the estimated duration of the REM sleep period and the value derived from the UK study data. The NREM duration is for the NREM period just before the REM period.

Note again that in the Massaquoi and McCarley model time is measured in units and 1 unit is equal to 10.7 minutes.

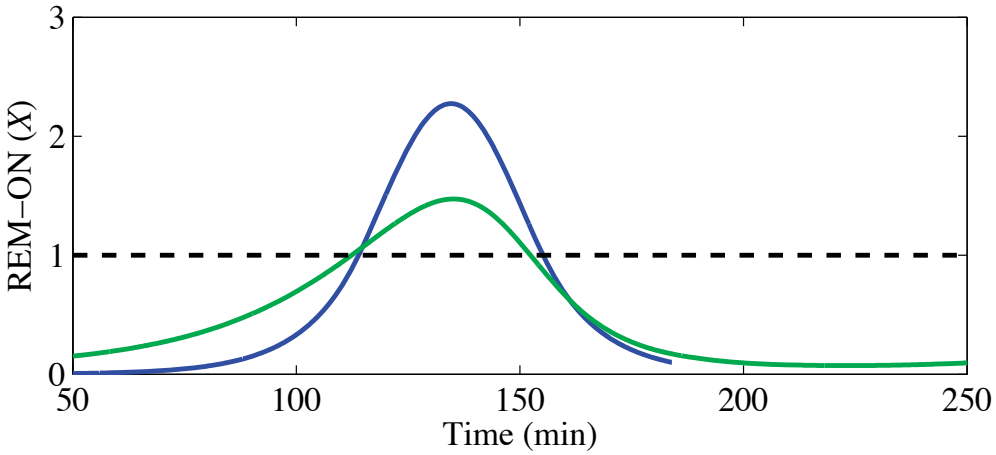

Figure 7.36. The created REM signal based on data and a simplified REM model (Equations 7.31 and 7.32) (blue/dark gray) and the simulated REM signal (green/light gray) using model parameters obtained from a linear fit to the study data.

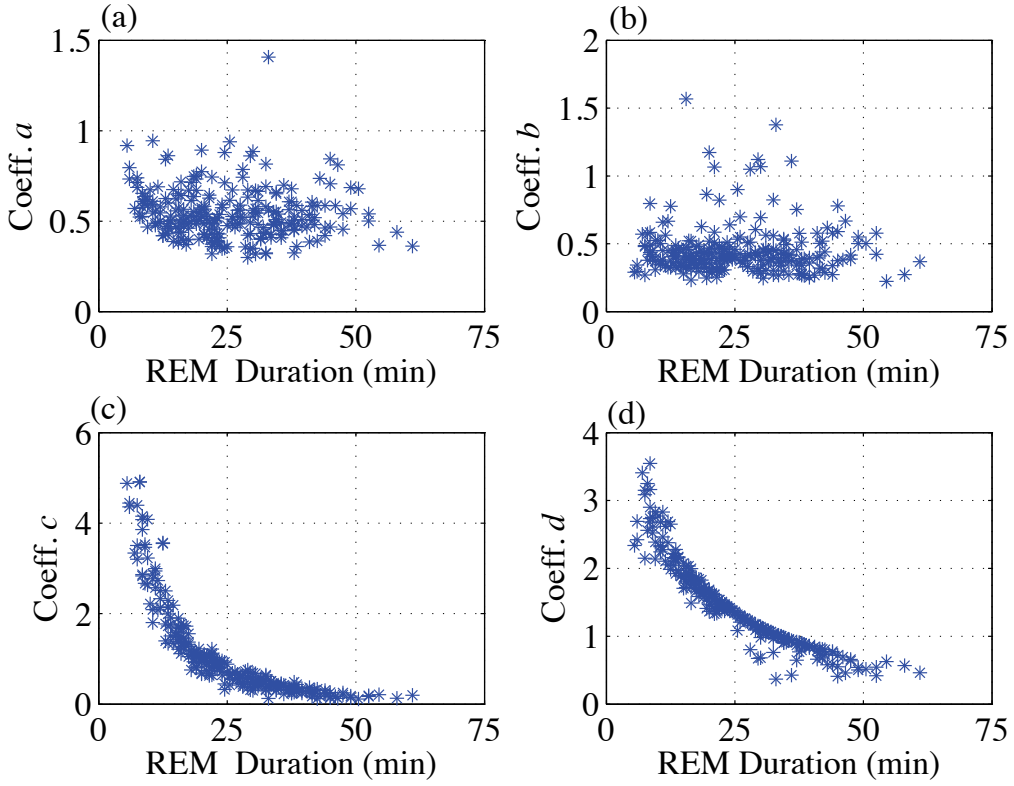

Figure 7.37. Estimated parameters of slow REM model versus the duration of REM sleep.

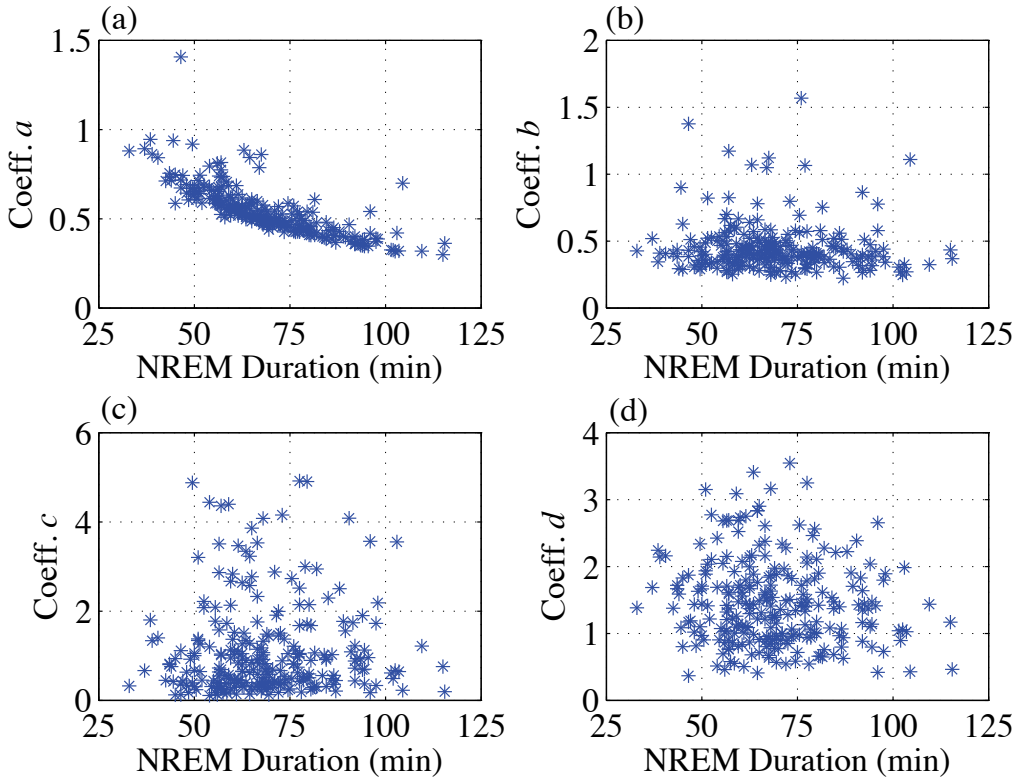

Figure 7.38. Estimated parameters of the slow REM model versus the duration of the NREM sleep period prior to the REM period.

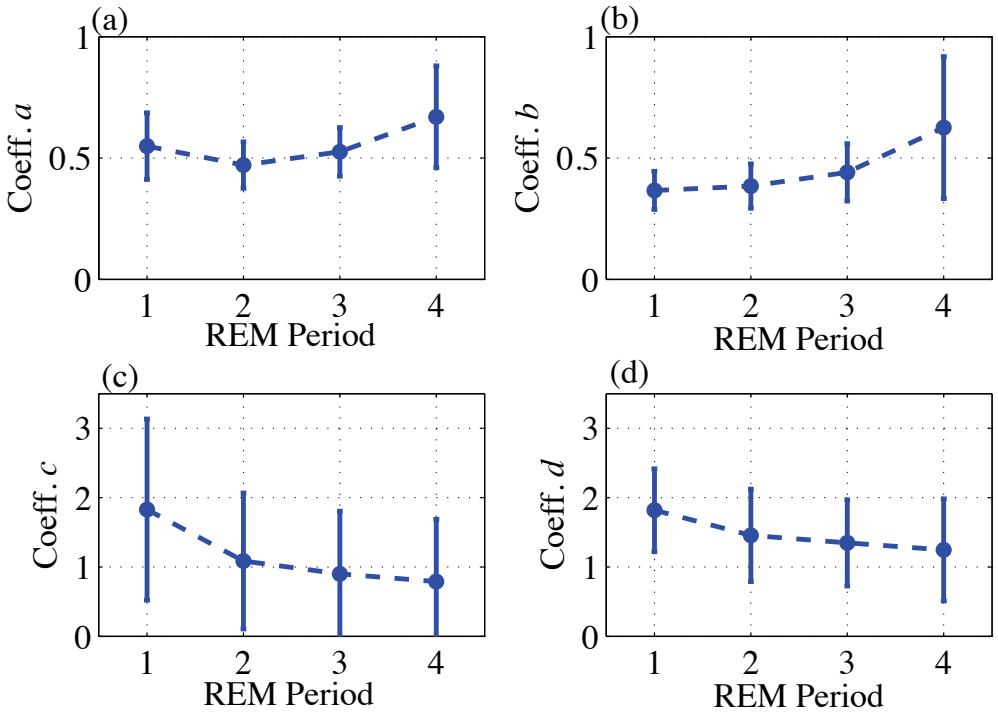

Figure 7.39. Mean and standard deviation of the estimated REM model parameters for each REM period.

7.5 Overview of The Model So Far

The complete nonlinear model is the result of all issues addressed and noted in this chapter and what follows in this and the following sections. So far, to recap, the SWA, S, the slow REM (X, Y) model and the fast REM model have been described. These models contain an impulsive term based on $N(t)$. $N(t)$ is a series of square pulses whose amplitudes and durations are Gaussian distributed, and the inter-arrival time has an exponential distribution. The parameters of these models have been estimated based on the data from the UK study. The following issues, though, still need to be resolved.

1. The desire is to have a model that results in the prediction of sleep stages. To calculate different stages, thresholds based on the level of SWA need to be assigned.

2. How should a noise event impact the sleep model? One possibility is to increase the number of excitations $N(t)$ and this will be a function of the L_{Amax} of the noise event.

These issues will be addressed in the following sections.

7.6 Thresholds for Scoring Sleep Stages

The output of the model being developed includes REM sleep, slow wave activity and awakenings. However, it is desired to also estimate different NREM stages (i.e. Stage 2 and Stage 3/4). In order to determine at what level to set the thresholds for this classification, first the mean, minimum and maximum level of SWA activity associated with Stage 3/4, Stage 2, and Stage 1/Wake were calculated for the 76 subject nights of the UK study. The results are listed in Table 7.5. Based on these levels a set of scoring rules were developed and are as follows:

1. Stage 3/4 was scored if SWA was greater than 2.75.

2. Stage Wake/1 was scored if SWA was less then 0.3.

3. Stage Wake/1 was scored if SWA was less than 1 and E was greater than 0.5.

4. At all other times when REM sleep was not occurring, stages were scored as Stage 2 sleep.

To evaluate the accuracy of these thresholds, simulations of slow wave activity for each subject night of data from the 1999 UK study, were completed using the model

parameters estimated in the previous sections, and the timing of REM sleep. The gamma activity for each subject was used to create the impulsive excitation term E. The fast REM model was not used for these simulations as the focus was on setting thresholds for scoring NREM sleep. Based on the thresholds and simulated levels of SWA, sleep stages were assigned to each 30 second epoch. The agreement between the actual scored sleep stages in the UK dataset and the simulated sleep stages was calculated. The agreement was defined as the fraction of all stages that were correctly identified. The overall agreement statistics are listed in Table 7.6 and the mean and standard deviation of the fraction of correctly identifying stages for each sleep stage is listed in Table 7.7. An example of the simulation that yielded the highest agreement is shown in Figure 7.40, and the simulation that had the lowest agreement is shown in Figure 7.41.

Table 7.5. Statistics of slow wave activity during different sleep stages for 76 subject nights in the 1999 UK dataset.

Sleep Stage	Mean (std. dev of data)	Min.	Max.
Stage Wake/1	0.42 (0.14)	0.14	1.24
Stage 2	1.06 (0.21)	0.67	1.53
Stage 3/4	3.41 (0.52)	1.86	5.08

Table 7.6. Overall statistics of the fraction of times there was agreement in sleep stage classification between scoring of the original data and automated scoring of simulated data for each of 76 subject nights.

mean	0.66
std. dev	0.07
max	0.79
min	0.43

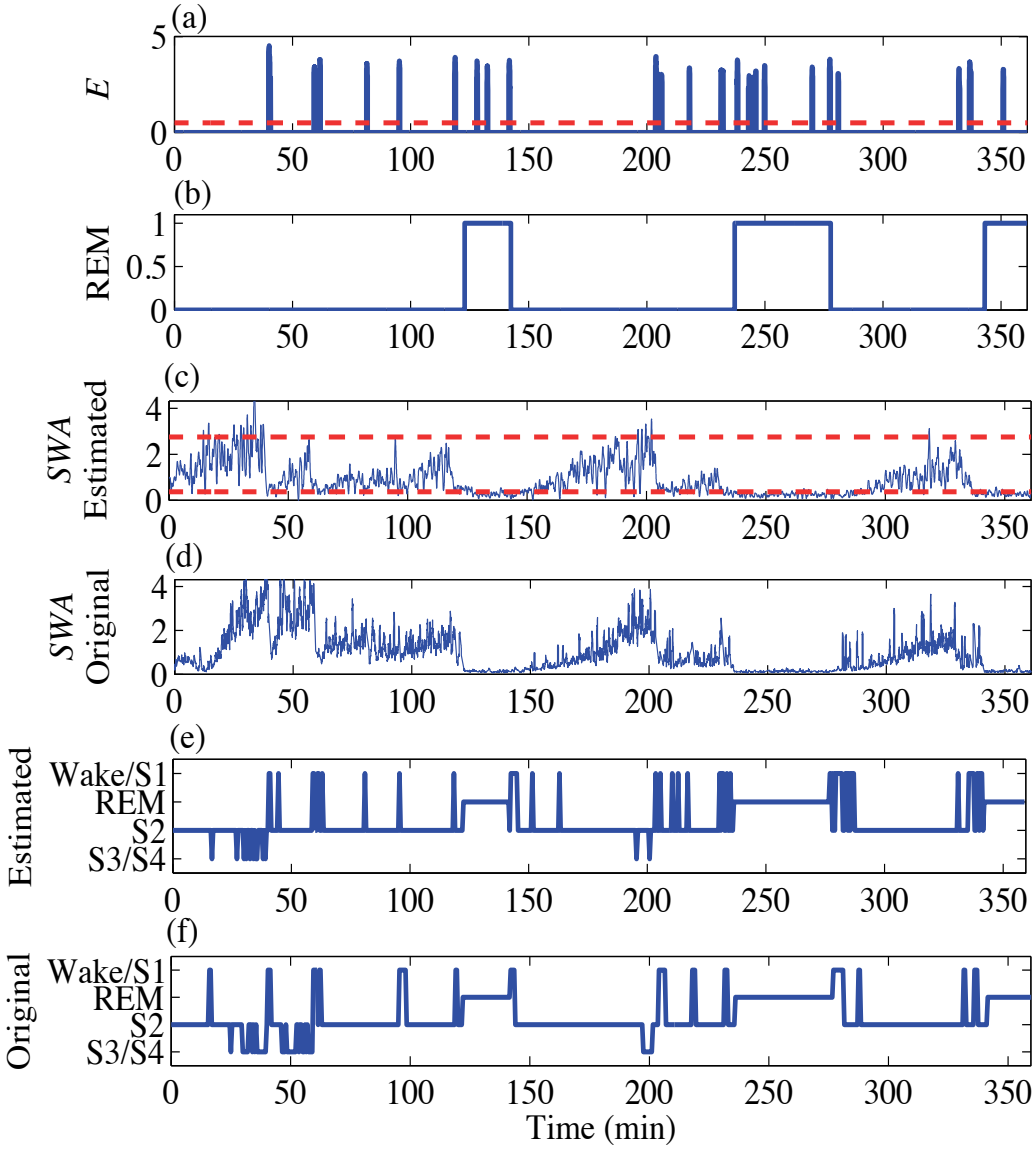

Figure 7.40. Best agreement between simulated and actual slow wave activity for one subject night of the 1999 UK dataset, thresholds used for scoring sleep stages (red-dashed lines).

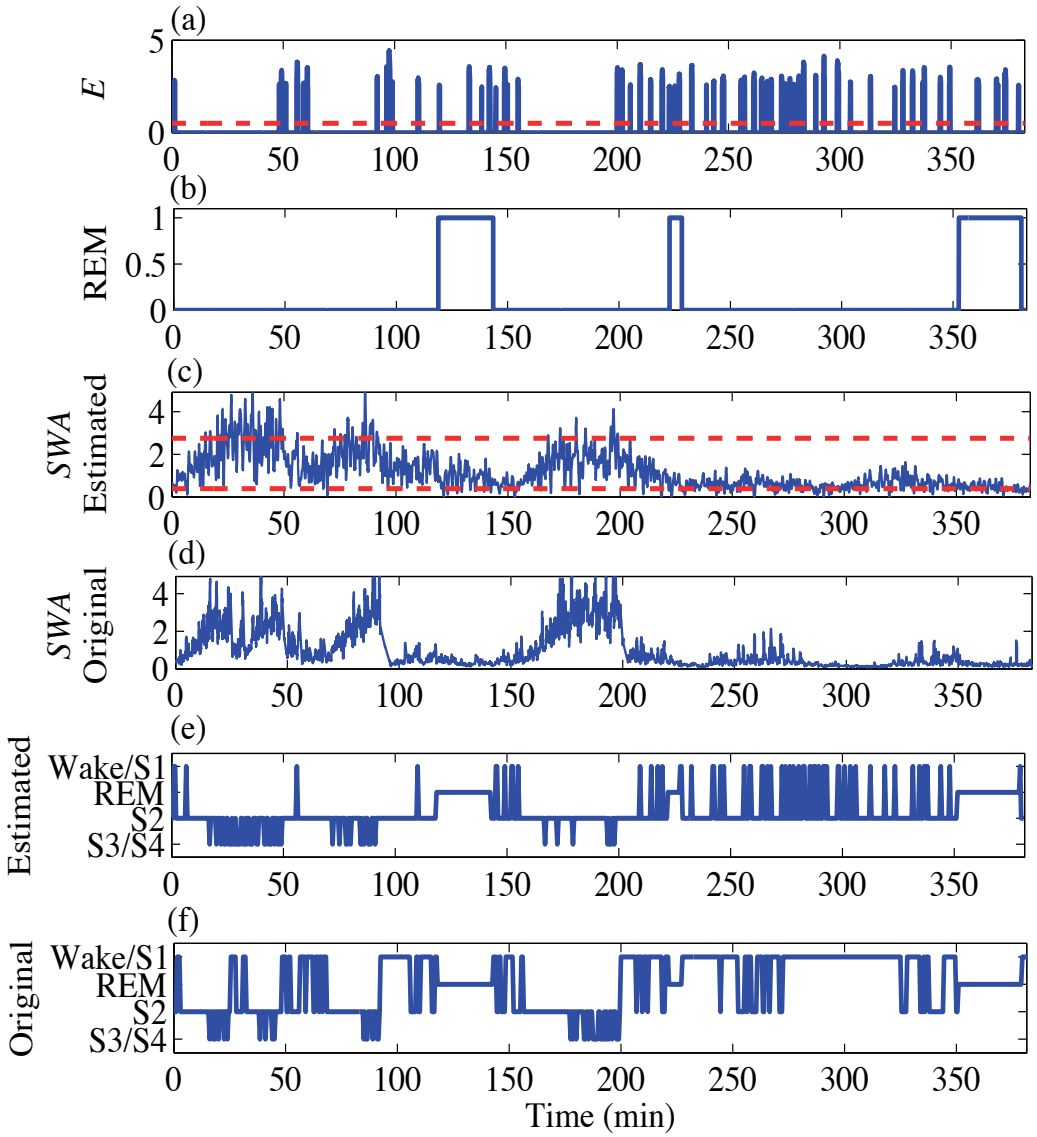

Figure 7.41. Worst agreement between simulated and actual slow wave activity for one subject night of the 1999 UK dataset, thresholds used for scoring sleep stages (red-dashed lines).

Table 7.7. Statistics of the fraction of times that there was agreement in sleep stage classification between scoring of the original data and automated scoring of simulated data for each of the 76 subject nights, for each sleep stage.

Sleep Stage	Mean (std)
Wake/S1	0.43 (0.17)
Stage 2	0.73 (0.09)
Stage 3/4	0.51 (0.29)

7.7 Adding Noise Dependence to Model

As discussed $N(t)$ is impulsive noise. The inter-arrival time of $N(t)$ is exponentially distributed and the amplitude and duration are both defined based on Gaussian distributions. The $N(t)$ term is low-pass filtered to obtain E which is used in the slow wave model and as mentioned in Section 7.3, is rescaled and also used in the fast REM model. Some of the examples shown for the fast REM model have used scaled versions of $N(t)$ (square impulses), not E. A diagram of the use of the impulsive terms is shown in Figure 7.42. The concept for introducing noise into the model was to create an excitation term for spontaneous (non-noise related excitations) and one for aircraft noise related excitations. The two components, both non-noise induced and noise induced excitations, are summed together and then fed into other parts of the model.

In order to determine how to add a noise level dependence to the nonlinear dynamic model, the amplitude of E from the UK data, was examined when noise events of different maximum levels occurred. Characteristics of E including the duration and amplitude of the events were examined, for every aircraft event that occurred during sleep Stage 2. Due to the limited amount of data, only two noise groups were examined: events which had a noise level below 50 dB(A) and events that had a maximum level greater than 50 dB(A). A small difference in amplitude of E was found,

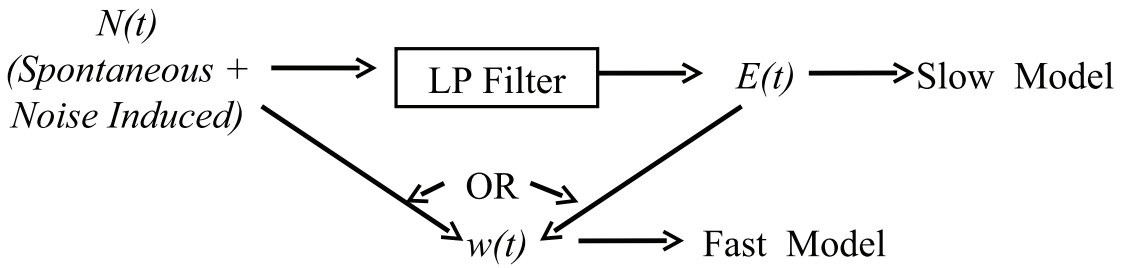

Figure 7.42. Diagram of impulsive noise as used in nonlinear dynamic model.

however, the primary difference was in the number of events that elicited additional impulses. Therefore, when modeling the effect of noise on sleep a linear relationship between the percentage of the population that will have a response to the noise event and the Indoor L_{Amax} of an event was created. The equation used is,

$$fraction\ \ responding = 0.0084 L_{Amax} - 0.1256. \tag{7.40}$$

Only L_{Amax} levels above 35 dB(A) cause a change in the fraction responding. Researchers have found from studies on aircraft noise and sleep that aircraft events with a L_{Amax} level below 35 dB(A) do not increase the probability of awakening (Basner, Buess, Elmenhorst, Gerlich, Luks, MaaB, Mawet, Müller, Müller, Plath, Quehl, Samel, Schulze, Vejvoda, and Wenzel, 2004). The percent increase in response with noise level was added based on existing awakening models (see Chapter 3 for more information) because the data from the UK study was limited and could not be used to create a reliable dose response relationship. The duration and height of $N(t)$ is assigned randomly based on normal distributions with mean and standard deviation as

defined in Table 7.8. Perhaps with more data, a variation in amplitude and duration with noise level will be identified and can be added to the model.

7.8 Combined Model

The components of the nonlinear dynamic model that was developed include a fast and a slow REM model, a SWA activity model, and impulsive excitations $N(t)$ for both spontaneous and noise induced awakenings. To simulate the sleep pattern of a person for a single night the following steps are performed:

1. The spontaneous excitation term $N(t)$ is generated based on an exponential inter-arrival time and Gaussian duration and amplitude distributions and is low-pass filtered to obtain $E(t)$.

2. If aircraft noise is present, the additional noise excitation term is generated and then the spontaneous and noise-induced excitation terms are summed together.

3. Both noise and spontaneous excitation terms are scaled to generate $w(t)$ for the fast REM model.

4. The excitation term $E(t)$, that includes both spontaneous and noise induced activity is fed into the slow REM activity model. The output of the slow REM model is REM-ON and REM-OFF activity which is used to generate a REM sleep indicator which is equal to 1 when the level of REM-ON X activity is above a level of 1. This REM indicator defines the REM periods.

5. The REM indicator that is generated is used to signal when to model fast REM activity. The term $w(t)$ is fed into the fast REM model in order to predict transitions to Stage Wake during a REM period.

6. The REM indicator and excitation term ($E(t)$) are fed into the Slow Wave Activity Model. For the SWA model, the rise and fall terms for the slow wave activity (fc, rc), and the mean, standard deviation, and skewness of the noise term ($n(t)$) are not varied for each simulation (one person night). The other parameters are varied according to Gaussian distributions, the mean and standard deviations of which are listed in Table 7.8.

7. Based on the SWA, REM-Indicator, excitation terms, and fast REM model, sleep stages are assigned for each 1 second. In order to compare predicted sleep stages though to other existing models, the probability of being in each sleep stage for each 30 second epoch is calculated from the 1-second sliding sleep stage classification and then a sleep stage is assigned according to the highest probability.

In Table 7.8 is a list of the model parameters and the values used in the simulations. An example of the individual output components of the combined model are shown in Figure 7.43. An example of sleep stages calculated from a simulation with and without aircraft noise is shown in Figure 7.44. For the simulation with aircraft events, there were 32 evenly spaced events with an L_{Amax} of 60 dB(A). Note the additional awakenings that occur during the REM sleep period.

The predictions of the nonlinear model were compared to those of Basner's Baseline Markov model (2006). Six hundred simulations, each simulation contains a different choice of random variables for parameters that are described by distributions, for baseline conditions without aircraft noise events were completed using the nonlinear model. The probability of being in each sleep stage was calculated. For these simulations the threshold used to assign Stage 3/4 was lowered to 2 instead of 2.75. The reason is that perhaps the properties of $N(t)$ are more time varying, with less excitations occurring during Stage 3/4, this should be explored in the future. The results

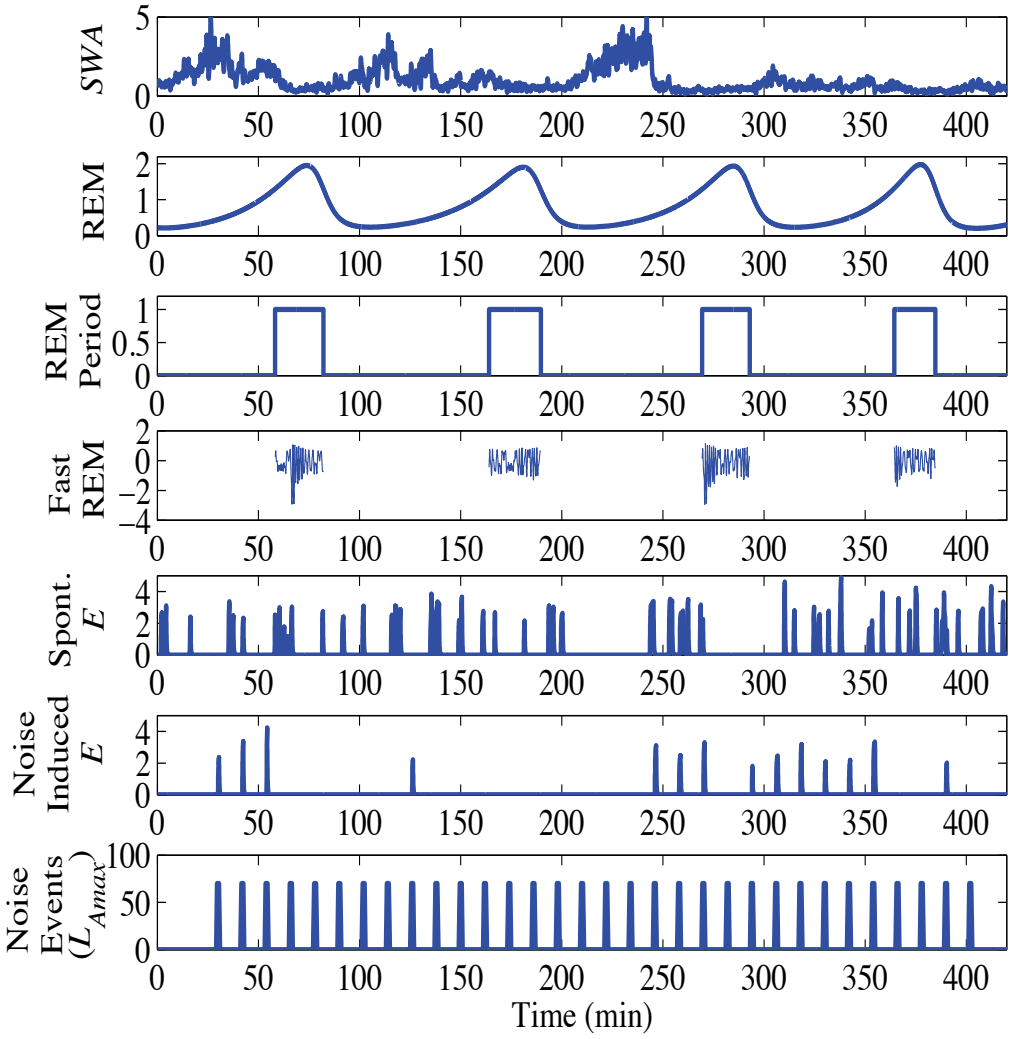

Figure 7.43. Example of the parameters for the developed nonlinear sleep model, which include slow wave activity (SWA), REM which is the X or REM-ON activity, REM sleep period indicator, Fast REM model and the spontaneous and noise induced excitation terms.

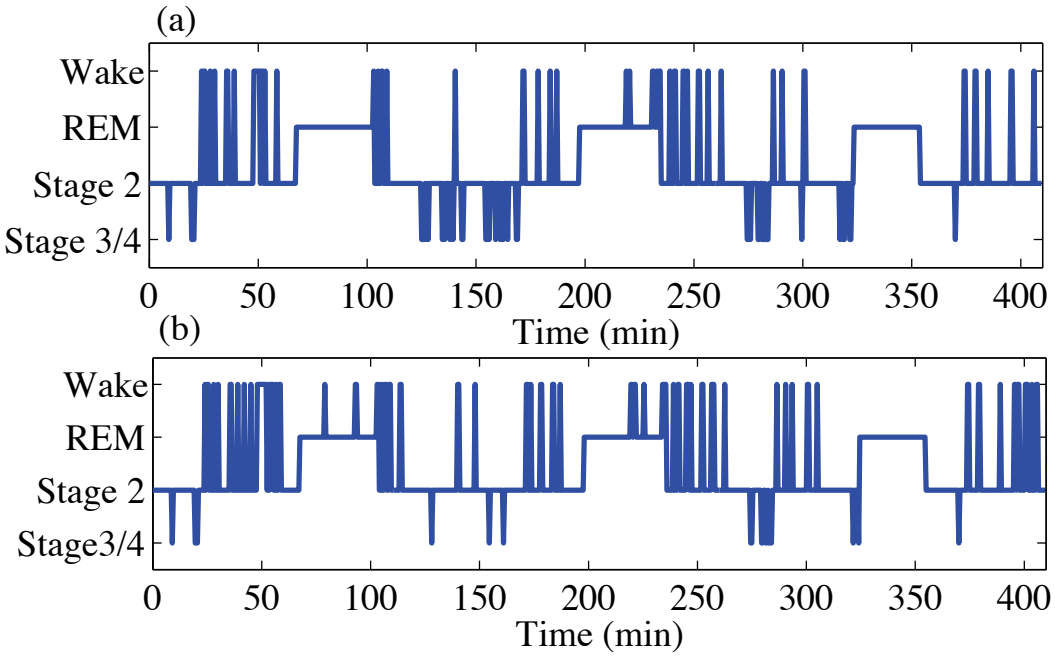

Figure 7.44. Sleep stages calculated using the developed nonlinear model. (a) No aircraft events, and (b) 32 events of an L_{Amax} of 60 dB(A).

Table 7.8. Parameters of the nonlinear model. *Parameters varied according to a Gaussian distribution, + parameters varied according to a uniform distribution, and x parameter varied according to an exponential distribution.

SWA		Slow REM		Fast REM		Excitations	
$^*S_o$	mean 3.75 std. dev 0.67	$^*a$	mean 0.47 std. dev 0.1	ω	2 π (0.3)	N	^{x}mean inter-arr 6.1 min
$^*SWA_o$	mean 0.78 std. dev 0.29	$^*b$	mean 0.41 std. dev 0.1	A	0.5		*dur.-mean 0.5 min
$^*gc$	mean 0.03 std. dev 0.01	$^*c$	mean 1.4 std. dev 0.15	δ	0.06		*dur.-std. dev 0.2 min
SWA_L	0.2	$^*d$	mean 1.83 std. dev 0.15	^+x_o	min -1.0 max 1.0		*amp.- mean 3.0
fc	2.0	e	0.05	^+y_o	min -1.0 max 1.0		*amp.-std. dev 0.65
fcw	4.0	^+X_o	min 0.15 max 0.3				amp.-max 5.0
rc	0.4	^+Y_o	min 0.5 max 3.0				
$n(t)$	mean 0 std. dev 0.2 skewness 0.53						

are shown in Figure 7.45. Similar predictions for time spent in Stage Wake/Stage 1 were obtained from both of the models. The Markov model did, however, predict a higher probability of being in Stage 3/4 at the start of the night and the increase in the probability of being in REM sleep toward the end of night was greater for that model. However, the subjects in the UK study did have less Stage 3/4 sleep than those in Basner's study which might explain some of the difference in predicted probabilities. Note that the nonlinear model has been tuned to the UK study data and the Basner model to data from a laboratory study (Basner et al., 2004).

Simulations with the nonlinear model were also conducted for scenarios with 16 and 32 noise events of different noise levels. For each simulation, the noise events

were all of the same level. Fifty simulations were conducted for each noise level which ranged from 40 to 90 dB(A), L_{Amax}. The increase in the predicted probability of being awakened with noise level is shown in Figure 7.46 and the change in duration spent in the Slow Wave, REM, and Wake states is shown in Figure 7.47. Fifty simulations for each condition were also completed using Basner's Markov model with added noise level dependence (see Chapter 4). The probability of awakening predicted by the nonlinear model did increase with noise level. Also an increase in duration spent in Stage Wake and a reduction in time spent in Stage 3/4 was found, and the changes were greater for nights when there were 32 events than for nights with only 16 events. The change in REM sleep was less predicable in that it did not vary with noise level. The results for the probability of awakening is in agreement with the modified version of Basner's Markov model. The nonlinear model does predict a higher duration spent awake and a greater reduction in slow wave sleep. However, in Basner's laboratory study (Basner and Samel, 2005) when subjects were exposed to 32 noise events at an L_{Amax} of 70 dB a reduction in Slow Wave Sleep of 10.7 minutes was found, the prediction of the nonlinear model is a reduction of 10 minutes. Also an increase in duration of time spent awake of 11.4 minutes, for the same number and level of events, was found in Basner's Laboratory study while the nonlinear model predicts 12.6 minutes. It is not clear whether the the nonlinear dynamic model needs to be altered to predict less change in sleep stage duration or if the altered version of Basner's Markov model needs to be modified further to predict a larger change in duration, perhaps both modifications are needed.

7.9 Conclusions

The Massaquoi and McCarley sleep model had two primary limitations: it had slow dynamics and could not predict brief awakenings during the night and it could not

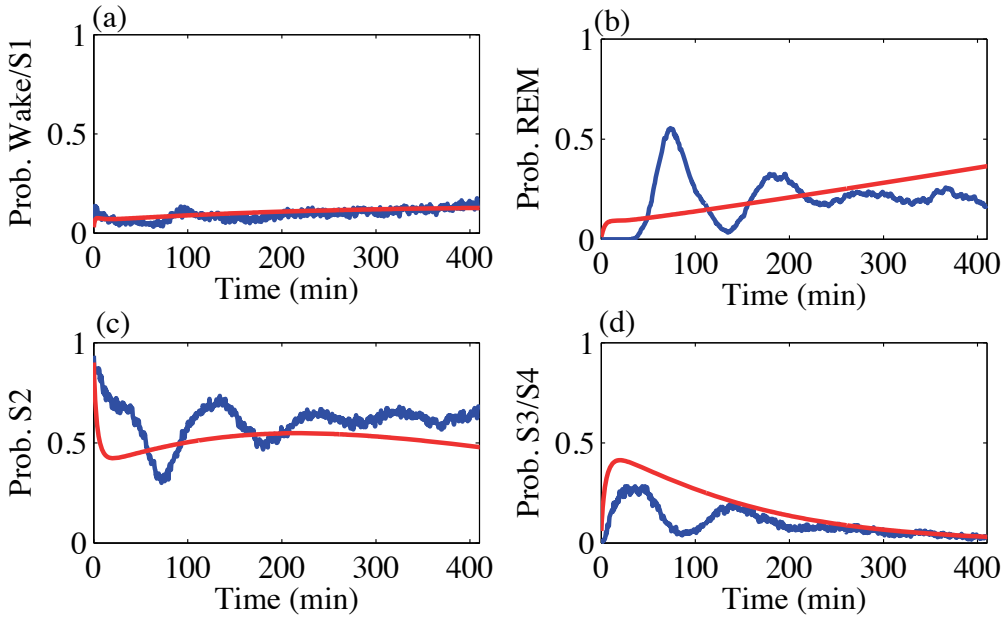

Figure 7.45. Probability of being in each sleep stage predicted for a baseline no noise night using the developed nonlinear model (blue) and Basner's Markov model (red): (a) Wake/S1, (b) REM, (c) S2, (d) S3/S4 Stages.

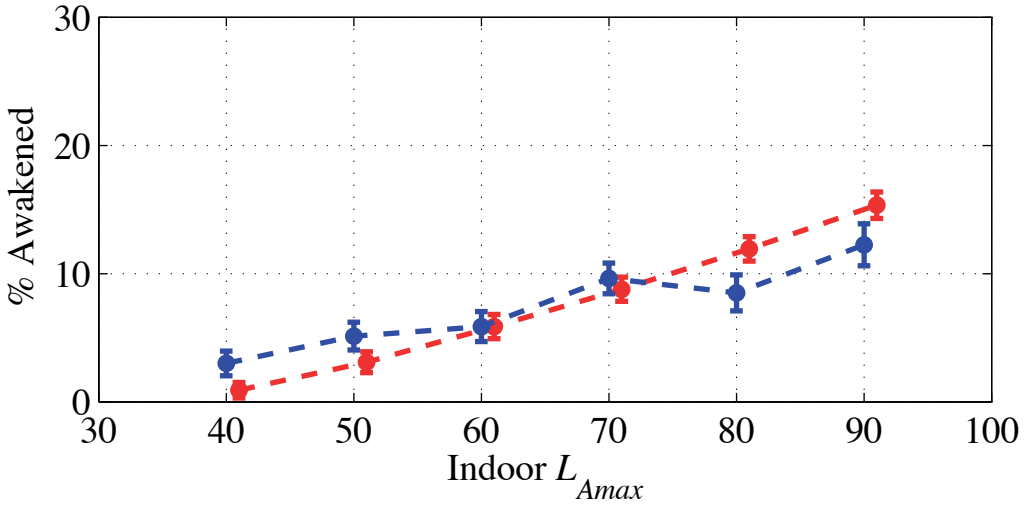

Figure 7.46. Percent awakened predicted with the nonlinear dynamic model developed in this research (blue/dark gray) and the modified version of Basner's Markov model (red/light gray).

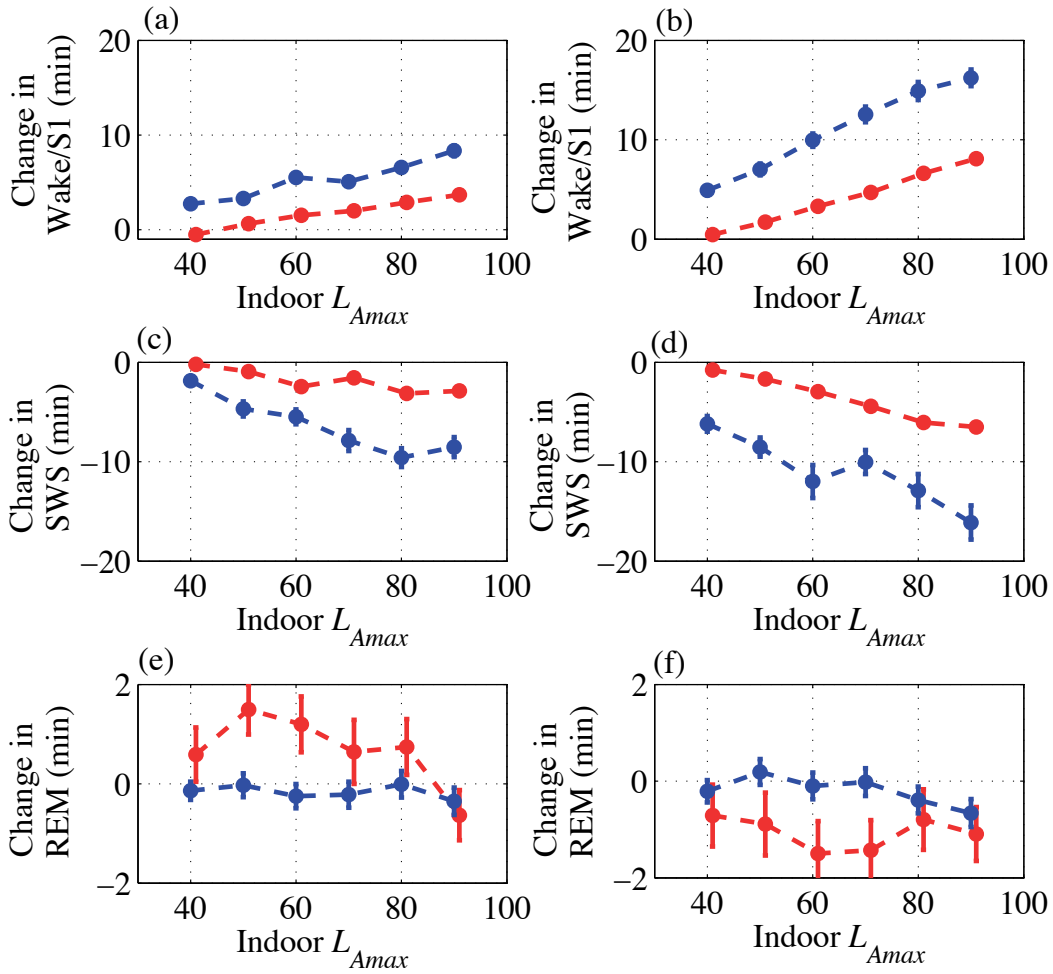

Figure 7.47. Change in duration of Wake/S1, SWS, and REM sleep for (a,c,e) 16 evenly spaced events and (b,d,f) 32 evenly spaced events. The nonlinear dynamic model predictions are shown in blue/dark gray and the predictions from the modified version of Basner's Markov model are shown in red/light gray.

predict awakenings during REM sleep. To overcome these challenges a modified version of the Massaquoi and McCarley sleep model was developed. With this model it is possible to predict spontaneous and noise induced awakenings, slow wave activity and fast and slow REM sleep. The parameters of the developed model were estimated using the data from the 1999 UK data. The predictions of changes in sleep stage duration and increase in probability of awakening for events of different noise levels, using the developed nonlinear model, was found to be similar to other sleep models.

8. NOISE MODEL COMPARISONS FOR AIRPORT OPERATIONS

Data on flight operations from two US airports, aircraft and flight tracks, were obtained. This was used as input to noise prediction software so that noise levels inside houses could be estimated for each aircraft event. By using this information, it is possible to compare sleep disturbance model predictions for different models and for different flight operation scenarios. Comparisons of both awakening model predictions and changes in sleep stages predicted using Basner's Markov model and the nonlinear dynamic sleep model developed in this research are described in this Chapter.

8.1 Airport Noise Modeling

Flight operations data were obtained for two US airports. The airports will be referred to as Airport A and Airport B. The data included the arrival and departure flight paths and the timing of aircraft events, whether they occurred during the day, evening, or night. The specific time of each flight operation was obtained for one of the airports. Information on type of aircraft and distance the aircraft was traveling was also obtained.

A list of aircraft responsible for approximately 90 percent of the operations at each airport was made, to reduce the amount of computation. This was not felt to be a significant problem because a few aircraft made up the majority of operations. By having a smaller number of aircraft it was feasible to calculate the noise for these aircraft on many different flight paths. For Airport A there were 3 runways, 89 arrival and 80 departure flight paths. For Airport B there were 4 runways, 44 arrival and 76 departure flight paths. The primary aircraft for Airport A are given in Table 8.1 and

the primary aircraft for Airport B are listed in Table 8.2. The departure standard, in both tables, refers to how far an aircraft is traveling. The higher the departure standard the farther the aircraft is traveling. In general an aircraft that is flying farther will be heavier at takeoff due to a greater amount of fuel and it will take longer for the aircraft to reach higher altitudes. Therefore, for the same aircraft, as the departure standard increases so do the noise levels on the ground.

Table 8.1. Aircraft at Airport A.

INM Aircraft ID	Description	Departure Standards
757PW	Boeing 757-200/PW2037	1, 2, 3, 4
757RR	Boeing 757-200/RB211-535E4	1, 2, 3, 4
7373B2	Boeing 737-300/CFM56-3B-2	1, 2, 3, 4
737300	Boeing 737-300/CFM56-3B-1	1, 2, 3, 4
737700	Boeing 737-700/CFM56-7B24	1, 2, 3, 4
747400	Boeing 747-400/PW4056	1, 2, 3, 4, 5
767300	Boeing 767-300/PW4060	1, 2, 3, 4
A300-622R	Airbus A300-622R/PW4158	1, 2, 3, 4
BEC190	Beech 1900	1
CL601	CL601/CF34-3A	1
CNA560	Cessna 560 Citation V	1
EMB145	Embraer 145 ER/Allison AE3007	1
EMB170	Embraer EMB-170	1
FAL20	FALCON 20/CF700-2D-2	1
MD11GE	MD-11/CF6-80C2D1F	1, 2
MD82	MD-82/JT8D-217A	1, 2
SD360	SD360	1

For the consolidated list of aircraft, the L_{Amax} and *SELA* noise levels for single event operations on every flight path were calculated by using the Federal Aviation Administration's Integrated Noise Model (INM) (FAA, 2007). The grid size used for the calculations was 0.1 by 0.1 nautical mile. Different flight operation scenarios were created based on the single event data and then sleep disturbance was predicted using

Table 8.2. Aircraft at Airport B.

INM Aircraft ID	Description	Departure Standards
757PW	Boeing 757-200/PW2037	1, 2, 3, 4, 5
757RR	Boeing 757-200/RB211-535E4	1, 2, 3, 4
767CF6	Boeing 767-200/CF6-80A	1, 2, 3, 4, 5, 6
737300	Boeing 737-300/CFM56-3B-1	1, 2, 3, 4
737400	Boeing 737-400/CFM56-3C-1	1, 2, 3, 4
737500	Boeing 737-500/CFM56-3C-1	1, 2, 3, 4
737700	Boeing 737-700/CFM56-7B24	1, 2, 3, 4
737800	Boeing 737-800/CFM56-7B26	1, 2, 3, 4
747400	Boeing 747-400/PW4056	1, 2, 4, 7
767300	Boeing 767-300/PW4060	1, 2, 3, 4, 5, 6, 7
777200	Boeing 777-200ER/GE90-90B	1, 2, 3, 4, 7
A319-131	Airbus A319-131/V2522-A5	1, 2, 3, 4
A320-232	Airbus A320-232/V2527-A5	1, 2, 3, 4
A321-232	Airbus A321-232/IAE V2530-A5	1, 2, 3, 4
A340-211	Airbus A340-211/CFM 56-5C2	1, 2, 3, 4, 5, 6, 7
CL600	CL600/ALF502L	1
CLREGJ	Canadair Regional Jet	1
DHC8	DASH 8-100/PW121	1
EMB14L	Embraer 145 LR / Allison AE3007A1	1
EMB120	Embraer 120 ER Pratt and Whitney PW118	1
MD82	MD-82/JT8D-217A	1, 2, 3, 4
MD83	MD-83/JT8D-219	1, 2, 3, 4
SF340	SF340B/CT7-9B	1

different models including the ANSI sleep model, Basner's Markov Model, and the nonlinear dynamic model developed in this research.

8.2 Awakening Model Comparisons

A baseline scenario for Airport A and Airport B was created. The scenario for Airport A had 150 operations and the scenario for Airport B had 281 operations. These numbers were the same for all the different scenarios investigated at each airport.

The aircraft and flight paths used were assigned randomly after calculating usage statistics for both airports. The percentage of the population awakened at least once for the airport scenarios was predicted using the ANSI standard method, however no time dependence was used, and different dose-response relationships were used (see Chapter 3) in order to compare models in a more comprehensive manner. Also as the sleep models are based on indoor noise levels and INM only predicts outdoor levels, for all simulations an outdoor to indoor noise attenuation of 25 dB(A) was used. In the future, it would be desirable to improve the outdoor-to-indoor prediction using characteristics of typical houses, window opening habits, house orientation, etc. This 25 dB(A) level of attenuation is similar to the reduction in noise level found in numerous studies (WHO, 2009).

The results for the baseline scenario for Airport A is shown in Figure 8.1 (a,b,c) for predictions calculated using the the ANSI (2008), FICAN (1997), and Basner et al. (2004) awakenings models. The results in Figure 8.1 (d,e,f) are percent awakened at least once predictions for a scenario in which 25 of the 150 operations were assigned to the third cross runway. For comparison, the 40 and 55 dB(A) $L_{night,outside}$ contours are shown. According to the WHO Night Noise Guidelines for Europe (2009) an $L_{night,outside}$ of 40 dB(A) should not be exceeded in order to prevent adverse health effects caused by noise. However, as this contour encompasses a large area and it would be difficult to reduce noise levels below this level, reducing nighttime noise to levels below an $L_{night,outside}$ of 55 dB(A) is the target goal. The ANSI standard model was found to predict the lowest percent awakened at least once. This is due to the fact that the model is based on behavioral awakening data. This low prediction (compared to that of other models) is particularly noticeable for the scenario in which there were 25 events on the cross runway.

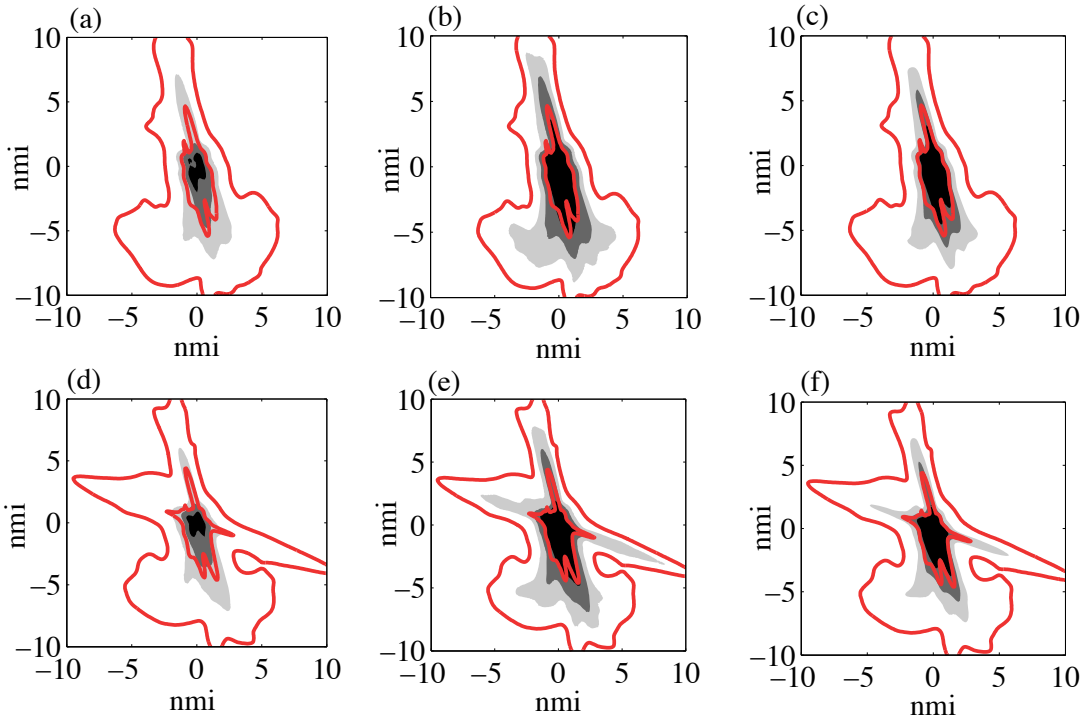

Figure 8.1. Gray-scale shading indicates percent awakened at least once. Black to dark gray 75%, dark gray to light gray 50%, and light gray to white 25%. (a,b,c) Scenario 1 and (d,e,f) Scenario 2 for Airport A. (a,d) ANSI, (b,e) FICAN and (c,f) Basner et al. model. Red contours are the 40 and 55 dB(A) $L_{night,outside}$ contours.

The number of people predicted to be awakened in communities surrounding Airport A and Airport B was also calculated. Population data was obtained from the US census and the number of people living within each 0.1 by 0.1 nautical mile block was calculated. The number of people in each block was then multiplied by the percent awakened at least once predicted using Basner et al.'s dose-response model. In Figure 8.2, the number of people living in each block for both Airport A and Airport B are shown and in Figure 8.3 the number of people predicted to be awakened at least once is shown. For comparison the $L_{night,outside}$ 40 to 55 dB(A) contours are also plotted. People living outside the WHO guideline of 55 dB(A) are clearly still awakened, this is especially noticeable at Airport B which has a larger population of people living near the airport. Awakenings occurred out to the 40 dB(A) contour.

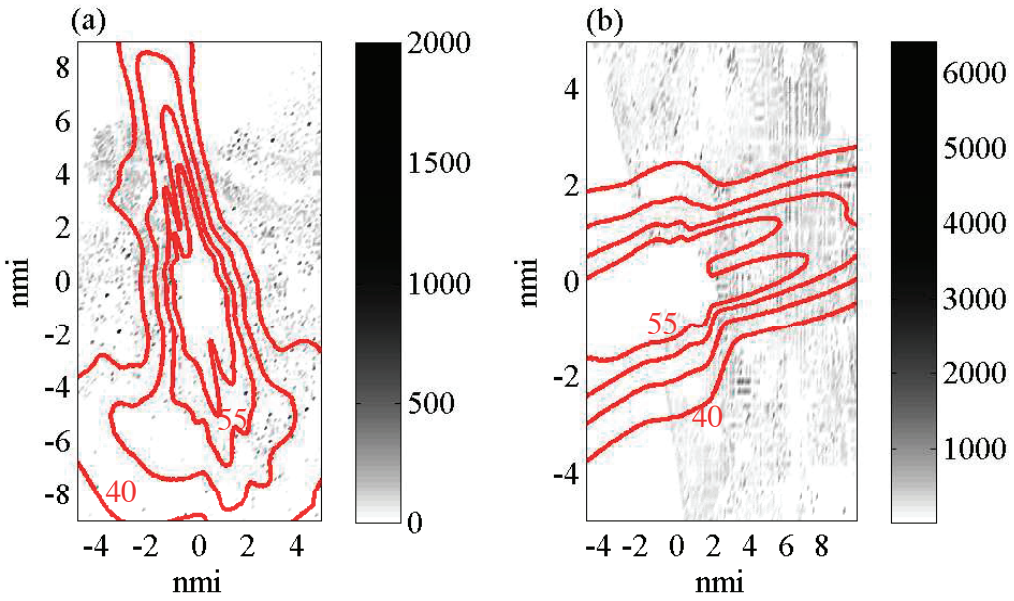

Figure 8.2. Population distribution living around the Airports. (a) Airport A and (b) Airport B. Red contours are the 40 to 55 dB(A) $L_{night,outside}$ contours.

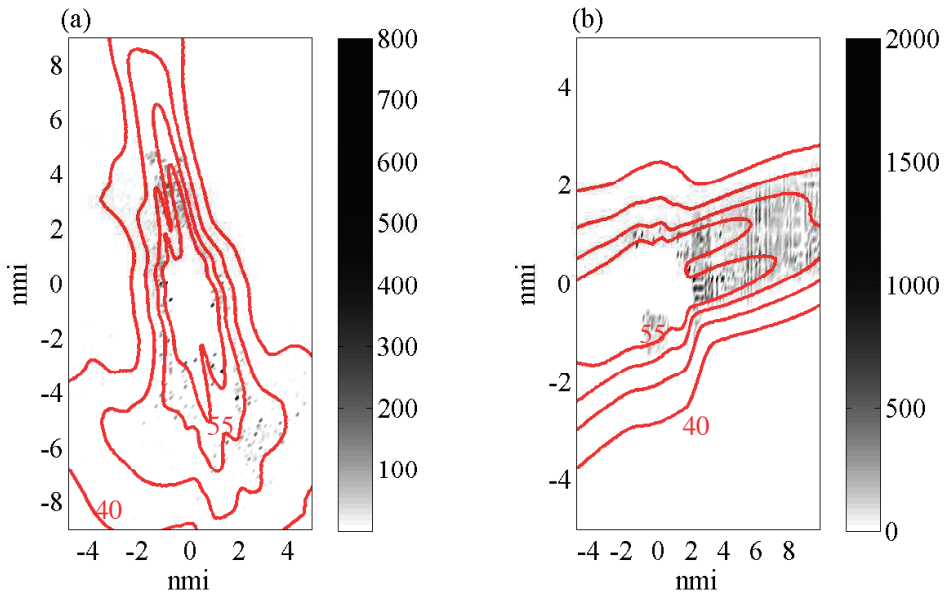

Figure 8.3. Number of people awakened at least once around the Airports, predicted using Basner et al.'s awakening model. (a) Airport A and (b) Airport B. Red contours are the 40 to 55 dB(A) $L_{night,outside}$ contours.

8.3 Sleep Disturbance Comparisons for Different Time Scenarios

Sleep disturbance predictions for different distributions of aircraft events during the night were also examined. Comparisons of sleep disturbance predictions made using the ANSI standard model with time dependence, a modified version of Basner's Markov model and the nonlinear dynamic model developed in this research are discussed.

8.3.1 Addition of Quadratic Dependence on Noise Level to Markov Model

In Chapter 4, a linear dependence on noise level was added to Basner et al.'s Markov model. For this analysis it was decided to add a quadratic dependence on level in order to better match Basner et al.'s dose-response awakening model. The equation for Basner et al.'s (2004) dose-response model is,

$$\%Awake = (1.894e^{-3})L_{Amax}^2 + (4.008e^{-2})L_{Amax} - 3.3243. \tag{8.1}$$

To determine how to change the coefficient values in the Markov model in order to obtain this same relationship, simulations of the same person nights as in Basner's study were completed. Events were evenly spaced throughout the night and the model coefficients, all denoted by a generic coefficient name c were varied for each simulation according to the following:

$$\begin{aligned} c = NoNoisemodelCoeff + \\ (NoiseModelCoeff - NoNoiseModelCoeff)mult, \end{aligned} \tag{8.2}$$

where $mult$ is a multiplier. The coefficients associated with a dependence on time t were not varied with noise level. The time dependence needed to stay as close to the original model as possible, as the focus was on comparing predictions for

different time scenarios, and the change in coefficients made for different noise levels are based on assumptions and not actual data. The relationship between the predicted percent awakened and different values of the multiplier *mult* are shown in Figure 8.4. The value of the multiplier was then compared to the L_{Amax} level (determined from Basner's dose-response relationship) that was associated with the same percent awake, this is shown in Figure 8.4.

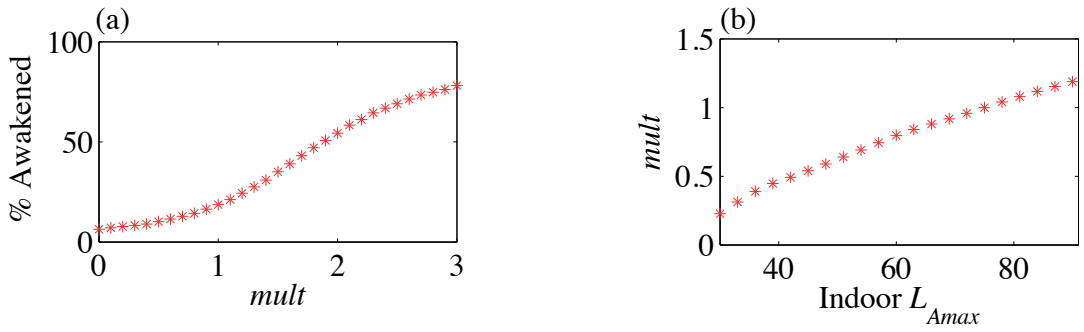

Figure 8.4. (a) Percent awakened predicted when using Basner's Markov model for different values of the multiplier. (b) The relationship between L_{Amax} and the multiplier, based on Basner's field dose-response relationship.

The data, shown in Figure 8.4 (b), was fit with a quadratic function, and the obtained equation was:

$$mult = (-8.1508e^{-5})L_{Amax}^2 + (2.5274e^{-2})L_{Amax} - 0.4321. \tag{8.3}$$

To verify that this change in the Markov Model coefficient values resulted in the desired percent awakened dose-response curve, a simulation was performed using the coefficients with the added noise level dependence. Simulations of 50 person nights with 32 evenly spaced noise events for each L_{Amax} noise level from 35 to 90 dB(A) in increments of 5 dB(A) were completed. The percent awakened was calculated for each noise level based on the simulated dataset. This simulation process was than repeated

100 times and the mean was calculated and variation of the results examined. The results from this verification are shown in Figure 8.5.

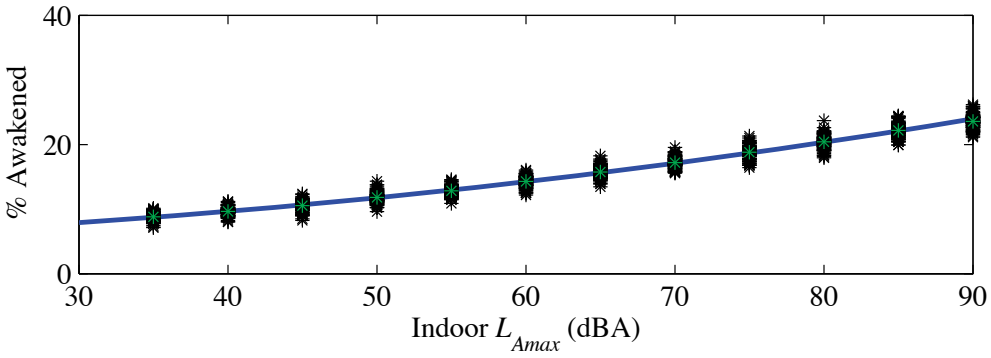

Figure 8.5. The obtained relationship between L_{Amax} and the percent awakened using the modified version of Basner's Markov model. Basner et al.'s (2004) dose-response curve is shown in blue,the mean of the simulated results in (green/light gray), and the results of 100 simulations in black.

The equation for the probability of sleep stage transitions with the added quadratic dependence on noise level has the form:

$$p(s_i|s_j) = \frac{e^X}{\sum_{i=0}^{5} e^X}, \tag{8.4}$$

where

$$\begin{aligned} X = A(s_i) + A_{N1}(s_i)L_{Amax} + A_{N2}(s_i)L_{Amax}^2 + Bt + C(s_i, s_j) \\ + C_{N1}(s_i, s_j)L_{Amax} + C_{N2}(s_i, s_j)L_{Amax}^2. \end{aligned} \tag{8.5}$$

8.3.2 Time-Dependent Model Comparisons

Sleep disturbance, using different models, was predicted for 6 nighttime operation scenarios. The distributions of aircraft events are shown in Figure 8.6. These time scenarios were chosen in order to determine the largest difference in sleep disturbance predictions that might be expected with various scenarios.

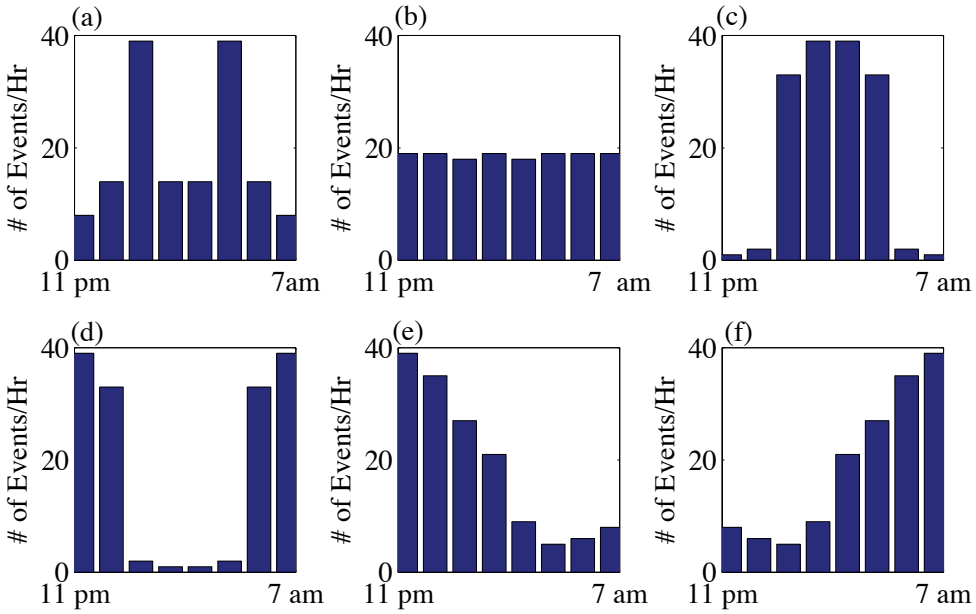

Figure 8.6. The occurrence of events for six nighttime scenarios that were examined. Each bar represents the number of events during an hour of the night. There are eight bars per scenario representing each hour from 11 pm to 7 am. (a) Peak in operations in two hours in the middle of the night, (b) an even distribution, (c) most events in the middle of the night, (d) a U-shaped distribution, (e) most events at the beginning of the night, and (f) most events occurring at the end of the night.

The average number of awakenings for the six scenarios was calculated using the ANSI standard model with time dependence. The results are shown in Figure 8.7. The ANSI standard has a time dependence which results in events at the beginning

of the night having the lowest probability of causing an awakening and events at the end of the night having the highest probability of causing an awakening. Scenarios 1, 2, 3 in which most of the events are in the middle of the night all caused similar number of awakenings.

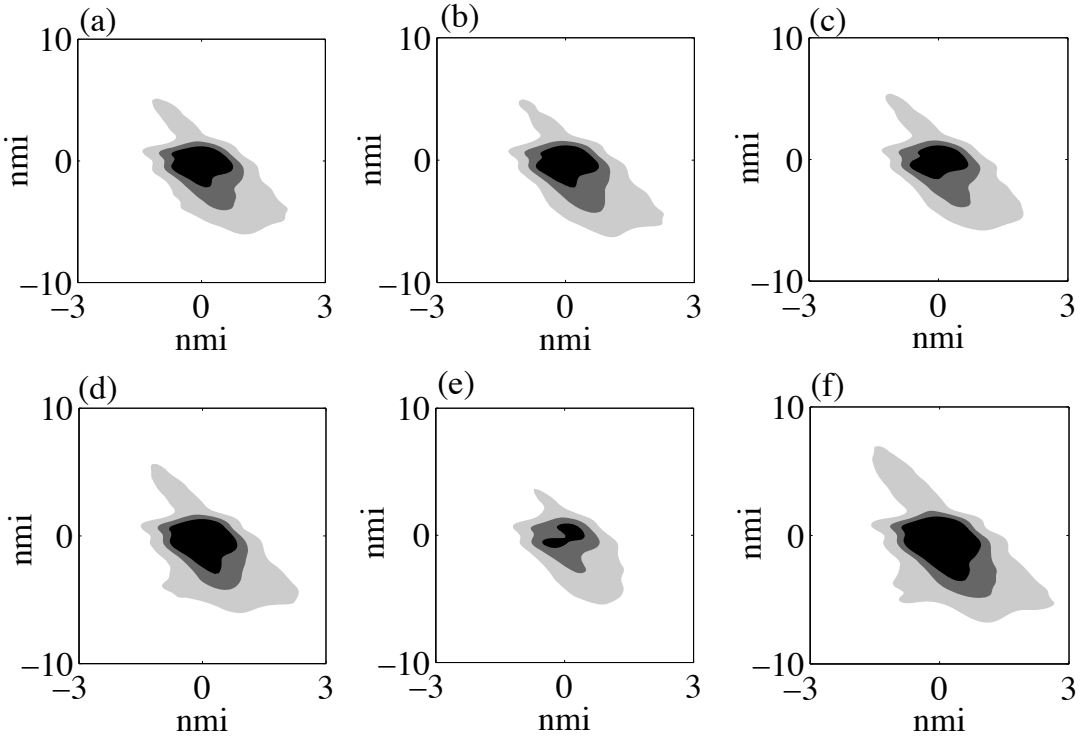

Figure 8.7. Average number of awakenings for the 6 time scenarios predicted using the ANSI standard model with time dependence. Black to dark gray 1.5, dark gray to light gray 1.0 and light gray to white 0.5 awakenings. (a) Peak in operations in two hours in the middle of the night, (b) an even distribution, (c) most events in the middle of the night, (d) a U-shaped distribution, (e) most events at the beginning of the night, and (f) most events occurring at the end of the night.

Using Basner's Markov model with the added quadratic dependence on noise level described earlier in this chapter, the average number of awakenings in 50 simulations at each grid point was calculated for the six time scenarios. The results are shown in

Figure 8.8. The awakenings that are calculated are EEG, not behavioral awakenings, they must occur within 90 seconds or three epoch of the start of the aircraft event and the minimum duration of an awakening is 30 seconds. The results are opposite to those of the ANSI standard model, more awakenings were predicted when most events were at the beginning of the night. This difference in predictions is partly due to the time dependent coefficients of the Markov model. While the baseline no-noise model predicts an increase in awakenings, the time dependence coefficients of the first and second noise models are negative. This decrease in awakening response to events with time is supported by other models (Brink, Lercher, Eisenmann, and Schierz, 2008). In addition, more spontaneous awakenings tend to occur at the end of the night and therefore more noise-induced and spontaneous awakenings may be jointly occurring. In Figure 8.9, the results for the beginning of the night and end of the night scenarios for both Basner's Markov model and the ANSI Standard model with time dependence are shown. The differences in percent awakened do appear small for the two time scenarios. However, when the number of people living within each contour are calculated the difference is more substantial, these results are given in Table 8.3.

Table 8.3. Number of people within awakening contours for Airport A, with 150 events during the night.

Average Number of Awakenings Per Night	Basner Beginning of the Night	Basner End of the Night	ANSI Beginning of the Night	ANSI End of the Night
0.5 Awakenings	40,276	35,514	14,302	39,531
1.0 Awakenings	27,281	11,772	2,790	7,657
1.5 Awakenings	17,288	6,513	10	4,829

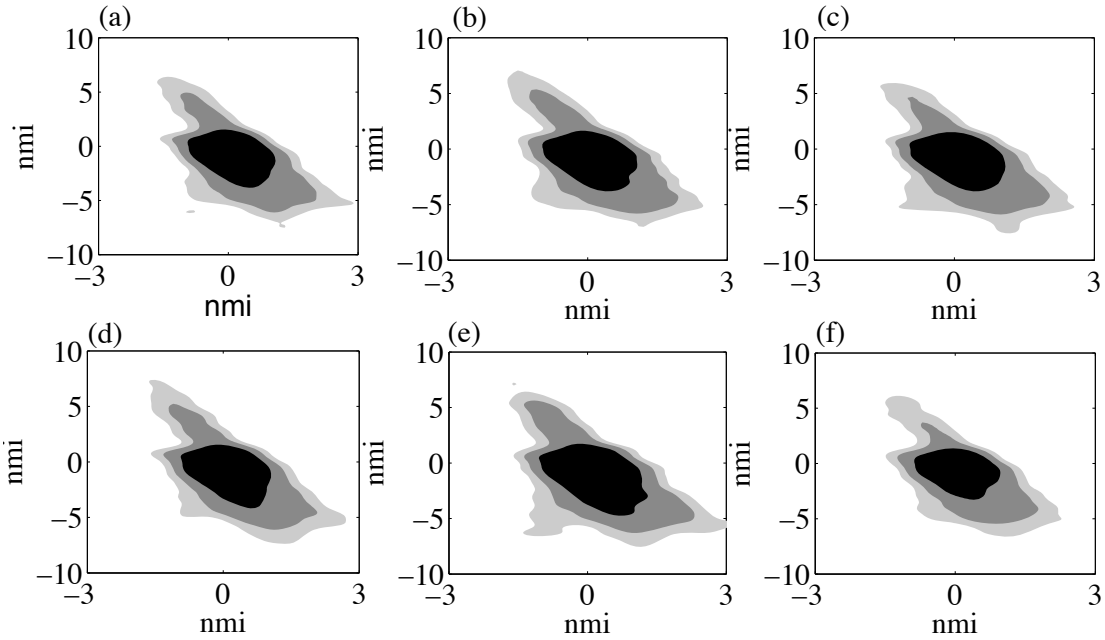

Figure 8.8. Average number of awakenings for the 6 time scenarios predicted using Basner's Markov model with added quadratic dependence on noise level. Black to dark gray 1.5, dark gray to light gray 1.0, and light gray to white 0.5 awakenings. (a) Peak in operations in two hours in the middle of the night, (b) an even distribution, (c) most events in the middle of the night, (d) a U-shaped distribution, (e) most events at the beginning of the night, and (f) most events occurring at the end of the night.

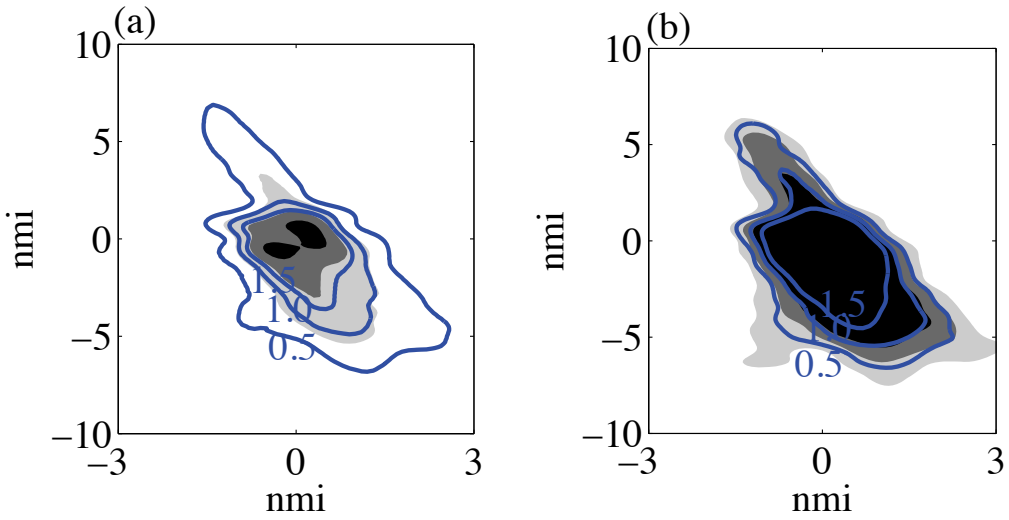

Figure 8.9. Average number of awakenings for the beginning of the night (black to dark gray 1.5, dark gray to light gray 1.0 and light gray to white 0.5 awakenings) and end of the night (blue contours) for (a) the ANSI standard model with time dependence and (b) Basner's Markov model with added quadratic dependence on noise level.

As the the use of $L_{night,\ outside}$ is advocated by WHO, contours for the scenario in which most events occurred at the beginning of the night calculated using Basner's Markov model and the $L_{night,outside}$ contours is shown in Figure 8.10. In addition to the WHO guidelines, recommendations have also been made based on the acceptable number of awakenings per night such that 0.5 (Schrenkenberg, Meis, Kahl, Peschel, and Eikmann, 2010) or 1.0 (Basner, Samel, and Isermann, 2006) additional awakening on average should be prevented in order to protect communities from the adverse effects of nighttime noise. Both limits, based on number of average awakenings, were found to be more protective than the WHO Guideline of $L_{night,outside}$=55 dB(A).

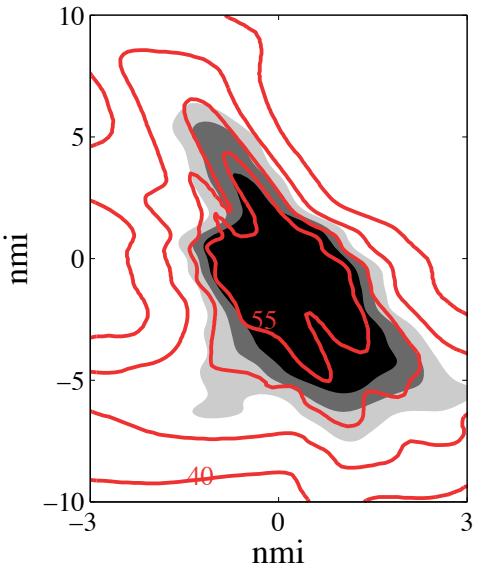

Figure 8.10. Predictions of the average number of awakenings using Basner's Markov model with added quadratic dependence on noise level for the scenario in which most events are at the beginning of the night (black to dark gray 1.5, dark gray to light gray 1.0 and light gray to white 0.5 awakenings) and the $L_{night,outside}$ contours (red).

The change in duration of sleep stages predicted using the modified version of Basner's Markov model was also examined. The Sleep Quality Index (SQI) (Basner,

2006) was calculated based on the duration of time spent in the different sleep stages. The SQI is defined as,

$$SQI = 0.657\ S2 + 0.840\ REM + 0.879\ S3 + S4, \tag{8.6}$$

where $S2$, $S3$, $S4$, andREM are the duration of these stages in minutes. The equation for SQI linearly weights the duration spent in different stages of sleep. The highest weighting is for the duration spent in Stage 4 sleep and lowest is for Stage 2 sleep. Time spent in Stage 1 and Wake are not included in the equation as they are not restorative. A lower value of the SQI corresponds with worse sleep as REM, $S3$, and $S4$ in the equation would have lower durations. The SQI values for the 6 nighttime operation scenarios are shown in Figure 8.11. The scenario in which most events were at the beginning of the night resulted in the lowest SQI values due to a greater reduction in Stage 3 and 4 sleep. The reduction in Stage 3 and 4 sleep and the increase in Stage Wake for the 6 time scenarios are also shown in Figures 8.12 and 8.13, respectively.

Due to increased computational complexity of the developed nonlinear model, full contours for the six scenarios were not able to be generated with the model in time for inclusion in this thesis. However, simulations for the six different scenarios for a few grid points was completed. For each of these grid points, 50 simulations were completed for each noise scenario. For each simulation a different set of random parameters were selected as described in Chapter 7. For two grid points, the average number of additional awakenings calculated by taking the difference between the number of awakenings occurring when noise events are present and the number that would occur at the same time spontaneously without noise present, are shown in Figure 8.14.

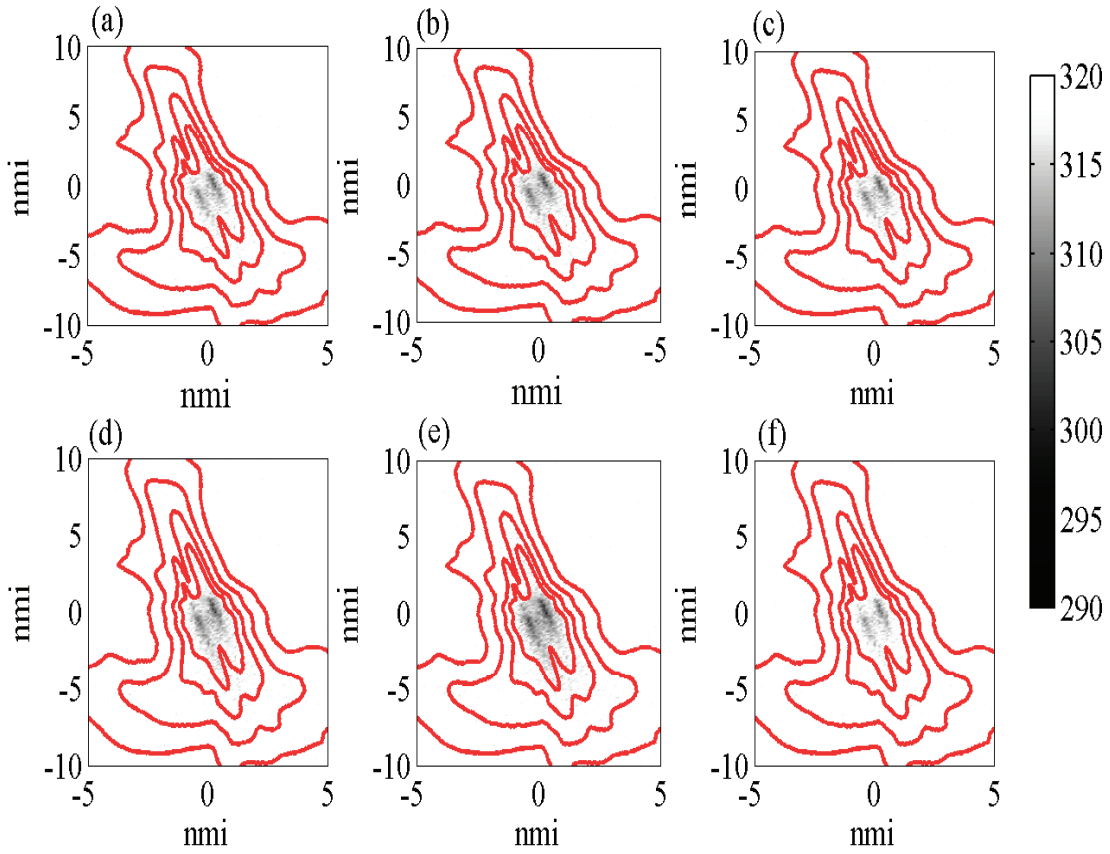

Figure 8.11. *SQI* predictions for the 6 nighttime flight operation scenarios. (a) Peak in operations in two hours in the middle of the night, (b) an even distribution, (c) most events in the middle of the night, (d) a U-shaped distribution, (e) most events at the beginning of the night, and (f) most events occurring at the end of the night. Red contours are the 40 to 55 dB(A) $L_{night,outside}$ contours.

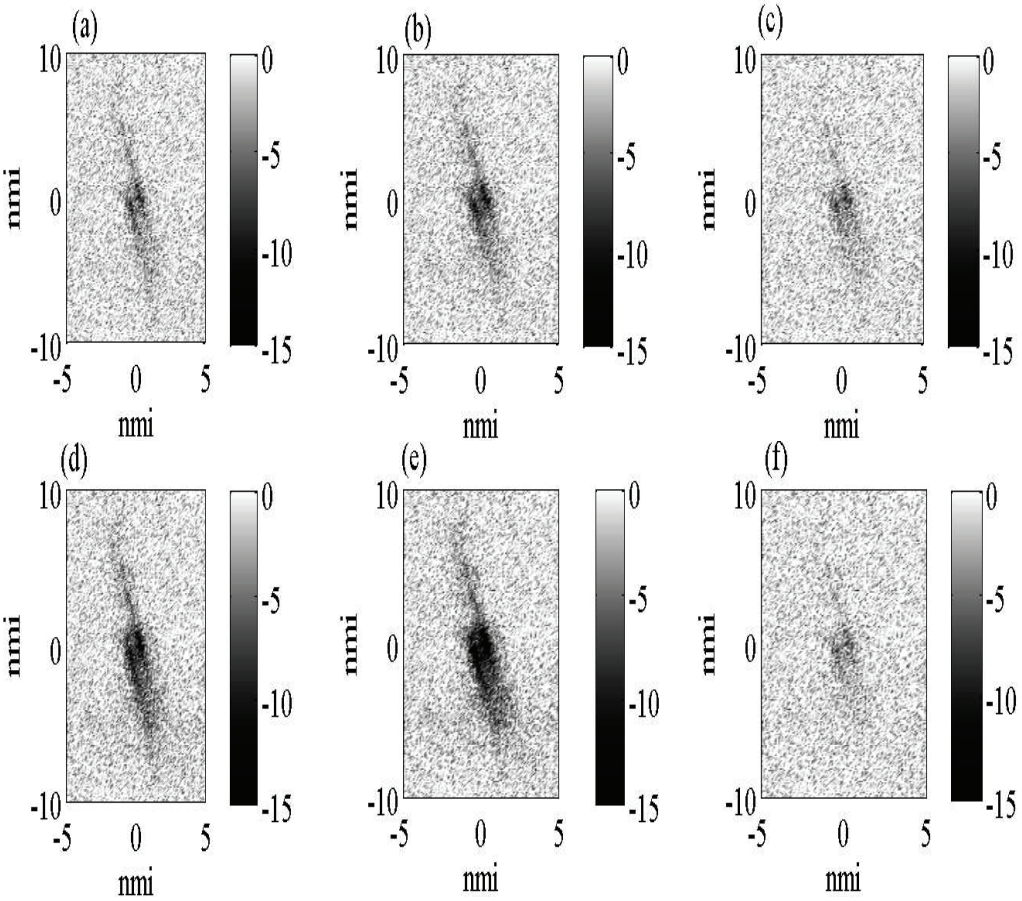

Figure 8.12. Reduction in time spent (minutes) in slow wave sleep for the 6 nighttime flight operation scenarios. (a) Peak in operations in two hours in the middle of the night, (b) an even distribution, (c) most events in the middle of the night, (d) a U-shaped distribution, (e) most events at the beginning of the night, and (f) most events occurring at the end of the night.

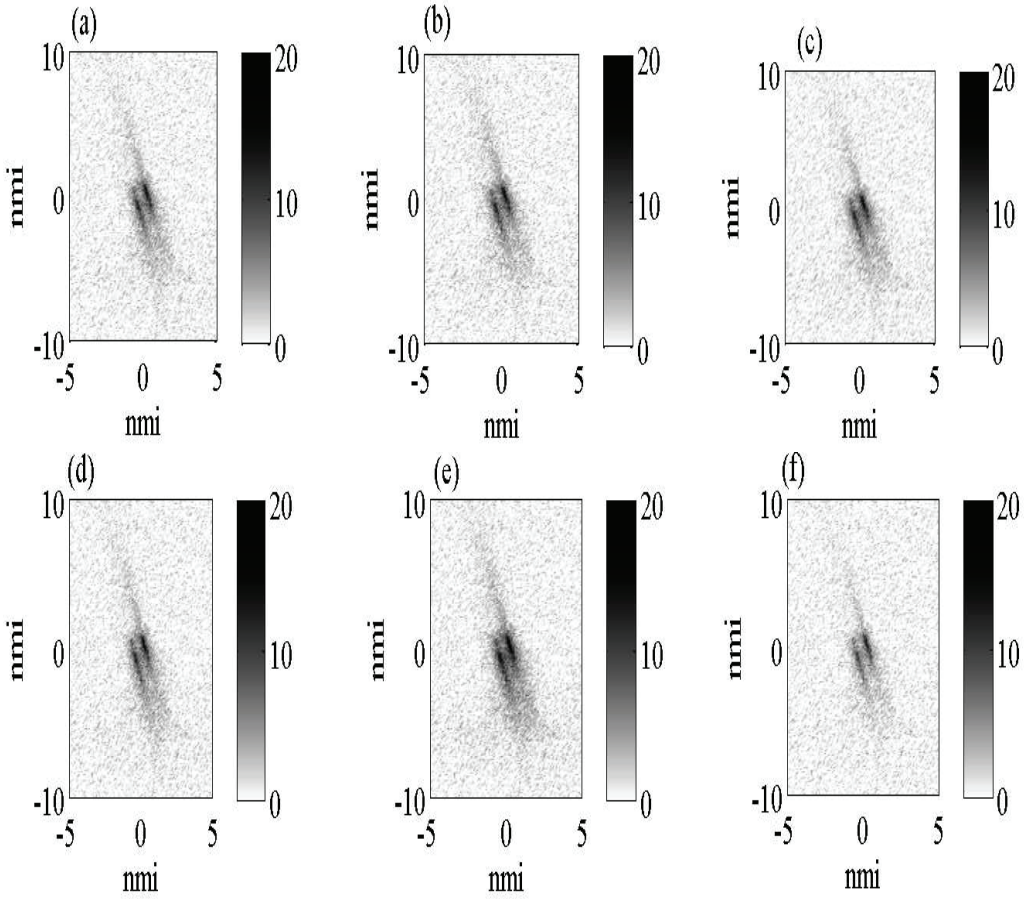

Figure 8.13. Increase in time spent (minutes) in Wake for the 6 night-time flight operation scenarios. (a) Peak in operations in two hours in the middle of the night, (b) an even distribution, (c) most events in the middle of the night, (d) a U-shaped distribution, (e) most events at the beginning of the night, and (f) most events occurring at the end of the night.

As with modified version of Basner's Markov model a greater number of additional awakenings occurred when most of the events were at the beginning of the night than when most events were at the end of the night. The change in sleep stage durations, compared to nights without aircraft events, for the two grid points is shown in Figure 8.15. The change in sleep stage durations did not vary greatly between the six scenarios. The largest difference occurred between the scenario when most of the events were at the end of the night and the scenario in which most events were at the beginning of the night. When most events were at the beginning of the night, there was a greater reduction in slow wave sleep. However, unlike with the modified version of Basner's Markov model predictions, there was not a greater increase in Stage Wake. A possible reason for this result is that the events at the end of the night, for the nonlinear dynamic model, might have caused a greater reduction in slow wave activity than when the events were at the beginning of the night, which might have increased the duration spent awake due to both spontaneous and noise excitations.

8.4 Conclusions

Sleep disturbance in communities was predicted for realistic airport operations scenarios. Models based on behavioral awakenings were found to predict a low number of awakenings compared to those based on polysomnography data and may, particularly, under-predict the impact of nighttime noise on communities for scenarios in which there are only a few events on a runway or flight-path. For different distributions of aircraft events during the night, the ANSI standard model predicted opposite results, in terms of the average number of awakenings, when compared to predictions from Basner's Markov model with added quadratic dependence on noise level and the nonlinear model developed in this research. A possible explanation for this result

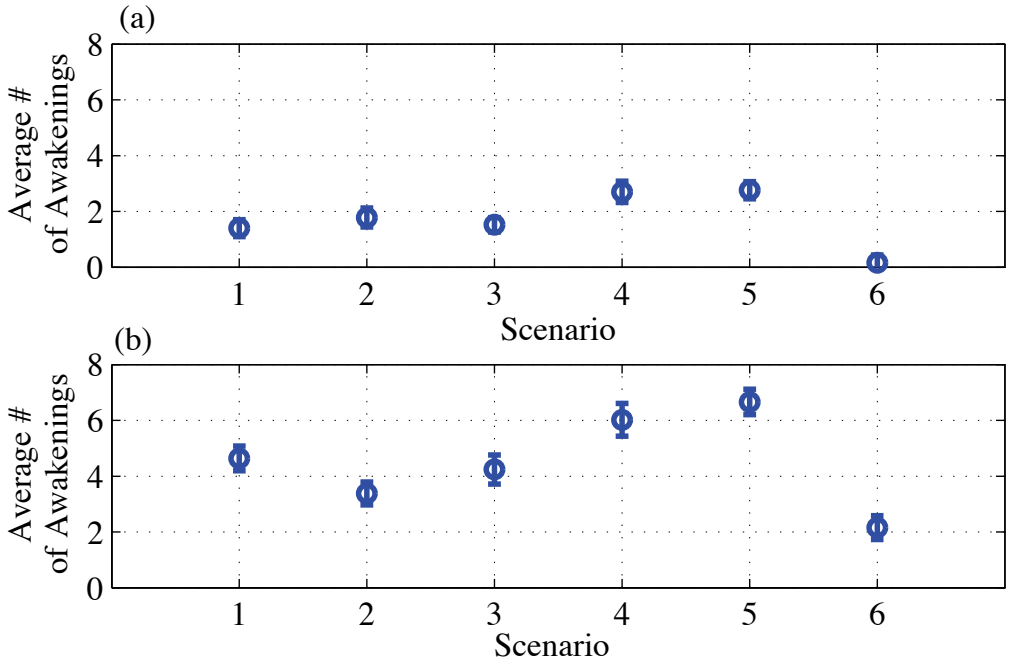

Figure 8.14. Average number of awakenings for 6 flight operation scenarios predicted using the nonlinear dynamic model for (a) grid point at (-1 nmi, 5 nmi) and (b) grid point at (1 nmi, -4 nmi). The scenarios are: (1) Peak in operations in two hours in the middle of the night, (2) an even distribution, (3) most events in the middle of the night, (4) a U-shaped distribution, (5) most events at the beginning of the night, and (6) most events occurring at the end of the night.

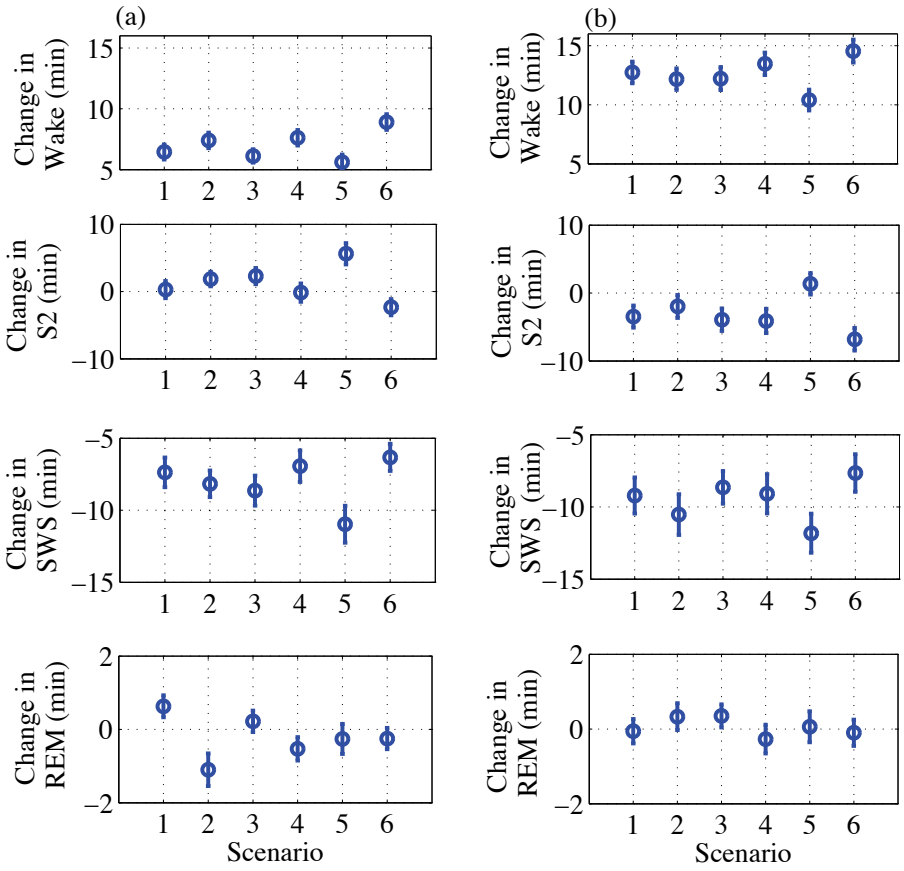

Figure 8.15. Change in sleep stage durations for the 6 flight operation scenarios predicted using the nonlinear dynamic model for (a) grid point at (-1 nmi, 5 nmi) and (b) grid point at (1 nmi, -4 nmi). The scenarios are: (1) Peak in operations in two hours in the middle of the night, (2) an even distribution, (3) most events in the middle of the night, (4) a U-shaped distribution, (5) most events at the beginning of the night, and (6) most events occurring at the end of the night.

is that the ANSI standard model does not take into account the difference between normal and noise disturbed sleep. Also, while the differences in disturbance between more events at the the beginning and more events at the end of the night scenarios appeared small for predictions calculated using both the ANSI standard model and the modified version of Basner's Markov model when translated into the number of people impacted differences were quite large for the two scenarios. Therefore, the number of people awakened by noise as well as contour size should be considered when evaluating sleep disturbance in communities.

While similar trends were found in the number of additional awakenings and the reduction in slow wave sleep calculated using the nonlinear dynamic model and the modified version of Basner's Markov model, there were differences in the predicted total duration of being awake due to noise events. For the Markov Model a noise event impacts the model predictions for 3 epochs, while for the nonlinear model the noise events can impact the predictions of sleep for a longer duration. This difference and its impact on predictions needs to be examined further. In addition, methods for increasing the computation speed of the nonlinear dynamic model need to be examined so that, in the future, it can be used to predict sleep disturbance contours.

9. SUMMARY, OUTCOMES AND RECOMMENDATIONS FOR FUTURE WORK

Nighttime aircraft noise can disturb sleep in communities, causing a decrease in rapid eye movement and slow wave sleep and an increase in the number of awakenings and time spent awake. These changes in sleep may lead to both next day and long term health effects. There have been several models developed to predict noise induced sleep disturbance. Most of the models, however, are limited because they only predict the number of awakenings and not a change in sleep structure which may be important when relating noise-induced sleep disturbance to potential health effects. A Markov model which can be used to predict changes in sleep structure has been developed by Basner (2006). However, the model does not have a noise level dependence and it has many coefficients which makes it difficult to validate due to a large amount of data being needed to produce estimates of the model parameters.

Nonlinear dynamic models have been developed to predict normal, non-noise induced sleep patterns. This type of model was examined to determine if it could be used to predict noise induced sleep disturbance. The nonlinear models have limitations: they cannot predict awakenings during REM sleep or brief awakenings during both NREM and REM sleep as observed in data from sleep studies. Approaches to modifying a nonlinear dynamic model in order to be able to predict this type of behavior was examined. This resulted in the development of a model that could predict slow wave, and slow and fast REM activity.

9.1 Outcomes of This Research

To determine how to introduce faster dynamics into the Massaquoi and McCarley model, first a sleep stage classification algorithm was developed. This algorithm includes methods for removing artifacts and for identifying specific features of polysomnography data including rapid eye movement and sleep spindles. Based on the extracted features, a sleep stage classification algorithm in which sleep stages are classified for each 1 second in time was developed. The standard method for scoring sleep is to assign a sleep stage to each 30 second epoch. The algorithm that was developed provides a more continuous evaluation of sleep stages than this standard method. While in this research 30 second epochs were used at 1 second intervals (sliding through the data), the algorithm is flexible so that shorter or longer epochs could be used and the amount of overlap of segments changed.

To predict brief awakenings during REM sleep using the Massaquoi and McCarley model (1992), a fast REM activity model was added. The occurrence of rapid eye movements, identified using the sleep stage classification algorithm, was used to classify when an individual was awake, in Tonic REM or in Phasic REM sleep. Based on this classification, the fast REM activity was modeled by using a Duffing equation with a 5th order stiffness term, undergoing periodic excitations in a region where chaotic responses are occurring. The Duffing system has 3 stable and 2 unstable equilibrium positions. When responses were in the regions of the stable equilibria sleep was classified as being in Stage Wake, Phasic REM, or Tonic REM. The unstable equilibrium position between Wake and Tonic stable equilbria is a function of the impulsive excitation in the sleep model.

To introduce aircraft noise into the model, extra impulsive excitations were added. The probability of having a non-zero excitation response to a noise event increased from its no-noise/external stimulus level with the maximum A-weighted Sound Pres-

sure Level (L_{Amax}) of the noise event. The complete nonlinear model has 5 components: fast and slow REM sleep, slow wave activity and spontaneous and aircraft-noise induced excitation models. The parameters of this model were estimated by using the 1999 UK sleep study data (Flindell et al., 2000). This model can predict similar durations of sleep stages for baseline non-noise nights as other existing sleep stage models.

To compare predictions of noise induced sleep disturbance for different models, two approaches for adding a noise level dependence to Basner's Markov model were examined. The coefficients of the three noise models were made a function of the maximum A-weighted indoor noise level during a noise event. Both a linear and quadratic dependence on noise level were examined. By using the modified version of Basner's Markov Model, with a quadratic dependence on noise level, and the nonlinear model developed in this research, changes in sleep structure were predicted for different airport noise scenarios. Both models predicted an increase in awakenings with noise level, and a decrease in time spent in slow wave sleep. However, the magnitude of these changes varied between the two models. A further refinement of the model parameters used in the nonlinear model, and further examination of the coefficients of the Markov model is still needed.

It should be noted that Basner's model was tuned using the data the he had available, the data from the DLR laboratory study. The model developed in this research was tuned to the 1999 UK study, a relatively small dataset. Therefore some differences may be due to the unique conditions in the two studies. There is clearly a need with both models to have data from more studies to make the models more generally applicable. Having emphasized the differences between the Markov and nonlinear model predictions in terms of absolute levels it should be noted that while tuned with different study data, the trends predicted agree very well with each other,

perhaps evidence that they are predicting more generally observable trends in sleep behavior.

In summary, the nonlinear dynamic model developed in this research with further refinement can be a useful tool for predicting sleep disturbance in communities around airports. One of the advantages of this type of model is that model coefficients can be related to specific physiological processes and unlike Markov models which require a large amount of data to estimate the large number of model parameters, the parameters of the nonlinear model can be estimated using data for each subject night. This perhaps will allow sleep disturbance to be able to be predicted for different subgroups of the populations such as children, elderly, and individuals with preexisting sleep problems, by estimating and using a different set of model parameters for each group.

9.2 Recommendations for Future Work

There are many areas in which research on the development of sleep disturbance models should be conducted. Suggested areas of future research are provided below.

1. *Further validation of the nonlinear model.* The nonlinear dynamic sleep model was developed based on one dataset the 1999 UK sleep study. This model should be further validated by estimating parameters using additional sleep datasets. In addition, further work should be done on validating and defining the thresholds used to score sleep stages.

2. *Incorporate additional noise characteristics into the model.* Only the maximum indoor noise level was considered in the model. However, researchers examining the effects of noise on sleep have found that the rise time of the event as well as spectral characteristics of the sound affect whether an individual will be awakened. The incorporation of these characteristics into the model through modification of the excitation term should be explored.

3. *Examine use of the model for predicting sleep in different subgroups of the population.* An advantage of the nonlinear dynamic model is that the parameters can be changed on a more intuitive basis than those of Markov sleep models. For example, as individuals age the depth of sleep lightens therefore the decay parameters for slow wave activity can be altered to reflect these changes. In addition, individuals with sleep apnea have more awakenings during the night which could potentially be modeled by increasing the rate of the excitation term. An examination of how to change the model parameters in order to predict sleep in different populations should be examined.

4. *Improve predictions of indoor noise levels.* For the airport noise simulations that were conducted, outdoor noise levels, L_{Amax} and $SELA$, were predicted and an outdoor to indoor noise attenuation of 25 dB(A) was assumed. However, one-third octave band levels can be predicted using noise prediction software, though it is computationally intensive. By using sound transmission software and housing construction data, house transfer filters could be developed and perhaps a better prediction of indoor noise levels could be obtained. Effects of house orientation and window opening would be interesting issues to explore in communities around airports and this would be possible with improved sound transmission models.

5. *Perform simulations of surveys around airports.* There are very few large aircraft noise and sleep field studies and so there is a limited number of datasets that can be used to further validate the developed models. As part of designing a future survey, simulations of the outcomes of different survey designs together with predictions of sleep disturbance from existing models for current airport operations should be completed. This will enable researchers/survey designers to determine if the resulting datasets would provide robust estimates of the parameters of existing sleep models.

LIST OF REFERENCES

LIST OF REFERENCES

P. Achermann and A. A. Borbély. Simulation of human sleep: ultradian dynamics of electroencephalographic slow-wave activity. *Journal of Biological Rhythms*, 5(2): 141–157, 1990.

P. Achermann and A. A. Borbély. Combining different models of sleep regulation. *Journal of Sleep Research*, 1:144–147, 1992.

P. Achermann, D. G. M. Beersma, and A. A. Borbély. The two-process model: Ultradian dynamics of sleep. In *Sleep 90': proceedings of the tenth European Congress on Sleep Research*, Strasbourg, France, May 1990.

P. Achermann, D. J. Dijk, D. P. Brunner, and A. A. Borbély. A model of human sleep homeostasis based on EEG slow-wave activity: Quantitative comparison of data and simulations. *Brain Research Bulletin*, 31(1-2):97–113, 1993.

R. Agarwal and J. Gotman. Computer-assisted sleep staging. *IEEE Transactions on Biomedical Engineering*, 48(12):1412–1423, 2001.

R. Agarwal, T. Takeuchi, S. Laroche, and J. Gotman. Detection of rapid-eye movement in sleep studies. *IEEE Transactions on Biomedical Engineering*, 52(8):1390–1396, 2005.

T. Åkerstedt and M. Gillberg. Subjective and objective sleepiness in the active individual. *International Journal of Neuroscience*, 52:29–37, 1990.

P. Anderer, S. Roberts, A. Schlögl, G. Gruber, G. Klösch, W. Herrmann, P. Rappelsberger, O. Filz, M. J. Barbanoj, G. Dorffner, and B. Saletu. Artifact processing in computerized analysis of sleep EEG - A review. *Neuropsychobiology*, 40(3):150–157, 1999.

G. S. Anderson and N. Miller. A pragmatic re-analysis of sleep disturbance data. In *Noise-Con 2005*, Minneapolis, Minnesota, Oct. 2005.

G. S. Anderson and N. Miller. Alternative analysis of sleep-awakening data. *Noise Control Engineering Journal*, 55(2):224–245, 2007.

ANSI. S12.9-2008, Quantities and procedures for description and measurement of environmental sound - Part 6: Methods for estimation of awakenings associated with outdoor noise events heard in homes. American National Standards Institute, 2008.

I. Bankman, V. G. Sigillito, R. A. Wise, and P. L. Smith. Feature-based detection of the K-Complex using neural networks. *IEEE Transactions on Biomedical Engineering*, 39(12):1305–1310, 1992.

M. Basner. Markov state transition models for the prediction of changes in sleep structure induced by aircraft noise. Technical report, German Aerospace Center (DLR), Institute of Aerospace Medicine, Cologne, Germany, 2006.

M. Basner. Nocturnal aircraft noise exposure increases objectively assessed daytime sleepiness. *Somnologie*, 12:110–117, 2008.

M. Basner. Arousal threshold determination in 1862: Kohlschütters measurements on the firmness of sleep. *Sleep Medicine*, 11:417–422, 2010.

M. Basner and A. Samel. Nocturnal aircraft noise effects. *Noise & Health*, 6(22): 83–93, 2004.

M. Basner and A. Samel. Effects of nocturnal aircraft noise on sleep structure. *Somnologie*, 9:84–95, 2005.

M. Basner, H. Buess, D. Elmenhorst, A. Gerlich, N. Luks, H. MaaB, L. Mawet, E. W. Müller, U. Müller, G. Plath, J. Quehl, A. Samel, M. Schulze, M. Vejvoda, and J. Wenzel. Effects of nocturnal aircraft noise, Volume 1, Executive Summary. Technical report, German Aerospace Center (DLR), Institute of Aerospace Medicine, Cologne, Germany, 2004.

M. Basner, A. Samel, and U. Isermann. Aircraft noise effects on sleep: Application of the results of a large polysomnographic field study. *Journal of the Acoustical Society of America*, 119(5):2772–2784, 2006.

M. Basner, E. M. Elmenhorst, H. Maass, U. Müller, J. Quehl, and M. Vejvoda. Single and combined effects of air, road and rail traffic noise on sleep. In *9th International Congress on Noise as a Public Health Problem (ICBEN)*, Foxwoods, Ct., July 2008a.

M. Basner, C. Glatz, B. Griefahn, T. Penzel, and A. Samel. Aircraft noise: Effects on macro- and microstructure of sleep. *Sleep Medicine*, 9:382–387, 2008b.

M. Basner, U. Müller, E. M. Elmenhorst, G. Kluge, and B. Griefahn. Aircraft noise effects on sleep: a systematic comparison of EEG awakenings and automatically detected cardiac activations. *Physiological Measurement*, 29:1089–1103, 2008c.

G. Becq, S. Charbonnier, F. Chapotot, A. Buguet, L. Bourdon, and P. Baconnier. Comparison between five classifiers for automatic scoring of human sleep recordings. *Studies in Computational Intelligence*, 4:113–127, 2005.

M. Bonnet and D. L. Arand. EEG arousal norms by age. *Journal of Clinical Sleep Medicine*, 3(3):271–274, 2007.

M. Bonnet, D. Carley, M. Carkskadon, P. Easton, C. Guilleminault, R. Harper, B. Hayes, M. Hirshkowitz, P. Ktonas, S. Keenan, M. Pressman, T. Roehrs, J. Smith, J. Walsh, S. Weber, and P. Westbrook. EEG arousals: Scoring rules and examples. *Sleep*, 15(2):173–184, 1992.

A. A. Borbély, F. Baumann, D. Brandeis, I. Strauch, and D. Lehmann. Sleep deprivation: effect on sleep stages and EEG power density in man. *Electroencephalography and Clinical Neurophysiology*, 51:483–495, 1981.

J. Born and H. L. Fehm. The neuroendocrine recovery function of sleep. *Noise & Health*, 2(7):25–37, 2000.

A. M. Boukadoum and P. Y. Ktonas. EOG-based recording and automated detection of sleep rapid eye movements: A critical review and some recommendations. *Psychophysiology*, 23(5):598–611, 1986.

A. M. Boukadoum and P. Y. Ktonas. Non-random patterns of REM occurrences during REM sleep in normal human subjects: an automated second-order study using Markovian modeling. *Electroencephalography and Clinical Neurophysiology*, 70(5):404–416, 1988.

G. Bremer, J. R. Smith, and I. Karacan. Automatic detection of the K-complex in sleep electroencephalograms. *IEEE Transactions on Bio-Medical Engineering*, 17 (4):314–323, 1970.

M. Brink and M. Basner. Determination of awakening probabilities in night time noise effects research. In *Proceedings of Euronoise 2009*, Edinburgh, Scotland, Oct. 2009.

M. Brink, C. H. Müller, and C. Schierz. Contact-free measurement of heart rate, respiration rate, and body movements during sleep. *Behavior Research Methods*, 38 (3):511–521, 2006.

M. Brink, P. Lercher, A. Eisenmann, and C. Schierz. Influence of slope of rise and event order of aircraft noise events on high resolution actimetry parameters. *Somnologie*, 12:118–128, 2008.

D. Bruck, M. Ball, I. Thomas, and V. Rouillard. How does the pitch and pattern of a signal affect auditory arousal thresholds? *Journal of Sleep Research*, 18:196–203, 2009.

D. P. Brunner, R. C. Vasko, C. S. Detka, J. P. Monahan, C. F. Reynolds III, and D. J. Kupfer. Muscle artifacts in the sleep EEG: Automated detection and effect on all-night EEG power spectra. *Journal of Sleep Research*, 5:155–164, 1996.

M. A. Carskadon and W. C. Dement. Normal human sleep: an overview. In M. H. Kryer, T. Roth, and W. C. Dement, editors, *Principles and Practice of Sleep Medicine*. Elsevier, Philadelphia, Pennsylvania, 4th edition, 2005.

N. Carter, R. Henderson, S. Lal, M. Hart, S. Booth, and S. Hunyor. Cardiovascular and autonomic response to environmental noise during sleep in night shift workers. *Sleep*, 25(4):444–451, 2002.

N. L. Carter, S. N. Hunyor, G. Crawford, D. Kelly, and A. J. M. Smith. Environmental noise and sleep, a study of arousals, cardiac arrhythmia, and urinary catecholamines. *Sleep*, 17(4):298–307, 1994.

A. Coenen. Subconscious stimulus processing recognition and processing during sleep. *Psyche*, 16(2):90–97, 2010.

J. C. Comte, M. Schatzman, P. Ravassard, P. H. Luppi, and P. A. Salin. A three states sleep-waking model. *Chaos, Solitons, Fractals*, 29:808–815, 2006.

C. Curtco, S. Sakata, S. Marguet, V. Itskov, and K. D. Harris. A simple model of cortical dynamics explains variability and state dependence of sensory response in urethane-anesthetized auditory cortex. *The Journal of Neuroscience*, 29(34):10600–10612, 2009.

M. Czisch, T. C. Wetter, C. Kaufmann, T. Pollmächer, F. Holsboer, and D. P. Auer. Altered processing of acoustic stimuli during sleep: Reduced auditory activation and visual deactivation detected by a combined fMRI/EEG study. *NeuroImage*, 16:251–258, 2002.

A. C. Da Rosa, B. Kemp, T. Paiva, F. H. Lopes da Silva, and H. A. Kamphuisen. A model-based detector of vertex waves and K-complexes in sleep electroencephalogram. *Electroencephalography and Clinical Neurophysiology*, 78(1):71–79, 1991.

T. T. Dang-Vu, S. M. McKinney, O. M. Buxton, J. M. Solet, and J. M. Ellenbogen. Spontaneous brain rhythms predict sleep stability in the face of noise. *Current Biology*, 20(15):R626–R627, 2010.

H. Davis, P. A. Davis, A. L. Loomis, E. N. Harvey, and G. Hobart. Changes in human brain potentials during the onset of sleep. *Science*, 86(2237):448–450, 1937.

J. L. DeVore. *Probability and Statistics*. Thomson, Belmont, California, 7th edition, 2008.

S. Devuyst, T. Dutoit, J. F. Didier, F. Meers, E. Stanus, P. Stenuit, and M. Kerkhofs. Automatic sleep spindle detection in patients with sleep disorders. In *Proceedings of the 28th IEEE EMBS Annual International Conference*, New York City, Aug.-Sept.3 2006.

S. Devuyst, T. Dutoit, P. Stenuit, M. Kerkhofs, and E. Stanus. Removal of ECG artifacts from EEG using a modified Independent Component Analysis approach. In *Proceedings of the 30th Annual International IEEE EMBS Conference*, Vancouver, British Columbia, Canada, Aug. 2008.

S. Devuyst, T. Dutoit, P. Stenuit, and M. Kerkhofs. Automatic K-complexes detection in sleep EEG recordings using likelihood thresholds. In *Proceedings of the 32nd Annual International Conference of the IEEE EMBS*, Buenos Aires, Argentina, Aug. 31-Sept. 4 2010.

J. Di Nisi, A. Muzet, J. Ehrhart, and J. P. Libert. Comparison of cardiovascular responses to noise during waking and sleeping in humans. *Sleep*, 13(2):108–120, 1990.

D. J. Dijk, D. G. M. Beersma, and R. H. van den Hoofdakker. All night spectral analysis of EEG sleep in young adult and middle-aged male subjects. *Neurobiology of Aging*, 10(6):677–682, 1989.

I. DiMatteo, C. R. Genovese, and R. E. Kass. Bayesian curve-fitting with free-knot splines. *Biometrika*, 88(4):1055–1071, 2001.

C. G. Diniz Behn and V. Booth. Simulating microinjection experiments in a novel model of the rat sleep-wake regulatory network. *Journal of Neurophysiology*, 103: 1937–1953, 2010.

C. G. Diniz Behn, E. N. Brown, T. E. Scammell, and N. J. Kopell. Mathematical model of network dynamics governing mouse sleep-wake behavior. *Journal of Neurophysiology*, 97:3828–3840, 2007.

J. B. Dixon, L. M. Schachter, and P. E. O'Brien. Polysomnography before and after weight loss in obese patients with severe sleep apnea. *International Journal of Obesity*, 29:1048–1054, 2005.

M. Domjan, J. W. Grau, and M. A. Krause. *The Principles of Learning and Behavior*. Wadsworth, Belmont, California, 2010.

DORA. Aircraft noise and sleep disturbance: final report. Technical Report DORA report no. 8008, Directorate of Operational Research and Analysis, Civil Aviation Authority, U.K., 1980.

T. A. Doughty, P. Davies, and A. K. Bajaj. A comparison of three techniques using steady state data to identify non-linear modal behavior of an externally excited cantilever beam. *Journal of Sound and Vibration*, 249(4):785–813, 2002.

M. Ekstedt, T. Åkerstedt, and M. Söderström. Microarousals during sleep are associated with increased levels of lipids, cortisol, and blood pressure. *Psychosomatic Medicine*, 66:925–931, 2004.

E. M. Elmenhorst and M. Basner. Fluglärmwirkungen band 5 leistung. Technical report, German Aerospace Center (DLR), Institute of Aerospace Medicine, Cologne, Germany, 2008.

U. Ermis, K. Krakow, and U. Voss. Arousal thresholds during human tonic and phasic REM sleep. *Journal of Sleep Research*, 19:400–406, 2010.

T. P. Exarchos, A. T. Tzallas, D. I. Fotiadis, S. Konitsiotis, and S. Giannopoulos. EEG transient event detection and classification using association rules. *IEEE Transactions on Information Technology in Biomedicine*, 10(3):451–457, 2006.

FAA. *Integrated Noise Model (INM) Version 7.0 User's Guide*. Federal Aviation Administration, 2007.

F. Ferrillo, S. Donadio, F. De Carli, S. Garbarino, and L. Nobili. A model-based approach to homeostatic and ultradian aspects of nocturnal sleep structure in narcolepsy. *Sleep*, 30(2):157–165, 2007.

FICAN. Effects of aviation noise on awakenings from sleep, 1997. URL http:\\www.fican.org/pdf/Effects_AviationNoise_Sleep.pdf.

FICON. Federal agency review of selected airport noise analysis issues, 1992. URL http://www.fican.org/pdf/nai-8-92.pdf.

S. Fidell, K. Pearsons, B. Tabachnick, R. Howe, L. Silvati, and D. S. Barber. Field study of noise-induced sleep disturbance. *Journal of the Acoustical Society of America*, 98(2):1025–1033, 1995.

S. Fidell, K. Pearsons, B. G. Tabachnick, and R. Howe. Effects on sleep disturbance of changes in aircraft noise near three airports. *Journal of the Acoustical Society of America*, 107(5):2535–2547, 2000.

J. M. Fields, R. G. De Jong, T. Gjestland, I. H. Flindell, R. F. S. Job, S. Kurra, P. Lercher, M. Vallet, T. Yano, R. Guski, U. Felscher-suhr, and R. Schumer. Standardized general-purpose noise reaction questions for community noise surveys research and a recommendation. *Journal of Sound and Vibration*, 242(4):641–679, 2001.

L. S. Finegold and B. Elias. A predictive model of noise induced awakenings from transportation noise sources. In *Proceedings of Internoise 2002*, Dearborn, Michigan, Aug. 2002.

L. S. Finegold, C. S. Harris, and H. E. von Gierke. Community annoyance and sleep disturbance: Updated criteria for assessing the impacts of general transportation noise on people. *Noise Control Engineering Journal*, 42(1):25–30, 1994.

R. S. Fisher and S. Cordova. EEG for beginners. In G. L. Krauss and R. S. Fisher, editors, *The John Hopkins Atlas of Digital EEG: An Interactive Training Guide*, pages 11–76. The John Hopkins University Press, Baltimore, Maryland, 2006.

I. H. Flindell, A. J. Bullmore, K. A. Robertson, N. A. Wright, C. Turner, C. L. Birch, M. Jiggins, B. F. Berry, M. Davison, and N. Dix. Aircraft noise and sleep, 1999 UK trial methodology study. Technical report, ISVR Consultancy Services, Institute of Sound and Vibration Research, University of Southampton, UK, 2000.

J. Foret, N. Touron, O. Clodoré, Benoit, and G. Bouard. Modification of sleep structure by brief forced awakenings at different times of the night. *Electroencephalography and Clinical Neurophysiology*, 75:141–147, 1990.

P. Fort, C. L. Bassetti, and P. H. Luppi. Alternating vigilance states: new insights regarding neuronal networks and mechanisms. *European Journal of Neuroscience*, 29:1741–1753, 2009.

D. J. Frey, P. Badia, and K. P. Wright Jr. Inter- and intra-individual variability in performance near the circadian nadir during sleep deprivation. *Journal of Sleep Research*, 13:305–315, 2004.

B. D. Fulcher, A. J. K. Phillips, and P. A. Robinson. Modeling the impact of impulsive stimuli on sleep-wake dynamics. *Physical Review E*, 78:051920, 2008.

K. H. Fuller, W. F. Waters, P. Binks, and T. Anderson. Generalized anxiety and sleep architecture: A polysomnographic investigation. *Sleep*, 20(5):370–376, 1997.

A. Garcés Correa, E. Laciar, H. D. Patiño, and M. E. Valentinuzzi. Artifact removal from EEG signals using adaptive filters in cascade. In *In Proceedings of the 16th Argentine Bioengineering Congress and the 5th Conference of Clinical Engineering*, 2007.

W. Gerstner and W. Kistler. *Spiking Neuron Model*. Cambridge University Press, New York, 1996.

I. S. Gopal and G. G. Haddad. Automatic detection of eye movements in REM sleep using the electrooculogram. *American Journal of Physiology*, 241(3):R217–21, 1981.

D. J. Gottlieb, N. M. Punjabi, A. B. Bewman, H. E. Resnick, S. Redline, C. M. Baldwin, and F. J. Nieto. Association of sleep time with diabetes mellitus and impaired glucose tolerance. *Archives of Internal Medicine*, 165:863–868, 2005.

J. M. A. Graham, S. A. Janssen, J. Vos, and H. M. E. Miedema. Habitual traffic noise at home reduces cardiac parasympathetic tone during sleep. *International Journal of Psychophysiology*, 72:179–186, 2009.

B. Griefahn. Long-term exposure to noise-aspects of adaptation, habituation and compensation. *Waking and Sleeping*, 1:383–386, 1977.

B. Griefahn and A. Muzet. Noise-induced sleep disturbances and their effects on health. *Journal of Sound and Vibration*, 59(1):99–106, 1978.

B. Griefahn, A. Schuemer-Kohrs, R. Schuemer, U. Moehler, and P. Mehnert. Physiological, subjective, and behavioural responses during sleep to noise from rail and road traffic. *Noise & Health*, 3(9):59–71, 2000.

B. Griefahn, A. Marks, and S. Robens. Noise emitted from road, rail, and air traffic and their effects on sleep. *Journal of Sound and Vibration*, 295:129–140, 2006.

B. Griefahn, P. Bröde, A. Marks, and M. Basner. Autonomic arousals related to traffic noise during sleep. *Sleep*, 31(4):569–577, 2008a.

B. Griefahn, S. Robens, P. Bröde, and M. Basner. The sleep disturbance index-a measure for structural alterations of sleep due to environmental influences. In *Proceedings of the 9th International Congress on Noise as a Public Health Problem (ICBEN)*, Foxwoods, Connecticut, July 2008b.

C. Guilleminault and R. Stoohs. Arousals increased respiratory efforts, blood pressure and obstructive sleep apnoea. *Journal of Sleep Research*, 4(Supplement 1): 117–124, 1995.

C. Guilleminault, V. C. Abad, P. Philip, and R. Stoohs. The effect of CNS activation versus EEG arousal during sleep on heart rate response and daytime tests. *Clinical Neurophysiology*, 117:731–739, 2006.

A. S. Haralabidis, K. Dimakopoulou, F. Vigna-Taglianti, M. Giampaolo, A. Borgini, M. L. Dudley, G. Pershagen, G. Bluhm, D. Houthuijs, W. Babisch, M. Velonakis, K. Katsouyanni, and L. Jarup. Acute effects of night-time noise exposure on blood pressure in populations living near airports. *European Heart Journal*, 29:658–664, 2008.

N. Hatzilabrou, N. Greenberg, R. J. Sclabassi, T. Carroll, R. D. Guthrie, and M. S. Scher. A comparison of conventional and matched filtering techniques for rapid eye movement detection of the newborn. *IEEE Transactions on Biomedical Engineering*, 41(10):990–995, 1994.

S. Haykin. *Adaptive Filter Theory*. Prentice Hall, Upper Saddle River, New Jersey, 3rd edition, 1996.

P. He, G. Wilson, and C. Russell. Removal of ocular artifacts from electroencephalogram by adaptive filtering. *Medical and Biological Engineering and Computing*, 42: 407–412, 2004.

J. A. Hobson, R. W. McCarley, and P. W. Wyzinski. Sleep cycle oscillation: reciprocal discharge by two brainstem neuronal groups. *Science*, 189:55–58, 1975.

A. Huss, A. Spoerri, M. Egger, and M. Röösli. Aircraft noise, air pollution, and mortality from myocardial infarction. *Epidemiology*, 21(6):829–836, 2010.

C. Iber, S. Redline, A. M. Kaplan Gilpin, S. F. Quan, L. Zhang, D. G. Gottlieb, D. Rapoport, H. Resnick, M. Sanders, and P. Smith. Polysomnography performed in the unattended home versus the attended laboratory setting, Sleep Heart Health Study Methodology. *Sleep*, 27(3):536–540, 2004.

G. Inuso, F. La Foresta, N. Mammone, and F. Carlo Morabito. Wavelet-ICA methodology for efficient artifact removal from electroencephalographic recordings. In *Proceedings of International Joint Conference on Neural Networks*, Orlando, Florida, Aug. 2007.

H. Ising and M. Ising. Chronic cortisol increases in the first half of the night caused by road traffic noise. *Noise & Health*, 4(16):13–21, 2002.

E. B. Issa and X. Wang. Altered neural responses to sounds in primate primary auditory cortex during slow-wave sleep. *The Journal of Neuroscience*, 31(8):2965–2973, 2011.

E. M. Izhikevich. Which model to use for cortical spiking neurons? *IEEE Transactions on Neural Networks*, 15(5):1063–1070, 2004.

L. Jarup, W. Babisch, D. Houthuijs, G. Pershagen, K. Katsouyanni, E. Cadum, M. L. Dudley, P. Savigny, I. Seiffert, W. Swart, O. Brugelmans, G. Bluhm, J. Selander, A. Haralabidis, K. Dimakopolou, P. Sourtzi, M. Velonakis, and F. Vigna-Taglianti. Hypertension and exposure to noise near airports: the HYENA study. *Environmental Health Perspective*, 116(3):329–333, 2008.

M. W. Johns. A new method for measuring daytime sleepiness: The Epworth Sleepiness Scale. *Sleep*, 14(6):540–545, 1991.

T. P. Jung, S. Makeig, C. Humphries, T. W. Lee, M. J. McKeown, V. Iragui, and T. J. Sejnowski. Removing electroencephalographic artifacts by blind source separation. *Psychophysiology*, 37:163–178, 2000.

A. Kales and J. Kales. Evaluation, diagnosis, and treatment of clinical conditions related to sleep. *Journal of the American Medical Association*, 213(13):2229–2235, 1970.

B. Kemp and H. A. Kamphuisen. Simulation of human hypnograms using a Markov chain model. *Sleep*, 9(3):405–414, 1986.

T. Kobayashi. Sleep Package Model. *Computers and Industrial Engineering*, 27: 385–388, 1994.

M. Kuroiwa, P. Xin, S. Suzuki, Y. Saszawa, and T. Kawada. Habituation of sleep to road traffic noise observed not by polygraphy but by perception. *Journal of Sound and Vibration*, 250(1):101–106, 2002.

H. Kuwahara, H. Higashi, Y. Mizuki, S. Matsunari, M. Tanaka, and K. Inanaga. Automatic real-time analysis of human sleep stages by an interval histogram method. *Electroencephalography and Clinical Neurophysiology*, 70:220–229, 1988.

R. E. Lawder. A proposed mathematical model for sleep patterning. *Journal of Biomedical Engineering*, 6:63–69, 1984.

T. E. LeVere, R. T. Bartus, and F. D. Hart. The relation between time of presentation and the sleep disturbing effects of nocturnally occurring jet aircraft flyovers. Technical Report NASA/ CR-2036, National Aeronautics and Space Administration, Washington, D. C., 1972.

T. E. LeVere, R. T. Bartus, G. W. Morlock, and F. D. Hart. Arousal from sleep: Responsiveness to different auditory frequencies equated for loudness. *Physiological Psychology*, 10(3):53–57, 1973.

T. E. LeVere, G. W. Morlock, L. P. Thomas, and F. Hart. Arousal from sleep: The differential effect of frequencies equated for loudness. *Physiological Psychology*, 12 (4):573–582, 1974.

T. E. Levere, N. Davis, J. Mills, E. H. Berger, and W. F. Reiter. Arousal from sleep: The effects of the rise-time of auditory stimuli. *Physiological Psychology*, 4 (2):213–218, 1976.

G. X. Li and F. C. Moon. Criteria for chaos of a three-well potential oscillator with homoclinic and heteroclinic orbits. *Journal of Sound and Vibration*, 136(1):17–34, 1990.

R. R. Llinas and D. Pare. Of dreaming and wakefulness. *Neuroscience*, 44(3):521–535, 1991.

C. C. Lo, L. A. Nunes Amaral, S. Havlin, P. C. Ivanov, T. Penzel, J. H. Peter, and H. E. Stanley. Dynamics of sleep-wake transitions during sleep. *Europhysics Letters*, 57(5):625–631, 2002.

J. S. Loredo, S. Ancoli-Israel, and J. E. Dimsdale. Sleep quality and blood pressure dipping in obstructive sleep apnea. *American Journal of Hypertension*, 14(9):887–892, 2001.

J. S. Loredo, R. Nelesen, S. Ancoli-Israel, and J. E. Dimsdale. Sleep quality and blood pressure dipping in normal adults. *Sleep*, 27(6):1097–1103, 2004.

J. Lu, D. Sherman, M. Devor, and C. B. Saper. A putative flip-flop switch for control of REM sleep. *Nature*, 44(1):589–594, 2006.

J. S. Lukas. Effects of aircraft noise on human sleep. *American Industrial Hygiene Association Journal*, 33(5):298–303, 1972.

G. Luz, D. Nykaza, C. Stewart, and L. Pater. Use of actimeters to determine awakenings by sounds of large guns. *Noise Control Engineering Journal*, 56(3): 211–217, 2008.

H. MaaB and M. Basner. Effects of nocturnal aircraft noise: Volume 3 stress hormones. Technical report, German Aerospace Center (DLR), Institute of Aerospace Medicine, 2006.

A. Marks and B. Griefahn. Railway noise - its effects on sleep, mood, subjective sleep quality, and performance. *Somnologie*, 9:68–75, 2005.

A. Marks and B. Griefahn. Associations between noise sensitivity and sleep, subjectively evaluated sleep quality, annoyance, and performance after exposure to nocturnal traffic noise. *Noise & Health*, 9:1–7, 2007.

A. Marks, B. Griefahn, and M. Basner. Event-related awakenings caused by nocturnal transportation noise. *Noise Control Engineering Journal*, 56(1):52–62, 2008.

S. Massaquoi and R. McCarley. Resetting the REM sleep oscillator. In *Sleep 90': proceedings of the tenth European Congress on Sleep Research*, Strasbourg, France, May 1990.

S. G. Massaquoi and R. W. McCarley. Extension of the limit cycle reciprocal interaction model of REM cycle control. An integrated sleep control model. *Journal of Sleep Research*, 1:138–143, 1992.

R. W. McCarley. Neurobiology of REM and NREM sleep. *Sleep Medicine*, 8:302–330, 2007.

R. W. McCarley and J. A. Hobson. Single neuron activity in cat gigantocellular tegmental field: Selectivity of discharge in desynchronized sleep. *Science*, 174:1250–1252, 1971.

R. W. McCarley and J. A. Hobson. Neuronal excitability modulation over the sleep cycle: A structure and mathematical model. *Science*, 189:58–60, 1975.

R. W. McCarley and S. G. Massaquoi. A limit cycle mathematical model of the REM sleep oscillator system. *American Journal of Physiology- Regulatory, Integrative, and Comparative Physiology*, 251:1011–1029, 1986.

R. J. McPartland, D. J. Kupfer, and F. G. Foster. Rapid eye movement analyzer. *Electroencephalography and Clinical Neurophysiology*, 34(3):317–320, 1973.

W. C. Meecham and H. G. Smith. Effects of jet aircraft noise on mental hospital admissions. *British Journal of Audiology*, 11(3):81–85, 1977.

H. M. E. Miedema and C. G. M. Oudshoorn. Annoyance from transportation noise: Relationships with exposure metrics DNL and DENL and their confidence intervals. *Environmental Health Perspectives*, 109(4):409–416, 2001.

H. M. E. Miedema, W. Passchier-Vermeer, and H. Vos. Elements for a position paper on night-time transportation noise and sleep disturbance. Technical Report TNO report 2002-59, TNO, Delft, Nederland, 2002.

F. C. Moon and P. J. Holmes. A magnetoelastic strange attractor. *Journal of Sound and Vibration*, 65(2):275–296, 1979.

NIH. National sleep disorders research plan. Technical report, National Institute of Health, 2003. URL http://www.nhlbi.nih.gov/health/prof/sleep/res_plan/sleep-rplan.pdf.

E. Öhrström. Effects of low levels of road traffic noise during the night: A laboratory study on number of events, maximum noise levels, and noise sensitivity. *Journal of Sound and Vibration*, 179(4):603–615, 1995.

E. Öhrström and M. Björkman. Effects of noise-disturbed sleep-A laboratory study on habituation and subjective noise sensitivity. *Journal of Sound and Vibration*, 122 (2):277–290, 1988.

E. Öhrström, E. Hadzibajramovic, M. Holmes, and H. Svensson. Effects of road traffic noise on sleep: studies on children and adults. *Journal of Environmental Psychology*, 26:116–126, 2006.

E. Olbrich and P. Achermann. Analysis of oscillatory patterns in the human sleep EEG using a novel detection algorithm. *Journal of Sleep Research*, 14:337–346, 2005.

E. Olbrich and P. Achermann. Analysis of the temporal organization of sleep spindles in the human sleep EEG using a phenomenological modeling approach. *Journal of Biological Physiology*, 34:341–349, 2008.

J. B. Ollerhead, C. J. Jones, R. E. Cadoux, A. Woodley, B. J. Atkinson, J. A. Horne, F. Pankhurst, L. Reyner, K. I. Hume, F. Van, I. D. Watson, A. Diamond, P. Egger, D. Holmes, and J. McKean. Report of a field study of aircraft noise and sleep disturbance. Technical report, Department of Safety, Environment, and Engineering, Civil Aviation Authority, UK, 1992.

I. Oswald, A. M. Taylor, and M. Treisman. Discriminative responses to stimulation during human sleep. *Brain*, 83:440–453, 1960.

W. Passchier-Vermeer, H. Vos, J. H. M. Steenbekkers, F. D. van der Ploeg, and K. Froothuis-Oudshoorn. Sleep disturbance and aircraft noise exposure: Exposure-effect relationships. Technical report, TNO, Leiden, the Netherlands, 2002.

K. S. Pearsons, D. S. Barber, B. G. Tabachnick, and S. Fidell. Predicting noise-induced sleep disturbance. *Journal of the Acoustical Society of America*, 97(1): 331–338, 1995.

A. J. K. Phillips and P. A. Robinson. A quantitative model of sleep-wake dynamics based on the physiology of the brainstem ascending arousal system. *Journal of Biological Rhythms*, 22(2):167–179, 2007.

A. J. K. Phillips and P. A. Robinson. Sleep deprivation in a quantitative physiologically based model of the ascending arousal system. *Journal of Theoretical Biology*, 255:413–423, 2008.

C. M. Portas, K. Karakow, P. Allen, O. Josephs, J. L. Armony, and C. D. Frith. Auditory processing across the sleep-wake cycle: simultaneous EEG and fMRI monitoring in humans. *Neuron*, 28(3):991–999, 2000.

J. Quehl and M. Basner. Annoyance from nocturnal aircraft noise exposure: Laboratory and field-specific dose-response curves. *Journal of Environmental Psychology*, 26(2):127–140, 2006.

L. B. Ray, S. M. Fogel, C. T. Smith, and K. R. Peters. Validating an automated sleep spindle detection algorithm using an individualized approach. *Journal of Sleep Research*, 19(2):374–378, 2010.

A. Rechtschaffen, P. Hauri, and M. Zeitlin. Auditory awakening thresholds in REM and NREM sleep stages. *Perceptual and Motor Skills*, 22(3):927–942, 1966.

A. Rechtschaffen, A. Kales, R. J. Berger, W. C. Dement, A. Jacobson, L. C. Johnson, M. Jouvet, L. J. Monroe, I. Oswald, H. P. Roffwarg, B. Roth, and R. D. Walter. *A Manual of Standardized Terminology, Techniques and Scoring System for Sleep Stages of Human Subjects*. Public Health Service, Washington, D. C., 1968.

M. J. Rempe, J. Best, and D. Terman. A mathematical model of the sleep/wake cycle. *Journal of Mathematical Biology*, 60(5):615–644, 2010.

A. Sadeh, R. Gruber, and A. Raviv. Sleep, neurobehavioral functions, and behavior problems in school-age children. *Child Development*, 73(2):405–417, 2002.

M. Sallinen, J. Kaartinen, and H. Lyytine. Processing of auditory stimuli during tonic and phasic periods of REM sleep as revealed by event-related brain potentials. *Journal of Sleep Research*, 5(4):220–228, 1996.

S. Sanei and J. A. Chambers. *EEG Signal Processing*. John Wiley & Sons, West Sussex, England, 2007.

C. B. Saper, T. C. Chou, and T. E. Scammell. The sleep switch: Hypothalamic control of sleep and wakefulness. *TRENDS in Neurosciences*, 24(12):726–731, 2001.

M. Saremi, J. Grenéche, A. Bonnefond, O. Rohmer, A. Eschenlauer, and P. Tassi. Effects of nocturnal railway noise on sleep fragmentation in young and middle-aged subjects as a function of type of train and sound level. *International Journal of Psychophysiology*, 70(3):184–191, 2008.

S. A. Schapkin, M. Falkenstein, A. Marks, and B. Griefahn. After effects of noise-induced sleep disturbances on inhibitory functions. *Life Sciences*, 78(10):1135–1142, 2006.

P. Schimcek, J. Zeitlhofer, P. Anderer, and B. Saletu. Automatic sleep spindle detection procedure: aspects of reliability and validity. *Clinical Electroencephalography*, 25:26–29, 1994.

A. Schlögl, P. Anderer, M. J. Barbanoj, G. Klösch, G. Gruber, J. L. Lorenzo, O. Filz, M. Koivuluoma, I. Rezek, S. J. Roberts, A. Värri, P. Rappelsberger, G. Pfurtscheller, and G. Dorffner. Artifact processing of the sleep EEG in the SIESTA Project. In *Proceedings of the EMBEC*, pages 1644–1645, Edinburgh, Scotland, 1999.

D. Schreckenberg, G. Thomann, and M. Basner. FFI and FNI-two effect based aircraft noise indices at Frankfurt Airport. In *Proceedings of Euronoise 2009*, Edinburgh, Scotland, Oct. 2009.

D. Schrenkenberg, M. Meis, C. Kahl, C. Peschel, and T. Eikmann. Aircraft noise and quality of life around Frankfurt Airport. *International Journal of Environmental Research and Public Health*, 7(9):3382–3405, 2010.

T. J. Schultz. Synthesis of social surveys on noise annoyance. *Journal of the Acoustical Society of America*, 64:377–405, 1978.

J. M. Seigl. Normal human sleep: an overview. In M. H. Kryer, T. Roth, and W. C. Dement, editors, *Principles and Practice of Sleep Medicine*. Elsevier, Philadelphia, Pennsylvania, 4th edition, 2005.

M. H. Silber, S. Ancoli-Israel, M. H. Bonnet, S. Chokroverty, M. M. Grigg-Damberger, M. Hirshkowitz, S. Kapen, S. A. Keenan, M. H. Kryger, T. Penzel, M. R. Pressman, and C. Iber. The visual scoring of sleep in adults. *Journal of Clinical Sleep Medicine*, 3(2):121–135, 2007.

A. Skånberg and E. Öhrström. Sleep disturbances from road traffic noise: A comparison between laboratory and field settings. *Journal of Sound and Vibration*, 290 (1-2):3–16, 2006.

J. R. Smith, M. J. Cronin, and I. Karacan. A multichannel hybrid system for rapid eye movement detection (REM detection). *Computers and Biomedical Research*, 4 (3):275–290, 1971.

M. Sørensen, M. Hvidberg, Z. J. Andersen, R. B. Nordsborg, K. G. Lillelund, J. Jakobsen, A. Tjønneland, K. Overvad, and O. Raaschou-Nielsen. Road traffic noise and stroke: a prospective cohort study. *European Heart Journal*, 32(6):737–744, 2011.

K. Spiegel, R. Leproult, and E. Van Cauter. Impact of sleep debt on metabolic and endocrine function. *The Lancet*, 354:1435–1439, 1999.

K. Spiegel, E. Tasali, P. Penev, and E. Van Cauter. Brief communication: Sleep curtailment in healthy young men is associated with decreased leptin levels, elevated ghrelin levels, and increased hunger and appetite. *Annals of Internal Medicine*, 141 (11):846–850, 2004.

M. Spreng. Noise induced nocturnal cortisol secretion and tolerable overhead flights. *Noise & Health*, 6(22):35–47, 2004.

W. H. Spriggs. *Essentials of Polysomnography: A Training Guide and Reference for Sleep Technicians*. Sleep Ed, LLC, Carrollton, Texas, 2008.

R. Srebro. The Duffing oscillator: a model for the neuronal groups comprising the transient evoked potential. *Electroencephalography and Clinical Neurophysiology*, 96: 561–573, 1995.

S. A. Stansfeld and M. P. Matheson. Noise pollution: non-auditory effects on health. *British Medical Bulletin*, 68:243–257, 2003.

S. A. Stansfeld, C. Clark, R. M. Cameron, T. Alfred, J. Head, M. M. Haines, I. van Kamp, E. van Kempen, and I. Lopez-Barrio. Aircraft and road traffic noise exposure and children's mental health. *Journal of Environmental Psychology*, 29:203–207, 2009.

N. J. Stevenson, M. Mesbah, G. B. Boylan, P. B. Colditz, and B. Boashash. Nonlinear model of newborn EEG. *Annals of Biomedical Engineering*, 38(9):3010–3021, 2010.

J. V. Stone. Independent component analysis: an introduction. *TRENDS in Cognitive Sciences*, 6(2):203–207, 2009.

S. H. Strogatz. *Nonlinear Dynamics and Chaos, With Applications to Physics, Biology, Chemistry, and Engineering*. Westview Press, Cambridge, Massachusetts, 2000.

S. Taheri, L. Lin, D. Austin, T. Young, and E. Mignot. Short sleep duration is associated with reduced Leptin, elevated Ghrelin, and increased Body Mass Index. *Public Library of Science Medicine*, 1(3):210–217, 2004.

E. Tasali, R. Leproult, D. A. Ehrmann, and E. Van Cauter. Slow-wave sleep and the risk of type 2 diabetes in humans. *Proceedings of the National Academy of Science*, 105(3):1044–1049, 2008.

G. J. Thiessen. Disturbance of sleep by noise. *Journal of the Acoustical Society of America*, 64(1):216–222, 1978.

J. Trammell and P. Ktonas. A simple nonlinear deterministic process may generate the timing of rapid eye movements during human REM sleep. In *Proceedings of the 1st International IEEE EMBS Conference on Neural Engineering*, Capri Island, Italy, Oct. 2003.

M. Vallet, J. M. Gagneux, V. Blanchet, B. Favre, and G. Labiale. Long term sleep disturbance due to traffic noise. *Journal of Sound and Vibration*, 90(2):173–191, 1983.

M. van de Velde, G. van Erp, and P. J. M. Cluitmans. Detection of muscle artifact in the normal human awake EEG. *Electroencephalography and Clinical Neurophysiology*, 107(2):149–158, 1998.

P. Venkatakrishnan, S. Sangeetha, and R. Sukanesh. Detection of sleep spindles from electroencephalogram (EEG) signals using auto-recursive (AR) model. In *First International Conference on Emerging Trends in Engineering and Technology*, July 2008.

R. Vigário, J. Särelä, V. Jousmäki, M. Hämäläinen, and E. Oja. Independent Component Approach to the analysis of EEG and MEG recordings. *IEEE Transactions on Biomedical Engineering*, 47(5):589–593, 2000.

J. Virkkala, J. Hasan, A. Värri, S.-L. Himanen, and M. Härmä. The use of two-channel electro-oculography in automatic detection of unintentional sleep onset. *Journal of Neuroscience Methods*, 163(1):137–144, 2007.

G. L. Wallstrom, R. E. Kass, A. Miller, J. F. Cohn, and N. A. Fox. Automatic correction of ocular artifacts in the EEG: a comparison of regression-based and component-based methods. *International Journal of Psychophysiology*, 53:105–119, 2004.

R. Wehrle, C. Kaufmann, T. C. Wetter, F. Holsboer, D. P. Auer, T. Pollmächer, and M. Czisch. Functional microstates within human REM sleep: first evidence from fMRI of a thalamocortical network specific for phasic REM periods. *European Journal of Neuroscience*, 25:863–871, 2007.

R. A. Wever. Mathematical models of circadian one and multi-oscillator systems. In G. A. Carpenter, editor, *Lectures on Mathematics in the Life Sciences Volume 19. Some Mathematical Questions in Biology, Circadian rhythms*. American Mathematical Society, Providence, Rhode Island, 1980.

WHO. Night noise guidelines for Europe. Technical report, 2009. URL http://www.euro.who.int/__data/assets/pdf_file/0017/43316/E92845.pdf.

R. T. Wilkinson and K. B. Campbell. Effects of traffic noise on quality of sleep: Assessment by EEG, subjective report, or performance the next day. *Journal of the Acoustical Society of America*, 75(2):468–475, 1984.

R. L. Williams, I. Karacan, and C. J. Hursch. *Electroencephalography (EEG) of human sleep: Clinical applications*. Wiley, New York, 1974.

M. C. K. Yang and C. J. Hursch. The use of a Semi-Markov model for describing sleep patterns. *Biometrics*, 29(4):667–676, 1973.

E. C. Zeeman. Brain modelling. *Lecture Notes in Mathematics*, 525:367–372, 1976.

H. Zeplin, C. S. McDonald, and G. K. Zammit. Effects of age on auditory awakening thresholds. *Journal of Gerontology*, 39(3):294–300, 1984.

W. K. Zung, T. H. Naylor, D. T. Gianturco, and W. P. Wilson. Computer simulation of sleep EEG patterns with a markov chain model. *Recent Advances in Biological Psychiatry*, 8:335–355, 1965.

APPENDICES

Appendix A. Noise Metrics

The following are noise metrics that were used in this report.

Cumulative Metrics:

1. Day Night Average Sound Pressure Level (DNL or L_{dn}):

$$DNL = 10log_{10}\left[\frac{1}{24}\left(\int_{7:00}^{22:00}\frac{{p_A}^2}{{p_o}^2}dt + 10\int_{22:00}^{7:00}\frac{{p_A}^2}{{p_o}^2}dt\right)\right], \tag{A.1}$$

   p_A is the A-weighted sound pressure level.

2. L_{night}:

$$L_{night} = 10log_{10}\left[\frac{1}{8}\left(\int_{23:00}^{7:00}\frac{{p_A}^2}{{p_o}^2}dt\right)\right]. \tag{A.2}$$

Single Event Metrics:

1. L_{Amax}: Maximum A-weighted noise level.

2. $SELA$: Sound Exposure Level:

$$SELA = 10log_{10}\left(\int_{t_1}^{t_2}\frac{{p_A}^2}{{p_o}^2}dt\right), \tag{A.3}$$

   where t_1 and t_2 are defined in Figure A.1.

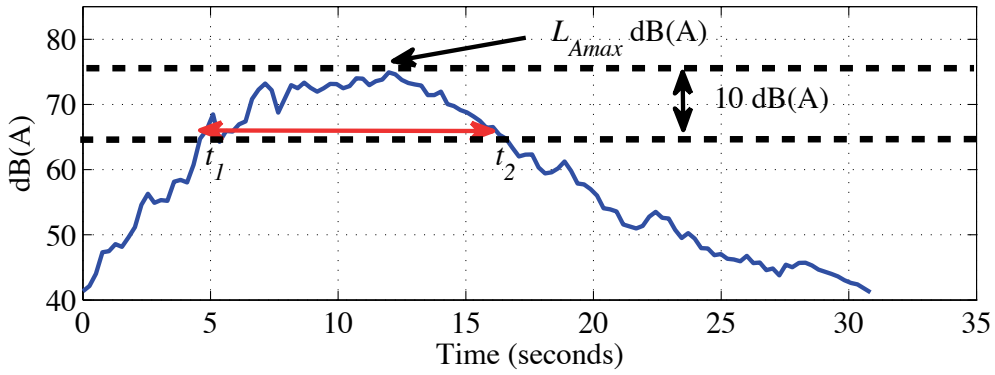

Figure A.1. A-weighted noise level (dB(A)) of aircraft noise event. The maximum noise level (L_{Amax}) and the portion of the sound used to calculate the Sound Exposure Level ($SELA$) (red arrow) are indicated.

Appendix B. Laboratory and Field Studies

This appendix contains tables which list the survey data available for laboratory and field studies on the effects of aircraft noise on sleep.

Table B.1. Laboratory studies-sleep measurements.

Study	# of People	am/pm Surveys	Behav. Awake	Acti-metry	Motility-Other	Polysom-nography
Basner et al. (2004)	128	X		X		X
Basner et al. (2008)	72	X		X		X
Carter et al. (1994)	9					X
Carter et al. (2002)	9					X
Dinisi et al. (1990)	20				X	X
Flindell et al. (2000)	9	X		X		X
Levere et al. (1972)	6					X (EEG)
Levere & Davis (1977)	12	X				X (EEG, EOG)
Lukas & Kryter (1970)	6		X			X (EEG, EOG)
Lukas et al. (1971)	12	X	X			X
Lukas & Dobbs (1972)	8	X	X			X
Marks et al. (2008)	24	X				X

Table B.2. Laboratory studies-additional measurements.

Study	# of People	ECG	Blood Pressure	Hormone Levels, etc	Sleepiness (Objective)	Performance
Basner et al. (2004)	128	X		X	PST (24)	X
Basner et al. (2008)	72	X		X		X
Carter et al. (1994)	9	X		X		
Carter et al. (2002)	9	X	X			
Dinisi et al. (1990)	20	X				
Flindell et al. (2000)	9	X			MSLT	X
Levere et al. (1972)	6					X
Levere & Davis (1977)	12					
Lukas & Kryter (1970)	6					
Lukas et al. (1971)	12					
Lukas & Dobbs (1972)	8					
Marks et al. (2008)	24	X				X

Table B.3. Field studies-sleep measurements.

Study	Location	# of People	Social Survey	am/pm Survey	Behav. Awake	Acti-metry
Basner et al. (2004)	Cologne-Bonn	64		X		X
Borksy (1976)	JFK	1500	X			
Brink et al. (2008)	Zurich	60		X		
DORA (1980)	Heathrow Gatwick	4153	X			
Fidell & Jones (1975)	LAX	1417	X			
Fidell et al. (1995)	Castle Air Force Base LAX	85		X	X	
Fidell et al. (2000)	Stapleton Denver	77		X	X	X
Fidell et al. (2000)	DeKalb-Peachtree	22		X	X	X
Flindell et al. (2000)	Manchester	18		X		X
Haral-abidis et al. (2008)	Athens Arlanda Heathrow Malpensa	140	X			
Ollerhead et al. (1992) Hume et al. (2003)	Heathrow Gatwick Stansted Manchester	400-Act. 46-Poly. 1636-Social Survey	X			X
Passchier-Vermeer et al. (2002)	Schiphol	418		X	X	X

Table B.4. Field studies-additional sleep measurements.

Study	Motility-Other	Polysomnography	ECG	Blood Pressure	Hormone Levels, etc	Performance
Basner et al. (2004)		X	X		X	X
Borksy (1976)						
Brink et al. (2008)	X					
DORA (1980)						
Fidell & Jones (1975)						
Fidell et al. (1995)						
Fidell et al. (2000)						
Fidell et al. (2000)						
Flindell et al. (2000)		X	X			X
Haral-abidis et al. (2008)				X		
Ollerhead et al. (1992) Hume et al. (2003)		X				
Passchier-Vermeer et al. (2002)						X

Table B.5. Field studies-noise measurements.

Surveys	Metrics-# of Locations	Measurement of Outdoor Noise	Measurement of Indoor Noise	Noise Metrics
Basner et al. (2004)	64	X	X	A-weighted time histories
Borksy (1976)	1500			
Brink et al. (2008)	60		X	
DORA (1980)	29	X		L_{Aeq}, L_{Amax}, *SELA*, "number above" and "level exceeded"
Fidell & Jones (1975)	3	X		L_{dn}
Fidell et al. (1995)	45	X	X	A-weighted time histories, L_{Amax}, *SELA*
Fidell et al. (2000)	38	X	X	A-weighted time histories, L_{Amax}, *SELA*
Fidell et al. (2000)	12	X	X	A-weighted time histories, L_{Amax}, *SELA*
Flindell et al. (2000)	18	X	X	1-sec A-weighted time histories
Haralabidis et al. (2008)	140		X	A-weighted time histories
Ollerhead et al. (1992) Hume et al. (2003)	8	X		L_{Amax}, *SELA*, Hourly L_{Aeq}
Passchier-Vermeer et al. (2002)	418	X	X	1 sec A-weighted time histories

Table B.6. Field studies-additional noise measurements.

Surveys	Noise Recordings (e.g. .wav)	Flight Operations Data
Basner et al. (2004)	X	
Borksy (1976)		Distance from airport
Brink et al. (2008)	Played recordings in each subject's home	
DORA (1980)		Flight paths, Location of surveyed areas
Fidell & Jones (1975)		
Fidell et al. (1995)		
Fidell et al. (2000)		
Fidell et al. (2000)		
Flindell et al. (2000)	10 sec .wav recordings for 4 locations	List of aircraft by time of arrival and departure
Haralabidis et al. (2008)	X	
Ollerhead et al. (1992) Hume et al. (2003)		Maps indicating flight paths and study locations
Passchier-Vermeer et al. (2002)		Obtained data from flight track monitoring system indicating aircraft noise events

Appendix C. Coefficients of Basner's Markov Model

Table C.1. Coefficients for Basner's Four Markov Models (2006).

Coefficient/s_j	s_i	Baseline	Noise 1	Noise 2	Noise 3
Intercept	0	1.2144	2.3013	0.7674	0.9691
	1	-0.4702	-0.4125	-0.4415	-0.3739
	3	-3.6542	-4.0295	-3.8388	-3.8809
	4	-6.2984	-12.6277	-14.1409	-5.0150
	5	-1.3717	-1.0818	-1.6914	-2.2264
S1	0	-2.7472	-1.8124	-2.9919	-2.8770
	1	0.2838	0.4352	0.0584	-0.3877
	3	-2.5433	-0.4452	-9.0011	-1.9712
	4	-6.9807	-1.1678	-1.6087	-8.7818
	5	-1.3017	-1.5643	-0.0583	-1.2233
S2	0	-4.8576	-3.5524	-3.8725	-4.6710
	1	-4.6860	-3.3554	-4.2785	-4.7750
	3	0.8986	1.6156	0.8650	1.2007
	4	0.2586	4.8135	6.9155	-3.3496
	5	-3.0316	-3.3679	-2.1935	-1.9309
S3	0	-3.4514	-2.4651	-2.9214	-3.2425
	1	-6.7253	-3.6566	-4.7870	-4.9466
	3	5.7615	5.9772	4.9008	5.8730
	4	6.5807	12.6037	12.5687	4.9879
	5	-3.8353	-4.9858	-5.2357	-2.6269
S4	0	-0.7784	-0.4093	-1.0691	-0.5785
	1	-3.5858	-2.5576	-3.5520	-9.9189
	3	6.5302	6.5707	5.6143	6.9644
	4	11.5460	17.2381	17.5938	10.6345
	5	-3.0085	-10.3476	-10.8294	-8.2248
REM	0	-1.0655	-0.9722	-0.8380	-1.0694
	1	-1.2599	-0.3825	-1.2592	-1.5366
	3	-2.0445	-9.1235	-8.4853	-8.2782
	4	-6.1652	8.0627	-1.0821	-6.7936
	5	4.5398	3.9654	4.6170	4.9946
Transition	0	0.000452	-0.00025	-0.00004	0.000401
	1	-0.00026	-0.00030	-0.0013	0.000277
	3	-0.00147	-0.00135	-0.00125	-0.00190
	4	-0.00273	-0.00187	-0.00150	-0.00285
	5	0.000869	0.000337	0.000822	0.000896

Appendix D. Model Parameters Estimated for Each Subject

The model coefficient values listed in the following tables were calculated for 76 subject nights from the 1999 UK sleep study (Flindell et al., 2000). The methods used to calculate these coefficients are discussed in Chapter 7. For the slow REM sleep model, the coefficients were not calculated if the REM period defined in the original dataset was less than 5 minutes in duration or if the NREM period before or after a REM period was less than 15 minutes. Also the coefficients of the slow REM model were not calculated if the duration of the prior NREM period or the duration of the REM period was considered an outlier, which was defined as:

$$Lower\ Outliers < 25th\ percentile - 1.5(75th\ percentile - 25th\ percentile), \quad \text{(D.1)}$$

$$Upper\ Outliers > 75th\ percentile + 1.5(75th\ percentile - 25th\ percentile), \quad \text{(D.2)}$$

here the 75th and 25th percentiles were calculated based on all NREM or REM periods during the night for all 76 subject nights. The subject nights for which the coefficients were not calculated are indicated by gray/blank entries in the following tables.

Table D.1. Estimated parameters for Process S and SWA models for field subjects 1 through 12 in the 1999 UK study.

Subject	Night	S_o	gc	SWA_L	rc	fc	SWA_o
1	2	3.3365	0.0391	0.2384	0.1064	4.1062	1.5094
1	4	4.1180	0.0497	0.1725	0.2324	1.4241	1.0915
2	1	3.3673	0.0248	0.1094	0.4977	3.2499	0.8288
2	3	3.7074	0.0304	0.1411	0.3090	1.1422	1.1137
2	4	3.5105	0.0307	0.1501	0.3532	3.0706	0.9375
3	3	3.8628	0.0306	0.2220	0.2636	1.0852	0.9697
3	4	2.8551	0.0265	0.1641	0.8013	1.9962	0.5251
6	1	4.3358	0.0442	0.1103	0.2309	1.7047	1.0080
6	2	4.0398	0.0441	0.1010	0.2930	2.1427	1.1029
6	3	5.4750	0.0544	0.1075	0.1779	2.5459	1.1783
8	4	2.9164	0.0240	0.2467	0.3148	1.1791	0.9923
9	1	4.2406	0.0350	0.1879	0.2398	1.0777	0.9125
9	3	5.8348	0.0461	0.1513	0.2348	1.4101	0.6386
9	4	4.9060	0.0410	0.1532	0.3571	1.7851	0.6713
10	0	3.0004	0.0155	0.1751	0.5186	2.3834	0.7325
10	1	3.3971	0.0251	0.1691	0.3169	4.6552	1.0097
10	3	3.0035	0.0175	0.1817	0.4090	2.8392	0.8222
12	0	2.6382	0.0084	0.2029	0.6562	1.7541	0.6065
12	1	3.5689	0.0268	0.2300	0.2968	1.9174	0.6616
12	2	3.6195	0.0290	0.2220	0.3064	2.4094	0.6035
12	3	3.2195	0.0272	0.2102	0.3388	0.8993	0.8086
12	4	3.2789	0.0346	0.2216	0.5200	1.6621	0.6518

Table D.2. Estimated parameters for Process S and SWA Models for field subjects 13 through 18 in the 1999 UK study.

Subject	Night	S_o	gc	SWA_L	rc	fc	SWA_o
13	1	3.6619	0.0391	0.2099	0.3742	2.3962	0.9962
13	2	3.2038	0.0368	0.2127	0.6463	1.4571	1.0797
13	3	3.6877	0.0396	0.1749	0.4544	2.6606	0.9135
13	4	3.6919	0.0384	0.2346	0.3296	1.7203	0.8148
14	0	3.1813	0.0191	0.2252	0.5168	1.3479	0.4149
14	1	3.6535	0.0378	0.2081	0.3027	2.4437	0.4495
14	3	3.4100	0.0349	0.1948	0.4929	3.1263	0.4518
14	4	3.5922	0.0260	0.2182	0.4196	1.3223	0.3784
15	0	4.0728	0.0448	0.1920	0.2650	1.6454	0.8416
15	1	3.4671	0.0380	0.1849	0.4188	0.8472	0.8556
15	2	5.1299	0.0526	0.1491	0.2146	2.2660	1.0116
15	3	3.5554	0.0316	0.1909	0.3501	2.1493	0.8968
15	4	2.8822	0.0237	0.2099	0.3902	2.8141	0.9586
16	2	3.7999	0.0511	0.1885	0.3281	2.4172	0.6750
16	3	2.5900	0.0132	0.2515	0.4534	2.3607	0.7207
16	4	4.1062	0.0329	0.2400	0.4131	1.1499	0.6461
17	2	3.1666	0.0085	0.1984	0.6205	2.5602	0.1973
17	4	3.5993	0.0111	0.1903	0.2904	1.8888	0.7340
18	0	3.9134	0.0293	0.1481	0.5266	0.9661	0.3428
18	1	4.0829	0.0277	0.1769	0.4777	1.5498	0.6446
18	3	3.8975	0.0259	0.1720	0.5255	1.1675	1.3014

Table D.3. Estimated parameters to define the random noise term $n(t)$ for field subjects 1 through 12 in the 1999 UK study.

Subject	Night	mean	std. dev	skew	kurtosis
1	2	-0.0137	0.2052	0.6424	3.1467
1	4	-0.0162	0.2376	0.7350	3.2077
2	1	-0.0249	0.3184	0.5866	3.0170
2	3	-0.0233	0.3076	0.5346	3.0197
2	4	-0.0270	0.3529	0.6954	3.0037
3	3	-0.0155	0.2619	0.6994	3.0650
3	4	-0.0183	0.2516	0.5569	3.1028
6	1	-0.0148	0.2358	0.4925	2.8902
6	2	-0.0163	0.2421	0.3801	2.7713
6	3	-0.0169	0.2414	0.4245	2.7671
8	4	-0.0131	0.2039	0.5482	3.0342
9	1	-0.0159	0.2125	0.4902	2.9049
9	3	-0.0153	0.2424	0.5413	3.0465
9	4	-0.0221	0.2908	0.4896	2.8882
10	0	-0.0166	0.2699	0.4735	3.0702
10	1	-0.0217	0.3305	0.5821	3.0052
10	3	-0.0231	0.2896	0.5359	2.9910
12	0	-0.0115	0.1989	0.4082	2.9315
12	1	-0.0126	0.2057	0.3081	2.8874
12	2	-0.0109	0.1999	0.4820	3.0699
12	3	-0.0127	0.2363	0.4677	2.8805
12	4	-0.0152	0.2335	0.5244	3.0019

Table D.4. Estimated parameters to define the random noise term $n(t)$ for field subjects 13 through 18 in the 1999 UK study.

Subject	Night	mean	std. dev	skew	kurtosis
13	1	-0.0150	0.2333	0.4922	2.7396
13	2	-0.0126	0.2398	0.4638	2.7454
13	3	-0.0147	0.2262	0.4192	2.6815
13	4	-0.0117	0.2101	0.4216	2.7749
14	0	-0.0194	0.2653	0.6029	3.1969
14	1	-0.0188	0.2689	0.5385	3.2537
14	3	-0.0176	0.2690	0.6065	3.2100
14	4	-0.0171	0.2430	0.6088	3.3874
15	0	-0.0176	0.2389	0.5988	3.2506
15	1	-0.0148	0.2298	0.6067	2.9735
15	2	-0.0165	0.2028	0.5076	3.0437
15	3	-0.0144	0.2079	0.5460	2.9984
15	4	-0.0181	0.2209	0.6691	3.2496
16	2	-0.0152	0.2316	0.4356	2.7253
16	3	-0.0094	0.2039	0.3273	2.8323
16	4	-0.0110	0.2145	0.2778	2.7091
17	2	-0.0123	0.1875	0.3502	2.8473
17	4	-0.0113	0.1788	0.2057	2.7489
18	0	-0.0129	0.2000	0.4971	2.8332
18	1	-0.0187	0.2207	0.5803	3.1554
18	3	-0.0132	0.2158	0.5883	3.1180

Table D.5. Estimated Slow REM parameters for the 1st REM period for field subjects 1 through 12 in the 1999 UK study.

Subject	Night	a	b	c	d
1	2	0.9449	0.3452	1.8029	2.2423
1	4	0.4772	0.3628	0.4370	1.0013
2	1				
2	3				
2	4	0.5625	0.3310	0.5577	1.2185
3	3				
3	4				
6	1	0.6171	0.3082	2.6341	2.1381
6	2	0.7395	0.2693	3.5046	2.1494
6	3	0.5880	0.5230	3.2306	2.8342
8	4	0.6009	0.3204	1.7271	1.9237
9	1	0.5630	0.2888	0.9491	1.4708
9	3	0.4375	0.3988	1.6747	1.8993
9	4	0.4624	0.2723	0.2468	0.7767
10	0	0.5033	0.2472	1.0223	1.4101
10	1	0.7957	0.2963	4.4418	2.4240
10	3				
12	0	0.5003	0.2333	1.4639	1.4902
12	1	0.5599	0.3768	0.4808	1.1372
12	2	0.4742	0.3416	0.3624	0.8917
12	3	0.4671	0.3713	4.0835	2.3865
12	4				

Table D.6. Estimated Slow REM parameters for the 1st REM period for field subjects 13 through 18 in the 1999 UK study.

Subject	Night	a	b	c	d
13	1	0.8421	0.4053	1.3973	2.1578
13	2	0.3383	0.4697	2.9938	2.9428
13	3	0.6519	0.4009	1.3782	1.9353
13	4	0.5565	0.4542	1.5234	2.0760
14	0	0.4277	0.3275	1.0295	1.5120
14	1	0.5209	0.3732	0.8963	1.4355
14	3	0.6248	0.3588	1.7732	2.0457
14	4	0.4921	0.3768	0.9242	1.5152
15	0				
15	1	0.4890	0.4508	2.9965	2.4623
15	2	0.4987	0.3260	2.5135	2.0515
15	3	0.4328	0.3804	0.5348	1.0644
15	4				
16	2	0.5231	0.5728	4.9164	3.2492
16	3	0.5326	0.5202	1.2638	1.9961
16	4	0.6534	0.4220	2.8619	2.6845
17	2	0.4584	0.3948	2.1441	2.1096
17	4	0.4532	0.2789	0.3634	0.8962
18	0	0.4601	0.3255	1.6773	1.7843
18	1	0.4294	0.2975	0.9734	1.4024
18	3	0.5304	0.4369	1.0966	1.8001

Table D.7. Estimated Slow REM parameters for the 2nd REM period for field subjects 1 through 12 in the 1999 UK study.

Subject	Night	a	b	c	d
1	2	0.4639	0.3865	0.5274	1.0631
1	4	0.5053	0.3594	1.9105	1.9666
2	1	0.4896	0.4300	0.8211	1.4968
2	3	0.4815	0.3023	0.5093	1.0836
2	4	0.4277	0.2928	1.0524	1.4569
3	3	0.3494	0.2807	0.6846	1.1034
3	4	0.4522	0.2536	1.0486	1.3399
6	1	0.4283	0.4861	3.2037	3.1510
6	2	0.3507	0.3839	0.9261	1.3689
6	3	0.6365	0.3903	1.0005	1.7083
8	4	0.5400	0.3777	4.9061	2.5620
9	1				
9	3	0.4857	0.2791	0.3239	0.9093
9	4	0.3462	0.3166	0.6968	1.1381
10	0	0.3200	0.2705	0.6440	1.0248
10	1	0.3870	0.3070	0.9110	1.3715
10	3	0.4808	0.4389	0.4637	0.9781
12	0	0.3189	0.3230	1.2159	1.4351
12	1				
12	2	0.4674	0.3754	0.2581	0.7168
12	3				
12	4				

Table D.8. Estimated Slow REM parameters for the 2nd REM period for field subjects 13 through 18 in the 1999 UK study.

Subject	Night	a	b	c	d
13	1	0.5208	0.4153	0.6243	1.2152
13	2				
13	3	0.5909	0.3677	2.7721	2.3193
13	4	0.5863	0.3894	0.2723	0.8640
14	0	0.4264	0.3666	0.5073	1.0169
14	1	0.4901	0.4151	0.5836	1.1526
14	3	0.4566	0.4687	0.8856	1.5078
14	4	0.4850	0.4171	0.6355	1.2381
15	0	0.4898	0.5628	2.7293	2.6201
15	1	0.5081	0.2515	0.2453	0.8591
15	2	0.5007	0.4217	0.1873	0.5431
15	3	0.4853	0.3430	0.3609	0.9168
15	4	0.3844	0.3957	0.3694	0.7949
16	2	0.5862	0.2872	0.1222	0.8035
16	3	0.7002	0.3297	0.1092	0.5507
16	4	0.5370	0.4100	0.7989	1.4283
17	2	0.5171	0.3613	1.2800	1.7625
17	4	0.3584	0.3965	0.8833	1.3490
18	0	0.4221	0.4101	0.5928	1.1745
18	1	0.3666	0.2230	0.2092	0.6277
18	3	0.5499	0.3413	0.3794	1.0031

Table D.9. Estimated Slow REM parameters for the 3rd REM period for field subjects 1 through 12 in the 1999 UK study.

Subject	Night	a	b	c	d
1	2	0.5024	0.3216	1.1445	1.5797
1	4	0.4838	0.5494	0.6685	1.2813
2	1	0.5188	0.3152	0.2316	0.8083
2	3	0.4390	0.5583	0.4880	0.9656
2	4	0.4011	0.4044	1.7710	1.9035
3	3	0.4550	0.3972	4.6822	2.9365
3	4				
6	1	0.7139	0.4861	3.2037	3.1510
6	2	0.4969	0.4907	1.1780	3.1510
6	3	0.5158	0.5850	0.9091	1.6064
8	4	0.4733	0.4081	1.4409	1.8836
9	1				
9	3	0.3599	0.2662	0.4348	0.8829
9	4	0.4198	0.3390	0.3032	0.7564
10	0	0.5402	0.5777	0.1713	0.4179
10	1	0.3928	0.4597	0.9503	1.4718
10	3	0.6591	0.4520	0.1129	0.4489
12	0	0.4552	0.3867	0.2471	0.6599
12	1	0.4861	0.4889	1.9929	2.2783
12	2	0.4854	0.3978	0.6604	1.2595
12	3				
12	4				

Table D.10. Estimated Slow REM parameters for the 3rd REM period for field subjects 13 through 18 in the 1999 UK study.

Subject	Night	a	b	c	d
13	1	0.5238	0.4283	1.0469	1.7118
13	2	0.6365	0.4470	3.4673	2.7505
13	3	0.4666	0.3557	0.7078	1.2666
13	4	0.5455	0.4493	2.3287	2.3778
14	0	0.5051	0.4106	0.2837	0.7724
14	1	0.5639	0.4553	0.3234	0.8716
14	3	0.6588	0.5353	0.3121	0.9028
14	4				
15	0	0.6721	0.4306	0.3627	1.1717
15	1	0.3238	0.2679	0.4875	0.8953
15	2	0.5598	0.4507	0.3937	1.0072
15	3	0.5276	0.6923	0.4838	0.9810
15	4	0.5040	0.4025	0.8526	1.4848
16	2	0.3968	0.3456	1.5555	1.7050
16	3	0.4699	0.4098	2.1466	2.1424
16	4	0.4970	0.2984	0.3987	0.9866
17	2	0.5683	0.5020	0.1770	0.5425
17	4	0.5104	0.4287	0.6854	1.3078
18	0	0.5262	0.4634	0.9469	1.6672
18	1	0.3623	0.3685	0.1945	0.4621
18	3	0.4293	0.3853	0.8116	1.4171

Table D.11. Estimated Slow REM parameters for the 4th REM period for field subjects 1 through 12 in the 1999 UK study.

Subject	Night	a	b	c	d
1	2	0.5365	0.5782	0.2852	0.6619
1	4	1.5974	1.3901	0.1178	0.2581
2	1	0.6074	0.7519	0.3061	0.6471
2	3	1.4069	1.3761	0.1261	0.3670
2	4	0.8437	0.7795	0.1388	0.4083
3	3	0.8604	1.1212	0.3128	0.6724
3	4				
6	1	0.6818	0.3391	0.1062	0.5235
6	2	0.5887	0.3292	0.4522	1.2172
6	3	0.7326	0.3834	0.8000	1.6670
8	4	0.5739	0.6394	0.6444	1.3707
9	1				
9	3	0.3905	0.4391	0.3334	0.7305
9	4	0.5724	1.5681	1.2130	1.7177
10	0				
10	1	0.5912	0.4784	0.7260	1.4171
10	3	0.8150	0.8238	0.3115	0.7617
12	0	0.7859	1.0489	0.3869	0.8025
12	1	0.6698	0.3620	0.1179	0.5445
12	2	0.5553	0.6585	2.5723	2.8309
12	3	0.7427	0.5116	0.4340	1.1898
12	4				

Table D.12. Estimated Slow REM parameters for the 4th REM period for field subjects 13 through 18 in the 1999 UK study.

Subject	Night	a	b	c	d
13	1	0.5669	0.4338	1.0256	1.6158
13	2	0.6722	0.6984	0.5466	1.2074
13	3	0.4981	0.5578	3.3427	3.3730
13	4	0.6880	0.4682	0.1152	0.4618
14	0	0.8844	1.0687	0.2996	0.6810
14	1	0.6790	0.5767	0.2644	0.7689
14	3	0.6432	0.3055	0.6329	1.4333
14	4				
15	0	0.5792	0.6659	2.1312	2.6890
15	1	0.4194	0.7760	3.5629	2.6521
15	2	0.7735	1.1726	0.6910	1.3673
15	3	0.8922	0.5190	0.6672	1.6873
15	4				
16	2	1.1560	1.1883	0.1378	0.1548
16	3	0.5448	0.4312	0.4498	1.0866
16	4				
17	2	0.6413	0.5223	1.2624	2.0347
17	4	0.5594	0.3957	0.2866	0.8331
18	0	0.8106	0.6671	0.1257	0.4598
18	1				
18	3	0.5416	0.4163	0.2068	0.6370

Table D.13. Estimated parameters for Process S and SWA Models for laboratory subjects in the 1999 UK study.

Subject	Night	S_o	gc	SWA_L	rc	fc	SWA_o
19	0	4.4617	0.0388	0.1322	0.2723	2.7529	0.7880
19	1	4.1486	0.0416	0.1389	0.5287	2.3165	0.6207
19	2	4.4169	0.0377	0.1574	0.3119	1.8867	0.7717
20	1	3.7485	0.0301	0.1414	0.2021	1.2187	0.7005
20	2	4.4947	0.0510	0.1266	0.3502	1.9782	0.6344
20	3	4.5684	0.0447	0.1118	0.3991	0.9658	1.0292
22	0	3.6723	0.0302	0.1618	0.2413	0.8112	0.8331
22	1	2.7767	0.0224	0.1888	0.5033	0.6205	1.0756
22	2	2.9903	0.0215	0.1799	0.4356	3.9335	0.5538
22	3	3.3267	0.0247	0.1887	0.2465	0.5896	1.4638
22	4	3.2060	0.0299	0.1781	0.3031	1.4033	1.1598
23	0	4.3522	0.0437	0.1360	0.2274	1.5741	0.5255
23	1	3.6144	0.0427	0.1253	0.5919	3.0516	0.5897
23	2	3.5923	0.0458	0.1170	0.4904	3.2262	0.9388
23	3	3.9107	0.0403	0.1123	0.4474	0.7768	0.7866
23	4	4.2102	0.0408	0.0962	0.4243	5.2869	0.1287
24	1	3.7697	0.0262	0.1946	0.3005	1.2354	0.9240
24	2	3.6909	0.0287	0.1616	0.3345	1.2877	0.7526
24	3	3.5164	0.0242	0.1131	0.1927	2.1170	1.0128
24	4	3.3937	0.0310	0.1446	0.3861	2.5985	0.7584
25	0	4.4544	0.0408	0.1317	0.3577	3.0195	0.5270
25	1	5.5164	0.0423	0.1339	0.3528	1.8326	0.3762
25	3	4.1590	0.0326	0.1568	0.3428	1.7633	0.5745
25	4	4.6178	0.0388	0.1379	0.3817	4.4222	0.5808
26	0	4.1647	0.0367	0.2180	0.3898	1.8732	0.8575
26	1	3.5370	0.0251	0.1832	0.5734	2.5480	0.2611
26	2	3.5335	0.0148	0.2155	0.4978	3.5402	0.6858
26	3	3.0433	0.0285	0.2277	0.5752	1.0266	0.5940
26	4	3.3089	0.0247	0.1842	0.8444	3.5710	0.5459
27	0	3.7023	0.0310	0.1469	0.1939	2.1031	1.3816
27	1	4.2429	0.0291	0.1901	0.5101	2.4893	0.3781
27	2	3.6894	0.0174	0.1578	0.7144	3.8975	0.6864
27	3	2.2853	0.0092	0.1519	0.5768	1.3976	1.3098

Table D.14. Estimated parameters to define the random noise term $n(t)$ for laboratory subjects in the 1999 UK study.

Subject	Night	mean	std. dev	skew	kurtosis
19	0	-0.0230	0.2976	0.4820	2.9347
19	1	-0.0238	0.3001	0.4651	3.0426
19	2	-0.0223	0.3166	0.7243	3.4013
20	1	-0.0248	0.3499	0.7557	3.2273
20	2	-0.0208	0.3163	0.6404	2.9809
20	3	-0.0282	0.3209	0.7196	3.2341
22	0	-0.0102	0.1855	0.3313	2.5732
22	1	-0.0122	0.2177	0.4288	2.6868
22	2	-0.0139	0.2222	0.3567	2.7088
22	3	-0.0089	0.2127	0.3329	2.5741
22	4	-0.0126	0.1957	0.3300	2.6127
23	0	-0.0230	0.2794	0.6314	3.2467
23	1	-0.0270	0.3284	0.6696	3.2777
23	2	-0.0264	0.3022	0.7096	3.3291
23	3	-0.0269	0.3437	0.7923	3.4239
23	4	-0.0259	0.3180	0.6423	3.3163
24	1	-0.0215	0.2784	0.5800	3.2364
24	2	-0.0209	0.2496	0.7014	3.3164
24	3	-0.0246	0.2742	0.5689	3.1053
24	4	-0.0183	0.2503	0.6000	3.1454
25	0	-0.0153	0.2173	0.4594	3.1641
25	1	-0.0179	0.2804	0.4747	2.9093
25	3	-0.0153	0.2127	0.5792	3.0931
25	4	-0.0148	0.2390	0.4520	2.9289
26	0	-0.0138	0.2104	0.6281	3.2015
26	1	-0.0168	0.2368	0.6540	3.1220
26	2	-0.0135	0.2158	0.5218	2.8605
26	3	-0.0119	0.1976	0.3841	2.7699
26	4	-0.0180	0.2549	0.5501	2.9491
27	0	-0.0156	0.2358	0.4369	2.8233
27	1	-0.0206	0.2284	0.4893	2.7561
27	2	-0.0200	0.2304	0.4844	2.8232
27	3	-0.0157	0.2285	0.4956	2.8772

Table D.15. Estimated Slow REM parameters for the 1st REM period for laboratory subjects in the 1999 UK study.

Subject	Night	a	b	c	d
19	0				
19	1	0.4251	0.2834	4.9021	2.2987
19	2	0.3810	0.3050	1.0263	1.3982
20	1	0.6702	0.3544	0.9204	1.6302
20	2	0.7062	0.5900	0.1642	0.5507
20	3	0.6909	0.4573	0.3386	1.0201
22	0	0.6138	0.3478	1.1979	1.6893
22	1	0.9176	0.2900	4.8776	2.3368
22	2	0.7329	0.3431	4.3607	2.6913
22	3	0.4388	0.2721	0.1291	0.5678
22	4	0.7147	0.2939	0.7556	1.5869
23	0	0.4287	0.4356	2.5031	2.2213
23	1				
23	2	0.6862	0.4797	4.3969	3.0872
23	3	0.4092	0.5104	1.0667	1.6152
23	4	0.6191	0.3796	2.6691	2.5219
24	1	0.3248	0.3053	0.6152	1.0414
24	2				
24	3	0.3725	0.3171	1.0875	1.4275
24	4	0.3869	0.3413	2.1844	1.8916
25	0	0.5445	0.3723	2.8765	2.3358
25	1	0.4892	0.4575	1.4841	1.9746
25	3	0.4685	0.3327	1.5071	1.8612
25	4	0.6223	0.2788	1.5787	1.7070
26	0	0.3708	0.3830	1.7241	1.7961
26	1	0.4198	0.3258	3.5515	1.9850
26	2				
26	3	0.4386	0.3382	1.7017	1.8136
26	4				
27	0	0.6900	0.3382	2.0799	2.1056
27	1				
27	2	0.5655	0.3170	1.3695	1.7208
27	3	0.7115	0.4085	0.4487	1.3780

Table D.16. Estimated Slow REM parameters for the 2nd REM period for laboratory subjects in the 1999 UK study.

Subject	Night	a	b	c	d
19	0	0.4803	0.5197	0.3091	0.6831
19	1	0.3598	0.3574	1.1256	1.4724
19	2	0.3997	0.3644	0.5559	1.0828
20	1	0.4260	0.2717	0.3975	0.9515
20	2	0.7553	0.4345	0.8170	1.7184
20	3	0.5803	0.3985	0.3900	1.0402
22	0	0.4607	0.4267	1.3724	1.8195
22	1	0.3668	0.5099	0.9374	1.4428
22	2	0.5261	0.7963	4.1544	3.5468
22	3	0.3817	0.4728	1.9004	2.0365
22	4	0.4082	0.4221	0.4460	0.9360
23	0	0.6101	0.4355	2.8321	2.7324
23	1	0.3572	0.2965	0.7228	1.1619
23	2	0.6739	0.5253	2.2173	2.7709
23	3	0.6715	0.3244	1.0515	1.6653
23	4	0.5010	0.4570	1.7549	2.1579
24	1	0.4336	0.4467	2.2907	2.2103
24	2	0.5105	0.3927	1.3382	1.8843
24	3	0.4776	0.3814	2.9425	2.2768
24	4	0.4261	0.3919	1.1084	1.5847
25	0	0.4851	0.4419	1.0678	1.7222
25	1	0.5728	0.3633	1.0387	1.5875
25	3	0.4326	0.4155	0.8186	1.4586
25	4	0.3923	0.3724	1.7375	1.8288
26	0	0.4667	0.2680	0.2915	0.8435
26	1	0.4088	0.2678	0.5056	1.0000
26	2	0.3176	0.2458	0.6736	1.0591
26	3	0.4307	0.3001	0.6203	1.1292
26	4	0.2989	0.4336	0.7549	1.1672
27	0	0.4469	0.3773	0.4208	0.9390
27	1	0.4478	0.4120	0.4503	0.9404
27	2				
27	3	0.5702	0.5707	3.3406	3.4079

Table D.17. Estimated Slow REM parameters for the 3rd REM period for laboratory subjects in the 1999 UK study.

Subject	Night	a	b	c	d
19	0	0.6687	0.4552	0.3896	1.1010
19	1	0.4728	0.3570	0.3457	0.8511
19	2	0.4754	0.4595	0.6974	1.3590
20	1	0.3470	0.4226	0.9595	1.4112
20	2	0.5526	0.3769	1.1329	1.6898
20	3	0.5821	0.5023	0.2380	0.7116
22	0				
22	1	0.6749	0.3394	1.3436	1.8864
22	2	0.8796	0.4257	0.3223	1.3819
22	3	0.6144	0.4661	0.4351	1.0741
22	4	0.5689	0.4450	0.4569	1.1015
23	0	0.5458	0.3444	0.4666	1.1157
23	1	0.4042	0.4423	0.5583	1.0675
23	2	0.6268	0.3094	0.6703	1.4387
23	3	0.4075	0.3986	0.8956	1.4221
23	4	0.5821	0.4232	1.0106	1.6091
24	1	0.5238	0.2789	0.2633	0.8962
24	2	0.5222	0.5068	0.5811	1.2142
24	3	0.5527	0.5264	0.6560	1.2955
24	4	0.5049	0.3868	0.3160	0.8776
25	0	0.5605	0.3765	0.5711	1.2564
25	1	0.4855	0.3871	0.4313	0.9964
25	3	0.5264	0.3732	0.6560	1.2955
25	4	0.4878	0.4818	0.8249	1.5370
26	0				
26	1				
26	2	0.6989	1.1090	0.2242	0.4263
26	3	0.4499	0.5123	0.3603	0.7970
26	4	0.6328	0.6036	0.4991	1.0923
27	0	0.5763	0.5844	4.0785	3.1609
27	1	0.5280	0.4658	1.5061	2.1693
27	2				
27	3	0.7172	0.3840	1.1155	1.8699

Table D.18. Estimated Slow REM parameters for the 4th REM period for laboratory subjects in the 1999 UK study.

Subject	Night	a	b	c	d
19	0				
19	1				
19	2	0.6152	0.5341	0.6383	1.3189
20	1	0.5484	0.3193	1.1088	1.5594
20	2	0.5387	0.4948	0.3856	0.9102
20	3	0.7437	0.8210	0.6442	1.4124
22	0	0.6091	0.5014	2.0878	2.6806
22	1	0.5382	1.0653	0.7443	1.3323
22	2	0.6858	0.5499	0.1414	0.5037
22	3	0.5855	0.3806	0.1708	0.6939
22	4	0.7367	0.6174	0.1708	0.5800
23	0	0.5867	0.5784	0.2321	0.5851
23	1				
23	2	0.3950	0.4652	1.0138	1.5328
23	3	0.6093	0.4891	3.8592	2.9005
23	4	0.5175	0.3944	0.8351	1.4474
24	1	0.4008	0.8642	1.2226	1.6379
24	2	0.6070	0.3593	0.2406	0.9023
24	3	0.6052	0.3211	0.1749	0.8150
24	4	0.5982	0.4042	3.5296	2.6082
25	0	0.4848	0.4690	0.9139	1.6335
25	1	0.4930	0.3682	0.3855	0.9550
25	3	0.5087	0.4269	0.4168	0.9627
25	4	0.6791	0.5020	0.115	0.5144
26	0	0.9384	0.8990	0.4220	1.0837
26	1				
26	2				
26	3	0.6516	0.4208	0.3062	0.9689
26	4				
27	0	0.7471	0.6266	0.9356	1.8275
27	1	0.6651	0.5636	0.3960	1.0266
27	2	0.8620	0.4098	1.3385	2.1424
27	3	0.4858	0.4788	1.3242	1.8655

Appendix E. Range for Nonlinear Model Parameters Estimated for Each Subject

Table E.1. Range of estimated parameter values for Process S and SWA Models for all field subject nights in the 1999 UK study.

	Range min to max
S_o	2.5900 to 5.8348
gc	0.0084 to 0.0544
SWA_L	0.1010 to 0.2515
rc	0.1064 to 0.8013
fc	0.8472 to 4.6552
SWA_o	0.1973 to 1.5094

Table E.2. Range of estimated parameter values for $n(t)$ for all field subject nights in the 1999 UK study.

	Range min to max
mean	-0.0094 to -0.0270
standard deviation	0.1788 to 0.3529
skew	0.2057 to 0.7350
kurtosis	2.6815 to 3.3874

Table E.3. Range of estimated parameter values for the Slow REM model for all field subject nights in the 1999 UK study.

REM Period	a min to max	b min to max	c min to max	d min to max
1	0.3383 to 0.9449	0.2333 to 0.5728	0.2468 to 4.9164	0.7767 to 3.2492
2	0.3189 to 0.7002	0.2230 to 0.5628	0.1092 to 4.9061	0.5431 to 3.1510
3	0.3238 to 0.7139	0.2662 to 0.6923	0.1129 to 4.6822	0.4179 to 3.1510
4	0.3905 to 1.5974	0.3055 to 1.5681	0.1062 to 3.5629	0.1548 to 3.3730

Table E.4. Range of estimated parameter values for Process S and SWA Models for all laboratory subject nights in the 1999 UK study.

	Range min to max
S_o	2.2853 to 5.5164
gc	0.0092 to 0.0510
SWA_L	0.0962 to 0.2277
rc	0.1927 to 0.8444
fc	0.5896 to 5.2869
SWA_o	0.1287 to 1.4638

Table E.5. Range of estimated parameter values for $n(t)$ for all laboratory subject nights in the 1999 UK study.

	Range min to max
mean	-0.0089 to -0.0282
standard deviation	0.1788 to 0.3529
skew	0.2057 to 0.7923
kurtosis	2.5732 to 3.4239

Table E.6. Range of estimated parameter values for the Slow REM model for all laboratory subject nights in the 1999 UK study.

REM Period	a min to max	b min to max	c min to max	d min to max
1	0.3248 to 0.9176	0.2721 to 0.5900	0.1291 to 4.9021	0.5507 to 3.0872
2	0.2986 to 0.7553	0.2458 to 0.7963	0.2915 to 4.1544	0.6831 to 3.5468
3	0.3470 to 0.8796	0.2789 to 1.1090	0.2242 to 4.0785	0.4263 to 3.1609
4	0.3950 to 0.9384	0.3193 to 1.0653	0.1115 to 3.8592	0.5037 to 2.9005

Appendix F. Equations and Coefficients of Nonlinear Dynamic Models

F.1 Massaquoi and McCarley Model

The Massaquoi and McCarley model (1992) has 4 main components. The first part of the model is the reciprocal interaction REM model. The equation for REM promoting neuron activity is,

$$\dot{X} = a(X)S_1(X)X - b(X)XY, \tag{F.1}$$

and the equation for REM inhibiting neuron activity is,

$$\dot{Y} = -cY + d_{circ}S_2(Y)(X + E)Y, \tag{F.2}$$

where,

$$d_{circ} = 0.975(1 + 0.125sin(0.0467 + 2.3)), \tag{F.3}$$

and E is defined in Equation F.11. The equations for the coefficients of the REM model are,

$$a(X) = 2 - 1.8\left(1 - \frac{1}{1 + e^{-4(X-0.5)}}\right), \tag{F.4}$$

$$b(X) = \frac{2}{1 + e^{-80(X-0.1)}}, \tag{F.5}$$

$$S_1(X) = 1 - 1.4\left(\frac{1}{1 + e^{-0.8(X-2.5)}}\right) + 0.167, \tag{F.6}$$

$$S_2(Y) = 1 - 1.5\left(\frac{1}{1 + e^{-20(Y-2)}}\right). \tag{F.7}$$

The equations for the Process S and SWA models are:

$$\dot{SWA} = rc\, SWA(1 - SWA/SWA_{max}) + SWA\, n(t), \tag{F.8}$$

and

$$\dot{S} = -gc\, SWA + rs(1 - S), \tag{F.9}$$

where SWA_{max} is defined as,

$$SWA_{max} = max(S(1 - 0.95\ min(X^4 + E/2, 1.0)), 0.05), \tag{F.10}$$

and $n(t)$ is a uniformly distributed random noise signal. The excitation term E in the above equations is filtered Poisson noise (N) which has an exponentially distributed arrival time, and uniformly distributed amplitude and duration, the equation for E is,

$$\dot{E} = N - kE. \tag{F.11}$$

Sleep stages during the night are scored according to the following rules:

1. If X >1.4 score as stage REM,
2. If SWA <0.1 and E >0.5 score as Wake,
3. Else score as NREM sleep.

The values of the model parameters are in Table F.1. An example of the output of the model is shown in Figure F.1.

F.2 The Nonlinear Model Developed as Part of This Research.

The following are the equations for the modified version of the Massaquoi and McCarley model that was developed as part of this research. The equations used for the slow wave activity model are,

$$\dot{S} = -gc\, SWA, \tag{F.12}$$

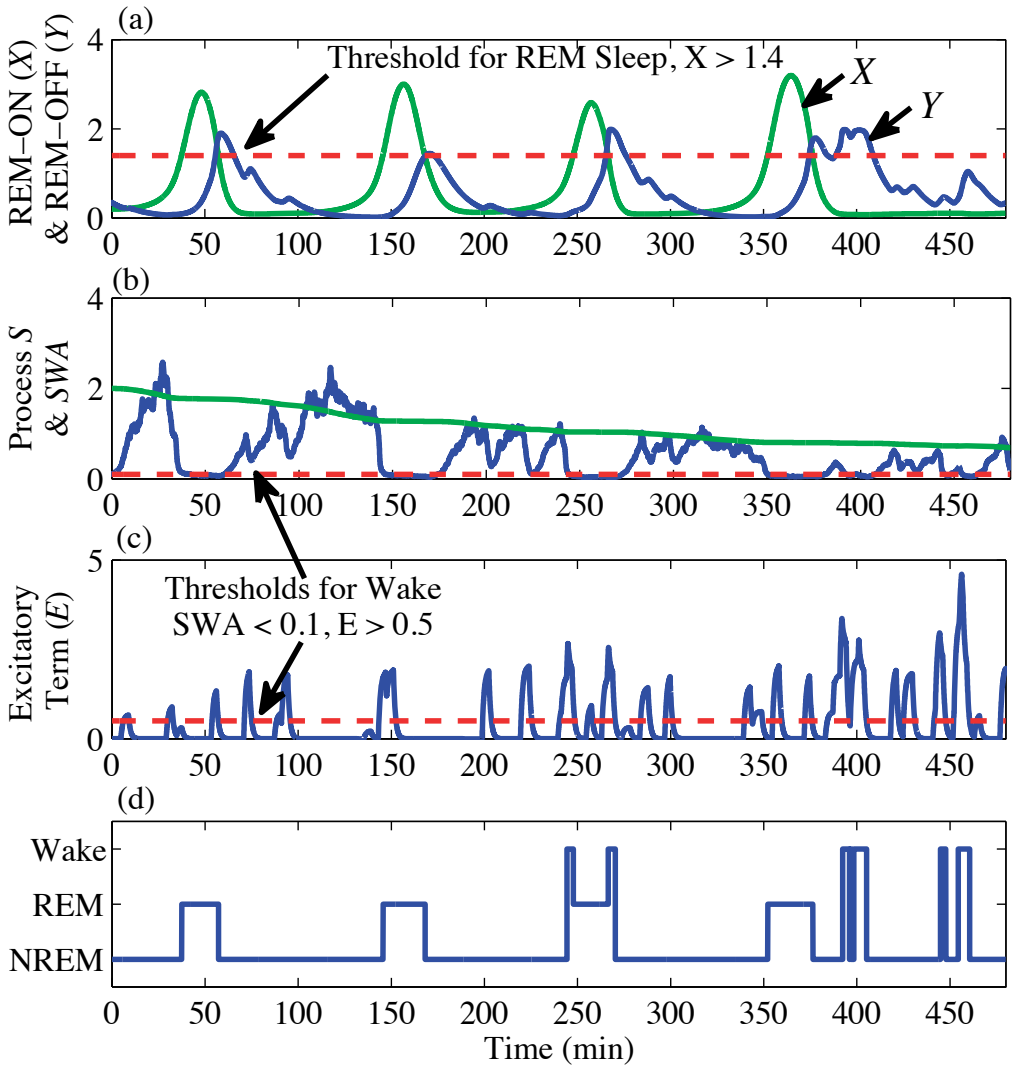

Figure F.1. An example of using Massaquoi and McCarley's LCRIM/I model to classify sleep stages, (a) REM-ON (X) (green) and REM-OFF(X) (blue) activity, (b) Process S (green) and SWA (blue), (c) Excitatory activity E, and (d) sleep stages. Thresholds used for scoring sleep stages (red-dashed lines).

and

$$\dot{SWA} = rc\, SWA\ (S - SWA) - fc\,(SWA - SWA_L)REMT - fcw\,(SWA - SWA_L)E, \tag{F.13}$$

Table F.1. Coefficients of Massaquoi and McCarley's LCRIM/I Model (1992).

Model Parameters	Original Values
c	1
gc	0.05
k	10
rc	3.0
rs	0.005
E_o	0.001
X_o	0.12
Y_o	0.35
S_o	2.0
SWA_o	0.1
N Amplitude	Uniformly distributed between 1.25 and 25
N Duration	Uniformly distributed between 0.25 and 0.5
N Inter-arrival Time	Exponentially distributed with mean of 1.1
$n(t)$	Uniformly distributed between -10 and 10

and

$$SWA = SWA(1 + n(t)). \tag{F.14}$$

The equations for the Slow REM model are similar to those of the Massaquoi and McCarley model but without the saturation functions. The equation for REM promoting neuron activity is thus,

$$\dot{X} = (aX - bXY)dc, \tag{F.15}$$

where dc is a sinusoidal term with a period of 24 hours,

$$dc = 1.55 + 0.8sin(0.0467t + 4), \tag{F.16}$$

where t is measured in units rather than seconds with 1 unit equal to 10.7 minutes. The equation for the REM inhibiting neuron activity is,

$$\dot{Y} = -cY + d(X + eE)Y. \tag{F.17}$$

The equation for the fast REM model is,

$$\ddot{x} + \delta\dot{x} + (x + 2.5)(x - (-2 + \gamma w(t)))(x + 0.5)(x)(x - 0.5) = Acos(\omega t), \tag{F.18}$$

where $w(t)$ in the equation is typically the excitation term $E(t)$. An example of the output of the model when noise events are occurring is shown in Figure F.2. The model parameter values are listed in Table F.2. The following rules were used for assigning NREM sleep stages:

1. If SWA >2.0 score as Stage 3/4,
2. If SWA <0.3 score as Stage Wake/1 ,
3. If SWA <1 and E >0.5 score as Stage Wake/1,
4. All other times when REM sleep is not occurring are scored as Stage 2 sleep.

The following rules were used to assign REM sleep stages according to the value of x of the fast REM model:

1. If x >0 score as Phasic REM sleep,
2. If x <-2 and an excitation is occurring score as Wake,
3. All other times are scored as Tonic REM sleep.

REM sleep periods were defined by the level of REM promoting activity X in the slow REM model. When X is greater than 1, REM sleep periods was considered to be occurring.

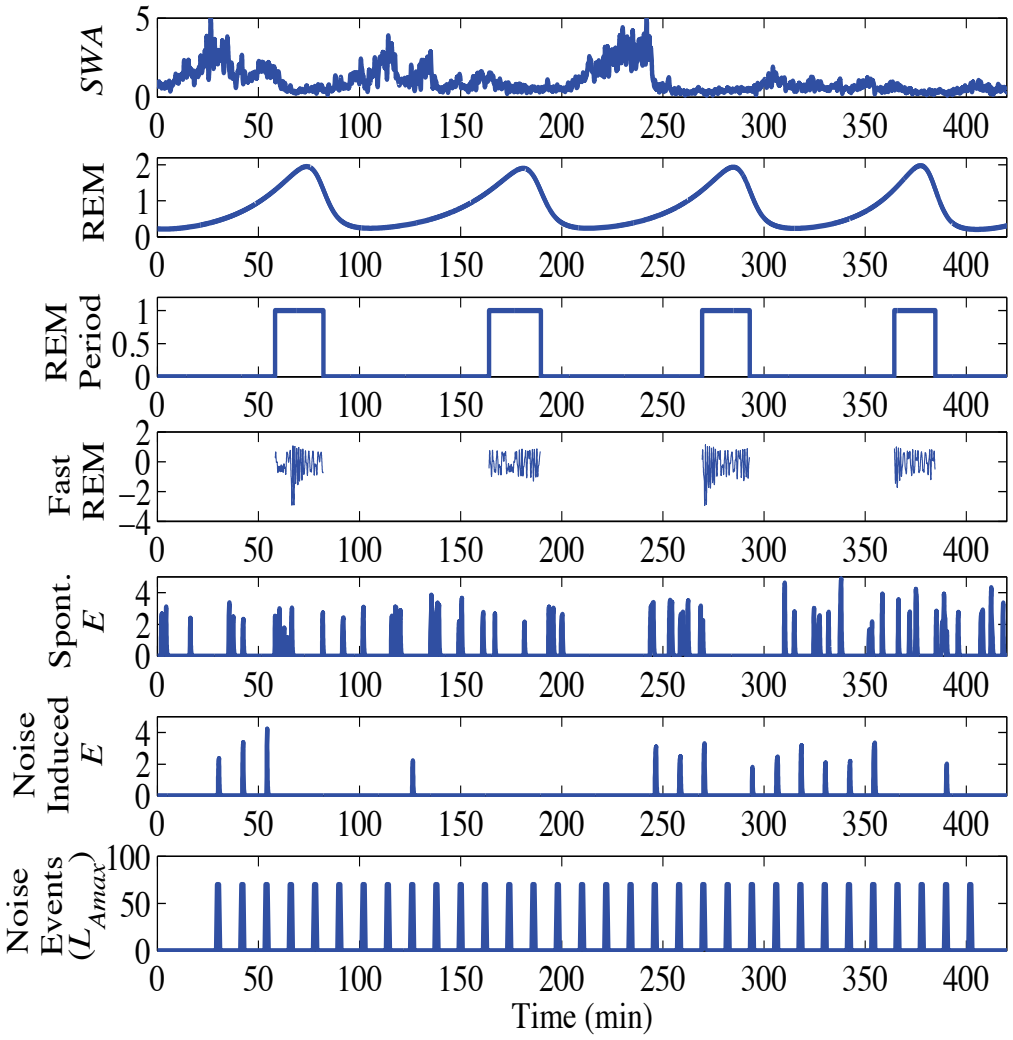

Figure F.2. An example of the parameters for the developed nonlinear sleep model, which include slow wave activity (SWA), REM, REM sleep period indicator, fast REM model and the spontaneous and noise induced excitation terms.

Table F.2. Parameters of the nonlinear model. *Parameters varied according to a Gaussian distribution and + parameters varied according to a uniform distribution, x parameter varied with an exponential distribution.

SWA		Slow REM		Fast REM		Excitations	
$*S_o$	mean 3.75 std. dev 0.67	$*a$	mean 0.47 std. dev 0.1	ω	2 π (0.3)	N	^{x}mean inter-arr 6.1 min
$*SWA_o$	mean 0.78 std. dev 0.29	$*b$	mean 0.41 std. dev 0.1	A	0.5		*dur.-mean 0.5 min
$*gc$	mean 0.03 std. dev 0.01	$*c$	mean 1.4 std. dev 0.15	δ	0.06		*dur.-std. dev 0.2 min
SWA_L	0.2	$*d$	mean 1.83 std. dev 0.15	^+x_o	min -1.0 max 1.0		*amp.- mean 3.0
fc	2.0	e	0.05	^+y_o	min -1.0 max 1.0		*amp.-std. dev 0.65
fcw	4.0	^+X_o	min 0.15 max 0.3				amp.-max 5.0
rc	0.4	^+Y_o	min 0.5 max 3.0				
$n(t)$	mean 0 std. dev 0.2 skewness 0.53						

Appendix G. Code for Nonlinear Dynamic Model

The following is the Matlab program for the nonlinear dynamic sleep model that was developed as part of this research. The components of the model are the slow and fast REM model, slow wave activity model, and spontaneous and aircraft noise induced excitation terms. Based on these components sleep stages are predicted. In Table G.1 is a list of subroutines in this program and the functions they call.

Table G.1. Subroutines of the nonlinear dynamic model.

Subroutine Name	Is Called By	Makes Calls to
Input_Parameters	Model_Main	None
Create_Aircraft Input	Model_Main	None
Generate_Random_Input_Variables	Model_Main	None
Create_Spontaneous	Model_Main	None
Create_Aircraft_Awakenings	Model_Main	None
E_Calc	Model_Main	None
REM_Calc	Model_Main	None
Create_REM_INPUT	Model_Main	None
SWA_Calc	Model_Main	None
NREM_Sleep_Stage_Classify	Model_Main	None
Fast_REM_Main	Model_Main	calc_tonic_phasic_int Phasic_Tonic_Calc
Phasic_Tonic_Calc	Fast_REM_Main	None
calc_tonic_phasic_int	Fast_REM_Main	None
Calc_30_Sec_Stages	Model_Main	None

The following are the inputs to the model:

1. optionN: which is used if a noise scenario is being run,
2. position: the x,y grid position,
3. LAMAX: the maximum noise levels of sound events during the night. This term is a vector and its length is equal to the length of the number of events during the night,
4. Numpeople: is the number of people to simulate for each location point,
5. Timing: the time of each noise event during the night in minutes.

An example of an input to the model is the following if the events were of all the same noise level during the night,

```
optionN={'Noise'};%%Run for noise events
position=[0 0];%%X,Y position
LAMAX=40*ones(1,16);%%LAMAX and timing must be equal in length
Numpeople=50;%%Number of people at grid point
Timing=30:24:402;%%Time of events in minutes
```

Function Model_Main: This is the main code for the nonlinear dynamic model.

```
%%%-------------------------------------------------------------------------%%
%%%-------------------------------------------------------------------------%%
%%%Function Model_Main
%%%Main code for the nonlinear dynamic sleep model
%%%Note 1 Unit in the model is equal to 10.7 minutes
%%%
%%%Input:  LAMAX-noise level for each nighttime event
%%%        Timing-timing of aircraft events in minutes
%%%        Numpeople-number of people at a location point
%%%        optionN: is used if a noise scenario is being run
%%%        position: x,y location for grid point
%%%-------------------------------------------------------------------------%%
%%%-------------------------------------------------------------------------%%
function Model_Main(LAMAX,Timing,Numpeople,optionN,position)
warning off;
len=48;
Fs=640;

[Data]=Input_Parameters;%%Obtain model parameter values

if strcmp(optionN,'Noise')
  %%Run simulation once for baseline conditions and once for
  %%Noise event conditions
  Repeat=2;

  %%Create aircraft noise input
  [Events]=Create_Aircraft_Input(Data,LAMAX,Numpeople);
else
  Repeat=1;
end

for ink=1:Numpeople
  display(ink)
  time=0:1/Fs:len;
```

```
%%Relationship between NREM excitation amplitude
%%and fast REM sleep excitation amplitude
REM=[.5 1.45];
NREM=[.5 5];
pr=polyfit(NREM,REM,1);

%%Spontaneous awakenings
[Nt,NtREM]=Create_Spontaneous(Fs,len,Data,pr);

%%Limit amplitude of REM and NREM excitation terms
if max(NtREM)>1.45
  I=find(NtREM>1.45);
  NtREM(I)=1.45;
end
if max(Nt)>5
  I=find(Nt>5);
  Nt(I)=5;
end

[Data,nt,initRx,initRy]=Generate_Random_Input_Variables(Data,len,Fs);

for ii=1:Repeat
  tic
  if strcmp(optionN,'Noise') && ii==2
    %%Create excitation term (N(t)) for
    %%noise-induced awakenings
    [aircraftREM aircraft]=...
    Create_Aircraft_Awakenings(Data,Timing,len,Fs,pr,ink,Events);

    %%Add spontaneous and noise-induced excitation terms
    Nt=Nt+aircraft;
    NtREM=NtREM+aircraftREM;

    if max(NtREM)>1.45
      I=find(NtREM>1.45);
      NtREM(I)=1.45;
    end
    if max(Nt)>5
      I=find(Nt>5);
      Nt(I)=5;
    end
  end

  %%Low-pass filter N(t) to obtain E(t)
  [T,Wake]=E_Calc(Nt,Fs,len);
  [T,WakeREM]=E_Calc(NtREM,Fs,len);

  %%Calculate REM promoting (X) and
  %%REM inhibiting activity (Y)
  [T,X]=REM_Calc(Data,Wake,Fs,len);
  REM=X(:,1);%%REM-ON activity
```

```
  %%Create REM sleep indicator (REMT)
  [REM_NEW,st_new,ff_new]=Create_REM_INPUT(REM,Fs,len);
  toc

  %%Calculate SWA activity
  tic
  [T,X]=SWA_Calc(Data,REM_NEW,Wake,Fs,len);
  SWA=X(:,1).*(1+nt(1:length(X(:,1))))';
  toc

  %%Assign 1 second NREM sleep stages based on SWA and E(t)
  Est_Stage=zeros(1,960);
  tic
  [Est_Stage]=NREM_Sleep_Stage_Classify(Est_Stage,SWA,Wake,REM_NEW);

  %%Calculate Fast REM activity and assign 1 second REM sleep stages
  [Est_Stage]=Fast_REM_Main(Est_Stage,initRx,initRy,Fs,st_new,ff_new,WakeREM);

  %%Calculate 30 second sleep stages
  [tempstage,tempstage30plot]=Calc_30_Sec_Stages(Est_Stage);
  toc

  %%Calculate duration of each sleep stage
  for jj=1:4
    I=find(tempstage(1:960)==jj);
    dur_stage(jj,ink,ii)=length(I)/2;
  end

  %%Calculate percent of events individual awakened
  %%to during the night
  if strcmp(optionN,'Noise')
    perawake1=0;
    for jj=1:length(Timing)
      I=find(tempstage(Timing(jj)*2:Timing(jj)*2+3)==1);
      if length(I)>0 && tempstage(Timing(jj)*2-1)~=1
        perawake1=perawake1+1;
      end
    end
    perawake(ink,ii)=perawake1/length(Timing);
  end
  Full_Stages(1:length(tempstage30plot),ink,ii)=tempstage30plot';
end

%%Calculate difference in sleep stage duration
%%and probability of awakening at the time of noise events
%%for (1) baseline no-noise nights and (2)
%%nights with aircraft noise exposure
if strcmp(optionN,'Noise') && ii==2
  change(1:4,ink)=dur_stage(:,ink,2)-dur_stage(:,ink,1);
  changeperawake(ink)=(perawake(ink,2)-perawake(ink,1))
end
```

```
end

%%Save data
if strcmp(optionN,'Noise')
total_awake(1)=...
sum(perawake(1:Numpeople,1)*length(Timing))/(Numpeople*length(Timing));
total_awake(2)=...
sum(perawake(1:Numpeople,2)*length(Timing))/(Numpeople*length(Timing));
totalchangeper=mean(changeperawake)';
totalchangedur(1:4)= mean(change');
save(['Ntotal_awake_LAmax' num2str(LAMAX(1)) ...
'NumEvents' num2str(length(Timing)) 'Numpeop' num2str(Numpeople) ...
'position' num2str(position(1)) '_' num2str(position(2)) '.mat'],'total_awake')
save(['Ntotalchangeper_LAmax' num2str(LAMAX(1)) ....
'NumEvents' num2str(length(Timing)) 'Numpeop' num2str(Numpeople)...
'position' num2str(position(1)) '_' num2str(position(2)) '.mat'],'totalchangeper')
save(['Ntotalchangedur_LAmax' num2str(LAMAX(1)) ...
'NumEvents' num2str(length(Timing)) 'Numpeop' num2str(Numpeople)...
'position' num2str(position(1)) '_' num2str(position(2)) '.mat'],'totalchangedur')
save(['Ntotal_awake_LAmax' num2str(LAMAX(1)) ...
'NumEvents' num2str(length(Timing)) 'Numpeop' num2str(Numpeople)...
'position' num2str(position(1)) '_' num2str(position(2)) '.mat'],'total_awake')
save(['Nchange_LAmax' num2str(LAMAX(1)) ...
'NumEvents' num2str(length(Timing)) 'Numpeop' num2str(Numpeople) ...
'position' num2str(position(1)) '_' num2str(position(2)) '.mat'],'change')
save(['Nchangeperawake_LAmax' num2str(LAMAX(1)) ...
'NumEvents' num2str(length(Timing)) 'Numpeop' num2str(Numpeople)...
'position' num2str(position(1)) '_' num2str(position(2)) '.mat'],'changeperawake')
end

save(['NFull_Stages_LAmax' num2str(LAMAX(1)) ...
'NumEvents' num2str(length(Timing)) 'Numpeop' num2str(Numpeople)...
'position' num2str(position(1)) '_' num2str(position(2)) '.mat'],'Full_Stages')
%%%-------------------------------------------------------------------------%%
%%%-------------------------------------------------------------------------%%
```

Function Input_Parameters: This function contains the values for the parameters of the model.

```
%%%-------------------------------------------------------------------------%%
%%%-------------------------------------------------------------------------%%
%%%Function Input_Parameters
%%%Contains values of most model inputs-these values are based on the 1999
%%%UK data
%%%
%%%Output: Data-contains model parameters used
%%%-------------------------------------------------------------------------%%
%%%-------------------------------------------------------------------------%%
function [Data]=Input_Parameters
```

```
%%Noise n(t) model parameters
Data.ntmean=0;
Data.ntstd=0.20;
Data.ntskew=0.5269;
Data.ntkurtosis=3;

%%wt/E model parameters
%%divide by 10.7 to convert parameters from
%%minutes to units
Data.wtintarr=6.1/10.7;
Data.wtstddur=0.20/10.7;
Data.wtmeandur=0.5/10.7;
Data.wtmindur=0.05/10.7;

Data.wtminamp=0.5;
Data.wtmaxamp=5.0;
Data.wtmeanamp=3.0;
Data.wtstdamp=0.65;

%%Slow REM model parameters
Data.amean=0.47;
Data.astd=0.1;
Data.bmean=0.41;
Data.bstd=0.1;
Data.cmean=1.4;
Data.cstd=0.15;
Data.dmean=1.83;
Data.dstd=0.15;
Data.yomin=0.5;
Data.yomax=3;
Data.xomin=0.15;
Data.xomax=0.3;

%%SWA model parameters
Data.SWAL=0.2;
Data.fc=2.0;
Data.rc=0.4;
Data.fcw=2*Data.fc;
Data.Somean=3.75;
Data.Sostd=0.67;
Data.Somin=2.3;
Data.Somax=5.8;
Data.gcmax=0.05;
Data.gcmin=0.008;
Data.gcstd=0.011;
Data.gcmean=0.0320;
Data.SWAomin=0.13;
Data.SWAomax=1.51;
Data.SWAomean=0.78;
Data.SWAostd=0.29;
%%%-------------------------------------------------------------------------%%
```

```
%%%-------------------------------------------------------------------------%%
```

Function Generate_Random_Input_Variables: The following program is used to generate all model parameters for one person night based on uniform and Gaussian distributions.

```
%%%-------------------------------------------------------------------------%%
%%%-------------------------------------------------------------------------%%
%%%Function Generate_Random_Input_Variables
%%%Code for generating all random inputs to the model
%%%
%%%Input:  Data-contains model parameters used
%%%        len-length of night that is being simulated
%%%        Fs-sampling rate
%%%
%%%Output: Data-contains model parameter values for subject
%%%        nt-noise term applied to SWA
%%%        initRx-initial xo values for fast REM model
%%%        initRy-initial yo values for fast REM model
%%%-------------------------------------------------------------------------%%
%%%-------------------------------------------------------------------------%%
function [Data,nt,initRx,initRy]=Generate_Random_Input_Variables(Data,len,Fs)

%%Minimum and maximum values are used to
%%limit current range of parameters
%%note: acceptable range of parameters will be
%%further explored in the future

%%SWA and Process S model parameters
Data.SWAo=normrnd(Data.SWAomean,Data.SWAostd,1,1);
if Data.SWAo<Data.SWAomin
  Data.SWAo=Data.SWAomin;
elseif Data.SWAo>Data.SWAomax
  Data.SWAo=Data.SWAomax;
end

Data.So=normrnd(Data.Somean,Data.Sostd,1,1);
if Data.So<Data.Somin
  Data.So=Data.Somin;
elseif Data.So>Data.Somax
  Data.So=Data.Somax;
end

Data.gc=normrnd(Data.gcmean,Data.gcstd,1,1);
if Data.gc<Data.gcmin
  Data.gc=Data.gcmin;
elseif Data.gc>Data.gcmax
  Data.gc=Data.gcmax;
```

```
end

%%More restrictive on range for
%%slow REM sleep models as certain
%%combinations of a,b,c,d will result
%%in no REM cycling

%%Slow REM sleep model parameters
Data.a=normrnd(Data.amean,Data.astd,1,1);
if Data.a<Data.amean-Data.astd
  Data.a=Data.amean-Data.astd;
elseif Data.a>Data.amean+Data.astd
  Data.a=Data.amean+Data.astd;
end

Data.b=normrnd(Data.bmean,Data.bstd,1,1);
if Data.b<Data.bmean-Data.bstd
  Data.b=Data.bmean-Data.bstd;
elseif Data.b>Data.bmean+Data.bstd
  Data.b=Data.bmean+Data.bstd;
end

Data.c=normrnd(Data.cmean,Data.cstd,1,1);
if Data.c<Data.cmean-Data.cstd
  Data.c=Data.cmean-Data.cstd;
elseif Data.c>Data.cmean+Data.cstd
  Data.c=Data.cmean+Data.cstd;
end

Data.d=normrnd(Data.dmean,Data.dstd,1,1);
if Data.d<Data.dmean-Data.dstd
  Data.d=Data.dmean-Data.dstd;
elseif Data.d>Data.dmean+Data.dstd
  Data.d=Data.dmean+Data.dstd;
end

%%Slow and Fast REM sleep model initial conditions
Data.yo=Data.yomin+(Data.yomax-Data.yomin)*rand(1,1);
Data.xo=Data.xomin+(Data.xomax-Data.xomin)*rand(1,1);
initRx=-1+2*rand(1,10);
initRy=-1+2*rand(1,10);

%%Random noise term n(t)
cc=pearsrnd(Data.ntmean,Data.ntstd,Data.ntskew,Data.ntkurtosis, 1,len*Fs);
[b,a]=butter(3,10/(Fs/2));
nt=filter(b,a,cc);
nt=nt*(max(cc)/max(nt));
%%%-------------------------------------------------------------------------%%
%%%-------------------------------------------------------------------------%%
```

Function Create_Aircraft_Input: The following program is used to generate a matrix which contains, for each person and aircraft event, the amplitude of the associated excitation based on the maximum noise level of the event.

```
%%%-------------------------------------------------------------------------%%
%%%-------------------------------------------------------------------------%%
%%%Function Create_Aircraft_Input
%%%Code for assigning excitation values for aircraft events
%%%for every subject
%%%
%%%Input:  Data-contains model parameters used
%%%        LAMAX-noise level for each nighttime event
%%%        Numpeople-number of people at location point
%%%
%%%Output: Events-amplitudes of excitation N for all subjects for all
%%%        aircraft events during the night
%%%-------------------------------------------------------------------------%%
%%%-------------------------------------------------------------------------%%

function [Events]=Create_Aircraft_Input(Data,LAMAX,Numpeople)

%%linear relationship between noise level and
%%fraction responding
Noise=[35 80];%%Lamax level
per=[.17 .55];%%percent nonzero response(above baseline)
p=polyfit(Noise,per,1);

%%Cycle through for each noise event
for ii=1:length(LAMAX)
  %%These are nonzero responses hence value not zero
  rel=p(1)*LAMAX(ii)+p(2);
  val = normrnd(Data.wtmeanamp,Data.wtstdamp,floor(Numpeople*rel),1);
  I=find(val<Data.wtminamp);

  %%Limit range of excitations
  if length(I)>0
    val(I)=val;
  end

  I=find(val>Data.wtmaxamp);
  if length(I)>0
    val(I)=Data.wtmaxamp;
  end

  %%Nonzero and zero aircraft responses
  Total=[val(:); zeros(Numpeople,1)];
  Total=Total(1:Numpeople);
  rr=randperm(Numpeople);
  for jj=1:length(rr)
```

```
    Events(jj,ii)=Total(rr(jj));
  end
end
%%%-------------------------------------------------------------------------%%
%%%-------------------------------------------------------------------------%%
```

Function Create_Spontaneous: The following program is used to generate $N(t)$ for spontaneous awakenings for one subject night.

```
%%%-------------------------------------------------------------------------%%
%%%-------------------------------------------------------------------------%%
%%%Function Create_Spontaneous
%%%Code for generating spontaneous excitations N(t)
%%%
%%%Input:  Fs-sampling rate
%%%        len-length of night that is being simulated
%%%        Data-contains model parameters used
%%%        pr-relationship between noise amplitudes during slow and
%%%        fast models
%%%
%%%Output: Nt-amplitudes of excitation N(t) for slow models
%%%        NtREM-amplitudes of excitation N(t) for fast REM model
%%%
%%%-------------------------------------------------------------------------%%
%%%-------------------------------------------------------------------------%%
function [Nt,NtREM]=Create_Spontaneous(Fs,len,Data,pr)

delta=1/Fs;
time=0:delta:len;
Nt=zeros(1,1.1*len*Fs);
NtREM=zeros(1,1.1*len*Fs);

%%Create vectors of amplitudes and durations
Amp=normrnd(Data.wtmeanamp,Data.wtstdamp,1,length(time)*1.1);
I=find(Amp < Data.wtminamp);
Amp(I)=Data.wtminamp;

duration=normrnd(Data.wtmeandur,Data.wtstddur,1,length(time)*1.1);
I=find(duration < Data.wtmindur);
duration(I)=Data.wtmindur;

%%Time between pulses are exponentially distributed
int_arr=exprnd(Data.wtintarr,1,length(time)*1.1);
total_dur=0;
ii=1;

%%Create N(t) for slow models
%%Assuming inter-arrival time is between the start of each pulse
while (total_dur <len)
```

```
  beg=round(sum(int_arr(1:ii))/delta);
  if beg==0
    beg=1;
  end
  fin=beg+round(duration(ii)/delta);
  Nt(beg:fin)=Nt(beg:fin)+Amp(ii).*ones(1,round(duration(ii)/delta)+1);

  %%Create N(t) for fast models
  Aramp=pr(1)*Amp(ii)+pr(2);
  NtREM(beg:fin)=NtREM(beg:fin)+Aramp.*ones(1,round(duration(ii)/delta)+1);
  ii=ii+1;
  total_dur=sum(int_arr(1:ii))+duration(ii);
end
%%%-------------------------------------------------------------------------%%
%%%-------------------------------------------------------------------------%%
```

Function Create_Aircraft_Awakenings: The following program is used to generate $N(t)$ for aircraft noise events.

```
%%%-------------------------------------------------------------------------%%
%%%-------------------------------------------------------------------------%%
%%%Function Create_Aircraft_Awakenings
%%%Code for creating excitations N(t) associated with the occurrence
%%%of aircraft events
%%%
%%%Input:  Data-contains model parameters used
%%%        Timing-timing of aircraft events in minutes
%%%        len-length of night that is being simulated
%%%        Fs-sampling rate
%%%        pr-relationship between noise amplitudes during slow and
%%%        fast models
%%%        ink-subject number
%%%        Events-amplitudes of excitation N(t) for all subjects for all
%%%        events during the night
%%%
%%%Output: aircraftREM-amplitudes of excitation N(t) for fast REM model for
%%%        aircraft events
%%%        aircraft-amplitudes of excitation N(t) for slow models
%%%        aircraft events
%%%-------------------------------------------------------------------------%%
%%%-------------------------------------------------------------------------%%
function [aircraftREM aircraft]=Create_Aircraft_Awakenings(Data,Timing,...
len,Fs,pr,ink,Events)
aircraft=zeros(1,1.1*len*Fs);
aircraftREM=zeros(1,1.1*len*Fs);

for ii=1:length(Timing)
  if Events(ink,ii)>0
    dur=normrnd(Data.wtmeandur,Data.wtstddur,1,1);
```

```
    if dur<Data.wtmindur
      dur(1)= Data.wtmindur;
    end

    %%Create N(t) for slow models
    beg=round((Timing(ii)/10.7)*Fs);
    fin=beg+round(dur*Fs);
    aircraft(beg:fin)=aircraft(beg:fin)+Events(ink,ii).*ones(1,round(dur*Fs)+1);

    %%Create N(t) for fast models
    Aramp=pr(1)*Events(ink,ii)+pr(2);
    aircraftREM(beg:fin)=aircraftREM(beg:fin)+Aramp.*ones(1,round(dur*Fs)+1);
    end
  end
%%%-------------------------------------------------------------------------%%
%%%-------------------------------------------------------------------------%%
```

Function E_Calc: The following program is used to generate $E(t)$ by low pass filtering $N(t)$, which is the summation of the aircraft noise induced and spontaneous excitation terms.

```
%%%-------------------------------------------------------------------------%%
%%%-------------------------------------------------------------------------%%
%%%Function E_Calc
%%%Code for low-pass filtering the excitation term N(t)
%%%
%%%Input:  Wake-this is the Poisson Noise (N(t))
%%%        Fs-sampling rate
%%%        len-length of night that is being simulated
%%%
%%%Output: T-time
%%%        X-low pass filtered noise process E(t)
%%%-------------------------------------------------------------------------%%
%%%-------------------------------------------------------------------------%%
function [T,X]=E_Calc(Wake,Fs,len)
options = odeset('RelTol',1e-6);
[T,X]=ode45(@(t,x) fun(t,x,Wake,Fs),1/Fs:1/Fs:len,[.001],options);
end

function dxdt=fun(t,x,Wt,Fs)
dxdt=zeros(1,1);
time=(0:1:(length(Wt)-1))/Fs;
w=interp1(time,Wt,t);
dxdt(1)=(64)*w-(64)*x(1);%%Lowpass below 10 seconds
end
%%%-------------------------------------------------------------------------%%
%%%-------------------------------------------------------------------------%%
```

Function REM_Calc: The following program is used to calculate the slow REM activity, both X REM promoting activity and Y REM inhibiting activity.

```
%%%-------------------------------------------------------------------------%%
%%%-------------------------------------------------------------------------%%
%%%Function REM_Calc
%%%Code for calculating slow REM activity-based on the Massaquoi and
%%%McCarley model.
%%%
%%%Reference:S. G. Massaquoi and R. W. McCarley. Extension of the limit
%%%cycle reciprocal interaction model of REM cycle control. An integrated
%%%sleep control model, 1:138-143,1992.
%%%
%%%Input:  REM_Param-data for REM model
%%%        Wake-excitation term E(t)
%%%        Fs-sampling rate
%%%        len-length of night that is being simulated
%%%
%%%Output: T-time
%%%        X-slow REM model
%%%-------------------------------------------------------------------------%%
%%%-------------------------------------------------------------------------%%
function [T,X]=REM_Calc(REM_Param,Wake,Fs,len)
options = odeset('RelTol',1e-6);
[T,X]=ode45(@(t,x) fun(t,x,REM_Param,Wake,Fs),1/Fs:1/Fs:len,...
[REM_Param.xo REM_Param.yo],options );
end

function dxdt=fun(t,x,REM_Param,Wake,Fs)
dxdt=zeros(2,1);
time=(0:1:(length(Wake)-1))/Fs;
w=interp1(time,Wake,t);

dc2=(1.55+0.8*sin(.0467*t+4));%%24 hour circadian variation
dc=1;

%%REM-ON (X)
dxdt(1)=REM_Param.a*x(1)*dc2-x(1)*x(2)*REM_Param.b*dc2;

%%REM-OFF (Y)
dxdt(2)=-x(2)*REM_Param.c*dc+dc*(x(1)+(0.25/max(Wake))*w)*x(2)*REM_Param.d;
end
%%%-------------------------------------------------------------------------%%
%%%-------------------------------------------------------------------------%%
```

Function Create_REM_INPUT: The following program is used to calculate the start and end of each REM period based on the level of X, REM-promoting activity, from the slow REM model.

```
%%%-------------------------------------------------------------------------%%
%%%-------------------------------------------------------------------------%%
%%%Function Create_REM_INPUT
%%%Program for determining the beginning and end of each REM period
%%%based on the level of slow REM activity
%%%%
%%%Input:  REM-slow REM model activity
%%%        Fs-sampling rate
%%%        len-length of night that is being simulated
%%%
%%%Output: st_new-start of each REM period
%%%        ff_new-end of each REM period
%%%        REM_NEW-REM-indicator, 1 during REM sleep and zero during NREM
%%%        sleep
%%%-------------------------------------------------------------------------%%
%%%-------------------------------------------------------------------------%%
function [REM_NEW,st_new,ff_new]=Create_REM_INPUT(REM,Fs,len)
ii=1;
if max(REM)<1.5
  valgreat=.5*(max(REM)-min(REM));
else
  valgreat=1;
end

%%Calculate Multipliers
tempShift=REM;
Ind=find(tempShift>=valgreat);
st(ii)=Ind(1);
tempShift=tempShift(Ind(1):length(tempShift));
Ind=find(tempShift<valgreat);
maxval=max(tempShift(1:Ind(1)));
ff(ii)=Ind(1)+st(ii);
sc(ii)=1.5/maxval;
tempShift=tempShift(Ind(1):length(tempShift));
Ind=find(tempShift>=valgreat);

while(ff(ii)<len*Fs && length(Ind)>0)
  ii=ii+1;
  st(ii)=Ind(1)+ff(ii-1);
  tempShift=tempShift(Ind(1):length(tempShift));
  Ind=find(tempShift<valgreat);
 if length(Ind)>0
   maxval=max(tempShift(1:Ind(1)));
   ff(ii)=Ind(1)+st(ii);
   sc(ii)=1.5/maxval;
```

```
   tempShift=tempShift(Ind(1):length(tempShift));
else
  ff(ii)=len*Fs ;
  maxval=max(tempShift(1:length(tempShift)));
  sc(ii)=1.5/maxval;
end
  Ind=find(tempShift>=valgreat);
end

%%Cycle through and find start points for the scaled REM signal
REM_NEW=zeros(1,length(REM));
for ii=1:length(st)
  if ii==1
    temp=REM(1:ff(1)+(st(2)-ff(1))/2)*sc(ii);
    Ind=find(temp>=1);
    REM_NEW(Ind)=1;
    st_new(ii)=Ind(1);
    ff_new(ii)=Ind(length(Ind));
  elseif ii<length(st)
    temp=REM(ff(ii-1)+(st(ii)-ff(ii-1))/2:ff(ii)+(st(ii+1)-ff(ii))/2)*sc(ii);
    Ind=find(temp>=1);
    REM_NEW(round(Ind+ff(ii-1)+(st(ii)-ff(ii-1))/2-1))=1;
    st_new(ii)=round(Ind(1)+ff(ii-1)+(st(ii)-ff(ii-1))/2-1);
    ff_new(ii)=round(Ind(length(Ind))+ff(ii-1)+(st(ii)-ff(ii-1))/2-1);
  else
    temp=REM(ff(ii-1)+(st(ii)-ff(ii-1))/2:length(REM))*sc(ii);
    Ind=find(temp>=1);
    REM_NEW(round(Ind+ff(ii-1)+(st(ii)-ff(ii-1))/2-1))=1;
    st_new(ii)=round(Ind(1)+ff(ii-1)+(st(ii)-ff(ii-1))/2-1);
    ff_new(ii)=round(Ind(length(Ind))+ff(ii-1)+(st(ii)-ff(ii-1))/2-1);
  end
end
%%%-------------------------------------------------------------------------%%
%%%-------------------------------------------------------------------------%%
```

Function SWA_Calc: The following program is used to calculate the slow wave activity (SWA) and Process S.

```
%%%-------------------------------------------------------------------------%%
%%%-------------------------------------------------------------------------%%
%%%Function SWA_Calc
%%%Program for calculating slow wave activity based on Achermann et al.'s
%%%model
%%%
%%%Reference: P. Achermann, D. J. Dijk, D. P. Brunner and A. A. Borbly.  A
%%%model of human sleep homeostasis based on EEG slow-wave activity:
%%%Quantitative comparison of data and simulations. Brain Research
%%%Bulletin. 31: 97-113, 1993.
%%%
```

```
%%%Input:  Param-model parameters
%%%        REM-indicator of REM periods
%%%        Wake-aircraft and spontaneous excitations, E(t)
%%%        Fs-sampling rate
%%%        len-length of night that is being simulated
%%%
%%%
%%%Output: T-time vector
%%%        X-SWA and Process S
%%%
%%%-------------------------------------------------------------------------%%
%%%-------------------------------------------------------------------------%%
function [T,X]=SWA_Calc(Param,REM,Wake,Fs,len)
options = odeset('RelTol',1e-6);
[T,X]=ode45(@(t,x) fun(t,x,Param,REM,Wake,Fs),1/Fs:1/Fs:len,...
[Param.SWAo  Param.So],options);
end

function dxdt = fun(t,x,Param,REM,Wake,Fs)
dxdt=zeros(2,1);
timew=(0:1:(length(Wake)-1))/Fs;
timeR=(0:1:(length(REM)-1))/Fs;
w=interp1(timew,Wake,t);
R=interp1(timeR,REM,t);

%%dxdt(1) and x(1) is for SWA (slow wave activity)
%%dxdt(2) and x(2) is for process S
dxdt(1)=(Param.rc)*x(1)*x(2)*(1-x(1)/x(2))-(Param.fc)*(x(1)-Param.SWAL)*R...
-(x(1)-Param.SWAL)*(Param.fcw)*w;
dxdt(2)=-Param.gc*x(1);
end
%%%-------------------------------------------------------------------------%%
%%%-------------------------------------------------------------------------%%
```

Function NREM_Sleep_Stage_Classify: The following program is used to classify NREM sleep stages based on the level of SWA and the excitation term E.

```
%%%-------------------------------------------------------------------------%%
%%%-------------------------------------------------------------------------%%
%%%Function NREM_Sleep_Stage_Classify
%%%Program for calculating NREM sleep stages based on SWA activity
%%%and excitation values
%%%
%%%Input:  Est_Stage-empty vector for sleep stage assignment
%%%        SWA-Slow wave activity
%%%        Wake-excitation term
%%%        REM-NEW-indicator of REM periods
%%%
%%%Output: Est_Stage-assigned NREM sleep stages
```

```
%%%-------------------------------------------------------------------------%%
%%%-------------------------------------------------------------------------%%
function [Est_Stage]=NREM_Sleep_Stage_Classify(Est_Stage,SWA,Wake,REM_NEW)

for ii=1:length(SWA)
  if REM_NEW(ii)==0
    if SWA(ii)>=2.0
      Est_Stage(ii)=3;%%Stage 3/4
    elseif SWA(ii)<1.0 && Wake(ii)>=.5
      Est_Stage(ii)=1;%%Stage Wake/S1
    elseif SWA(ii)<0.3
      Est_Stage(ii)=1;%%Stage Wake/S1
    else
      Est_Stage(ii)=2;%%Stage 2
    end
  else
    Est_Stage(ii)=5;%%Temporary place holder
  end
end
%%%-------------------------------------------------------------------------%%
%%%-------------------------------------------------------------------------%%
```

Function Fast_REM_Main: The following program is the main program for calculating fast REM activity.

```
%%%-------------------------------------------------------------------------%%
%%%-------------------------------------------------------------------------%%
%%%Function Fast_REM_Main
%%%Program for calculating fast REM activity
%%%
%%%
%%%Input:  Est_Stage-vector containing sleep stages
%%%        initRx-initial xo values for fast REM model
%%%        initRy-initial yo values for fast REM model
%%%        Fs-sampling rate
%%%        st_new-start of each REM period
%%%        ff_new-end of each REM period
%%%        WakeREM-excitation term for fast REM model
%%%
%%%Output: Est_Stage-assigned sleep stages
%%%-------------------------------------------------------------------------%%
%%%-------------------------------------------------------------------------%%
function [Est_Stage]=Fast_REM_Main...
(Est_Stage,initRx,initRy,Fs,st_new,ff_new,WakeREM)

%%Moving unstable equilibrium position
Eq_Wake=2-(WakeREM);

%%Cycle through for each REM period
```

```
for ii=1:length(st_new)
  Wake_Seg=Eq_Wake(st_new(ii):ff_new(ii));

  %%t of fast REM model is on a different scale
  t=0:1/Fs:(ff_new(ii)-st_new(ii))/Fs;
  tnew=0:1/(10.7*Fs*5):(ff_new(ii)-st_new(ii))/Fs;
  Wake_Seg_sp = spline(t,Wake_Seg,tnew);

  lenT=(ff_new(ii)-st_new(ii)+1)/Fs*10.7*5;
  initREM(1)=initRx(ii);
  initREM(2)=initRy(ii);

  delta=.06;
  w=0.3*2*pi;
  A=0.50;

  %%Calculate Duffing oscillator solution
  [T,X]=Phasic_Tonic_Calc(delta,w,Wake_Seg_sp,A,Fs,lenT-1,initREM);

  %%Initial assignment of REM sleep stages
  %%1-Tonic, 0-Phasic, -1-Wake
  X=X(:,1);
  REM_Stage=0;
  I=find(X>=0);
  REM_Stage(I)=1;
  I=find(X<0 & X>-2);
  REM_Stage(I)=0;
  I=find(X<=-2);
  for jj=1:length(I)
    if Wake_Seg_sp(I(jj))<1.9
      REM_Stage(I(jj))=-1;
    else
      REM_Stage(I(jj))=0;
    end
  end

  [st, ff]=calc_tonic_phasic_int(REM_Stage);
  REM_Stage_New=REM_Stage;

  %%Correction for Tonic REM
  if st(1)~=0 && ff(1)~=0
    for jj=1:length(ff)
      if min(X(st(jj):ff(jj)))>=-.25
        REM_Stage_New(st(jj):ff(jj))=1;
      end
    end
  end
  [st, ff]=calc_tonic_phasic_int(REM_Stage_New);

  %%Tonic REM period less than 15 seconds is equal to previous stage
  if st(1)~=0 && ff(1)~=0
   for jj=1:length(ff)
```

```
    if ff(jj)-st(jj)<.25*5*Fs && st(jj)>1
      REM_Stage_New(st(jj):ff(jj))=REM_Stage_New(st(jj)-1);
    end
  end
end

%%Correct for Phasic period in which max is not near 0.5
TempREM_Phasic=ones(1,length(REM_Stage_New));
I=find(REM_Stage_New==1);
TempREM_Phasic(I)=zeros(1,length(I));
[st, ff]=calc_tonic_phasic_int(TempREM_Phasic);
if st(1)~=0 && ff(1)~=0
  for jj=1:length(ff)
    if max(X(st(jj):ff(jj)))<.25
      REM_Stage_New(st(jj):ff(jj))=0;
    end
  end
end

%%Correct if awakening started during noise event-find its end
tempEvents=ones(1,length(REM_Stage_New));
I=find(Wake_Seg_sp<1.9);
tempEvents(I)=zeros(1,length(I));
[stN, ffN]=calc_tonic_phasic_int(tempEvents);

if ffN(1)~=0 && ffN(length(ffN))<length(X)
  for jj=1:length(ffN)
    if X(ffN(jj))<-2 && X(ffN(jj)+1)<-2
      I=find(X(ffN(jj):length(X))>-2);
      if length(I)~=0
        REM_Stage_New(ffN(jj):ffN(jj)-1+I(1))=-1;
      end
    end
  end
end

%%Determine sleep stage- five points for every one point in slow models.
stageREM=[-1 0 1];
REM_StageFinal=0;
for jj=1:length(X)/(5*10.7)
  for kk=1:3
    I=length(find(REM_Stage_New((jj-1)*5*10.7+1:jj*5*10.7)==stageREM(kk)));
    perseg(kk)=I/length(REM_Stage_New((jj-1)*5*10.7+1:jj*5*10.7));
  end
  I=find(perseg==max(perseg));
  REM_StageFinal(jj)=stageREM(I(1));
  if REM_StageFinal(jj)==-1
    Est_Stage(st_new(ii)+jj-1)=1;%%Stage Wake/S1
  else
    Est_Stage(st_new(ii)+jj-1)=5;%%Stage REM
  end
end
```

```
end
%%%-------------------------------------------------------------------------%%
%%%-------------------------------------------------------------------------%%
```

Function Phasic_Tonic_Calc: The following program is used to calculate the fast REM activity based on the Duffing model with the 5th order stiffness term.

```
%%%-------------------------------------------------------------------------%%
%%%-------------------------------------------------------------------------%%
%%%Function Phasic_Tonic_Calc
%%%Program for Duffings system with a 5th order stiffness term
%%%
%%%Reference:G. X. Li and F. C. Moon.  Criteria for chaos of a three-well
%%%potential oscillator with homoclinic and heteroclinic orbits. Journal
%%%of Sound and Vibration. 136(1): 17-34, 1990.
%%%
%%%Input:  delta-damping
%%%        w-drive frequency
%%%        Wake-spontaneous and aircraft excitations
%%%        A-drive amplitude
%%%        Fs-sampling rate
%%%        len-length of night that is being simulated
%%%        init-inital conditions
%%%
%%%Output: X-fast REM model
%%%-------------------------------------------------------------------------%%
%%%-------------------------------------------------------------------------%%
function [T,X]=Phasic_Tonic_Calc(delta,w,Wake,A,Fs,len,init)
options = odeset('RelTol',1e-6);
[T,X]=ode45(@(t,X) fun(t,X,delta,w,Wake,A,Fs),1/Fs:1/Fs:len,init,options);
end

function dxdt=fun(t,X,delta,w,Wake,A,Fs)
time=(0:1:(length(Wake)-1))/Fs;
m=interp1(time,Wake,t);
dxdt=zeros(2,1);

dxdt(1)=X(2);
dxdt(2)=-1*((X(1)-0.5)*(X(1)-0))*(X(1)+0.5)*(X(1)+m)*(X(1)+2.5)...
-delta*X(2)+A*cos(w*t);
end
%%%-------------------------------------------------------------------------%%
%%%-------------------------------------------------------------------------%%
```

Function Phasic_Tonic_Calc: The following program is used to calculate the inter-arrival times of Phasic or Tonic REM sleep.

```
%%%-------------------------------------------------------------------------%%
%%%-------------------------------------------------------------------------%%
%%%Function Phasic_Tonic_Calc
%%%Program for determing start and end points of certain activity, for
%%%example calculating the inter-arrival time of phasic activity
%%%
%%%Input:  REM_Dens-fast REM model sleep stages
%%%
%%%Output: st-start
%%%        ff-end
%%%-------------------------------------------------------------------------%%
%%%-------------------------------------------------------------------------%%
function [st, ff]=calc_tonic_phasic_int(REM_Dens)
st=0;
ff=0;
ink(1:2)=1;%%ink(1) start, %%ink(2)=fin
for kk=1:length(REM_Dens)
  if REM_Dens(kk)==0 && kk <length(REM_Dens)
    if kk==1
      st(ink(1))=kk;
      ink(1)=ink(1)+1;
    elseif REM_Dens(kk-1)~=0
      st(ink(1))=kk;
      ink(1)=ink(1)+1;
    end
    if REM_Dens(kk+1)~=0
      ff(ink(2))=kk;
      ink(2)=ink(2)+1;
   end
  elseif REM_Dens(kk)==0 && kk ==length(REM_Dens)
   if REM_Dens(kk-1)~=0
     st(ink(1))=kk;
     ff(ink(2))=kk;
     ink(1)=ink(1)+1;
     ink(2)=ink(2)+1;
   else
     ff(ink(2))=kk;
     ink(2)=ink(2)+1;
     end
  end
end
%%%-------------------------------------------------------------------------%%
%%%-------------------------------------------------------------------------%%
```

Function Calc_30_Sec_Stages: The following program is used to calculate 30 second sleep stages.

```
%%%-------------------------------------------------------------------------%%
%%%-------------------------------------------------------------------------%%
```

```
%%%Function Calc_30_Sec_Stages
%%%Program for calculating 30 second sleep stages
%%%
%%%Input:  Est_Stage-1 second sleep stages
%%%
%%%Output: tempstage-30 second sleep stages
%%%        tempstage30plot-30 second sleep stages for plotting
%%%-------------------------------------------------------------------------%%
%%%-------------------------------------------------------------------------%%
function [tempstage,tempstage30plot]=Calc_30_Sec_Stages(Est_Stage)
val=[1 2 3 5];

tempstage=0;
tempstage30plot=0;
for ii=1:length(Est_Stage)/(30)
  for kk=1:length(val)
    I=find(Est_Stage((ii-1)*30+1:ii*30-1)==val(kk));
    per(ii,kk)=length(I)/(30);
  end

  maxval=max(per(ii,:));
  I=find(per(ii,:)==maxval);
  tempstage(ii)=I(1);

  if tempstage(ii)==4
    tempstage30plot(ii)=3;
  elseif tempstage(ii)==3
    tempstage30plot(ii)=1;
  elseif tempstage(ii)==2
    tempstage30plot(ii)=2;
  elseif tempstage(ii)==1
    tempstage30plot(ii)=4;
  end
end
%%%-------------------------------------------------------------------------%%
%%%-------------------------------------------------------------------------%%
```

Appendix H. Code for Feature Extraction and Sleep Stage Scoring

The following is the Matlab program used for extracting different features of the polysomnography data and for scoring sleep stages. The first part of the program extracts characteristics such as the occurrence of movement artifacts, level of EMG activity, correlation of EOG channels, power in EEG frequency bands, and the frequency with the lowest decay rate identified using Auto-Regressive modeling. An example of some of the features that were extracted for one subject night is shown in Figure H.1. Sleep stages are assigned for each second based on the extracted features using a classification algorithm that was developed and the probability of being in different sleep stages was calculated for each 30 seconds of scored sleep stages, an example for one subject night is shown in Figure H.2. An overview of the subroutines of the program is in Table H.1.

Table H.1. Subroutines of the feature extraction code and sleep stage scoring algorithm.

Subroutine Name	Is Called By	Makes Calls to
Movement_Artifacts_Threshold	Main_Feature_Calc	None
Dominant_Band_AR	Main_Feature_Calc	None
Calc_Correlation	Main_Feature_Calc	None
RLS_Calc	Main_Feature_Calc	None
Amplitude_Time_Exceeded	Main_Feature_Calc	None
Per_Power	Main_Feature_Calc	None
Power_Welch	Main_Feature_Calc	None
Classify_Stage	None	Calc_REM_Periods
Calc_REM_Periods	Classify_Stage	None

Function Main_Feature_Calc: This is the main program for extracting features of polysomnography data for later use. The data is saved and then imported into the separate sleep stage classification program.

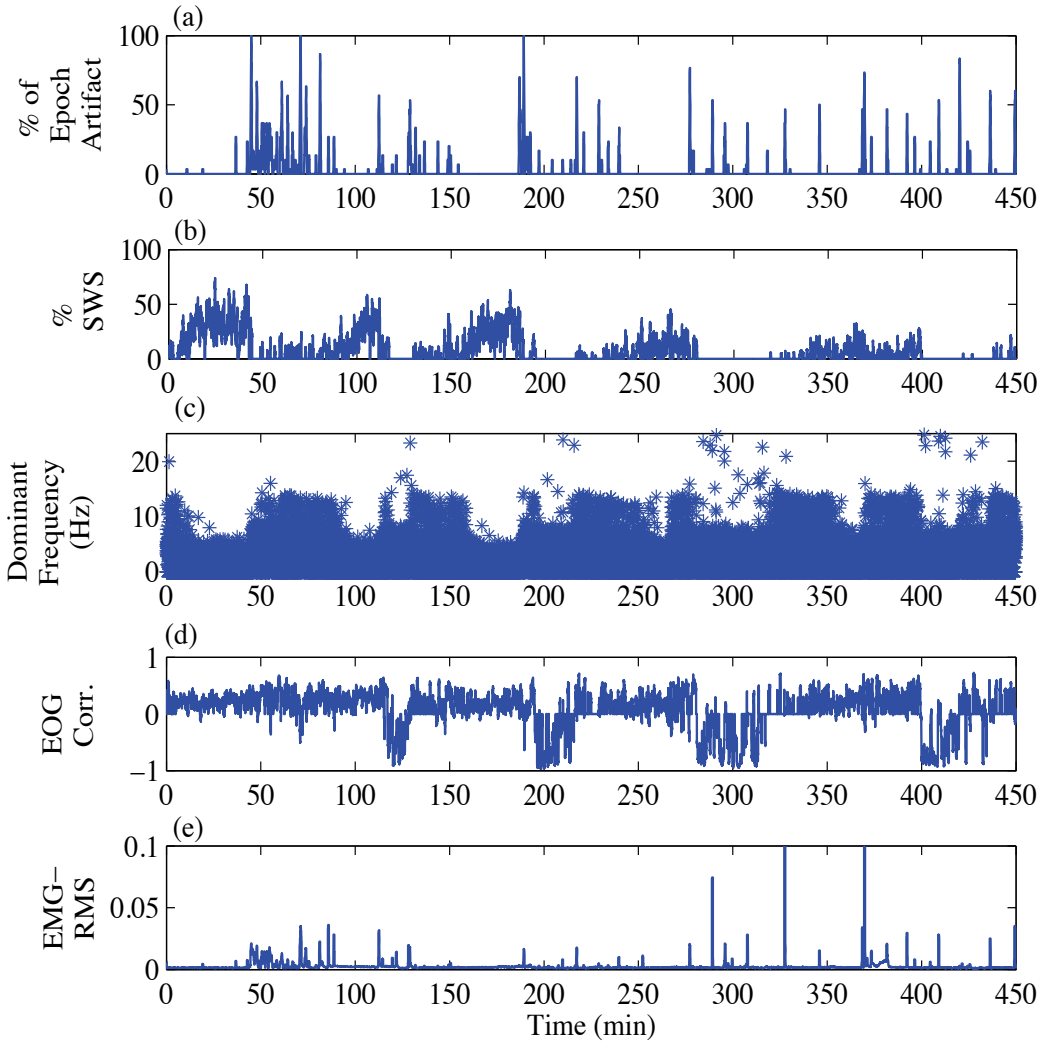

Figure H.1. An example of some of the characteristics that are extracted including; (a) the percent of an epoch occupied by movement artifacts, (b) the percent of an epoch occupied by Slow Wave Sleep (SWS), (c) the frequency that has the lowest decay rate identified using an AR(4) model, (d) correlation between the right and left EOG channels, and (e) the root-mean-square (RMS) of the EMG activity for each epoch.

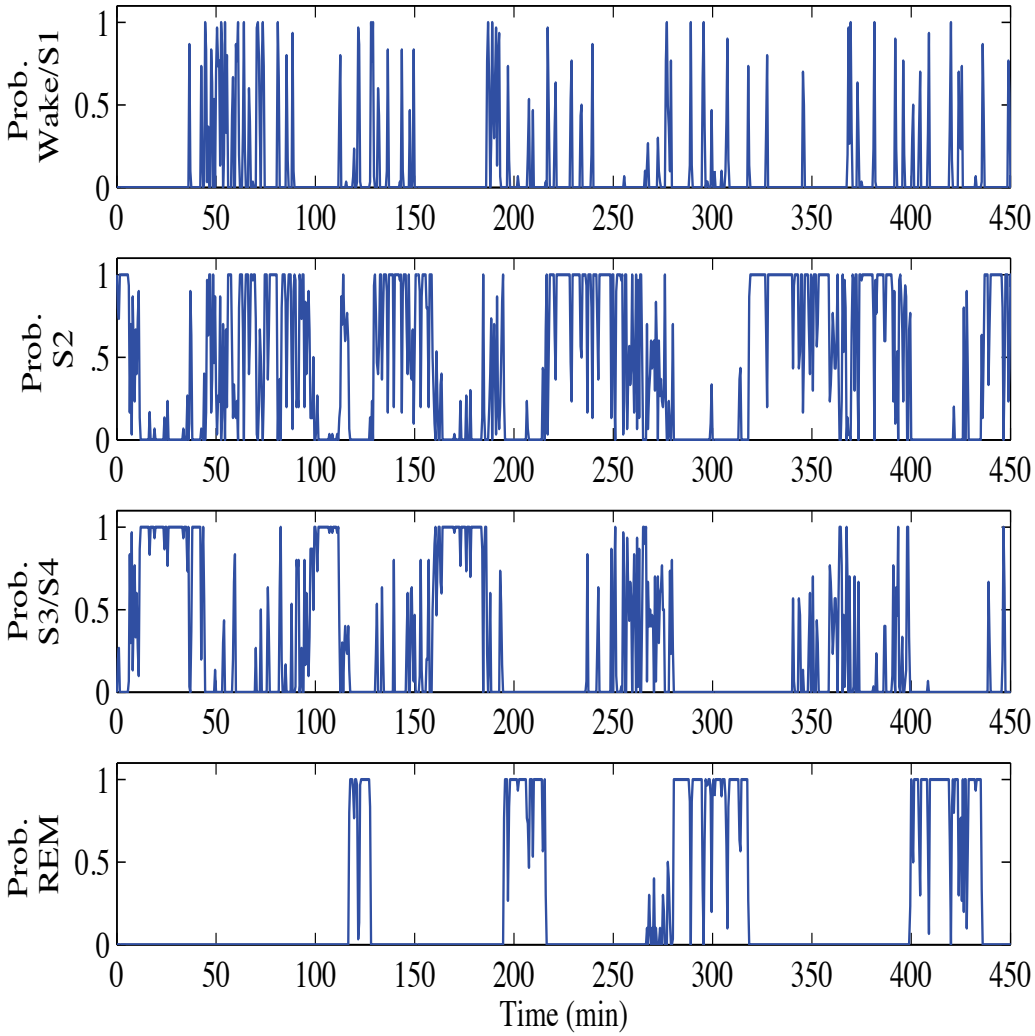

Figure H.2. Probability of being in Stage Wake/S1, Stage 2, Stage 3/4, and REM sleep calculated using the developed sleep stage scoring algorithm.

```
%%%-------------------------------------------------------------------------%%
%%%-------------------------------------------------------------------------%%
%%%Function Main_Feature_Calc
%%%Main code for extracting and saving signal characteristics for later
%%%analysis
%%%Input:  subject_num-subject number
%%%        night_num-night number
%%%        Seg_Len-length of moving signal (i.e. usually 15 or 30 seconds)
%%%        inc_Len-length of increment in time (i.e. usually 1 for 1 second)
%%%        Fs-sampling rate
%%%        correct_option-'correct' if EKG and EOG artifact corrections
%%%        are going to be applied to the EEG data
%%%        EKG_File-indicates whether the EKG file is usuable or not for
%%%        correction, equal to 0 if it is fine to use, 1 if it contains
%%%        artifacts
%%%
%%%Output: The data is saved as .mat files within this
%%%        program
%%%-------------------------------------------------------------------------%%
%%%-------------------------------------------------------------------------%%
function Main_Feature_Calc...
(subject_num, night_num,Seg_Len,inc_Len,Fs,correct_option,EKG_File)

%%Read in the Physiological Data from 1999 UK dataset
choice={'C4-A1','C3-A2','EMG','EOG-L','EOG-R','EKG','Stages'};
[Signals, Stages, Missing_Data]=Load_Signals(subject_num,night_num,choice);

%%For EOG and EKG Corrections
lambda = .9999; %%Forgetting Factor
delta = .01; %%Initial Value
M=3;%%Filter Order

%%Indentify movement artifacts
%%ART indicates whether a 1 second epoch was above the threshold (1 there
%%is an artifact and 0 there is not an artifact.)
%%Cycle through twice for both EEG channels
for ii=1:2
  [ART_Thres(:,ii),ART_Thres_onesec(:,ii)]...
  =Movement_Artifacts_Threshold(Signals(:,ii),Fs,inc_Len);
end

%%Frequency Bands
bandHigh= [ 2 4.5 4.5 8 12 16 25  35 45 15 14 45];
bandlow=  [.5 2  .5  4.5 8 12 16  25 35 11 12 .5];

%%Save AR Model for every increment
Band=[.5 45];
Size=1;
for jj=1:2
  [Damp_AR(:,jj) Freq_AR(:,jj)]=Dominant_Band_AR...
  (Signals(:,jj),Band,floor(length(Signals(:,1))/(Fs)),Size,inc_Len,Fs);
```

```
end

%%Incase I want to run for multiple segment lengths
for ink=1:length(Seg_Len)
  %%Preallocate Space
  SWS=zeros((length(ART_Thres(:,1)))-Seg_Len,2);
  ART=zeros((length(ART_Thres(:,1)))-Seg_Len,2);
  Pow=zeros((length(ART_Thres(:,1)))-Seg_Len,length(bandHigh),2);
  Pow_Welch=zeros((length(ART_Thres(:,1)))-Seg_Len,length(bandHigh),2);
  EOG_Corr=zeros((length(ART_Thres(:,1)))-Seg_Len,1);
  maxEOG=zeros((length(ART_Thres(:,1)))-Seg_Len,2);
  EMG_RMS=zeros((length(ART_Thres(:,1)))-Seg_Len,1);
  K_Complex=zeros((length(ART_Thres(:,1)))-Seg_Len,30,1);
  inc=1;
 for kk=1:(length(ART_Thres(:,1)))-Seg_Len
   display(kk)
   for jj=1:2%%Cycle twice for both EEG channels
    Seg=Signals((kk-1)*inc_Len*Fs+1:(kk-1)*inc_Len*Fs+Seg_Len(ink)*Fs,jj);
    ART(kk,jj)=sum(ART_Thres((kk-1)*1+1:(kk-1)*1+Seg_Len(ink),jj));
    EKG=Signals((kk-1)*inc_Len*Fs+1:(kk-1)*inc_Len*Fs+Seg_Len*Fs,6);
    EOGL=Signals((kk-1)*inc_Len*Fs+1:(kk-1)*inc_Len*Fs+Seg_Len*Fs,4);
    EOGR=Signals((kk-1)*inc_Len*Fs+1:(kk-1)*inc_Len*Fs+Seg_Len*Fs,5);
    EMG=Signals((kk-1)*inc_Len*Fs+1:(kk-1)*inc_Len*Fs+Seg_Len*Fs,3);

    if jj==1;%%Don't need this step for both cycles through
      Band=[.5 5];
      Thresholds=[25 250];
      %%Calculate EOG_Corr
      [EOG_Corr(kk) maxEOG(kk,1:2)]=Calc_Correlation...
      (EOGL,EOGR,Thresholds,Band,Fs);
      %%Calculate EMG RMS
      EMG_RMS(kk)=sqrt(mean(abs(EMG).^2));
    end

    %%If the EEG signal is going to be corrected for EKG and EOG artifacts
    if strcmp(correct_option,'correct')
    %%if EKG signal is usuable && low amount of movement artifacts
       if EKG_File==0 && ART(kk,jj)<15
         %%For EKG Correction
         %%Determine if segment contains EKG
         [CC]=...
         Calc_Correlation(Seg,EKG,[0 1.1*max([max(Seg) max(EKG)])],[.5 40],Fs);

         if abs(CC)>=.2 %%If EEG and EKG are Correlated
           %%EKG input signal measured in mV, EEG is measured in micro volts
           u=EKG*1000;
           d=Seg;%%Contaminated/desired EEG signal
           %%use RLS to correct EEG signal
           %%"Fixed Signal" is the output error of RLS
           [Seg,w,h]=RLS_Calc(lambda,M,u,d,delta);
         end
       end
```

```
        %%For EOG Correction
        %%Determine if segment contains eye mvmts
        %%if eye Movement && low amount of EEG artifacts
        if EOG_Corr(kk)<=-.2 && ART(kk,jj)<15
          Band=[.5 5];
          Thresholds=[25 250];

          %%Corr between EEG and EOGL
          [CCL]=Calc_Correlation(EOGL,Seg,Thresholds,Band,Fs);
          %%Corr between EEG and EOGR
          [CCR]=Calc_Correlation(EOGR,Seg,Thresholds,Band,Fs);

           %%Determine if EEG and EOG signals are correlated
           if abs(CCL)>=abs(CCR) && abs(CCL)>=.2%%Use Signal most correlated
             u=EOGL;%%input signal
             d=Seg;%%Contaminated/desired EEG signal
             %%"Fixed Signal" is the output error of RLS
             [Seg,w,h]=RLS(lambda,M,u,d,delta);
           elseif abs(CCR)>=.2
             u=EOGR;%%input signal
             d=Seg;%%Contaminated desired EEG signal
             [Seg,w,h]=RLS_Calc(lambda,M,u,d,delta);
           end
        end
    end

    %%Detect SWS
    Threshold_SWS=[75 250];
    [DataSWS]=Amplitude_Time_Exceeded(Seg,Threshold_SWS,[.5 2],Fs);
    SWS(kk,jj)=sum(DataSWS.Time_Above)/DataSWS.Total_Time;

    %%Power for segment
    [Pow(kk,1:length(bandHigh),jj)]=Per_Power(Seg,bandHigh,bandlow,Fs);

    %%Power using Welch Method
    Band=[.5 45];
    [Pow_Welch(kk,1:length(bandHigh),jj)]=...
    Power_Welch(Seg,bandHigh,bandlow,Band,Fs);
    end
  end
end


%%Save files
save(['Seg_Len_' num2str(Seg_Len(1)) 's' num2str(subject_num) '_n' ...
num2str(night_num) '_Damp_ARburg.mat'],'Damp_AR')
save(['Seg_Len_' num2str(Seg_Len(1)) 's' num2str(subject_num) '_n'...
num2str(night_num) '_Freq_ARburg.mat'],'Freq_AR')
save(['Seg_Len_' num2str(Seg_Len(ink)) 's' num2str(subject_num) '_n'...
num2str(night_num) '_SWS.mat'],'SWS')
save(['Seg_Len_' num2str(Seg_Len(ink)) 's' num2str(subject_num) '_n' ...
```

```
num2str(night_num) '_EOG_Corr.mat'],'EOG_Corr')
save(['Seg_Len_' num2str(Seg_Len(ink)) 's' num2str(subject_num) '_n'...
num2str(night_num) '_ART.mat'],'ART')
save(['Seg_Len_' num2str(Seg_Len(ink)) 's' num2str(subject_num) '_n' ...
num2str(night_num) '_EMG_RMS.mat'],'EMG_RMS')
save(['Seg_Len_' num2str(Seg_Len(ink)) 's' num2str(subject_num) '_n'...
num2str(night_num) '_Pow.mat'],'Pow')
save(['Seg_Len_' num2str(Seg_Len(ink)) 's' num2str(subject_num) '_n'...
num2str(night_num) '_Pow_Welch.mat'],'Pow_Welch')
save(['Seg_Len_' num2str(Seg_Len(ink)) 's' num2str(subject_num) '_n'...
num2str(night_num) '_maxEOG.mat'],'maxEOG')
save(['Seg_Len_' num2str(Seg_Len(ink)) 's' num2str(subject_num) '_n'...
num2str(night_num) '_ART_Thres.mat'],'ART_Thres')
save(['Seg_Len_' num2str(Seg_Len(ink)) 's' num2str(subject_num) '_n'...
num2str(night_num) '_ART_Thres_onesec.mat'],'ART_Thres_onesec')
end
%%%-------------------------------------------------------------------------%%
%%%-------------------------------------------------------------------------%%
```

Function Movement_Artifacts_Threshold: This program is used to identify when movement artifacts are occurring based on activity in the gamma frequency band of the EEG signal.

```
%%%-------------------------------------------------------------------------%%
%%%-------------------------------------------------------------------------%%
%%%Function Movement_Artifacts_Threshold
%%%Code for calculating thresholds which are used to identify movement
%%%artifacts.  The method used is based on the work of Brunner et al.
%%%
%%%Reference: D. P. Brunner, R. C. Vasko, C. S. Detka, J. P. Monahan, C. F.
%%%Reynolds III and D. J. Kupfer.  Muscle artifacts in the sleep EEG:
%%%Automated detection and effect on all-night EEG power spectra.  J. Sleep
%%%Res. 5: 155-164, 1996.
%%%
%%%Input:  Signal-typically the EEG channel
%%%        Fs-is the sampling frequency
%%%        inc_Len-size of increment in time (i.e. usually 1 for 1 second)
%%%
%%%Output: ART-indicator of artifacts, 1 if there is an artifact and 0 if
%%%        there is not an artifact
%%%        ART_Thres_re-threshold used for defining artifacts
%%%-------------------------------------------------------------------------%%
%%%-------------------------------------------------------------------------%%
function [ART,ART_Thres_re]=Movement_Artifacts_Threshold(Signal,Fs,inc_Len)

%%Consider only activity from 26 to 32 Hz
[b,a]=butter(4,[26 32]./(Fs/2),'bandpass');
Filt_Signal=filtfilt(b,a,Signal);
```

```
%%Calculate average power every 4 seconds
meanval=zeros(1,length(Signal)/(4*Fs));

for ii=1:length(Signal)/(4*Fs)
  meanval(ii)=mean(abs(Filt_Signal((ii-1)*4*Fs+1:ii*4*Fs)).^2);
end

pow_smooth=medfilt1(meanval,45); %%Brunner smoothed out the spectrum for the
                                 %%threshold using the
                                 %%surrounding three minutes
                                 %%three minutes divided by 4 second epochs
                                 %%is 45 points

ART_Thres_4sec=pow_smooth.*4;%%Brunner found that 4* the smoothed threshold
                             %%provided the best results

%%Resample threshold
len=length(Signal)/(inc_Len*Fs)-(4/inc_Len);
t=(0:1:length(ART_Thres_4sec)-1)*4;
tnew=(0:1:(len-1))*inc_Len;
ART_Thres_re=spline(t,ART_Thres_4sec,tnew);

%%Cycle through signal and and determine if the mean of the
%%signal is above the smoothed out threshold
for ii=1:length(ART_Thres_re)
  meanval(ii)=mean(abs(Filt_Signal((ii-1)*inc_Len*Fs+1:ii*inc_Len*Fs)).^2);
  if meanval(ii)> ART_Thres_re(ii)
    ART(ii)=1;
  else
    ART(ii)=0;
  end
end
end
%%%-------------------------------------------------------------------------%%
%%%-------------------------------------------------------------------------%%
```

Function Dominant_Band_AR: This program is used to determine the frequency with the lowest decay rate using an AR model.

```
%%%-------------------------------------------------------------------------%%
%%%-------------------------------------------------------------------------%%
%%%Function Dominant_Band_AR
%%%Code for calculating the frequencies that have the least damping
%%%identified using an AR model. The approach is based on Olbrich and
%%%Achermann.
%%%
%%%Reference: E. Olbrich and P. Achermann. Analysis of the temporal
%%%organization of sleep spindles in the human sleep EEG using a
```

```
%%%phenomenological modeling approach. Journal of Biological Physiology,
%%%34:341349, 2008.
%%%
%%%Input:  Signal-the EEG signal
%%%        Band-frequency band limits for filtering
%%%        Seg_Len-length of signal being used
%%%        Size-length of sub-segment
%%%        inc_Len-length of increment in time (i.e. usually 1 for 1 second)
%%%        Fs-the sampling frequency
%%%
%%%Output: max_freq-frequency associated with the minimum damping
%%%        max_damp-minimum damping value.
%%%-------------------------------------------------------------------------%%
%%%-------------------------------------------------------------------------%%

function [max_damp,max_freq]=Dominant_Band_AR(Signal,Band,Seg_Len,Size,inc_Len,Fs)
[b,a]=butter(4,[Band(1) Band(2)]./(Fs/2),'bandpass');
Seg=filtfilt(b,a,Signal);

N=4;%%Order of AR filter

%%preallocate space
max_damp=zeros((Seg_Len/inc_Len)-Size,1);
max_freq=zeros((Seg_Len/inc_Len)-Size,1);

%%Determine frequency and damping
for ii=1:floor(Seg_Len/inc_Len)-Size
  [a,e]=arburg(Seg((ii-1)*Fs*inc_Len+1:(ii-1)*Fs*inc_Len+1+Fs*Size),N);
  damping=abs(roots(a));
  freq=rad2deg(abs(angle(roots(a))))*(Fs/2)/180;

  %%find maximum value
  maxval=max(damping);
  I=0;
  I=find(damping==maxval);
  if length(I)>1
    I2=find(freq(I)>=.5 & freq(I)<45);
    if length(I2)>0
      freqval=min(freq(I(I2)));
    else
      freqval=min(freq(I));
    end
  else
    freqval=freq(I(1));
  end
  if freqval>=Band(1) &&  freqval<Band(2)
    max_damp(ii)=maxval;
    max_freq(ii)=freqval;
  else
    max_damp(ii)=0;
    max_freq(ii)=0;
  end
```

```
end
%%%-------------------------------------------------------------------------%%
%%%-------------------------------------------------------------------------%%
```

Function RLS_Calc: This program is used to create a Recursive Least Squares Filter (RLS) for removing eye movement and ECG artifacts from EEG data.

```
%%%-------------------------------------------------------------------------%%
%%%-------------------------------------------------------------------------%%
%%%Function RLS_Calc
%%%Code for Recursive Least Squares Filter
%%%
%%%Reference: S. Haykin Adaptive Filter Theory. Prentice Hall, Upper Saddle
%%%River, New Jersey, 3rd edition, 1996.
%%%
%%%Input:  Lambda=forgetting factor
%%%        M = filter order
%%%        x=input signal (ECG or EOG)
%%%        d=desired signal (contaminated EEG)
%%%        delta=initial value
%%%
%%%Output: e = error estimate (corrected signal)
%%%        h = filter coefficients
%%%-------------------------------------------------------------------------%%
%%%-------------------------------------------------------------------------%%
function [e,w,h]=RLS_Calc(lambda,M,x,d,delta)
w=zeros(M,1);
P=eye(M)/delta;

x=x(:);
d=d(:);
len=length(x);

%%error vector
e=d;

for ii=M:len
  x_est=x(ii:-1:ii-M+1);
  k=P*x_est/(lambda+x_est'*P*x_est);
  e(ii)=d(ii)-w'*x_est;
  w=w+k*conj(e(ii));
  h(:,ii)=w;
  P=lambda^(-1)*P-lambda^(-1)*k*x_est'*P;
end
%%%-------------------------------------------------------------------------%%
%%%-------------------------------------------------------------------------%%
```

Function Calc_Correlation: This program is used to calculate the correlation between two signals.

```
%%%-------------------------------------------------------------------------%%
%%%-------------------------------------------------------------------------%%
%%%Function Calc_Correlation
%%%Code for calculating the correlation between two signals
%%%
%%%Input:  Seg1-Signal 1
%%%        Seg2-Signal 2
%%%        Thresholds-minimum and maximum amplitude of signal
%%%        primarily used for EOG to eliminate artifacts
%%%        Band-frequency band limits
%%%        Fs-the sampling frequency
%%%
%%%Output: CC-correlation of the two channels
%%%-------------------------------------------------------------------------%%
%%%-------------------------------------------------------------------------%%
function [CC,maxval]=Calc_Correlation(Seg1,Seg2,Thresholds,Band,Fs)

if Band(1)~=0
   [b,a]=butter(4,[Band(1) Band(2)]./(Fs/2),'bandpass');
   temp1=filtfilt(b,a,Seg1);
   temp2=filtfilt(b,a,Seg2);
else
  [b,a]=butter(4,Band(2)./(Fs/2),'low');
  temp1=filtfilt(b,a,EOGL);
  temp2=filtfilt(b,a,EOGR);
end

maxval(1)=max(abs(temp1));
maxval(2)=max(abs(temp2));

if maxval(1)<Thresholds(2) && maxval(2)<Thresholds(2) && ...
maxval(1)>Thresholds(1) && maxval(2)>Thresholds(1)
 C=corrcoef(temp1,temp2);
 CC=C(1,2);
else
 CC=0;
end
%%%-------------------------------------------------------------------------%%
%%%-------------------------------------------------------------------------%%
```

Function Amplitude_Time_Exceeded: This program is used to calculate the percent of each epoch occupied by slow wave sleep.

```
%%%-------------------------------------------------------------------------%%
%%%-------------------------------------------------------------------------%%
%%%Function Amplitude_Time_Exceeded
%%%Code for calculating peak to peak amplitude critera
%%%
%%%Reference: H. Kuwahara, H. Higashi, Y. Mizuki, S. Matsunari, M. Tanaka,
%%%and K. Inanaga.  Automatic real-time analysis of human sleep stages by
%%%an interval histogram method. Electroencephalography and Clinical
%%%Neurophysiology, 70: 220-229,1988.
%%%
%%%Input:  Signal-either the EOG, EEG, or EMG signal
%%%        Thresholds-vector containing the minimum and maxmium amplitude
%%%        Band-frequency band limits
%%%        Fs-sampling frequency
%%%
%%%Output: Data.Time_Above-time the signal is within the specified thresholds
%%%        Data.Total_Time-total time of segment
%%%        Data.Range-maximum value of signal between zero crossings
%%%        Data.Duration-duration of the signal between zero crossings
%%%        Data.Start_Time-start time of each zero crossing
%%%        Data.End_Time-end time of each zero crossing
%%%-------------------------------------------------------------------------%%
%%%-------------------------------------------------------------------------%%
function [Data]= Amplitude_Time_Exceeded(Signal,Thresholds,Band,Fs)
[b,a]=butter(4,[Band(1) Band(2)]./(Fs/2),'bandpass');
Seg=filtfilt(b,a,Signal);

greater=[];
greater=find(Seg>=0);%%Find values greater then 0

incpos=1;
crossingpos=[];
incneg=1;
crossingneg=[];

%%Find all zero crossings
for ii=1:length(greater)
  if (greater(ii)-1)>0 && (greater(ii)+1)<length(Seg)
    if Seg(greater(ii)-1)<0 && Seg(greater(ii)+1)>0 %%make sure it is a crossing
      crossingpos(incpos)=greater(ii);
      incpos=incpos+1;
    end
    if Seg(greater(ii)+1)<0 && Seg(greater(ii)-1)>0
      crossingneg(incneg)=greater(ii);
      incneg=incneg+1;
    end
  end
end

%%Find the start, end, range, and duration for each crossing
ink=1;
if crossingpos(1)<crossingneg(1)
```

```
  lenval= length(crossingpos)-1;
else
  lenval= length(crossingneg)-1;
end
for ii=1:lenval
  if crossingpos(1)<crossingneg(1)
    temp=abs(Seg(crossingpos(ii):crossingneg(ii)));
    Data.Range(ink)=max(abs(Seg(crossingpos(ii):crossingneg(ii))));
    Data.Duration(ink)=(crossingneg(ii)-crossingpos(ii))/Fs;
    Data.Start_Time(ink)=crossingpos(ii)/Fs;
    Data.End_Time(ink)=crossingneg(ii)/Fs;
    ind=[];
    ind=find(temp==Data.Range(ink));
    Data.Max_Time(ink)=(ind(1)-1)/Fs;
    ink=ink+1;

    temp=abs(Seg(crossingneg(ii):crossingpos(ii+1)));
    Data.Range(ink)=max(abs(Seg(crossingneg(ii):crossingpos(ii+1))));
    Data.Duration(ink)=(crossingpos(ii+1)-crossingneg(ii))/Fs;
    Data.Start_Time(ink)=crossingneg(ii)/Fs;
    Data.End_Time(ink)=crossingpos(ii+1)/Fs;
    ind=[];
    ind=find(temp==Data.Range(ink));
    Data.Max_Time(ink)=(ind(1)-1)/Fs;
    ink=ink+1;
  else
    temp=abs(Seg(crossingneg(ii):crossingpos(ii)));
    Data.Range(ink)=max(abs(Seg(crossingneg(ii):crossingpos(ii))));
    Data.Duration(ink)=(crossingpos(ii)-crossingneg(ii))/Fs;
    Data.Start_Time(ink)=crossingneg(ii)/Fs;
    Data.End_Time(ink)=crossingpos(ii)/Fs;
    ind=[];
    ind=find(temp==Data.Range(ink));
    Data.Max_Time(ink)=(ind(1)-1)/Fs;
    ink=ink+1;

    temp=abs(Seg(crossingpos(ii):crossingneg(ii+1)));
    Data.Range(ink)=max(abs(Seg(crossingpos(ii):crossingneg(ii+1))));
    Data.Duration(ink)=(crossingneg(ii+1)-crossingpos(ii))/Fs;
    Data.Start_Time(ink)=crossingpos(ii)/Fs;
    Data.End_Time(ink)=crossingneg(ii+1)/Fs;
    ind=[];
    ind=find(temp==Data.Range(ink));
    Data.Max_Time(ink)=(ind(1)-1)/Fs;
    ink=ink+1;
  end
end
ii=length(crossingpos);
if crossingpos(1)<crossingneg(1)  && length(crossingneg)==length(crossingpos)
  temp=abs(Seg(crossingpos(ii):crossingneg(ii)));
  tempSign=Seg(crossingpos(ii):crossingneg(ii));
  Data.Range(ink)=max(abs(Seg(crossingpos(ii):crossingneg(ii))));
```

```
  Data.Duration(ink)=(crossingneg(ii)-crossingpos(ii))/Fs;
  Data.Start_Time(ink)=crossingpos(ii)/Fs;
  Data.End_Time(ink)=crossingneg(ii)/Fs;
  ind=[];
  ind=find(temp==Data.Range(ink));
  Data.Max_Time(ink)=(ind(1)-1)/Fs;
  Data.Range_Sign(ink)=tempSign(ind(1));
elseif length(crossingneg)==length(crossingpos)
  temp=abs(Seg(crossingneg(ii):crossingpos(ii)));
  tempSign=Seg(crossingneg(ii):crossingpos(ii));
  Data.Range(ink)=max(abs(Seg(crossingneg(ii):crossingpos(ii))));
  Data.Duration(ink)=(crossingpos(ii)-crossingneg(ii))/Fs;
  Data.Start_Time(ink)=crossingneg(ii)/Fs;
  Data.End_Time(ink)=crossingpos(ii)/Fs;
  ind=[];
  ind=find(temp==Data.Range(ink));
  Data.Max_Time(ink)=(ind(1)-1)/Fs;
  Data.Range_Sign(ink)=tempSign(ind(1));
end

%%Determine time when peak to peak amplitude is greater than the threshold
Data.Total_Time=sum(Data.Duration);
Data.Time_Above=zeros(1,length(Data.Range));
for ii=1:length(Data.Range)-1
  if (Data.Range(ii)+Data.Range(ii+1))>=Thresholds(1) &&...
   (Data.Range(ii)+Data.Range(ii+1))<=Thresholds(2)
   %%Make sure that half of wave is not contributing to the entire peak to
   %%peak amplitude
   if Data.Range(ii)>=Thresholds(1)*.25 && Data.Range(ii+1)>=Thresholds(1)*.25
     if (Data.Duration(ii)+Data.Duration(ii+1))>=1/Band(2) &&...
      (Data.Duration(ii)+Data.Duration(ii+1))<=1/Band(1)
       Data.Time_Above(ii)=Data.Duration(ii);
       Data.Time_Above(ii+1)=Data.Duration(ii+1);
     end
   end
  end
end
%%%-------------------------------------------------------------------------%%
%%%-------------------------------------------------------------------------%%
```

Function Per_Power: This program is used to calculate the root-mean-square value for the power in each frequency band.

```
%%%-------------------------------------------------------------------------%%
%%%-------------------------------------------------------------------------%%
%%%Function: Per_Power
%%%Code for calculating RMS values for each frequency band
%%%
%%%Input:  EEG-EEG segment
```

```
%%%        BandHigh-upper frequency band limit
%%%        BandLow-lower frequency band limit
%%%        Fs-sampling frequency
%%%
%%%Output: pow-RMS value for each of the specified frequency bands
%%%-------------------------------------------------------------------------%%
%%%-------------------------------------------------------------------------%%
function [pow]=Per_Power(EEG,bandHigh,bandlow,Fs)
pow=zeros(1,length(bandlow));
for ii=1:length(bandlow) %%Cycle through and calculate
  [b,a]=butter(4,[bandlow(ii) bandHigh(ii)]./(Fs/2),'bandpass');
  temp=filtfilt(b,a,EEG);
  pow(ii)=sqrt(mean(abs(temp).^2));
end
end
%%%-------------------------------------------------------------------------%%
%%%-------------------------------------------------------------------------%%
```

Function Power_Welch: This program is used to calculate power in each frequency band.

```
%%%-------------------------------------------------------------------------%%
%%%-------------------------------------------------------------------------%%
%%%Function: Power_Welch
%%%Code for calculating power spectral density
%%%
%%%Reference: F. Ferrillo, S. Donadio, F. De Carli, S. Gabarino, and
%%%L. Nobili. A model-based approach to homeostatic and ultradian
%%%aspects of nocturnal sleep structure in narcolepsy.
%%%Sleep, 30(2):157165, 2007.
%%%
%%%Input:  EEG-EEG segment
%%%        BandHigh-upper frequency band limits
%%%        BandLow-lower frequency band limits
%%%        Band-cutoff frequencies for filter
%%%        Fs-sampling frequency
%%%
%%%Output: Pow-power for each of the specified frequency bands
%%%-------------------------------------------------------------------------%%
%%%-------------------------------------------------------------------------%%
function [Pow]=Power_Welch(EEG,bandHigh,bandlow,Band,Fs)

%%Method is Similar to Ferrillo et al.  Calculate PSD using
%%Welch method.

%%Filter EEG
[b,a]=butter(4,[Band(1)  Band(2)]./(Fs/2),'bandpass');
EEG_filt=filtfilt(b,a,EEG);
```

```
%%Calculate power spectra using the Welch method
%%Use 4 second segments, apply hamming window
%%Use 75% overlap
%%Sum power in each frequency band
window=4*Fs;
noverlap=.75*window;
nfft=2^(nextpow2(8*window));
[Sxx,f] = pwelch(EEG_filt,window,noverlap,nfft,Fs,'onesided');

%%Calculate power in each frequency Band
for ii=1:length(bandHigh)
  start=find(f>=bandlow(ii));
  fin=find(f<bandHigh(ii));
  Pow(ii)=sum(Sxx(start(1):fin(length(fin))));
end
%%%-------------------------------------------------------------------------%%
%%%-------------------------------------------------------------------------%%
```

Function Calc_REM_Periods: This program is used to identify the start and end of each REM period.

```
%%%-------------------------------------------------------------------------%%
%%%-------------------------------------------------------------------------%%
%%%Function Calc_REM_Periods
%%%Code for calculating potential REM sleep periods as part of
%%%sleep stage classification algorithm
%%%
%%%Input:  Stages-sleep stages
%%%        inc_len-sliding increment used
%%%
%%%Output: start-start of each potential REM period
%%%        fin-end of each potential REM period
%%%-------------------------------------------------------------------------%%
%%%-------------------------------------------------------------------------%%
function [start,fin]=Calc_REM_Periods(Stages,inc_len)

%%Find start and finish for each REM period
starti=[];
fini=[];
starti=0;
fini=0;
I=find(Stages==5);
starti(1)=I(1);
ink=1;

for kk=2:length(I);
  durStage=length(find(Stages(I(kk-1):I(kk))<5));
  %%definition need greater then 15 minutes
  if durStage>15*floor(60/inc_len)%
```

```
    fini(ink)=I(kk-1);
    ink=ink+1;
    starti(ink)=I(kk);
  end
end

%%Can happen if REM sleep period is at end of night
if length(starti)>length(fini)
  fini(length(starti))=I(length(I));
end

%%Eliminate very brief REM sleep periods
start=[];
fin=[];
ink=1;
for kk=1:length(starti)
  lenREM=length(find(Stages(starti(kk):fini(kk))==5));
  if lenREM>=1*floor(60/inc_len) && fini(kk)-starti(kk)>=2.0*floor(60/inc_len)
    start(ink)=starti(kk);
    fin(ink)=fini(kk);
    ink=ink+1;
  end
end
%%%-------------------------------------------------------------------------%%
%%%-------------------------------------------------------------------------%%
```

Function Classify_Stage: This program is used to automatically classify sleep stages.

```
%%%-------------------------------------------------------------------------%%
%%%-------------------------------------------------------------------------%%
%%%Classify_Stage
%%%Code for automatically classifying sleep stages
%%%
%%%Input:  ART-artifact signal
%%%        SWS-percent of epoch occupied by SWS
%%%        EOG_Corr-correlation between left and right EOG channels
%%%        EMG-RMS-root mean square of EMG activity
%%%        Freq-AR-dominant frequency in the EEG signal
%%%        Alpha-power in the alpha frequency band
%%%        Delta-power in the delta frequency band
%%%        Sigma-power in the sigma frequency band
%%%        Theta-power in the theta frequency band
%%%        Seg-Size-size of segment that sleep stages are being scored
%%%        for
%%%        inc_len-sliding increment used
%%%
%%%Output: Est_Stage-sleep stages for each time increment
%%%        Per_Stage-probility of sleep stage
%%%        Hyp-hypnogram for plotting
%%%        Count_AR-percent of epoch dominated by each frequency
```

```
%%%-------------------------------------------------------------------------%%
%%%-------------------------------------------------------------------------%%

function [Est_Stage,Per_Stage,Hyp,Count_AR]=Classify_Stage...
(ART,SWS,EOG_Corr,EMG_RMS,Freq_AR,Alpha,Delta,Sigma,Theta,Seg_Size,inc_len)
I=find(EMG_RMS>0);
a=sort(EMG_RMS(I));
per_85=a(round(.85*length(a)));%%Most EMG_RMS is below 85 percentile
Est_Stage=85.*ones(1,length(SWS));
ink=1;
Est_Stage(1)=2;
jj=1;
Count_AR=0;

for ii=2:length(Alpha)
  bandHigh= [ 4.5 8 12 16 25  35 ];
  bandlow=  [ .5 4.5 8 12 16  25 ];

  for jj=1:length(bandlow)
    tempFreq_Ar=Freq_AR(ii:ii+floor(Seg_Size/inc_len)-1);
    I=find(tempFreq_Ar>=bandlow(jj) & tempFreq_Ar< bandHigh(jj));
    if length(I)~=0
      Count_AR(ii,jj)=length(I)/Seg_Size;
    else
      Count_AR(ii,jj)=0;
    end
  end
  Count_AR(ii,:)=Count_AR(ii,:)./sum(Count_AR(ii,:));

  if  ART(ii,1)>=5 || Count_AR(ii,3)>=.5
    Est_Stage(ii)=0;

  %%If there is not an artifact
  else
    if EOG_Corr(ii)>-.2 %%no eye movements
    %%.15 is from 2 standard deviations for Stage 2 sleep
      if (SWS(ii)>=.15 || Delta(ii)>=0.7 )
        Est_Stage(ii)=3;
      elseif (SWS(ii)>=.05 && SWS(ii)<.15 ) || (Count_AR(ii,4)>=1/Seg_Size )
        if Est_Stage(ii-1)==3 && Delta(ii)>=0.65 ...
        && Count_AR(ii,4)<=1/Seg_Size && Sigma(ii)<=1/Seg_Size
          Est_Stage(ii)=3;
        else
          Est_Stage(ii)=2;
        end
      else
        if Alpha(ii)/Theta(ii) >=1.5
          Est_Stage(ii)=0;
        elseif Est_Stage(ii-1)==5
          if EMG_RMS(ii)<=per_85 && SWS(ii)<=1/Seg_Size && Delta(ii)<0.45
            Est_Stage(ii)=5;
          else
```

```
            Est_Stage(ii)=0;
          end
        else
          Est_Stage(ii)=2;
        end
      end
    %%Eye Movement
    elseif EOG_Corr(ii)<=-.2
     if EMG_RMS(ii)<=per_85  &&  (Alpha(ii)/Theta(ii))< 1.5 && Delta(ii)<0.45
        Est_Stage(ii)=5;
     else
       Est_Stage(ii)=0;
     end
    end
  end
end

%%Get rid of brief eye movements (single eye movements
%%with no other activity around it)
for ii=floor(61/inc_len):length(Est_Stage)-floor(60/inc_len)
   I=find(Est_Stage(ii-floor(60/inc_len):ii+floor(60/inc_len))==5);
   if length(I)<floor(3/inc_len) && Est_Stage(ii)==5
     Est_Stage(ii)=0;
   end
end

%%Correction for rapid eye movements at the beginning of the
%%night
I=find(Est_Stage(1:30*floor(60/inc_len))==5);
for ii=1:length(I)
  if Est_Stage(I(ii)-1)==0
    Est_Stage(I(ii))=0;
  else
    Est_Stage(I(ii))=2;
  end
end

%%Correct for Stage 2 sleep during REM periods
[start,fin]=Calc_REM_Periods(Est_Stage,inc_len);
ink=1;

for ii=1:length(start)
  for jj=start(ii):fin(ii)
    if Est_Stage(jj)==2  && SWS(jj)<2/30 && Count_AR(jj,4)<=.05
      Est_Stage(jj)=5;
    elseif Est_Stage(jj)==2 && Est_Stage(jj-1)==0  && Alpha(ii)/Theta(ii) >=1.5
      Est_Stage(jj)=0;
    elseif Est_Stage(jj)==2 && Est_Stage(jj-1)==0 && Count_AR(jj,3)>Count_AR(jj,2)
      Est_Stage(jj)=0;
    end
  end
end
```

```
%%Get rid of eye movements not between end points
for ii=1:length(start)
    if ii==1
      I=find(Est_Stage(1:start(ii)-1)==5);
      Est_Stage(I)=0;
    elseif ii<=length(start)
      I=find(Est_Stage(fin(ii-1)+1:start(ii)-1)==5);
      Est_Stage(fin(ii-1)+I)=zeros(1,length(I));
    end
end
if fin(length(fin))+1<length(Est_Stage)
  I=find(Est_Stage(fin(length(fin))+1:length(Est_Stage))==5);
  Est_Stage(fin(length(fin))+I)=0;
end

val=[0 2 3 5];
%%Calc_30 second sleep stages
for ii=1:length(Est_Stage)/floor(30/inc_len)
  for jj=1:length(val)
    Per_Stage(ii,jj)=...
    length(find(Est_Stage((ii-1)*floor(30/inc_len)+1:ii*floor(30/inc_len))...
    ==val(jj)))/floor(30/inc_len);
  end

  maxval=max(Per_Stage(ii,:));
  ind=find(Per_Stage(ii,:)==maxval);
  if length(ind)>1
    if ii~=1
      Hyp(ii)=Hyp(ii-1);
    else
      Hyp(ii)=val(ind(1));
    end
  elseif length(ind)==1
     Hyp(ii)=val(ind(1));
  end
end
%%%-------------------------------------------------------------------------%%
%%%-------------------------------------------------------------------------%%
```